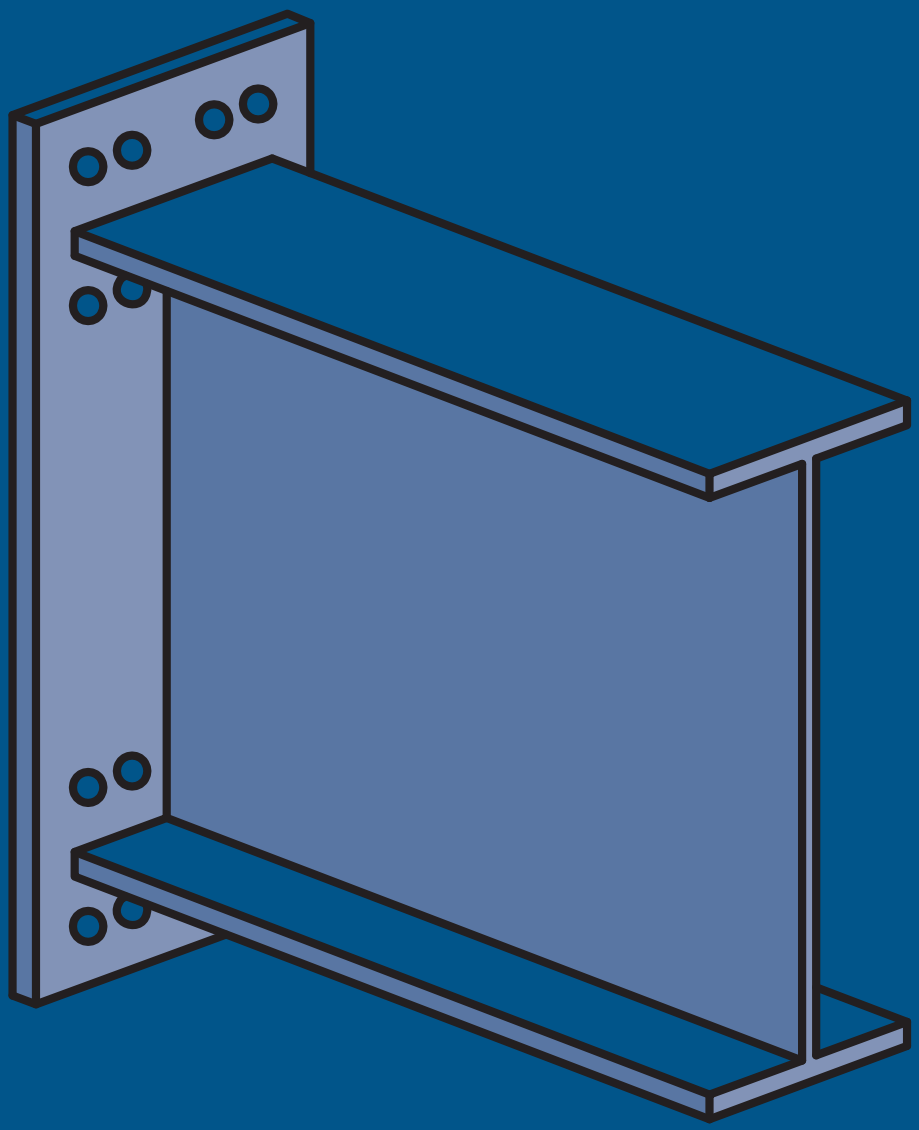

Design Guide 39

End-Plate Moment Connections

Smarter. Stronger. Steel.

Design Guide 39

End-Plate Moment Connections

Matthew R. Eatherton, SE, PhD
Thomas M. Murray, PE, PhD

American Institute of Steel Construction

© AISC 2023

by

American Institute of Steel Construction

All rights reserved. This book or any part thereof must not be reproduced in any form without the written permission of the publisher. The AISC logo is a registered trademark of AISC.

The information presented in this publication has been prepared following recognized principles of design and construction. While it is believed to be accurate, this information should not be used or relied upon for any specific application without competent professional examination and verification of its accuracy, suitability and applicability by a licensed engineer or architect. The publication of this information is not a representation or warranty on the part of the American Institute of Steel Construction, its officers, agents, employees or committee members, or of any other person named herein, that this information is suitable for any general or particular use, or of freedom from infringement of any patent or patents. All representations or warranties, express or implied, other than as stated above, are specifically disclaimed. Anyone making use of the information presented in this publication assumes all liability arising from such use.

Caution must be exercised when relying upon standards and guidelines developed by other bodies and incorporated by reference herein since such material may be modified or amended from time to time subsequent to the printing of this edition. The American Institute of Steel Construction bears no responsibility for such material other than to refer to it and incorporate it by reference at the time of the initial publication of this edition.

Printed in the United States of America

Second Printing

Authors

Matthew R. Eatherton, Ph.D., S.E., is an Associate Professor, Department of Civil and Environmental Engineering, Virginia Tech, Blacksburg, Va. He is a member of the AISC task committee on Seismic Systems and the AISC Connection Prequalification Review Panel. He is also a member of the AISC Committee on Manuals and its seismic subcommittee.

Thomas M. Murray, Ph.D., P.E., is an Emeritus Professor of Structural Steel Design, Department of Civil and Environmental Engineering, Virginia Tech, Blacksburg, Va. He is an emeritus member of the AISC Committee on Specifications and its task committee on Connection Design. He is also an emeritus member of the AISC Committee on Manuals and its subcommittee on bolts, welds, and connection elements.

Acknowledgments

The authors thank the American Institute of Steel Construction for funding the development of this document and for assistance in its preparation. The authors also wish to thank the following reviewers and AISC staff members, whose contributions significantly improved the document.

Allen Adams
Eric Bolin
Roger Brockenbrough
Maria Mercado Celin
Dustin Cole
Brad Davis
Carol Drucker
Patrick Fortney
Mark Holland
Rene Jacir
Laura Johnson
Larry Kruth
Igor Marinovic
Margaret Matthew
Ron Meng
Larry Muir
John Rolfes
Victor Shneur
Lee Shoemaker
Jeff Walsh
Dennis Watson
Ronald Yeager

Preface

This Design Guide includes a compilation and enhancement of the design procedures and design examples in AISC Design Guide 4, *Extended End-Plate Moment Connections—Seismic and Wind Applications,* published in 2004 and AISC Design Guide 16, *Flush and Extended Multiple-Row Moment End-Plate Connections,* published in 2002. Since Design Guides 4 and 16 were written, a large volume of research has been conducted, and literature has been published on the analysis and design of end-plate moment connections, much of which has been incorporated into this Design Guide. In addition, the number of end-plate configurations has been expanded from the 10 configurations in Design Guides 4 and 16 to 15 in this Design Guide. This Design Guide has an extensive literature review, an overview of design concepts, a review of the use of yield line analysis to determine end-plate strength, and design procedures for determining required bolt strength. It also includes 15 design examples for gravity, wind, and low-seismic-ductility design and three examples for high-seismic-ductility design.

Table of Contents

CHAPTER 1 INTRODUCTION 1

1.1 TYPICAL APPLICATIONS 1
1.2 OVERVIEW OF THIS DESIGN GUIDE. 1
1.3 CLASSIFICATIONS OF END-PLATE MOMENT CONNECTIONS 3
1.4 INTRODUCTION TO SEISMIC CONSIDERATIONS 4

CHAPTER 2 BACKGROUND. 7

2.1 INTRODUCTION 7
2.2 DEVELOPMENT OF DESIGN PROCEDURES 8
2.2.1 Experiments Used to Validate Design Procedures in This Design Guide 8
2.2.2 Development of Design Procedures 8
2.3 SELECTED KEY EXPERIMENTAL PROGRAMS AROUND THE WORLD 11
2.4 INVESTIGATIONS FOR SPECIFIC TOPICS 12
2.4.1 Experiments Focused on Bolt Behavior in End-Plate Moment Connections 12
2.4.2 Experiments with Variations on the Flange-to-End-Plate Welds 12
2.4.3 Investigations for Combined Bending and Axial Force 13
2.4.4 Panel Zone Behavior and Tension Field Action Adjacent to an End Plate. 13
2.4.5 Connection to Minor Axis of an I-Shaped Column 14
2.4.6 Connection to HSS Column 15
2.4.7 Column Flange Washer Plates 15
2.4.8 Effect of Composite Slab 15
2.4.9 Stiffener Geometry for Stiffened Extended End Plates 16
2.4.10 Sloping End-Plate Moment Connections. 17
2.4.11 Additional Topics 18
2.5 COMPUTATIONAL SIMULATION AND ANALYTICAL METHODS 19
2.5.1 Finite Element Method. 19
2.5.2 Component Stiffness Models of End-Plate Moment Connections. 20

CHAPTER 3 OVERVIEW OF DESIGN CONCEPTS 23

3.1 OVERVIEW 23
3.2 CONNECTION STIFFNESS AND USE AS FULLY RESTRAINED CONNECTION 25
3.3 DESIGN FOR END-PLATE FLEXURAL YIELDING 26
3.4 DESIGN OF BOLTS TO RESIST FLEXURE IN THE CONNECTION 33
3.5 DESIGN FOR AXIAL AND SHEAR FORCES 36
3.6 APPLYING DESIGN PRINCIPLES TO SLOPED CONNECTIONS. 37
3.7 ADDITIONAL LIMIT STATES AND ASSUMPTIONS 38
3.7.1 Limit State Checklist 38
3.7.2 Assumptions 39
3.7.3 Column Panel Zone Strength. 40
3.7.4 End-Plate Stiffener Requirements. 43
3.7.5 Beam and Stiffener Welds to End Plate. 44
3.7.6 Column-Side Limit States. 46

CHAPTER 4 DESIGN CONSIDERATIONS 49

4.1 DESIGN CHOICES 49
4.1.1 Thick vs. Thin End-Plate Design for Gravity, Wind, and Low-Seismic-Ductility Design 49
4.1.2 Limits on Parameters Based on Range Tested 49
4.1.3 Materials. 49
4.2 DETAILING ISSUES 50
4.2.1 Fit-Up Issues 50
4.2.2 Bolt and End-Plate Detailing. 50
4.2.3 Welds and Weld Access Holes 52
4.2.4 Composite Slabs. 52
4.2.5 Stiffener and Cap Plate Detailing 53

CHAPTER 5 GRAVITY, WIND, AND LOW-SEISMIC-DUCTILITY DESIGN 55

5.1 DESIGN EQUATIONS 55
5.1.1 Thick End-Plate Design Procedure 55
5.1.2 Thin End-Plate Design Procedure. 56
5.1.3 Design Procedure 58
5.2 FLUSH END-PLATE CONNECTIONS 59
5.2.1 Design Tables and Limitations. 59
5.2.2 Flush Thick End-Plate Analysis Examples 66
Example 5.2-1—Two-Bolt Flush Unstiffened Thick End-Plate Example 66
Example 5.2-2—Four-Bolt Flush Unstiffened Thick End-Plate Example 77

Example 5.2-3—Four-Bolt Flush Stiffened with Web Stiffener Plates between the Tension Bolts Thick End-Plate Example 83
Example 5.2-4—Four-Bolt Flush Stiffened with Web Stiffeners below the Tension Bolts Thick End-Plate Example 91
Example 5.2-5—Six-Bolt Flush Unstiffened Thick End-Plate Example 99
Example 5.2-6—Six-Bolt Flush Four-Wide/ Two-Wide Unstiffened Thick End-Plate Example. 105
5.3 EXTENDED END-PLATE CONNECTIONS 112
5.3.1 Design Tables and Limitations. 112
5.3.2 Extended Thick End-Plate Analysis Examples 122
Example 5.3-1—Four-Bolt Extended Unstiffened Thick End-Plate Example 123
Example 5.3-2—Four-Bolt Extended Stiffened Thick End-Plate Example 138
Example 5.3-3—Multiple-Row Extended 1/2 Unstiffened Thick End-Plate Example 153
Example 5.3-4—Multiple-Row Extended 1/3 Unstiffened Thick End-Plate Example 159
Example 5.3-5—Multiple-Row Extended 1/3 Stiffened Thick End-Plate Example 166
Example 5.3-6—Eight-Bolt Extended Four-Wide Unstiffened Thick End-Plate Example 174
Example 5.3-7—Eight-Bolt Extended Stiffened Thick End-Plate Example. . . . 180
Example 5.3-8—12-Bolt Multiple-Row Extended 1/3 Four-Wide/Two-Wide Unstiffened Thick End-Plate Example 188
Example 5.3-9—12-Bolt Extended Stiffened Thick End-Plate Example 195

CHAPTER 6 HIGH-SEISMIC-DUCTILITY DESIGN. 205

6.1 INTRODUCTION AND DESIGN APPROACH 205
6.2 DESIGN REQUIREMENTS. 205
6.2.1 General 205
6.2.2 Geometric Limitations for Beams, Columns, Bolts, and End Plates 206
6.2.3 Design Requirements for Bolts 208
6.2.4 Design Requirements for End Plates 210
6.2.5 Design Requirements for End-Plate Stiffeners. 213
6.2.6 Detailing of Composite Slabs at End-Plate Connections. 213
6.2.7 Weld Design and Detailing Requirements 213
6.2.8 Column-Side Limit States. 214
6.3 DESIGN EXAMPLES. 218
Example 6.3-1—Four-Bolt Extended Unstiffened End-Plate Example. 218
Example 6.3-2—Four-Bolt Extended Stiffened End-Plate Example. 234
Example 6-3-3—Eight-Bolt Extended Stiffened End-Plate Example. 247

APPENDIX A COLUMN-SIDE YIELD LINE PARAMETERS. 263

APPENDIX B GRAVITY, WIND, AND LOW-SEISMIC-DUCTILITY THIN END-PLATE DESIGN EXAMPLES 277

B.1 CONNECTION EXAMPLES 277
B.2 FLUSH THIN END-PLATE CONNECTIONS 277
Example B.2-1—Two-Bolt Flush Unstiffened Thin End-Plate Example 277
Example B.2-2—Four-Bolt Flush Unstiffened Thin End-Plate Example . . 282
Example B.2-3—Four-Bolt Flush Stiffened with Web Stiffener between the Tension Bolts Thin End-Plate Example 287
Example B.2-4—Four-Bolt Flush Stiffened with Web Stiffener below the Tension Bolts Thin End-Plate Example 292
Example B.2-5—Six-Bolt Flush Unstiffened Thin End-Plate Example 297
Example B.2-6—Six-Bolt Flush Four-Wide/ Two-Wide Unstiffened Thin End-Plate Example. 302
B.3 EXTENDED THIN END-PLATE CONNECTIONS 307
Example B.3-1—Four-Bolt Extended Unstiffened Thin End-Plate Example . . 307
Example B.3-2—Four-Bolt Extended Stiffened Thin End-Plate Example 314

Example B.3-3—Multiple-Row Extended 1/2 Unstiffened Thin End-Plate Example 321
Example B.3-4—Multiple-Row Extended 1/3 Unstiffened Thin End-Plate Example 328
Example B.3-5—Multiple-Row Extended 1/3 Stiffened Thin End-Plate Example 334
Example B.3-6—Eight-Bolt Extended Four-Wide Unstiffened Thin End-Plate Example 340
Example B.3-7—Eight-Bolt Extended Stiffened Thin End-Plate Example 347
Example B.3-8—12-Bolt Multiple-Row Extended 1/3 Four-Wide/ Two-Wide Unstiffened Thin End-Plate Example. 357
Example B.3-9—12-Bolt Extended Stiffened Thin End-Plate Example 363

SYMBOLS 371

REFERENCES. 377

Chapter 1
Introduction

1.1 TYPICAL APPLICATIONS

An end-plate moment connection is made when a steel plate is shop welded to the end of a beam or the top of a column and then the plate is field bolted to the connecting member using high-strength bolts. One of the biggest advantages of the end-plate moment connection is that it allows fast erection of rigid joints without requiring any field welding. With advances in 3D detailing software and automated shop fabrication equipment, end-plate moment connections can be fabricated efficiently and with tolerances that create good fit-up in the field. The following summarizes some of the advantages of end-plate moment connections:

- A moment connection that does not require field welding. This can be especially advantageous in cases with high field labor costs, difficulties getting qualified field welders, unfavorable environmental conditions such as low temperatures or high winds, or galvanized structures for which welding requires special accommodations.
- The end-plate connection does not need to be designed as slip-critical, thus allowing relaxed surface preparation as compared to other bolted moment connections such as bolted flange plate connections.
- End-plate moment connections are not as affected by flange out-of-square imperfections (i.e., flange tilt) as other bolted moment connections such as bolted flange plate connections.
- A moment connection that is faster to erect than field-welded connections.

End-plate moment connections are used in a variety of steel structures from nonbuilding framework to complex building structures, low-rise to taller buildings, low-seismic to high-seismic sites, and in structures with low to extremely large loads. The most common application for end-plate moment connections in the United States are metal buildings; however, use in conventionally fabricated structures is becoming more common. This Design Guide can be used for many of these connections, including conventional steel buildings with end-plate moment connections between hot-rolled steel sections [Figure 1-1(a)], metal buildings with end-plate moment connections at rafter-to-column [Figure 1-1(b)], rafter-on-column connections [Figure 1-1(c)], or beam-to-beam splice connections [Figure 1-1(d)]. Figure 1-2 shows examples of end-plate moment connections being erected in the field.

Connections between steel members can be categorized as simple, partially restrained (PR), or fully restrained (FR). Simple connections are defined as transmitting negligible moment, whereas FR connections are defined as transmitting moment with negligible rotation between the connected members. End-plate moment connections designed according to this Design Guide are intended for FR construction. For purposes of structural analysis, therefore, end-plate moment connections can be considered as fully fixed.

1.2 OVERVIEW OF THIS DESIGN GUIDE

The purpose of this Design Guide is to provide a convenient source of information for the design of end-plate moment connections. End-plate moment connections are subject

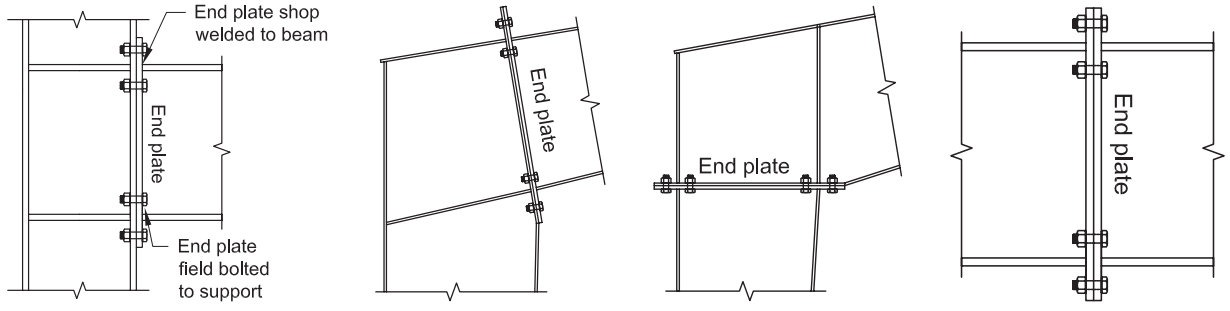

(a) Beam-to-column *(b) Rafter-to-column* *(c) Rafter-on-column* *(d) Beam-to-beam*

Fig. 1-1. Schematic drawings of typical end-plate moment connections.

to a set of limit states associated with the end plate, bolts, welds, and column that have unique aspects. For instance, the application of yield line analysis to calculate end-plate and column flange flexural strength and the application of the effective tee-stub analogy to calculate prying forces require careful consideration. This Design Guide attempts to summarize and simplify the design concepts and limit state checks into coherent design procedures. The design procedures for the 15 end-plate moment connection configurations presented herein have been validated by testing.

The scope of this Design Guide includes the development of fundamental concepts, conversion of these concepts into design equations, and design examples. Gravity, wind, and low-seismic-ductility applications are covered, as well as high-seismic-ductility applications. Both allowable strength design (ASD) and load and resistance factor design (LRFD) procedures are discussed and illustrated throughout this Design Guide. While some concepts are unique to built-up members, the design procedures can be applied to both conventional hot-rolled steel sections or built-up steel sections.

Two previous AISC Design Guides were consolidated and updated in this Design Guide. Design Guide 16, *Flush and Extended Multiple-Row Moment End-Plate Connections* (Murray and Shoemaker, 2002), provided information, concepts, design procedures, and examples for nine end-plate moment connection configurations. Design Guide 16 was intended for use in low-seismic-ductility applications. The second edition of Design Guide 4, *Extended End-Plate Moment Connections, Seismic and Wind Applications* (Murray and Sumner, 2004), included seismic design procedures and examples for three end-plate moment connection configurations.

Besides consolidating information from the previous AISC Design Guides 4 and 16, some of the changes and additions incorporated into the current Design Guide are:

- Expanded background chapter with more information on past testing.
- Added fundamental information on how to conduct yield line analysis.
- Included development of prying action forces.
- Added more information about how to handle specific conditions such as sloping connections and large axial forces.
- Added more information on column-side limit states.
- Added more discussion of design and detailing considerations.
- Added more connection configurations to go from nine configurations in the previous Design Guide 16 to 15 in this Design Guide.
- Expanded discussion of seismic design issues and new design examples demonstrating seismic design procedures.

Design procedures in this Design Guide are based on the AISC *Specification for Structural Steel Buildings,* ANSI/AISC 360-22 (AISC, 2022d); AISC *Seismic Provisions for Structural Steel Buildings,* ANSI/AISC 341-22 (AISC, 2022c); and AISC *Prequalified Connections for Special and*

(a) Conventional steel building (photo from Matt Eatherton collection)

(b) Metal building (photo courtesy of MBMA)

Fig. 1-2. Erection of beams with end-plate moment connections.

Intermediate Steel Moment Frames for Seismic Applications, ANSI/AISC 358-22 (AISC, 2022b), and are hereafter referred to as the AISC *Specification,* the AISC *Seismic Provisions,* and AISC *Prequalified Connections*, respectively, in the remainder of this Design Guide.

The AISC 15th Edition *Steel Construction Manual* (AISC, 2017a) and the companion *Design Examples* version 15.0 (AISC, 2017b), are resources for connection limit states. As a companion to the AISC *Seismic Provisions* and AISC *Prequalified Connections*, the AISC *Seismic Design Manual*, 3rd Edition (AISC, 2018), is a resource for design aids and examples. Another resource for seismic design of end-plate moment connections is the *Seismic Design Guide for Metal Building Systems: Based on the 2019 IBC*, 3rd Edition, published by the International Code Council (MBMA, 2019).

This Design Guide is organized into six chapters and two appendices. The content is arranged as follows:

1. Chapter 1 gives an introduction to end-plate moment connections and their typical classifications and sets the scope of this Design Guide.
2. Chapter 2 presents a review of past experimental programs. There has been substantial previous testing on end-plate moment connections, and the goal of this chapter is to review that past work in an organized way such that the reader can identify experiments done on specific connection configurations or with specific conditions.
3. Chapter 3 develops the design concepts, including an introduction to yield line analysis, bolt prying forces, sloping connections, welds, and column-side limit states.
4. Chapter 4 includes a discussion of several design and detailing considerations intended to help engineers and detailers make informed choices.
5. Chapter 5 covers gravity, wind, and low-seismic-ductility design of end-plate moment connections. The chapter starts with design equations used for thick and thin end-plate and bolt design methods. The following two sections provide thick end-plate design examples for six flush and nine extended connection configurations. Most examples show the design of the end plate, bolts, and welds, but three examples, the first in Section 5.2, Flush End-Plate Connections, and the first two in Section 5.3, Extended End-Plate Connections, include design checks for column-side limit states.
6. Chapter 6 discusses the seismic design procedures and gives three relatively complete design examples.
7. Appendix A is a collection of column-side yield line parameters.
8. Appendix B has thin end-plate design examples for 15 configurations. These connections have the same geometry as the corresponding connections in Chapter 5 with the exception of Example B.3.7.
9. A Symbols list and References follow Appendix B.

1.3 CLASSIFICATIONS OF END-PLATE MOMENT CONNECTIONS

End-plate moment connections are classified as flush or extended, stiffened or unstiffened, and are further classified by the number and configuration of bolts at the tension flange. Depending on the direction of the moment and whether the connection will see a moment reversal, the bolted end plate may be designed to carry tension at the top flange, bottom flange, or both. Consequently, connections may have a combination of configurations, such as an extended end plate at the top flange and a flush end plate at the bottom flange.

A flush connection is detailed such that the end plate does not appreciably extend beyond the beam flanges with all bolts located between the beam flanges. An extended end plate is one that extends beyond the tension flange a sufficient distance to allow one or more bolt rows outside the beam flange. Flush end-plate connections are typically used in frames subject to light lateral loads or near inflection points of gable frames. Extended end plates are typically used for beam-to-column moment connections. However, flush end plates are sometimes used for beam-to-column moment connections when a plate extension would interfere with other members or the roof deck.

Six flush and nine extended end-plate connections are within the scope of this Design Guide. The flush end-plate configurations are shown in Figure 1-3. Figures 1-3(a) and 1-3(b) show unstiffened flush end-plate connections with two and four bolts near the tension flange. Figures 1-3(c) and 1-3(d) show stiffened flush end-plate connections with four bolts near the tension flange. In Figure 1-3(c), a web stiffener plate is located on both sides of the web between the two tension bolt rows, while in Figure 1-3(d), the web stiffener plates are located below the two tension bolt rows. For both connections, the stiffener plates are welded to both the end plate and the beam web. Figure 1-3(e) shows a six-bolt flush end-plate connection with three rows of bolts, and Figure 1-3(f) shows a six-bolt configuration with four bolts in the first row and two bolts in the second row.

The nine extended end-plate configurations are shown in Figure 1-4. Figure 1-4(a) shows an extended, unstiffened end-plate connection with four bolts at the tension flange, which is probably the most commonly used configuration. Figure 1-4(b) shows the same connection with an end-plate to beam flange stiffener. A connection with eight bolts in two rows of four bolts each is shown in Figure 1-4(c).

Six multiple-row extended (MRE) end-plate configurations are shown in Figures 1-4(d) through 1-4(i). These configurations have three or more rows of bolts. They are identified with the notation x/y, where "x" is the number of bolt rows outside the tension flange and "y" is the number of bolt rows inside the tension flange. The connection shown in Figure 1-4(d) is designated as the unstiffened MRE 1/2 configuration, while the connections shown in Figures 1-4(e) and 1-4(f) are designated as unstiffened and stiffened MRE 1/3 configurations, respectively. The connection shown in Figure 1-4(g) is referred to as the eight-bolt extended stiffened (8ES) configuration. A 12-bolt unstiffened MRE 1/3 configuration is shown in Figure 1-4(h) that has four bolts in the two outer rows and two bolts in the two inner rows. A 12-bolt MRE 2/2 stiffened configuration is shown in Figure 1-4(i) that has two and four bolt outer and inner rows.

1.4 INTRODUCTION TO SEISMIC CONSIDERATIONS

There are fundamental differences in the design and expected behavior of lateral force-resisting systems designed for seismic ductility as opposed to systems designed for gravity or wind loading. For gravity and wind loads, a structure is designed to have sufficient strength to resist moment, shear, and axial force on a member or a connection. When subjected to full service loads, the structure is expected to remain essentially elastic.

The goal of seismic design is to provide sufficient deformation capacity (elastic and inelastic) to survive the maximum considered earthquake with a low probability of collapse. Design seismic lateral loads do not represent the forces that are produced during an earthquake. Instead, design seismic lateral loads are calibrated forces, much smaller than the forces that would develop in an elastic structure that, in combination with proper detailing requirements, will result in a structure with sufficient deformation capacity to survive a rare earthquake without collapse. Actual forces and drifts will be considerably larger than the design lateral loads and associated elastic displacements suggest. During large earthquakes, substantial inelasticity is expected to occur in members and connections throughout the structure. Seismic design centers around ensuring nonductile parts of the load path can resist the larger forces that develop, and that brittle limit states are prevented while the structure is subjected to the larger inelastic drifts.

Regardless of the type of loading, moment frames are often drift-controlled, meaning that the beam and column sizes are selected to limit the lateral drifts below the applicable limit. For gravity and wind loading, the connection is then designed such that the flexural strength of the connection, as calculated for all applicable limit states, is greater

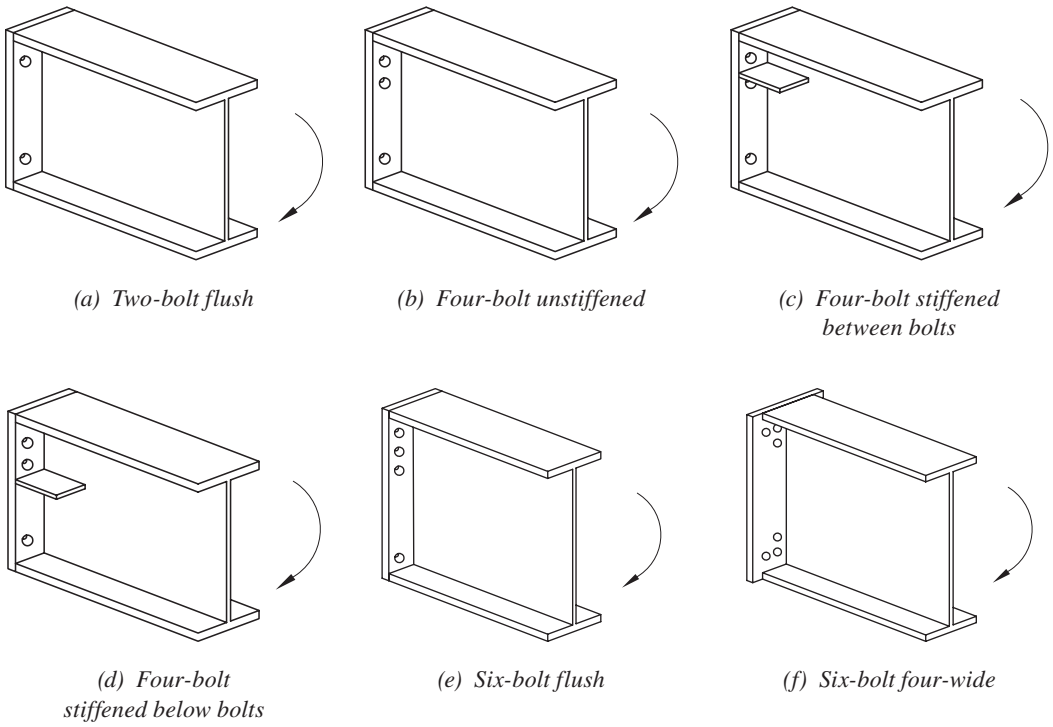

Fig. 1-3. Flush end-plate moment connections.

than the required flexural strength. Common limit states that control an end-plate connection design include end-plate flexural yielding; bolt rupture; weld rupture; panel zone yielding; column flange yielding; and column web yielding, crippling, or buckling. The resulting connection generally has smaller flexural strength than the flexural strength of the beam, meaning that the connection may fail before the beam.

Conversely, when designing for seismic ductility, the goal is to create a flexural plastic hinge in the beam and prevent all connection limit states. Plastic hinging of the beam creates considerably more inelastic rotation capacity than limit states like end-plate yielding or bolt yielding. After selecting the beam size based on drift requirements, the largest moment the beam can produce is calculated considering likely material over-strength and strain-hardening. All parts of the end-plate moment connection and column are designed to resist the largest moment the beam can create. This design approach is referred to as capacity design, and it can result in connections that are significantly stronger than nonseismic design.

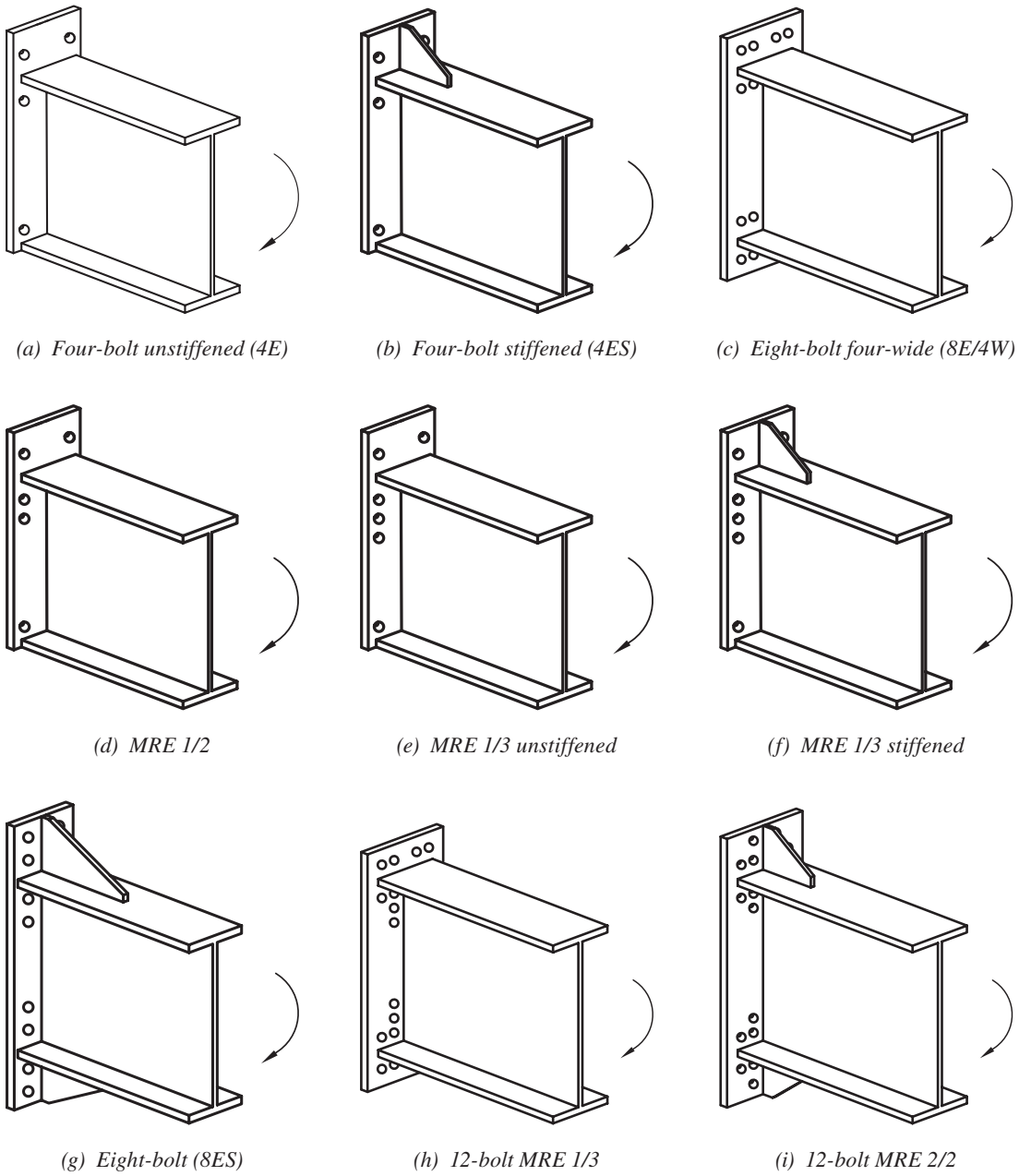

(a) Four-bolt unstiffened (4E) *(b) Four-bolt stiffened (4ES)* *(c) Eight-bolt four-wide (8E/4W)*

(d) MRE 1/2 *(e) MRE 1/3 unstiffened* *(f) MRE 1/3 stiffened*

(g) Eight-bolt (8ES) *(h) 12-bolt MRE 1/3* *(i) 12-bolt MRE 2/2*

Fig. 1-4. Extended end-plate moment connections.

Beyond providing sufficient design strength to cause a beam plastic hinge, it is necessary to detail the connection so that fracture is avoided. Because it is difficult to determine through equations or computational simulation whether specific details will result in premature fracture, full-scale experiments are required. The AISC *Seismic Provisions* allow two approaches for showing that a connection configuration has sufficient ductility to be used in an intermediate moment frame (IMF) or a special moment frame (SMF)—qualification and prequalification. A connection can be qualified for a specific project if two full-scale tests with identical details to the actual building are successfully performed. The criterion for successful SMF qualification is that the connection must undergo 0.04 rad of rotation, while an IMF must only reach 0.02 rad. Both types must resist 80% of the nominal beam plastic moment strength at the respective rotation requirements.

If a sufficient number of full-scale tests have been performed on a particular connection configuration using consistent design and detailing, a connection can be prequalified for the range of parameters that have been tested. AISC *Seismic Provisions* Section K1.2b states that prequalification shall be established by a connection prequalification review panel (CPRP). The only currently recognized CPRP, that the authors are aware of, is the AISC Connection Prequalification Review Panel. AISC *Prequalified Connections* contains design and detailing requirements for three prequalified end-plate moment connection configurations as shown in Figure 1-5. Therefore, instead of project-specific tests, structural engineers can follow the procedures in that standard to design a connection for IMF or SMF. These end-plate configurations—the four-bolt extended unstiffened, four-bolt extended stiffened, and the eight-bolt extended stiffened—represent a subset of the 15 connection configurations described in this Design Guide for gravity, wind, and low-seismic-ductility applications. Design and detailing requirements for the three prequalified connections are described and demonstrated in Chapter 6 of this Design Guide.

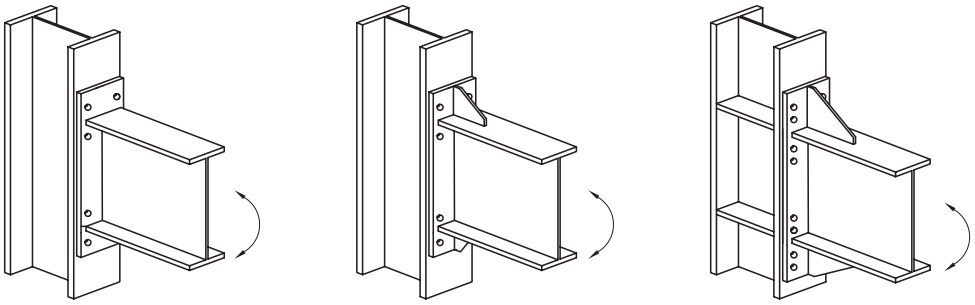

(a) Four-bolt extended unstiffened

(b) Four-bolt extended stiffened

(c) Eight-bolt extended stiffened

Fig. 1-5. End-plate moment connections prequalified for use in intermediate or special moment frames.

Chapter 2
Background

2.1 INTRODUCTION

While it is conceptually simple to create a moment connection using an end plate, the end-plate moment connection is highly indeterminate and has a deceptively complex behavior that is subject to a whole host of limit states associated with the beam, welds, end plate, bolts, and column. Many types of loading are also possible, including axial forces in addition to moment and shear, out-of-plane loads, static loads versus dynamic loads, and elastic stresses versus large inelastic strains due to earthquakes. The moment connection behavior can be further complicated by the presence of composite concrete slabs or the use of beams or columns other than I-shapes bent about their major axis. A substantial number of studies have been performed to understand the range of end-plate moment connection behavior as subjected to different types of loading.

Approaches to studying the behavior of end-plate moment connections include experiments, computational simulation, and analytical modeling (i.e., equations or component models). This literature review focuses more on experimental studies. Types of experiments include beam-to-column experiments, beam-to-beam splice experiments, tee-joint tests to investigate bolt behavior with prying action, knee joint tests that implicitly include axial force, and full-frame tests. These types of testing configurations are illustrated in Figure 2-1.

There has been considerable research conducted on end-plate moment connections, including work conducted on all continents except Antarctica. While it is not necessary to understand the literature to use the design procedures presented in this Design Guide, an understanding of the literature is useful. For design configurations or loading outside the typical design procedures, the literature can be used for guidance. For example, there is considerable research on end-plate moment connections with large axial forces and behavior of end-plate moment connections with concrete slabs that are composite with the beam up to the face of the column—neither of which is covered by the design procedures herein.

This literature review builds on past literature reviews. For instance, Murray (1988) presents a review that includes an overview of end-plate moment connections, literature

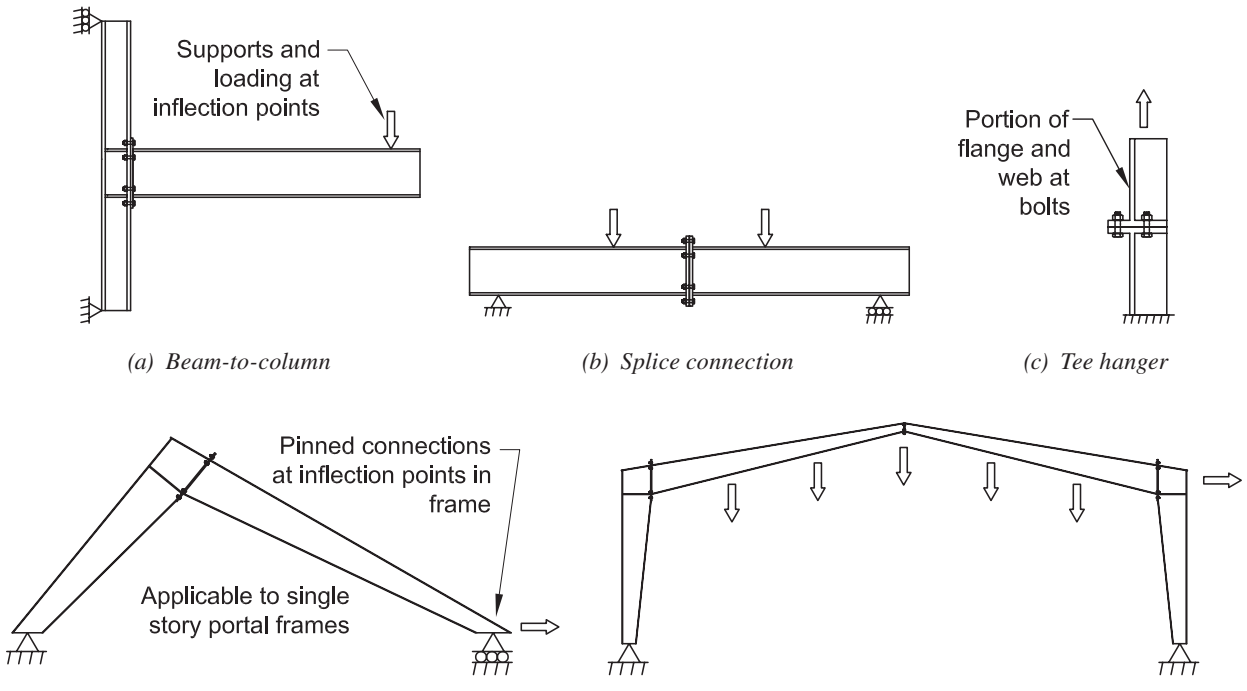

(a) Beam-to-column *(b) Splice connection* *(c) Tee hanger*

(d) Knee connection *(e) Full frame*

Fig. 2-1. Types of experimental assemblies.

review, and discussion of the design procedures that were available at the time. Sumner (2003) summarizes the literature up to 2003. Hasan et al. (1997) created a database of end-plate moment connection tests, including 112 specimens to study the stiffness of the connections.

This chapter starts with information about the tests used to validate the design procedures in this Design Guide, followed by a history of the development of the design procedures. Then a handful of other key experimental programs are described before covering specific topics. The objective of this review is to give the reader general information about the literature on varying topics so further information can be found if required. Although this chapter attempts to give an overview of the body of knowledge, it is not intended to be exhaustive in its scope or description of the work.

2.2 DEVELOPMENT OF DESIGN PROCEDURES

2.2.1 Experiments Used to Validate Design Procedures in This Design Guide

The development of the design procedures included herein are based primarily on a large set of tests conducted at the University of Oklahoma and Virginia Tech. More than one-third of the over 700 end-plate moment connection tests found in the literature were conducted by or involved the second author of this Design Guide. The design procedures included in this document have been developed based on and validated against this large body of work. Furthermore, throughout their development, these design procedures were checked against experiments conducted around the world to ensure the design procedures capture the correct limit states and reasonably predict flexural strength (e.g., Hendrick, 1983; Hendrick et al., 1985; Sumner, 2003).

Some of the experiments found in the literature are not useful in examining U.S. design procedures. If the detailing is different than that used in the United States, it can be difficult to determine how the detailing affected strength. In some cases, the specimens produce limit states that do not occur when using the design procedures in this Design Guide, such as connections controlled by panel zone shear deformations or excessive local buckling. Other tests in the literature exhibit multiple limit states that are hard to decouple, or there is incomplete information or insufficient instrumentation to verify connection behavior. For these reasons, only selected tests are reviewed in the following.

Table 2-1 lists some of the specimens used to validate the design procedures herein. This list is limited to tests conducted by the authors on end-plate moment connection configurations included in this Design Guide.

In addition to the tests tabulated in Table 2-1, a number of full metal building frames with end-plate connections have been tested as described in Section 2.3.

2.2.2 Development of Design Procedures

This section provides a brief background on the development of design procedures in the U.S. and focuses on design procedures for end-plate thickness and bolt size.

End-plate moment connections were included in the AISC *Steel Construction Manual,* 7th Ed. (1970), based largely on the work of Douty and McGuire (1965). As discussed by Griffiths (1984), this first attempt to standardize the design resulted in conservatively thick end plates and large bolts. Packer and Morris (1977) and Mann and Morris (1979) were among the first to use yield line analysis for end-plate and column flange design, which led to more economical end plates.

Some early design procedures for end-plate moment connections used results of parametric finite element studies to calibrate design equations (e.g., Krishnamurthy, 1978; Ahuja et al., 1982; Ghassemieh et al., 1983; Murray and Kukreti, 1988). Multi-variate regression analysis was used to create equations for end-plate thickness and maximum bolt force as a function of the connection geometry and materials. This approach was abandoned in favor of mechanics based approaches.

One of the first concerted efforts to unify design procedures for multiple configurations of end-plate moment connections was Srouji et al. (1983, 1984). Yield line analysis was used to evaluate the end-plate flexural yielding. The method for analyzing bolt forces was based on a split-tee model from Kennedy et al. (1981). These mechanics based approaches laid the foundation for the current design procedures. Srouji et al. (1983, 1984) verified the design procedures against test data for the two-bolt flush and four-bolt flush end-plate configurations.

Hendrick et al. (1985) expanded on this work by adding procedures for the four-bolt flush end-plate configuration with stiffeners between the tension bolt rows and outside the tension bolt rows. Furthermore, they also developed an empirical equation, based on results of 21 tests, for the distance between the bolt center line to the point of application of the prying force.

The design procedures were expanded to include multiple-row extended end-plate moment connection configurations by Morrison et al. (1985, 1986). Morrison et al. (1985) also proposed separately evaluating prying for bolts inside the flange versus bolts outside the flange. This split-tee analogy allows calculation of unique prying forces for the two different bolt locations.

The next major advance in the end-plate design procedures was by Borgsmiller (1995) and Murray and Borgsmiller (1995), which further refined the bolt force assumptions. It was determined that for thick end-plate behavior, all of the bolts reach their ultimate strength and the flexural strength associated with no prying action is calculated accordingly.

Table 2-1 Summary of Experiments Used to Validate the Design Procedures in This Design Guide					
Reference	**Configuration**	**Number of Tests**	**Rafter Size or Depth**	**Test Setup**	**Notes**
Abel and Murray, 1994	4E	4	W16×67 or 18" built-up	Monotonic splice	
Abel and Murray, 1992	MRE 1/2	2	26" built-up	Monotonic splice	
Blumenbaum and Murray, 2004	MRE 1/2, 4ES, MRE 1/3	11	24" up to 72" built-up	Cyclic beam-to-column	MRE 1/3 stiffened and unstiffened
Blumenbaum and Murray, 2003	4E	4	W18×35 up to W27×84	Cyclic beam-to-column	
Bond and Murray, 1989	6Bolt Flush	5	28" and 36" built-up	Monotonic splice	
Boorse and Murray, 1999	2Bolt Flush	4	16" built-up	Cyclic beam-to-column	
Borgsmiller et al., 1995	4E, MRE 1/2, MRE 1/3	7	16.5" up to 64" built-up	Monotonic splice	
Curtis and Murray, 1989	4E, 8ES	13	W24×100 and W27×114	Double-sided push column	Investigate column flange flexure
Eatherton et al., 2013	4E, 8ES	6	W24×62 and W36×150	Cyclic beam-to-column	Fasteners and welds in plastic hinge
Eatherton et al., 2017	4E	3	48" built-up	Cyclic beam-to-column	Noncompact beam webs
Ghassemieh et al., 1983	8ES	2	W24×100	Monotonic splice	
Hendrick et al., 1984	4Bolt Flush Stiffened	8	16" up to 24" built-up	Monotonic splice	Stiffened flush configurations
Italiano and Murray, 2001	4Bolt Flush	6	28" built-up	Monotonic knee	Diagonal end plate
Jain et al., 2015	6Bolt-4Wide/2Wide, 12Bolt-MRE 1/3, 8ES	10	36" up to 60" built-up	Monotonic splice	
Jenner et al., 1985a	2 and 4Bolt Flush, 4E, MRE 1/2	8	10" up to 48" built-up	Monotonic knee	Diagonal end plate
Kline et al., 1995	2 and 4Bolt Flush, 4E, 4ES, MRE 1/3	11	16" up to 30" built-up	Monotonic and dynamic splice	Snug tight bolts
Kukreti et al., 1987	2Bolt Flush	8	10" to 24" built-up	Monotonic splice	
Kukreti et al., 1990	8ES	6	W24×100 to W24×162	Monotonic splice	
Meng, 1996	4E, 4ES	20	W18×35 up to W24×76	Cyclic beam-to-column	Tried weld access holes and shims
Meng and Murray, 1996	8Bolt/4Wide	2	W36×135	Cyclic beam-to-column	Stiffened and unstiffened

Table 2-1 continues on next page

Table 2-1 Summary of Experiments Used to Validate the Design Procedures in This Design Guide (continued)					
Reference	**Configuration**	**Number of Tests**	**Rafter Size or Depth**	**Test Setup**	**Notes**
Morrison et al., 1985	4ES	6	16" to 24" built-up	Monotonic splice	
Morrison et al., 1986	MRE 1/3	7	30" to 62" built-up	Monotonic splice	
Murray, 1989	4E	4	W18×50 and 18" built-up	Monotonic splice	Grade A490 bolts
Murray and Sumner, 1999	8Bolt/4Wide	1	W30×99	Cyclic beam-to-column	
Rodkey and Murray, 1993b	MRE 1/3	1	33" built-up	Monotonic splice	
Ryan and Murray, 1999	4E, 4ES, MRE 1/3	7	24" and 55" built-up	Cyclic beam-to-column	
Seek and Murray, 2008	8ES	1	W27×84 composite slab	Cyclic beam-to-column	Composite slab
Srouji et al., 1983, 1984	2 and 4Bolt Flush	14	10" to 24" built-up	Monotonic splice	
Stevens et al., 2020	4ES and 8ES	4	W24×76 and W36×150	Cyclic beam-to-column	
Structural Engineers Inc., 1984	MRE 1/3	3	62" built-up	Monotonic splice	
Sumner and Murray, 2002	4E, 8ES	6	W24×68 up to W36×150	Cyclic beam-to-column	
Sumner and Murray, 2002	4E	2	W24×68 composite slab	Cyclic beam-to-column	Composite slab
Sumner et al., 2000	8Bolt/4Wide	4	W30×99 and W36×150	Cyclic beam-to-column	
Sumner and Murray, 2001a	MRE 1/2	6	30" built-up	Monotonic splice	
Sumner and Murray, 2001b	8Bolt/4Wide	3	62" built-up	Monotonic splice	
Sumner et al., 1995	4Bolt Flush, MRE 1/2, MRE 1/3	8	24" and 44" built-up	Monotonic and cyclic knee	Diagonal end plate
Szabo et al., 2017	12Bolt MRE 2/2	4	24" and 44" built-up	Monotonic and cyclic beam-to-column	
Thompson and Murray, 1975	2Bolt Flush, 4ES	8	16" and 20" built-up	Monotonic beam-to-column and splice	
Young and Murray, 1997	4E	4	26" to 43" built-up	Monotonic knee	Diagonal end plate
Zarat-Basir et al., 2020	12ES and 12E	4	44" built-up	Cyclic beam-to-column	

Thinner end plates are assumed to conform to the thin plate model from Kennedy et al. (1981), and thus the maximum prying force, Q_{max}, is assumed for all bolts. However, bolt forces in some locations (e.g., the innermost bolts in an MRE 1/3 configuration) were shown not to increase beyond their pretension force. Murray and Borgsmiller (1995) therefore proposed that the bolt force for thin end-plate behavior should be taken as the larger of either the bolt tensile strength less the prying force, Q_{max}, or the bolt pretension force. Borgsmiller (1995) verified the proposed design procedures for the nine end-plate moment connection configurations included in AISC Design Guide 16 (Murray and Shoemaker, 2002). Sumner (2003) further evaluated the design procedures against a set of 90 test specimens found in the literature.

2.3 SELECTED KEY EXPERIMENTAL PROGRAMS AROUND THE WORLD

Douty and McGuire (1965) and Tsai and Popov (1990) represent important early testing programs that contributed to the development of end-plate moment connections. Douty and McGuire explored bolted moment connections using high strength bolts, which were relatively new at the time. They tested seven end-plate moment connections and determined that bolts undergo prying action and can be designed using a tee-stub analogy. It was determined that bolts closer to the flange were more effective in resisting moment, and thus, the four-bolt extended configuration was recommended over the six-bolt flush configuration that was tested, and a design approach was developed.

Tsai and Popov's study was one of the first research programs investigating seismic resistance of end-plate moment connections. In a large testing program on moment connections, three tests were end-plate moment connections, including both four-bolt extended unstiffened and four-bolt extended stiffened configurations. The bolts fractured in one of the three specimens, severely limiting the ductility of the specimen. It was determined that designing the bolts to resist the nominal plastic moment strength was insufficient.

In the early 1990s, there were more than 20 tests by Ghobarah and associates in Canada studying a range of topics, including seismic behavior, panel zone behavior, and end-plate connections on eccentrically braced frame links (Ghobarah et al., 1990; Korol et al., 1990; Osman, 1991; Mourad et al., 1994; Ramadan and Ghobarah, 1995). Adey et al. (2000), also in Canada, conducted a series of 15 tests investigating the cyclic behavior of the four-bolt extended unstiffened, four-bolt stiffened, and eight-bolt extended stiffened configurations. The majority of the specimens were designed for end-plate failure, and four specimens were designed for beam plastic hinging.

In the late 1990s and early 2000s, there were approximately 26 tests and associated finite element modeling conducted by Wheeler et al. (1997, 1998, 2000, 2003) in Australia, investigating end-plate moment connections on rectangular hollow structural section (HSS) members. In the past 20 years, Simoes da Silva, Coelho, and associates in Portugal conducted 58 tests and substantial investigation on topics including axial and bending interaction, high-strength end plates, effect of concrete slabs, and use of the component method for design (Simoes da Silva and Coelho, 2001; Simoes da Silva, Lima, et al., 2001, 2004; Simoes da Silva, Simoes, et al., 2001; Coelho et al., 2004, 2006; Coelho and Bijlaard, 2007, 2010; Simoes da Silva, 2008; Augusto et al., 2017, 2019).

Recently, there has been a substantial amount of research in China on end-plate moment connections. One particularly large study was conducted by Chen and Wang (2009), which used 30 end-plate connection tests to study the effect of different types of welds [complete-joint-penetration (CJP) groove welds, partial-joint-penetration (PJP) groove welds, and fillet welds] between the beam flange and end plate. Other studies in China account for more than 100 tests studying topics such as the use of shape memory alloy bolts, high-strength connections with up to 16 bolts, panel zone behavior, end-plate connections to HSS or concrete filled tube (CFT) columns, and more (Shi et al., 2004; Guo et al., 2006; Shi et al., 2007a, 2007b, 2010, 2017, 2019; Wang and Chen, 2012; Wang and Guo, 2012; Wang et al., 2012a, 2012b, 2009a, 2009b, 2016b, 2017, 2021; Wang and Spencer, 2013; Fang et al., 2014; Tao et al., 2017; Wang and Pang, 2017; Wang and Zhang, 2017; Chen and Shi, 2018; Xu et al., 2018, 2019; Guo et al., 2020).

A large research program called the EQUALJOINTS project supported by the European Community's Research Fund for Coal and Steel has developed prequalification procedures in Europe for seismic steel moment connections. Design procedures for end-plate moment connections were developed (D'Aniello et al., 2017), tests were conducted (Straten et al., 2016; D'Aniello et al., 2018), and finite element studies were used to evaluate aspects of the design procedures (Tartaglia et al., 2018a, 2018b, 2019).

In addition to the large testing programs described in the previous paragraphs, there have been several projects of note wherein portions of full 3D buildings have been tested. Forest and Murray (1982) and Davis et al. (1995a, 1995b) conducted full-scale tests on one-bay sections of metal buildings to evaluate design procedures. Hong and Uang (2012) conducted shake table tests on a one-bay section of a metal building. Braconi et al. (2008) and Wang et al. (2017) subjected multistory moment frames with end-plate moment connections to lateral loading.

Jerez and Murray (1980a, 1980b) and Forest and Murray (1982) conducted eight tests on full-scale one-bay buildings (i.e., each specimen includes two frames connected by purlins and roof deck) having 50 ft to 60 ft spans, with the

objective of evaluating the design procedures of the time. Davis et al. (1995a, 1995b) conducted similar tests, and then Davis (1996) used those results to evaluate contemporary AISC ASD and LRFD design checks. Uang et al. (2011) conducted shake table tests (Uang et al., 2011; Smith and Uang, 2011), and cyclic testing (Hong and Uang, 2012) on a full bay of a metal building. These studies found that the tested metal building frames subjected to large cyclic loading failed due to lateral torsional buckling of the rafters or panel zone shear buckling. Although these are not high ductility limit states, the specimens, designed as ordinary moment frames (OMF), were found to stay relatively elastic up to 2% story drift and survived ground motions between 150% and 290% of the design basis earthquake without collapse. Braconi et al. (2008) conducted cyclic and pseudo-dynamic testing of a two-story, two-bay by two-bay building with a composite slab at the elevated floor, composite columns, and end-plate moment connections at all beam-to-column connections. The tested structure exhibited ductile behavior up to 4% story drift with beam yielding, column panel zone yielding, column base plastic hinging, and yielding of the slab reinforcement. An inspection of the connections after cycles larger than 4% story drift revealed a number of fractures at the lower beam flange-to-end-plate welds. Wang et al. (2017) subjected reduced-scale two-story, one-bay frames with CFT columns and composite slab to pseudo-dynamic loading. At large story drifts, the end plates, which were not designed per AISC *Prequalified Connections*, experienced large inelastic flexural deformations near the bottom flange.

2.4 INVESTIGATIONS FOR SPECIFIC TOPICS

2.4.1 Experiments Focused on Bolt Behavior in End-Plate Moment Connections

Prying action in bolted connections is a well-studied topic. Several research projects have focused specifically on bolt prying forces in end-plate moment connections. Agerskov (1976) conducted 15 end-plate moment connection tests and derived equations for prying forces. Others at the time suggested that prying forces might be calculated as a percentage of bolt force calculated without prying action (Packer and Morris, 1977; Mann and Morris, 1979). Kennedy et al. (1981) evaluated eight previous methods for predicting prying forces and developed new equations that have been further validated in the studies described in Section 2.2.1.

More recently, several studies examined prying action and overall connection behavior when bolts are snug-tightened instead of fully pretensioned (Fleischman et al., 1989, 1991; Chasten et al., 1992; Kline et al., 1995). Between these studies, 18 tests were conducted on end-plate moment connections with snug-tight and pretensioned bolts. Chasten et al. conducted quasi-static tests, while Kline et al. conducted both quasi-static and cyclic tests. It was determined that the behavior, and in particular the strength, of end-plate moment connections with snug-tight bolts is not significantly different than those with pretensioned bolts. While the studies by Fleischman et al. found little change in stiffness, Kline et al. found slightly reduced stiffness with snug tight bolts.

Murray (1989) examined the use of Grade A490 bolts in end-plate connections and, based on a limited set of four specimens, observed that the equations for flexural strength associated with bolt rupture were equally valid for Grade A490 bolts as they were for Grade A325 bolts. Since that time, many tests have further validated this conclusion (e.g., Sumner, 2003; Blumenbaum and Murray, 2004; Szabo et al., 2017; Stevens et al., 2020; Zarat-Basir et al., 2020).

2.4.2 Experiments with Variations on the Flange-to-End-Plate Welds

There are examples of fractures at the flange-to-end-plate weld occurring during tests. Examples from specimens cyclically loaded to large inelastic strains (i.e., seismic testing) include Korol et al. (1990), Meng and Murray (1996), Shi et al. (2007a), Braconi et al. (2008), and Saberi et al. (2016). Korol et al. tested specimens with thick and thin end plates, and the latter experienced cracking at the toe of the weld between the beam flange and end plate. It was concluded that thicker end plates can reduce the potential for this cracking. Meng and Murray found that the use of a weld access hole for the beam flange-to-end-plate weld led to brittle fracture of the beam flange, and thus, weld access holes should not be used in end-plate connections to members likely to undergo significant inelastic demand, such as those in OMF, IMF, and SMF. Shi et al. observed cracks initiating at the beam flange-to-end-plate CJP groove welds, but the cause was not identified. Braconi et al. observed cracking of welds at the bottom flange-to-end-plate weld in a composite beam connection after large inelastic cycles. The demands at the beam bottom flange weld were exacerbated by the higher neutral axis location due to composite beam action and panel zone yielding. Saberi et al. observed fracture in a single-sided PJP groove weld between the beam flange and end plate in one specimen, whereas similar specimens with CJP groove welds did not fracture.

A similar conclusion was reached in a large study conducted at Tongji University by Chen and Wang (2009). Monotonic and cyclic tests were conducted on 30 specimens to specifically study the use of fillet welds and PJP and CJP groove welds for the beam flange-to-end-plate weld. It was determined that the stress distribution in the flange weld is highly nonuniform for thinner end plates. The study recommended that the weld be designed to be stronger than the connected beam flange, but that the weld can be a double fillet or a PJP or CJP groove weld.

Double fillet welds and single-sided PJP groove welds have also been studied by others. Ramseyer and Sherry

(2019) examined the use of PJP groove welds for seismic end-plate connections. The welds were cut and examined along many locations to determine the weld penetration and actual weld size. Coelho and Bijlaard (2007) and Shek et al. (2012, 2013) are examples of testing programs that used double-sided fillet welds between the beam flange to the end plate. Two of the specimens tested by Coelho and Bijlaard experienced cracking in the heat affected zone of the welds.

2.4.3 Investigations for Combined Bending and Axial Force

There have been some investigations into the combined effect of axial and bending forces on end-plate moment connections. De Lima et al. (2004) conducted seven monotonic tests on identical four-bolt extended end-plate specimens with constant axial forces ranging from 27% of the beam's plastic compression strength to 20% of the beam's plastic tension strength. Axial forces (both tension and compression) were shown to substantially reduce flexural stiffness with the tension force producing the largest effect equal to a 27% reduction in initial stiffness. The difference in peak moment was less significant; there was a negligible reduction in peak moment for the specimens subjected to tension and up to a 13% increase in peak moment for specimens subjected to compression. Simoes da Silva et al. (2004) conducted a companion study on nine two-bolt flush end-plate moment connections. Unlike the extended end-plate connections, the flush connections with axial force exhibited larger initial stiffness than the specimen without axial force. However, specimens with large axial tension force experienced a sharp loss of stiffness at a relatively small moment. The peak moment was approximately 10% larger and 15% smaller than the specimen without axial force for specimens with axial compression equal to 20% of the plastic axial strength and axial tension of the same magnitude, respectively.

A more common type of test setup that subjects end-plate moment connections to both axial force and bending are knee joint tests (Beamish and Butterworth, 1984; Jenner et al., 1985a; Masika and Dunai, 1995; Sumner and Murray, 1995; Sumner et al., 1995; Young and Murray, 1997; Italiano and Murray, 2001; Wald and Švarc, 2001; Redmond, 2007; Cristutiu and Dubina, 2010; Smith et al., 2013). In a typical knee joint test setup, a beam-to-column subassemblage is subjected to forces along a diagonal line connecting the column inflection point to the beam inflection point. These diagonal forces produce an axial force at the end plate that is proportional to the moment applied to the end plate. Many of these test specimens were designed to examine limit states outside the end plate, such as panel zone buckling, panel zone yielding, local buckling, and lateral torsional buckling.

There have been several finite element studies that examined the interaction of axial forces and bending in end-plate moment connections (Urbonas and Daniunas, 2006; Baei et al., 2012; Goudarzi et al., 2012; Ghassemieh et al., 2014a; Shaker and Elrahman, 2014b; El-Khoriby et al., 2017). Many of the simulated configurations studied limit states associated with the beam (e.g., local buckling), but a few examined end-plate yielding in the presence of axial forces. Baei et al. and Shaker and Elrahman show that extended end-plate moment-rotation behavior is less affected by axial compression forces than flush end-plate connections but that flush end-plate connections experience more reduction in stiffness and strength with axial tension forces. Flush end-plate configurations subjected to 20% of the plastic tension force developed 10% to 20% less flexural strength as compared to specimens with no tension. Compression forces tend to increase the flexural strength.

There has also been significant work conducted to develop component models that capture the combined effects of axial and bending forces (Jaspart et al., 1999; Simeos da Silva and Coelho, 2001; Cerfontaine and Jaspart, 2002; Sokol et al., 2002; De Lima et al., 2004; Urbonas and Daniunas, 2005, 2006; Nunes et al., 2007; Del Savio et al., 2010).

2.4.4 Panel Zone Behavior and Tension Field Action Adjacent to an End Plate

Shear yielding of panel zones has been studied for moment connections in general (e.g., Krawinkler, 1978). In this section, the behavior of thin panel zones adjacent to an end plate is briefly discussed, including tension field action.

For end-plate moment connections to columns that are continuous through the connection, the panel zone is an interior panel; thus, the top and bottom of the panel zone are anchored well enough to develop tension field action, and the consideration of tension field action is allowed in the AISC *Specification*. Tests on end-plate moment connections have demonstrated tension field action with continuous columns (Ghobarah et al., 1992; Shi et al., 2007a).

On the other hand, even though the AISC *Specification* allows tension field action in some end panels, it does not directly address tension field action in the panel zone of knee joints where the column is not continuous. However, studies have shown that under certain conditions, tension field action can be reliably developed in these panel zones and thus can be used in design. Jenner et al. (1985a) and Scheer et al. (1991) conducted knee joint tests that showed that while panel zones with partial depth column web stiffeners did not obtain full tension field action, specimens with full-depth column web stiffeners subjected to negative moment could develop the full tension field action strength of their panel zones. Negative moment is defined as moment that produces compression in the interior flanges of the beam and column.

A follow-up study by Young and Murray (1997) showed that knee joint specimens subjected to positive moment were not able to develop the full tension field action strength of their panel zones because the exterior corner of the panel

zone is often not stiff enough or strong enough to anchor the tension field. A study by Wei et al. (2019) derived a formula to predict the post-buckling strength associated with partial tension field action and validated the formula against 98 computational models of gable frame panel zones of various configurations.

Beamish and Butterworth (1984) conducted three tests to study the effect of stiffeners such as the diagonal stiffeners proposed by Mann and Morris (1979) on increasing the shear strength of the panel zone. Elastic shear buckling was observed in panel zones of the structure subjected to shake table testing at 100% of the design basis earthquake by Uang et al. (2011). Subsequently, the visual appearance of a tension field could be observed.

2.4.5 Connection to Minor Axis of an I-Shaped Column

Different approaches for connecting an end plate to the minor axis of an I-shaped column have been attempted. Dominesse and Murray (2004) and Tahir et al. (2011) connected the end plate directly to the column web as shown in Figure 2-2(a). Three tests by Dominesse and Murray, one including a composite slab, and five tests by Tahir et al. showed that the response was governed by a significant amount of column web deformation. Dominesse and Murray found that the flexural strength of the column web was larger than yield line analysis predicted due to catenary action, and Tahir et al. found similar difficulties in capturing experimental behavior with finite element models.

Loureiro et al. (2012) created an end-plate moment connection to the minor axis of an I-shaped column by welding a plate to the column flange tips as shown in Figure 2-2(b). It was found that in addition to increasing the strength and stiffness of the minor axis connection as compared to connecting to the column web, the stiffness of connections to the major axis of the same columns increased. The plate welded across the flange tips stiffens the column flanges for the major axis connection. A similar configuration was explored by Shi et al. (2019) wherein the plate was located several inches from the column flanges and connected through horizontal stiffeners at the top and bottom and a vertical stiffener between the plate and column web.

As shown in Figure 2-2(c), Shek et al. (2011) created a cruciform column by welding tee shapes to the middle of the column web on both sides. The results of two specimens

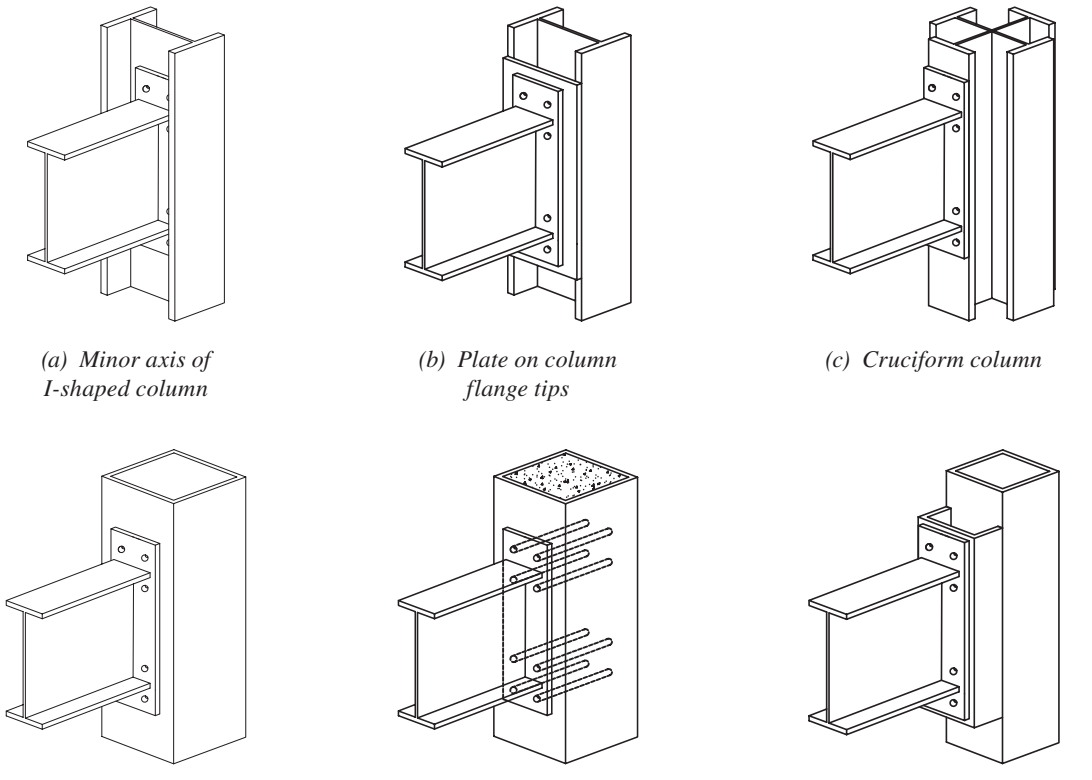

(a) Minor axis of I-shaped column

(b) Plate on column flange tips

(c) Cruciform column

(d) Blind bolts to HSS

(e) Through bolts to CFT

(f) Channel connection to HSS

Fig. 2-2. End-plate moment connections to different types of column.

indicated that the limit states were not related to the column and instead were typical end-plate moment connection limit states such as end-plate yielding and bolt rupture.

2.4.6 Connection to HSS Column

HSS columns and concrete filled HSS columns are more common in Asia and Europe than they are in the United States. A large number of tests have been performed on end-plate moment connections with blind bolts (bolts that only require access to one side) to HSS columns as shown in Figure 2-2(d) (Mourad et al., 1994, 1996; Wang et al., 2009a, 2009b, 2011, 2016b, 2017, 2018; Wang and Chen, 2012; Wang and Guo, 2012; Wang and Spencer, 2013; Ataei et al., 2015b; Wang and Pang, 2017; Wang and Zhang, 2017; Tahir et al., 2018; Guo et al., 2020). These tests have shown that with proper detailing, blind bolts can be successfully used in end-plate moment connections. A set of tests was conducted with blind bolts to a thin-walled box section built up of four light-gage metal sections (Wang and Guo, 2012; Wang et al., 2012a, 2012b; Wang et al., 2016a). In this case, the column walls were too thin, and the connection failed before developing the beam strength.

Alternatively, studies have shown that bolts passing through a CFT can be used in end-plate moment connections as shown in Figure 2-2(e) (Sheet and Gunasekaran, 2013; Van-Long et al., 2015; Tao et al., 2017; Al-Rifaie et al., 2018; Xu et al., 2018, 2019). For single-sided connections, a thick plate was installed on the back side of the tube to increase the flexural strength of the tube wall and spread out the bearing force. End-plate moment connections with through bolts to CFTs exhibited high strength and ductility.

As shown in Figure 2-2(f), Alhendi and Celikag (2015a, 2015b, 2015c) used a channel welded to the HSS column tips first to create a surface for which to make an end-plate moment connection. A testing program and associated finite element study showed the connection to be viable, but that it is important to have a channel with an adequately thick web to resist flexure associated with bolt tension forces. Another option for an end-plate connection to an HSS column, not depicted in Figure 2-2, involves cutting windows into the sides of the HSS to allow access to the back of the bolt (Chen and Shi, 2018).

2.4.7 Column Flange Washer Plates

Column flange flexural strength can control the required size of the column. Sometimes, changes to projects occur after material has been ordered and/or fabricated, and increasing the column size is not a practical option. In such cases, adding column web stiffeners or column flange washer plates can provide a practical solution. As shown in Figure 2-3, column flange washer plates are located behind the column flange and act to spread out the bolt forces. Design procedures for column flange washer plates are not included in this Design Guide, but previous studies provide guidance on their use.

Curtis (1985) explored the use of column flange washer plates with an experimental program consisting of 13 tests that showed an increase in column flange flexural strength of 14% to 35% with the addition of column flange washers. Design procedures were developed in which the flexural strength of the column flange washer is added to the flexural strength of the column flange. Yield line analysis was conducted to calculate the flexural strength of column flange washer plates for typical four-bolt and eight-bolt connection patterns. For bolt forces, it was assumed that the bolt prying forces associated with an unstiffened column flange would be larger (i.e., conservative) for use with column flange washer plates. This assumption was challenged by Moore and Sims (1986) as their tests on end-plate moment connections and tee stubs showed larger bolt forces with flange washer plates than without. It was concluded that bolt prying forces were larger in the presence of column flange washers.

In addition to prying forces, Moore and Sims (1986) also explored the importance of the washer plate length. They determined that there is a minimum and maximum length, outside of which the washer plate does not increase column flange flexural strength significantly. Other studies included Wang and Chen (2009), who attempted to use the component method to calculate connection stiffness with column washer plates; Fink et al. (2001), who used flange washer plates in rack structure connections; and Grogan and Surtees (1999), who used angles instead of plates as the column flange washers. Grogran and Surtees found that angles increased the panel zone shear strength in addition to the column flange flexural strength.

2.4.8 Effect of Composite Slab

Adding a composite concrete slab to a beam can significantly alter the flow of forces through and the overall behavior of an end-plate moment connection. The effect of composite slabs on seismic moment connections was studied as part of the SAC project after the Northridge earthquake (FEMA, 2000), and it was found that the strains at the beam bottom flange can be several times larger than the top flange strains (Hajjar et al., 1988; Leon et al., 1988). Seismic design procedures for end-plate moment connections try to minimize this effect by eliminating studs at the end of the beam and blocking out the concrete slab around the column (AISC, 2022b). Experiments by Sumner (2003) and Seek and Murray (2008) showed this approach to be effective.

Outside of the United States, there has been considerably more research on end-plate moment connections with composite slabs (Anderson and Najafi, 1994; Li et al., 1996a; Xiao et al., 1996; Aribert and Dinga, 2000; Liew et al., 2000, 2004; Brown and Anderson, 2001; Simoes da Silva, Simoes,

et al., 2001; Lachal et al., 2004; Loh et al., 2004, 2006; Fu and Lam, 2006; Fu et al., 2008; Braconi et al., 2010; Wang, 2010, 2012; Vega and Xiao, 2014). The many tests that have been conducted have shown the asymmetric behavior of the composite end-plate moment connection (Liew et al., 2004). They have also demonstrated a range of limit states, the most common of which were concrete slab cracking and reinforcing steel yielding and fracture (Brown and Anderson, 2001; Fu and Lam, 2006). Limit states typical to bare steel end-plate moment connections were also observed but were more severe at the bottom flange of the composite connection, such as weld fracture (Lachal et al., 2004) and beam flange local buckling (Anderson and Najafi, 1994).

Continuous composite slabs can increase the flexural strength of the end-plate moment connection. The strength increase is particularly substantial when a continuous composite slab is added to a relatively weak end-plate moment connection on a shallow beam. For example, tests on shallow beams with two-bolt flush end-plate connections developed two to four times larger flexural strength with a continuous composite slab (Brown and Anderson, 2001; Loh et al., 2004). Anderson and Najafi (1994) further identified the importance of slab reinforcement. Because continuous slab reinforcement through the connection region and parallel to the beam adds to the tension area of the composite section for hogging (negative) moment, continuous slab reinforcement is a key component of the connection flexural strength. However, the strength and stiffness of the connection undergoes substantial degradation as the concrete slab cracks, crushes, and spalls (Dominesse and Murray, 2004; Braconi et al., 2010). This degradation has been found to be more severe for high strength concretes (Braconi et al., 2010).

Beyond experimental programs, several researchers have used finite element models and component models to investigate the effect of composite slabs on end-plate moment connections (Li et al., 1996b; Xiao et al., 1996; Fu et al., 2008; Wang, 2010, 2012; Vega and Xiao, 2014). In general, it is challenging to accurately capture the behavior of the composite connection, including nonlinear concrete cracking behavior (e.g., see Vega and Xiao, 2014). Other studies about the behavior of end-plate moment connections in the presence of composite slabs have included the use of bolted deconstructable slabs (Ataei et al., 2015a, 2015b, 2016a, 2017), composite beams with corrugated webs (Anis et al., 2011), composite beam connections with weak panel zones (Gracia et al., 2010a, 2010b), and composite beam connections to the weak axis of the column (Dominesse and Murray, 2004).

2.4.9 Stiffener Geometry for Stiffened Extended End Plates

For extended stiffened end-plate moment connections, the shape of the stiffener affects the flow of forces, the magnitude of stress concentrations, the potential for fracture, and the ease of fabrication. Many end-plate moment connections have used triangular-shaped stiffeners with a slope of approximately 45° as shown in Figure 2-4(a). Studies in the United States that have used this type of stiffener geometry include Thompson and Murray (1975), Structural Engineers Inc. (1984), Morrison et al. (1985), Curtis and Murray (1989), Kukreti et al. (1990), Sumner and Murray (1995), and Meng and Murray (1996) at approximately 40°. Studies around the world that have used triangular-shaped stiffeners include Ghobarah et al. (1990, 1992), Korol et al. (1990),

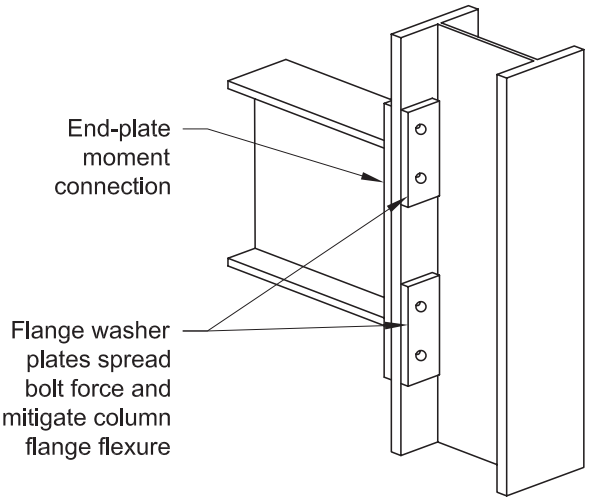

Fig. 2-3. Column flange washer plates.

Adey et al. (2000), Shi et al. (2007a, 2007b), Abidelah et al. (2012), D'Aniello et al. (2017) at 40°, and Garoosi et al. (2018).

Several tests on end-plate moment connections with 45° triangular stiffeners have experienced cracking or fracture, especially when subjected to large inelastic loading cycles (Ghobarah et al., 1990; Korol et al., 1990; Adey et al., 2000; Shi et al., 2007a). A research program using rectangular stiffeners [see Figure 2-4(b)] also experienced fractures at the stiffeners in more than one specimen (Ryan, 1999; Ryan and Murray, 1999). The nature of the fractures varied, but most often occurred at the toe of the welds at the flange.

Two research projects modified the stiffener geometry to be somewhere between rectangular and triangular. Tsai and Popov (1990) and Guo et al. (2006) used stiffeners such as shown in Figure 2-4(c). The landings were large relative to the sloped part of the stiffener. Fracture at the weld to the flange occurred in two of the specimens subjected to large inelastic cyclic loading by Guo et al.

Computational studies have investigated the stiffener angle and resulting stress and strain distributions (Wei and Qian, 2011; Zhuling et al., 2012; Ismail et al., 2015). Zhuling et al. and Ismail et al. both showed that the magnitude of localized stresses were decreased and the flexural strength of the connection was slightly increased with stiffeners that are at a 30° angle instead of 45°.

Research by Sumner (2003) developed the current stiffener geometry shown in Figure 2-4(d) and used in AISC *Prequalified Connections* and this Design Guide. The angle was softened to 30°, similar to the angle at which stresses are assumed to spread in the Whitmore section. Landings that are 1 in. at both the end-plate side and the beam flange side allow for full-size fillet welds over the length and height of the stiffener and make it easier to cut the stiffener to the correct overall dimensions (i.e., if the diagonal is off, the size of the landings deviates from 1 in., but the overall dimensions can still be cut accurately). Tests by Sumner (2003), Blumenbaum and Murray (2004), Eatherton et al. (2013), and Stevens et al. (2020) have shown that specimens having hot-rolled beams and this stiffener geometry are capable of large inelastic rotations without fracture at the stiffener. Conversely, tests on connections with built-up beam shapes have experienced brittle fracture of the beam flange at the toe of the stiffener at relatively small inelastic rotations (Szabo et al., 2017; Zarat-Basir et al., 2020). The cause for the difference in behavior is currently under investigation.

2.4.10 Sloping End-Plate Moment Connections

The majority of end-plate moment connection tests have end plates perpendicular to the axis of the beam as shown in Figure 2-1(a) and 2-1(b). Because end-plate moment connections are commonly used in metal buildings, there have been several studies using a knee joint test setup [see Figure 2-1(d)] with end plates that are sloping relative to the beam axis or diagonal.

Knee joint testing programs that used vertical end plates (i.e., end plates parallel to the outer face of the column) included Beamish and Butterworth (1984) and Young and Murray (1997). In these cases, the end-plate moment connection was not perpendicular to the beam axis because the beam was set along a roof slope as shown in Figure 2-5(a). Conversely, the end plate can be perpendicular to the top flange of the beam as shown in Figure 2-5(b) (Jenner et al., 1985a, 1985b, 1985c).

Diagonal end-plate moment connections as shown in Figure 2-5(c) have been used extensively in knee joint tests (Beamish and Butterworth, 1984; Davis et al., 1995a, 1995b; Sumner et al., 1995; Sumner and Murray, 1995; Italiano and Murray, 2001; Redmond, 2007). Diagonal end plates have the advantage of a larger moment arm between the center of the compression flange and the tension bolts. This typically results in smaller diameter bolts and thinner end plates than those that are vertical or perpendicular to the beam axis. However, diagonal end plates are considerably longer, which is associated with more plate material and weld. Few tests (e.g., Uang et al., 2011) have been conducted on end-plate

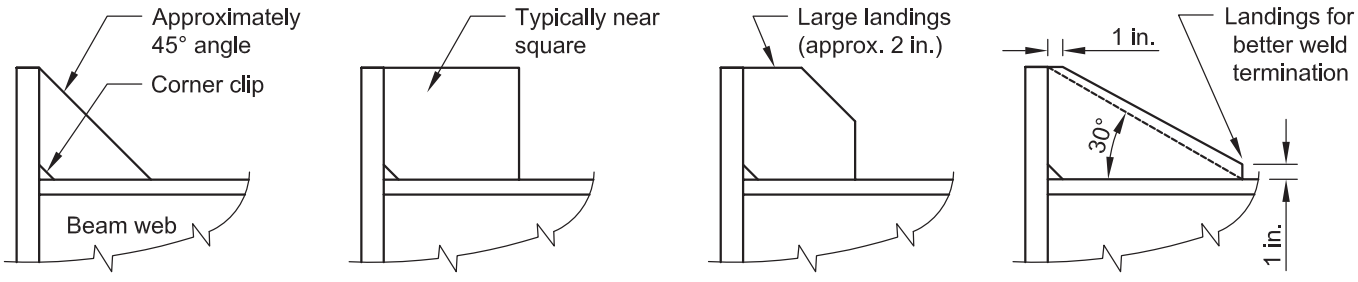

(a) Triangular *(b) Rectangular* *(c) Large landings* *(d) Current geometry*

Fig. 2-4. Variations in stiffener geometry for extended end plates.

moment connections with horizontal end plates as shown in Figure 2-5(d), which are sometimes used in metal buildings.

2.4.11 Additional Topics

Shape Memory Alloy Bolts for Seismic Joints

Several research projects have evaluated the use of shape memory alloy bolts for use in end-plate moment connections to increase the rotation capacity for use in seismic regions. Fang et al. (2014) conducted a set of eight tests where the shape memory alloy bolts had stand offs under their head to increase their deformable length. Computational studies by Yam et al. (2015), Fanaie and Monfared (2016), Farmani and Ghassemieh (2016), and Nia and Moradi (2020) have built on the experimental work to further explore behavior.

End-Plate Moment Connections in Fire

There have been a considerable number of experimental, analytical, and computational studies on the behavior of end-plate moment connections subjected to fire. For more information, the reader is directed to the following references: Al-Jabri et al. (1998, 2006), Wang and Davies (2003), Qian et al. (2009), Zahmatkesh and Talebi (2010), Strejcek et al. (2011), Li et al. (2012a, 2012b), Qiang et al. (2014a, 2014b, 2015, 2016), and Khonsari et al. (2018).

End-Plate Moment Connections Subjected to Impact Loading

Recently, several researchers have used drop hammer test configurations to investigate the behavior of end-plate moment connections subjected to impact loading with conventional connections (Al-Rifaie et al., 2017), with connections to CFT columns (Al-Rifaie et al., 2018), and including a composite slab (Wang et al., 2021).

Column Removal Scenarios

Researchers have also been studying the behavior of frames that have end-plate moment connections when subjected to column removal scenarios. Experiments with composite slabs (Yang and Tan, 2014; Yang et al., 2016) and without slabs (Xu et al., 2018) show that end-plate moment connections can support catenary action while undergoing large rotations and create substantial ductility prior to failure, which is typically associated with bolt rupture. Computational studies using finite element models and component models support these results (Yang et al., 2015; Dinu et al., 2017; Tartaglia et al., 2019; Wang et al., 2020).

Atypical Beam or Column Sections

End-plate moment connections with beams having corrugated webs have been studied by Anis et al. (2011) and Aydin et al. (2015). Spangler and Murray (1989a, 1989b) studied end-plate moment connections attached to the end of truss sections. End-plate moment connections at the end of channels were studied by Structural Engineers Inc. (1986) and for the ends of HSS sections by Wheeler et al. (1997, 1998, 2000, 2003). Researchers have also studied the use of end-plate moment connections at the ends of replaceable links in eccentrically braced frames (Ghobarah and Ramadan, 1994; Ramadan and Ghobarah, 1995), moment frames (Garoosi et al., 2018; Zhang et al., 2020), and the linked column frame system (Malakoutian et al., 2013). Dunai et al. (1996) used conventional I-shaped beams but made the end-plate moment connection to the side of a reinforced concrete girder.

Noncompact or Slender Beam Webs in Seismic Connections

Because end-plate moment connections are commonly used in metal buildings where beams can have noncompact or

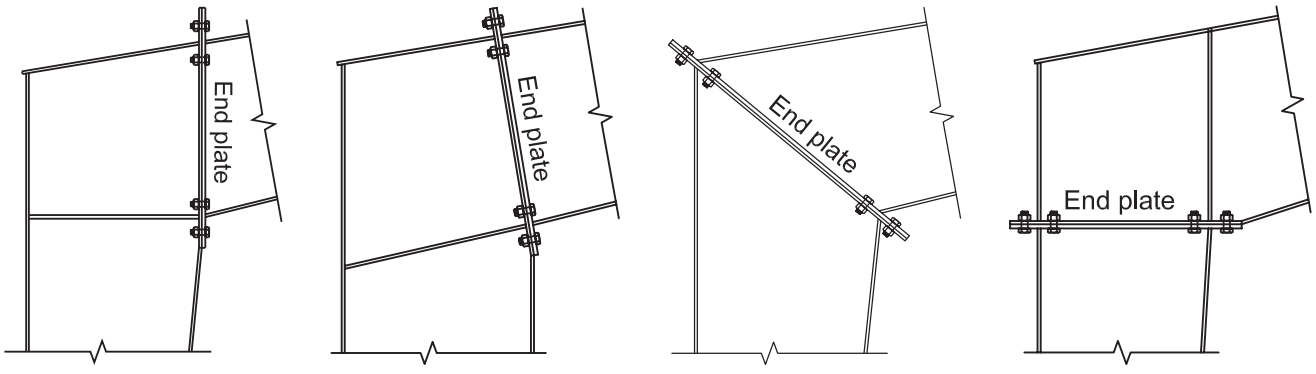

(a) Vertical *(b) Perpendicular to top flange of beam* *(c) Diagonal* *(d) Horizontal*

Fig. 2-5. Sloping end-plate moment connections.

slender webs, it is desirable to develop ductile seismic connections that work with thinner beam webs. Sherry (2016) conducted cyclic testing on end-plate moment connections with noncompact beams that showed limited ductility before the test was stopped. Eatherton et al. (2017) developed a preliminary design approach where longitudinal stiffeners are welded to the beam web to reduce the web slenderness in the vicinity of the connection. A limited set of tests and a parametric computational study showed this to be a promising approach.

Circular Bolt Pattern

Kiamanesh (2011) and Kiamanesh et al. (2013) investigated a circular bolt pattern of eight bolts around the tension flange that makes the bolt forces more uniform. A large computational study showed that the circular pattern is most effective for large bolts and thinner end plates. Morrison et al. (2017, 2019) refer to this as an octagonal arrangement of bolts and studied its behavior through finite element study and an experiment. The experimental specimen also included a heat-treated beam section intended to move the plastic hinge away from the end plate, which was shown to reach 6% story drift during cyclic loading for the specimen with a 30 in. deep beam (Morrison et al., 2019).

High Strength End-Plate Moment Connections

A 12-bolt extended unstiffened end-plate configuration was tested by Rodkey and Murray (1993a). The connection had five rows of bolts inside the tension flange; the innermost two rows were found to be ineffectual. Sumner and Murray (2001b) tested a 12-bolt extended unstiffened end-plate configuration with three rows (one outside and two inside the tension flange) of four bolts each. The outer bolts in the innermost row were found to be ineffectual, and a second test was run with 10 bolts. A 16-bolt flush configuration was tested by Schnupp and Murray (2003) with four rows of four bolts all inside the tension flange. Shi et al. (2017) conducted three tests on a 16-bolt extended stiffened configuration with two rows of four bolts outside and two rows of four bolts inside the tension flange. After finding the corner bolts did not resist much load, a fourth specimen was tested with 12 bolts eliminating the corner bolts. That same configuration of 12 bolts in a cruciform pattern around the stiffened tension flange was investigated by Szabo et al. (2017). This 12-bolt configuration is shown in Figure 1-4(i), and related design procedures in this Design Guide include design examples presented in Chapter 5 and Appendix B.

Coelho and Bijlaard (2007, 2010) and Ataei et al. (2016b) investigated the use of high-strength steel for the end plate. Material with a nominal yield stress between 100 ksi and 139 ksi was used. Some cracking occurred in the heat affected zone, but the authors concluded that the concept was promising and deserved further research.

2.5 COMPUTATIONAL SIMULATION AND ANALYTICAL METHODS

2.5.1 Finite Element Method

The end-plate moment connection is highly indeterminate, and the flow of forces across the interface between the end-plate and the face of the supporting element can be quite complex. Capturing the forces at this interface is just one of the many challenges associated with creating finite element models that can accurately capture end-plate moment connection behavior. Aspects of the model that can be important to accurately capture behavior include:

1. Contact at the interface between the end plate and the supporting element, including friction and slip at this interface.
2. Initial bolt pretension force and inelasticity in the bolts that causes loss of pretension during large inelastic cycles.
3. Material hardening with proper cyclic hardening rules (e.g., kinematic vs. isotropic).
4. Geometric nonlinearity (e.g., second-order effects can create geometric hardening due to catenary action in the end plate).
5. Residual stresses affect when the material starts yielding and thus the initiation of nonlinearity in the response.
6. Initial imperfections that have substantial effect on buckling of thin plates. This can be important for buckling of panel zones or local buckling of the beam or column.
7. Weld filler material is different from the base metal.
8. Fracture—to understand ultimate behavior, it is important to know when fracture initiates.
9. Sufficient mesh refinement for the intended purpose. Mesh size should be different for moment-rotation than for capturing local stresses, strains, or fracture.
10. Composite slab if present. It is necessary to capture nonlinear behavior of concrete, including cracking, effect of confinement, effect of cracks closing upon load reversals, and the degree of composite action between beam and slab.

Many research reports and papers are dedicated to working out the challenges associated with finite element modeling of end-plate moment connections. These works include Krishnamurthy and Graddy (1976), Bahaari and Sherbourne (1994), Shi et al. (2008), Gerami et al. (2011), Balc et al. (2012), Liu and Li (2012), Buzuleac (2013), Reza et al. (2013), Ghassemieh et al. (2014b), Vega and Xiao (2014), Zeinoddini-Meimand et al. (2014), Muresan and Balc

(2015), Krolo et al. (2016), and Thai et al. (2017). Once finite element models are developed that can capture the salient features of end-plate moment response, some researchers conduct parametric studies to evaluate the effect of basic parameters such as end-plate thickness, bolt size and layout, and stiffeners on the behavior of the connection. These studies include Sherbourne and Bahaari (1997), Mashaly et al. (2011), Ataei and Bradford (2014), Saberi et al. (2014a, 2014b), Shaker and Elraham (2014a), Ismail et al. (2015), El Sabbagh et al. (2019), and Sun et al. (2020).

Finite element models have been used to develop or validate design equations and design procedures. Ahuja et al. (1982) and Abolmaali et al. (1984) used multivariate regression analysis on the results of a suite of finite element models to develop empirical equations for stiffness, bolt forces, and required end-plate thickness. Bahaari and Sherbourne (1997), Abolmaali et al. (2005), Mohamadi-Shooreh and Mofid (2008), Diaz et al. (2011), Mohamadi-Shooreh et al. (2013), Zhao (2013), and Ataei et al. (2015a) used multivariate regression analysis on finite element results to develop equations for the moment-rotation behavior of end-plate moment connections. Instead of creating design equations, others use finite element modeling to validate existing design procedures (Mays and Murray, 1999; Sullivan et al., 2006; Bai et al., 2015; D'Aniello et al., 2017, 2018; Francavilla et al., 2018; Tartaglia et al., 2018a; Augusto et al., 2019; Radmehr and Homami, 2020).

The moment-rotation behavior of end-plate moment connections is especially important for semi-rigid connections. Several computational studies have shown the importance of capturing semi-rigid connection flexibility on overall frame behavior (Ioannides and Tarpy, 1980; Xu, 2001; Ghassemieh et al., 2015). Ioannides and Tarpy found that semi-rigid end-plate connection flexibility can lead to 20% larger lateral drift and as much as 50% larger beam deflections due to lateral loads. Ghassemieh et al. found that nonlinear response history analyses overpredict the ground motion intensity associated with a particular performance level by 6% to 46% if connection flexibility is ignored. Xu concluded that it is critical to incorporate the flexibility of semi-rigid connections into structural analysis models to capture global stability.

Finite element models have been used to investigate a specific aspect of connection behavior such as Sherbourne and Bahaari (1994), Bahaari and Sherbourne (1996), and Choi and Chung (1996) examining prying action and bolt bending in end-plate moment connections. Baei et al. (2012) used finite element models to examine the effect of axial force, and Vulcu et al. (2017) and Tartaglia et al. (2018b) investigated the effect of a composite slab. Gillman (2004), Baumberger (2005), and Augusto et al. (2017) investigated panel zone shear strength using finite element models. Hoseinzadeh et al. (2019) studied skewed connections with up to 45° skew angle.

Another use of finite element models is to evaluate a new configuration or application of end-plate moment connections. Mays et al. (2000) and Chen and Shi (2016) separately used finite element models to evaluate a 16-bolt extended stiffened end-plate connection configuration. Without having to conduct any costly experiments, both concluded that the 16-bolt configuration was not efficient because the four corner bolts did not take any load if the end plate was relatively thin. Instead, a 12-bolt end-plate configuration was recommended, which eliminates the corner bolts. Erfani et al. (2016) used finite element models to evaluate an end-plate connection to a stub beam welded to a box column, and Ataei et al. (2016b, 2017) evaluated high-strength steel end-plate connections in the presence of a deconstructable composite slab. Kiamanesh (2011) and Kimanesh et al. (2013) developed a circular bolt pattern, which finite element models showed to create more uniform bolt forces at the tension flange. Keikha and Mofid (2020) and Lopez et al. (2021) used finite element models to examine splice connections from a single beam to a double beam and between beams on opposite sides of a girder, respectively.

More recently, researchers have attempted to use finite element models to predict fracture initiation. One of the first examples of capturing fracture in finite element models of end-plate moment connections was Kukreti and Biswas (1997). Lim (2009) and Lim et al. (2012) attempted to capture low-cycle fatigue fracture of end-plate connections subjected to large amplitude cyclic loading. Szabo et al. (2017) and Abar et al. (2020) used a parameter called the rupture index to evaluate fracture potential for a set of end-plate detailing options, while Ghaderi et al. (2020) implemented the cyclic void growth model to predict fracture.

2.5.2 Component Stiffness Models of End-Plate Moment Connections

As specified in Eurocode 3 (CEN, 2005), the European method of designing end-plate moment connections is based on the component method where a connection is represented by a series of springs that capture the response of different parts of the connection. Figure 2-6 shows an example of a component model. Some general studies on the behavior of the components and component model of end-plate moment connections were conducted by Yee and Melchers (1986) and Coelho et al. (2006).

The component model has been used extensively to study the interaction of axial forces and moment in end-plate moment connections, including the development of interaction curves (Jaspart et al., 1999; Simoes da Silva and Coelho,

2001; Cerfontaine and Jaspart, 2002; Urbonas and Daniunas, 2005, 2006; Nunes et al., 2007; Simoes da Silva, 2008). Component models have been extended to composite connections including springs to represent the concrete slab and the interface between slab and beam (Anderson and Najafi, 1994; Aribert and Dinga, 2000), have been used to capture weak panel zone behavior (Augusto et al., 2017), have been extended to capture cyclic behavior (Nemati et al., 2000; Yang and Eatherton, 2014), and have been compared to finite element models (Luo et al., 2020). The component model method has been computerized (Steenhuis et al., 1994) and used to model column removal scenarios (Yang et al., 2015).

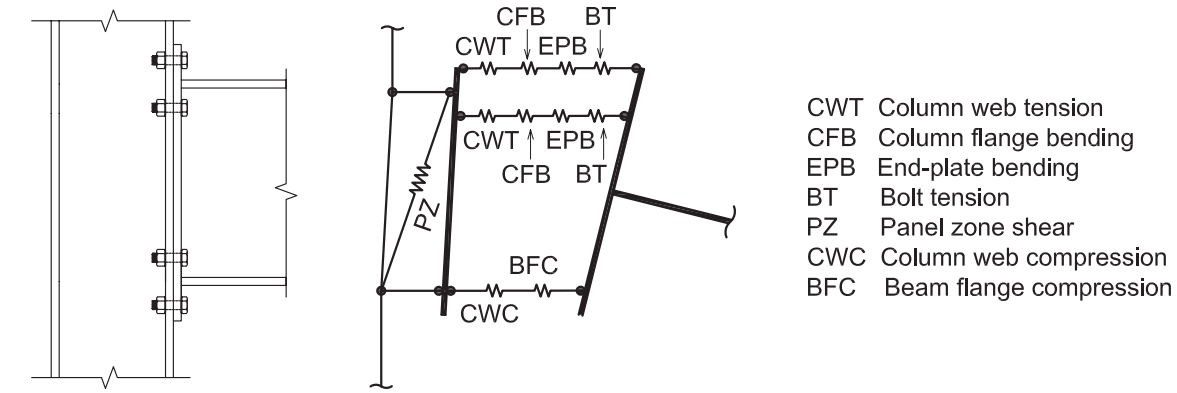

(a) Beam-to-column connection *(b) Component model* *(c) Key*

Fig. 2-6. Typical component model for end-plate moment connections.

Chapter 3
Overview of Design Concepts

3.1 OVERVIEW

End-plate moment connections can be designed to have three distinct types of behavior as demonstrated graphically in Figure 3-1—thin end-plate behavior, thick end-plate behavior, and plastic hinging of the beam.

Thin end-plate behavior is characterized by end-plate yielding and an associated post-yield reduction in stiffness. End-plate yielding progresses until either the tension bolts that are subjected to prying forces rupture, lateral instability of the beam occurs, or the beam begins to yield. Designing a moment connection to exhibit thin end-plate behavior results in thinner end plates, but typically larger bolts than thick end-plate design.

Thick end-plate behavior is characterized by the end plate pulling away from the supporting member (gap formation), followed by bolt rupture without bolt axial force amplification due to prying action. End plates designed for thick behavior typically allow smaller bolts than those designed for thin end-plate behavior, but the end plate is generally thicker.

End-plate moment connections designed for plastic hinging of the beam must have a sufficiently thick end plate to prevent end-plate yielding and sufficiently large bolts to prevent bolt rupture. The end plate and bolts are designed to develop larger flexural strength than the strain-hardened plastic section strength of the beam. After some amount of plastic rotation, the flanges experience local buckling, which results in softening of the moment-rotation behavior (loss of moment-carrying strength). Design for plastic hinging is the preferred option for seismic load-resisting connections because it can sustain the plastic moment through large inelastic rotations, thus dissipating large amounts of seismic energy.

Design procedures have been developed that produce each type of behavior and are presented in this Design Guide. The design procedures for the 15 end-plate configurations presented in this Design Guide are based primarily on research conducted at the University of Oklahoma and Virginia Tech. See Chapter 2 for more information about the experimental programs used to validate these design methods. The design procedures center on predicting the following:

1. Flexural strength associated with end-plate yielding, which is determined using yield-line theory. This leads to a strength criterion used to find the minimum end-plate thickness.
2. Flexural strength associated with bolt rupture without prying action based on an idealized bolt force model. This leads to a strength criterion used to find the minimum bolt diameter for thick end-plate behavior.
3. Flexural strength associated with bolt rupture with prying action based on a split-tee model. This leads to a

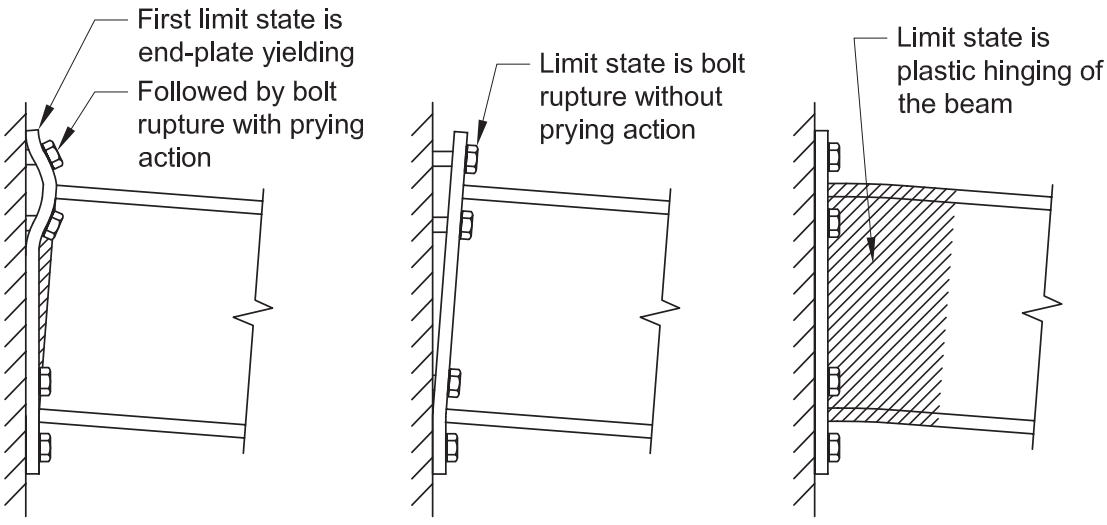

(a) Thin end-plate behavior *(b) Thick end-plate behavior* *(c) Plastic hinging behavior*

Fig. 3-1. Three categories of end-plate moment connection behavior.

strength criterion used to find the minimum bolt diameter for thin end-plate behavior.

4. Plastic moment strength of the beam calculated based on strain-hardened plastic stress distribution. This is used as required flexural strength in the strength criteria for end-plate thickness and bolt diameter in seismic connections designed for plastic hinging.
5. An assessment of the stiffness of the connection to determine for which construction types the connection is applicable (e.g., FR vs. PR). This is a stiffness criterion.
6. Other limit states associated with stiffeners or continuity plates, welds, local column strength, and others are strength criteria that are evaluated for forces consistent with the assumed mechanism (thin end-plate behavior, thick end-plate behavior, or plastic hinging of the beam).

There are fundamental differences in the way structures are designed to resist seismic loading and wind loading, some of which are demonstrated in Figure 3-2. Structures designed for wind loading are expected to remain elastic during design wind events and as such, the resulting peak drifts, Δ_{actual}, should be similar in magnitude to the calculated elastic design drifts, $\Delta_{elastic\ design}$. The actual drifts during earthquakes, Δ_{actual}, are expected to be much larger because structures are allowed to become inelastic, which protects them from collapse. Steel moment frames can be detailed to exhibit a wide range of ductility (i.e., the ability to deform inelastically without failure) including highly ductile SMF, IMF, lower ductility OMF, and steel systems not specifically detailed for seismic resistance.

A seismic response modification factor, R, is assigned to each type of steel moment frame in ASCE/SEI 7, *Minimum Design Loads and Associated Criteria for Buildings and Other Structures* (ASCE, 2022), hereafter referred to as ASCE/SEI 7, based on the amount of ductility and overstrength the structural system possesses: SMF R = 8, IMF $R = 4\frac{1}{2}$, OMF $R = 3\frac{1}{2}$, and for steel systems not specifically detailed for seismic resistance, R = 3. In calculating seismic forces per ASCE/SEI 7, the elastic seismic forces are divided by the response modification factor, R. For schematic representation of these force levels, F, see the seismic loading curves in Figure 3-2. However, to allow these reductions in seismic demands (except for R = 3), the structural system must be detailed according to the AISC *Seismic Provisions* and AISC *Prequalified Connections* to produce the required level of ductility.

For wind design or R = 3 design, the connections may be designed to be weaker than the beams and columns, which may result in less ductility. In these cases, end-plate moment connections can be designed to exhibit thick or thin end-plate behavior. For OMF, the beam-to-column connection has to be stronger than the maximum forces that can be transferred to the connection, forcing the inelasticity into the members that may be more ductile. For IMF and SMF, the beam-to-column connection not only has to be stronger than the strain-hardened flexural strength of the beam, it also has to be shown by qualification testing to be capable of undergoing cyclic rotations up to 0.02 and 0.04 rad, respectively, while maintaining at least 80% of the nominal plastic

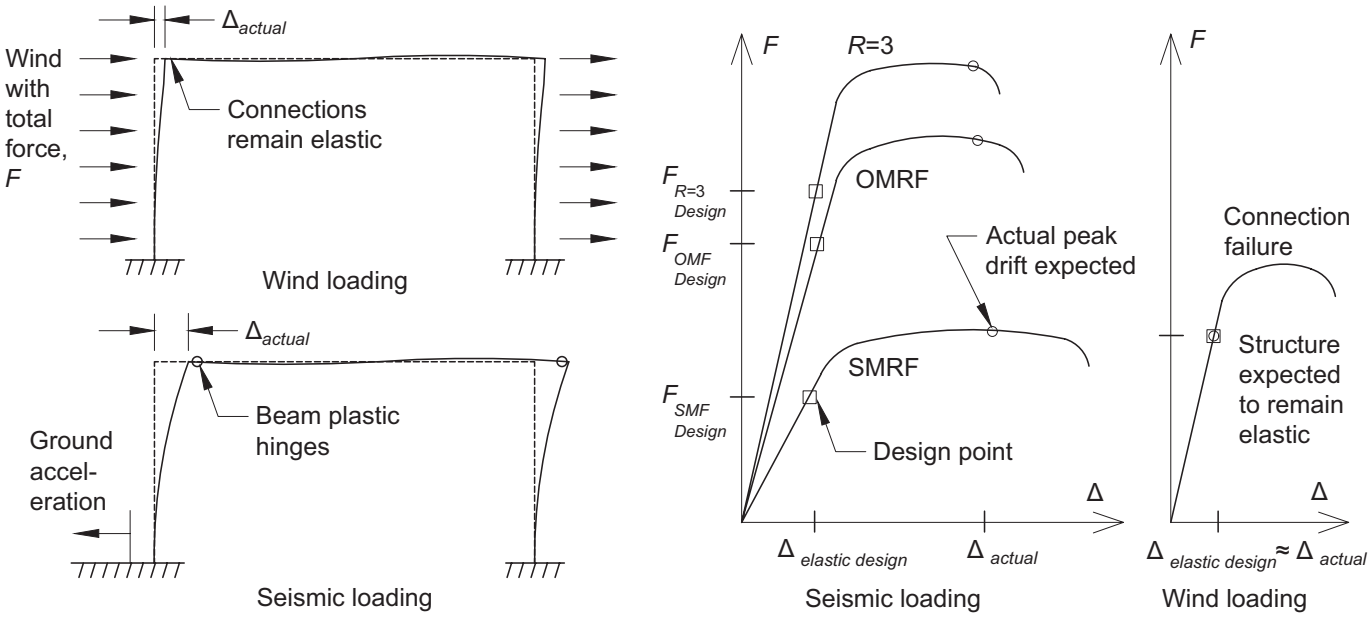

Fig. 3-2. Differences between wind design and seismic design.

moment strength of the beam section (see AISC *Seismic Provisions* Section K2). Design and detailing requirements for three types of end-plate moment connections have been prequalified for SMF, meaning they have been subjected to enough previous testing to allow their general use, and are included in AISC *Prequalified Connections*.

There is also a difference in resistance factors, ϕ, used for high-seismic-ductility design compared to gravity, wind, and low-seismic-ductility design. For wind or low-seismic design, resistance factors from the AISC *Specification* are used, such as $\phi = 0.90$ for end-plate yielding and $\phi = 0.75$ for bolt rupture. In seismic design, on the other hand, the resistance factors are larger because (1) the design demand for the connection is determined based on the maximum force that can be delivered by the beam, including expected yield stress and a factor for strain-hardening, and (2) the materials, detailing, and workmanship of the connection are more rigorously controlled than for typical structural steel elements. For those reasons, AISC *Prequalified Connections* allows seismic end-plate moment connections to be designed with $\phi_d = 1.00$ for ductile limit states such as end-plate yielding and $\phi_n = 0.90$ for nonductile limit states such as bolt rupture with some exceptions.

3.2 CONNECTION STIFFNESS AND USE AS FULLY RESTRAINED CONNECTION

Another design consideration for low seismic and wind design is connection stiffness and whether the connection qualifies as fully restrained. Connection stiffness is the rotational resistance of a connection to applied moment. This connection characteristic is often described with a moment versus rotation or M-θ diagram. The initial slope of the M-θ curve, typically obtained from experimental end-plate test data, is an indication of the rotational stiffness of the connection, (i.e., the greater the slope of the curve, the greater the stiffness of the connection).

This stiffness is reflected in the three types of construction defined in AISC *Specification* Section B3.4 and demonstrated in Figure 3-3—simple connections, PR moment connections, and FR moment connections. Simple connections are defined as transmitting negligible moment between connected members, and it is stated that these connections must be designed to have sufficient rotation capacity to accommodate the rotation determined by analysis of the structure, which the AISC *Specification* Commentary explains should be evaluated at the strength limit state (i.e., for LRFD factored load combinations). On the other hand, FR connections are defined as transmitting moment with negligible rotation between the connected members. FR connections need to be designed to have sufficient flexural strength and stiffness to maintain the angle between the connected members at the strength limit states, (i.e., rotation associated with LRFD factored load combinations or 1.6 times ASD load combinations).

Moment-rotation curves representing the three types of connections are shown in Figure 3-3. Note that the moment-rotation curve for an ideally fixed connection is a line along

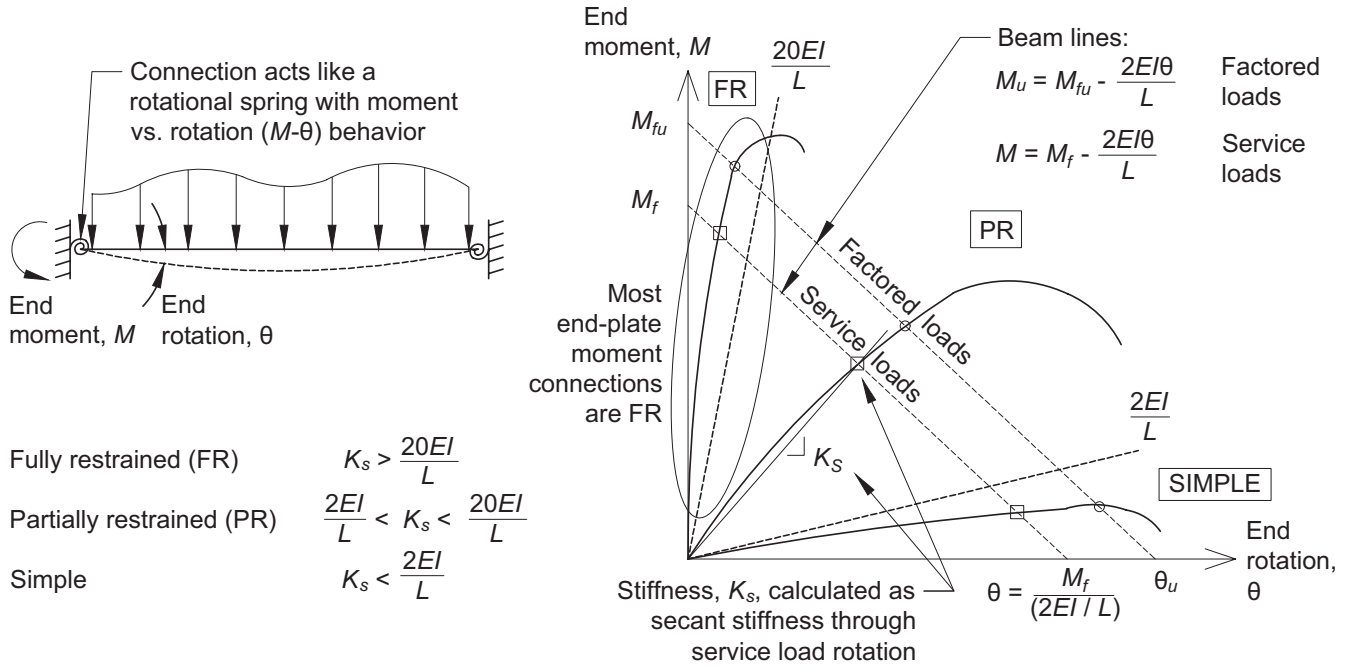

Fig. 3-3. Evaluating connection stiffness for classification as simple, PR, or FR.

the vertical axis of the M-θ diagram, whereas a truly pinned connection is a line along the horizontal axis of the M-θ diagram.

For beams, guidelines have been suggested by Bjorhovde, et al. (1987, 1990) and Salmon et al. (2009) to correlate moment-rotation behavior with connection type. Traditionally, the criterion for FR moment connections is that it be stiff enough to develop an end moment at service loads that is greater than 90% of the fixed end moment associated with a fully rigid connection ($M_s > 0.9\ M_f$ in Figure 3-3, where M_s is the moment associated with the M-θ curve intersecting the service load beam line). The criterion for simple connections is that it should be flexible enough that, at service loads, it does not develop more than 20% of the fixed end moment associated with a rigid connection ($M_s < 0.2\ M_f$ in Figure 3-3). If K_s is the rotational stiffness of the connection, calculated as the secant stiffness through the service load rotation (see Figure 3-3), then the criteria for fully rigid moment connections and simple connections can be restated as $K_s > 20EI/L$ and $K_s < 2EI/L$ respectively, as shown graphically in Figure 3-3.

Salmon et al. (2009) describes the development of the beam lines shown in Figure 3-3. The beam lines are useful tools for understanding the relationship between moment and rotation demands. As the required flexural strength decreases, the required rotational demand increases. For instance, the actual required flexural strength, M_u, for an FR connection is represented by the circle in Figure 3-3 at the intersection of the FR M-θ curve with the beam line (although FR connections are typically designed for the fixed end moment, M_{fu}). The rotational demand for a simple connection can be obtained at the intersection of the M-θ curve with the factored load beam line. Equations for the beam lines associated with service loads and factored loads are given in Figure 3-3.

To determine whether end-plate moment connections are FR or PR type connections, it is necessary to analyze their stiffness. Hendrick et al. (1985) evaluated the stiffness of approximately 20 flush end-plate connections and found that the moment-rotation curves crossed the beam line at an average of 83% of the values required to be considered FR. Another way to look at this result is that the connections were stiff enough to be considered FR up to a moment equal to 83% of the end-plate flexural strength. Hendrick et al., therefore, recommended that the end-plate design flexural strength be reduced by 0.80 (slightly reduced from 83% because of variability in results) so the connection would behave as FR when subjected to factored loads. This shows up in the end-plate design procedures as a reduction factor of $\gamma_r = 0.80$ applied to the flexural strength associated with end-plate flexural yielding for flush end-plate connections. It is noted that this reduction factor is equivalent to dividing by 1.25, which was used in the previous edition of this Design Guide.

Hasan et al. (1997) evaluated the moment-rotation stiffness of 80 extended end-plate moment connection experiments. In addition, three frames were analyzed with varying connection stiffness representing extended end-plate connections. It was concluded that almost all of the extended end-plate connections possessed sufficient stiffness to be considered FR. The reduction factor to ensure connections behave as FR is therefore taken as $\gamma_r = 1.0$ for extended end-plate connections.

3.3 DESIGN FOR END-PLATE FLEXURAL YIELDING

In the recommended design procedures, the end-plate and column flange bending strengths are determined using yield line analysis. Yield lines are the continuous formation of plastic hinges along a straight or curved line. It is assumed that yield lines divide a plate into rigid facets. Although the failure mechanism of a plate using yield line theory was initially developed for reinforced concrete, the principles and findings are also applicable to steel plates. There are also many parallels between yield line analysis of plates and plastic analysis for beams. Concepts related to yield line analysis are presented in this section, but because yield line solutions are presented in later chapters for the 15 connection configurations included in this Design Guide, it is not necessary to perform yield line analysis while applying the design procedures presented in later chapters.

The analysis of a yield line mechanism can be performed by two different methods—the equilibrium method or the virtual work energy method. The latter method is more suitable for the end-plate application, but the equilibrium method is presented briefly for completeness.

The two methods will be demonstrated using the following example. Consider a square plate with side dimensions equal to L subjected to uniform pressure, q, as shown in Figure 3-4. First a yield line mechanism is assumed, which in this case consists of a pair of intersecting diagonal yield lines. The moment along each yield line is assumed to be equal to the plastic moment per unit length, m_p, given by Equation 3-2 as a function of the end-plate yield stress, F_{yp}, the length of the yield line, L_n, and the plastic section modulus along the yield line, Z_p, given by Equation 3-1. To be a valid yield line mechanism for the equilibrium method, the yield criterion must not be violated anywhere—that is, the moment must be less than or equal to the plastic moment everywhere in the plate. Using equilibrium equations, such as setting the moment about line A-A equal to zero, a pressure, q, that causes collapse can be calculated as given in Equation 3-3.

$$Z_p = \frac{L_n t_p^2}{4} \tag{3-1}$$

$$m_p = \frac{F_{yp} Z_p}{L_n} = \frac{F_{yp} t_p^2}{4} \quad (3\text{-}2)$$

$$\sum M_{A-A} = 0 \quad \Rightarrow \quad q = \frac{24 m_p}{L} \quad (3\text{-}3)$$

Equilibrium is referred to as a lower-bound method because the collapse load associated with incorrectly assumed yield line mechanisms will always be smaller than the theoretically correct collapse load. Another way to look at this is that if all possible yield line patterns were analyzed, the one producing the largest collapse load would be correct. However, equilibrium can be difficult to apply to complex yield line patterns such as those required for end-plate moment connections because it would often require solving multiple equilibrium equations simultaneously. A virtual work solution on the other hand results in a single equation.

In the virtual work method, the external work done by the applied load moving through a small arbitrary virtual deflection field is equated to the internal work done as the plate

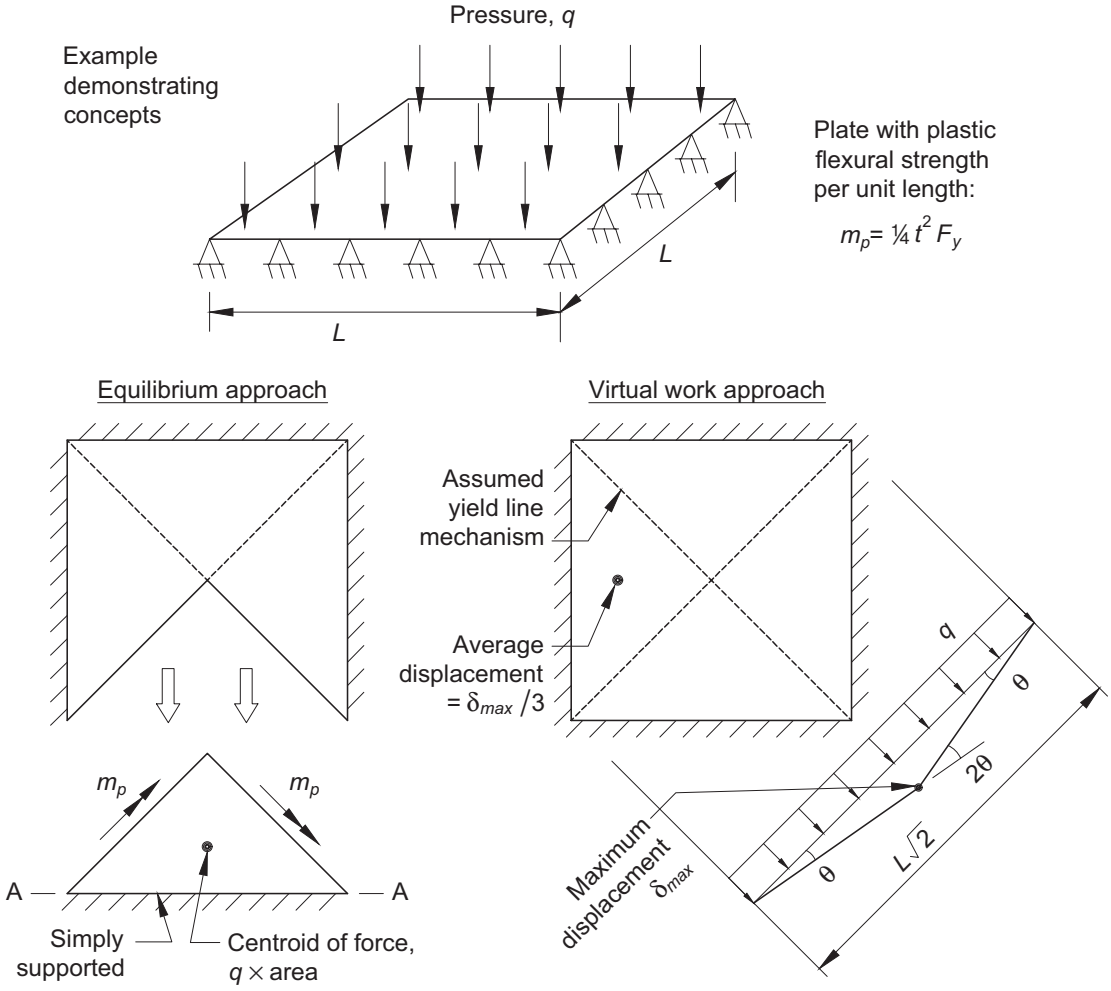

Notes:
1. Result is lower bound: q will always be greater if wrong mechanism was guessed.
2. The equiplibrium approach is not commonly used for yield line analysis because it generally requires more calculations.

Notes:
1. Result is upper bound: actual q will be less if wrong mechanism was guessed.
2. The virtual work approach is typically used for yield line analysis, which requires evaluations of different mechanisms until the minimum strength is found.

Fig. 3-4. Yield line analysis concepts.

rotates at the yield lines to facilitate this virtual deflection field. Although the virtual deflections represent a small additional deflection after the yield line mechanism has formed, this distinction is often neglected for simplicity. Figure 3-5 demonstrates the virtual change in rotations, $\delta\theta$, and the typical notation neglecting the distinction, θ.

Virtual work requires three basic steps: (1) assumption of a yield line pattern, (2) generation of equations for internal and external work, and (3) equating internal and external work to obtain collapse load. The internal work is equal to the summation over all yield lines of internal moments multiplied by their respective rotations. In the case of the square plate shown in Figure 3-4, all yield lines are subjected to a rotation, 2θ, where θ is defined in the figure. The internal work, therefore, is given by Equation 3-4. The external work is given by the total force, qL^2, multiplied by the average displacement, δ_{max}, which is given in Equation 3-5, assuming small rotation. The resulting external work is given by Equation 3-6, and equating the internal work and external work results in the pressure that causes collapse, q, given in Equation 3-7.

$$W_I = (m_p L\sqrt{2})(2\theta)(2\text{ lines}) \tag{3-4}$$
$$= 4\sqrt{2}m_p L\theta$$

$$\delta_{max} = \theta\frac{L\sqrt{2}}{2} \tag{3-5}$$
$$= \frac{L\theta}{\sqrt{2}}$$

$$W_E = (qL^2)\left(\frac{\delta_{max}}{3}\right) \tag{3-6}$$
$$= \frac{1}{3\sqrt{2}}qL^3\theta$$

$$W_I = W_E \quad \Rightarrow \quad q = \frac{24m_p}{L^2} \tag{3-7}$$

For the same loading, other yield line patterns will result in a larger collapse load, q. Hence, the appropriate pattern is the one which produces the smallest collapse load. Virtual work is therefore an upper-bound method. It is noted that the virtual work method produced the same collapse load as the equilibrium method. Because the equilibrium method produces a lower bound and the virtual work method produces an upper bound, the yield line pattern assumed for the square plate must be the correct one. In plastic analysis, this concept is referred to as the uniqueness theorem. However, because the equilibrium method can be onerous for complex yield line patterns, the uniqueness theorem is rarely applied in yield line analysis.

Instead, multiple yield line patterns are considered based on engineering judgment, and the associated collapse loads are calculated using virtual work only. The yield line pattern that creates the smallest collapse load is assumed to be correct. It is noted that the actual proof of whether a yield line solution is valid lies in its comparison with experimental data. If a yield line solution produces collapse loads that match experiments, then it can be considered appropriate for predicting strength. The controlling yield line mechanisms presented in later chapters were all derived using virtual work and validated by comparison with experiments.

When performing yield line analysis, it is important to be aware of the implicit assumptions:

1. Inelasticity is assumed to only exist in the plastic hinge along the yield line. It is assumed that there is no spread of inelasticity outside these lines.
2. The rotation angles are assumed to be small in the calculation of displacements.

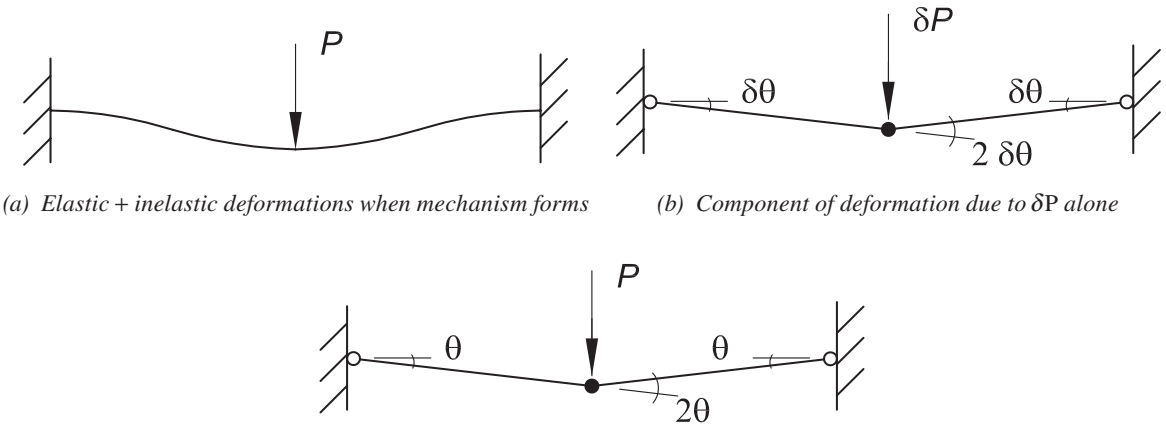

(a) Elastic + inelastic deformations when mechanism forms

(b) Component of deformation due to δP alone

(c) Typical to neglect the δ in the yield line analysis notation

Fig. 3-5. Typical yield line analysis notation does not identify loads and displacements as virtual.

3. It is assumed that there is no work associated with elastic deformations. In idealized cases, such as demonstrated in Figure 3-5, there will be little or no additional elastic deformations due to the added virtual load.
4. If a set of well-selected yield line patterns are analyzed, the correct mechanism, or close to it, will be captured. Ideally, the resulting collapse load is always verified by experiment.
5. For end-plate yield line analysis, it is often assumed that the beam is only subjected to moment/shear and that axial forces are negligible. If the axial tension forces are significant, the yield line mechanism will change as demonstrated in Figure 3-6(c). If the axial force is compression, the flexural deformation shown in Figure 3-6(b) will be reduced.
6. For yield line analysis of end-plate moment connections, the yield line along the compression flange is typically left out because it is subjected to negligible rotation.
7. For yield line analysis of end-plate moment connections, the thickness of the web is typically neglected, and the yield lines are assumed to be located at the center of the web.
8. To simplify the calculations the section at the yield lines is not reduced to account for bolt holes. The effect is generally negligible.

For the complex yield line patterns such as those required for end-plate moment connections, it is convenient to break the internal work down into Cartesian (x and y) components. The internal work done by a single yield line such as shown in Figure 3-7(a) is given by Equation 3-8. Although it can be shown mathematically, Figure 3-7(b) shows graphically that the moments and rotations are vectors that can be broken into Cartesian components. The internal work can thus be expressed in terms of Cartesian components as given in Equation 3-9. This is a useful form for the calculation of internal work and is used in the yield line derivations given in Eatherton et al. (2021).

$$W_I = m_p \theta L \tag{3-8}$$

$$W_I = m_p (\theta_x L_x + \theta_y L_y) \tag{3-9}$$

Another key concept necessary to perform yield line analysis is that for a yield line pattern to be valid, two criteria must be satisfied: (1) All facets in the yield line pattern must be planar, and (2) displacements along the boundary of two facets must be compatible. The yield line pattern shown in Figure 3-8(a) is not valid because it cannot meet both criteria simultaneously. For facet A to be a plane, point 1 must displace more than point 2 because it is further from the line of rotation along the simply supported edge. The reverse is true for facet B, wherein point 2 must displace more than point 1. Because the facets cannot remain planar while holding the displacements along the edge of facet A equal to those along the edge of facet B, this yield line pattern is not possible; therefore, it is inadmissible. Similar logic holds for the yield line pattern shown in Figure 3-8(b), wherein the facets cannot be planar, and thus the yield line pattern is inadmissible. Figure 3-8(c) is also inadmissible because the facets interior to the bolts cannot remain planar. As the beam rotates about a line at its bottom flange, the beam web becomes inclined relative to the surface to which the end plate attaches. The line on the side of the web is therefore inclined relative to the line through the bolts, which remains at zero displacement. As a result, the facet cannot be planar. A yield line pattern with additional intermediate facets is instead required as shown in Figure 3-8(d).

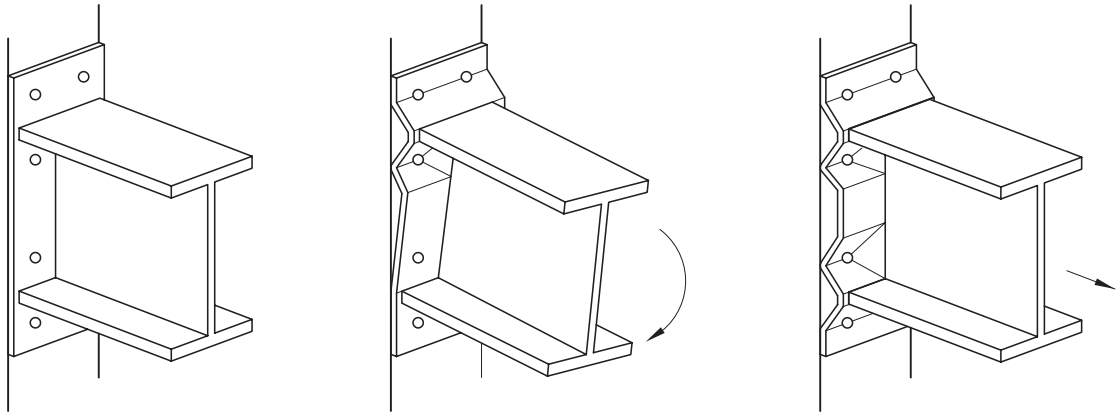

(a) End-plate connection configuration

(b) Yield line mechanism due to moment

(c) Yield line mechanism due to axial tension force

Fig. 3-6. Transition in yield line pattern from moment to axial tension force.

An example of the application of yield line analysis to find the moment associated with end-plate yielding, M_{pl}, is presented for the four-bolt extended unstiffened end-plate connection shown in Figure 3-9.

As the connection is subjected to a moment, the beam is assumed to rotate about the center of the compression flange through an angle, θ, as shown on the right side of Figure 3-9. A yield line pattern was assumed as shown in the left side of Figure 3-9 by dashed lines. It is noted that although there would be a yield line along the centerline of the compression flange, this yield line is typically neglected because the rotation is relatively small compared to the other yield lines. It is also noted that the dimension, *s*, is unknown and will need to be determined as part of the yield line solution.

This is a valid yield line pattern because all facets remain planar, and the displacements at the edges of adjacent facets are consistent with one another. In some cases, proving the yield line pattern is valid can be difficult without drawing or physically creating the 3D displaced shape such as Figure 3-6. In some cases, deriving the rotations of facets or yield lines can expose parts of the yield line pattern that are invalid.

The yield line pattern creates six facets as identified in Figure 3-9. The rotation of each facet, *n*, about the *x*- and *y*-axes is given by θ_{nx} and θ_{ny}, respectively, in Table 3-1. Positive values represent rotation that is in the same direction as the rotation, θ. The internal work of each yield line is given in Table 3-2, wherein, for example, yield line 1/2 is defined as the yield line between facet 1 and facet 2. It is noted that the thickness of the web is neglected in these calculations and that yield lines are assumed to extend to the center of the web thickness. This simplifying assumption can greatly reduce the complexity of the resulting yield line parameters without significant loss of accuracy.

Determining the rotation of each facet simplifies the calculation of internal work for each yield line. For example, the rotation of yield line 1/2 is the difference in rotation between facet 1 and facet 2. The internal work for yield lines that are rotating in both the *x*- and *y*-directions is calculated using components as given by Equation 3-9. For instance, the expression in brackets for the internal work of yield line 2/3 in Table 3-2 consists of the *x*-component of the yield line length multiplied by the rotation about the *x*-axis added to the *y*-component of length multiplied by rotation about the *y*-axis.

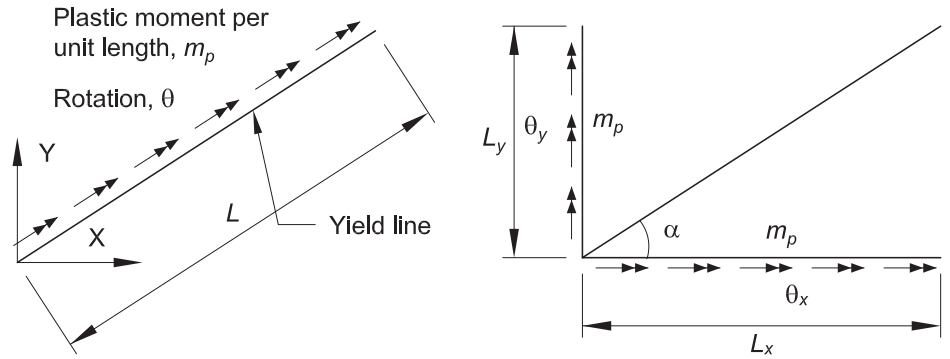

(a) Yield line along angle *(b) Yield line resolved into components*

Fig. 3-7. Resolving yield line into Cartesian components.

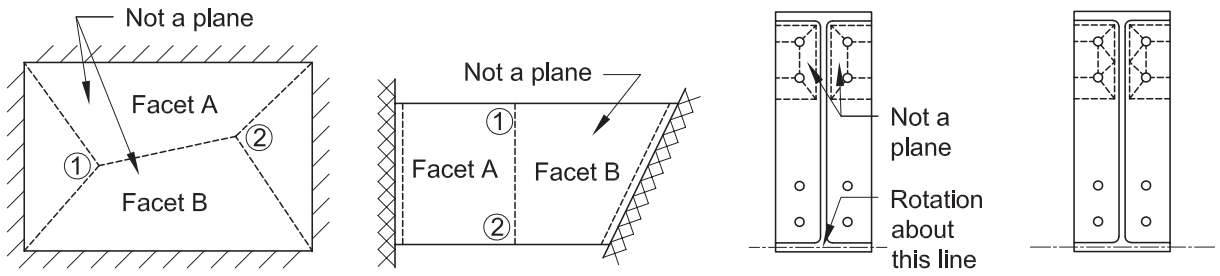

(a) Inadmissible mechanism *(b) Inadmissible mechanism* *(c) Inadmissible* *(d) Admissible*

Fig. 3-8. Inadmissible yield line mechanisms.

The internal work for each yield line is simplified in Table 3-2 as a function of $b_p/2$, $g/2$, or $2/g$. Summing the internal work given in Table 3-2 results in Equation 3-10, where the terms multiplied by $g/2$ cancel out.

$$W_I = m_p\left[\frac{b_p}{2}\left(\frac{4\delta_a}{p_{fi}}+\frac{4\delta_a}{s}+\frac{4\delta_b}{p_{fo}}-2\theta\right)+\frac{2}{g}(4\delta_a p_{fi}+4\delta_a s)\right] \quad (3\text{-}10)$$

Substituting $\delta_a = h_2\theta$ and $\delta_b = h_1\theta$ results in Equation 3-11:

$$W_I = 4m_p\theta\left\{\frac{b_p}{2}\left[h_2\left(\frac{1}{p_{fi}}+\frac{1}{s}\right)+h_1\left(\frac{1}{p_{fo}}\right)-\frac{1}{2}\right]+\frac{2}{g}\left[h_2(p_{fi}+s)\right]\right\} \quad (3\text{-}11)$$

The external work, W_E, is given by Equation 3-12:

$$W_E = M_{pl}\theta \quad (3\text{-}12)$$

When the internal work is set equal to the external work, the arbitrary angle of rotation, θ, cancels out leaving Equation 3-13. Equation 3-13 can be further simplified into the form given in Equation 3-15 by substituting the flexural strength per unit length, m_p, from Equation 3-2, and defining the yield line parameter, Y_p, as given in Equation 3-14. The moment, M_{pl}, can now be calculated as given in Equation 3-15 based on the geometry and yield stress of the end plate and represents the moment that will cause the yield line pattern shown in Figure 3-9 to form.

$$M_{pl} = 4m_p\left\{\frac{b_p}{2}\left[h_1\left(\frac{1}{p_{fo}}\right)+h_2\left(\frac{1}{p_{fi}}+\frac{1}{s}\right)-\frac{1}{2}\right]+\frac{2}{g}\left[h_2(p_{fi}+s)\right]\right\} \quad (3\text{-}13)$$

$$Y_p = \frac{b_p}{2}\left[h_1\left(\frac{1}{p_{fo}}\right)+h_2\left(\frac{1}{p_{fi}}+\frac{1}{s}\right)-\frac{1}{2}\right]+\frac{2}{g}\left[h_2(p_{fi}+s)\right] \quad (3\text{-}14)$$

$$M_{pl} = F_{yp}t_p^2 Y_p \quad (3\text{-}15)$$

To finish the yield line solution, it is necessary to determine the value of the dimension s that creates the smallest moment, M_{pl}. To do this, the yield line parameter, Y_p, is differentiated with respect to the dimension s and set equal to

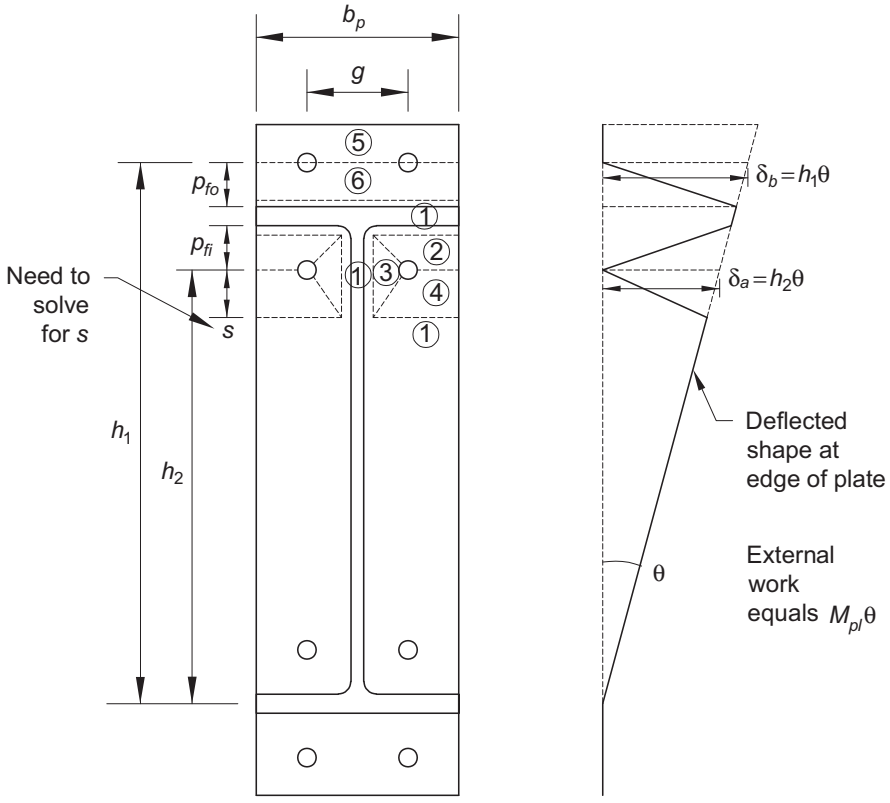

Fig. 3-9. Yield line pattern for the four-bolt extended unstiffened end plate.

Table 3-1. Rotation for Each Panel in the Four-Bolt Extended Unstiffened End Plate		
Facet	**θ_{nx}**	**θ_{ny}**
1	θ	0
2	$(\delta_a + p_{fi}\theta)/p_{fi}$	0
3	θ	$2\delta_a/g$
4	$-(\delta_a + s\theta)/s$	0
5	0	0
6	$-(\delta_b - p_{fo}\theta)/p_{fo}$	0

Table 3-2. Internal Work Associated with Each Yield Line in the Four-Bolt Extended Unstiffened End Plate			
Yield Line	**Internal Work**	**Simplified Internal Work**	**Number of Lines**
1/2	$m_p\left(\frac{b_p}{2}\right)\left(\frac{\delta_a + p_{fi}\theta}{p_{fi}} - \theta\right)$	$m_p\left[\left(\frac{b_p}{2}\right)\frac{\delta_a}{p_{fi}}\right]$	2
2/3	$m_p\left[\frac{g}{2}\left(\frac{\delta_a + p_{fi}\theta}{p_{fi}} - \theta\right) + p_{fi}\frac{2\delta_a}{g}\right]$	$m_p\left[\left(\frac{g}{2}\right)\frac{\delta_a}{p_{fi}} + \left(\frac{2}{g}\right)\delta_a p_{fi}\right]$	2
3/4	$m_p\left[\frac{g}{2}\left(\frac{\delta_a - s\theta}{s} + \theta\right) + s\frac{2\delta_a}{g}\right]$	$m_p\left[\left(\frac{g}{2}\right)\frac{\delta_a}{s} + \left(\frac{2}{g}\right)\delta_a s\right]$	2
2/4	$m_p\left(\frac{b_p - g}{2}\right)\left[\left(\frac{\delta_a + p_{fi}\theta}{p_{fi}}\right) + \left(\frac{\delta_a - s\theta}{s}\right)\right]$	$m_p\left(\frac{b_p}{2} - \frac{g}{2}\right)\left(\frac{\delta_a}{p_{fi}} + \frac{\delta_a}{s}\right)$	2
4/1	$m_p\left(\frac{b_p}{2}\right)\left(\frac{\delta_a + s\theta}{s} + \theta\right)$	$m_p\left(\frac{b_p}{2}\right)\left(\frac{\delta_a}{s}\right)$	2
1/6	$m_p(b_p)\left(\frac{\delta_b - p_{fo}\theta}{p_{fo}} + \theta\right)$	$m_p\left(\frac{b_p}{2}\right)\left(\frac{2\delta_b}{p_{fo}}\right)$	1
6/5	$m_p(b_p)\left(\frac{\delta_b - p_{fo}\theta}{p_{fo}}\right)$	$m_p\left(\frac{b_p}{2}\right)\left(\frac{2\delta_b}{p_{fo}} - 2\theta\right)$	1
1/3	$m_p(p_{fi} + s)\left(\frac{2\delta_a}{g}\right)$	$m_p\left(\frac{2}{g}\right)(\delta_a p_{fi} + \delta_a s)$	2

zero to find the value that creates the minimum yield line parameter, which corresponds to the minimum flexural strength. The derivative of the yield line parameter with respect to s is given in Equation 3-16, which simplifies to the value given by Equation 3-17.

$$\frac{dY_p}{ds} = \frac{-b_p h_2}{2} s^{-2} + \frac{2h_2}{g} = 0 \tag{3-16}$$

$$s = \frac{\sqrt{b_p g}}{2} \tag{3-17}$$

The yield line parameters for all the configurations discussed in this Design Guide are given in tables included in Chapters 5 and 6. All yield line parameters were derived using virtual work similar to the preceding example and are available in Eatherton et al. (2021). Understanding the yield line patterns is useful so that conditions that might alter the yield line pattern (e.g., adding or subtracting stiffeners, adding or subtracting bolts, excessively shallow beams, etc.) can be identified.

3.4 DESIGN OF BOLTS TO RESIST FLEXURE IN THE CONNECTION

As described at the beginning of this chapter, end-plate moment connections can be designed to exhibit three distinct types of behavior—thick end-plate behavior, thin end-plate behavior, and plastic hinging behavior of the beam. For thin end-plate behavior, the end plate is allowed to yield and prying forces develop in the bolts. Prying forces are additional tension forces in the bolts due to the yielded end plate acting as a lever to pry the bolts out of the support. End-plate moment connections designed for thick end-plate behavior or plastic hinging behavior are designed so that the end plate does not yield and, thus, prying forces are considered negligible.

Numerous studies have been conducted to investigate the behavior of bolts in end-plate moment connections with the goal of measuring and predicting the bolt prying forces. The majority of the bolt force prediction methods were developed using an analogy between a portion of the end plate around the tension flange and an equivalent tee stub as shown in Figure 3-10(a) and Figure 3-10(b). The design model developed by Kennedy et al. (1981) is used for determining the bolt forces in end-plate moment connections. Hendrick (1983), Srouji et al. (1983, 1984), Hendrick et al. (1985), Morrison et al. (1986), Borgsmiller (1995), and Jain et al. (2015) all used a modified Kennedy approach to predict the bolt forces in flush, extended, stiffened, and unstiffened end-plate moment connection configurations. The modifications to the Kennedy method include an adjustment to the location of prying forces and to the distribution of the flange force to multiple bolt rows.

Kennedy et al. (1981) identified three types of tee-stub flange plate behavior. Thick plate behavior is characterized by elastic behavior of the tee-stub flange and bolt forces that sum to the applied load as illustrated in Figure 3-10(c). For thick plate behavior, it is assumed that there are no prying forces and the tension force is divided evenly among the bolts. It is noted that all tee stubs will exhibit thick plate behavior for small loads. As the load is increased, the tee-stub flange may behave as a thick plate up to bolt rupture or enter intermediate or thin plate behavior, depending on the relative strength of the bolts and plate.

If the load is increased and the bolts possess sufficient strength, plastic hinges will form in the tee-stub flange plate at the base of the tee stem as shown in Figure 3-10(d). The plate is said to be of intermediate thickness and prying forces, Q, are present.

The third type of plate behavior occurs if the bolts have sufficient strength to allow the load to be further increased, leading to the formation of additional plastic hinges at the bolt line. The plate is classified as thin and prying forces are at a maximum, Q_{max}. Figure 3-10(e) shows this condition.

It is noted that a plate may exhibit one type of behavior at factored loads, but the ultimate failure of that plate may be governed by another type of behavior depending on the relative strength of the bolts and plate. For instance, a plate may

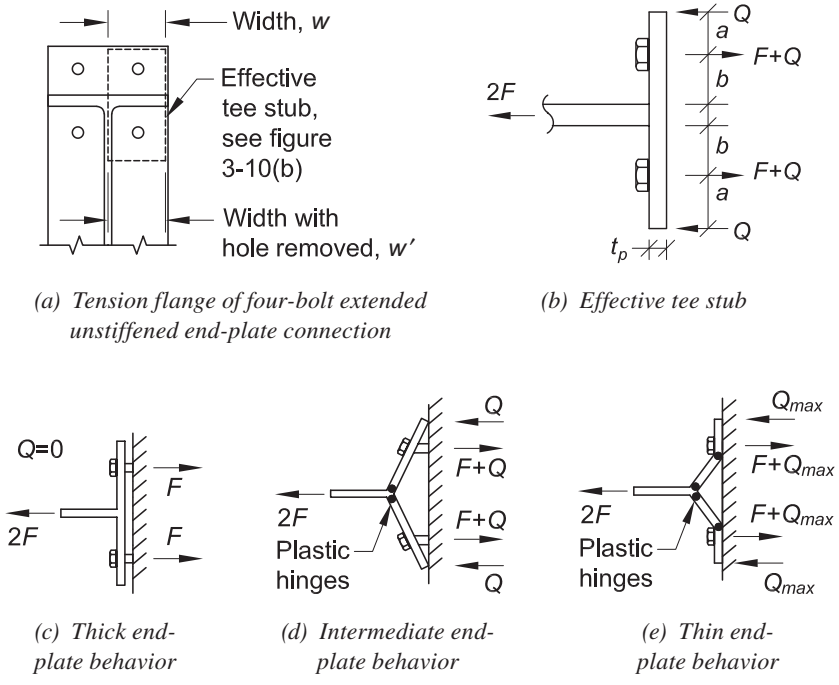

(a) Tension flange of four-bolt extended unstiffened end-plate connection

(b) Effective tee stub

(c) Thick end-plate behavior

(d) Intermediate end-plate behavior

(e) Thin end-plate behavior

Fig. 3-10. Tee-stub analogy for bolt prying forces.

be designed to exhibit thick plate behavior at factored loads, but if the bolts have substantial overstrength, the plate may ultimately yield, leading to intermediate or thin behavior.

The Kennedy model was modified by Srouji et al. (1983), Hendrick et al. (1985), and Morrison et al. (1986) to adjust the location of the prying forces and to modify the distribution of the flange tension force to the various bolt rows. Borgsmiller (1995) presented a simplified version of the modified Kennedy method to predict the bolt strength, including the effects of prying. The simplified method considers only two stages of plate behavior—thick plate behavior with no prying forces, and thin plate behavior with maximum prying forces. The intermediate plate behavior, as defined in the Kennedy model, is not considered. This simplification allows for a direct solution of the bolt forces and is included in this Design Guide.

The threshold between thick and thin plate behavior was established as the point where the bolt prying forces are negligible. Based upon past experimental test results, Borgsmiller (1995) determined this threshold to be when the bolts can develop 90% of the end-plate yield strength. If the flexural strength of the connection based on bolt rupture without prying action, M_{np}, is less than 90% of the flexural strength associated with end-plate yielding, M_{pl}, then the end plate is considered to be "thick," and no prying forces are considered. Conversely, when the flexural strength based on bolt rupture without prying action, M_{np}, is greater than 90% of the end-plate flexural strength, M_{pl}, the end plate is considered to be "thin," and the prying forces are assumed to be at a maximum. If Equation 3-18 is satisfied, the end plate can be considered "thick." If Equation 3-19 is satisfied, where M_{cf} is the column flange flexural strength, the column flange acts as a "thick" plate, and if both are satisfied, then M_{np} represents the flexural strength of the bolted end-plate connection. In both equations, 1.10 is the approximate inverse of 0.90.

$$M_{pl} \geq 1.10 M_{np} \tag{3-18}$$

$$M_{cf} \geq 1.10 M_{np} \tag{3-19}$$

The modified Kennedy method and the simplified method were developed to predict the bolt forces in tee-stub and end-plate moment connections subjected to monotonic loading. Connections designed for high-seismic-ductility force inelasticity in ductile elements such as the beam plastic hinge or panel zones. All other elements are designed to remain essentially elastic. Applying this philosophy to the connection requires that the end plate and column flange be designed to exhibit thick plate behavior. This will ensure that the end plate and column flange remain elastic and that the bolts are not subject to any significant prying forces. Note, if one of the inequalities is not satisfied for that element, the end plate, column flange, or possibly both, must be evaluated as a thin end plate and/or column flange.

For thick plate behavior, the flexural strength associated with bolt rupture without prying action, M_{np}, is determined by taking the static moment of the bolt forces about the centerline of the compression flange. Figure 3-11 demonstrates this bolt force model for the four-bolt extended unstiffened connection configuration. The no-prying bolt rupture flexural strength, M_{np}, is given by Equation 3-20 based on the bolt tension strength, P_t, which is given by Equation 3-21.

$$M_{np} = P_t \sum_i n_i h_i \tag{3-20}$$

$$P_t = F_{nt} A_b \tag{3-21}$$

where

A_b = nominal unthreaded body area of bolt, in.^{2}

F_{nt} = specified nominal tensile strength from the AISC *Specification* (90 ksi for Group 120, 108 ksi for Group 144, and 113 ksi for Group 150 high-strength bolts), kips

M_{np} = flexural strength for bolt rupture with no prying action, kip-in.

P_t = bolt tension strength, kips

h_i = distance from the centerline of the compression flange to the center of bolt row i, in.

n_i = number of bolts in row i

The no-prying bolt rupture flexural strength utilizes the full tensile strength of each bolt within the connection. Assuming that the end plate remains relatively planar for thick end plates implies that the outermost bolts will reach their tensile strength first. The underlying assumption in the simplified model is that the outer bolts will yield and provide enough deformation to develop the full tensile force in each of the inner connection bolt rows. This assumption has been investigated in multiple row extended connections by Sumner and Murray (2001a) and was determined to be valid.

The maximum prying force is developed based on the assumed forces and moments shown in Figure 3-12. The

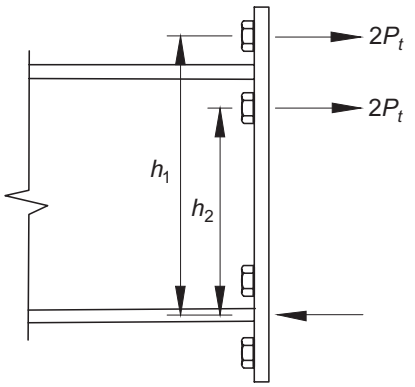

Fig. 3-11. Thick plate bolt force design model (4E shown).

derivation of the maximum prying force is presented here in a general form from Kennedy et al. (1981), and more specific equations will be presented later.

The maximum prying force, Q_{max}, is calculated as given in Equation 3-22 considering equilibrium of the flange tip shown in Figure 3-12. The resulting maximum prying force, Q_{max}, is given in Equation 3-23. If the expression under the radical in Equation 3-23 is negative, this means the average shear stress associated with the plastic mechanism is so large that there is no stress available to resist bending and, thus, the end-plate geometry is not appropriate for thin end-plate behavior.

$$Q_{max} = \frac{M_{p2}}{a} = \frac{Z_{2effective}\sigma_{effective}}{a} \tag{3-22}$$

$$Q_{max} = \frac{w't_p^2}{4a}\sqrt{F_{yp}^2 - 3\left(\frac{F'}{w't_p}\right)^2} \tag{3-23}$$

where

F' = bolt force associated with the tee-stub plastic mechanism, kips

F_{yp} = end-plate yield stress, ksi

M_{p2} = plastic moment at the bolt line, kip-in.

Q_{max} = maximum prying force, kips

$Z_{2effective} = \frac{w't_p^2}{4}$ effective plastic section modulus at the bolt line, in.^{3}

a = distance from prying reaction to bolt line shown in Figure 3-12, in.

t_p = thickness of the end plate, in.

w' = width of the effective tee stub after subtracting the bolt hole diameter, in.

$\sigma_{effective}$ = effective yield stress considering reduction for applied shear stress, ksi

The distance, a, from the bolt centerline to the reaction force applied to the tee stub by the support, is calculated using Equation 3-24 (Hendrick, 1985), as limited by the distance from the bolt centerline to the edge of the plate. The bolt force associated with the tee-stub plastic mechanism shown in Figure 3-12 using equilibrium of the tee-stub flange over the length, b, as subjected to the plastic moments, M_{p1} and M_{p2}, reduced for shear stress, and the bolt moment, M_b, is found from Equation 3-25. The effective yield stress reduced due to the effect of shear is estimated by Kennedy et al. (1981) to be $0.85F_{yp}$, and $0.80F_{yp}$ for the plastic hinges, M_{p1}, and M_{p2}, respectively. For two bolts in a row, the width, w, is taken as $b_p/2$, and for interior and exterior bolts, the distance, b, is equivalent to the dimensions p_{fi} and p_{fo}, respectively.

$$a = 3.62\left(\frac{t_p}{d_b}\right)^3 - 0.085 \;\leq\; \text{Distance to edge of end plate} \tag{3-24}$$

$$F' = \frac{M_{p1} + M_{p2} + M_b}{b} \tag{3-25}$$

$$F' = \frac{1}{b}\left[\frac{t_p^2 F_{yp}}{4}(0.85w + 0.8w') + \frac{\pi d_b^3 F_{nt}}{32}\right] \tag{3-26}$$

where

M_b = bolt moment, kip-in.

M_{p1} = plastic moment at face of the tee stem, kip-in.

b = distance from bolt line to face of the tee stem as shown in Figure 3-12, in.

d_b = nominal diameter of the bolt shank, in.

w = width of the effective tee stub, in.

Using Equations 3-23, 3-24, and 3-26, the maximum prying force on the bolt is calculated. The flexural strength for bolt rupture with prying action, M_q, is then calculated using Equations 3-27 and 3-28. Bolts can either rupture due to

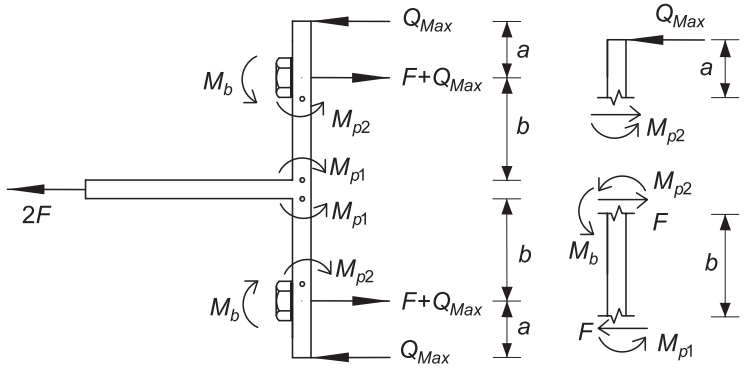

Fig. 3-12. Tee-stub model used by Kennedy et al. (1981) to derive maximum prying force.

Table 3-3. Bolt Pretension Force, kips				
	Group 120 Bolts[1]			Group 144 and Group 150 Bolts[2]
Bolt Diameter	Pretensioned Bolts Pretension, $T_{b,full}$[3]	Snug-Tight Pretension, T_b	Snug-Tight Pretension, T_b	Pretensioned Bolts Pretension, $T_{b,full}$[3]
d_b = ⅝ in.	19	0.75 $T_{b,full}$	14.3	24
d_b = ¾ in.	28	0.50 $T_{b,full}$	14.0	35
d_b = ⅞ in.	39	0.375 $T_{b,full}$	14.6	49
d_b = 1 in.	51	0.25 $T_{b,full}$	12.8	64
d_b = 1⅛ in.	64	N/A[4]	N/A[4]	80
d_b = 1¼ in.	81	N/A[4]	N/A[4]	102
d_b = 1⅜ in.	97	N/A[4]	N/A[4]	121
d_b = 1½ in.	118	N/A[4]	N/A[4]	148

[1] Includes ASTM F3125/F3125M Grade A325 bolts and ASTM F3125/F3125M Grade F1852 bolts

[2] Includes ASTM F3125/F3125M Grade A490 bolts, ASTM F3125/F3125M Grade F2280 bolts, and ASTM F3148 Grade 144 bolts

[3] $T_{b,full}$ = Minimum bolt pretension for fully pretensioned bolts in the AISC *Specification*

[4] N/A = Data is not available for the snug-tight pretension force

prying action forces, or if the bolt pretension force, T_b, is large enough, the end plate does not separate from the support and no prying forces develop. Bolt pretension forces, T_b, are given in the AISC *Specification* for fully pretensioned bolts. In Table 3-3, the pretension forces for snug-tight bolts are based on the work of Kline et al. (1995). The factor, α, in Equation 3-28 is a number less than or equal to 1.0 and accounts for the reduction in the contribution of some bolts that are far from the center of the tension flange and, therefore, may not reach their tensile strength before the first bolts rupture.

$$P_{qi} = \max\left(P_{t,i} - Q_{max,i},\ T_{b,i}\right) \tag{3-27}$$

$$M_q = \sum_i \alpha_i P_{qi} n_i h_i \tag{3-28}$$

where

M_q = flexural strength for bolt rupture with prying action, kip-in.

P_{qi} = bolt strength adjusted for prying forces for bolt position i, kips

$T_{b,i}$ = bolt pretension for bolt position i, kips

n_i = number of bolts in position i

α_i = adjustment factor for bolt position contribution

3.5 DESIGN FOR AXIAL AND SHEAR FORCES

In a moment-resisting frame, all lateral loads must transfer through the end-plate moment connection to become shear in the columns. The horizontal forces collect along the beam length and are transferred through the end-plate moment connections as axial force in the beams. Additionally, end-plate connections that are sloped relative to vertical are subjected to axial forces associated with gravity loads. Section 3.6 includes examples for resolving gravity and lateral loads into axial, shear, and moment for end plates that are sloped relative to vertical.

Past experimental and finite element studies of end-plate moment connections subjected to combined axial force and bending (see Chapter 2) show that while axial tensile force can significantly reduce the flexural strength of flush end-plate connections, extended end-plate connections are less susceptible to loss of flexural strength due to axial tension. Both flush and extended end-plate connections show increased flexural strength in the presence of axial compression forces (assuming no local buckling in the beam) because the compression acts to counteract the tension flange force, which leads to most of the major limit states associated with the end-plate connection.

A simplified approach to incorporating axial force into the design procedures is presented here based on the concept of distributing half of the axial force to each flange, as shown in Figure 3-13. In this discussion, T_r and M_r are used to denote the demands, required axial strength and required flexural strength, respectively, which are T_u and M_u for LRFD and T_a and M_a for ASD.

As shown in Figure 3-13, this concept for including axial forces assumes that the section is symmetric and that the axial force is concentrated in two equal forces centered on the flanges. For nonsymmetric sections, the axial force could be distributed to the flanges based on the ratio of flange areas. The tensile force distributed to the compression flange acts to reduce the demand, which can be neglected. The half of the tensile force that goes to the tension flange acts to increase the tensile demand. The effect on the bolt rupture and end-plate yielding limit states is similar to an

added moment equal to half the tensile force multiplied by the moment arm, as given by Equation 3-30. This effective moment due to axial force is added to the applied moment, M_r, that is used to calculate the bolt diameter and end-plate thickness. Several examples are presented in Chapter 5 that demonstrate this procedure.

$$M_{r,eq} = M_r + \frac{T_r}{2}(d - t_{bf}) \tag{3-30}$$

Axial forces that are large compared to the applied moment will change the yield line pattern as shown in Figure 3-6(c). For example, if the effective moment due to axial force, $M_{r,axial}$, is equal to the applied moment, M_r, then the compression flange will experience zero force, which will invalidate the assumed point of rotation about the compression flange shown in Figure 3-6(b). Because no testing or computational simulations exist for such large axial forces, an investigation of the yield line pattern is warranted if the effective moment due to axial force, $M_{r,axial}$, is large (e.g., greater than $M_r/2$).

If the end-plate moment connection is subjected to axial compression forces, a similar model as shown in Figure 3-13 is used. In this case, half the beam compression force should be added to the compression flange force used to calculate whether column web stiffeners (continuity plates) are required on the column side. It is conservative to neglect the beneficial effect of beam axial compression on end-plate flexural strength.

Bolts acting in bearing are used to resist the shear force at the interface of the end plate and column flange. Slip critical end-plate connections are not required for static (temperature, wind, and snow) or seismic loading.

In the design of bolts for shear forces, it is commonly assumed that all the shear force is resisted by the bolts at the compression flange. This is a convenient assumption that allows the tension and shear forces to be separated to different groups of bolts. Because the bolt tension produced by the moment is coupled with a compensating compression force on the other side of the axis of bending, the net clamping force does not reduce with applied moment, and the equivalent bolt pretension force from all bolts is active in resisting the shear force due to friction, although this resistance is not considered in design. However, if the connection is subjected to axial tension, it may be necessary to design the bolts for the combined effects of shear and tension.

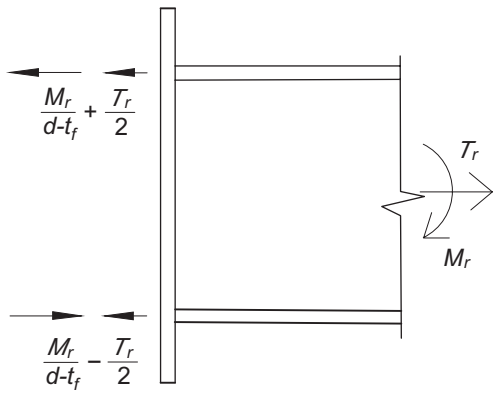

Fig. 3-13. Model for considering axial forces.

3.6 APPLYING DESIGN PRINCIPLES TO SLOPED CONNECTIONS

In gable frames and similar applications, the longitudinal axis of the rafter is not commonly perpendicular to the columns. As a result, the end plates may not be perpendicular to the beam axis, such as shown in Figure 3-14(b) and Figure 3-14(c). There are several unique considerations for sloped end-plate connections, including resolving the beam forces into components parallel and perpendicular to the end plate, panel zone geometry, bolt position in the plane of the end plate, and weld detailing.

Experiments have been conducted on specimens with end plates sloped relative to the beam axis. Knee joint tests were conducted on specimens with diagonal end plates such as shown in Figure 3-14(c) (Beamish and Butterworth, 1984; Sumner et al., 1995). Models for calculating forces in a knee joint with a diagonal stiffener are discussed in Fisher et al. (1963). Knee joint type tests have also been conducted on specimens with vertical end plates that were sloped relative to the beam axis as shown in Figure 3-14(b) (Beamish and Butterworth, 1984; Young and Murray, 1997).

If the end plate is not perpendicular to the beam axis, the beam resultant forces must be resolved into components that are parallel and perpendicular to the end plate, as shown in Figure 3-14(d). If θ is defined as the angle between the beam axis and the end plate, then the components of force that are perpendicular and parallel to the end plate are given by P_r^* and V_r^* in Equations 3-31 and 3-32, respectively. The required flexural strength, M_r^* as given in Equation 3-33, remains the same regardless of the angle the end plate makes relative to the beam.

$$P_r^* = P_r \sin\theta + V_r \cos\theta \tag{3-31}$$

$$V_r^* = P_r \cos\theta + V_r \sin\theta \tag{3-32}$$

$$M_r^* = M_r \tag{3-33}$$

While the required flexural strength may stay the same with sloping end plates, the flexural strength increases. The dimensions from the center of the compression flange to the bolt row lines (e.g., h_1 and h_2) are measured along the end plate as shown in Figure 3-14(d). This leads to larger flexural strength for bolt rupture and end-plate yielding limit states.

Another consideration for sloped beams or sloped end plates such as those shown in Figure 3-14(a) and

Figure 3-14(b) is the design of the panel zone. The panel zone demands may be calculated based on beam forces similar to procedures discussed in the next section for nonsloped connections. The panel zone strength, however, depends on the geometry. It is appropriate in the calculation of available panel zone shear strength to use the largest panel zone dimension, h, to determine the shear buckling stress, but to use the actual dimension of the panel zone in the direction of shear to determine the web area.

Another important consideration for sloped end plates is the detailing of the welds from the flange to the end plate and from the column stiffener to the column flange. Welds should satisfy the requirements of AWS D1.1/D1.1M and all specifications therein related to welding a skewed T-joint (AWS, 2020; Green and Schlafly, 2011).

3.7 ADDITIONAL LIMIT STATES AND ASSUMPTIONS

3.7.1 Limit State Checklist

There are multiple limit states, both those unique to end-plate connections and those that apply to other types of moment connections, that must be considered in the design

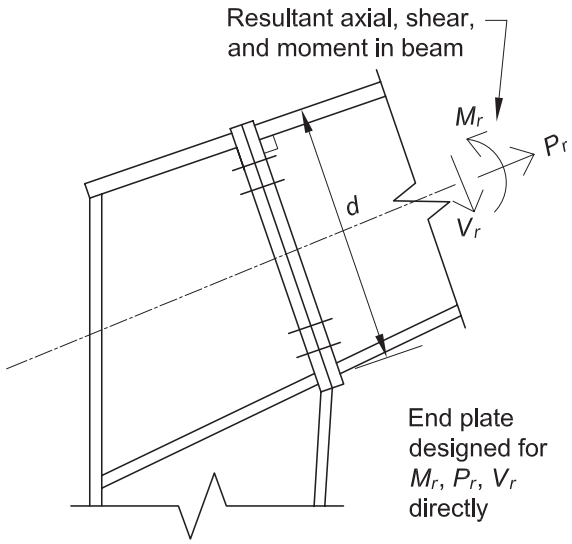

(a) End plate perpendicular to the beam axis

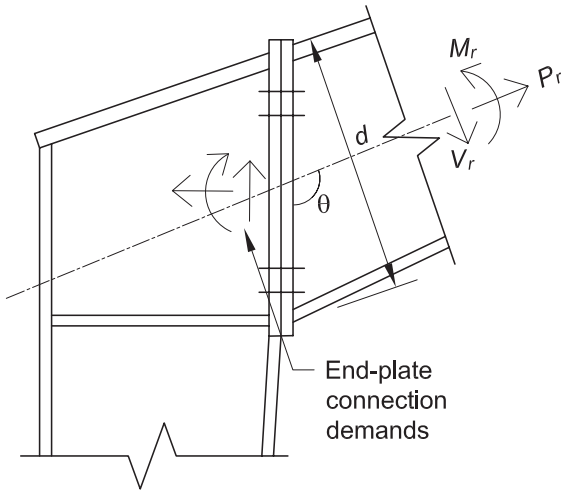

(b) Vertical end plate sloped relative to beam axis

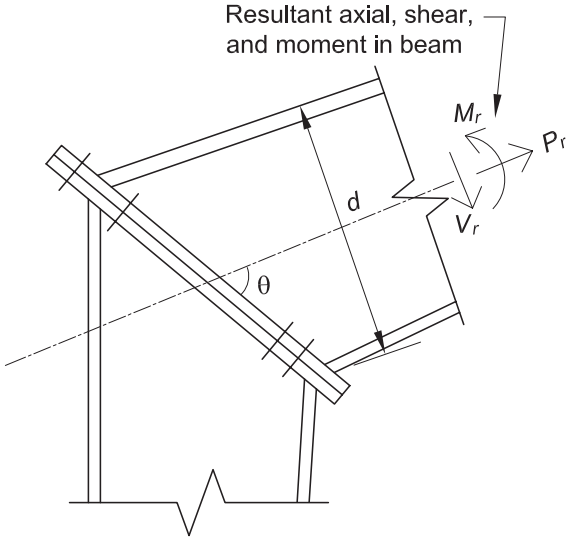

(c) End plate sloped relative to vertical and beam axis

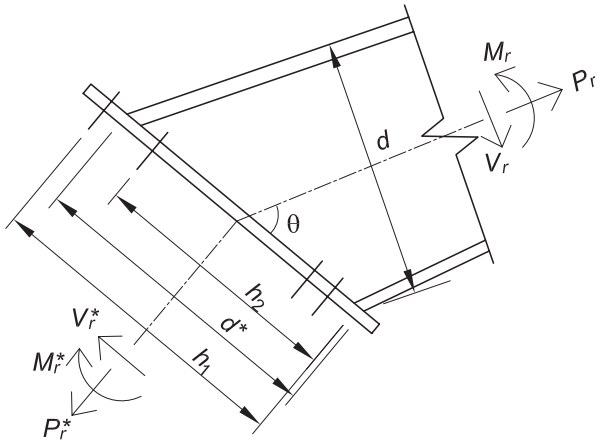

(d) Resolving forces into end-plate demands

Fig. 3-14. Resolving forces in sloped connections into end-plate forces.

of an end-plate moment connection. Limit states that are unique to end-plate type moment connections are discussed in the following:

Beam Limit States:

1. Plastic hinging of the beam. This is a ductile limit state for seismic design.

End-Plate Limit States:

2. Flexural yielding of the end-plate material near the tension flange bolts. This limit state in itself does not lead to a loss of load-carrying strength, but end-plate yielding results in a rapid increase in tensile bolt forces.
3. Shear yielding of the end-plate material. This limit state is not typically observed, but shear in combination with bending can result in reduced flexural strength and stiffness.
4. Shear yielding or rupture of the extended portion of an unstiffened extended end plate. It is explicitly required to check these two limit states in high-seismic-ductility design.

Bolt-Related Limit States:

5. Bolt tension rupture considering prying forces if applicable. This limit state is obviously a brittle failure mode and is the most critical limit state in an end-plate connection.
6. Bolt shear rupture due to shear at the interface between the end plate and column flange.
7. Bearing/tearout failure of the end plate or column flange at a bolt hole.

Weld-Related Limit States:

8. If fillet welds or PJP groove welds are used, rupture of the beam tension flange to end-plate welds or the beam web tension region to end-plate welds.
9. If fillet welds or PJP groove welds are used, shear rupture of the beam web to end-plate weld or the beam web base metal.

Column-Side Limit States:

10. Column web local yielding opposite either the tension or compression flange of the connected beam.
11. Column web crippling opposite the compression flange of the connected beam.
12. Column web compression buckling opposite the compression flange of the connected beam.
13. Flexural yielding of the column flange in the vicinity of the tension bolts. As with flexural yielding of the end plate, this limit state in itself does not result in loss of load-carrying capacity, but results in rapid increases in tensile bolt forces and excessive rotation at the connection.
14. Column transverse web stiffener (continuity plate) failure due to yielding, local buckling, or weld failure.
15. Column panel zone failure due to shear yielding or web plate buckling.

3.7.2 Assumptions

A list of the assumptions made in the design procedures follows:

1. Group 120, Group 144, or Group 150 high-strength bolts of a diameter not greater than 1½ in. must be used.
2. The specified minimum yield stress of the end-plate material must be 50 ksi or less.
3. The distance from the face of the beam flange to the nearest bolt centerline (the vertical bolt pitch) should allow for the required tightening clearances found in AISC *Manual* Part 7. However, many fabricators prefer to use a standard pitch dimension of 2 in. or 2½ in. for all bolt diameters.
4. Generally, the shear force at a connection can be resisted by the compression side bolts. End-plate connections need not be designed as slip-critical connections, and it is noted that shear is rarely a major concern in the design of moment end-plate connections.
5. The end-plate width effective in resisting the applied moment must be taken as not greater than the beam flange width, b_{bf}, plus 1 in. or the end-plate thickness, whichever is greater.
6. The distance between the outer bolt hole centerlines must not be greater than the width of the beam flange.
7. When CJP groove welds are used, it is recommended that weld access holes not be used. The groove weld should be made from the outside face of the flange, and the weld between beam flange-to-web fillets should be treated as a PJP groove weld relative to fabrication.
8. For gravity loading, wind loading, or low-seismic-ductility systems, normally the beam flange to end-plate weld is designed to develop the yield strength of the connected beam flange. This is generally done with CJP groove welds but, alternatively, fillet welds or any combination of groove and fillet welds may be used. When the required moment is less than the available flexural strength of the beam, the beam flange to end-plate connections should be designed for the required moment, but not less than 60% (LRFD) or 40% (ASD) of the specified minimum yield strength of the connected beam flange. This minimum demand is intended

to account for uneven stress distributions that can occur across the flange at end-plate welds.

9. Beam web to end-plate welds in the vicinity of the tension bolts, taken as extending from the flange to 6 in. inside the innermost row of bolts, are designed to develop the yield strength of the beam web, unless the available strength of the beam is not required. When the required connection moment is less than the available flexural strength of the beam, the beam web to end-plate welds in the vicinity of the tension bolts should be designed for the required moment, but not less than 60% (LRFD) or 40% (ASD) of the specified minimum yield strength of the beam web.
10. The length of web to end-plate weld available to resist shear is assumed to be the lesser of (a) the weld from the end of the assumed web tension length to the inside face of the beam compression flange and (b) the weld between the mid-depth of the beam and the inside face of the beam compression flange.
11. For doubly symmetric beam sections, the required connection axial forces can be treated as an additional required moment equal to half the required axial force multiplied by the distance between the flange centroids. The design procedures may not be applicable for large axial forces where the additional required moment associated with axial force is greater than half the original required moment. Required connection axial forces are also considered when checking column-side limit states.

3.7.3 Column Panel Zone Strength

The panel zone is the portion of the column web that extends over the height of the beam. The demands on the panel zone are shown graphically in Figures 3-15(a) and 3-15(b) for a double-sided joint and in Figures 3-15(c) and 3-15(d) for a gable frame knee joint. The panel zone shear demand for the joint and sign convention shown in Figure 3-15(a) is given by Equation 3-34, and the panel zone shear demand for a gable frame connection simplifies to the expression given in Equation 3-35. It is noted that the column shear, V_{rc}, and the axial forces in the beams, P_r, (associated with collector forces) are acting in the opposite direction of the shear associated with beam moments, M_r.

$$R_r = \frac{M_{r1}}{d_1 - t_{f1}} + \frac{M_{r2}}{d_2 - t_{f2}} - V_{rc} - \frac{P_{r1} + P_{r2}}{2} \qquad (3\text{-}34)$$

$$R_r = \frac{M_r}{d - t_f} - \frac{P_r}{2} \qquad (3\text{-}35)$$

AISC *Specification* Section J10.6 provides equations for the available strength of the panel zone to resist shear. These equations apply specifically to the limit state of shear yielding, and P_r in these equations is the required axial strength for the column using LRFD or ASD load combinations.

(a) When the effect of panel zone deformation on frame stability is not considered in the analysis:

for $\alpha P_r \le 0.4 P_y$

$$R_n = 0.60 F_{yw} d_c t_w \qquad (\textit{Spec.}\ \text{Eq. J10-9})$$

for $\alpha P_r > 0.4 P_y$

$$R_n = 0.60 F_{yw} d_c t_w \left(1.4 - \frac{\alpha P_r}{P_y}\right) \qquad (\textit{Spec.}\ \text{Eq. J10-10})$$

(b) When the effect of panel zone deformation on frame stability is considered in the analysis:

for $\alpha P_r \le 0.75 P_y$

$$R_n = 0.60 F_{yw} d_c t_w \left(1 + \frac{3 b_{cf} t_{cf}^2}{d_b d_c t_w}\right) \qquad (\textit{Spec.}\ \text{Eq. J10-11})$$

for $\alpha P_r > 0.75 P_y$

$$R_n = 0.60 F_{yw} d_c t_w \left(1 + \frac{3 b_{cf} t_{cf}^2}{d_b d_c t_w}\right)\left(1.9 - \frac{1.2 \alpha P_r}{P_y}\right) \qquad (\textit{Spec.}\ \text{Eq. J10-12})$$

In buildings using built-up columns with noncompact to slender webs, other limit states are possible, such as elastic plate buckling, inelastic plate buckling, and post-buckling strength due to formation of a tension field. For negative moment (tension on the outside of the knee area) such as shown in Figure 3-16(a), all of these limit states are possible. As shown in Figure 3-16(a), a tension field can develop because it is anchored by stiff corners of the panel zone. It has been shown that tension field action will not develop if partial depth stiffeners are used, such as shown in Figure 3-16(c) (Jenner et al., 1985a). For a buckled web plate to develop tension field action, the tension field must be anchored at both ends, locations A and B in Figure 3-16(a) for negative moment. Tests have shown that if partial depth stiffeners are used, the tension field will not anchor at location A, and the additional strength associated with a tension field will not develop. Similarly, anchorage at the outside corner of the knee area is not sufficient to fully develop a tension field if positive moment exists as shown in Figure 3-16(d) (Young and Murray, 1997). A method has been developed to predict the amount of added panel zone shear strength due to partial tension field action in gable frame connections subjected to positive moment as described by Wei et al. (2019).

The equations for panel zone strength in the AISC *Specification* are primarily intended for beam-to-column joints in multistory frames. The assumed limit state in those equations

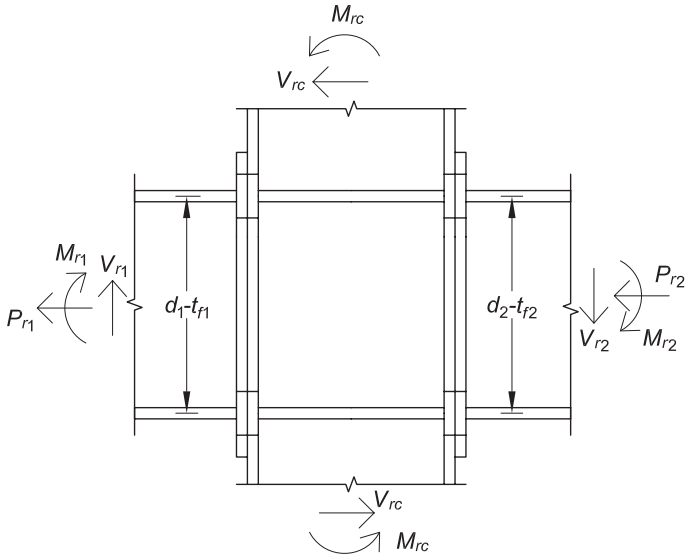

(a) Four-way joint

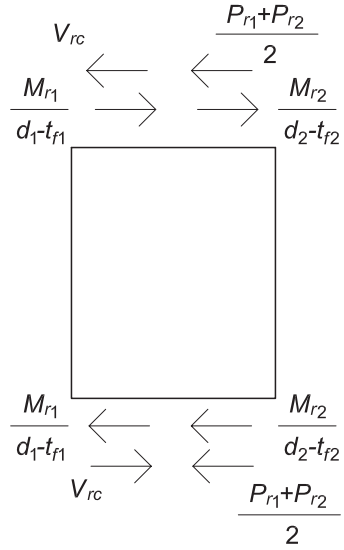

(b) Panel zone forces

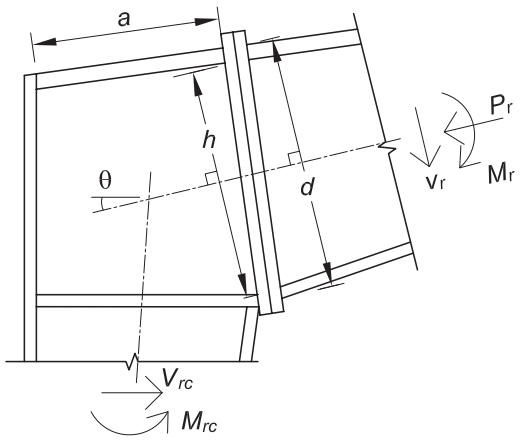

(c) Knee joint

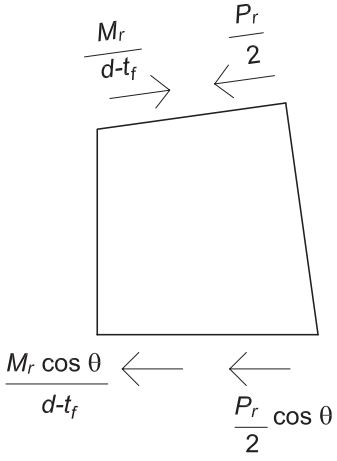

(d) Panel zone forces

Fig. 3-15. Panel zone demands.

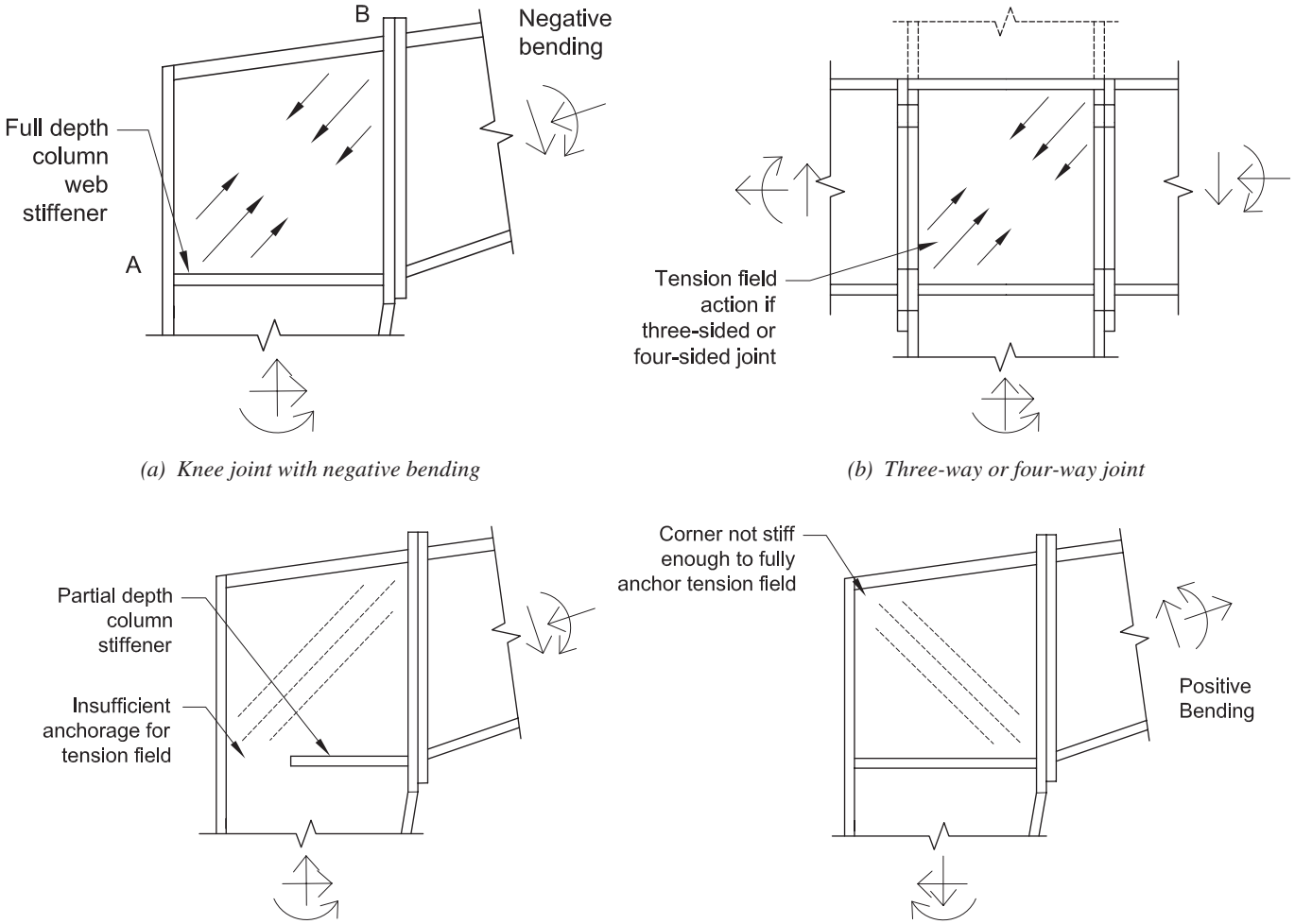

(a) Knee joint with negative bending

(b) Three-way or four-way joint

(c) Partial depth column stiffener

(d) Positive bending

Fig. 3-16. Panel zone tension field action.

is shear yielding, and plate buckling checks are not required. However, plate buckling is usually the controlling limit state of panel zone plates in gable frames using built-up columns and rafters. Design rules for such plates have been developed (Murray, 1988; Murray and Shoemaker, 2002) as follows.

The shear area, A_w, is calculated as the panel zone thickness multiplied by the dimension, a_v, along a line even with the top of the beam. If, on the other hand, the required shear strength is calculated along the vertical edge of the panel zone (e.g., for horizontal end-plate connections in a gable frame where the beam rests on top of the column), then the shear area used to calculate available shear strength is based on the dimension along the vertical edge of the panel zone. The dimensions a and h used in the equations in AISC *Specification* Chapter G are taken as the width and height of the panel zone, respectively. This is demonstrated in Example 5.3-1.

For panel zones with $a/h \leq 3$, subjected to negative moment and having full-depth column web stiffeners, the shear strength of the panel zone is calculated using AISC *Specification* Section G2.2 for shear strength on an interior web panel considering tension field action. The column stiffener should be welded to both column flanges and the panel zone plate. Treating the panel zone as an interior panel rather than an end panel per Section G2.3 has been validated against test data (Jenner et al., 1985a).

For panel zones subjected to negative moment with partial depth column web stiffeners, or with $a/h > 3$, the use of tension field action is not allowed, and the provisions of AISC *Specification* Section G2.1 apply. Partial depth column web stiffeners must terminate within 1 in. of the outside column flange and be welded to the inside column flange and the panel zone plate. For panel zones subjected to positive moment, panel zones may be designed without consideration of tension field action or considering partial tension field action as described in Wei et al. (2019).

Use of these design rules requires that the combined width of the panel zone web stiffeners be approximately the same as the rafter flange width and of the same thickness as the rafter flange. Stiffener-to-column flange welds must be large enough to develop the yield strength of the portion of the stiffener in contact with the column flange (stiffener width minus clip required for web-to-column flange clearance). The stiffener-to-column web weld must be sufficient to resist the yield strength of the stiffener.

3.7.4 End-Plate Stiffener Requirements

There are two types of stiffeners included in the end-plate moment connection configurations shown in Chapter 1—the end-plate stiffeners used in the extended stiffened end-plate configurations and the beam web stiffener plates for two of the flush end-plate connections.

The end-plate stiffener must have adequate strength to transfer a portion of the beam flange force from the beam flange to the bolts on the extended portion of the end plate. To provide a consistent load path through the end-plate connection when the beam and end-plate stiffeners have the same material strengths, the thickness of the stiffeners must be greater than or equal to the beam web thickness. If the beam and end-plate stiffener have different material strengths, the thickness of the stiffener, t_s, must be greater than the ratio of the beam-to-stiffener plate material yield stress, F_{yb}/F_{ys}, multiplied by the beam web thickness, t_{bw}, as given by Equation 3-36.

$$t_s \geq t_{bw}\left(\frac{F_{yb}}{F_{ys}}\right) \tag{3-36}$$

The end-plate yield line models and bolt force models assume that the connection rotation has a pivot point at the center of the compression flange, thus not relying on the end-plate stiffener for compression rigidity. The end-plate stiffener is not typically designed to resist compression, but for high-seismic-ductility applications, the stiffener must satisfy the slenderness limit given in Equation 3-37 to provide a minimum level of local buckling resistance.

$$\frac{h_{st}}{t_s} \leq 0.56\sqrt{\frac{E}{F_{ys}}} \tag{3-37}$$

Chapter 4 includes detailing requirements for end-plate stiffeners.

Web stiffener plates help transfer tension load from the beam web to the end plate in the vicinity of the tension bolts, and as such, their area is included with the beam web area in the check of web tension yielding. The required strength for beam web tension yielding is given by Equation 3-40 and checked for an area equal to the web stiffeners cross-sectional area plus a height of the web extending from the inside of the tension beam flange to 6 in. inside the innermost tension bolt row. Design of web stiffeners is demonstrated in Example 5.2-3 and 5.2-4.

3.7.5 Beam and Stiffener Welds to End Plate

The appropriate design and detailing of the welds is critical for an end-plate moment connection to realize its full flexural strength. Welds in a seismic resisting connection can be subjected to inelastic strain demands and thus must be designed to develop the full strength of the connecting part with filler metal and detailing that promote ductility. There are more options for welds in end-plate connections designed for gravity, wind, and low-seismic-ductility applications. Regardless of whether the connection is designed for high-seismic-ductility or not, the design of welds must be based on configurations that have been tested in full-scale experimental programs. This section discusses guidelines for welding based on prior testing and is split into two subsections based on design for gravity, wind, and low-seismic-ductility applications versus design for high-seismic-ductility applications.

Welds for Gravity, Wind, and Low-Seismic-Ductility Applications

Normally, the beam flange to end-plate weld is designed to develop the yield strength of the connected beam flange. This is typically done with CJP groove welds, but alternatively, PJP groove welds or fillet welds may be used for thin flanges. However, when the applied moment is less than the design flexural strength of the beam, the beam flange to end-plate weld can be designed for the required flexural strength, but not less than 60% (LRFD) or 40% (ASD) of the specified minimum yield strength of the connected beam flange. The required tensile strength, R_u (LRFD) or R_a (ASD), is therefore calculated using Equations 3-38 as a function of the required flexural strength, M_u (LRFD) or M_a (ASD); required axial tensile strength, T_u (LRFD) or T_a (ASD); and the beam flange yield stress, F_y, width, b_f, and thickness, t_f.

LRFD	ASD
$R_u = \max\left(\frac{M_u}{d-t_f}+\frac{T_u}{2}, 0.60F_y b_f t_f\right)$ (3-38a)	$R_a = \max\left(\frac{M_a}{d-t_f}+\frac{T_a}{2}, 0.40F_y b_f t_f\right)$ (3-38b)

The beam web, and in some cases the beam web plus web stiffeners, is checked for tension yielding in the vicinity of the tension bolts with the required strength equal to the calculated beam flange force, $T_{r,calc}$, given by Equation 3-39 multiplied by the number of tension bolts adjacent to the web, n_{trib}, divided by the total number of tension bolts, n. The required strength for beam web tension yielding is given by Equation 3-40 and checked for a length of the web extending from the inside of the tension beam flange to 6 in. beyond the last tension bolt row.

$$T_{r,calc} = \frac{M_r}{d-t_{bf}} + \frac{T_r}{2} \tag{3-39}$$

$$T_{rw} = \left(\frac{n_{trib}}{n}\right) T_{r,calc} \tag{3-40}$$

The beam web to end-plate welds are separately checked for (1) tension rupture in the region around the tension bolt holes (extending 6 in. beyond the tension bolt holes), and (2) the rest of the web to end-plate weld is checked for shear. If moment reversal is expected, both the top and bottom of the beam web to end-plate welds are designed for tension. The portions of the weld used to resist tension and shear are demonstrated in Figure 3-17.

Beam web to end-plate welds in the vicinity of the tension bolts, taken as extending from the flange to 6 in. beyond the innermost row of bolts, are to be designed to develop the yield strength of the beam web, unless the full design strength of the beam is not required. If the applied moment is less than the design flexural strength, the beam web to end-plate welds in the vicinity of the tension bolts are designed for the same required strength as the beam web, T_{rw}, except that the required strength must be at least 60% (LRFD) or 40% (ASD) of the minimum specified yield strength of the beam web (reference AISC *Manual* Part 12). The required strength for the beam web to end-plate welds in the vicinity of the tension bolts is therefore given by Equations 3-41.

LRFD	ASD
$T_{uwd} = \max(T_{uw}, 0.60F_y t_{bw} l_{wt})$ (3-41a)	$T_{awd} = \max(T_{aw}, 0.40F_y t_{bw} l_{wt})$ (3-41b)

Alternate approaches may be reasonable, such as designing the flange and web tension welds together as an effective tee section, but the required strength must always be at least 60% (LRFD) or 40% (ASD) of the minimum specified yield strength of the flange and web.

The length of web to end-plate weld available to resist shear, as demonstrated in Figure 3-17, is assumed to be the lesser of (1) the weld from the end of the assumed web tension length to the inside face of the beam compression flange and (2) the weld between the mid-depth of the beam and the inside face of the beam compression flange. The shear strength of this portion of weld is compared to the required shear applied to the connection.

The connection of the end-plate stiffener to the outside face of the beam flange and to the face of the end plate may be made using groove welds or fillet welds. The stiffener to end-plate weld is designed to develop the tensile yield strength of the stiffener plate, and the stiffener to the beam flange weld is designed for the shear yield strength of the stiffener.

Welds for High-Seismic-Ductility Applications

The requirements for end-plate moment connection welds are described in AISC *Prequalified Connections* Section 6.6.6. There are a number of welds that require careful detailing including (1) weld from the beam flange to the end plate, (2) weld from the beam web to the end plate, (3) stiffener to beam flange and stiffener to end plate, and (4) weld from the beam web to beam flange in built-up beam sections.

The beam flange to end-plate weld must be a CJP groove weld made from the outside of the flanges except directly over the beam web. Weld access holes and backing bars are not permitted. The root along the inside of the flanges must be backgouged, except at the web where access makes this impossible, and then a 5⁄16 in. reinforcing fillet weld must be added on the inside of the beam flanges. At the web locations, the weld is not considered a CJP groove weld because it does not satisfy the prequalified CJP groove weld requirements, but instead is considered a full-depth PJP groove weld.

The weld of the beam flange to the end plate is a demand critical weld for OMF, IMF, and SMF, which must satisfy the associated requirements of AWS D1.8/D1.8M (AWS, 2016). As part of the demand critical requirements, the filler metal must have a

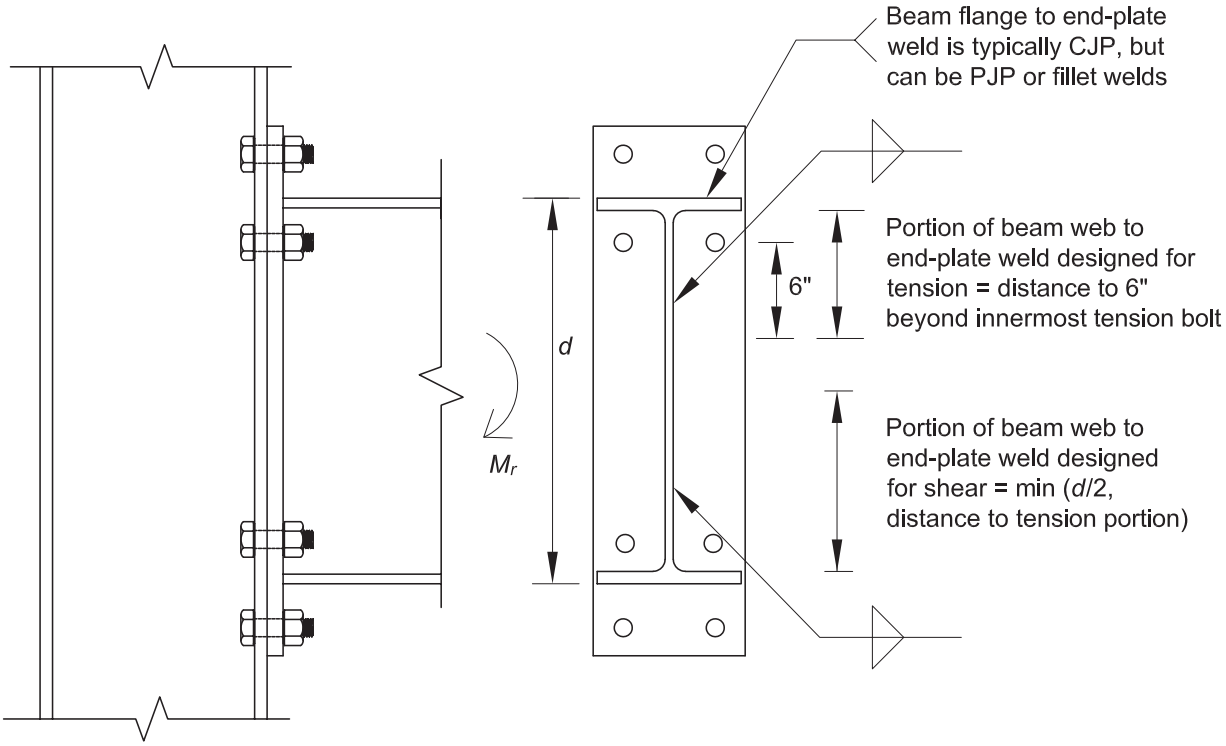

Fig. 3-17. Beam to end-plate welds.

minimum Charpy V-notch (CVN) toughness of 20 ft-lb at 0°F and must also satisfy requirements for heat input envelope testing, unless it is a filler metal listed in the exceptions of AWS D1.8/D1.8M.

The beam web to end plate weld is separately checked for (1) tension rupture in the region around the tension bolts extending 6 in. beyond the bolt row farthest from the beam flange, and (2) the remainder of the web to end-plate weld is checked for shear. The weld of the beam web to the end plate in the tension region (taken as the portion of web from the inside face of the flange to 6 in. beyond the bolt row farthest from the beam flange) must develop the full yield strength of the beam web in tension. This can be accomplished using either fillet welds or CJP groove welds. For shear, the beam web to end-plate weld in one of the tension regions plus the weld between the two tension regions is available to resist beam shear.

The weld from any stiffeners to the end plate must be made using CJP groove welds, unless the stiffener is less than or equal to ⅜ in. thick, then double-sided fillet welds are allowed that develop tensile yield strength of the stiffener plate. Similarly, the weld of the stiffener to the beam flange must develop the shear yield strength of the stiffener plate. This can be accomplished using CJP groove welds or double-sided fillet welds.

In built-up beam sections, the weld between the beam web and beam flange must be sufficiently strong in the moment connection region. For a distance equal to the lesser of the beam depth, d, or three times the flange width, $3b_f$, the beam web to beam flange weld must either be a pair of fillet welds each having a size 75% of the beam web thickness (but not less than ¼ in.), or CJP groove welds. For the rest of the beam, the web to flange weld is designed based on shear transfer between the web and flange.

3.7.6 Column-Side Limit States

Column-side limit states directly associated with end-plate moment connections include (1) flexural yielding of the column flange in the vicinity of the tension bolts; (2) column web local yielding, web local crippling, or compression web buckling; (3) failure of the column web stiffeners due to yielding, local buckling, or weld fracture; and (4) panel zone shear yielding or buckling. Depending on the column section, column bracing, and frame configuration, other limit states may require considerations associated with column and frame stability.

There have been relatively few studies conducted to determine the column flange strength in beam-to-column end-plate moment connections. In a beam-to-column end-plate moment connection, the beam flange tensile forces are transmitted directly to the column flange by the connection bolts. The column flange must provide adequate strength to resist the applied bolt tensile forces. The column flanges can be configured as stiffened or unstiffened, as shown in Figure 3-18. A stiffened column flange has web stiffener plates, often called continuity plates, installed perpendicular to the column web and in line with the connecting beam flanges. An unstiffened column flange does not have stiffener plates.

Yield line analysis has been used to develop solutions for the stiffened and unstiffened column flange configurations for the end-plate moment connection configurations included in this Design Guide. For example, the column flange unstiffened and stiffened yield line pattern for the four-bolt end-plate connection (either four-bolt extended unstiffened or four-bolt extended stiffened) is shown in Figure 3-18. The flexural strength associated with column flange yielding is calculated as given in Equation 3-43, where the yield line parameter for this specific type of connection is given in Equation 3-44 and Equation 3-45 for the unstiffened and stiffened conditions, respectively. Yield line solutions for the column-side yield line parameters for all the end-plate configurations considered in this Design Guide are included in Appendix A and derived in Eatherton et al. (2021). The available axial tensile strength given by Equation 3-42 is used later in conjunction with the resistance factor and safety factor in AISC *Specification* Section J10.1 in the check for required column web stiffeners.

$$R_n = \frac{M_{cf}}{(d - t_{bf})} \tag{3-42}$$

$$M_{cf} = F_{yc} t_{cf}^2 Y_c \tag{3-43}$$

For unstiffened column flange and four-bolt connection:

$$Y_c = \frac{b_{fc}}{2}\left[h_2\left(\frac{1}{s}\right) + h_1\left(\frac{1}{s}\right)\right] + \frac{2}{g}\left[h_2\left(\frac{3c}{4} + s\right) + h_1\left(\frac{c}{4} + s\right) + \frac{c^2}{2}\right] + \frac{g}{2} \tag{3-44}$$

For stiffened column flange and four-bolt connection:

$$Y_c = \frac{b_{fc}}{2}\left[h_2\left(\frac{1}{p_{si}}+\frac{1}{s}\right)+h_1\left(\frac{1}{p_{so}}+\frac{1}{s}\right)\right]+\frac{2}{g}\left[h_2(p_{si}+s)+h_1(p_{so}+s)\right] \tag{3-45}$$

The column web yielding strength is given by Equation 3-46 with bearing width, l_b, given by Equation 3-47, where $C_t = 0.5$ if the distance from the top of the column to the beam flange in question is less than the depth of the column, and $C_t = 1.0$ otherwise; k_c = distance from outer face of column flange to web toe of fillet (design value, k_{des}) or fillet weld; and w is the leg size of the double fillet weld if used in the beam flange-to-end-plate weld. The calculated column web yielding strength is used in conjunction with the resistance factor, $\phi = 1.00$, and safety factor, $\Omega = 1.50$, in AISC *Specification* Section J10.2.

$$R_n = (6C_t k_c + l_b)F_{yc}t_{cw} \tag{3-46}$$

$$l_b = t_{bf} + 2w + 2t_p \tag{3-47}$$

The column web crippling strength at the beam compression flange is given by the following, which is used in conjunction with the resistance factor and safety factor in AISC *Specification* Section J10.3:

(a) When F_{fu} is applied at a distance greater than or equal to $d_c/2$ from the end of the column

$$R_n = 0.80t_{cw}^2\left[1+3\left(\frac{l_b}{d_c}\right)\left(\frac{t_{cw}}{t_{cf}}\right)^{1.5}\right]\sqrt{\frac{EF_{yc}t_{cf}}{t_{cw}}} \qquad (\textit{Spec}.\text{ Eq. J10-4})$$

(b) When F_{fu} is applied at a distance less than $d_c/2$ from the end of the column

(i) for $l_b/d_c \le 0.2$,

$$R_n = 0.40\,t_{cw}^2\left[1+3\left(\frac{l_b}{d_c}\right)\left(\frac{t_{cw}}{t_{cf}}\right)^{1.5}\right]\sqrt{\frac{EF_{yc}t_{cf}}{t_{cw}}} \qquad (\textit{Spec}.\text{ Eq. J10-5a})$$

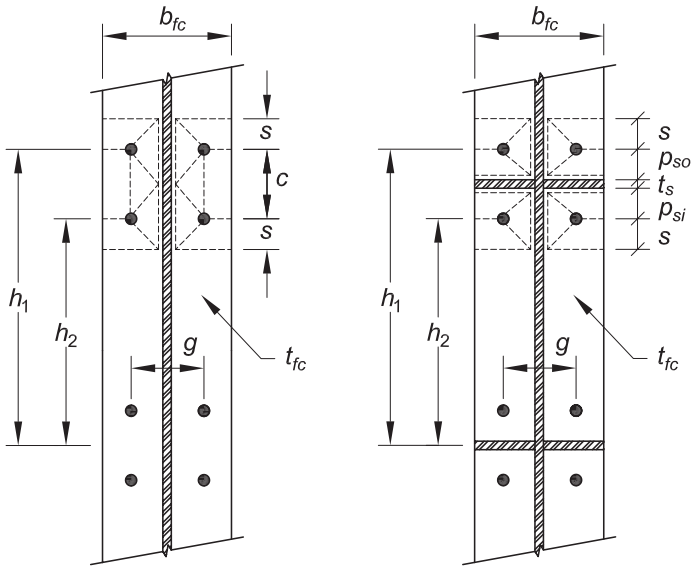

(a) Unstiffened column flange *(b) Stiffened column flange*

Fig. 3-18. Example yield line pattern for column flange.

(ii) for $l_b/d_c > 0.2$,

$$R_n = 0.40t_{cw}^2\left[1+\left(\frac{4l_b}{d_c}-0.2\right)\left(\frac{t_{cw}}{t_{cf}}\right)^{1.5}\right]\sqrt{\frac{EF_{yc}t_{cf}}{t_{cw}}} \qquad \text{(}Spec\text{. Eq. J10-5b)}$$

where

d_c = overall depth of column, in.

t_p = end-plate thickness, in.

w = leg size of double fillet weld if used in the beam flange to end-plate weld, in.

If the column has moment connections on both sides and is loaded such that compressive forces are developed at the opposing flanges (e.g., opposing moment connections both subjected to gravity loading only), then web compression buckling must also be checked in accordance with AISC *Specification* Section J10.5.

Determining whether column web stiffeners are required depends on whether the column has sufficient strength to resist flange flexure, web local yielding, web local crippling, and web compression buckling (if applicable). If the column strength is insufficient for any of these limit states, then column web stiffeners are required and need to satisfy the requirements of AISC *Specification* Section J10.8. If column web stiffeners are required for any of the column-side limit states, the required strength, $T_{u,stiff}$ (LRFD) or $T_{a,stiff}$ (ASD), is given by Equations 3-48, where $T_{u,calc}$ (LRFD) and $T_{a,calc}$ (ASD) are the flange forces given by Equation 3-39 (except for high-seismic-ductility design, where this is replaced with F_{fu} from AISC *Prequalified Connections* Equation 6.7-6), and ϕR_n (LRFD) and R_n/Ω (ASD) are the design strengths for each of the four limit states.

LRFD	ASD
$T_{u,stiff} = T_{u,calc} - \min(\phi R_n)$ (3-48a)	$T_{a,stiff} = T_{a,calc} - \min\left(\frac{R_n}{\Omega}\right)$ (3-48b)

For high-seismic-ductility design, the web stiffener plates must also follow the requirements in AISC *Seismic Provisions* Section E3.6f and AISC *Prequalified Connections* Section 6.4(3).

Chapter 4
Design Considerations

4.1 DESIGN CHOICES

4.1.1 Thick vs. Thin End-Plate Design for Gravity, Wind, and Low-Seismic-Ductility Design

The design concepts presented in Chapter 3 are organized into thin end-plate and thick end-plate design procedures in Chapter 5 based on whether the controlling limit state is end-plate yielding or bolt rupture without prying action, respectively. Both design procedures are valid, but there are several considerations that may affect the decision to choose one or the other.

By using the required flexural strength, M_u (LRFD) and M_a (ASD), as the demand for end-plate flexure in Equations 5-4, the end plate will not reach a plastic hinge before reaching the required flexural strength. The end plate will, therefore, exhibit thick end-plate behavior at factored loads but may transition into intermediate or thin end-plate behavior at failure. This approach results in connections that have thicker end plates but smaller bolts than those designed using the thin end-plate design procedures.

If either the end plate or the column flange do not qualify as a thick plate, then the bolts should be designed for the worst case prying forces associated with the two.

4.1.2 Limits on Parameters Based on Range Tested

For gravity, wind, and low-seismic-ductility design, the range of end-plate parameters that have been previously tested are tabulated in Chapter 5 for flush and extended end-plate connections. The design procedures have been validated for this range of parameters, and thus it is recommended that end plates be designed within these bounds. It is stated in Chapter 5 that a variation of plus or minus 10% applies to the design equations. However, in the event that an end-plate configuration falls outside the tested parameters, it is worth examining which parameters are more likely to significantly change connection behavior and invalidate the design procedures.

Reducing the beam depth, d, below the tested range may alter the yield line pattern and invalidate the design equations. On the other hand, increasing the beam depth, d, above the tested range is less likely to alter the yield line pattern. Similarly, if the interior bolts are pushed too far away from the inside of the flange, the yield line pattern can change, and the end plate may not be sufficiently stiff for the interior bolts to contribute to flexural strength. Increasing bolt hole spacing on the interior side of the flange outside the tested range can therefore invalidate the design procedures. Pushing exterior bolt holes farther away from the outside of the beam flange is less likely to reduce design equation accuracy.

In a subsequent section on detailing, it is stated that the bolt hole gage should not be so large that the outer bolt hole centerline is beyond the edge of the flange tip. The previous tests have used bolt gages that have ranged from the minimum bolt hole spacing up to this upper limit where bolt hole centerlines are just inside the edges of the flanges.

The beam flange thickness is related to the maximum forces that can be transferred by the beam flanges. The design equations have not been validated for required moment that is significantly larger or smaller than the flexural strength of the tested connections. Also, it has not been verified that the detailing requirements (e.g., beam to end-plate welds) are sufficient for larger beam flange thickness.

For high-seismic-ductility design, the range of tested end-plate parameters are given in AISC *Prequalified Connections* Table 6.1, Parametric Limitations on Prequalification. For an end-plate connection to be designed in accordance with the prequalification standard, the end-plate parameters must be within the limits given in this table. If project specific cyclic testing is conducted to demonstrate that an end-plate connection qualifies for use in SMF, then the ability to extrapolate beyond the tested beam and column size is described in AISC *Seismic Provisions* Chapter K. The tested depth of the beam, weight of the beam, and depth of the column are required to be at least 90%, 75%, and 90% of those used on the actual project, respectively. No specific provisions are given for extrapolating end-plate geometry, but a geometric scaling of the end-plate dimensions equal to the scaling of the beam depth may be reasonable.

4.1.3 Materials

The design procedures in this Design Guide have been validated for use with Group 120 ASTM F3125/F3125M (ASTM, 2019d) Grades A325 and F1852 and Group 150 ASTM F3125/F3125M Grades A490 and F2280 high-strength bolts. Fully threaded bolts are permitted. To the authors' knowledge, no tests on end-plate moment connections have been conducted using Group 144 or Group 200 high-strength bolts. Group 144 ASTM F3148 (ASTM, 2017) Grade 144 high-strength bolts, in the authors' opinion, are suitable for use in end-plate moment connections. The use of Group 200 ASTM F3043 (ASTM, 2015) and ASTM F3111 (ASTM, 2016) super high-strength bolts in end-plate

moment connections is not recommended unless validated by testing.

End-plate moment connections with snug-tight bolts have been shown to develop similar strength as connections with pretensioned bolts (Kline et al., 1995). Snug-tight bolts are allowed for end-plate connections with Grade A325 bolts that are not subjected to fatigue loading or significant load reversal (RCSC, 2020). Types of loading for which snug tight bolts are allowed, therefore, includes nonfatigue gravity loads (e.g., dead, live, and snow), some lateral loads (e.g., wind and low-seismic ductility systems such as $R = 3$), and other relatively static loads (e.g., temperature). End-plate connections with snug-tight bolts are not recommended for members where fatigue is a design consideration or loosening due to vibratory loading is a concern, such as heavy crane runways and supporting structures for machinery and equipment because the AISC *Specification* requires the use of pretensioned connections for such applications. Pretensioned bolts are required for all connections in the seismic force-resisting system including end-plate moment connections according to the AISC *Seismic Provisions*.

Tests have been conducted with end plates that are a different material than the beam or column. In particular, end plates of ASTM A36/A36M (ASTM, 2019a) material have been tested with Grade 50 beams and columns. There have been tests by others that explored the use of high-strength steel for the end plate with yield stresses between 100 ksi and 139 ksi (Coelho and Bijlaard, 2007, 2010; Ataei et al., 2016b), but the use of higher strength steels with a specified minimum yield stress greater than 55 ksi for the end plate, beam, or column have not been evaluated with the design procedures in this Design Guide. Cracking has been observed in the heat affected zone of the specimens with higher strength end plates (Coelho and Bijlaard, 2007, 2010). Conversely, local failure of the end-plate material may be possible if the beam is significantly higher strength than the end plate.

4.2 DETAILING ISSUES

4.2.1 Fit-Up Issues

Beam length and column depth tolerances and column flange out of straightness are concerns in the fabrication and erection of structural steel moment frames utilizing end-plate moment connections. The end plates are welded to the beam or girder in the fabrication shop, and the column flanges are drilled to match the end-plate bolt pattern. This results in a connection with very little adjustment.

The AISC *Code of Standard Practice for Steel Buildings and Bridges* (AISC, 2022a) gives allowable mill, fabrication, and erection tolerances, whereas ASTM A6/A6M, *Standard Specification for General Requirements for Rolled Structural Steel Bars, Plates, Shapes, and Sheet Piling* (ASTM, 2019b), specifies mill tolerances for rolled shapes. The AISC *Code of Standard Practice* states that the accumulation of the mill tolerances and fabrication tolerances shall not cause the erection tolerances to be exceeded.

To solve the tolerance problem, the beam or girder may be detailed and fabricated 3⁄16 in. to 3⁄8 in. short, and then any gaps between the end plate and column flange filled using finger shims. Finger shims are thin steel plates, usually 1⁄16 in. thick, that are cut to match the connection bolt pattern so that they can be inserted between the column flange and the end plate. Figure 4-1 illustrates the use of finger shims inserted from the sides, although finger shims may also be inserted from the top. A tilted column flange or end plate can be corrected by inserting more or thicker shims on one side of the connection than the other. Experimental tests have been performed with finger shims, and no adverse consequences or differences in connection behavior were observed (Sumner et al., 2000). If the shim thickness exceeds ¼ in., the bolt shear strength must be adjusted according to AISC *Specification* Section J5.2.

Contact is required around bolts, but gaps are permitted, and shimming is not required for gaps between plies between the tension and compression bolts (RCSC, 2020).

It is recommended that beams with end-plate connections not be cambered because the resulting beam end rotation may cause field fit-up problems.

4.2.2 Bolt and End-Plate Detailing

Detailing the bolts to be as close to the flange and web as possible results in the most economical connection. However, small bolt hole spacing can also cause difficulties with fit-up and bolt tightening during erection. AISC *Manual* Part 7 gives guidance on entering and tightening clearances. The distance from the bolt holes to the face of the flange and web should be sufficient to allow tightening clearance (see Figure 4-2). Also, the washer, or bolt head if washers are not used, should sit flat against the end plate without interfering with the fillet welds between the beam and end plate or a stiffener. The spacing between bolt holes must not be less than required by the AISC *Specification*, which is 2⅔ times the nominal bolt diameter, although three times the bolt diameter is preferred. Edge distances must also conform to the minimum edge distances given in the AISC *Specification*.

The bolt gage should be selected to allow for adequate clearance to install and tighten the connection bolts. For end plates bolted to hot rolled columns, the distance between the inner bolt hole centerlines, g, generally should not be less than the workable gage as listed in AISC *Manual* Part 1. For built-up columns, the minimum gage should be determined considering the entering and tightening clearances in AISC *Manual* Part 7 and the size of the beam to end-plate fillet welds.

Further, the distance between the outer bolt hole centerlines should not be greater than the width of the beam flange,

as shown graphically in Figure 4-2. This restriction is to ensure a favorable load path between the beam flange and the connection bolts. For two bolts in a row, this requirement simplifies to the bolt gage should be less than the beam flange width as given in Equation 4-1. For four bolts in a row, this requirement is given in Equation 4-2.

For two bolts in a row

$$b_f \geq g \tag{4-1}$$

For four bolts in a row

$$b_f \geq g + 2g_o \tag{4-2}$$

In design calculations, the effective end plate or column flange width is limited to the connected beam flange width plus the larger of 1 in. or the end-plate thickness. This provision ensures that the end-plate material outside the beam flange width, which may not be effective, is not considered

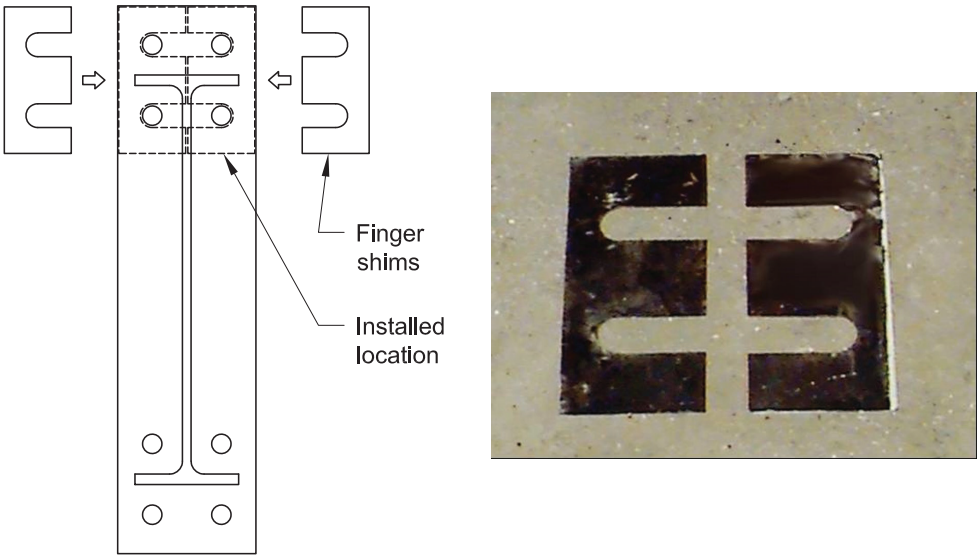

(a) Application of finger shims *(b) Picture of finger shims (Sumner, 2003)*

Fig. 4-1. Typical use of finger shims.

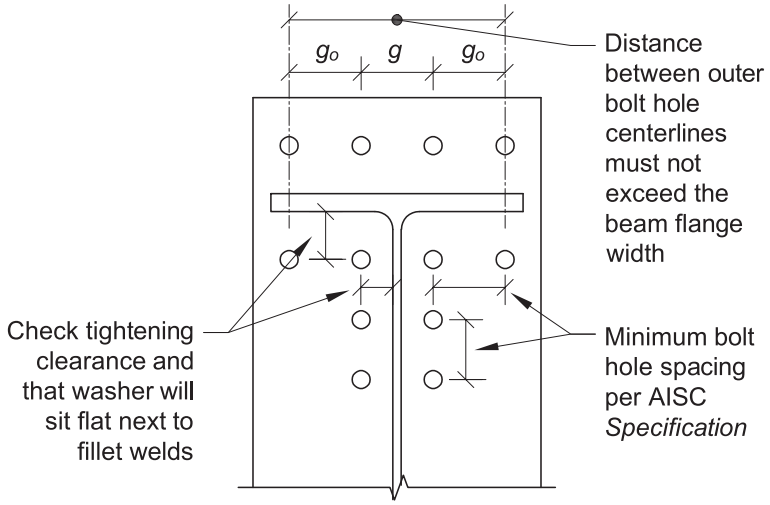

Fig. 4-2. Bolt hole detailing.

in the end-plate or column flange strength calculations. Calculations for the column-side yield line parameter assume that if stiffeners are present, they extend to within ½ in. of the flange tips.

$$b_{p,eff} \le b_f + \max(t_p, 1 \text{ in.}) \quad (4\text{-}3)$$

Some fabricators and many metal building manufacturers prefer to use a limited number of bolt lengths and use fully threaded bolts, which are permitted. It is also permitted to place washers under the bolt head or nut.

4.2.3 Welds and Weld Access Holes

For the beam flange to end-plate welds, no weld access holes should be used. Groove welds between the beam flange and end plate should be made from the outside face of the flange. This requires the beam to be flipped over between welds to allow both flange welds to be made in the flat position. The exception is gravity, wind, and low-seismic-ductility applications with extended stiffened end plates, for which the use of weld access holes is acceptable. In this case, weld access hole geometry should conform to the requirements of AWS D1.1/D1.1M or AISC *Specification* Section J1.6 and associated Commentary.

Run-off tabs, sometimes referred to as weld tabs, allow the lower-quality weld at the weld start and stop to be located outside the beam flange width. Run-off tabs are not explicitly required by AWS D1.1/D1.1M or AWS D1.8/D1.8M for the beam flange to end-plate weld, but they are recommended by the authors. For unstiffened end-plate connections in high-seismic-ductility applications, run-off tabs are recommended because the weld undergoes inelastic strains. In accordance with AWS D1.1/D1.1M, if used, run-off tabs can be left in place for statically loaded structures, but should be removed for any structures subjected to cyclic loading (e.g., fatigue or seismic loading). When run-off tabs are removed, the welds must be ground smooth and flush with the edges of the beam flange.

Backing bars at the beam flange to end-plate groove weld are not allowed for high-seismic-ductility applications, but acceptable for gravity, wind, and low-seismic-ductility applications. For high-seismic-ductility applications, there are additional requirements for the beam flange to end plate weld; see Section 3.7.5.

The beam web to end-plate weld should be completed before the beam flange to end-plate welds to avoid introduction of additional stresses in the beam flange to end-plate weld due to shrinkage of the web welds. For extended stiffened end-plate connection configurations, the beam flange is welded to the end plate prior to installing the stiffener. This allows the weld passes to be continuous across the flange width instead of piling up all the weld terminations at the middle of the flange where the corner clip on the stiffener is not intended to be a weld access hole.

End-plate warping during welding is a concern for extended end-plate connection configurations whether they are stiffened or unstiffened. Temporary strong-backs that restrain out-of-plane deformations of the end plate may be required to mitigate warping.

CJP groove welds are common at the beam flange to end-plate joint. Prequalified CJP groove welds require either a backing bar or that the root be backgouged. For most of the flange width, this is not a problem. However, for the portion of the weld over the web, there is no way to use a backing bar or backgouge because the web is in the way. At this location, the weld is considered a full-depth PJP groove weld. For high-seismic-ductility applications, AISC *Prequalified Connections* states that backgouging of the root is not required in the flange directly above and below the beam web for a length equal to 1.5 k_1, where k_1 is the distance from the beam centerline to the edge of the fillet in rolled sections (or edge of the web-to-flange fillet weld for built-up sections).

4.2.4 Composite Slabs

The design procedures in this Design Guide assume that if a concrete slab is present, it does not contribute significantly to the moment connection behavior. The composite slab should therefore be detailed with a block out around the end plate and column flange to permit insertion of compressible material as shown in Figure 6-7. For high-seismic design, it is also not permitted to have any steel headed stud anchors within the protected zone (the region of the beam where the plastic hinge forms with extents as given in AISC *Prequalified Connections*). This requirement is partially intended to reduce the possibility of fracture during large inelastic deformations of the plastic hinge; a tested moment connection fracture was attributed to steel headed stud anchors as described by Ricles et al. (2002). Excluding steel headed stud anchors in the portion of the beam near the column also reduces the amount of composite action at the connection and is recommended for gravity, wind, and low-seismic-ductility applications as well. The slab reinforcement should be minimized in the zone two times the depth of the connecting beam from the face of the column. Experimental programs by Sumner (2003) and Seek and Murray (2008) showed this approach to be effective in mitigating the effect of a composite slab on end-plate moment connection behavior.

Design procedures for end-plate moment connections with a fully composite beam participating in the connection (i.e., not following the requirements in the previous paragraph) are not included in this Design Guide. A composite slab can greatly increase the flexural strength of the beams and connection. However, they also change the flow of forces, increase demands at the bottom flange, and add limit states associated with concrete and reinforcing steel. Section 2.4.8 of this Design Guide gives some information about associated research.

4.2.5 Stiffener and Cap Plate Detailing

Three common types of stiffeners in end-plate moment connections include extended end-plate stiffeners between the end plate and beam flange, flush end-plate stiffeners between the end plate and beam web, and column web stiffeners between the column flange and column web.

To facilitate welding of the stiffener, a corner clip is necessary to prevent the stiffener and the connected element welds from conflicting. Additionally, the trimmed corner of the stiffener plate provides a consistent termination point for the stiffener plate and the welds. A diagonal clip across the corner to allow clearance and provide weld stop-start points is commonly used. Another method that has recently been introduced is a radiused cut for the "clip." The advantage of the radiused cut is the edge for start and stop is normal to the connected surfaces. The radius shape also provides better distribution of stresses and reduces stress risers and potential for cracks. If a radiused cut is used, a minimum radius of ½ in. is recommended, which is consistent with AWS D1.8/D1.8M, Figure C-4-1.

Extended End-Plate Stiffeners

Four of the nine extended end-plate moment connections shown in Figure 1-4 have a stiffener between the beam flange and end plate. The stiffening of the end plate increases the flexural strength and results in a thinner end plate as compared to an equivalent unstiffened connection. Stiffened extended end-plate configurations facilitate the use of a second row of bolts outside the flange, which further increases flexural strength by spreading out the beam tension flange force to more bolts. Also, column flange flexural demand is reduced, which may eliminate the need for column web stiffeners. The end-plate stiffener acts like a portion of the beam web to transfer part of the beam flange tensile force to the end plate and then to the connection bolts.

For seismic design, detailing of the extended end-plate stiffener must follow the requirements in AISC *Prequalified Connections*. Some of the reasoning for those requirements is given here. Analytical and experimental studies have shown that a concentrated stress applied to an unsupported edge of a gusset plate is distributed out from that point towards the supported edge at an angle of approximately 30°. This force distribution model is commonly referred to as the Whitmore Section (see AISC *Manual* Part 9 for more details). The same force distribution model is applied to the detailing of the end-plate stiffeners. The portion of the flange force that is transferred to the stiffener is assumed to distribute into the stiffener plate at an angle of 30°. Using this model, the required length of the stiffener along the outside face of the beam flange is

$$L_{st} = \frac{h_{st}}{\tan 30^\circ} \tag{4-4}$$

where h_{st} is the height of the end plate from the outside face of the beam flange to the end of the end plate (see Figure 4-3). The same geometry can be used to design triangular beam web stiffeners.

To facilitate welding of the stiffener, the stiffener plates should be terminated at the beam flange and at the end of the end plate with landings approximately 1 in. long. The landings provide a consistent termination point for the stiffener plate and the welds. The stiffener should be clipped where it meets the beam flange and end plate to provide clearance between the stiffener and the beam flange weld. Figure 4-3 illustrates the required layout of the end-plate stiffener geometry.

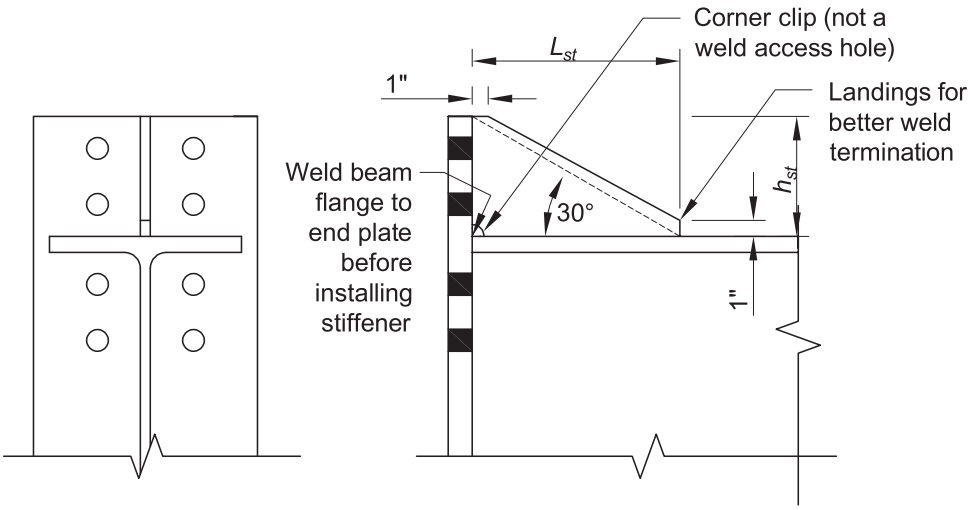

Fig. 4-3. Stiffener geometry.

For end-plate moment connections designed for gravity, wind, or low-seismic-ductility, there is more flexibility in the detailing of the extended end-plate stiffener because the connection is expected to remain elastic during service level demands. Many of the monotonic tests conducted to validate nonseismic design procedures used triangular- or rectangular-shaped stiffeners as shown in Figure 2-4(a) and Figure 2-4(b), respectively. Triangular-shaped stiffeners with an angle no larger than 45° and rectangular stiffeners with a height to length ratio no larger than 1.0 are expected to produce adequate behavior for gravity, wind, and low-seismic-ductility design.

Flush End-Plate Stiffeners

Most end-plate moment connection tests use beam specimens with relatively thick webs to avoid premature web failure. In a number of tests, beam webs near the tension bolts have been instrumented with strain gages with yielding of the beam web reported at moments smaller than the plastic moment strength of the beam (40% of M_p in some cases). For example, the distribution of longitudinal strain in the beam web was measured over the depth of the beam at a location 2 in. from the end plate by Hendrick et al. (1984). The measured strain distribution showed that the web longitudinal stresses were considerably larger in the vicinity of the bolts than those predicted by a linear stress distribution and that web yielding occurred even though the applied moment was less than the yield moment for the beam section.

The experimental program conducted by Hendrick et al. (1984), which included eight successful tests on specimens with web stiffeners, provides some useful information about the effectiveness of flush end-plate web stiffeners. For beams of depth 16 in. to 24 in., the web thicknesses were either ¼ in. or ⅜ in. thick, with ⅜-in.-thick web stiffeners for all specimens. The stiffeners were either square or triangular with an approximately 45° angle. Stiffeners between the tension bolts produced approximately 22% larger flexural strength than a similar end-plate configuration with stiffeners outside the bolts and approximately 45% larger than unstiffened configurations. Additionally, the bolt forces were found to be smaller when the stiffener was located between the bolts rather than outside the bolts.

Although Hendrick et al. (1984) did not explicitly develop design procedures for the web stiffeners, their longitudinal web strain measurements suggest that it is reasonable to design the portion of the beam web in the vicinity of the tension bolts and the web stiffener for the total tensile bolt force. The design examples in Sections 5.2-3 and 5.2-4 adopt this design approach and check the combined web plus stiffener area and their welds to the end plate for the total tensile bolt force.

Column Web Stiffeners (Continuity Plates)

The third type of stiffener common in end-plate moment connections is the column web stiffener, referred to as continuity plates in seismic design. Column web stiffeners are required if the unstiffened column has insufficient strength to resist the concentrated force associated with the beam flange force. The applicable limit states are column flange bending, column web yielding, column web crippling, and for a column with double-sided moment connections subject to gravity loading only, column web buckling. If the design strength for all four limit states are greater than the effects of the beam flange force, then continuity plates are not required. Conversely, if the unstiffened column strength is less than necessary to resist the beam flange force, the continuity plate required strength is calculated as the difference between the beam flange force and the unstiffened column's resistance to this force. This procedure is detailed in AISC *Prequalified Connections* for seismic design. The same procedure is applicable to gravity, wind, and low-seismic-ductility design as described in AISC *Specification* Section J10. The examples in Section 6.3 demonstrate these calculations for cases where continuity plates are both required and not required.

If continuity plates are required in seismic design, full-depth stiffeners are required and must follow the requirements of the AISC *Seismic Provisions*. For gravity, wind, and low-seismic-ductility design, the column web stiffeners can be partial depth and the stiffener plates and welds would be designed for the forces described in the previous paragraph. As described in Section 3.7.3, full-depth column web stiffeners are required if tension field action is used to resist panel zone shear in the presence of negative bending.

Cap Plates

Cap plates are horizontal plates welded to the top of the column and act to stiffen the column section at a roof beam to column connection (see Example 5.2-1 for recommended details). If the cap plate is in line with the beam flange, the cap plate and the welds to the column web must be capable of transferring the full beam flange force. The cap plate also braces the column flange against translation and rotation so that the column flange can develop a yield line mechanism with larger strength.

Chapter 5
Gravity, Wind, and Low-Seismic-Ductility Design

This chapter contains design guidance and examples for end-plate moment connections that are not subjected to large inelastic deformations, which includes design for gravity loads and wind loads. This type of design is also applicable for seismic loads in low-ductility seismic force-resisting systems, such as OMF and moment frames designed with a response modification factor $R = 3$.

The chapter is organized into three sections, the first summarizes the design procedures for both flush and extended thick and thin end-plate connections, the second provides design tables and examples for the six flush end-plate moment connections shown in Figure 1-3, and the third gives design tables and examples for the nine extended end-plate moment connections shown in Figure 1-4. For all end-plate connection configurations, an example is provided demonstrating the checks for plate thickness and bolt diameter for the thick end-plate design procedure as well as checks for the beam to end-plate welds. Three of the examples—the two-bolt flush, the four-bolt extended unstiffened, and the four-bolt extended stiffened—include additional design checks for the column-side limit states. The four-bolt extended unstiffened example is configured to have the geometry of a gable frame knee joint. Appendix B includes design examples demonstrating the thin end plate/larger bolt design procedure for all flush and extended end-plate configurations.

5.1 DESIGN EQUATIONS

Design concepts from Chapter 3 are presented in this section in the format of a design procedure for both thick end-plate behavior (thicker end plate with smaller bolts not subjected to prying action), and thin end-plate behavior (thinner end plate and larger bolts to resist prying action).

As discussed in Section 3.2, flush end-plate moment connections can be too flexible to qualify as an FR connection. To qualify as an FR connection, the end plate is made thicker through the use of a plate strength reduction factor, γ_r. The end-plate flexural yielding strength is reduced by the factor, γ_r, for the calculation of required end-plate thickness. If the flexural strength is reduced by 20%, the connection rotation at the required flexural strength is expected to be limited to 10% of the simple span beam rotation. The factor, γ_r, is therefore given by Equation 5-1.

$\gamma_r = 0.80$ for flush end-plate configurations (5-1)
$\gamma_r = 1.0$ for extended end-plate configurations

Both the bolt strength and the yield line parameter are necessary for design regardless of whether a thick or thin end-plate approach is selected. The bolt strength, P_t, is given in AISC *Manual* Table 7-2 (includes the value of ϕ or Ω which must be removed), or it can be obtained using Equation 5-2 and AISC *Specification* Table J3.2. The yield line parameter, Y_p, is calculated per the equations provided in Tables 5-2 through 5-7 and Tables 5-10 through 5-18 for the specific bolt configuration selected.

$$P_t = F_{nt}A_b \tag{5-2}$$

where

A_b = nominal area of the bolt, in.^{2}
F_{nt} = nominal tensile strength of bolts, ksi
= 90 ksi for Group 120 ASTM F3125/F3125M Grade A325 and Grade F1852 bolts
= 108 ksi for Group 144 ASTM F3148 Grade 144
= 113 ksi for Group 150 ASTM F3125/F3125M Grade A490 and Grade F2280 bolts

5.1.1 Thick End-Plate Design Procedure

Equations 5-3 give the minimum bolt diameter for a thick end-plate design and were developed by combining Equation 3-20, Equation 5-2, and the inequality that the design flexural strength associated with bolt rupture, ϕM_{np} or M_{np}/Ω, is greater than the required flexural strength, M_u or M_a.

LRFD		ASD	
$d_{b,reqd} = \sqrt{\dfrac{4M_u}{\pi\phi F_{nt}\left(\sum_i n_i h_i\right)}}$ $\phi = 0.75$	(5-3a)	$d_{b,reqd} = \sqrt{\dfrac{4M_a}{\dfrac{\pi F_{nt}}{\Omega}\left(\sum_i n_i h_i\right)}}$ $\Omega = 2.00$	(5-3b)

The minimum end-plate thickness calculated using Equations 5-4 is found by substituting the value of M_{pl} from Equation 3-15 into Equation 3-18 and including the factor, γ_r, that increases the stiffness of flush end-plate connections to be FR.

LRFD		ASD	
$t_{p,reqd} = \sqrt{\dfrac{1.10M_u}{\gamma_r\phi_b F_{yp} Y_p}}$ $\phi_b = 0.90$	(5-4a)	$t_{p,reqd} = \sqrt{\dfrac{1.10M_a}{\gamma_r F_{yp} Y_p / \Omega_b}}$ $\Omega_b = 1.67$	(5-4b)

By using the required flexural strength, M_u (LRFD) or M_a (ASD), as the demand for end-plate flexure, the end plate will not yield before reaching the required flexural strength. The end plate will, therefore, exhibit thick end-plate behavior at factored loads but may transition into intermediate or thin end-plate behavior at failure.

5.1.2 Thin End-Plate Design Procedure

A similar equation is used to find the minimum end-plate thickness for thin end-plate design, except the 1.10 factor associated with ensuring thick end-plate behavior is removed.

LRFD		ASD	
$t_{p,reqd} = \sqrt{\dfrac{M_u}{\gamma_r\phi_b F_{yp} Y_p}}$ $\phi_b = 0.90$	(5-5a)	$t_{p,reqd} = \sqrt{\dfrac{\Omega_b M_a}{\gamma_r F_{yp} Y_p}}$ $\Omega_b = 1.67$	(5-5b)

The minimum bolt diameter is calculated based on satisfying the inequality given in Equations 5-6, where the flexural strength for bolt rupture with prying action must be greater than the required flexural strength.

LRFD		ASD	
$\phi M_q > M_u$ $\phi = 0.75$	(5-6a)	$\dfrac{M_q}{\Omega} > M_a$ $\Omega = 2.00$	(5-6b)

The flexural strength for bolt rupture with prying action, M_q, is given by Equation 3-28 and subsequent equations. P_{qi} is the bolt force considering prying force and is calculated for each bolt position. The factor, α_i, reduces the contribution of some bolts toward M_q. The value of α_i was calibrated for each bolt position based on testing and is given in the center column of Tables 5-2 to 5-7 and 5-10 to 5-18. The parameter α_i is equal to 1.0, except for some bolts in configurations with four-bolt horizontal rows where the value is less than 1.0 for some bolt positions.

$$M_q = \sum_i \alpha_i P_{qi} n_i h_i \tag{3-28}$$

The maximum bolt strength is the maximum of the bolt rupture strength considering prying and the bolt pretension force, T_b. As discussed in Section 3.4, if the bolt pretension is larger than the bolt rupture strength reduced for prying, then the plates will not separate, and prying forces do not develop. Therefore, it is the maximum of the two that is used as given in Equation 3-27.

For bolt position *i*:

$$P_{qi} = \max\left(P_{t,i} - Q_{\max,i},\ T_{b,i}\right) \tag{3-27}$$

Connections are designed using either pretensioned or snug-tightened bolts. For pretensioned bolts, the pretension force, T_b, from AISC *Specification* Table J3.1 is used. For Grade A325 snug-tightened bolts, the pretension force, T_b, can be taken as a percentage of the AISC specified pretension as indicated in Table 3-3.

The prying action force, Q_{max}, is based on modeling the end plate as the flange of an effective tee section. The orientation of the tee stem, and thus the direction in which prying occurs, can vary depending on the bolt location. The rules for applying prying action are demonstrated in Figure 5-1 and are given by the following:

1. If the bolt is next to the flange, the tee stub is oriented vertically perpendicular to the flange. This is demonstrated in Figure 5-1(a) bolt locations 2 and 3 and Figure 5-1(b) bolt locations 1 and 2.
2. If the bolt is next to the web or end-plate stiffener, but not next to the flange, the tee stub is oriented horizontally perpendicular to the web or end-plate stiffener. This is demonstrated in Figure 5-1(a) bolt locations 1 and 4 and Figure 5-1(b) bolt location 3.
3. In configurations with three interior bolt rows, the bolts in the second interior row have been shown in experiments not to undergo prying or significant plate separation. This is shown in Figure 5-1(c) by the lack of plate separation at the second interior bolt line. In these cases, the bolt force is taken as $P_{qi} = T_{b,i}$ in the calculation of the flexural strength for prying action, M_q (Borgsmiller et al., 1995).

Equation 3-23 estimates the prying force. It is noted that the expression for $Q_{max,i}$ in Equation 3-23 contains a negative term in the radical. If the quantity inside the radical is negative, the configuration is such that end-plate failure at that bolt location is dominated by shear and no flexural strength is available to develop the prying force at that location. Therefore, the end plate is not adequate. Either the bolt distance, b_i, or the end-plate thickness, t_p, must be increased.

$$Q_{max,i} = \frac{w_i' t_p^2}{4a_i}\sqrt{F_{yp}^2 - 3\left(\frac{F_i'}{w_i' t_p}\right)^2} \qquad \text{(from Eq. 3-23)}$$

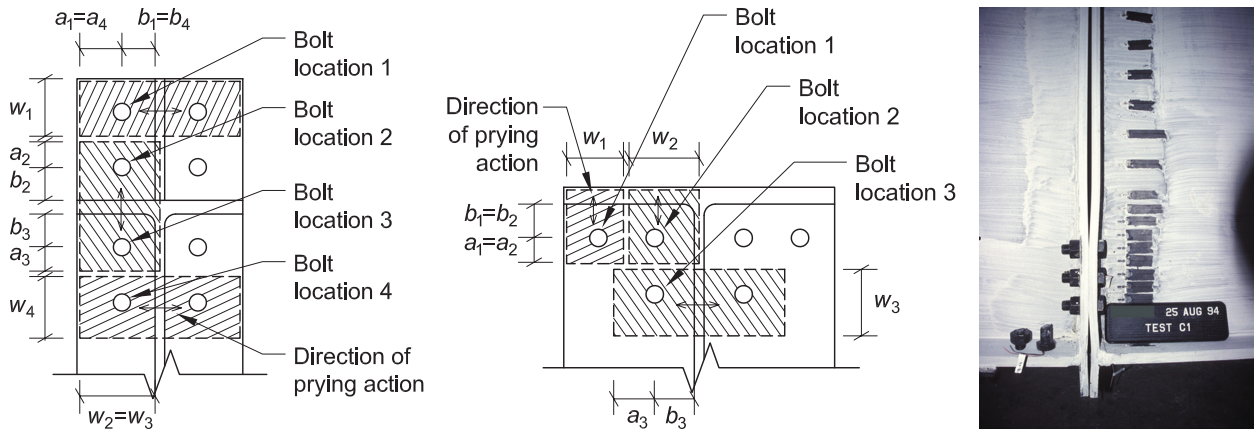

(a) Eight-bolt extended stiffened

(b) Six-bolt flush

(c) No prying for middle row of interior bolts (Borgsmiller et al., 1995)

Fig. 5-1. Demonstrating rules for calculating prying forces.

The distance, a, from the bolt line to the reaction force is calculated by Equation 3-24 as limited by the distance from the bolt line to the edge of the plate or to the interior stiffener in the case of the four-bolt flush with web stiffener between the bolts configuration.

$$a = 3.62\left(\frac{t_p}{d_b}\right)^3 - 0.085 \le \text{distance to plate edge or intermediate stiffener} \qquad \text{(from Eq. 3-24)}$$

The tee-stem force, F_i', is given by Equation 3-26, which is a function of b_i, the distance from the bolt to the tee stem, as demonstrated in Figure 5-1.

$$F_i' = \frac{1}{b_i}\left[\frac{t_p^2 F_{yp}}{4}(0.85w_i + 0.8w_i') + \frac{\pi d_b^3 F_{nt}}{32}\right] \qquad \text{(from Eq. 3-26)}$$

The effective width of each tee stub, w_i, depends on the geometry as shown in Figure 5-1. The effective net width of the tee stub, w_i', is the effective width less the effective bolt hole diameter, d_h:

$$w_i' = w_i - d_h \qquad (5\text{-}7)$$

where

$d_h = d_b + 1/16$ in. if $d_b < 1$ in.

$= d_b + 1/8$ in. if $d_b \ge 1$ in.

5.1.3 Design Procedure

The following are the steps in the thick end-plate design process as followed in the examples in this chapter.

A. End Plate and Bolt Design
   1. Design bolts to satisfy required bolt diameter using Equations 5-3.
   2. Design end plate to satisfy required end-plate thickness using Equations 5-4.
   3. Check shear yielding and shear rupture of the extended portion of the end plate (for unstiffened extended end-plate configurations only).
   4. Check shear transfer for compression bolts considering bolt shear rupture and bearing/tear-out at end-plate and column flange bolt holes.

B. Beam to End-Plate Welds
   1. Design the beam flange to end-plate weld.
   2. Design the stiffener welds (for stiffened configurations only).
   3. Check the beam web yield strength near the tension bolts.
   4. Design the beam web to end-plate weld near the tension bolts.
   5. Design the beam web to end-plate weld away from the tension bolts for shear.

C. Column-Side Limit States
   1. Design cap plate welds if applicable—column flange to cap plate weld and cap plate to column web weld.
   2. Check column limit states associated with concentrated forces such as flange flexural strength, column web local crippling, column web local yielding, and column local buckling if applicable.

Table 5-1. Tested Parameter Range for Flush End-Plate Connections		
Parameter	**Low (in.)**	**High (in.)**
p_f	1 5/16	2 1/4
p_b	1 7/8	3 1/2
g	2 1/4	4 1/2
g_o	3	3
d	16[1]	24[2,3]
b_p	5	14
t_f	3/16	3/4

[1] Two-bolt flush, lower limit is 8 in.
[2] Six-bolt 4W/2W, upper limit is 60 in.
[3] Six-bolt 3 row flush, upper limit is 36 in.

3. Check column web stiffener geometric requirements per AISC *Specification* Section J10.8 and stiffener local buckling per AISC *Specification* Table B4.1a, Case 2.
4. Calculate required strength for column web stiffeners as the beam flange force less the minimum strength determined in Step C.2.
5. Design column web stiffener welds to the column flange and column web.
6. Check column panel zone shear and provide doubler plates if necessary.

For thin end-plate design examples in Appendix B, substitute the following for the first two steps:

A. End-Plate and Bolt Design
   1. Design end plate to satisfy required end-plate thickness using Equations 5-5.
   2. Design bolts to satisfy flexural strength considering prying action using Equations 5-6.

   The remaining steps are the same as the thick end-plate design process.

Member-related limit states such as yielding, lateral torsional buckling, or local buckling of the beams and columns are not listed as part of this connection design procedure.

5.2 FLUSH END-PLATE CONNECTIONS

5.2.1 Design Tables and Limitations

The analytical procedures for the six flush end-plate connections shown in Figure 1-3 were verified through tests by Srouji et al. (1983, 1984), Hendrick et al. (1984, 1985), and Jain et al. (2015) in which geometric parameters were varied among the test configurations. Significant changes in the geometry could affect the mechanism configuration and thus the predicted strength. Therefore, the tested parameter ranges given in Table 5-1 with a variation of plus or minus 10% apply to the design equations for the flush end-plate configurations. The allowance for 10% variation from the tested values is consistent with the qualification requirements for IMF and SMF given in the AISC *Seismic Provisions*. The variables are defined in Tables 5-2 through 5-7.

Design equations for the six flush end-plate configurations are summarized in Tables 5-2 through 5-7. It is noted that in AISC Design Guide 16 (Murray and Shoemaker, 2002), d is the distance to bolt forces and h the depth of the beam. For consistency with AISC Design Guide 4 (Murray and Sumner, 2004) and the AISC *Seismic Provisions*, these symbols are reversed in the tables.

Table 5-2. Summary of Design Equations for Two-Bolt Flush Unstiffened End Plate

Geometry	Yield-Line Mechanism	Bolt Force Model
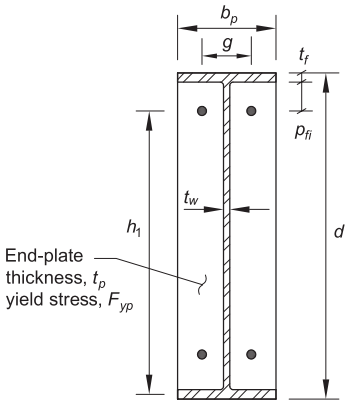	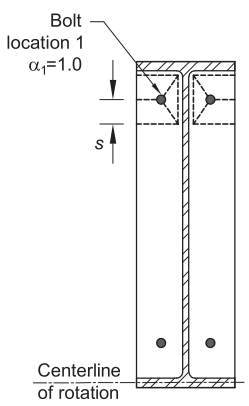	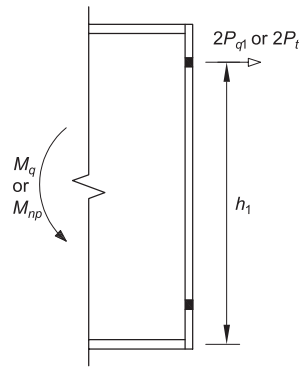

End-Plate Yield	$\phi M_n = \phi_b M_{pl} = \phi_b F_{yp} t_p^2 Y_p$ $Y_p = \frac{b_p}{2}\left[h_1\left(\frac{1}{p_{fi}}+\frac{1}{s}\right)\right]+\frac{2}{g}\left[h_1(p_{fi}+s)\right]$	$\phi_b = 0.90$ $s = \frac{\sqrt{b_p g}}{2}$ Note: Use $p_{fi} = s$ if $p_{fi} > s$
Bolt Rupture with Prying Action	$\phi M_n = \phi_r M_q = \phi \sum_i \alpha_i n_i P_{qi} h_i = \phi_r 2 P_{q1} h_1$ $P_{qi} = \max(P_t - Q_{max,i}, T_b)$	P_t = nominal bolt tensile strength $Q_{max,i}$ = prying force for bolt location i T_b = bolt pretension force n_i = number of bolts in bolt location i ϕ_r = 0.75
Bolt Rupture without Prying Action	$\phi M_n = \phi_r M_{np} = \phi_r P_t \sum_i n_i h_i = \phi_r 2 P_t h_1$	$\phi_r = 0.75$

Table 5-3. Summary of Design Equations for Four-Bolt Flush Unstiffened End Plate

Geometry	Yield-Line Mechanism	Bolt Force Model
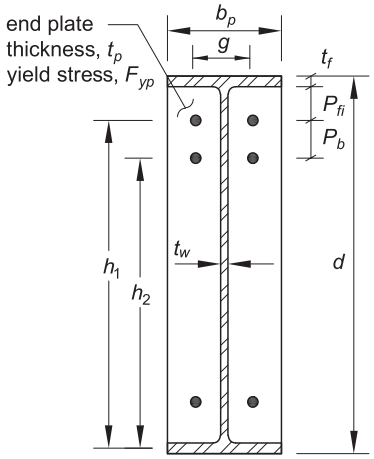	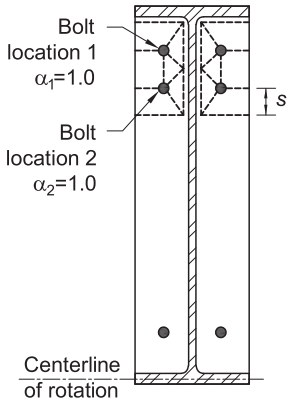	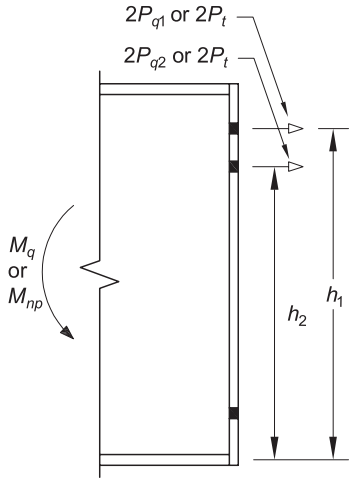

End-Plate Yield	$\phi M_n = \phi_b M_{pl} = \phi_b F_{yp} t_p^2 Y_p$ $Y_p = \frac{b_p}{2}\left[h_1\left(\frac{1}{p_{fi}}\right) + h_2\left(\frac{1}{s}\right)\right]$ $+ \frac{2}{g}\left[h_1\left(p_{fi} + \frac{3p_b}{4}\right) + h_2\left(s + \frac{p_b}{4}\right)\right] + \frac{g}{2}$	$\phi_b = 0.90$ $s = \frac{\sqrt{b_p g}}{2}$ Note: Use $p_{fi} = s$ if $p_{fi} > s$
Bolt Rupture with Prying Action	$\phi M_n = \phi_r M_q = \phi_r \sum_i \alpha_i n_i P_{qi} h_i = \phi_r (2P_{q1}h_1 + 2P_{q2}h_2)$ $P_{qi} = \max(P_t - Q_{max,i}, T_b)$	P_t = nominal bolt tensile strength $Q_{max,i}$ = prying force for bolt location i T_b = bolt pretension force n_i = number of bolts in bolt location i ϕ_r = 0.75
Bolt Rupture without Prying Action	$\phi M_n = \phi_r M_{np} = \phi_r P_t \sum_i n_i h_i = \phi_r P_t (2h_1 + 2h_2)$	$\phi_r = 0.75$

Table 5-4. Summary of Design Equations for Four-Bolt Flush Stiffened Stiffener between the Tension Bolt Rows

Geometry	Yield-Line Mechanism	Bolt Force Model
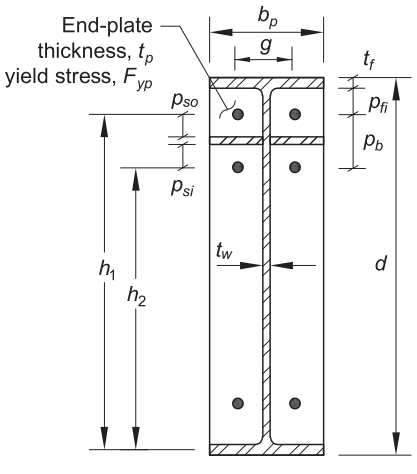	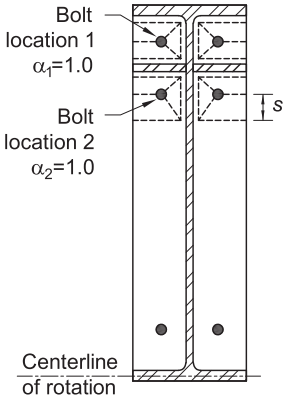	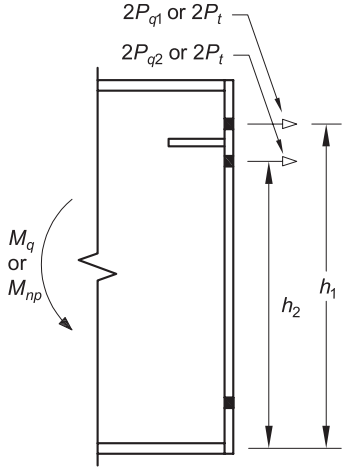

End-Plate Yield	$\phi M_n = \phi_b M_{pl} = \phi_b F_{yp} t_p^2 Y_p$ $Y_p = \frac{b_p}{2}\left[h_1\left(\frac{1}{p_{fi}}+\frac{1}{p_{so}}\right)+h_2\left(\frac{1}{s}+\frac{1}{p_{si}}\right)\right]$ $+\frac{2}{g}\left[h_1(p_{fi}+p_{so})+h_2(s+p_{si})\right]$	$\phi_b = 0.90$ $s = \frac{\sqrt{b_p g}}{2}$ Note: Use $p_{fi} = s$ if $p_{fi} > s$ Use $p_{so} = s$ if $p_{so} > s$ Use $p_{si} = s$ if $p_{si} > s$
Bolt Rupture with Prying Action	$\phi M_n = \phi_r M_q = \phi_r \sum_i \alpha_i n_i P_{qi} h_i = \phi_r (2P_{q1}h_1 + 2P_{q2}h_2)$ $P_{qi} = \max(P_t - Q_{max,i}, T_b)$	P_t = nominal bolt tensile strength $Q_{max,i}$ = prying force for bolt location i T_b = bolt pretension force n_i = number of bolts in bolt location i ϕ_r = 0.75
Bolt Rupture without Prying Action	$\phi M_n = \phi_r M_{np} = \phi_r P_t \sum_i n_i h_i = \phi_r P_t (2h_1 + 2h_2)$	$\phi_r = 0.75$

Table 5-5. Summary of Design Equations for Four-Bolt Flush Stiffened Stiffener below the Tension Bolt Rows

Geometry	Yield-Line Mechanism	Bolt Force Model
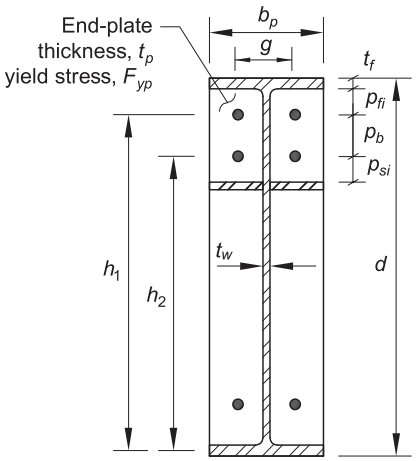	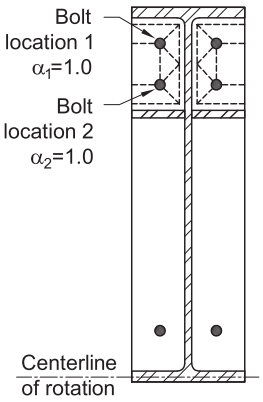	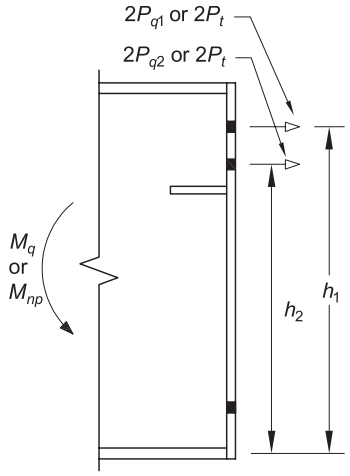

End-Plate Yield	$\phi M_n = \phi_b M_{pl} = \phi_b F_{yp} t_p^2 Y_p$ $Y_p = \frac{b_p}{2}\left[h_1\left(\frac{1}{p_{fi}}\right) + h_2\left(\frac{1}{p_{si}}\right)\right]$ $+ \frac{2}{g}\left[h_1\left(p_{fi} + \frac{3p_b}{4}\right) + h_2\left(p_{si} + \frac{p_b}{4}\right)\right] + \frac{g}{2}$	$\phi_b = 0.90$ $s = \frac{\sqrt{b_p g}}{2}$ Note: Use $p_{fi} = s$ if $p_{fi} > s$ Use $p_{si} = s$ if $p_{si} > s$
Bolt Rupture with Prying Action	$\phi M_n = \phi_r M_q = \phi_r \sum_i \alpha_i n_i P_{qi} h_i = \phi_r (2P_{q1}h_1 + 2P_{q2}h_2)$ $P_{qi} = \max(P_t - Q_{max,i}, T_b)$	P_t = nominal bolt tensile strength $Q_{max,i}$ = prying force for bolt location i T_b = bolt pretension force n_i = number of bolts in bolt location i ϕ_r = 0.75
Bolt Rupture without Prying Action	$\phi M_n = \phi_r M_{np} = \phi_r P_t \sum_i n_i h_i = \phi_r P_t (2h_1 + 2h_2)$	$\phi_r = 0.75$

Table 5-6. Summary of Design Equations for Six-Bolt Flush Unstiffened End Plate

Geometry	Yield-Line Mechanism	Bolt Force Model
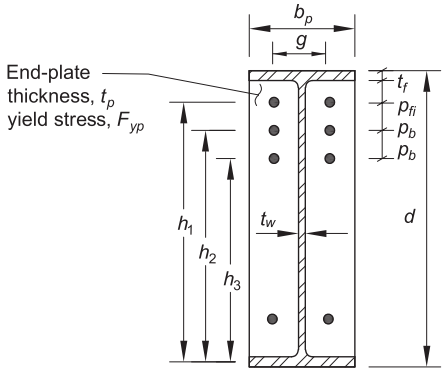	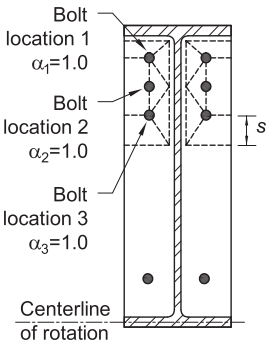	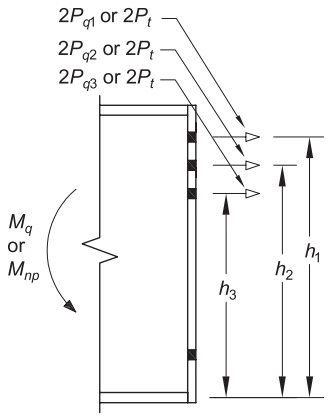

End-Plate Yield	$\phi M_n = \phi_b M_{pl} = \phi_b F_{yp} t_p^2 Y_p$ $Y_p = \frac{b_p}{2}\left[h_1\left(\frac{1}{p_{fi}}\right) + h_3\left(\frac{1}{s}\right)\right]$ $+ \frac{2}{g}\left[h_1\left(p_{fi} + \frac{3p_b}{2}\right) + h_3\left(s + \frac{p_b}{2}\right)\right] + \frac{g}{2}$	$\phi_b = 0.90$ $s = \frac{\sqrt{b_p g}}{2}$ Note: Use $p_{fi} = s$ if $p_{fi} > s$
Bolt Rupture with Prying Action	$\phi M_n = \phi_r M_q = \phi_r \sum_i \alpha_i n_i P_{qi} h_i = \phi_r (2P_{q1}h_1 + 2P_{q2}h_2 + 2P_{q3}h_3)$ $P_{qi} = \max(P_t - Q_{max,i}, T_b)$	P_t = nominal bolt tensile strength $Q_{max,i}$ = prying force for bolt location i T_b = bolt pretension force n_i = number of bolts in bolt location i ϕ_r = 0.75
Bolt Rupture without Prying Action	$\phi M_n = \phi_r M_{np} = \phi_r P_t \sum_i n_i h_i = \phi_r P_t (2h_1 + 2h_2 + 2h_3)$	$\phi_r = 0.75$

Table 5-7. Summary of Design Equations for Six-Bolt Flush Four-Wide/Two-Wide Unstiffened End Plate

Geometry	Yield-Line Mechanism	Bolt Force Model
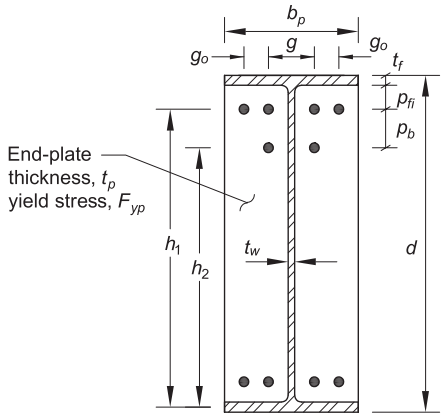	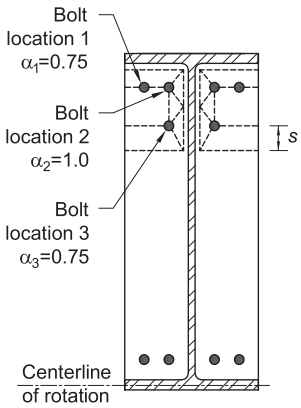	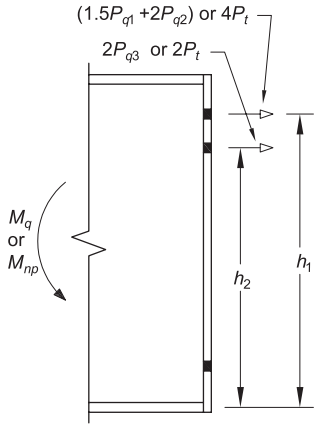

End-Plate Yield	$\phi M_n = \phi_b M_{pl} = \phi_b F_{yp} t_p^2 Y_p$ $Y_p = \frac{b_p}{2}\left[h_1\left(\frac{1}{p_{fi}}\right) + h_2\left(\frac{1}{s}\right)\right]$ $+ \frac{2}{g}\left[h_1\left(p_{fi} + \frac{3p_b}{4}\right) + h_2\left(s + \frac{p_b}{4}\right)\right] + \frac{g}{2}$	$\phi_b = 0.90$ $s = \frac{\sqrt{b_p g}}{2}$ Note: Use $p_{fi} = s$ if $p_{fi} > s$
Bolt Rupture with Prying Action	$\phi M_n = \phi_r M_q = \phi_r \sum_i \alpha_i n_i P_{qi} h_i = \phi_r \left(1.5P_{q1}h_1 + 2P_{q2}h_1 + 1.5P_{q3}h_2\right)$ $P_{qi} = \max\left(P_t - Q_{max,i}, T_b\right)$	P_t = nominal bolt tensile strength $Q_{max,i}$ = prying force for bolt location i T_b = bolt pretension force n_i = number of bolts in bolt location i ϕ_r = 0.75
Bolt Rupture without Prying Action	$\phi M_n = \phi_r M_{np} = \phi_r P_t \sum_i n_i h_i = \phi_r P_t (4h_1 + 2h_2)$	$\phi_r = 0.75$

Table 5-8. Flush Thick End-Plate Analysis Examples						
Example	**End-Plate Configuration**	**Beam**	**Column**	**Bolts**	**Weld Calculations**	**Column-Side Limit States**
5.2-1	Two-bolt flush unstiffened thick end plate	W18×35	W12×35	Grade A325 ¾ in. snug-tightened	Yes	Yes
5.2-2	Four-bolt flush unstiffened thick end plate	W18×35	—	Grade A325 ¾ in. snug-tightened	Yes	No
5.2-3	Four-bolt flush stiffened with web stiffener plates between the tension bolts thick end plate	Built-up[1] 6" × 20"	—	Grade A325 ⅞ in. snug-tightened	Yes	No
5.2-4	Four-bolt flush stiffened with web stiffeners below the tension bolts thick end plate	Built-up[1] 6" × 20"	—	Grade A325 ⅞ in. snug-tightened	Yes	No
5.2-5	Six-bolt flush unstiffened thick end plate	Built-up[1] 10" × 36"	—	Grade A490 1 in. pretensioned	Yes	No
5.2-6	Six-bolt flush four-wide/two-wide unstiffened thick end plate	Built-up[1] 12" × 48"	—	Grade A490 1 in. pretensioned	Yes	No

[1] Flange width, in. × beam depth, in.

5.2.2 Flush Thick End-Plate Analysis Examples

This section has thick end-plate/smaller bolt analysis examples for the six flush end-plate configurations shown in Figure 1-3. Table 5-8 summarizes the relevant parameters for each example. Appendix B has thin end-plate/larger bolt diameter examples for the same configurations. Calculations are shown for both LRFD and ASD designs.

EXAMPLE 5.2-1—Two-Bolt Flush Unstiffened Thick End-Plate Example

Given:

The connection shown in Figure 5-2 is a two-bolt flush unstiffened end-plate connection for a W18×35 beam to the top of a W12×35 column. The beam and column are ASTM A992/A992M (ASTM, 2020) steel, and the plate steel is ASTM A572/A572M Grade 50 (ASTM, 2021). Bolts are Group 120 ASTM F3125/F3125M Grade A325, snug-tightened. Weld electrodes are E70XX. Note that the end-plate width is greater than the beam flange width. The connection is to be evaluated as a thick end-plate design for the following required moments and forces.

	LRFD	ASD
Moment	$M_u = 800$ kip-in.	$M_a = 533$ kip-in.
Axial tension	$T_u = 3.30$ kips	$T_a = 2.20$ kips
Shear force	$V_u = 25.8$ kips	$V_a = 17.2$ kips

Solution:

From AISC *Manual* Table 2-4, the material properties are as follows:

ASTM A992/A992M
F_y = 50 ksi
F_u = 65 ksi

ASTM A572/A572M Grade 50
F_y = 50 ksi
F_u = 65 ksi

From AISC *Specification* Table J3.2, the material properties of the bolts are as follows:

Group 120 ASTM F3125/F3125M ¾-in.-diameter Grade A325 snug-tightened
F_{nt} = 90 ksi
F_{nv} = 54 ksi (Group 120 bolts with threads not excluded from the shear plane; thread condition N)

From AISC *Manual* Table 1-1, the geometric properties are as follows:

Beam: W18×35
d = 17.7 in. t_{bw} = 0.300 in.
b_{bf} = 6.00 in. t_{bf} = 0.425 in. k_1 = ¾ in.

Column: W12×35
d_c = 12.5 in. t_{cw} = 0.300 in.
b_{cf} = 6.56 in. t_{cf} = 0.520 in.
k_{des} = 0.820 in. k_1 = ¾ in.

End-plate geometric properties:
b_p = 7 in.
t_p = 9/16 in.
g = 3½ in.
p_{fi} = 1½ in.
d_p = 18¾ in.

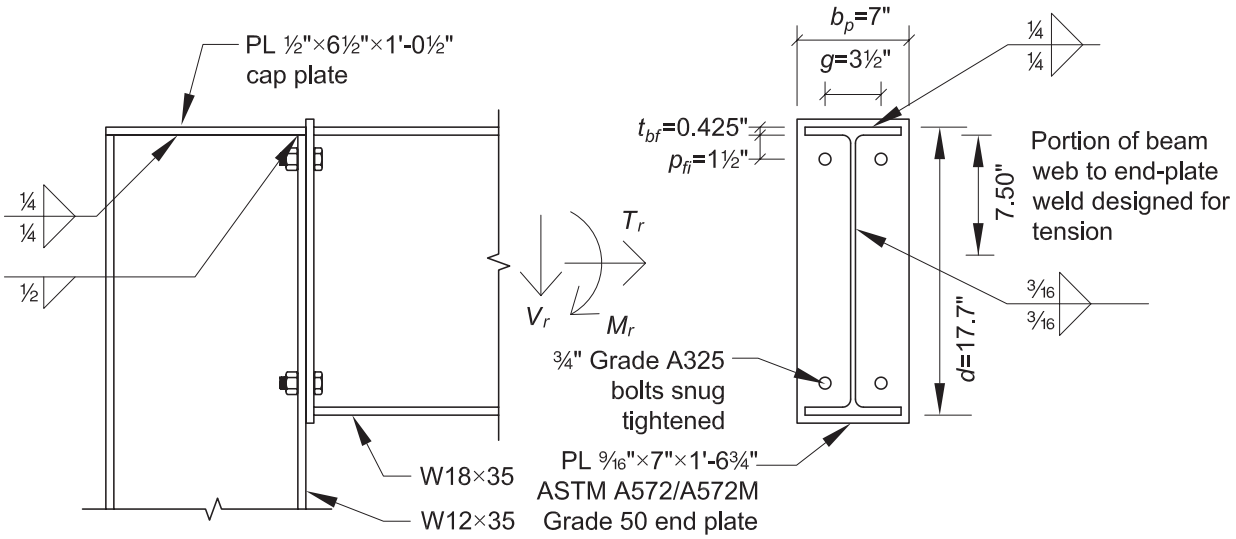

Fig. 5-2. Two-bolt unstiffened thick end-plate configuration for Example 5.2-1.

The distance from the centerline of the compression flange to the bolt line, h_1, is depicted in Table 5-2 and computed as:

$$h_1 = d - \frac{3}{2}t_{bf} - p_{fi}$$
$$= 17.7 \text{ in.} - \frac{3(0.425 \text{ in.})}{2} - 1\text{½ in.}$$
$$= 15.6 \text{ in.}$$

$$b_{p,eff} \le b_{bf} + \max(t_p, 1 \text{ in.}) \quad (4\text{-}3)$$
$$\le 6.00 \text{ in.} + \max(\text{9⁄16 in.}, 1 \text{ in.})$$
$$\le 7.00 \text{ in.}$$

$b_p = 7 \text{ in.} \le 7.00 \text{ in.}$ **o.k.**

$$b_{bf} \ge g \quad (4\text{-}1)$$
$6.00 \text{ in.} \ge 3\text{½ in.}$ **o.k.**

A. End-Plate and Bolt Design Verification

Calculate the equivalent required moment considering the effect of the required tension force using Equation 3-30.

LRFD	ASD
$M_{u,eq} = M_u + (T_u/2)(d - t_{bf})$ $= 800 \text{ kip-in.} + (3.30 \text{ kips}/2)(17.7 \text{ in.} - 0.425 \text{ in.})$ $= 829 \text{ kip-in.}$	$M_{a,eq} = M_a + (T_a/2)(d - t_{bf})$ $= 533 \text{ kip-in.} + (2.20 \text{ kips}/2)(17.7 \text{in.} - 0.425 \text{in.})$ $= 552 \text{ kip-in.}$

Determine if the specified ¾-in.-diameter Grade A325 snug-tightened bolts and 9⁄16 in. end-plate thickness are sufficient using the thick end-plate/smaller bolt diameter procedure.

Solve for the required bolt diameter using Equations 5-3. For Grade A325 bolts, the nominal tensile stress is $F_{nt} = 90$ ksi.

LRFD	ASD
$d_{b,reqd} = \sqrt{\frac{4M_{u,eq}}{\pi\phi F_{nt}\left(\sum_i n_i h_i\right)}}$ $= \sqrt{\frac{4(829 \text{ kip-in.})}{\pi(0.75)(90 \text{ ksi})(2)(15.6 \text{ in.})}}$ $= 0.708 \text{ in.} \le$ ¾ in. **o.k.**	$d_{b,reqd} = \sqrt{\frac{4M_{a,eq}}{\frac{\pi F_{nt}}{\Omega}\left(\sum_i n_i h_i\right)}}$ $= \sqrt{\frac{4(552 \text{ kip-in.})}{\frac{\pi(90 \text{ ksi})}{2.00}(2)(15.6 \text{ in.})}}$ $= 0.708 \text{ in.} \le$ ¾ in. **o.k.**

Solve for the required end-plate thickness using Equations 5-4. First solve for the distance, s, and yield line parameter, Y_p, using Table 5-2.

$$s = \frac{\sqrt{b_p g}}{2}$$
$$= \frac{\sqrt{(7 \text{ in.})(3\text{½ in.})}}{2}$$
$$= 2.47 \text{ in.}$$

Because $s \geq p_{fi} = 1\frac{1}{2}$ in., the dimension p_{fi} is used in the equation for the yield line parameter.

$$Y_p = \frac{b_p}{2}\left[h_1\left(\frac{1}{p_{fi}}+\frac{1}{s}\right)\right]+\frac{2}{g}\left[h_1(p_{fi}+s)\right]$$

$$=\left(\frac{7\text{ in.}}{2}\right)\left[(15.6\text{ in.})\left(\frac{1}{1\frac{1}{2}\text{ in.}}+\frac{1}{2.47\text{ in.}}\right)\right]+\left(\frac{2}{3\frac{1}{2}\text{ in.}}\right)\left[(15.6\text{ in.})(1\frac{1}{2}\text{ in.}+2.47\text{ in.})\right]$$

$$= 93.9\text{ in.}$$

Determine the required end-plate thickness using Equations 5-4. For flush end-plate configurations, $\gamma_r = 0.80$.

LRFD	ASD
$t_{p,reqd} = \sqrt{\frac{1.10M_{u.eq}}{\gamma_r\phi_b F_y Y_p}}$	$t_{p,reqd} = \sqrt{\frac{1.10M_{a.eq}}{\gamma_r F_y Y_p/\Omega_b}}$
$= \sqrt{\frac{1.10(829\text{ kip-in.})}{0.80(0.90)(50\text{ ksi})(93.9\text{ in.})}}$	$= \sqrt{\frac{1.10(552\text{ kip-in.})}{0.80(50\text{ ksi})(93.9\text{ in.})/1.67}}$
$= 0.519\text{ in.} \leq \frac{9}{16}\text{ in.}$ **o.k.**	$= 0.520\text{ in.} \leq \frac{9}{16}\text{ in.}$ **o.k.**

Check Shear Transfer at the Bottom Holes

Shear at the faying surface, V_u, is assumed to be resisted only by the two compression side bolts. The shear transfer strength at each bolt hole is the minimum of the end-plate bearing/tearout strength, the bolt shear rupture strength, and the column flange bearing/tearout strength. See the User Note in AISC *Specification* Section J3.7.

The nominal unthreaded body area of a ¾ in. bolt is $A_b = 0.442\text{ in.}^2$ The nominal shear strength of a ¾-in.-diameter Grade A325 bolt is:

$$R_{n,bt} = F_{nv}A_b \qquad \text{(from } \textit{Spec.} \text{ Eq. J3-1)}$$

$$= (54\text{ ksi})0.442\text{ in.}^2$$

$$= 23.9\text{ kips}$$

The nominal bearing/tearout strength is given by AISC *Specification* Section J3.11. The bolt shear force acting on the end plate is up toward the middle of the end plate, and therefore, tearout will not control. The bolt shear force acting on the column flange is down, and again, tearout will not control. The end plate is 9/16 in. thick and the column flange is 0.520 in. thick; therefore, the column flange will control the bearing/tearout strength at the bottom bolt holes. The bearing strength at a bolt hole is:

$$R_{n,brg} = 2.4d_b t_{cf} F_u \qquad \text{(from } \textit{Spec.} \text{ Eq. J3-6a)}$$

$$= 2.4(\tfrac{3}{4}\text{ in.})(0.520\text{ in.})(65\text{ ksi})$$

$$= 60.8\text{ kips}$$

The shear transfer strength at each bolt hole is then the minimum of the column flange bearing strength and the bolt shear rupture strength, hence $R_n = 23.9$ kips.

Therefore, the nominal shear transfer strength at the two bottom bolt holes is:

$$V_n = (2\text{ bolts})R_n$$

$$= (2\text{ bolts})23.9\text{ kips}$$

$$= 47.8\text{ kips}$$

LRFD	ASD
$\phi V_n = 0.75(47.8 \text{ kips})$ $= 35.9 \text{ kips} \quad \geq \quad V_u = 25.8 \text{ kips}$ **o.k.**	$\frac{V_n}{\Omega} = \frac{47.8 \text{ kips}}{2.00}$ $= 23.9 \text{ kips} \quad \geq \quad V_a = 17.2 \text{ kips}$ **o.k.**

The specified ASTM A572/A572M Grade 50 9⁄16 in. end plate and ¾-in.-diameter Grade A325 snug-tightened bolts are sufficient.

B. Check Beam to End-Plate Welds

The minimum weld size in AISC *Specification* Table J2.4 is determined from the material thickness of the thinner part joined. The weld sizes shown in Figure 5-2 satisfy the requirements in Table J2.4.

Check Beam Flange to End-Plate Weld

The weld from the beam flange to the end plate is shown in Figure 5-2 as a double-sided ¼ in. fillet weld. Determine if this weld is adequate. First, find the required tensile force as the maximum of either the calculated flange tensile force or 60% of the flange tensile strength for LRFD and 40% of the flange tensile strength for ASD (Equations 3-38), but not greater than the yield strength of the tension flange.

LRFD	ASD
$T_{u,calc} = \frac{M_u}{d - t_{bf}} + \frac{T_u}{2}$ $= \frac{800 \text{ kip-in.}}{17.7 \text{ in.} - 0.425 \text{ in.}} + \frac{3.30 \text{ kips}}{2}$ $= 48.0 \text{ kips}$ $T_{yf} = F_y b_{bf} t_{bf}$ $= (50 \text{ ksi})(6.00 \text{ in.})(0.425 \text{ in.})$ $= 128 \text{ kips}$ $T_{u,min} = 0.60 F_y b_{bf} t_{bf}$ $= 0.60(50 \text{ ksi})(6.00 \text{ in.})(0.425 \text{ in.})$ $= 76.5 \text{ kips}$ $T_{uf} = \max(T_{u,calc}, T_{u,min})$ $= 76.5 \text{ kips} \leq T_{yf} = 128 \text{ kips}$	$T_{a,calc} = \frac{M_a}{d - t_{bf}} + \frac{T_a}{2}$ $= \frac{533 \text{ kip-in.}}{17.7 \text{ in.} - 0.425 \text{ in.}} + \frac{2.20 \text{ kips}}{2}$ $= 32.0 \text{ kips}$ $\frac{T_{yf}}{1.50} = \frac{F_y}{1.50} b_{bf} t_{bf}$ $= \frac{50 \text{ ksi}}{1.50}(6.00 \text{ in.})(0.425 \text{ in.})$ $= 85.0 \text{ kips}$ $T_{a,min} = 0.40 F_y b_{bf} t_{bf}$ $= 0.40(50 \text{ ksi})(6.00 \text{ in.})(0.425 \text{ in.})$ $= 51.0 \text{ kips}$ $T_{af} = \max(T_{a,calc}, T_{a,min})$ $= 51.0 \text{ kips} \quad \leq \quad \frac{T_{yf}}{1.50} = 85.0 \text{ kips}$

Calculate the strength of the double-sided ¼ in. fillet weld. Because the weld is loaded perpendicular to its longitudinal axis, the angle of loading, θ, is 90°. The length of the weld is two times the width of the beam flange, b_{bf}, minus two times the beam k_1 distance.

$$l_w = 2b_{bf} - 2k_1$$
$$= 2(6.00 \text{ in.}) - 2(¾ \text{ in.})$$
$$= 10.5 \text{ in.}$$

$$R_n = 0.60F_{EXX}\frac{t_{weld}}{\sqrt{2}}l_w(1.0+0.5\sin^{1.5}\theta) \quad \text{(from } \textit{Spec.} \text{ Eq. J2-4)}$$
$$= 0.60(70\text{ ksi})\left(\frac{\frac{1}{4}\text{ in.}}{\sqrt{2}}\right)(10.5\text{ in.})(1.0+0.5\sin^{1.5}90°)$$
$$= 117\text{ kips}$$

Compare the weld strength to the required tensile strength.

LRFD	ASD
$\phi R_n = 0.75(117\text{ kips})$ $= 87.8\text{ kips} \quad \geq \quad T_{uf} = 76.5\text{ kips}$ **o.k.**	$\frac{R_n}{\Omega} = \frac{117\text{ kips}}{2.00}$ $= 58.5\text{ kips} \quad \geq \quad T_{af} = 51.0\text{ kips}$ **o.k.**

The flange to end-plate weld consisting of a double-sided ¼ in. fillet weld is adequate. (A CJP or PJP groove weld are alternate options.)

Check Beam Web to End-Plate Weld

The beam web to end-plate weld is shown in Figure 5-2 as a double-sided 3⁄16 in. fillet weld over the full height of the web. However, the weld is separately checked for (1) tension rupture in the region around the tension bolts (extending 6 in. to the inside of the tension bolts), and (2) the remainder of the web to end-plate weld is checked for shear.

As explained in Section 3.7.5, the demand for the tension web area, T_{uw} (LRFD) or T_{aw} (ASD), for this connection is the number of tension bolts adjacent to the web, n_{trib}, divided by the total number of tension bolts, n, multiplied by the calculated beam flange force, $T_{u,calc}$ (LRFD) or $T_{a,calc}$ (ASD), from the beam flange to end-plate weld demand calculations. Using Equation 3-40:

LRFD	ASD
$T_{uw} = (n_{trib}/n)T_{u,calc}$ $= (2/2)(48.0\text{ kips})$ $= 48.0\text{ kips}$	$T_{aw} = (n_{trib}/n)T_{a,calc}$ $= (2/2)(32.0\text{ kips})$ $= 32.0\text{ kips}$

The length of the web tension region is measured from the inside of the beam flange to 6 in. inside the tension bolt row:

$l_{wt} = p_{fi} + 6\text{ in.}$
$= 1½\text{ in.} + 6\text{ in.}$
$= 7.50\text{ in.}$

The nominal web yield strength in the tension region is:

$$T_{yw} = F_yA_g \quad \text{(from } \textit{Spec.} \text{ Eq. J4-1)}$$
$$= F_yt_{bw}l_{wt}$$
$$= (50\text{ ksi})(0.300\text{ in.})(7.50\text{ in.})$$
$$= 113\text{ kips}$$

Check that the web design tensile yield strength of the web is sufficient.

LRFD	ASD
$\phi T_{yw} = 0.90(113 \text{ kips})$ $= 102 \text{ kips} \quad \geq \quad T_{uw} = 48.0 \text{ kips}$ **o.k.**	$\frac{T_{yw}}{\Omega} = \frac{113 \text{ kips}}{1.67}$ $= 67.7 \text{ kips} \quad \geq \quad T_{aw} = 32.0 \text{ kips}$ **o.k.**

Check that the required strength is at least 60% (LRFD) or 40% (ASD) of the web tensile strength from Equations 3-41.

LRFD	ASD
$0.60T_{yw} = 0.60(113 \text{ kips})$ $= 67.8 \text{ kips}$ $T_{uwd} = \max(T_{uw},\ 0.60T_{yw})$ $= \max(48.0 \text{ kips}, 67.8 \text{ kips})$ $= 67.8 \text{ kips}$	$0.40T_{yw} = 0.40(113 \text{ kips})$ $= 45.2 \text{ kips}$ $T_{awd} = \max(T_{aw}, 0.40T_{yw})$ $= \max(32.0 \text{ kips}, 45.2 \text{ kips})$ $= 45.2 \text{ kips}$

Check the web to end-plate weld around the tension bolts. Because the weld is loaded perpendicular to its longitudinal axis, the angle of loading, θ, is 90°.

$$R_n = (2 \text{ welds})0.60F_{EXX}\frac{t_{weld}}{\sqrt{2}}l_{wt}(1.0 + 0.5\sin^{1.5}\theta) \qquad \text{(from } \textit{Spec.} \text{ Eq. J2-4)}$$

$$= (2 \text{ welds})(0.60)(70 \text{ ksi})\left(\frac{3/16 \text{ in.}}{\sqrt{2}}\right)(7.50 \text{ in.})(1.0 + 0.5\sin^{1.5}90°)$$

$$= 125 \text{ kips}$$

LRFD	ASD
$\phi R_n = 0.75(125 \text{ kips})$ $= 93.8 \text{ kips} \quad \geq \quad T_{uwd} = 67.8 \text{ kips}$ **o.k.**	$\frac{R_n}{\Omega} = \frac{125 \text{ kips}}{2.00}$ $= 62.5 \text{ kips} \quad \geq \quad T_{awd} = 45.2 \text{ kips}$ **o.k.**

Check the web to end-plate weld away from the tension bolts. Only the web to end-plate weld between the mid-depth of the beam and the inside face of the beam compression flange or the weld between the end of the assumed web tension length and the inside face of the bottom beam compression flange, whichever is smaller, is considered effective in resisting the beam end shear. The shear strength of this weld is compared to the required shear applied to the connection.

$$l_t = d - 2t_{bf} - l_{wt}$$
$$= 17.7 \text{ in.} - 2(0.425 \text{ in.}) - 7.50 \text{ in.}$$
$$= 9.35 \text{ in.}$$

$$l_{0.5w} = d/2 - t_{bf}$$
$$= (17.7 \text{ in.})/2 - 0.425 \text{ in.}$$
$$= 8.43 \text{ in.}$$

$$l_{wv} = \min(l_t,\ l_{0.5w})$$
$$= \min(9.35 \text{ in.}, 8.43 \text{ in.})$$
$$= 8.43 \text{ in.}$$

$$R_n = (2\text{ welds})0.60F_{EXX}\frac{t_{weld}}{\sqrt{2}}l_{wv}\left(1.0+0.5\sin^{1.5}\theta\right) \quad \text{(from } \textit{Spec.} \text{ Eq. J2-4)}$$

$$= (2\text{ welds})(0.60)(70\text{ ksi})\left(\frac{3/16\text{ in.}}{\sqrt{2}}\right)(8.43\text{ in.})(1.0+0.5\sin^{1.5}0°)$$

$$= 93.9\text{ kips}$$

LRFD	ASD
$\phi R_n = 0.75(93.9\text{ kips})$ $= 70.4\text{ kips} \geq V_u = 25.8\text{ kips}$ **o.k.**	$\frac{R_n}{\Omega} = \frac{93.9\text{ kips}}{2.00}$ $= 47.0\text{ kips} \geq V_a = 17.2\text{ kips}$ **o.k.**

Check that the shear rupture strength of the beam web at the weld using AISC *Specification* Equation J4-4 is sufficient.

$$R_n = 0.60F_uA_{nv} \quad \text{(}\textit{Spec.}\text{ Eq. J4-4)}$$

$$= 0.60F_ul_{wv}t_{bw}$$

$$= 0.60(65\text{ ksi})(8.43\text{ in.})(0.300\text{ in.})$$

$$= 98.6\text{ kips}$$

LRFD	ASD
$\phi R_n = 0.75(98.6\text{ kips})$ $= 74.0\text{ kips} \geq V_u = 25.8\text{ kips}$ **o.k.**	$\frac{R_n}{\Omega} = \frac{98.6\text{ kips}}{2.00}$ $= 49.3\text{ kips} \geq V_a = 17.2\text{ kips}$ **o.k.**

The double-sided 3/16 in. fillet welds from the web to the end plate are sufficient.

C. Check Column-Side Limit States

The cap plate size, ½ in. by 6½ in., is larger than the beam flange, 0.425 in. by 6.00 in., and therefore is sufficient by inspection.

Check Column Flange to Cap Plate Weld

The weld at the column cap plate to flange is shown in Figure 5-2 as a single-sided ½ in. fillet weld. The required tensile force is the same as it is for the beam flange to end-plate force, found in Part B to be 76.5 kips (LRFD) or 51.0 kips (ASD).

Calculate the strength of the fillet weld. Because the weld is loaded perpendicular to its longitudinal axis, the angle of loading, θ, is 90°. The length of the weld is the width of cap plate, b_{cp}, minus two times the column web fillet dimension, k_1.

$$l_w = b_{cp} - 2k_1$$

$$= 6½\text{ in.} - 2(¾\text{ in.})$$

$$= 5.00\text{ in.}$$

$$R_n = 0.60F_{EXX}\frac{t_{weld}}{\sqrt{2}}l_w(1.0+0.5\sin^{1.5}\theta) \quad \text{(from } \textit{Spec.} \text{ Eq. J2-4)}$$

$$= 0.60(70\text{ ksi})\left(\frac{½\text{ in.}}{\sqrt{2}}\right)(5.00\text{ in.})(1.0+0.5\sin^{1.5}90°)$$

$$= 111\text{ kips}$$

Compare the weld strength to the required tensile strength.

LRFD	ASD
$\phi R_n = 0.75(111 \text{ kips})$ $= 83.3 \text{ kips} \quad \geq \quad T_u = 76.5 \text{ kips}$ **o.k.**	$\frac{R_n}{\Omega} = \frac{111 \text{ kips}}{2.00}$ $= 55.5 \text{ kips} \quad \geq \quad T_a = 51.0 \text{ kips}$ **o.k.**

The cap plate to column flange weld consisting of a single-sided ½ in. fillet weld is adequate.

Check Cap Plate to Column Web Weld

The cap plate to column web weld required strength is conservatively taken as that for the column flange to cap plate weld, 76.5 kips (LRFD) or 51.0 kips (ASD). The nominal weld rupture strength for the double-sided ¼ in. fillet weld shown in Figure 5-2 is:

$$l_w = 2(d_c - 2t_{cf})$$
$$= 2\left[12.5 \text{ in.} - 2(0.520 \text{ in.})\right]$$
$$= 22.9 \text{ in.}$$

$$R_n = 0.60F_{EXX}\frac{t_{weld}}{\sqrt{2}}l_w(1.0 + 0.5\sin^{1.5}\theta) \qquad \text{(from } \textit{Spec.} \text{ Eq. J2-4)}$$
$$= 0.60(70 \text{ ksi})\left(\frac{¼ \text{ in.}}{\sqrt{2}}\right)(22.9 \text{ in.})(1.0 + 0.5\sin^{1.5} 0°)$$
$$= 170 \text{ kips}$$

LRFD	ASD
$\phi R_n = 0.75(170 \text{ kips})$ $= 128 \text{ kips} \quad \geq \quad T_u = 76.5 \text{ kips}$ **o.k.**	$\frac{R_n}{\Omega} = \frac{170 \text{ kips}}{2.00}$ $= 85.0 \text{ kips} \quad \geq \quad T_a = 51.0 \text{ kips}$ **o.k.**

Check that the shear rupture strength of the column web at the weld using AISC *Specification* Equation J4-4 is sufficient.

$$R_n = 0.60F_uA_{nv} \qquad \text{(Spec. Eq. J4-4)}$$
$$= 0.60F_u(d_c - 2t_{cf})t_{cw}$$
$$= 0.60(65 \text{ ksi})\left[12.5 \text{ in.} - 2(0.520 \text{ in.})\right](0.300 \text{ in.})$$
$$= 134 \text{ kips}$$

LRFD	ASD
$\phi R_n = 0.75(134 \text{ kips})$ $= 101 \text{ kips} \quad \geq \quad V_u = 76.5 \text{ kips}$ **o.k.**	$\frac{R_n}{\Omega} = \frac{134 \text{ kips}}{2.00}$ $= 67.0 \text{ kips} \quad \geq \quad V_a = 51.0 \text{ kips}$ **o.k.**

The cap plate to column web weld consisting of a double-sided ¼ in. fillet weld is sufficient.

Check Column Flange Flexural Strength

Check the column flange for flexural yielding. The column flange yield line parameter, Y_{cu}, is taken from Appendix A, Table A-1, Figure A-1(d). The resulting design moment strength is compared to $1.10M_{u,eq}$ or $1.10M_{a,eq}$ to prevent prying action on the bolts.

$$p_{cp} = t_{bf} + p_{fi} - t_{cap}$$
$$= 0.425 \text{ in.} + 1\text{½ in.} - \text{½ in.}$$
$$= 1.43 \text{ in.}$$

$$s = \frac{\sqrt{b_{cf} g}}{2}$$
$$= \frac{\sqrt{(6.56 \text{ in.})(3\text{½ in.})}}{2}$$
$$= 2.40 \text{ in.}$$

$$Y_c = \frac{b_{cf}}{2}\left[h_1\left(\frac{1}{p_{cp}} + \frac{1}{s}\right)\right] + \frac{2}{g}\left[h_1(p_{cp} + s)\right]$$
$$= \left(\frac{6.56 \text{ in.}}{2}\right)\left[(15.6 \text{ in.})\left(\frac{1}{1.43 \text{ in.}} + \frac{1}{2.40 \text{ in.}}\right)\right] + \left(\frac{2}{3\text{½ in.}}\right)\left[(15.6 \text{ in.})(1.43 \text{ in.} + 2.40 \text{ in.})\right]$$
$$= 91.2 \text{ in.}$$

$$M_{cf} = F_y t_{cf}^2 Y_c \quad (3\text{-}43)$$
$$= (50 \text{ ksi})(0.520 \text{ in.})^2 (91.2 \text{ in.})$$
$$= 1{,}230 \text{ kip-in.}$$

LRFD	ASD
$\phi M_{cf} = 0.90(1{,}230 \text{ kip-in.})$ $= 1{,}110 \text{ kip-in.} \quad \geq \quad 1.10M_{u,eq} = 912 \text{ kip-in.}$ **o.k.**	$\frac{M_{cf}}{\Omega} = \frac{1{,}230 \text{ kip-in.}}{1.67}$ $= 737 \text{ kip-in.} \quad \geq \quad 1.10M_{a,eq} = 607 \text{ kip-in.}$ **o.k.**

The column flange flexural strength is sufficient to resist flexural yielding.

Check for Column Web Stiffeners Opposite the Beam Bottom Flange

Check web yielding and web crippling to determine if stiffeners are required for the column web opposite the beam bottom flange. The concentrated force delivered by the beam bottom flange to the column, conservatively neglecting the small tension force, is:

LRFD	ASD
$P_u = \frac{M_u}{d - t_{bf}}$ $= \frac{800 \text{ kip-in.}}{17.7 \text{ in.} - 0.425 \text{ in.}}$ $= 46.3 \text{ kips}$	$P_a = \frac{M_a}{d - t_{bf}}$ $= \frac{533 \text{ kip-in.}}{17.7 \text{ in.} - 0.425 \text{ in.}}$ $= 30.9 \text{ kips}$

Calculate the nominal column web local yielding strength opposite the bottom flange of the beam. Equations from Section 3.7.6 are used. The parameter C_t is 1.0 because the distance from the bottom of the beam to the top of the column is greater than the depth of the column. The bearing length, l_b, is calculated as follows, where ¼ in. is the distance from the outside of the beam flange fillet weld to the bottom edge of the end plate.

$$l_b = t_{bf} + 2t_{weld} + t_p + ¼ \text{ in.} \qquad \text{(from Eq. 3-47)}$$
$$= 0.425 \text{ in.} + 2(¼ \text{ in.}) + 9/16 \text{ in.} + ¼ \text{ in.}$$
$$= 1.74 \text{ in.}$$

Using $k_c = k_{des}$:

$$R_{n,lwy} = (6C_t k_c + l_b) F_y t_{cw} \qquad (3\text{-}46)$$
$$= \left[6(1.0)(0.820 \text{ in.}) + 1.74 \text{ in.}\right](50 \text{ ksi})(0.300 \text{ in.})$$
$$= 99.9 \text{ kips}$$

The available column web local yielding strength is then calculated and compared to the required strength.

LRFD	ASD
$\phi R_{n,lwy} = 1.00(99.9 \text{ kips})$ $= 99.9 \text{ kips} \quad \geq \quad P_u = 46.3 \text{ kips}$ **o.k.**	$\frac{R_{n,lwy}}{\Omega} = \frac{99.9 \text{ kips}}{1.50}$ $= 66.6 \text{ kips} \quad \geq \quad P_a = 30.9 \text{ kips}$ **o.k.**

The column web has sufficient yield strength to resist the concentrated force at the beam bottom flange location. [Note that the limit state of column web yielding also applies at the beam tension (top) flange. Because of the column cap plate, this limit state is satisfied by inspection.]

Calculate the column web local crippling strength. The flange force applied from the bottom of the beam is located more than the half the column depth from the end of the column, therefore use AISC *Specification* Equation J10-4 with $Q_f = 1.0$.

$$R_{n,lwc} = 0.80 t_{cw}^2 \left[1 + 3\left(\frac{l_b}{d_c}\right)\left(\frac{t_{cw}}{t_{cf}}\right)^{1.5}\right]\sqrt{\frac{EF_y t_{cf}}{t_{cw}}}\, Q_f \qquad \text{(from } \textit{Spec.} \text{ Eq. J10-4)}$$
$$= 0.80(0.300 \text{ in.})^2 \left[1 + 3\left(\frac{1.74 \text{ in.}}{12.5 \text{ in.}}\right)\left(\frac{0.300 \text{ in.}}{0.520 \text{ in.}}\right)^{1.5}\right]\sqrt{\frac{(29{,}000 \text{ ksi})(50 \text{ ksi})(0.520 \text{ in.})}{0.300 \text{ in.}}}\,(1.0)$$
$$= 135 \text{ kips}$$

The available column web local crippling strength is calculated and compared to the required compression force.

LRFD	ASD
$\phi R_{n,lwc} = 0.75(135 \text{ kips})$ $= 101 \text{ kips} \quad \geq \quad P_u = 46.3 \text{ kips}$ **o.k.**	$\frac{R_{n,lwc}}{\Omega} = \frac{135 \text{ kips}}{2.00}$ $= 67.5 \text{ kips} \quad \geq \quad P_a = 30.9 \text{ kips}$ **o.k.**

Because the column has sufficient strength for column web yielding and column web crippling, column web stiffeners are not required opposite the beam bottom flange. (If column web stiffeners are required, see Example 5.3-1 for calculation procedures.)

Check Column Panel Zone Shear

Check the column panel zone for shear strength. From Equation 3-35, the required shear strength is the beam flange force plus half the axial force. The beam axial force is shown in the same direction as the beam flange force.

LRFD	ASD
$V_u = \frac{M_u}{d - t_{bf}} + \frac{T_u}{2}$ $= \frac{800 \text{ kip-in.}}{17.7 \text{ in.} - 0.425 \text{ in.}} + \frac{3.30 \text{ kips}}{2}$ $= 48.0 \text{ kips}$	$V_a = \frac{M_a}{d - t_{bf}} + \frac{T_a}{2}$ $= \frac{533 \text{ kip-in.}}{17.7 \text{ in.} - 0.425 \text{ in.}} + \frac{2.20 \text{ kips}}{2}$ $= 32.0 \text{ kips}$

Calculate the panel zone shear strength using AISC *Specification* Section J10.6. Because the structural analysis did not include panel zone deformations and because the axial forces are small relative to the axial yield strength of the column, P_y, AISC *Specification* Equation J10-9 is used:

$$R_n = 0.60 F_y d_c t_{cw} \qquad \text{(Spec. Eq. J10-9)}$$
$$= 0.60(50 \text{ ksi})(12.5 \text{ in.})(0.300 \text{ in.})$$
$$= 113 \text{ kips}$$

Check that the available panel zone shear strength is greater than the required shear.

LRFD	ASD
$\phi R_n = 0.90(113 \text{ kips})$ $= 102 \text{ kips} \quad \geq \quad V_u = 48.0 \text{ kips}$ **o.k.**	$\frac{R_n}{\Omega} = \frac{113 \text{ kips}}{1.67}$ $= 67.7 \text{ kips} \quad \geq \quad V_a = 32.0 \text{ kips}$ **o.k.**

The column panel zone is sufficient to resist the required shear. (Note the column panel zone calculations shown are only applicable if there is a column cap plate.)

Summary

The connection shown in Figure 5-2 is adequate for the required moment and forces.

EXAMPLE 5.2-2—Four-Bolt Flush Unstiffened Thick End-Plate Example

Given:

The connection shown in Figure 5-3 is a four-bolt flush unstiffened end-plate moment connection to a W18×35. Beam material is ASTM A992/A992M, and end-plate material is ASTM A572/A572M Grade 50. Bolts are Group 120 ASTM F3125/F3125M Grade A325 snug-tightened, and weld electrodes are E70XX. The connection is to be evaluated as a thick end-plate design for the following required moments and shear forces.

	LRFD	ASD
Moment	$M_u = 1{,}500$ kip-in.	$M_a = 1{,}000$ kip-in.
Shear force	$V_u = 25.8$ kips	$V_a = 17.2$ kips

Solution:

From AISC *Manual* Table 2-4, the material properties are as follows:

ASTM A992/A992M
$F_y = 50$ ksi
$F_u = 65$ ksi

ASTM A572/A572M Grade 50
$F_y = 50$ ksi
$F_u = 65$ ksi

From AISC *Specification* Table J3.2, the material properties of the bolts are as follows:

Group 120 ASTM F3125/F3125M ¾-in.-diameter Grade A325 snug-tightened
F_{nt} = 90 ksi
F_{nv} = 54 ksi (Group 120 bolts with threads not excluded from the shear plane; thread condition N)

From AISC *Manual* Table 1-1, the geometric properties are as follows:

Beam: W18×35
d = 17.7 in. t_{bw} = 0.300 in.
b_{bf} = 6.00 in. t_{bf} = 0.425 in.
k_1 = ¾ in.

End-plate geometric properties:
b_p = 6 in.
t_p = ¾ in.
g = 3 in.
p_{fi} = 1½ in.
p_b = 3 in.
d_p = 18¾ in.

The distances from the centerline of the compression flange to the bolt lines, h_1 and h_2, are depicted in Table 5-3 and computed as:

$$h_1 = d - \frac{3}{2}t_{bf} - p_{fi}$$

$$= 17.7 \text{ in.} - \frac{3(0.425 \text{ in.})}{2} - 1\text{½ in.}$$

$$= 15.6 \text{ in.}$$

$$h_2 = d - \frac{3}{2}t_{bf} - p_{fi} - p_b$$

$$= 17.7 \text{ in.} - \frac{3(0.425 \text{ in.})}{2} - 1\text{½ in.} - 3 \text{ in.}$$

$$= 12.6 \text{ in.}$$

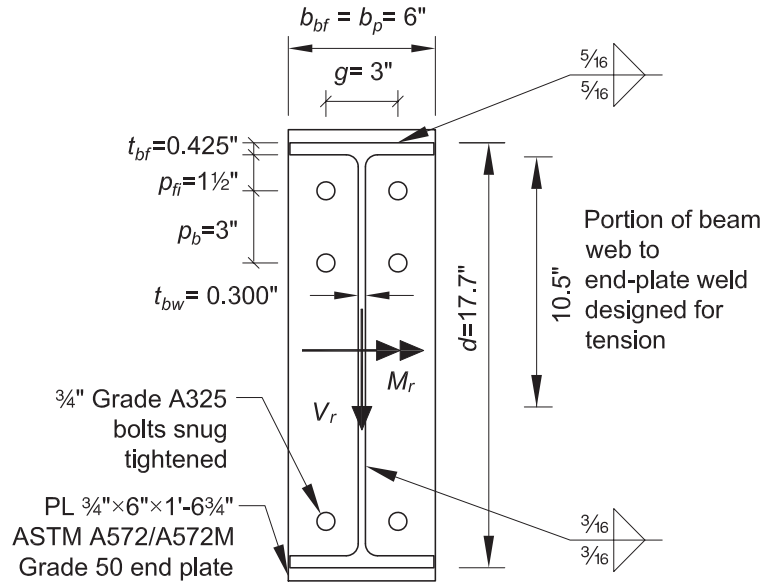

Fig. 5-3. Four-bolt unstiffened end-plate configuration for Example 5.2-2.

$$b_{p,eff} \le b_{bf} + \max(t_p, 1 \text{ in.}) \quad (4\text{-}3)$$
$$\le 6.00 \text{ in.} + \max(¾ \text{ in.}, 1 \text{ in.})$$
$$\le 7.00 \text{ in.}$$

$b_p = 6$ in. $\le$ 7.00 in. **o.k.**

$$b_{bf} \ge g \quad (4\text{-}1)$$

6.00 in. ≥ 3 in. **o.k.**

A. End-Plate and Bolt Design Verification

Determine if the specified ¾-in.-diameter Grade A325 snug-tightened bolts and ¾ in. end-plate thickness are sufficient using the thick end-plate/smaller bolt diameter procedure.

Solve for the required bolt diameter using Equations 5-3. For Grade A325 bolts, the nominal tensile stress is $F_{nt} = 90$ ksi.

LRFD	ASD
$d_{b,reqd} = \sqrt{\dfrac{4M_u}{\pi\phi F_{nt}\left(\sum_i n_i h_i\right)}}$	$d_{b,reqd} = \sqrt{\dfrac{4M_a}{\dfrac{\pi F_{nt}}{\Omega}\left(\sum_i n_i h_i\right)}}$
$= \sqrt{\dfrac{4(1{,}500 \text{ kip-in.})}{\pi(0.75)(90 \text{ ksi})\left[2(15.6 \text{ in.}) + 2(12.6 \text{ in.})\right]}}$	$= \sqrt{\dfrac{4(1{,}000 \text{ kip-in.})}{\dfrac{\pi(90 \text{ ksi})}{2.00}\left[2(15.6 \text{ in.}) + 2(12.6 \text{ in.})\right]}}$
$= 0.708$ in. $\le$ ¾ in. **o.k.**	$= 0.708$ in. $\le$ ¾ in. **o.k.**

Solve for the required end-plate thickness using Equations 5-4. First determine the distance, s, and yield line parameter, Y_p, using Table 5-3.

$$s = \frac{\sqrt{b_p g}}{2}$$
$$= \frac{\sqrt{(6 \text{ in.})(3 \text{ in.})}}{2}$$
$$= 2.12 \text{ in.}$$

Because $s \ge p_{fi} = 1½$ in., the dimension p_{fi} is used in the equation for the yield line parameter.

$$Y_p = \frac{b_p}{2}\left[h_1\left(\frac{1}{p_{fi}}\right) + h_2\left(\frac{1}{s}\right)\right] + \frac{2}{g}\left[h_1(p_{fi} + 0.75p_b) + h_2(s + 0.25p_b)\right] + \frac{g}{2}$$
$$= \left(\frac{6 \text{ in.}}{2}\right)\left[(15.6 \text{ in.})\left(\frac{1}{1½ \text{ in.}}\right) + (12.6 \text{ in.})\left(\frac{1}{2.12 \text{ in.}}\right)\right]$$
$$+ \left(\frac{2}{3 \text{ in.}}\right)\left\{(15.6 \text{ in.})\left[1½ \text{ in.} + 0.75(3 \text{ in.})\right] + (12.6 \text{ in.})\left[2.12 \text{ in.} + 0.25(3 \text{ in.})\right]\right\} + \frac{3 \text{ in.}}{2}$$
$$= 114 \text{ in.}$$

Determine the required end-plate thickness using Equations 5-4. For flush end-plate configurations, $\gamma_r = 0.80$.

LRFD	ASD
$t_{p,reqd} = \sqrt{\dfrac{1.10M_u}{\gamma_r \phi_b F_y Y_p}}$ $= \sqrt{\dfrac{1.10(1{,}500 \text{ kip-in.})}{0.80(0.90)(50 \text{ ksi})(114 \text{ in.})}}$ $= 0.634 \text{ in.} \quad \leq \quad ¾ \text{ in.} \qquad \textbf{o.k.}$	$t_{p,reqd} = \sqrt{\dfrac{1.10M_a}{\gamma_r F_y Y_p / \Omega_b}}$ $= \sqrt{\dfrac{1.10(1{,}000 \text{ kip-in.})}{0.80(50 \text{ ksi})(114 \text{ in.})/1.67}}$ $= 0.635 \text{ in.} \quad \leq \quad ¾ \text{ in.} \qquad \textbf{o.k.}$

The specified ¾-in.-thick ASTM A572/A572M Grade 50 end plate and ¾-in.-diameter Grade A325 snug-tightened bolts are sufficient.

Check Shear Transfer Strength at the Bottom Holes

See Example 5.2-1 for calculation procedures.

B. Check Beam to End-Plate Welds

The minimum weld size in AISC *Specification* Table J2.4 is determined from the material thickness of the thinner part joined. The weld sizes shown in Figure 5-3 satisfy the requirements in Table J2.4.

Check Beam Flange to End-Plate Weld

The weld from the beam flange to the end plate is shown in Figure 5-3 as a double-sided 5⁄16 in. fillet weld. Determine if this weld is adequate. First, find the required tensile force as the maximum of either the calculated flange tensile force or 60% of the flange tensile strength for LRFD and 40% of the flange tensile strength for ASD (Equations 3-38), but not greater than the yield strength of the tension flange.

LRFD	ASD
$T_{u,calc} = \dfrac{M_u}{d - t_{bf}}$ $= \dfrac{1{,}500 \text{ kip-in.}}{17.7 \text{ in.} - 0.425 \text{ in.}}$ $= 86.8 \text{ kips}$ $T_{yf} = F_y b_{bf} t_{bf}$ $= (50 \text{ ksi})(6.00 \text{ in.})(0.425 \text{ in.})$ $= 128 \text{ kips}$ $T_{u,min} = 0.60 F_y b_{bf} t_{bf}$ $= 0.60(50 \text{ ksi})(6.00 \text{ in.})(0.425 \text{ in.})$ $= 76.5 \text{ kips}$ $T_{uf} = \max(T_{u,calc}, T_{u,min}) \quad \leq \quad T_{yf}$ $= 86.8 \text{ kips} \quad \leq \quad T_{yf} = 128 \text{ kips}$	$T_{a,calc} = \dfrac{M_a}{d - t_{bf}}$ $= \dfrac{1{,}000 \text{ kip-in.}}{17.7 \text{ in.} - 0.425 \text{ in.}}$ $= 57.9 \text{ kips}$ $\dfrac{T_{yf}}{1.50} = \dfrac{F_y}{1.50} b_{bf} t_{bf}$ $= \dfrac{50 \text{ ksi}}{1.50}(6.00 \text{ in.})(0.425 \text{ in.})$ $= 85.0 \text{ kips}$ $T_{a,min} = 0.40 F_y b_{bf} t_{bf}$ $= 0.40(50 \text{ ksi})(6.00 \text{ in.})(0.425 \text{ in.})$ $= 51.0 \text{ kips}$ $T_{af} = \max\left(T_{a,calc}, T_{a,min}\right) \quad \leq \quad T_{yf}/1.50$ $= 57.9 \text{ kips} \quad \leq \quad \dfrac{T_{yf}}{1.50} = 85.0 \text{ kips}$

Calculate the strength of the double-sided 5⁄16 in. fillet weld. Because the weld is loaded perpendicular to its longitudinal axis, the angle of loading, θ, is 90°. The length of the weld is two times the width of the beam flange, b_{bf}, minus two times the beam k_1 distance.

$$l_w = 2b_{bf} - 2k_1$$
$$= 2(6.00 \text{ in.}) - 2(¾ \text{ in.})$$
$$= 10.5 \text{ in.}$$

$$R_n = 0.60F_{EXX}\frac{t_{weld}}{\sqrt{2}}l_w(1.0 + 0.5\sin^{1.5}\theta) \quad \text{(from } Spec. \text{ Eq. J2-4)}$$
$$= 0.60(70 \text{ ksi})\left(\frac{5/16 \text{ in.}}{\sqrt{2}}\right)(10.5 \text{ in.})(1.0 + 0.5\sin^{1.5}90°)$$
$$= 146 \text{ kips}$$

Compare the weld strength to the required tensile strength.

LRFD	ASD
$\phi R_n = 0.75(146 \text{ kips})$ $= 110 \text{ kips} \geq T_{uf} = 86.8 \text{ kips}$ **o.k.**	$\frac{R_n}{\Omega} = \frac{146 \text{ kips}}{2.00}$ $= 73.0 \text{ kips} \geq T_{af} = 57.9 \text{ kips}$ **o.k.**

The flange to end-plate weld consisting of a double-sided 5/16 in. fillet weld is adequate. (A CJP or PJP groove weld are alternate options.)

Check Beam Web to End-Plate Weld

The beam web to end-plate weld is shown in Figure 5-3 as a double-sided 3/16 in. fillet weld over the full height of the web. However, the weld is separately checked for (1) tension rupture in the region around the tension bolts (extending 6 in. to the inside of the tension bolts), and (2) the remainder of the web to end-plate weld is checked for shear.

As explained in Section 3.7.5, the demand for the web tension area, T_{uw} (LRFD) or T_{aw} (ASD), for this connection is the number of tension bolts adjacent to the web, n_{trib}, divided by the total number of tension bolts, n, multiplied by the calculated beam flange force, $T_{uf,calc}$ (LRFD) or $T_{af,calc}$ (ASD), from the beam flange to end-plate weld demand calculations. Using Equation 3-40:

LRFD	ASD
$T_{uw} = (n_{trib}/n)T_{uf,calc}$ $= (4/4)(86.8 \text{ kips})$ $= 86.8 \text{ kips}$	$T_{aw} = (n_{trib}/n)T_{af,calc}$ $= (4/4)(57.9 \text{ kips})$ $= 57.9 \text{ kips}$

The length of the web tension region is measured from the inside of the beam flange to 6 in. inside the tension bolt row:

$$l_{wt} = p_{fi} + p_b + 6 \text{ in.}$$
$$= 1½ \text{ in.} + 3 \text{ in.} + 6 \text{ in.}$$
$$= 10.5 \text{ in.}$$

The nominal web yield strength in the tension region is:

$$T_{yw} = F_yA_g \quad \text{(from } Spec. \text{ Eq. J4-1)}$$
$$= F_yt_{bw}l_{wt}$$
$$= (50 \text{ ksi})(0.300 \text{ in.})(10.50 \text{ in.})$$
$$= 158 \text{ kips}$$

Check that the design tensile yield strength of the web is sufficient.

LRFD	ASD
$\phi T_{yw} = 0.90(158 \text{ kips})$ $= 142 \text{ kips} \quad \geq \quad T_{uw} = 86.8 \text{ kips}$ **o.k.**	$\frac{T_{yw}}{\Omega} = \frac{158 \text{ kips}}{1.67}$ $= 94.6 \text{ kips} \quad \geq \quad T_{aw} = 57.9 \text{ kips}$ **o.k.**

Check that the required strength is at least 60% (LRFD) or 40% (ASD) of the web tension strength from Equations 3-41.

LRFD	ASD
$0.60T_{yw} = 0.60(158 \text{ kips})$ $= 94.8 \text{ kips}$ $T_{uwd} = \max\left(T_{uw}, 0.60T_{yw}\right)$ $= \max(86.8 \text{ kips}, 94.8 \text{ kips})$ $= 94.8 \text{ kips}$	$0.40T_{yw} = 0.40(158 \text{ kips})$ $= 63.2 \text{ kips}$ $T_{awd} = \max(T_{aw}, 0.40T_{yw})$ $= \max(57.9 \text{ kips}, 63.2 \text{ kips})$ $= 63.2 \text{ kips}$

Check the web to end-plate weld around the tension bolts. Because the weld is loaded perpendicular to its longitudinal axis, the angle of loading, θ, is 90°.

$$R_n = (2 \text{ welds})0.60F_{EXX}\frac{t_{weld}}{\sqrt{2}}l_{wt}(1.0 + 0.5\sin^{1.5}\theta) \qquad \text{(from } \textit{Spec.} \text{ Eq. J2-4)}$$

$$= (2 \text{ welds})(0.60)(70 \text{ ksi})\left(\frac{\frac{3}{16} \text{ in.}}{\sqrt{2}}\right)(10.5 \text{ in.})(1.0 + 0.5\sin^{1.5} 90°)$$

$$= 175 \text{ kips}$$

LRFD	ASD
$\phi R_n = 0.75(175 \text{ kips})$ $= 131 \text{ kips} \quad \geq \quad T_{uwd} = 94.8 \text{ kips}$ **o.k.**	$\frac{R_n}{\Omega} = \frac{175 \text{ kips}}{2.00}$ $= 87.5 \text{ kips} \quad \geq \quad T_{awd} = 63.2 \text{ kips}$ **o.k.**

Check the web to end-plate weld away from the tension bolts. Only the web to end-plate weld between the mid-depth of the beam and the inside face of the beam compression flange or the weld between the end of the assumed web tension length and the inside face of the bottom beam compression flange, whichever is smaller, is considered effective in resisting the beam end shear. The shear strength of this weld is compared to the required shear applied to the connection.

$$l_t = d - 2t_{bf} - l_{wt}$$
$$= 17.7 \text{ in.} - 2(0.425 \text{ in.}) - 10.5 \text{ in.}$$
$$= 6.35 \text{ in.}$$

$$l_{0.5w} = d/2 - t_{bf}$$
$$= (17.7 \text{ in.})/2 - 0.425 \text{ in.}$$
$$= 8.43 \text{ in.}$$

$$l_{wv} = \min(l_t, l_{0.5w})$$
$$= \min(6.35 \text{ in.}, 8.42 \text{ in.})$$
$$= 6.35 \text{ in.}$$

$$R_n = (2\text{ welds})0.60F_{EXX}\frac{t_{weld}}{\sqrt{2}}l_{wv}(1.0+0.5\sin^{1.5}\theta) \quad \text{(from } \textit{Spec.} \text{ Eq. J2-4)}$$

$$= (2\text{ welds})(0.60)(70\text{ ksi})\left(\frac{3/16\text{ in.}}{\sqrt{2}}\right)(6.35\text{ in.})(1.0+0.5\sin^{1.5}0°)$$

$$= 70.7\text{ kips}$$

LRFD	ASD
$\phi R_n = 0.75(70.7\text{ kips})$ $= 53.0\text{ kips} \geq V_u = 25.8\text{ kips}$ **o.k.**	$\frac{R_n}{\Omega} = \frac{70.7\text{ kips}}{2.00}$ $= 35.4\text{ kips} \geq V_a = 17.2\text{ kips}$ **o.k.**

Check that the shear rupture strength of the beam web at the weld using AISC *Specification* Equation J4-4 is sufficient.

$$R_n = 0.60F_uA_{nv} \quad \text{(}\textit{Spec.}\text{ Eq. J4-4)}$$

$$= 0.60F_ul_{wv}t_{bw}$$

$$= 0.60(65\text{ ksi})(6.35\text{ in.})(0.300\text{ in.})$$

$$= 74.3\text{ kips}$$

LRFD	ASD
$\phi R_n = 0.75(74.3\text{ kips})$ $= 55.7\text{ kips} \geq V_u = 25.8\text{ kips}$ **o.k.**	$\frac{R_n}{\Omega} = \frac{74.3\text{ kips}}{2.00}$ $= 37.2\text{ kips} \geq V_a = 17.2\text{ kips}$ **o.k.**

The double-sided 3⁄16 in. fillet weld from the web to the end plate is sufficient.

C. Check Column-Side Limit States

See Example 5.2-1 for example column-side limit state check calculations.

Summary

The connection shown in Figure 5-3 is adequate for the required moment and shear force.

EXAMPLE 5.2-3—Four-Bolt Flush Stiffened with Web Stiffener Plates between the Tension Bolts Thick End-Plate Example

Given:

The connection shown in Figure 5-4 is a four-bolt flush, stiffened between the tension bolts, end-plate moment connection for a built-up beam. Beam and end-plate material are ASTM A572/A572M Grade 50. Bolts are Group 120 ASTM F3125/F3125M Grade A325 snug-tightened, and weld electrodes are E70XX. The connection is to be evaluated as a thick end-plate design for the following required moments and shear forces.

	LRFD	ASD
Moment	$M_u = 2{,}500$ kip-in.	$M_a = 1{,}670$ kip-in.
Shear force	$V_u = 25.8$ kips	$V_a = 17.2$ kips

Solution:

From AISC *Manual* Table 2-4, the material properties are as follows:

ASTM A572/A572M Grade 50
F_y = 50 ksi
F_u = 65 ksi

From AISC *Specification* Table J3.2, the material properties of the bolts are as follows:

Group 120 ASTM F3125/F3125M ⅞-in.-diameter Grade A325 snug-tightened
F_{nt} = 90 ksi
F_{nv} = 54 ksi (Group 120 bolts with threads not excluded from the shear plane; thread condition N)

Beam
d = 20 in. t_{bw} = ¼ in.
b_{bf} = 6 in. t_{bf} = ½ in.

End-plate geometric properties:
b_p = 6 in.
t_p = ¾ in.
g = 3½ in.
p_{fi} = 1½ in.
p_{so} = 1½ in.
p_{si} = 1½ in.
p_b = 3¼ in.
d_p = 21 in.

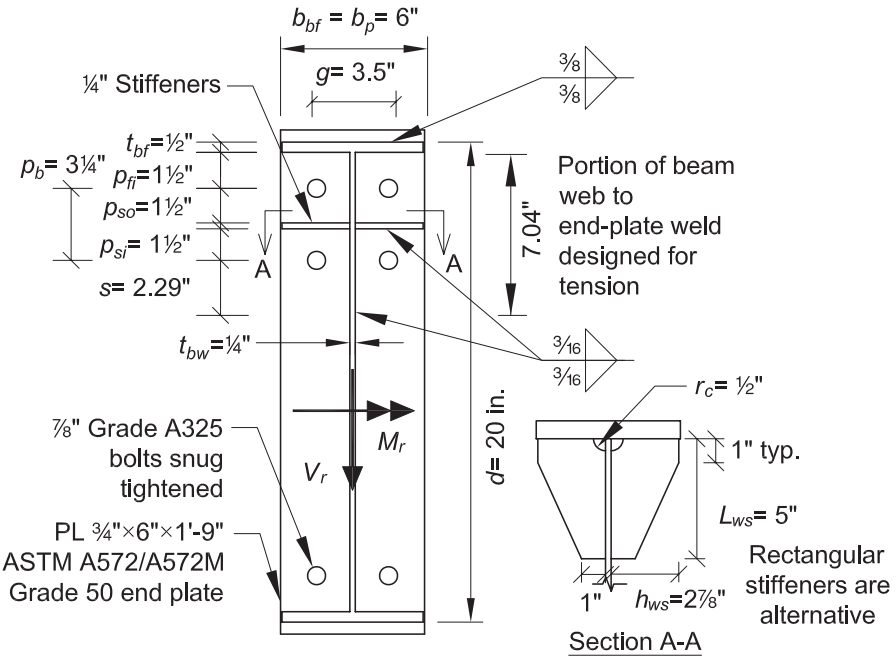

Fig. 5-4. Four-bolt stiffened with web stiffener plates between the tension bolts end-plate configuration for Example 5.2-3.

The distances from the centerline of the compression flange to the bolt lines, h_1 and h_2, are depicted in Table 5-4 and computed as:

$$h_1 = d - \frac{3}{2}t_{bf} - p_{fi}$$
$$= 20 \text{ in.} - \frac{3(½ \text{ in.})}{2} - 1½ \text{ in.}$$
$$= 17.8 \text{ in.}$$

$$h_2 = d - \frac{3}{2}t_{bf} - p_{fi} - p_b$$
$$= 20 \text{ in.} - \frac{3(½ \text{ in.})}{2} - 1½ \text{ in.} - 3¼ \text{ in.}$$
$$= 14.5 \text{ in.}$$

$$b_{p,eff} \le b_{bf} + \max(t_p, 1 \text{ in.}) \quad (4\text{-}3)$$
$$\le 6 \text{ in.} + \max(¾ \text{ in.}, 1 \text{ in.})$$
$$\le 7.00 \text{ in.}$$

$b_p = 6 \text{ in.} \le 7.00 \text{ in.}$ **o.k.**

$$b_{bf} \ge g \quad (4\text{-}1)$$

6 in. ≥ 3½ in. **o.k.**

Beam web stiffener geometric properties:

$$h_{ws} = (b_p - t_{bw})/2$$
$$= (6 \text{ in.} - ¼ \text{ in.})/2$$
$$= 2⅞ \text{ in.}$$

$$L_{ws} = h_{ws}/\tan 30° \quad (4\text{-}4)$$
$$= 2⅞ \text{ in.}/\tan 30°$$
$$= 4.98 \text{ in.} \le 5 \text{ in.} \quad \textbf{o.k.}$$

A. End-Plate and Bolt Design Verification

Determine if the specified ⅞-in.-diameter Grade A325 snug-tightened bolts and ¾ in. end-plate thickness are sufficient using the thick end-plate/smaller bolt diameter procedure.

Solve for the required bolt diameter using Equations 5-3. For Grade A325 bolts, the nominal tensile stress is $F_{nt} = 90$ ksi.

LRFD	ASD
$d_{b,reqd} = \sqrt{\frac{4M_u}{\pi\phi F_{nt}\left(\sum_i n_i h_i\right)}}$	$d_{b,reqd} = \sqrt{\frac{4M_a}{\frac{\pi F_{nt}}{\Omega}\left(\sum_i n_i h_i\right)}}$
$= \sqrt{\frac{4(2{,}500 \text{ kip-in.})}{\pi(0.75)(90 \text{ ksi})\left[2(17.8 \text{ in.}) + 2(14.5 \text{ in.})\right]}}$	$= \sqrt{\frac{4(1{,}670 \text{ kip-in.})}{\frac{\pi(90 \text{ ksi})}{2.00}\left[2(17.8 \text{ in.}) + 2(14.5 \text{ in.})\right]}}$
$= 0.854 \text{ in.} \le ⅞ \text{ in.}$ **o.k.**	$= 0.855 \text{ in.} \le ⅞ \text{ in.}$ **o.k.**

Solve for the required end-plate thickness using Equations 5-4. First solve for the distance, s, and check limits. Then calculate the yield line parameter, Y_p, using Table 5-4.

$$s = \frac{\sqrt{b_p g}}{2}$$
$$= \frac{\sqrt{(6\text{ in.})(3\text{½ in.})}}{2}$$
$$= 2.29\text{ in.}$$

Because $s \geq p_{fi} = 1\text{½}$ in., $p_{so} = 1\text{½}$ in., and $p_{si} = 1\text{½}$ in., the dimensions p_{fi}, p_{so}, and p_{si} are used in the equation for the yield line parameter.

$$Y_p = \frac{b_p}{2}\left[h_1\left(\frac{1}{p_{fi}} + \frac{1}{p_{so}}\right) + h_2\left(\frac{1}{s} + \frac{1}{p_{si}}\right)\right] + \frac{2}{g}\left[h_1(p_{fi} + p_{so}) + h_2(s + p_{si})\right]$$
$$= \left(\frac{6\text{ in.}}{2}\right)\left[(17.8\text{ in.})\left(\frac{1}{1\text{½ in.}} + \frac{1}{1\text{½ in.}}\right) + (14.5\text{ in.})\left(\frac{1}{2.29\text{ in.}} + \frac{1}{1\text{½ in.}}\right)\right]$$
$$+ \left(\frac{2}{3\text{½ in.}}\right)\left[(17.8\text{ in.})(1\text{½ in.} + 1\text{½ in.}) + (14.5\text{ in.})(2.29\text{ in.} + 1\text{½ in.})\right]$$
$$= 181\text{ in.}$$

Determine the required end-plate thickness using Equations 5-4. For flush end-plate configurations, $\gamma_r = 0.80$.

LRFD	ASD
$t_{p,reqd} = \sqrt{\frac{1.10M_u}{\gamma_r \phi_b F_y Y_p}}$	$t_{p,reqd} = \sqrt{\frac{1.10M_a}{\gamma_r F_y Y_p / \Omega_b}}$
$= \sqrt{\frac{1.10(2{,}500\text{ kip-in.})}{0.80(0.90)(50\text{ ksi})(181\text{ in.})}}$	$= \sqrt{\frac{1.10(1{,}670\text{ kip-in.})}{0.80(50\text{ ksi})(181\text{ in.})/1.67}}$
$= 0.650\text{ in.} \leq$ ¾ in. **o.k.**	$= 0.651\text{ in.} \leq$ ¾ in. **o.k.**

The specified ⅞-in.-diameter Grade A325 snug-tightened bolts and ¾ in. ASTM A572/A572M Grade 50 end plate are sufficient.

Check Shear Transfer Strength at the Bottom Holes

See Example 5.2-1 for calculation procedures.

B. Check Beam to End-Plate Welds

The minimum weld size in AISC *Specification* Table J2.4 is determined from the material thickness of the thinner part joined. The weld sizes shown in Figure 5-4 satisfy the requirements in Table J2.4.

Check Beam Flange to End-Plate Weld

The weld from the beam flange to the end plate is shown in Figure 5-4 as a double-sided ⅜ in. fillet weld. Determine if this weld is adequate. First, find the required tensile force as the maximum of either the calculated flange tensile force or 60% of the flange tensile strength for LRFD and 40% of the flange tensile strength for ASD (Equations 3-38), but not greater than the yield strength of the tension flange.

LRFD	ASD
$T_{u,calc} = \dfrac{M_u}{d - t_{bf}}$ $= \dfrac{2{,}500 \text{ kip-in.}}{20 \text{ in.} - ½ \text{ in.}}$ $= 128 \text{ kips}$ $T_{yf} = F_y b_{bf} t_{bf}$ $= (50 \text{ ksi})(6 \text{ in.})(½ \text{ in.})$ $= 150 \text{ kips}$ $T_{u,min} = 0.60 F_y b_{bf} t_{bf}$ $= 0.60(50 \text{ ksi})(6 \text{ in.})(½ \text{ in.})$ $= 90.0 \text{ kips}$ $T_{uf} = \max(T_{u,calc},\ T_{u,min}) \quad \le \quad T_{yf}$ $= \max(128 \text{ kips},\ 90.0 \text{ kips})$ $= 128 \text{ kips} \quad \le \quad T_{yf} = 150 \text{ kips}$	$T_{a,calc} = \dfrac{M_a}{d - t_{bf}}$ $= \dfrac{1{,}670 \text{ kip-in.}}{20 \text{ in.} - ½ \text{ in.}}$ $= 85.6 \text{ kips}$ $\dfrac{T_{yf}}{1.50} = \dfrac{F_y}{1.50} b_{bf} t_{bf}$ $= \dfrac{50 \text{ ksi}}{1.50}(6 \text{ in.})(½ \text{ in.})$ $= 100 \text{ kips}$ $T_{a,min} = 0.40 F_y b_{bf} t_{bf}$ $= 0.40(50 \text{ ksi})(6 \text{ in.})(½ \text{ in.})$ $= 60.0 \text{ kips}$ $T_{af} = \max(T_{a,calc},\ T_{a,min}) \quad \le \quad T_{yf}/1.50$ $= \max(85.6 \text{ kips},\ 60.0 \text{ kips})$ $= 85.6 \text{ kips} \quad \le \quad \dfrac{T_{yf}}{1.50} = 100 \text{ kips}$

Calculate the strength of the double-sided ⅜ in. fillet weld. Because the weld is loaded perpendicular to its longitudinal axis, the angle of loading, θ, is 90°. The length of the weld is two times the width of the beam flange, b_{bf}, minus the beam web thickness and two times the beam web to end-plate weld.

$$l_w = 2b_{bf} - t_{bw} - 2w$$
$$= 2(6 \text{ in.}) - ¼ \text{ in.} - 2(3/16 \text{ in.})$$
$$= 11.4 \text{ in.}$$

$$R_n = 0.60 F_{EXX} \frac{t_{weld}}{\sqrt{2}} l_w (1.0 + 0.5 \sin^{1.5} \theta) \qquad \text{(from } \textit{Spec.} \text{ Eq. J2-4)}$$
$$= 0.60(70 \text{ ksi}) \left(\frac{⅜ \text{ in.}}{\sqrt{2}} \right) (11.4 \text{ in.})(1.0 + 0.5 \sin^{1.5} 90°)$$
$$= 190 \text{ kips}$$

Compare the weld strength to the required tensile strength.

LRFD	ASD
$\phi R_n = 0.75(190 \text{ kips})$ $= 143 \text{ kips} \quad \ge \quad T_{uf} = 128 \text{ kips}$ **o.k.**	$\dfrac{R_n}{\Omega} = \dfrac{190 \text{ kips}}{2.00}$ $= 95.0 \text{ kips} \quad \ge \quad T_{af} = 85.6 \text{ kips}$ **o.k.**

The flange to end-plate weld consisting of a double-sided ⅜ in. fillet weld is adequate. (A CJP or PJP groove weld are alternate options.)

Check Beam Web to End-Plate Welds

The beam web to end-plate welds shown in Figure 5-4 are separately checked for (1) tension rupture in the region around the tension bolts, and (2) the remainder of the web is checked for shear strength. The region around the tension bolts includes the web stiffeners between the tension bolts as shown in Figure 5-5.

As explained in Section 3.7.5, the demand for the web tension area, T_{uw} (LRFD) or T_{aw} (ASD), is the calculated beam flange force, $T_{u,calc}$ (LRFD) or $T_{a,calc}$ (ASD). The web tension area is the area of the beam web from the inside of the beam tension flange to the s distance below the innermost bolt line plus the cross-sectional area of the web stiffeners.

$$\begin{aligned}A_{wt} &= t_{bw}(p_{fi} + p_b + s) + 2t_{ws}(h_{ws} - r_c)\\ &= (¼\text{ in.})(1½\text{ in.} + 3¼\text{ in.} + 2.29\text{ in.}) + 2(¼\text{ in.})(2⅞\text{ in.} - ½\text{ in.})\\ &= 2.95\text{ in.}^2\end{aligned}$$

The nominal web yield strength of the tension web area is

$$\begin{aligned}T_{yw} &= F_y A_{wt} \qquad \text{(from } \textit{Spec.} \text{ Eq. J4-1)}\\ &= (50\text{ ksi})(2.95\text{ in.}^2)\\ &= 148\text{ kips}\end{aligned}$$

Check that the design tensile yield strength of the web tension area is sufficient.

LRFD	ASD
$\phi T_{yw} = 0.90(148\text{ kips})$ $= 133\text{ kips} \quad \geq \quad T_{uw} = 128\text{ kips}$ **o.k.**	$\frac{T_{yw}}{\Omega} = \frac{148\text{ kips}}{1.67}$ $= 88.6\text{ kips} \quad \geq \quad T_{aw} = 85.6\text{ kips}$ **o.k.**

Check that the required strength is at least 60% (LRFD) or 40% (ASD) of the web tensile strength from Equations 3-41.

LRFD	ASD
$0.60T_{yw} = 0.60(148\text{ kips})$ $= 88.8\text{ kips}$ $T_{uwd} = \max(T_{uw},\ 0.60T_{yw})$ $= \max(128\text{ kips}, 88.8\text{ kips})$ $= 128\text{ kips}$	$0.40T_{yw} = 0.40(148\text{ kips})$ $= 59.2\text{ kips}$ $T_{awd} = \max(T_{aw},\ 0.40T_{yw})$ $= \max(85.6\text{ kips}, 59.2\text{ kips})$ $= 85.6\text{ kips}$

Check the web to end-plate weld in the tension area. Because the weld is loaded perpendicular to its longitudinal axis, the angle of loading, θ, is 90°.

The length of the specified double-sided 3⁄16 in. fillet welds is:

$$\begin{aligned}l_{wt} &= (2\text{ welds})(p_{fi} + p_b + s) + (4\text{ welds})(h_{ws} - r_c)\\ &= (2\text{ welds})(1½\text{ in.} + 3¼\text{ in.} + 2.29\text{ in.}) + (4\text{ welds})(2⅞\text{ in.} - ½\text{ in.})\\ &= 23.6\text{ in.}\end{aligned}$$

$$\begin{aligned}R_n &= 0.60F_{EXX}\frac{t_{weld}}{\sqrt{2}}l_{wt}(1.0 + 0.5\sin^{1.5}\theta) \qquad \text{(from } \textit{Spec.} \text{ Eq. J2-4)}\\ &= 0.60(70\text{ ksi})\left(\frac{3⁄16\text{ in.}}{\sqrt{2}}\right)(23.6\text{ in.})(1.0 + 0.5\sin^{1.5}90°)\\ &= 197\text{ kips}\end{aligned}$$

LRFD	ASD
$\phi R_n = 0.75(197 \text{ kips})$ $= 148 \text{ kips} \quad \geq \quad T_{uwd} = 128 \text{ kips}$ **o.k.**	$\frac{R_n}{\Omega} = \frac{197 \text{ kips}}{2.00}$ $= 98.5 \text{ kips} \quad \geq \quad T_{awd} = 85.6 \text{ kips}$ **o.k.**

Check the web to end-plate weld away from the tension bolts. Only the web to end-plate weld between the end of the assumed web tension length and the inside face of the bottom beam compression flange or the weld between the mid-depth of the beam and the inside face of the beam compression flange, whichever is smaller, is considered effective in resisting the beam end shear. The shear strength of this weld is compared to the required shear applied to the connection.

$$l_t = (d - 2t_{bf}) - (p_{fi} + p_b + s)$$
$$= \left[20 \text{ in.} - 2(\tfrac{1}{2} \text{ in.})\right] - (1\tfrac{1}{2} \text{ in.} + 3\tfrac{1}{4} \text{ in.} + 2.29 \text{ in.})$$
$$= 12.0 \text{ in.}$$

$$l_{0.5w} = d/2 - t_{bf}$$
$$= (20 \text{ in.})/2 - \tfrac{1}{2} \text{ in.}$$
$$= 9.50 \text{ in.}$$

$$l_{wv} = \min(l_t, l_{0.5w})$$
$$= \min(11.9 \text{ in.}, 9.50 \text{ in.})$$
$$= 9.50 \text{ in.}$$

$$R_n = (2 \text{ welds}) 0.60 F_{EXX} \frac{t_{weld}}{\sqrt{2}} l_{wv} (1.0 + 0.5 \sin^{1.5} \theta) \qquad \text{(from } \textit{Spec.} \text{ Eq. J2-4)}$$
$$= (2 \text{ welds})(0.60)(70 \text{ ksi}) \left(\frac{\tfrac{3}{16} \text{ in.}}{\sqrt{2}} \right) (9.50 \text{ in.})(1.0 + 0.5 \sin^{1.5} 0°)$$
$$= 106 \text{ kips}$$

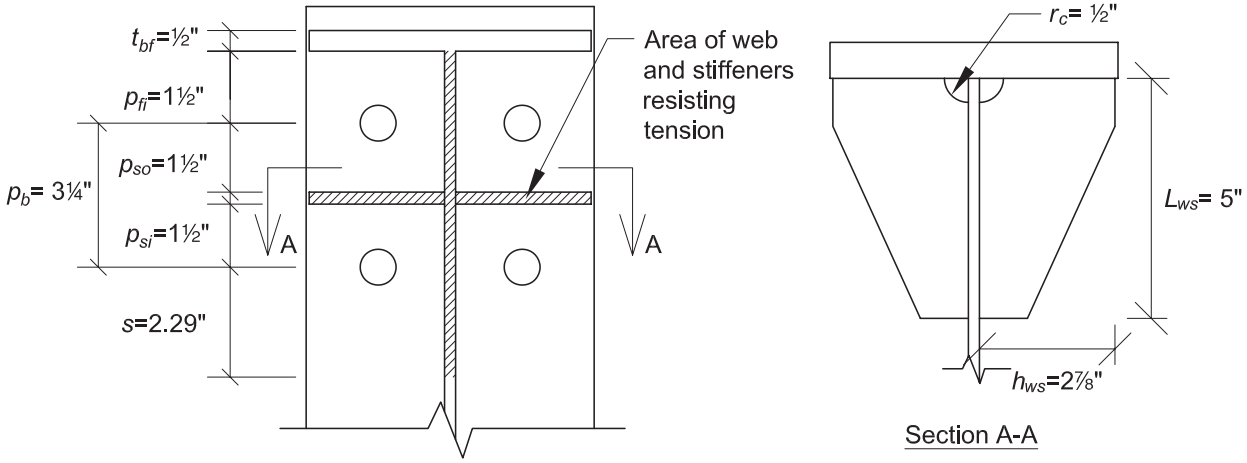

Fig. 5-5. Web and stiffener tension area for four-bolt stiffened configuration.

LRFD	ASD
$\phi R_n = 0.75(106 \text{ kips})$ $= 79.5 \text{ kips} \quad \geq \quad V_u = 25.8 \text{ kips}$ **o.k.**	$\frac{R_n}{\Omega} = \frac{106 \text{ kips}}{2.00}$ $= 53.0 \text{ kips} \quad \geq \quad V_a = 17.2 \text{ kips}$ **o.k.**

Check that the shear rupture strength of the beam web at the weld using AISC *Specification* Equation J4-4 is sufficient.

$R_n = 0.60 F_u A_{nv}$ (*Spec.* Eq. J4-4)

$= 0.60 F_u l_{wv} t_{bw}$

$= 0.60(65 \text{ ksi})(9.50 \text{ in.})(¼ \text{ in.})$

$= 92.6 \text{ kips}$

LRFD	ASD
$\phi R_n = 0.75(92.6 \text{ kips})$ $= 69.5 \text{ kips} \quad \geq \quad V_u = 25.8 \text{ kips}$ **o.k.**	$\frac{R_n}{\Omega} = \frac{92.6 \text{ kips}}{2.00}$ $= 46.3 \text{ kips} \quad \geq \quad V_a = 17.2 \text{ kips}$ **o.k.**

The double-sided 3⁄16 in. fillet weld from the web to the end plate is sufficient.

Check Web Stiffeners to Beam Web Welds

The web stiffener to beam web weld demand is the same as the demand resisted by the web stiffener to end-plate weld. The web stiffener to end-plate demand is taken as the area of the web stiffener in contact with the end plate divided by the total web tension area, A_{wt}, multiplied by the web tension area demand, T_{uw} (LRFD) and T_{aw} (ASD).

$A_{ws} = t_{bw}(b_p - t_{bw} - 2r_c)$

$= (¼ \text{ in.})\left[6 \text{ in.} - ¼ \text{ in.} - 2(½ \text{ in.})\right]$

$= 1.19 \text{ in.}^2$

LRFD	ASD
$T_{u,ws} = (A_{ws}/A_{wt})T_{uw}$ $= (1.19 \text{ in.}^2/2.95 \text{ in.}^2)(128 \text{ kips})$ $= 51.6 \text{ kips}$	$T_{a,ws} = (A_{ws}/A_{wt})T_{aw}$ $= (1.19 \text{ in.}^2/2.95 \text{ in.}^2)(85.6 \text{ kips})$ $= 34.5 \text{ kips}$

$R_n = (4 \text{ welds}) 0.60 F_{EXX} \frac{t_{weld}}{\sqrt{2}} (L_{ws} - r_c)(1.0 + 0.5 \sin^{1.5} \theta)$ (from *Spec.* Eq. J2-4)

$= (4 \text{ welds})(0.60)(70 \text{ ksi}) \left(\frac{3⁄16 \text{ in.}}{\sqrt{2}}\right) (5 \text{ in.} - ½ \text{ in.})(1.0 + 0.5 \sin^{1.5} 0°)$

$= 100 \text{ kips}$

LRFD	ASD
$\phi R_n = 0.75(100 \text{ kips})$ $= 75.0 \text{ kips} \quad \geq \quad T_{u,ws} = 51.6 \text{ kips}$ **o.k.**	$\frac{R_n}{\Omega} = \frac{100 \text{ kips}}{2}$ $= 50.0 \text{ kips} \quad \geq \quad T_{a,ws} = 34.5 \text{ kips}$ **o.k.**

The double-sided 3⁄16 in. fillet weld from the web stiffener to the beam web is sufficient.

Check that the shear rupture strength of the beam web and web stiffeners at the welds is sufficient using AISC *Specification* Equation J4-4. Because both the beam web and the web stiffeners thickness are the same, ¼ in., only the beam web is checked.

$$R_n = 0.60F_uA_{nv} \qquad \text{(Spec. Eq. J4-4)}$$
$$= 0.60F_u(L_{ws} - r_c)t_{bw}$$
$$= 0.60(65\text{ ksi})(2\text{ lines})(5\text{ in.} - ½\text{ in.})(¼\text{ in.})$$
$$= 87.8\text{ kips}$$

LRFD	ASD
$\phi R_n = 0.75(87.8\text{ kips})$ $= 65.9\text{ kips} \geq V_u = 51.6\text{ kips}$ **o.k.**	$\frac{R_n}{\Omega} = \frac{87.8\text{ kips}}{2.00}$ $= 43.9\text{ kips} \geq V_a = 34.5\text{ kips}$ **o.k.**

The web stiffener and beam web base metal adjacent to the web stiffener welds are sufficient.

C. Check Column-Side Limit States

See Example 5.2-1 for example column-side limit state check calculations.

Summary

The connection shown in Figure 5-4 is adequate for the required moment and shear force.

EXAMPLE 5.2-4—Four-Bolt Flush Stiffened with Web Stiffeners below the Tension Bolts Thick End-Plate Example

Given:

The connection shown in Figure 5-6 is a four-bolt flush, stiffened below the tension bolts, end-plate moment connection for a built-up beam. Beam and end-plate material are ASTM A572/A572M Grade 50. Bolts are Group 120 ASTM F3125/F3125M Grade A325 snug-tightened, and weld electrodes are E70XX. The connection is to be evaluated as a thick end-plate design for the following required moments and shear forces.

	LRFD	ASD
Moment	$M_u = 2{,}500$ kip-in.	$M_a = 1{,}670$ kip-in.
Shear force	$V_u = 25.8$ kips	$V_a = 13.8$ kips

Solution:

From AISC *Manual* Table 2-4, the material properties are as follows:

ASTM A572/A572M Grade 50
$F_y = 50$ ksi
$F_u = 65$ ksi

From AISC *Specification* Table J3.2, the material properties of the bolts are as follows:

Group 120 ASTM F3125/F3125M ⅞-in.-diameter Grade A325 snug-tightened
$F_{nt} = 90$ ksi
$F_{nv} = 54$ ksi (Group 120 bolts with threads not excluded from the shear plane; thread condition N)

Beam
$d = 20$ in. $\quad t_{bw} = ¼$ in.
$b_{bf} = 6$ in. $\quad t_{bf} = ½$ in.

End-plate geometric properties:
b_p = 6 in.
t_p = ⅞ in.
g = 3½ in.
p_{fi} = 1½ in.
p_b = 3 in.
p_{si} = 1½ in.
d_p = 21 in.
t_{ws} = 5⁄16 in.

The distances from the centerline of the compression flange to the bolt lines, h_1 and h_2, are depicted in Table 5-5 and computed as:

$$h_1 = d - \frac{3}{2}t_{bf} - p_{fi}$$
$$= 20 \text{ in.} - \frac{3(½ \text{ in.})}{2} - 1½ \text{ in.}$$
$$= 17.8 \text{ in.}$$

$$h_2 = d - \frac{3}{2}t_{bf} - p_{fi} - p_b$$
$$= 20 \text{ in.} - \frac{3(½ \text{ in})}{2} - 1½ \text{ in.} - 3 \text{ in.}$$
$$= 14.8 \text{ in.}$$

$$b_{p,eff} \le b_{bf} + \max(t_p, 1 \text{ in.}) \quad (4\text{-}3)$$
$$\le 6 \text{ in.} + \max(⅞ \text{ in.}, 1 \text{ in.})$$
$$\le 7.00 \text{ in.}$$

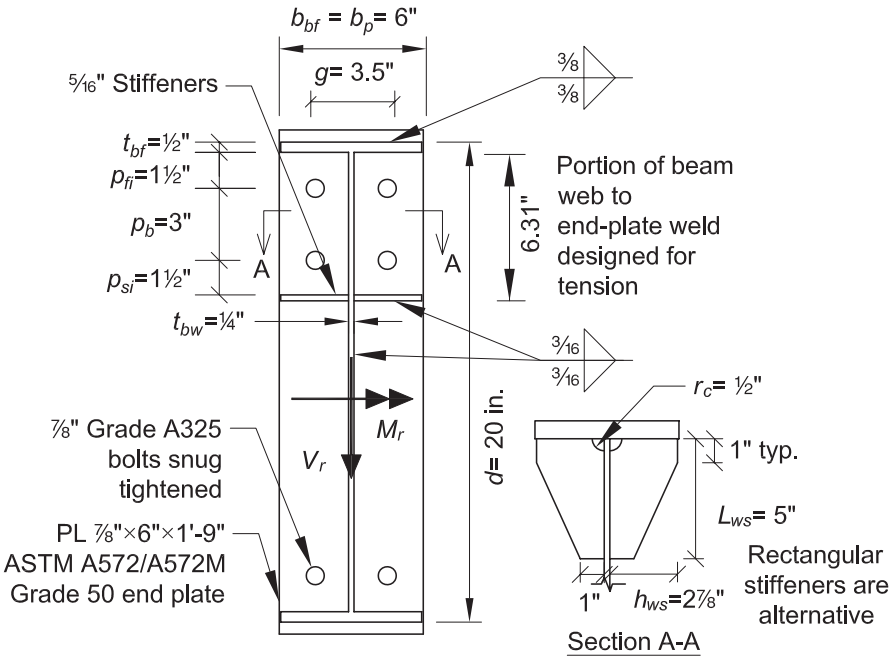

Fig. 5-6. Four-bolt stiffened with web stiffener below the tension bolts end-plate configuration for Example 5.2-4.

$b_p = 6 \text{ in.} \le 7.00 \text{ in.}$ **o.k.**

$$b_{bf} \ge g \tag{4-1}$$

$6 \text{ in.} \ge 3\frac{1}{2} \text{ in.}$ **o.k.**

Beam web stiffener geometric properties:

$$h_{ws} = (b_p - t_{bw})/2$$
$$= (6 \text{ in.} - \tfrac{1}{4} \text{ in.})/2$$
$$= 2\tfrac{7}{8} \text{ in.}$$

$$L_{ws} = h_{ws}/\tan 30^\circ \tag{4-4}$$
$$= 2\tfrac{7}{8} \text{ in.}/\tan 30^\circ$$
$$= 4.98 \text{ in.} \le 5 \text{ in.}$$ **o.k.**

A. End-Plate and Bolt Design Verification

Determine if the specified ⅞-in.-diameter Grade A325 snug-tightened bolts and ⅞ in. end-plate thickness are sufficient using the thick end-plate/smaller bolt diameter procedure.

Solve for the required bolt diameter using Equations 5-3. For Grade A325 bolts, the nominal tensile stress is $F_{nt} = 90$ ksi.

LRFD	ASD
$d_{b,reqd} = \sqrt{\dfrac{4M_u}{\pi\phi F_{nt}\left(\sum_i n_i h_i\right)}}$	$d_{b,reqd} = \sqrt{\dfrac{4M_a}{\dfrac{\pi F_{nt}}{\Omega}\left(\sum_i n_i h_i\right)}}$
$= \sqrt{\dfrac{4(2{,}500 \text{ kip-in.})}{\pi(0.75)(90 \text{ ksi})\left[2(17.8 \text{ in.}) + 2(14.8 \text{ in.})\right]}}$	$= \sqrt{\dfrac{4(1{,}670 \text{ kip-in.})}{\dfrac{\pi(90 \text{ ksi})}{2.00}\left[2(17.8 \text{ in.}) + 2(14.8 \text{ in.})\right]}}$
$= 0.850 \text{ in.} \le \tfrac{7}{8} \text{ in.}$ **o.k.**	$= 0.851 \text{ in.} \le \tfrac{7}{8} \text{ in.}$ **o.k.**

Solve for the required end-plate thickness using Equations 5-4. First solve for the distance, s, and yield line parameter, Y_p, using Table 5-5.

$$s = \frac{\sqrt{b_p g}}{2}$$
$$= \frac{\sqrt{(6 \text{ in.})(3\frac{1}{2} \text{ in.})}}{2}$$
$$= 2.29 \text{ in.}$$

Because $s \ge p_{fi} = 1\frac{1}{2}$ in., and $p_{si} = 1\frac{1}{2}$ in., the dimensions p_{fi} and p_{si} are used in the equation for the yield line parameter.

$$Y_p = \frac{b_p}{2}\left[h_1\left(\frac{1}{p_{fi}}\right) + h_2\left(\frac{1}{p_{si}}\right)\right] + \frac{2}{g}\left[h_1(p_{fi} + 0.75p_b) + h_2(p_{si} + 0.25p_b)\right] + \frac{g}{2}$$
$$= \left(\frac{6 \text{ in.}}{2}\right)\left[(17.8 \text{ in.})\left(\frac{1}{1\frac{1}{2} \text{ in.}}\right) + (14.8 \text{ in.})\left(\frac{1}{1\frac{1}{2} \text{ in.}}\right)\right]$$
$$+ \left(\frac{2}{3\frac{1}{2} \text{ in.}}\right)\left\{(17.8 \text{ in.})\left[1\tfrac{1}{2} \text{ in.} + (0.75)3 \text{ in.}\right] + (14.8 \text{ in.})\left[1\tfrac{1}{2} \text{ in.} + (0.25)3 \text{ in.}\right]\right\} + \frac{3\frac{1}{2} \text{ in.}}{2}$$
$$= 124 \text{ in.}$$

Determine the required end-plate thickness using Equations 5-4. For flush end-plate configurations, $\gamma_r = 0.80$.

LRFD	ASD
$t_{p,reqd} = \sqrt{\dfrac{1.10M_u}{\gamma_r \phi_b F_y Y_p}}$ $= \sqrt{\dfrac{1.10(2{,}500 \text{ kip-in.})}{0.80(0.90)(50 \text{ ksi})(124 \text{ in.})}}$ $= 0.785 \text{ in.} \quad \leq \quad ⅞ \text{ in.} \quad$ **o.k.**	$t_{p,reqd} = \sqrt{\dfrac{1.10M_a}{\gamma_r F_y Y_p / \Omega_b}}$ $= \sqrt{\dfrac{1.10(1{,}670 \text{ kip-in.})}{0.80(50 \text{ ksi})(124 \text{ in.})/1.67}}$ $= 0.786 \text{ in.} \quad \leq \quad ⅞ \text{ in.} \quad$ **o.k.**

The specified ⅞-in.-diameter Grade A325 snug-tightened bolts and ⅞ in. ASTM A572/A572M Grade 50 end plate are sufficient.

Check Shear Transfer Strength at the Bottom Holes

See Example 5.2-1 for calculation procedures.

B. Check Beam to End-Plate Welds

The minimum weld size in AISC *Specification* Table J2.4 is determined from the material thickness of the thinner part joined. The weld sizes shown in Figure 5-6 satisfy the requirements in Table J2.4.

Check Beam Flange to End-Plate Weld

The weld from the beam flange to the end plate is shown in Figure 5-6 as a double-sided ⅜ in. fillet weld. Determine if this weld is adequate. First, find the required tensile force as the maximum of either the calculated flange tensile force or 60% of the flange tensile strength for LRFD and 40% of the flange tensile strength for ASD (Equations 3-38), but not greater than the yield strength of the tension flange.

LRFD	ASD
$T_{u,calc} = \dfrac{M_u}{d - t_{bf}}$ $= \dfrac{2{,}500 \text{ kip-in.}}{20 \text{ in.} - ½ \text{ in.}}$ $= 128 \text{ kips}$ $T_{yf} = F_y b_{bf} t_{bf}$ $= (50 \text{ ksi})(6 \text{ in.})(½ \text{ in.})$ $= 150 \text{ kips}$ $T_{u,min} = 0.60 F_y b_{bf} t_{bf}$ $= 0.60(50 \text{ ksi})(6 \text{ in.})(½ \text{ in.})$ $= 90.0 \text{ kips}$ $T_{uf} = \max(T_{u,calc},\ T_{u,min}) \quad \leq \quad T_{yf}$ $= \max(128 \text{ kips},\ 90.0 \text{ kips})$ $= 128 \text{ kips} \quad \leq \quad T_{yf} = 150 \text{ kips}$	$T_{a,calc} = \dfrac{M_a}{d - t_{bf}}$ $= \dfrac{1{,}670 \text{ kip-in.}}{20 \text{ in.} - ½ \text{ in.}}$ $= 85.6 \text{ kips}$ $\dfrac{T_{yf}}{1.50} = \dfrac{F_y}{1.50} b_{bf} t_{bf}$ $= \dfrac{50 \text{ ksi}}{1.50}(6 \text{ in.})(½ \text{ in.})$ $= 100 \text{ kips}$ $T_{a,min} = 0.40 F_y b_{bf} t_{bf}$ $= 0.40(50 \text{ ksi})(6 \text{ in.})(½ \text{ in.})$ $= 60.0 \text{ kips}$ $T_{af} = \max(T_{a,calc},\ T_{a,min}) \quad \leq \quad T_{yf}/1.50$ $= \max(85.6 \text{ kips},\ 60.0 \text{ kips})$ $= 85.6 \text{ kips} \quad \leq \quad \dfrac{T_{yf}}{1.50} = 100 \text{ kips}$

Calculate the strength of the double-sided ⅜ in. fillet weld. Because the weld is loaded perpendicular to its longitudinal axis, the angle of loading, θ, is 90°. The length of the weld is two times the width of the beam flange, b_{bf}, minus the beam web thickness and two times the beam web to end-plate weld thickness.

$$l_w = 2b_{bf} - t_{bw} - 2w$$
$$= 2(6\text{ in.}) - ¼\text{ in.} - 2(3/16\text{ in.})$$
$$= 11.4\text{ in.}$$

$$R_n = 0.60F_{EXX}\frac{t_{weld}}{\sqrt{2}}l_w(1.0 + 0.5\sin^{1.5}\theta) \qquad \text{(from } \textit{Spec.}\text{ Eq. J2-4)}$$
$$= 0.60(70\text{ ksi})\left(\frac{⅜\text{ in.}}{\sqrt{2}}\right)(11.4\text{ in.})(1.0 + 0.5\sin^{1.5}90°)$$
$$= 190\text{ kips}$$

Compare the weld strength to the required tensile strength.

LRFD	ASD
$\phi R_n = 0.75(190\text{ kips})$ $= 143\text{ kips} \quad \geq \quad T_{uf} = 128\text{ kips}$ **o.k.**	$\frac{R_n}{\Omega} = \frac{190\text{ kips}}{2.00}$ $= 95.0\text{ kips} \quad \geq \quad T_{af} = 85.6\text{ kips}$ **o.k.**

The flange to end-plate weld consisting of a double-sided ⅜ in. fillet weld is adequate. (A CJP or PJP groove weld are alternate options.)

Check Beam Web to End-Plate Welds

The beam web to end-plate welds shown in Figure 5-6 are separately checked for (1) tension rupture in the region around the tension bolts, and (2) the remainder of the web for shear strength. The region around the tension bolts includes the stiffeners as shown in Figure 5-7.

As explained in Section 3.7.5, the demand for the web tension area, T_{uw} (LFD) or T_{aw} (ASD), is the calculated beam flange force, $T_{u,calc}$ (LRFD) or $T_{a,calc}$ (ASD). The web tension area is the area of the beam web from the inside of the beam tension flange to the underside of the stiffeners plus the cross-sectional area of the stiffeners.

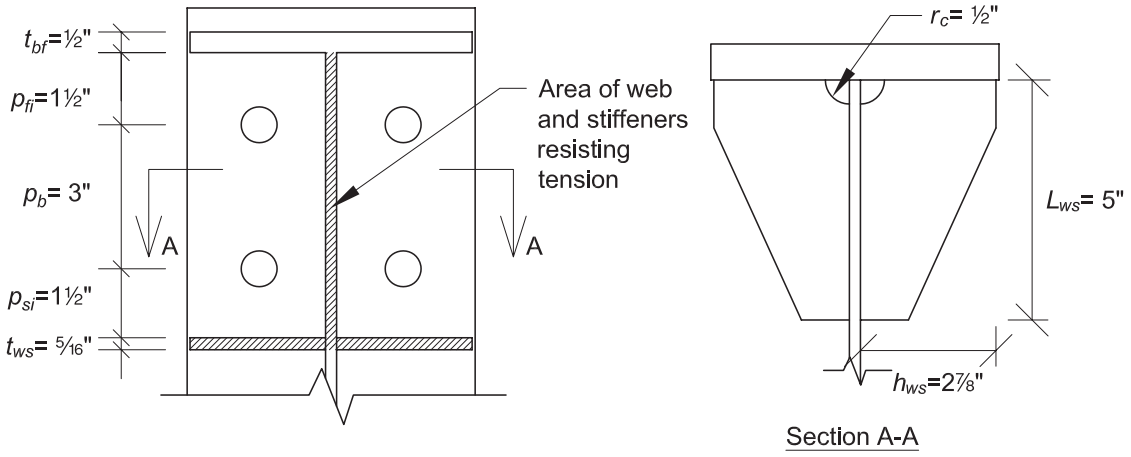

Fig. 5-7. Web and stiffener tension area for four-bolt stiffened configuration.

$$A_{wt} = t_{bw}(p_{fi} + p_b + p_s + t_{ws}) + 2t_{ws}(h_{ws} - r_c)$$
$$= (¼ \text{ in.})(1½ \text{ in.} + 3 \text{ in.} + 1½ \text{ in.} + 5⁄16 \text{ in.}) + 2(5⁄16 \text{ in.})(⅞ \text{ in.} - ½ \text{ in.})$$
$$= 3.07 \text{ in.}^2$$

The nominal web yield strength of the tension web region is

$$T_{yw} = F_y A_{wt} \qquad \text{(from } \textit{Spec.} \text{ Eq. J4-1)}$$
$$= (50 \text{ ksi})(3.07 \text{ in.}^2)$$
$$= 154 \text{ kips}$$

Check that the design tensile yield strength of the web tension area is sufficient.

LRFD	ASD
$\phi T_{yw} = 0.90(154 \text{ kips})$ $= 139 \text{ kips} \quad \geq \quad T_{uw} = 128 \text{ kips}$ **o.k.**	$\frac{T_{yw}}{\Omega} = \frac{154 \text{ kips}}{1.67}$ $= 92.2 \text{ kips} \quad \geq \quad T_{aw} = 85.6 \text{ kips}$ **o.k.**

Check that the required strength is at least 60% (LRFD) or 40% (ASD) of the web tensile strength from Equations 3-41.

LRFD	ASD
$0.60T_{yw} = 0.60(154 \text{ kips})$ $= 92.4 \text{ kips}$ $T_{uwd} = \max(T_{uw},\ 0.60T_{yw})$ $= \max(128 \text{ kips}, 92.4 \text{ kips})$ $= 128 \text{ kips}$	$0.40T_{yw} = 0.40(154 \text{ kips})$ $= 61.6 \text{ kips}$ $T_{awd} = \max(T_{aw},\ 0.40T_{yw})$ $= \max(85.6 \text{ kips}, 61.6 \text{ kips})$ $= 85.6 \text{ kips}$

Check the web to end-plate weld in the tension area. Because the weld is loaded perpendicular to its longitudinal axis, the angle of loading, θ, is 90°.

The length of the specified double-sided 3⁄16 in. fillet welds is:

$$l_{wt} = (2 \text{ welds})(p_{fi} + p_b + p_{si} + t_{ws}) + (4 \text{ welds})(h_{ws} - r_c)$$
$$= (2 \text{ welds})(1½ \text{ in.} + 3 \text{ in.} + 1½ \text{ in.} + 5⁄16 \text{ in.}) + (4 \text{ welds})(2⅞ \text{ in.} - ½ \text{ in.})$$
$$= 22.1 \text{ in.}$$

$$R_n = 0.60F_{EXX}\frac{t_{weld}}{\sqrt{2}} l_{wt}(1.0 + 0.5\sin^{1.5}\theta) \qquad \text{(from } \textit{Spec.} \text{ Eq. J2-4)}$$
$$= 0.60(70 \text{ ksi})\left(\frac{3⁄16 \text{ in.}}{\sqrt{2}}\right)(22.1 \text{ in.})(1.0 + 0.5\sin^{1.5} 90°)$$
$$= 185 \text{ kips}$$

LRFD	ASD
$\phi R_n = 0.75(185 \text{ kips})$ $= 139 \text{ kips} \quad \geq \quad T_{uwd} = 128 \text{ kips}$ **o.k.**	$\frac{R_n}{\Omega} = \frac{185 \text{ kips}}{2.00}$ $= 92.5 \text{ kips} \quad \geq \quad T_{awd} = 85.6 \text{ kips}$ **o.k.**

Check the web to end-plate weld away from the tension bolts. Only the web to end-plate weld between the end of the assumed web tension length and the inside face of the bottom beam compression flange or the weld between the mid-depth of the beam and the inside face of the beam compression flange, whichever is smaller, is considered effective in resisting the beam end shear. The shear strength of this weld is compared to the required shear applied to the connection.

$$l_t = (d - 2t_{bf}) - (p_{fi} + p_b + p_{si} + t_{ws})$$
$$= \left[20 \text{ in.} - 2(\tfrac{1}{2} \text{ in.})\right] - (1\tfrac{1}{2} \text{ in.} + 3 \text{ in.} + 1\tfrac{1}{2} \text{ in.} + \tfrac{5}{16} \text{ in.})$$
$$= 12.7 \text{ in.}$$

$$l_{0.5w} = d/2 - t_{bf}$$
$$= (20 \text{ in.})/2 - \tfrac{1}{2} \text{ in.}$$
$$= 9.50 \text{ in.}$$

$$l_{wv} = \min(l_t,\ l_{0.5w})$$
$$= \min(12.7 \text{ in.}, 9.50 \text{ in.})$$
$$= 9.50 \text{ in.}$$

$$R_n = (2 \text{ welds}) 0.60 F_{EXX} \frac{t_{weld}}{\sqrt{2}} l_{wv} (1.0 + 0.5 \sin^{1.5} \theta) \qquad \text{(from } \textit{Spec.} \text{ Eq. J2-4)}$$
$$= (2 \text{ welds})(0.60)(70 \text{ ksi}) \left(\frac{\tfrac{3}{16} \text{ in.}}{\sqrt{2}}\right) (9.50 \text{ in.})(1.0 + 0.5 \sin^{1.5} 0°)$$
$$= 106 \text{ kips}$$

LRFD	ASD
$\phi R_n = 0.75(106 \text{ kips})$ $= 79.5 \text{ kips} \quad \geq \quad V_u = 25.8 \text{ kips}$ **o.k.**	$\frac{R_n}{\Omega} = \frac{106 \text{ kips}}{2.00}$ $= 53.0 \text{ kips} \quad \geq \quad V_a = 17.2 \text{ kips}$ **o.k.**

Check that the shear rupture strength of the beam web at the weld using AISC *Specification* Equation J4-4 is sufficient.

$$R_n = 0.60 F_u A_{nv} \qquad \text{(}\textit{Spec.}\text{ Eq. J4-4)}$$
$$= 0.60 F_u l_{wv} t_{bw}$$
$$= 0.60(65 \text{ ksi})(9.50 \text{ in.})(\tfrac{1}{4} \text{ in.})$$
$$= 92.6 \text{ kips}$$

LRFD	ASD
$\phi R_n = 0.75(92.6 \text{ kips})$ $= 69.5 \text{ kips} \quad \geq \quad V_u = 25.8 \text{ kips}$ **o.k.**	$\frac{R_n}{\Omega} = \frac{92.6 \text{ kips}}{2.00}$ $= 46.3 \text{ kips} \quad \geq \quad V_a = 17.2 \text{ kips}$ **o.k.**

The double-sided $\frac{3}{16}$ in. fillet weld from the web to the end plate is sufficient.

Check Web Stiffeners to Beam Web Welds

The web stiffener to beam web weld demand is the same as the demand resisted by the web stiffener to end-plate weld. The web stiffener to end-pate demand is taken as the area of the web stiffener in contact with the end plate divided by the total web tension area, A_{wt}, multiplied by the web tension area demand, T_{uw} (LRFD) and T_{aw} (ASD).

$$A_{ws} = t_{ws}(b_p - t_{bw} - 2r_c)$$
$$= (5/16 \text{ in.})\left[6 \text{ in.} - 1/4 \text{ in.} - 2(1/2 \text{ in.})\right]$$
$$= 1.49 \text{ in.}^2$$

LRFD	ASD
$T_{u,ws} = (A_{ws}/A_{wt})T_{uw}$ $= (1.49 \text{ in.}^2/3.07 \text{ in.}^2)(128 \text{ kips})$ $= 62.1 \text{ kips}$	$T_{a,ws} = (A_{ws}/A_{wt})T_{aw}$ $= (1.49 \text{ in.}^2/3.07 \text{ in.}^2)(85.6 \text{ kips})$ $= 41.5 \text{ kips}$

$$R_n = (4 \text{ welds})0.60F_{EXX}\frac{t_{weld}}{\sqrt{2}}(L_{ws} - r_c)(1.0 + 0.5\sin^{1.5}\theta) \quad \text{(from } \textit{Spec.} \text{ Eq. J2-4)}$$
$$= (4 \text{ welds})(0.60)(70 \text{ ksi})\left(\frac{3/16 \text{ in.}}{\sqrt{2}}\right)(5 \text{ in.} - 1/2 \text{ in.})(1.0 + 0.5\sin^{1.5} 0°)$$
$$= 100 \text{ kips}$$

LRFD	ASD
$\phi R_n = 0.75(100 \text{ kips})$ $= 75.0 \text{ kips} \quad \geq \quad T_{u,ws} = 62.1 \text{ kips}$ **o.k.**	$\frac{R_n}{\Omega} = \frac{100 \text{ kips}}{2}$ $= 50.0 \text{ kips} \quad \geq \quad T_{a,ws} = 41.5 \text{ kips}$ **o.k.**

The double-sided 3/16 in. fillet weld from the web stiffener to the beam web is sufficient.

Check that the shear rupture strength of the beam web and web stiffeners at the welds is sufficient using AISC *Specification* Equation J4-4.

$$R_n = 0.60F_uA_{nv} \quad \text{(}\textit{Spec.}\text{ Eq. J4-4)}$$
$$= 0.60F_u(2 \text{ lines})(L_{ws} - r_c)t_{bw}$$
$$= 0.60(65 \text{ ksi})(2 \text{ lines})(5 \text{ in.} - 1/2 \text{ in.})(1/4 \text{ in.})$$
$$= 87.8 \text{ kips}$$

LRFD	ASD
$\phi R_n = 0.75(87.8 \text{ kips})$ $= 65.8 \text{ kips} \quad \geq \quad V_u = 62.1 \text{ kips}$ **o.k.**	$\frac{R_n}{\Omega} = \frac{87.8 \text{ kips}}{2.00}$ $= 43.9 \text{ kips} \quad \geq \quad V_a = 41.5 \text{ kips}$ **o.k.**

Because the web stiffeners thickness is 5/16 in., the shear rupture strength of the stiffeners is sufficient.

The web stiffener and beam web base metal adjacent to the web stiffener welds are sufficient.

C. Check Column-Side Limit States

See Example 5.2-1 for example column-side limit state check calculations.

Summary

The connection shown in Figure 5-6 is adequate for the required moment and shear force.

EXAMPLE 5.2-5—Six-Bolt Flush Unstiffened Thick End-Plate Example

Given:

The connection shown in Figure 5-8 is a six-bolt flush, unstiffened end-plate moment connection for a built-up beam. Beam and end-plate material are ASTM A572/A572M Grade 50. Bolts are ASTM F3125/F3125M Grade A490 pretensioned, and weld electrodes are E70XX. The connection is to be evaluated as a thick end-plate design for the following required moments and shear forces.

	LRFD	ASD
Moment	M_u = 14,000 kip-in.	M_a = 9,330 kip-in.
Shear force	V_u = 80.0 kips	V_a = 53.3 kips

Solution:

From AISC *Manual* Table 2-4, the material properties are as follows:

ASTM A572/A572M Grade 50
F_y = 50 ksi
F_u = 65 ksi

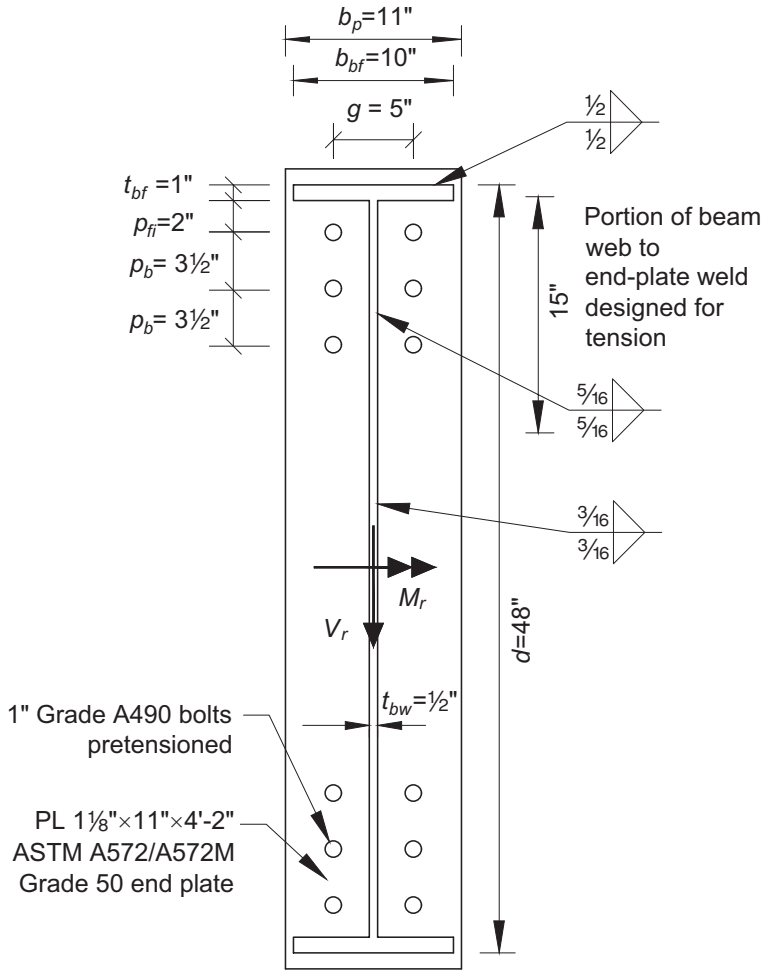

Fig. 5-8. Six-bolt unstiffened flush end-plate configuration for Example 5.2-5.

From AISC *Specification* Table J3.2, the material properties of the bolts are as follows:

Group 150 ASTM F3125/F3125M 1-in.-diameter Grade A490 pretensioned
F_{nt} = 113 ksi
F_{nv} = 68 ksi (Group 150 bolts with threads not excluded from the shear plane; thread condition N)

Beam
d = 48 in. t_{bw} = ½ in.
b_{bf} = 10 in. t_{bf} = 1 in.

End-plate geometric properties:
b_p = 11 in.
t_p = 1⅛ in.
g = 5 in.
p_{fi} = 2 in.
p_b = 3½ in.
d_p = 50 in.

The distances from the centerline of the compression flange to the bolt lines, h_1, h_2, and h_3, are depicted in Table 5-6 and computed as:

$$h_1 = d - \frac{3t_{bf}}{2} - p_{fi}$$
$$= 48 \text{ in.} - \frac{3(1 \text{ in.})}{2} - 2 \text{ in.}$$
$$= 44.5 \text{ in.}$$

$$h_2 = d - \frac{3t_{bf}}{2} - p_{fi} - p_b$$
$$= 48 \text{ in.} - \frac{3(1 \text{ in.})}{2} - 2 \text{ in.} - 3\text{½ in.}$$
$$= 41.0 \text{ in.}$$

$$h_3 = d - \frac{3t_{bf}}{2} - p_{fi} - 2p_b$$
$$= 48 \text{ in.} - \frac{3(1 \text{ in.})}{2} - 2 \text{ in.} - 2(3\text{½ in.})$$
$$= 37.5 \text{ in.}$$

$$b_{p,eff} \le b_{bf} + \max(t_p, 1 \text{ in.}) \quad (4\text{-}3)$$
$$\le 10 \text{ in.} + \max(1\text{⅛ in.}, 1 \text{ in.})$$
$$\le 11.1 \text{ in.}$$

b_p = 11 in. ≤ 11.1 in. **o.k.**

$$b_{bf} \ge g \quad (4\text{-}1)$$
10 in. ≥ 5 in. **o.k.**

A. End-Plate and Bolt Design Verification

Determine if the specified bolt diameter, 1 in., and end-plate thickness, 1⅛ in., are sufficient using the thick end-plate/smaller bolt diameter procedure.

Solve for the required bolt diameter using Equations 5-3. For Grade A490 bolts, the nominal tensile stress is F_{nt} = 113 ksi.

$$\sum_i n_i h_i = 2(44.5\text{ in.}) + 2(41.0\text{ in.}) + 2(37.5\text{ in.})$$
$$= 246\text{ in.}$$

LRFD	ASD
$d_{b,reqd} = \sqrt{\dfrac{4M_u}{\pi\phi F_{nt}\left(\sum_i n_i h_i\right)}}$ $= \sqrt{\dfrac{4(14{,}000\text{ kip-in.})}{\pi(0.75)(113\text{ ksi})(246\text{ in.})}}$ $= 0.925\text{ in.} \quad \le \quad 1\text{ in.} \quad$ **o.k.**	$d_{b,reqd} = \sqrt{\dfrac{4M_a}{\frac{\pi F_{nt}}{\Omega}\left(\sum_i n_i h_i\right)}}$ $= \sqrt{\dfrac{4(9{,}330\text{ kip-in.})}{\frac{\pi(113\text{ ksi})}{2.00}(246\text{ in.})}}$ $= 0.924\text{ in.} \quad \le \quad 1\text{ in.} \quad$ **o.k.**

Solve for the required end-plate thickness using Equations 5-4. First solve for the distance, s, and yield line parameter, Y_p, using Table 5-6.

$$s = \frac{\sqrt{b_p g}}{2}$$
$$= \frac{\sqrt{(11\text{ in.})(5\text{ in.})}}{2}$$
$$= 3.71\text{ in.}$$

Because $s \ge p_{fi} = 2.00$, the dimension p_{fi} is used in the equation for the yield line parameter.

$$Y_p = \frac{b_p}{2}\left[h_1\left(\frac{1}{p_{fi}}\right) + h_3\left(\frac{1}{s}\right)\right] + \frac{2}{g}\left[h_1(p_{fi} + 1.50p_b) + h_3(s + 0.50p_b)\right] + \frac{g}{2}$$
$$= \left(\frac{11\text{ in.}}{2}\right)\left[(44.5\text{ in.})\left(\frac{1}{2\text{ in.}}\right) + (37.5\text{ in.})\left(\frac{1}{3.71\text{ in.}}\right)\right]$$
$$+ \left(\frac{2}{5\text{ in.}}\right)\left\{(44.5\text{ in.})\left[2\text{ in.} + 1.50(3\text{½ in.})\right] + (37.5\text{ in.})\left[3.71\text{ in.} + 0.50(3\text{½ in.})\right]\right\} + \frac{5\text{ in.}}{2}$$
$$= 391\text{ in.}$$

Determine the required end-plate thickness using Equations 5-4. For flush end-plate configurations, $\gamma_r = 0.80$.

LRFD	ASD
$t_{p,reqd} = \sqrt{\dfrac{1.10M_u}{\gamma_r\phi_b F_{py} Y_p}}$ $= \sqrt{\dfrac{1.10(14{,}000\text{ kip-in.})}{0.80(0.90)(50\text{ ksi})(391\text{ in.})}}$ $= 1.05\text{ in.} \quad \le \quad 1\text{⅛ in.} \quad$ **o.k.**	$t_{p,reqd} = \sqrt{\dfrac{1.10M_a}{\gamma_r F_{py} Y_p/\Omega_b}}$ $= \sqrt{\dfrac{1.10(9{,}330\text{ kip-in.})}{0.80(50\text{ ksi})(391\text{ in.})/1.67}}$ $= 1.05\text{ in.} \quad \le \quad 1\text{⅛ in.} \quad$ **o.k.**

The specified 1-in.-diameter Grade A490 pretensioned bolts and 1⅛ in. ASTM A572/A572M Grade 50 end plate are sufficient.

Check Shear Transfer Strength at the Bottom Holes

See Example 5.2-1 for calculation procedures.

B. Check Beam to End-Plate Welds

The minimum weld size in AISC *Specification* Table J2.4 is determined from the material thickness of the thinner part joined. The weld sizes shown in Figure 5-8 satisfy the requirements in Table J2.4.

Check Beam Flange to End-Plate Weld

The weld from the beam flange to the end plate is shown in Figure 5-8 as a double-sided ½ in. fillet weld. Determine if this weld is adequate. First, find the required tensile force as the maximum of either the calculated flange tensile force from Equation 3-39 or 60% of the flange tensile strength for LRFD and 40% of the flange tensile strength for ASD (Equations 3-38), but not greater than the yield strength of the tension flange.

LRFD	ASD
$T_{u,calc} = \dfrac{M_u}{d - t_{bf}}$ $= \dfrac{14{,}000 \text{ kip-in.}}{48 \text{ in.} - 1 \text{ in.}}$ $= 298 \text{ kips}$ $T_{yf} = F_y b_{bf} t_{bf}$ $= (50 \text{ ksi})(10 \text{ in.})(1 \text{ in.})$ $= 500 \text{ kips}$ $T_{u,min} = 0.60 F_y b_{bf} t_{bf}$ $= 0.60(50 \text{ ksi})(10 \text{ in.})(1 \text{ in.})$ $= 300 \text{ kips}$ $T_{uf} = \max(T_{u,calc},\ T_{u,min}) \quad \le \quad T_{yf}$ $= 300 \text{ kips} \quad \le \quad T_{yf} = 500 \text{ kips}$	$T_{a,calc} = \dfrac{M_a}{d - t_{bf}}$ $= \dfrac{9{,}330 \text{ kip-in.}}{48 \text{ in.} - 1 \text{ in.}}$ $= 199 \text{ kips}$ $\dfrac{T_{yf}}{1.50} = \dfrac{F_y}{1.50} b_{bf} t_{bf}$ $= \dfrac{50 \text{ ksi}}{1.50}(10 \text{ in.})(1 \text{ in.})$ $= 333 \text{ kips}$ $T_{a,min} = 0.40 F_y b_{bf} t_{bf}$ $= 0.40(50 \text{ ksi})(10 \text{ in.})(1 \text{ in.})$ $= 200 \text{ kips}$ $T_{af} = \max(T_{a,calc},\ T_{a,min}) \quad \le \quad T_{yf}/1.50$ $= 200 \text{ kips} \quad \le \quad \dfrac{T_{yf}}{1.50} = 333 \text{ kips}$

Calculate the strength of the double-sided ½ in. fillet weld. Because the weld is loaded perpendicular to its longitudinal axis, the angle of loading, θ, is 90°. The length of the weld is two times the width of the beam flange, b_{bf}, minus the beam web thickness, and two times the beam web to end-plate weld.

$$l_w = 2b_{bf} - t_{bw} - 2w$$
$$= 2(10 \text{ in.}) - ½ \text{ in.} - 2(5⁄16 \text{ in.})$$
$$= 18.9 \text{ in.}$$

$$R_n = 0.60 F_{EXX} \frac{t_{weld}}{\sqrt{2}} l_w (1.0 + 0.5 \sin^{1.5} \theta) \qquad \text{(from } \textit{Spec.} \text{ Eq. J2-4)}$$
$$= 0.60(70 \text{ ksi}) \left(\frac{½ \text{ in.}}{\sqrt{2}} \right) (18.9 \text{ in.})(1.0 + 0.5 \sin^{1.5} 90°)$$
$$= 421 \text{ kips}$$

Compare the weld strength to the required tension strength.

LRFD	ASD
$\phi R_n = 0.75(421 \text{ kips})$ $= 316 \text{ kips} \quad \geq \quad T_{uf} = 300 \text{ kips}$ **o.k.**	$\frac{R_n}{\Omega} = \frac{421 \text{ kips}}{2.00}$ $= 211 \text{ kips} \quad \geq \quad T_{af} = 200 \text{ kips}$ **o.k.**

The flange to end-plate weld consisting of a double-sided ½ in. fillet weld is adequate. (A CJP or a PJP groove weld are alternate options.)

Check Beam Web to End-Plate Weld

The beam web to end-plate weld, shown in Figure 5-8, is separately checked for (1) tension rupture in the region around the tension bolts (extending 6 in. to the inside of the tension bolts), and (2) the remainder of the web to end-plate weld is checked for shear.

As explained in Section 3.7.5, the demand for the web tension area, T_{uw} (LFRD) or T_{aw} (ASD), for this connection is the number of tension bolts adjacent to the web, n_{trib}, divided by the total number of tension bolts, n, times the calculated beam flange force, $T_{u,calc}$ (LRFD) or $T_{a,calc}$, (ASD) from the beam flange to end-plate weld demand calculations. Using Equation 3-40:

LRFD	ASD
$T_{uw} = (n_{trib}/n)T_{u,calc}$ $= (6/6)(298 \text{ kips})$ $= 298 \text{ kips}$	$T_{aw} = (n_{trib}/n)T_{a,calc}$ $= (6/6)(199 \text{ kips})$ $= 199 \text{ kips}$

The length of the tension area region is measured from the inside of the beam flange to 6 in. inside the tension bolt row:

$$l_{wt} = p_{fi} + 2p_b + 6 \text{ in.}$$
$$= 2 \text{ in.} + 2(3\text{½ in.}) + 6 \text{ in.}$$
$$= 15.0 \text{ in.}$$

The nominal web yield strength in the tension region is

$$T_{yw} = F_y A_g \qquad \text{(from } \textit{Spec.} \text{ Eq. J4-1)}$$
$$= F_y t_{bw} l_{wt}$$
$$= (50 \text{ ksi})(\text{½ in.})(15.0 \text{ in.})$$
$$= 375 \text{ kips}$$

Check that the design tensile yield strength of the web is sufficient.

LRFD	ASD
$\phi T_{yw} = 0.90(375 \text{ kips})$ $= 338 \text{ kips} \quad \geq \quad T_{uw} = 298 \text{ kips}$ **o.k.**	$\frac{T_{yw}}{\Omega} = \frac{375 \text{ kips}}{1.67}$ $= 225 \text{ kips} \quad \geq \quad T_{aw} = 199 \text{ kips}$ **o.k.**

Check that the required strength is at least 60% (LRFD) or 40% (ASD) of the nominal web tensile strength from Equations 3-41.

LRFD	ASD
$0.60T_{yw} = 0.60(375 \text{ kips})$ $= 225 \text{ kips}$ $T_{uwd} = \max(T_{uw}, 0.60T_{yw})$ $= \max(298 \text{ kips}, 225 \text{ kips})$ $= 298 \text{ kips}$	$0.40T_{yw} = 0.40(375 \text{ kips})$ $= 150 \text{ kips}$ $T_{awd} = \max(T_{aw}, 0.40T_{yw})$ $= \max(199 \text{ kips}, 150 \text{ kips})$ $= 199 \text{ kips}$

Check the web to end-plate weld around the tension bolts. Because the weld is loaded perpendicular to its longitudinal axis, the angle of loading, θ, is 90°.

$$R_n = (2 \text{ welds})0.60F_{EXX}\frac{t_{weld}}{\sqrt{2}}l_{wt}(1.0 + 0.5\sin^{1.5}\theta) \quad \text{(from } \textit{Spec.} \text{ Eq. J2-4)}$$

$$= (2 \text{ welds})(0.60)(70 \text{ ksi})\left(\frac{5/16 \text{ in.}}{\sqrt{2}}\right)(15.0 \text{ in.})(1.0 + 0.5\sin^{1.5} 90°)$$

$$= 418 \text{ kips}$$

LRFD	ASD
$\phi R_n = 0.75(418 \text{ kips})$ $= 314 \text{ kips} \geq T_{uwd} = 298 \text{ kips}$ **o.k.**	$\frac{R_n}{\Omega} = \frac{418 \text{ kips}}{2.00}$ $= 209 \text{ kips} \geq T_{awd} = 199 \text{ kips.}$ **o.k.**

Only the web to end-plate weld between the mid-depth of the beam and the inside face of the beam compression flange or the weld between the end of the assumed web tension length and the inside face of the bottom beam compression flange, whichever is smaller, is considered effective in resisting the beam end shear. The shear strength of this weld is compared to the required shear applied to the connection.

$$l_t = (d - 2t_{bf}) - l_{wt}$$
$$= 48 \text{ in.} - 2(1 \text{ in.}) - 15.0 \text{ in.}$$
$$= 31.0 \text{ in.}$$

$$l_{0.5w} = d/2 - t_{bf}$$
$$= (48 \text{ in.})/2 - 1 \text{ in.}$$
$$= 23.0 \text{ in.}$$

$$l_{wv} = \min(l_t, l_{0.5w})$$
$$= \min(31.0 \text{ in.}, 23.0 \text{ in.})$$
$$= 23.0 \text{ in.}$$

$$R_n = (2 \text{ welds})0.60F_{EXX}\frac{t_{weld}}{\sqrt{2}}l_{wv}(1.0 + 0.5\sin^{1.5}\theta) \quad \text{(from } \textit{Spec.} \text{ Eq. J2-4)}$$

$$= (2 \text{ welds})(0.60)(70 \text{ ksi})\left(\frac{3/16 \text{ in.}}{\sqrt{2}}\right)(23.0 \text{ in.})(1.0 + 0.5\sin^{1.5} 0°)$$

$$= 256 \text{ kips}$$

LRFD	ASD
$\phi R_n = 0.75(256 \text{ kips})$ $= 192 \text{ kips} \quad \geq \quad V_u = 80.0 \text{ kips}$ **o.k.**	$\frac{R_n}{\Omega} = \frac{256 \text{ kips}}{2.00}$ $= 128 \text{ kips} \quad \geq \quad V_a = 53.3 \text{ kips}$ **o.k.**

Check that the shear rupture strength of the beam web at the weld using AISC *Specification* Equation J4-4 is sufficient.

$R_n = 0.60F_uA_{nv}$ (*Spec.* Eq. J4-4)
$= 0.60F_ul_{wv}t_{bw}$
$= 0.60(65 \text{ ksi})(23.0 \text{ in.})(\frac{1}{2} \text{ in.})$
$= 449 \text{ kips}$

LRFD	ASD
$\phi R_n = 0.75(449 \text{ kips})$ $= 337 \text{ kips} \quad \geq \quad V_u = 80.0 \text{ kips}$ **o.k.**	$\frac{R_n}{\Omega} = \frac{449 \text{ kips}}{2.00}$ $= 225 \text{ kips} \quad \geq \quad V_a = 53.3 \text{ kips}$ **o.k.**

The double-sided 5⁄16 in. fillet weld in the tension region and double-sided 3⁄16 in. fillet weld along the rest of the web to the end plate is sufficient.

C. Check Column-Side Limit States

See Example 5.2-1 for example column-side limit state check calculations.

Summary

The connection shown in Figure 5-8 is adequate for the required moment and shear force.

EXAMPLE 5.2-6—Six-Bolt Flush Four-Wide/Two-Wide Unstiffened Thick End-Plate Example

Given:

The connection shown in Figure 5-9 is a six-bolt flush, four-wide/two-wide, unstiffened end-plate moment connection for a built-up beam. Beam and end-plate material are ASTM A572/A572M Grade 50. Bolts are Group 150 ASTM F3125/F3125M Grade A490 pretensioned, and weld electrodes are E70XX. The connection is to be evaluated as a thick end-plate design for the following required moments and shear forces.

	LRFD	ASD
Moment	$M_u = 15{,}000$ kip-in.	$M_a = 10{,}000$ kip-in.
Shear force	$V_u = 87.9$ kips	$V_a = 58.6$ kips

Solution:

From AISC *Manual* Table 2-4, the material properties are as follows:

ASTM A572/A572M Grade 50
$F_y = 50$ ksi
$F_u = 65$ ksi

From AISC *Specification* Table J3.2, the material properties of the bolts are as follows:

Group 150 ASTM F3125/F3125M 1-in.-diameter Grade A490 pretensioned
F_{nt} = 113 ksi
F_{nv} = 68 ksi (Group 150 bolts with threads not excluded from the shear plane; thread condition N)

Beam
d = 48 in. t_{bw} = ½ in.
b_{bf} = 13 in. t_{bf} = ¾ in.

End-plate geometric properties:
b_p = 14 in.
t_p = 1⅛ in.
g = 4 in.
g_o = 3½ in.
p_{fi} = 2 in.
p_b = 3½ in.
d_p = 49 in.

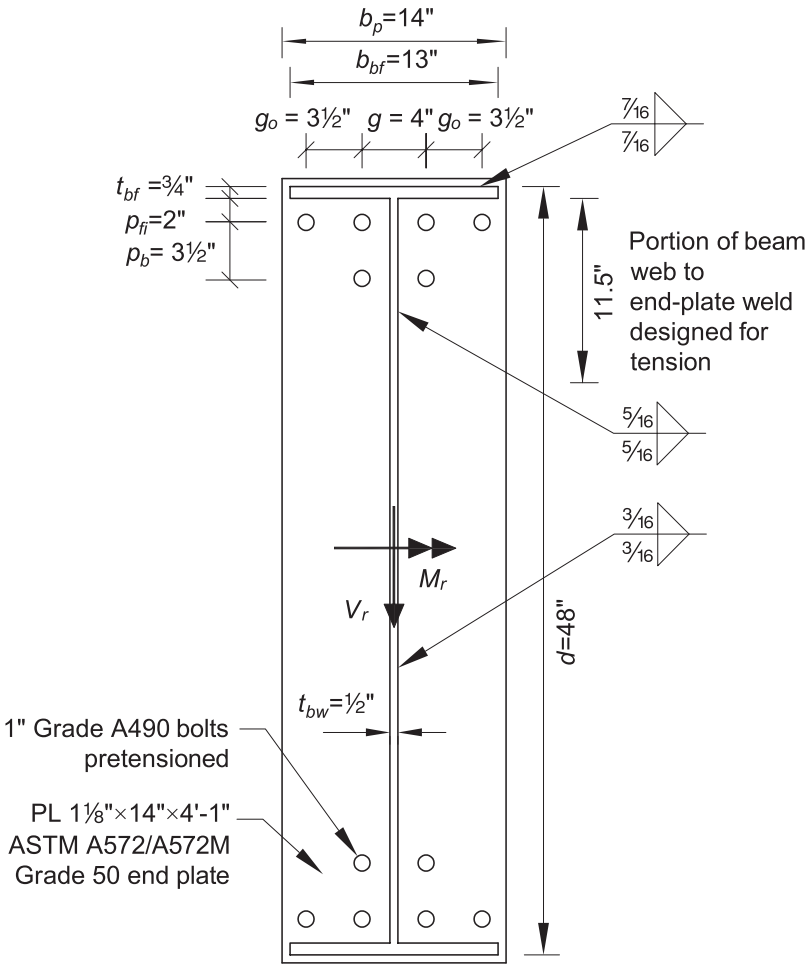

Fig. 5-9. Six-bolt flush four-wide/two-wide unstiffened end-plate configuration for Example 5.2-6.

The distances from the centerline of the compression flange to the bolt lines, h_1 and h_2, are depicted in Table 5-7 and computed as:

$$h_1 = d - \frac{3}{2}t_{bf} - p_{fi}$$
$$= 48 \text{ in.} - \frac{3(¾ \text{ in.})}{2} - 2 \text{ in.}$$
$$= 44.9 \text{ in.}$$

$$h_2 = d - \frac{3}{2}t_{bf} - p_{fi} - p_b$$
$$= 48 \text{ in.} - \frac{3(¾ \text{ in.})}{2} - 2 \text{ in.} - 3½ \text{ in.}$$
$$= 41.4 \text{ in.}$$

$$b_{p,eff} \le b_{bf} + \max(t_p, 1 \text{ in.}) \quad (4\text{-}3)$$
$$\le 13 \text{ in.} + \max(1⅛ \text{ in.}, 1 \text{ in.})$$
$$\le 14.1 \text{ in.}$$

$b_p = 14 \text{ in.} \le 14.1 \text{ in.}$ **o.k.**

$$b_{bf} \ge g + 2g_o \quad (4\text{-}2)$$
$$13 \text{ in.} \ge 4 \text{ in.} + 2(3½ \text{ in.})$$
$13 \text{ in.} \ge 11.0 \text{ in.}$ **o.k.**

A. End-Plate and Bolt Design Verification

Determine if the specified 1-in.-diameter Grade A490 pretensioned bolts and 1⅛ in. end-plate thickness are sufficient using the thick end-plate/smaller bolt diameter procedure.

Solve for the required bolt diameter using Equations 5-3. For Grade A490 bolts, the nominal tensile stress is $F_{nt} = 113$ ksi.

LRFD	ASD
$d_{b,reqd} = \sqrt{\frac{4M_u}{\pi\phi F_{nt}\left(\sum_i n_i h_i\right)}}$	$d_{b,reqd} = \sqrt{\frac{4M_a}{\frac{\pi F_{nt}}{\Omega}\left(\sum_i n_i h_i\right)}}$
$= \sqrt{\frac{4(15{,}000 \text{ kip-in.})}{\pi(0.75)(113 \text{ ksi})\left[4(44.9 \text{ in.}) + 2(41.4 \text{ in.})\right]}}$	$= \sqrt{\frac{4(10{,}000 \text{ kip-in.})}{\frac{\pi(113 \text{ ksi})}{2.00}\left[4(44.9 \text{ in.}) + 2(41.4 \text{ in.})\right]}}$
$= 0.927 \text{ in.} \le 1 \text{ in.}$ **o.k.**	$= 0.927 \text{ in.} \le 1 \text{ in.}$ **o.k.**

Solve for the required end-plate thickness using Equations 5-4. First solve for the distance, s, and yield line parameter, Y_p, using Table 5-7.

$$s = \frac{\sqrt{b_p g}}{2}$$
$$= \frac{\sqrt{(14 \text{ in.})(4 \text{ in.})}}{2}$$
$$= 3.74 \text{ in.}$$

Because $s \ge p_{fi} = 2$, the dimension p_{fi} is used in the equation for the yield line parameter.

$$Y_p = \frac{b_p}{2}\left[h_1\left(\frac{1}{p_{fi}}\right)+h_2\left(\frac{1}{s}\right)\right]+\frac{2}{g}\left[h_1\left(p_{fi}+0.75p_b\right)+h_2\left(s+0.25p_b\right)\right]+\frac{g}{2}$$

$$=\left(\frac{14\text{ in.}}{2}\right)\left[(44.9\text{ in.})\left(\frac{1}{2\text{ in.}}\right)+(41.4\text{ in.})\left(\frac{1}{3.74\text{ in.}}\right)\right]$$

$$+\left(\frac{2}{4\text{ in.}}\right)\left\{(44.9\text{ in.})\left[2\text{ in.}+0.75(3\text{½ in.})\right]+(41.4\text{ in.})\left[3.74\text{ in.}+0.25(3\text{½ in.})\right]\right\}+\frac{4\text{ in.}}{2}$$

$$=436\text{ in.}$$

Determine the required end-plate thickness using Equations 5-4. For flush end-plate configurations, $\gamma_r = 0.80$.

LRFD	ASD
$t_{p,reqd} = \sqrt{\dfrac{1.10M_u}{\gamma_r\phi_b F_{py}Y_p}}$	$t_{p,reqd} = \sqrt{\dfrac{1.10M_a}{\gamma_r F_{py}Y_p/\Omega_b}}$
$= \sqrt{\dfrac{1.10(15{,}000\text{ kip-in.})}{0.80(0.90)(50\text{ ksi})(436\text{ in.})}}$	$= \sqrt{\dfrac{1.10(10{,}000\text{ kip-in.})}{0.80(50\text{ ksi})(436\text{ in.})/1.67}}$
$= 1.03\text{ in.} \le 1\text{⅛ in.}$ **o.k.**	$= 1.03\text{ in.} \le 1\text{⅛ in.}$ **o.k.**

The specified 1-in.-diameter Grade A490 pretensioned bolts and 1⅛ in. ASTM A572/A572M Grade 50 end plate are sufficient.

Check Shear Transfer Strength at the Bottom Holes

See Example 5.2-1 for calculation procedures.

B. Check Beam to End-Plate Welds

The minimum weld size in AISC *Specification* Table J2.4 is determined from the material thickness of the thinner part joined. The weld sizes shown in Figure 5-9 satisfy the requirements in Table J2.4.

Check Beam Flange to End-Plate Weld

The weld from the beam flange to the end plate is shown in Figure 5-9 as a double-sided 7⁄16 in. fillet weld. Determine if this weld is adequate. First, find the required tensile force as the maximum of either the calculated flange tensile force or 60% of the flange tensile strength for LRFD and 40% of the flange tensile strength for ASD (Equations 3-38), but not greater than the yield strength of the tension flange.

LRFD	ASD
$T_{u,calc} = \dfrac{M_u}{d - t_{bf}}$ $= \dfrac{15{,}000 \text{ kip-in.}}{48 \text{ in.} - ¾ \text{ in.}}$ $= 317 \text{ kips}$ $T_{yf} = F_y b_{bf} t_{bf}$ $= (50 \text{ ksi})(13 \text{ in.})(¾ \text{ in.})$ $= 488 \text{ kips}$ $T_{u,min} = 0.60 F_y b_{bf} t_{bf}$ $= 0.60(50 \text{ ksi})(13 \text{ in.})(¾ \text{ in.})$ $= 293 \text{ kips}$ $T_{uf} = \max(T_{u,calc}, T_{u,min}) \quad \le \quad T_{yf}$ $= 317 \text{ kips} \quad \le \quad T_{yf} = 488 \text{ kips}$	$T_{a,calc} = \dfrac{M_a}{d - t_{bf}}$ $= \dfrac{10{,}000 \text{ kip-in.}}{48 \text{ in.} - ¾ \text{ in.}}$ $= 212 \text{ kips}$ $\dfrac{T_{yf}}{1.50} = \dfrac{F_y}{1.50} b_{bf} t_{bf}$ $= \dfrac{50 \text{ ksi}}{1.50}(13 \text{ in.})(¾ \text{ in.})$ $= 325 \text{ kips}$ $T_{a,min} = 0.40 F_y b_{bf} t_{bf}$ $= 0.40(50 \text{ ksi})(13 \text{ in.})(¾ \text{ in.})$ $= 195 \text{ kips}$ $T_{af} = \max(T_{a,calc}, T_{a,min}) \quad \le \quad T_{yf}/1.50$ $= 212 \text{ kips} \quad \le \quad \dfrac{T_{yf}}{1.50} = 325 \text{ kips}$

Calculate the strength of the double-sided 7⁄16 in. fillet weld. Because the weld is loaded perpendicular to its longitudinal axis, the angle of loading, θ, is 90°. The length of the weld is two times the width of the beam flange, b_{bf}, minus the beam web thickness, and two times the beam web to end-plate weld.

$$l_w = 2b_{bf} - t_{bw} - 2w$$
$$= 2(13 \text{ in.}) - ½ \text{ in.} - 2(5⁄16 \text{ in.})$$
$$= 24.9 \text{ in.}$$

$$R_n = 0.60 F_{EXX} \frac{t_{weld}}{\sqrt{2}} l_w (1.0 + 0.5 \sin^{1.5} \theta) \qquad \text{(from } \textit{Spec.} \text{ Eq. J2-4)}$$
$$= 0.60(70 \text{ ksi}) \left(\frac{7⁄16 \text{ in.}}{\sqrt{2}} \right) (24.9 \text{ in.})(1.0 + 0.5 \sin^{1.5} 90°)$$
$$= 485 \text{ kips}$$

Compare the weld strength to the required tensile strength.

LRFD	ASD
$\phi R_n = 0.75(485 \text{ kips})$ $= 364 \text{ kips} \quad \ge \quad T_{uf} = 317 \text{ kips}$ **o.k.**	$\dfrac{R_n}{\Omega} = \dfrac{485 \text{ kips}}{2.00}$ $= 243 \text{ kips} \quad \ge \quad T_{af} = 212 \text{ kips}$ **o.k.**

The flange to end-plate weld consisting of a double-sided 7⁄16 in. fillet weld is adequate. (A CJP or a PJP groove weld are alternate options.)

Check Beam Web to End-Plate Weld

The beam web to end-plate weld, shown in Figure 5-9, is separately checked for (1) tension rupture in the region around the tension bolts (extending 6 in. to the inside of the tension bolts), and (2) the remainder of the web to end-plate weld is checked for shear.

As explained in Section 3.7.5 the demand for the web tension area, T_{uw} (LRFD) or T_{aw} (ASD), for this connection is the number of tension bolts adjacent to the web, n_{trib}, divided by the total number of tension bolts, n, times the calculated beam flange force, $T_{u,calc}$ (LRFD) or $T_{a,calc}$, (ASD) from the beam flange to end-plate weld demand calculations. Using Equation 3-40:

LRFD	ASD
$T_{uw} = (n_{trib}/n)T_{u,calc}$ $= (4/6)(317 \text{ kips})$ $= 211 \text{ kips}$	$T_{aw} = (n_{trib}/n)T_{a,calc}$ $= (4/6)(212 \text{ kips})$ $= 141 \text{ kips}$

The length of the tension area region is measured from the inside of the beam flange to 6 in. inside the tension bolt row:

$l_{wt} = p_{fi} + p_b + 6 \text{ in.}$
$= 2 \text{ in.} + 3\text{½ in.} + 6 \text{ in.}$
$= 11.5 \text{ in.}$

The nominal web yield strength in the tension region is

$T_{yw} = F_y A_g$ (from *Spec.* Eq. J4-1)
$= F_y t_{bw} l_{wt}$
$= (50 \text{ ksi})(\text{½ in.})(11.5 \text{ in.})$
$= 288 \text{ kips}$

Check that the web design tensile yield strength of the web is sufficient.

LRFD	ASD
$\phi T_{yw} = 0.90(288 \text{ kips})$ $= 259 \text{ kips} \geq T_{uw} = 211 \text{ kips}$ **o.k.**	$\frac{T_{yw}}{\Omega} = \frac{288 \text{ kips}}{1.67}$ $= 172 \text{ kips} \geq T_{aw} = 141 \text{ kips}$ **o.k.**

Check that the required strength is at least 60% (LRFD) or 40% (ASD) of the nominal web tensile strength from Equations 3-41.

LRFD	ASD
$0.60T_{yw} = 0.60(288 \text{ kips})$ $= 173 \text{ kips}$ $T_{uwd} = \max(T_{uw}, 0.60T_{yw})$ $= \max(211 \text{ kips}, 173 \text{ kips})$ $= 211 \text{ kips}$	$0.40T_{yw} = 0.40(288 \text{ kips})$ $= 115 \text{ kips}$ $T_{awd} = \max(T_{aw}, 0.40T_{yw})$ $= \max(141 \text{ kips}, 115 \text{ kips})$ $= 141 \text{ kips}$

Check the web to end-plate weld around the tension bolts. Because the weld is loaded perpendicular to its longitudinal axis, the angle of loading, θ, is 90°.

$R_n = (2 \text{ welds})0.60F_{EXX}\frac{t_{weld}}{\sqrt{2}}l_{wt}(1.0 + 0.5\sin^{1.5}\theta)$ (from *Spec.* Eq. J2-4)
$= (2 \text{ welds})(0.60)(70 \text{ ksi})\left(\frac{\text{5⁄16 in.}}{\sqrt{2}}\right)(11.5 \text{ in.})(1.0 + 0.5\sin^{1.5}90°)$
$= 320 \text{ kips}$

LRFD	ASD
$\phi R_n = 0.75(320 \text{ kips})$ $= 240 \text{ kips} \quad \geq \quad T_{uwd} = 211 \text{ kips}$ **o.k.**	$\frac{R_n}{\Omega} = \frac{320 \text{ kips}}{2.00}$ $= 160 \text{ kips} \quad \geq \quad T_{awd} = 141 \text{ kips}$ **o.k.**

Only the web to end-plate weld between the mid-depth of the beam and the inside face of the beam compression flange or the weld between the end of the assumed web tension length and the inside face of the bottom beam compression flange, whichever is smaller, is considered effective in resisting the beam end shear. The shear strength of this weld is compared to the required shear applied to the connection.

$$l_t = (d - 2t_{bf}) - l_{wt}$$
$$= 48 \text{ in.} - 2(¾ \text{ in.}) - 11.5 \text{ in.}$$
$$= 35.0 \text{ in.}$$

$$l_{0.5w} = d/2 - t_{bf}$$
$$= (48 \text{ in.})/2 - ¾ \text{ in.}$$
$$= 23.3 \text{ in.}$$

$$l_{wv} = \min(l_t, l_{0.5w})$$
$$= \min(35.0 \text{ in.}, 23.3 \text{ in.})$$
$$= 23.3 \text{ in.}$$

$$R_n = (2 \text{ welds}) 0.60 F_{EXX} \frac{t_{weld}}{\sqrt{2}} l_{wv} (1.0 + 0.5 \sin^{1.5} \theta) \qquad \text{(from } \textit{Spec.} \text{ Eq. J2-4)}$$
$$= (2 \text{ welds})(0.60)(70 \text{ ksi}) \left(\frac{3/16 \text{ in.}}{\sqrt{2}} \right) (23.3 \text{ in.})(1.0 + 0.5 \sin^{1.5} 0°)$$
$$= 259 \text{ kips}$$

LRFD	ASD
$\phi R_n = 0.75(259 \text{ kips})$ $= 194 \text{ kips} \quad \geq \quad V_u = 87.9 \text{ kips}$ **o.k.**	$\frac{R_n}{\Omega} = \frac{259 \text{ kips}}{2.00}$ $= 130 \text{ kips} \quad \geq \quad V_a = 58.6 \text{ kips}$ **o.k.**

Check that the shear rupture strength of the beam web at the weld using AISC *Specification* Equation J4-4 is sufficient.

$$R_n = 0.60 F_u A_{nv} \qquad \text{(}\textit{Spec.}\text{ Eq. J4-4)}$$
$$= 0.60 F_u l_{wv} t_{bw}$$
$$= 0.60(65 \text{ ksi})(23.3 \text{ in.})(½ \text{ in.})$$
$$= 454 \text{ kips}$$

LRFD	ASD
$\phi R_n = 0.75(454 \text{ kips})$ $= 341 \text{ kips} \quad \geq \quad V_u = 87.9 \text{ kips}$ **o.k.**	$\frac{R_n}{\Omega} = \frac{454 \text{ kips}}{2.00}$ $= 227 \text{ kips} \quad \geq \quad V_a = 58.6 \text{ kips}$ **o.k.**

The double-sided 5/16 in. fillet weld in the tension region and double-sided 3/16 in. fillet weld along the rest of the web to the end plate is sufficient.

Table 5-9. Tested Parameter Range for Extended End-Plate Connections		
Parameter	**Low (in.)**	**High (in.)**
p_f	1	2½[1]
p_{ext}	2½	7½
g	2¾	7
g_o	2¼	3¾
d	15¾	72
b_p	5	10¼
t_f	⅜	1
[1] MRE 1/2 [Figure 1-4(d)], upper limit is 5 in.		

C. Check Column-Side Limit States

See Example 5.2-1 for example column-side limit state check calculations.

Summary

The connection shown in Figure 5-9 is adequate for the required moment and shear force.

5.3 EXTENDED END-PLATE CONNECTIONS

5.3.1 Design Tables and Limitations

The analytical procedures for the nine extended end-plate configurations shown in Figure 1-4 were verified through tests in which geometric parameters were varied among the test configurations (Structural Engineers Inc., 1984; Morrison et al., 1986; Abel and Murray, 1992, 1994; Rodkey and Murray, 1993b; Meng, 1996; Murray and Sumner, 1999; Blumenbaum and Murray, 2003; Jain et al., 2015; Szabo et al., 2017). Significant changes in the geometry could affect the mechanism configuration and thus the predicted strength. Therefore, the tested parameter ranges given in Table 5-9 with a variation of plus or minus 10% apply to the design equations for the extended end-plate configurations. The allowance for 10% variation from the tested values is consistent with the qualification requirements for IMF and SMF given in the AISC *Seismic Provisions*.

Design equations are given for each of the nine end-plate configurations in Tables 5-10 through 5-18. For the four-bolt extended stiffened, eight-bolt extended stiffened, and 12-bolt extended stiffened configurations, if the end-plate extension beyond the outermost tension bolt, d_e, is large (i.e., if d_e is greater than one to two times s), then the yield line pattern will change. See Eatherton et al. (2021) for an appropriate yield line parameter for these cases.

Table 5-10. Summary of Design Equations for Four-Bolt Extended Unstiffened End Plate

Geometry	Yield-Line Mechanism	Bolt Force Model
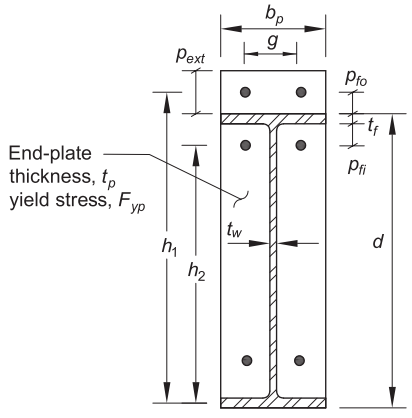	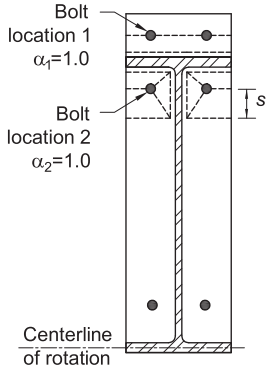	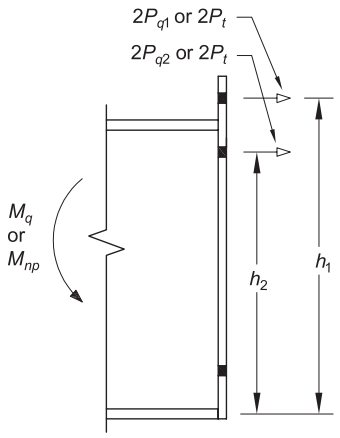

End-Plate Yield	$\phi M_n = \phi_b M_{pl} = \phi_b F_{yp} t_p^2 Y_p$ $Y_p = \frac{b_p}{2}\left[h_1\left(\frac{1}{p_{fo}}\right) + h_2\left(\frac{1}{p_{fi}} + \frac{1}{s}\right) - \frac{1}{2}\right] + \frac{2}{g}\left[h_2(s + p_{fi})\right]$	$\phi_b = 0.90$ $s = \frac{\sqrt{b_p g}}{2}$ Note: Use $p_{fi} = s$ if $p_{fi} > s$
Bolt Rupture with Prying Action	$\phi M_n = \phi_r M_q = \phi_r \sum_i \alpha_i n_i P_{qi} h_i = \phi_r (2P_{q1}h_1 + 2P_{q2}h_2)$ $P_{qi} = \max(P_t - Q_{max,i}, T_b)$	P_t = nominal bolt tensile strength $Q_{max,i}$ = prying force for bolt location i T_b = bolt pretension force n_i = number of bolts in bolt location i ϕ_r = 0.75
Bolt Rupture without Prying Action	$\phi M_n = \phi_r M_{np} = \phi_r P_t \sum_i n_i h_i = \phi_r P_t (2h_1 + 2h_2)$	$\phi_r = 0.75$

Table 5-11. Summary of Design Equations for Four-Bolt Extended Stiffened End Plate

Geometry	Yield-Line Mechanism	Bolt Force Model
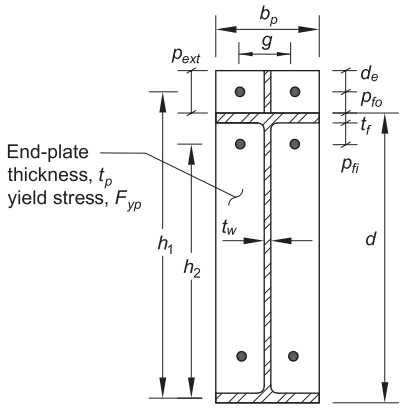	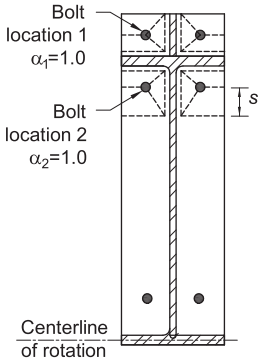	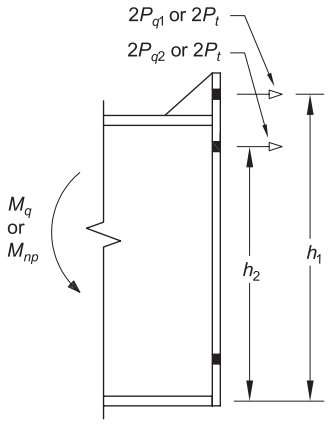

End-Plate Yield	$\phi M_n = \phi_b M_{pl} = \phi_b F_{yp} t_p^2 Y_p$ $Y_p = \frac{b_p}{2}\left[h_1\left(\frac{1}{p_{fo}}+\frac{1}{2d_e}\right)+h_2\left(\frac{1}{p_{fi}}+\frac{1}{s}\right)\right]$ $+\frac{2}{g}\left[h_1(p_{fo}+d_e)+h_2(p_{fi}+s)\right]$	$\phi_b = 0.90$ $s = \frac{\sqrt{b_p g}}{2}$ Applicable for $d_e < s$ Note: Use $p_{fi} = s$ if $p_{fi} > s$ Use $p_{fo} = s$ if $p_{fo} > s$
Bolt Rupture with Prying Action	$\phi M_n = \phi_r M_q = \phi_r \sum_i \alpha_i n_i P_{qi} h_i = \phi_r (2P_{q1}h_1 + 2P_{q2}h_2)$ $P_{qi} = \max(P_t - Q_{max,i}, T_b)$	P_t = nominal bolt tensile strength $Q_{max,i}$ = prying force for bolt location i T_b = bolt pretension force n_i = number of bolts in bolt location i ϕ_r = 0.75
Bolt Rupture without Prying Action	$\phi M_n = \phi_r M_{np} = \phi_r P_t \sum_i n_i h_i = \phi_r P_t (2h_1 + 2h_2)$	$\phi_r = 0.75$

Table 5-12. Summary of Design Equations for Multiple-Row Extended 1/2 Unstiffened End Plate

Geometry	Yield-Line Mechanism	Bolt Force Model
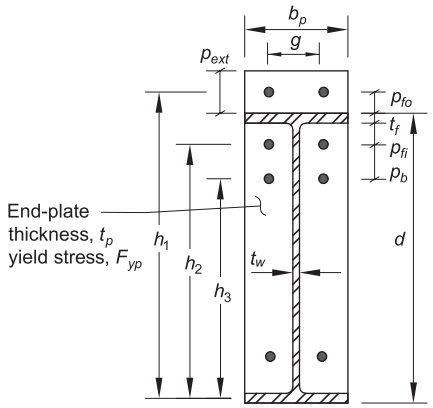	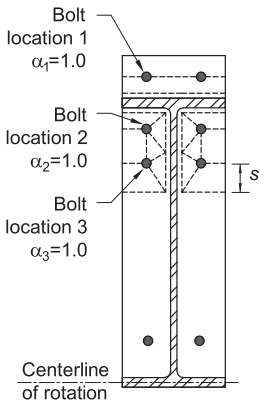	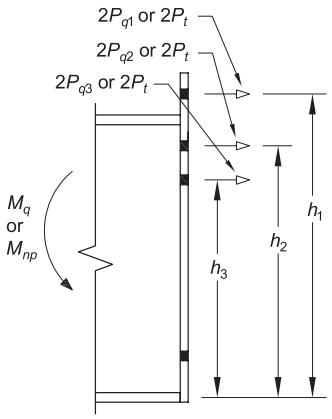

End-Plate Yield	$\phi M_n = \phi_b M_{pl} = \phi_b F_{yp} t_p^2 Y_p$ $Y_p = \frac{b_p}{2}\left[h_1\left(\frac{1}{p_{fo}}\right) + h_2\left(\frac{1}{p_{fi}}\right) + h_3\left(\frac{1}{s}\right) - \frac{1}{2}\right]$ $+ \frac{2}{g}\left[h_2\left(p_{fi} + \frac{3p_b}{4}\right) + h_3\left(s + \frac{p_b}{4}\right)\right] + \frac{g}{2}$	$\phi_b = 0.90$ $s = \frac{\sqrt{b_p g}}{2}$ Note: Use $p_{fi} = s$ if $p_{fi} > s$
Bolt Rupture with Prying Action	$\phi M_n = \phi_r M_q = \phi_r \sum_i \alpha_i n_i P_{qi} h_i = \phi_r (2P_{q1}h_1 + 2P_{q2}h_2 + 2P_{q3}h_3)$ $P_{qi} = \max(P_t - Q_{max,i}, T_b)$	P_t = nominal bolt tensile strength $Q_{max,i}$ = prying force for bolt location i T_b = bolt pretension force n_i = number of bolts in bolt location i ϕ_r = 0.75
Bolt Rupture without Prying Action	$\phi M_n = \phi_r M_{np} = \phi_r P_t \sum_i n_i h_i = \phi_r P_t (2h_1 + 2h_2 + 2h_3)$	$\phi_r = 0.75$

Table 5-13. Summary of Design Equations for Multiple-Row Extended 1/3 Unstiffened End Plate

Geometry	Yield-Line Mechanism	Bolt Force Model
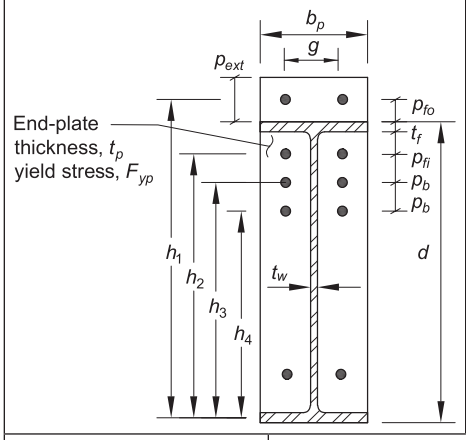	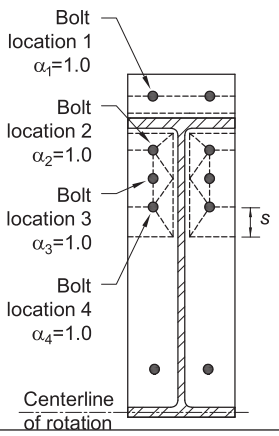	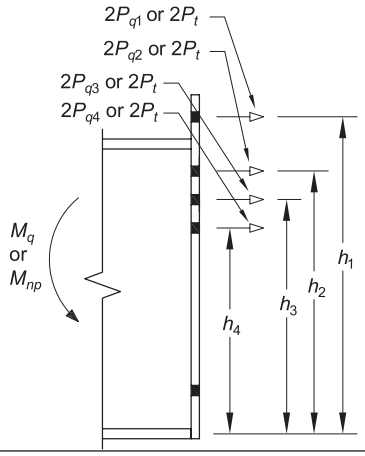

End-Plate Yield

$$\phi M_n = \phi_b M_{pl} = \phi_b F_{yp} t_p^2 Y_p$$

$$Y_p = \frac{b_p}{2}\left[h_1\left(\frac{1}{p_{fo}}\right) + h_2\left(\frac{1}{p_{fi}}\right) + h_4\left(\frac{1}{s}\right) - \frac{1}{2}\right] + \frac{2}{g}\left[h_2\left(p_{fi} + \frac{3p_b}{2}\right) + h_4\left(s + \frac{p_b}{2}\right)\right] + \frac{g}{2}$$

$\phi_b = 0.90$

$s = \dfrac{\sqrt{b_p g}}{2}$

Note: Use $p_{fi} = s$ if $p_{fi} > s$

Bolt Rupture with Prying Action

$$\phi M_n = \phi_r M_q = \phi_r \sum_i \alpha_i n_i P_{qi} h_i$$

$$= \phi_r (2P_{q1}h_1 + 2P_{q2}h_2 + 2P_{q3}h_3 + 2P_{q4}h_4)$$

$$P_{qi} = \max(P_t - Q_{max,i}, T_b)$$

P_t = nominal bolt tensile strength
$Q_{max,i}$ = prying force for bolt location i
T_b = bolt pretension force
n_i = number of bolts in bolt location i
$\phi_r = 0.75$

Bolt Rupture without Prying Action

$$\phi M_n = \phi_r M_{np} = \phi_r P_t \sum_i n_i h_i = \phi_r P_t (2h_1 + 2h_2 + 2h_3 + 2h_4)$$

$\phi_r = 0.75$

Table 5-14. Summary of Design Equations for Multiple-Row Extended 1/3 Stiffened End Plate

Geometry	Yield-Line Mechanism	Bolt Force Model
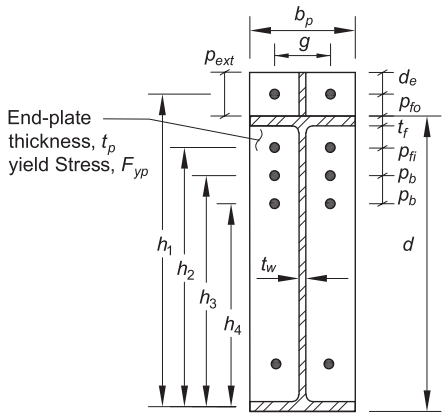	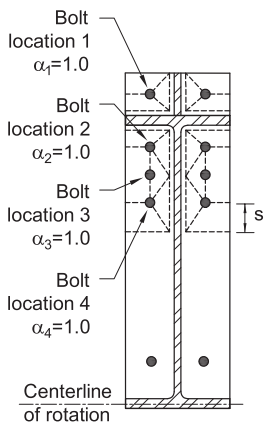	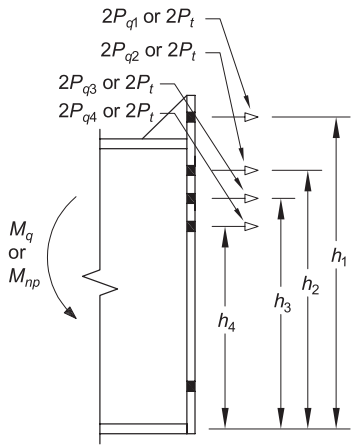

End-Plate Yield	$\phi M_n = \phi_b M_{pl} = \phi_b F_{yp} t_p^2 Y_p$ $Y_p = \frac{b_p}{2}\left[h_1\left(\frac{1}{p_{fo}}+\frac{1}{2d_e}\right)+h_2\left(\frac{1}{p_{fi}}\right)+h_4\left(\frac{1}{s}\right)\right]$ $+\frac{2}{g}\left[h_1(p_{fo}+d_e)+h_2\left(p_{fi}+\frac{3p_b}{2}\right)+h_4\left(\frac{p_b}{2}+s\right)\right]+\frac{g}{2}$	$\phi_b = 0.90$ $s = \frac{\sqrt{b_p g}}{2}$ Applicable for $d_e < s$ Note: Use $p_{fi} = s$ if $p_{fi} > s$ Use $p_{fo} = s$ if $p_{fo} > s$
Bolt Rupture with Prying Action	$\phi M_n = \phi_r M_q = \phi_r \sum_i \alpha_i n_i P_{qi} h_i$ $= \phi_r (2P_{q1}h_1 + 2P_{q2}h_2 + 2P_{q3}h_3 + 2P_{q4}h_4)$ $P_{qi} = \max(P_t - Q_{max,i}, T_b)$	P_t = nominal bolt tensile strength $Q_{max,i}$ = prying force for bolt location i T_b = bolt pretension force n_i = number of bolts in bolt location i ϕ_r = 0.75
Bolt Rupture without Prying Action	$\phi M_n = \phi_r M_{np} = \phi_r P_t \sum_i n_i h_i = \phi_r P_t (2h_1 + 2h_2 + 2h_3 + 2h_4)$	$\phi_r = 0.75$

Table 5-15. Summary of Design Equations for Eight-Bolt Extended Four-Wide Unstiffened End Plate

Geometry	Yield-Line Mechanism	Bolt Force Model
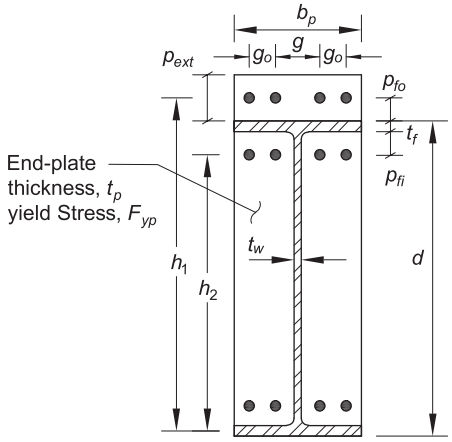	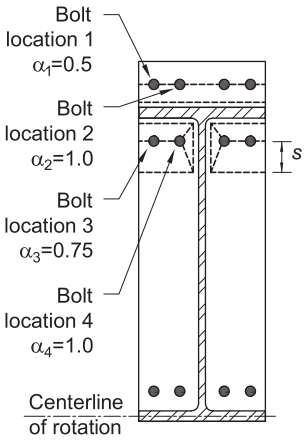	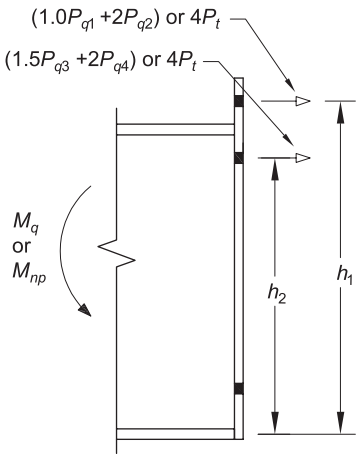

End-Plate Yield	$\phi M_n = \phi_b M_{pl} = \phi_b F_{yp} t_p^2 Y_p$ $Y_p = \frac{b_p}{2}\left[h_1\left(\frac{1}{p_{fo}}\right) + h_2\left(\frac{1}{p_{fi}} + \frac{1}{s}\right) - \frac{1}{2}\right] + \frac{2}{g}\left[h_2(p_{fi} + s)\right]$	$\phi_b = 0.90$ $s = \frac{\sqrt{b_p g}}{2}$ Note: Use $p_{fi} = s$ if $p_{fi} > s$
Bolt Rupture with Prying Action	$\phi M_n = \phi_r M_q = \phi_r \sum_i \alpha_i n_i P_{qi} h_i$ $= \phi_r (P_{q1} h_1 + 2P_{q2} h_1 + 1.5P_{q3} h_2 + 2P_{q4} h_2)$ $P_{qi} = \max(P_t - Q_{max,i}, T_b)$	P_t = nominal bolt tensile strength $Q_{max,i}$ = prying force for bolt location i T_b = bolt pretension force n_i = number of bolts in bolt location i ϕ_r = 0.75
Bolt Rupture without Prying Action	$\phi M_n = \phi_r M_{np} = \phi_r P_t \sum_i n_i h_i = \phi_r P_t (4h_1 + 4h_2)$	$\phi_r = 0.75$

Table 5-16. Summary of Design Equations for Eight-Bolt Extended Stiffened End Plate

Geometry	Yield-Line Mechanism	Bolt Force Model
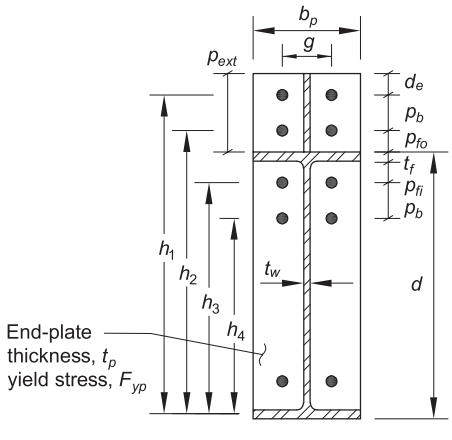	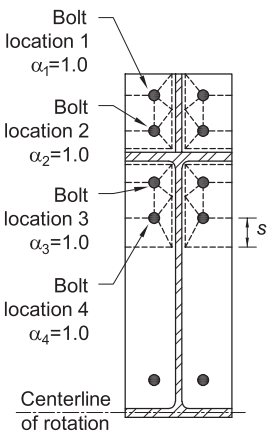	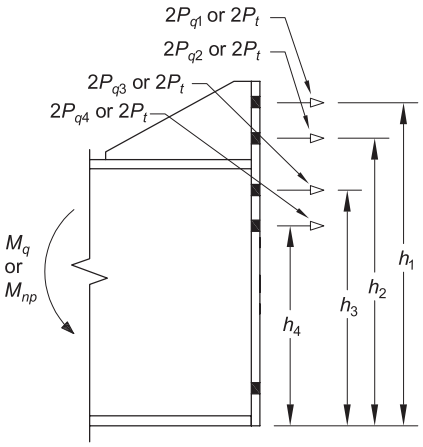

End-Plate Yield

$$\phi M_n = \phi_b M_{pl} = \phi_b F_{yp} t_p^2 Y_p$$

$$Y_p = \frac{b_p}{2}\left[h_1\left(\frac{1}{2d_e}\right) + h_2\left(\frac{1}{p_{fo}}\right) + h_3\left(\frac{1}{p_{fi}}\right) + h_4\left(\frac{1}{s}\right)\right] + \frac{2}{g}\left[h_1\left(d_e + \frac{3p_b}{4}\right) + h_2\left(p_{fo} + \frac{p_b}{4}\right) + h_3\left(p_{fi} + \frac{3p_b}{4}\right) + h_4\left(s + \frac{p_b}{4}\right)\right] + g$$

$\phi_b = 0.90$

$s = \dfrac{\sqrt{b_p g}}{2}$

Applicable for $d_e < s$

Note: Use $p_{fi} = s$ if $p_{fi} > s$

Use $p_{fo} = s$ if $p_{fo} > s$

Bolt Rupture with Prying Action

$$\phi M_n = \phi_r M_q = \phi_r \sum_i \alpha_i n_i P_{qi} h_i = \phi_r (2P_{q1}h_1 + 2P_{q2}h_2 + 2P_{q3}h_3 + 2P_{q4}h_4)$$

$$P_{qi} = \max(P_t - Q_{max,i}, T_b)$$

P_t = nominal bolt tensile strength

$Q_{max,i}$ = prying force for bolt location i

T_b = bolt pretension force

n_i = number of bolts in bolt location i

ϕ_r = 0.75

Bolt Rupture without Prying Action

$$\phi M_n = \phi_r M_{np} = \phi_r P_t \sum_i n_i h_i = \phi_r P_t (2h_1 + 2h_2 + 2h_3 + 2h_4)$$

$\phi_r = 0.75$

Table 5-17. Summary of Design Equations for 12-Bolt Multiple-Row Extended 1/3 Four-Wide/Two-Wide Unstiffened End Plate

Geometry	Yield-Line Mechanism	Bolt Force Model
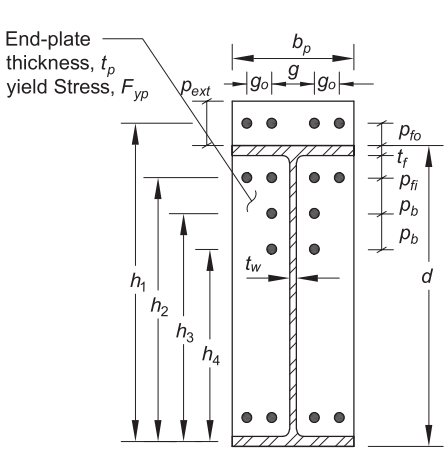	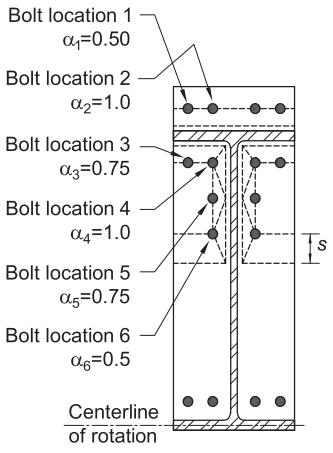	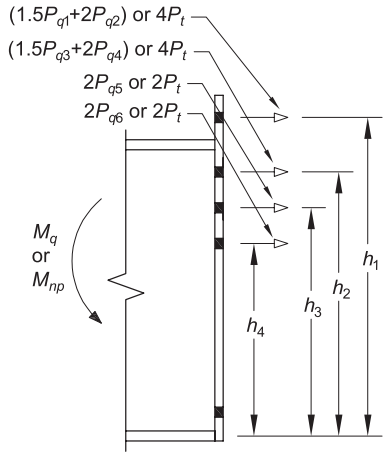

End-Plate Yield	$\phi M_n = \phi_b M_{pl} = \phi_b F_{yp} t_p^2 Y_p$ $Y_p = \frac{b_p}{2}\left[h_1\left(\frac{1}{p_{fo}}\right) + h_2\left(\frac{1}{p_{fi}}\right) + h_4\left(\frac{1}{s}\right) - \frac{1}{2}\right] + \frac{2}{g}\left[h_2\left(p_{fi} + \frac{3p_b}{2}\right) + h_4\left(s + \frac{p_b}{2}\right)\right] + \frac{g}{2}$	$\phi_b = 0.90$ $s = \frac{\sqrt{b_p g}}{2}$ Note: Use $p_{fi} = s$ if $p_{fi} > s$
Bolt Rupture with Prying Action	$\phi M_n = \phi_r M_q = \phi_r \sum_i \alpha_i n_i P_{qi} h_i$ $= \phi_r (P_{q1}h_1 + 2P_{q2}h_1 + 1.5P_{q3}h_2 + 2P_{q4}h_2 + 1.5P_{q5}h_3 + P_{q6}h_4)$ $P_{qi} = \max(P_t - Q_{max,i}, T_b)$	P_t = nominal bolt tensile strength $Q_{max,i}$ = prying force for bolt location i T_b = bolt pretension force n_i = number of bolts in bolt location i ϕ_r = 0.75
Bolt Rupture without Prying Action	$\phi M_n = \phi_r M_{np} = \phi_r P_t \sum_i n_i h_i = \phi_r P_t (4h_1 + 4h_2 + 2h_3 + 2h_4)$	$\phi_r = 0.75$

Table 5-18. Summary of Design Equations for 12-Bolt Extended Stiffened End Plate

Geometry	Yield-Line Mechanism	Bolt Force Model
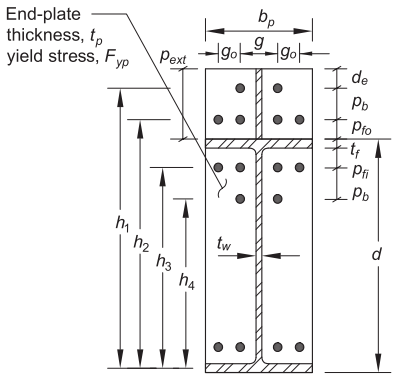	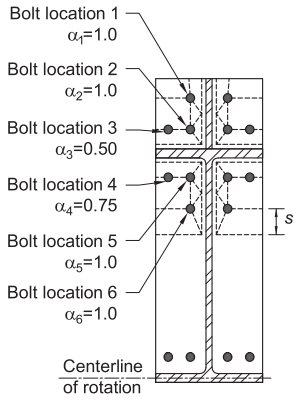	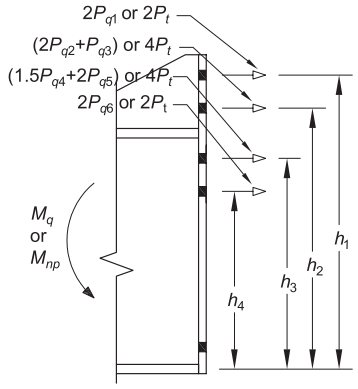

End-Plate Yield

$$\phi M_n = \phi_b M_{pl} = \phi_b F_{yp} t_p^2 Y_p$$

$$Y_p = \frac{b_p}{2}\left[h_2\left(\frac{1}{p_{fo}}\right)+h_3\left(\frac{1}{p_{fi}}\right)+h_4\left(\frac{1}{s}\right)-\frac{1}{2}\right] + \frac{2}{g}\left[h_1\left(d_e+\frac{3p_b}{4}\right)+h_2\left(p_{fo}+\frac{p_b}{4}\right) + h_3\left(p_{fi}+\frac{3p_b}{4}\right)+h_4\left(s+\frac{p_b}{4}\right)\right]+\frac{5g}{4}$$

$\phi_b = 0.90$

$s = \dfrac{\sqrt{b_p g}}{2}$

Note: Use $p_{fi} = s$ if $p_{fi} > s$

Use $p_{fo} = s$ if $p_{fo} > s$

Bolt Rupture with Prying Action

$$\phi M_n = \phi_r M_q = \phi_r \sum_i \alpha_i n_i P_{qi} h_i$$

$$= \phi_r (2P_{q1}h_1 + 2P_{q2}h_2 + P_{q3}h_2 + 1.5P_{q4}h_3 + 2P_{q5}h_3 + 2P_{q6}h_4)$$

$$P_{qi} = \max(P_t - Q_{max,i}, T_b)$$

P_t = nominal bolt tensile strength

$Q_{max,i}$ = prying force for bolt location i

T_b = bolt pretension force

n_i = number of bolts in bolt location i

$\phi_r = 0.75$

Bolt Rupture without Prying Action

$$\phi M_n = \phi_r M_{np} = \phi_r P_t \sum_i n_i h_i = \phi_r P_t (2h_1 + 4h_2 + 4h_3 + 2h_4)$$

$\phi_r = 0.75$

Table 5-19. Extended Thick End-Plate Analysis Examples						
Example	**End-Plate Configuration**	**Beam**	**Column**	**Bolts**	**Weld Calculations**	**Column-Side Limit States**
5.3-1	Four-bolt extended unstiffened thick end plate	Built-up[1] 8" × 24"	Built-up 8" × 26"	Grade A325 ¾ in. snug-tightened	Yes	Yes
5.3-2	Four-bolt extended stiffened thick end plate	W24×84	W14×99	Grade A490 1⅛ in. pretensioned	Yes	Yes
5.3-3	Multiple-row extended 1/2 unstiffened thick end plate	Built-up[1] 8" × 24"	—	Grade A325 ⅞ in. pretensioned	Yes	No
5.3-4	Multiple-row extended 1/3 unstiffened thick end plate	Built-up[1] 8" × 36"	—	Grade A325 ⅞ in. pretensioned	Yes	No
5.3-5	Multiple-row extended 1/3 stiffened thick end plate	Built-up[1] 8" × 36"	—	Grade A325 ⅞ in. pretensioned	Yes	No
5.3-6	Eight-bolt extended four-wide unstiffened thick end plate	Built-up[1] 14" × 24"	—	Grade A325 1 in. pretensioned	Yes	No
5.3-7	Eight-bolt extended stiffened thick end plate	W36×150	—	Grade A325 1⅛ in. pretensioned	Yes	No
5.3-8	12-bolt multiple-row extended 1/3 four-wide/two-wide unstiffened thick end plate	Built-up[1] 15" × 36"	—	Grade A325 1 in. pretensioned	Yes	No
5.3-9	12-bolt extended stiffened thick end plate	Built-up[1] 15" × 36"	—	Grade A325 1 in. pretensioned	Yes	No

[1] Flange width, in. × beam depth, in.

5.3.2 Extended Thick End-Plate Analysis Examples

This section has thick end-plate/smaller bolt analysis examples for the nine extended end-plate configurations shown in Figure 1-4. Table 5-19 summarizes the relevant parameters for each example. Appendix B has thin-end/larger bolt diameter examples for the same configurations, except for the eight bolt stiffened example where a built-up beam is used instead of the W36×150 beam. Calculations are shown for both LRFD and ASD designs.

EXAMPLE 5.3-1—Four-Bolt Extended Unstiffened Thick End-Plate Example

Given:

The connection shown in Figure 5-10 is a four-bolt unstiffened, extended (4E) gable frame connection of a built-up rafter and a built-up column. All plate steel is ASTM A572/A572M Grade 50. Bolts are ASTM F3125/F3125M Grade A325, snug-tightened. Weld electrodes are E70XX. The connection is to be evaluated as a thick end-plate design for the following required moments and forces.

	LRFD	ASD
Moment	M_u = 2,510 kip-in.	M_a = 1,670 kip-in.
Axial tension	T_u = 11.0 kips	T_a = 7.30 kips
Shear force	V_u = 33.8 kips	V_a = 22.5 kips

Solution:

From AISC *Manual* Table 2-4, the material properties are as follows:

ASTM A572/A572M Grade 50
F_y = 50 ksi
F_u = 65 ksi

From AISC *Specification* Table J3.2, the material properties of the bolts are as follows:

Group 120 ASTM F3125/F3125M ¾-in.-diameter Grade A325 snug-tightened
F_{nt} = 90 ksi
F_{nv} = 54 ksi (Group 120 bolts with threads not excluded from the shear plane; thread condition N)

Beam
d = 24 in. t_{bw} = ¼ in.
b_{bf} = 8 in. t_{bf} = ⅜ in.

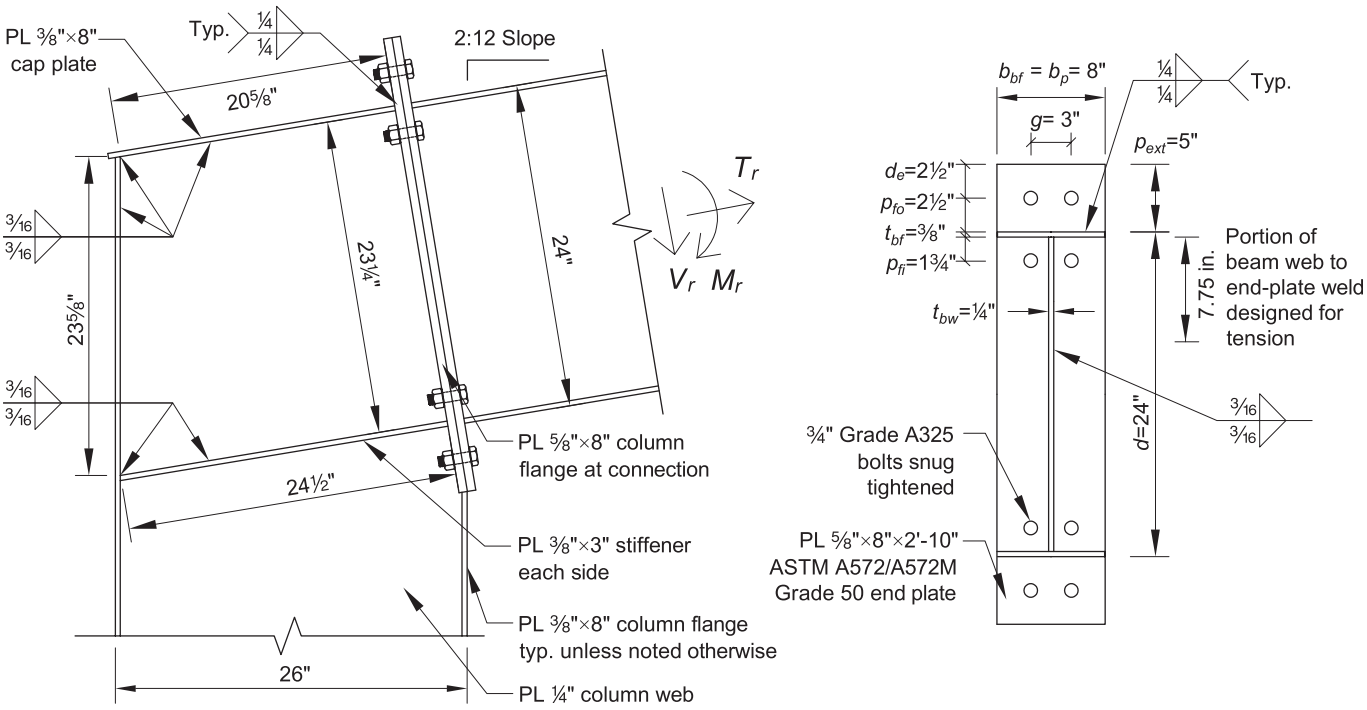

Fig. 5-10. Four-bolt unstiffened end-plate configuration for Example 5.3-1.

Column
d_c = 26 in. t_{cw} = ¼ in.
b_{cf} = 8 in. t_{cf} = ⅜ in.

End-plate geometric properties:
b_p = 8 in.
t_p = ⅝ in.
g = 3 in.
p_{ext} = 5 in.
d_e = 2½ in.
p_{fi} = 1¾ in.
p_{fo} = 2½ in.
d_p = 34 in.

The distances from the centerline of the compression flange to the bolt lines, h_1 and h_2, are depicted in Table 5-10 and computed as:

$$h_1 = d - \frac{t_{bf}}{2} + p_{fo}$$
$$= 24 \text{ in.} - \frac{⅜ \text{ in.}}{2} + 2½ \text{ in.}$$
$$= 26.3 \text{ in.}$$

$$h_2 = d - \frac{3t_{bf}}{2} - p_{fi}$$
$$= 24.0 \text{ in.} - \frac{3(⅜ \text{ in.})}{2} - 1¾ \text{ in.}$$
$$= 21.7 \text{ in.}$$

$$b_{p,eff} \le b_{bf} + \max(t_p, 1 \text{ in.}) \quad (4\text{-}3)$$
$$\le 8 \text{ in.} + \max(⅝ \text{ in.}, 1 \text{ in.})$$
$$\le 9.00 \text{ in.}$$

b_p = 8 in. ≤ 9.00 in. **o.k.**

$$b_{bf} \ge g \quad (4\text{-}1)$$
8 in. ≥ 3 in. **o.k.**

A. End-Plate and Bolt Design Verification

Calculate the equivalent required moment considering the effect of the required tensile force using Equation 3-30.

LRFD	ASD
$M_{u,eq} = M_u + (T_u/2)(d - t_{bf})$ $= 2{,}510 \text{ kip-in.} + (11.0 \text{ kips}/2)(24 \text{ in.} - ⅜ \text{ in.})$ $= 2{,}640 \text{ kip-in.}$	$M_{a,eq} = M_a + (T_a/2)(d - t_{bf})$ $= 1{,}670 \text{ kip-in.} + (7.30 \text{ kips}/2)(24 \text{ in.} - ⅜ \text{ in.})$ $= 1{,}760 \text{ kip-in.}$

Determine if the specified end-plate thickness, ⅝ in., and bolt diameter, ¾ in., are sufficient using the thick end-plate/smaller bolt diameter procedure.

Solve for the required bolt diameter using Equations 5-3. For Grade A325 bolts, the nominal tensile stress is F_{nt} = 90 ksi.

LRFD	ASD
$d_{b,reqd} = \sqrt{\dfrac{4M_{u,eq}}{\pi\phi F_{nt}\left(\sum_i n_i h_i\right)}}$	$d_{b,reqd} = \sqrt{\dfrac{4M_{a,eq}}{\dfrac{\pi F_{nt}}{\Omega}\left(\sum_i n_i h_i\right)}}$
$= \sqrt{\dfrac{4(2{,}640 \text{ kip-in.})}{\pi(0.75)(90 \text{ ksi})\left[2(26.3 \text{ in.}) + 2(21.7 \text{ in.})\right]}}$	$= \sqrt{\dfrac{4(1{,}760 \text{ kip-in.})}{\dfrac{\pi(90 \text{ ksi})}{2.00}\left[2(26.3 \text{ in.}) + 2(21.7 \text{ in.})\right]}}$
$= 0.720$ in. $\leq$ ¾ in. **o.k.**	$= 0.720$ in. $\leq$ ¾ in. **o.k.**

Solve for the required end-plate thickness using Equations 5-4. First solve for the distance, s, and yield line parameter, Y_p, using Table 5-10.

$$s = \frac{\sqrt{b_p g}}{2}$$
$$= \frac{\sqrt{(8 \text{ in.})(3 \text{ in.})}}{2}$$
$$= 2.45 \text{ in.}$$

Because $s \geq p_{fi} = 1¾$ in., the dimension p_{fi} is used in the equation for the yield line parameter.

$$Y_p = \frac{b_p}{2}\left[h_1\left(\frac{1}{p_{fo}}\right) + h_2\left(\frac{1}{p_{fi}} + \frac{1}{s}\right) - \frac{1}{2}\right] + \frac{2}{g}\left[h_2(s + p_{fi})\right]$$
$$= \left(\frac{8 \text{ in.}}{2}\right)\left[(26.3 \text{ in.})\left(\frac{1}{2½ \text{ in.}}\right) + (21.7 \text{ in.})\left(\frac{1}{1¾ \text{ in.}} + \frac{1}{2.45 \text{ in.}}\right) - \frac{1}{2}\right]$$
$$+ \left(\frac{2}{3 \text{ in.}}\right)\left[(21.7 \text{ in.})(2.45 \text{ in.} + 1¾ \text{ in.})\right]$$
$$= 186 \text{ in.}$$

Determine the required end-plate thickness using Equations 5-4. For extended end-plate configurations, $\gamma_r = 1.0$.

LRFD	ASD
$t_{p,reqd} = \sqrt{\dfrac{1.10M_{u,eq}}{\gamma_r \phi_b F_y Y_p}}$	$t_{p,reqd} = \sqrt{\dfrac{1.10M_{a,eq}}{\gamma_r F_y Y_p / \Omega_b}}$
$= \sqrt{\dfrac{1.10(2{,}640 \text{ kip-in.})}{1.0(0.90)(50 \text{ ksi})(186 \text{ in.})}}$	$= \sqrt{\dfrac{1.10(1{,}760 \text{ kip-in.})}{1.0(50 \text{ ksi})(186 \text{ in.})/1.67}}$
$= 0.589$ in. $\leq$ ⅝ in. **o.k.**	$= 0.590$ in. $\leq$ ⅝ in. **o.k.**

Check Shear Yielding/Shear Rupture of the Extended Portion of the End Plate

For extended end-plate moment connections that are unstiffened, potential limit states that must be checked are shear yielding and shear rupture of the extended portion of the end plate. For the 4E connection, the shear demand is taken as one-half of the tension flange force because this is the force that is transferred through the extended portion of the end plate to the exterior bolts. The shear strength is calculated in accordance with AISC *Specification* Section J4.2.

Calculate the shear demand on the extended portion of the end plate.

LRFD	ASD
$V_{up} = \frac{1}{2}\left(\frac{M_u}{d - t_{bf}} + \frac{T_u}{2}\right)$ $= \frac{1}{2}\left(\frac{2{,}510 \text{ kip-in.}}{24 \text{ in.} - \frac{3}{8} \text{ in.}} + \frac{11.0 \text{ kips}}{2}\right)$ $= 55.9 \text{ kips}$	$V_{ap} = \frac{1}{2}\left(\frac{M_a}{d - t_{bf}} + \frac{T_a}{2}\right)$ $= \frac{1}{2}\left(\frac{1{,}670 \text{ kip-in.}}{24 \text{ in.} - \frac{3}{8} \text{ in.}} + \frac{7.30 \text{ kips}}{2}\right)$ $= 37.2 \text{ kips}$

Calculate the nominal shear yielding strength.

$$R_n = 0.60 F_y A_{gv} \qquad \text{(Spec. Eq. J4-3)}$$
$$= 0.60 F_y b_p t_p$$
$$= 0.60(50 \text{ ksi})(8 \text{ in.})(\tfrac{5}{8} \text{ in.})$$
$$= 150 \text{ kips}$$

Compare the design shear yielding strength to the shear demand. According to AISC *Specification* Section J4.2 for yielding of elements in shear, the resistance factor is $\phi = 1.00$, and the safety factor is $\Omega = 1.50$.

LRFD	ASD
$\phi R_n = 1.00(150 \text{ kips})$ $= 150 \text{ kips} \quad \geq \quad V_{up} = 55.9 \text{ kips}$ **o.k.**	$\frac{R_n}{\Omega} = \frac{150 \text{ kips}}{1.50}$ $= 100 \text{ kips} \quad \geq \quad V_{ap} = 37.2 \text{ kips}$ **o.k.**

Calculate the nominal shear rupture strength. The width of the extended portion of the end plate for use in the net section area is the width minus two effective hole diameters. The effective hole diameter is the hole diameter from AISC *Specification* Table J3.3 plus 1/16 in. The additional 1/16 in. accounts for damage around the hole caused by drilling, punching, or thermal cutting. For 3/4-in.-diameter bolts, the standard hole diameter, d_h, is 13/16 in.

$$A_{nv} = \left[b_p - 2(d_h + \tfrac{1}{16} \text{ in.})\right] t_p$$
$$= \left[8 \text{ in.} - 2(\tfrac{13}{16} \text{ in.} + \tfrac{1}{16} \text{ in.})\right](\tfrac{5}{8} \text{ in.})$$
$$= 3.91 \text{ in.}^2$$
$$R_n = 0.60 F_u A_{nv} \qquad \text{(Spec. Eq. J4-4)}$$
$$= 0.60(65 \text{ ksi})(3.91 \text{ in.}^2)$$
$$= 152 \text{ kips}$$

Compare the design shear rupture strength to the shear demand. Using AISC *Specification* Section J4.2 for rupture of elements in shear, the resistance factor is $\phi = 0.75$, and the safety factor is $\Omega = 2.00$.

LRFD	ASD
$\phi R_n = 0.75(152 \text{ kips})$ $= 114 \text{ kips} \quad \geq \quad V_{up} = 55.9 \text{ kips}$ **o.k.**	$\frac{R_n}{\Omega} = \frac{152 \text{ kips}}{2.00}$ $= 76.0 \text{ kips} \quad \geq \quad V_{ap} = 37.2 \text{ kips}$ **o.k.**

The extended portion of the 5/8-in.-thick end plate has sufficient resistance to shear yielding and shear rupture.

Check Shear Transfer at the Bottom Holes

Shear at the faying surface, V_u, is assumed to be resisted only by the four compression side bolts. The shear transfer strength at each bolt hole is the minimum of the end-plate bearing/tearout strength, the bolt shear rupture strength, and the column flange bearing/tearout strength. See the User Note in AISC *Specification* Section J3.7.

The nominal unthreaded body area of a ¾ in. bolt is $A_b = 0.442$ in.^{2} The resulting nominal shear strength of a ¾-in.-diameter Grade A325 bolt is:

$$R_{n,bt} = F_{nv}A_b \qquad \text{(from } \textit{Spec.} \text{ Eq. J3-1)}$$
$$= (54 \text{ ksi})(0.442 \text{ in.}^2)$$
$$= 23.9 \text{ kips}$$

The nominal bearing/tearout strength is given by AISC *Specification* Section J3.11. The bolt shear force acting on the end plate is up toward the middle of the end plate, and therefore, tearout will not control. The bolt shear force acting on the column flange is down. Conservatively, the bottom of the sloping column flange is checked for both bearing and tearout. Because both the end plate and column flange are ⅝ in. thick, the column flange will be checked for bearing/tearout strength. The bearing strength at a bolt hole is:

$$R_{n,brg} = 2.4 d_b t_p F_u \qquad \text{(from } \textit{Spec.} \text{ Eq. J3-6a)}$$
$$= 2.4(¾ \text{ in.})(⅝ \text{ in.})(65 \text{ ksi})$$
$$= 73.1 \text{ kips}$$

The tearout strength at a bottom column flange bolt using the edge distance 2½ in. is:

$$R_{n,to} = 1.2 l_c t_p F_u \qquad \text{(from } \textit{Spec.} \text{ Eq. J3-6c)}$$
$$= 1.2\left[2½ - (¾ \text{ in.} + 1/16 \text{ in.})/2\right](⅝ \text{ in.})(65 \text{ ksi})$$
$$= 102 \text{ kips}$$

Because the tearout strength is greater than the bearing strength, bearing controls at the column flange. The shear transfer strength is then the minimum of the column flange bearing strength, the bolt shear rupture strength, and the end-plate bearing strength, which results in $R_n = 23.9$ kips.

Therefore, the nominal shear transfer strength at the four bottom bolt holes is

$$V_n = (4 \text{ bolts})R_n$$
$$= (4 \text{ bolts})(23.9 \text{ kips})$$
$$= 95.6 \text{ kips}$$

LRFD	ASD
$\phi V_n = 0.75(95.6 \text{ kips})$ $= 71.7 \text{ kips} \quad \geq \quad V_u = 33.8 \text{ kips}$ **o.k.**	$\frac{V_n}{\Omega} = \frac{95.6 \text{ kips}}{2.00}$ $= 47.8 \text{ kips} \quad \geq \quad V_a = 22.5 \text{ kips}$ **o.k.**

The specified ASTM A572/A572M Grade 50 ⅝-in.-thick end plate and ¾-in.-diameter Grade A325 snug-tightened bolts are sufficient.

B. Check Beam to End-Plate Welds

The minimum weld size in AISC *Specification* Table J2.4 is determined from the material thickness of the thinner part joined. The fillet weld sizes shown in Figure 5-10 satisfy the requirements in Table J2.4.

Check Beam Flange to End-Plate Weld

The weld from the beam flange to the end plate is shown in Figure 5-10 as a double-sided ¼ in. fillet weld. Determine if this weld is adequate. First, find the required tensile force as the maximum of either the calculated flange tensile force or 60% of the flange tensile strength for LRFD and 40% of the flange tensile strength for ASD (Equations 3-38), but not greater than the yield strength of the tension flange.

LRFD	ASD
$T_{u,calc} = \frac{M_u}{d - t_{bf}} + \frac{T_u}{2}$ $= \frac{2{,}510 \text{ kip-in.}}{24 \text{ in.} - \frac{3}{8} \text{ in.}} + \frac{11.0 \text{ kips}}{2}$ $= 112 \text{ kips}$ $T_{yf} = F_y b_{bf} t_{bf}$ $= (50 \text{ ksi})(8 \text{ in.})(\frac{3}{8} \text{ in.})$ $= 150 \text{ kips}$ $T_{u,min} = 0.60 F_y b_{bf} t_{bf}$ $= 0.60(50 \text{ ksi})(8 \text{ in.})(\frac{3}{8} \text{ in.})$ $= 90.0 \text{ kips}$ $T_{uf} = \max(T_{u,calc}, T_{u,min}) \leq T_{yf}$ $= \max(112 \text{ kips}, 90 \text{ kips})$ $= 112 \text{ kips} \leq T_{yf} = 150 \text{ kips}$	$T_{a,calc} = \frac{M_a}{d - t_{bf}} + \frac{T_a}{2}$ $= \frac{1{,}670 \text{ kip-in.}}{24 \text{ in.} - \frac{3}{8} \text{ in.}} + \frac{7.30 \text{ kips}}{2}$ $= 74.3 \text{ kips}$ $\frac{T_{yf}}{1.50} = \frac{F_y}{1.50} b_{bf} t_{bf}$ $= \frac{50 \text{ ksi}}{1.50}(8 \text{ in.})(\frac{3}{8} \text{ in.})$ $= 100 \text{ kips}$ $T_{a,min} = 0.40 F_y b_{bf} t_{bf}$ $= 0.40(50 \text{ ksi})(8 \text{ in.})(\frac{3}{8} \text{ in.})$ $= 60.0 \text{ kips}$ $T_{af} = \max(T_{a,calc}, T_{a,min}) \leq T_{yf}/1.50$ $= \max(74.3 \text{ kips}, 60.0 \text{ kips})$ $= 74.3 \text{ kips} \leq \frac{T_{yf}}{1.50} = 100 \text{ kips}$

Because the welds are loaded perpendicular to their longitudinal axis, the angle of loading, θ, is 90°. The length of the weld is two times the width of the beam flange, b_{bf}, less the beam web thickness, t_{bw}.

$$l_w = 2b_{bf} - t_{bw}$$
$$2(8 \text{ in.}) - \frac{1}{4} \text{ in.}$$
$$= 15.8 \text{ in.}$$

$$R_n = 0.60 F_{EXX} \frac{t_{weld}}{\sqrt{2}} l_w (1.0 + 0.5 \sin^{1.5} \theta) \qquad \text{(from } \textit{Spec.} \text{ Eq. J2-4)}$$
$$= 0.60(70 \text{ ksi}) \left(\frac{\frac{1}{4} \text{ in.}}{\sqrt{2}} \right) (15.8 \text{ in.})(1.0 + 0.5 \sin^{1.5} 90°)$$
$$= 176 \text{ kips}$$

LRFD	ASD
$\phi R_n = 0.75(176 \text{ kips})$ $= 132 \text{ kips} \geq T_{uf} = 112 \text{ kips}$ **o.k.**	$\frac{R_n}{\Omega} = \frac{176 \text{ kips}}{2.00}$ $= 88.0 \text{ kips} \geq T_{af} = 74.3 \text{ kips}$ **o.k.**

The flange to end-plate weld consisting of a double-sided ¼ in. fillet weld is adequate. (A CJP or a PJP groove weld are alternate options.)

Check Beam Web to End-Plate Weld

As explained in Section 3.7.5, the demand for the tension web area, T_{uw} (LRFD) or T_{aw} (ASD), for this connection is the number of tension bolts adjacent to the web, n_{trib}, divided by the total number of tension bolts, n, multiplied by the calculated beam flange force, $T_{u,calc}$ (LRFD) or $T_{a,calc}$ (ASD), from the beam flange to end-plate weld demand calculations. Using Equation 3-40:

LRFD	ASD
$T_{uw} = (n_{trib}/n)T_{u,calc}$	$T_{aw} = (n_{trib}/n)T_{a,calc}$
$= (2/4)(112 \text{ kips})$	$= (2/4)(74.3 \text{ kips})$
$= 56.0 \text{ kips}$	$= 37.2 \text{ kips}$

The length of the web tension region is measured from the inside of the beam flange to 6 in. inside the tension bolt row:

$l_{wt} = p_{fi} + 6 \text{ in.}$
$= 1¾ \text{ in.} + 6 \text{ in.}$
$= 7.75 \text{ in.}$

The nominal web yield strength in the tension region is:

$T_{yw} = F_y A_g$ (from *Spec.* Eq. J4-1)
$= F_y t_{bw} l_{wt}$
$= (50 \text{ ksi})(¼ \text{ in.})(7.75 \text{ in.})$
$= 96.9 \text{ kips}$

Check that the web design tensile yield strength of the web is sufficient.

LRFD	ASD
$\phi T_{yw} = 0.90(96.9 \text{ kips})$	$\frac{T_{yw}}{\Omega} = \frac{96.9 \text{ kips}}{1.67}$
$= 87.2 \text{ kips} \quad \geq \quad T_{uw} = 56.0 \text{ kips}$ **o.k.**	$= 58.0 \text{ kips} \quad \geq \quad T_{aw} = 37.2 \text{ kips}$ **o.k.**

Check that the required strength is at least 60% (LRFD) or 40% (ASD) of the web tensile strength from Equations 3-41.

LRFD	ASD
$0.60T_{yw} = 0.60(96.9 \text{ kips})$	$0.40T_{yw} = 0.40(96.9 \text{ kips})$
$= 58.1 \text{ kips}$	$= 38.8 \text{ kips}$
$T_{uwd} = \max(T_{uw}, 0.60T_{yw})$	$T_{awd} = \max(T_{aw}, 0.40T_{yw})$
$= \max(56.0 \text{ kips}, 58.1 \text{ kips})$	$= \max(37.2 \text{ kips}, 38.8 \text{ kips})$
$= 58.1 \text{ kips}$	$= 38.8 \text{ kips}$

Check the web to end-plate weld around the tension bolts. Because the weld is loaded perpendicular to its longitudinal axis, the angle of loading, θ, is 90°.

$R_n = (2 \text{ welds})0.60F_{EXX}\frac{t_{weld}}{\sqrt{2}}l_{wt}(1.0 + 0.5\sin^{1.5}\theta)$ (from *Spec.* Eq. J2-4)
$= (2 \text{ welds})(0.60)(70 \text{ ksi})\left(\frac{3/16 \text{ in.}}{\sqrt{2}}\right)(7.75 \text{ in.})(1.0 + 0.5\sin^{1.5}90°)$
$= 129 \text{ kips}$

LRFD	ASD
$\phi R_n = 0.75(129 \text{ kips})$ $= 96.8 \text{ kips} \quad \geq \quad T_{uwd} = 58.1 \text{ kips}$ **o.k.**	$\frac{R_n}{\Omega} = \frac{129 \text{ kips}}{2.00}$ $= 64.5 \text{ kips} \quad \geq \quad T_{awd} = 38.8 \text{ kips}$ **o.k.**

Check the web to end-plate weld away from the tension bolts. Only the web to end-plate weld between the end of the assumed web tension length and the inside face of the bottom beam compression flange or the weld between the mid-depth of the beam and the inside face of the beam compression flange, whichever is smaller, is considered effective in resisting the beam end shear. The shear strength of this weld is compared to the required shear applied to the connection.

$$l_t = (d - 2t_{bf}) - l_{wt}$$
$$= 24 \text{ in.} - 2(\tfrac{3}{8} \text{ in.}) - 7.75 \text{ in.}$$
$$= 15.5 \text{ in.}$$

$$l_{0.5w} = d/2 - t_{bf}$$
$$= (24 \text{ in.})/2 - \tfrac{3}{8} \text{ in.}$$
$$= 11.6 \text{ in.}$$

$$l_{wv} = \min(l_t, l_{0.5w})$$
$$= \min(15.5 \text{ in.}, 11.6 \text{ in.})$$
$$= 11.6 \text{ in.}$$

$$R_n = (2 \text{ welds}) 0.60 F_{EXX} \frac{t_{weld}}{\sqrt{2}} l_{wv} (1.0 + 0.5 \sin^{1.5} \theta) \qquad \text{(Spec. Eq. J2-4)}$$
$$= (2 \text{ welds})(0.60)(70 \text{ ksi}) \left(\frac{\tfrac{3}{16} \text{ in.}}{\sqrt{2}} \right) (11.6 \text{ in.})(1.0 + 0.5 \sin^{1.5} 0°)$$
$$= 129 \text{ kips}$$

LRFD	ASD
$\phi R_n = 0.75(129 \text{ kips})$ $= 96.8 \text{ kips} \quad \geq \quad V_u = 33.8 \text{ kips}$ **o.k.**	$\frac{R_n}{\Omega} = \frac{129 \text{ kips}}{2.00}$ $= 64.5 \text{ kips} \quad \geq \quad V_a = 22.5 \text{ kips}$ **o.k.**

Check that the shear rupture strength of the beam web at the weld using AISC *Specification* Equation J4-4 is sufficient.

$$R_n = 0.60 F_u A_{nv} \qquad \text{(Spec. Eq. J4-4)}$$
$$= 0.60 F_u l_{wv} t_{bw}$$
$$= 0.60(65 \text{ ksi})(11.6 \text{ in.})(\tfrac{1}{4} \text{ in.})$$
$$= 113 \text{ kips}$$

LRFD	ASD
$\phi R_n = 0.75(113 \text{ kips})$ $= 84.8 \text{ kips} \quad \geq \quad V_u = 33.8 \text{ kips}$ **o.k.**	$\frac{R_n}{\Omega} = \frac{113 \text{ kips}}{2.00}$ $= 56.5 \text{ kips} \quad \geq \quad V_a = 22.5 \text{ kips}$ **o.k.**

The double-sided $\tfrac{3}{16}$ in. fillet welds shown in Figure 5-10 from the web to the end plate are sufficient.

C. Column-Side Limit State Checks

The beam-to-column connection as shown in Figure 5-10 is similar to a splice connection between two beams. The column flange plate is similar to the end plate checked for the beam side in Part A. The column flange to column web welds are identical to those for the beam web to the end plate. The cap plate size is the same as the beam flange plate and therefore is sufficient, as well as the cap plate to column flange plate weld that is the same as the beam flange to end-plate weld. All of these welds were checked in Part B.

Check Cap Plate to Panel Zone Plate Weld

The cap plate to panel zone plate weld must resist the same force as that of the rafter flange, 112 kips (LRFD) or 74.3 kips (ASD) as determined in Part B. The nominal weld rupture strength for the double-sided 3⁄16 in. fillet weld across the panel zone plate shown in Figure 5-10 is:

$$l_w = 2a_v$$
$$= 2(20\tfrac{5}{8}\text{ in.})$$
$$= 41.3\text{ in.}$$

$$R_n = 0.60F_{EXX}\frac{t_{weld}}{\sqrt{2}}l_w(1.0+0.5\sin^{1.5}\theta) \qquad \text{(from } \textit{Spec.}\text{ Eq. J2-4)}$$
$$= 0.60(70\text{ ksi})\left(\frac{3/16\text{ in.}}{\sqrt{2}}\right)(41.3\text{ in.})(1.0+0.5\sin^{1.5}0°)$$
$$= 230\text{ kips}$$

LRFD	ASD
$\phi R_n = 0.75(230\text{ kips})$ $= 173\text{ kips} \geq T_u = 112\text{ kips}$ **o.k.**	$\frac{R_n}{\Omega} = \frac{230\text{ kips}}{2.00}$ $= 115\text{ kips} \geq T_a = 74.3\text{ kips}$ **o.k.**

Check that the shear rupture strength of the panel zone plate at the weld using AISC *Specification* Equation J4-4 is sufficient.

$$V_{nw} = 0.60F_uA_{nv} \qquad \text{(}\textit{Spec.}\text{ Eq. J4-4)}$$
$$= 0.60F_ua_vt_{cw}$$
$$= 0.60(65\text{ ksi})(20\tfrac{5}{8}\text{ in.})(1/4\text{ in.})$$
$$= 201\text{ kips}$$

LRFD	ASD
$\phi R_n = 0.75(201\text{ kips})$ $= 151\text{ kips} \geq V_u = 112\text{ kips}$ **o.k.**	$\frac{R_n}{\Omega} = \frac{201\text{ kips}}{2.00}$ $= 101\text{ kips} \geq V_a = 74.3\text{ kips}$ **o.k.**

The cap-plate to column panel zone plate weld consisting of a double-sided 3⁄16 in. fillet weld is adequate.

Check Strength of Column Web Stiffeners

Check web local yielding and web local crippling to determine if stiffeners are required for the column web opposite the beam bottom flange. The concentrated force delivered by the beam bottom flange to the column, conservatively neglecting the small tension force, is:

LRFD	ASD
$P_u = \dfrac{M_u}{d - t_{bf}}$ $= \dfrac{2{,}510 \text{ kip-in.}}{24 \text{ in.} - \frac{3}{8} \text{ in.}}$ $= 106 \text{ kips}$	$P_a = \dfrac{M_a}{d - t_{bf}}$ $= \dfrac{1{,}670 \text{ kip-in.}}{24 \text{ in.} - \frac{3}{8} \text{ in.}}$ $= 70.7 \text{ kips}$

Calculate the nominal column web local yielding strength opposite the bottom flange of the beam. Equations from Section 3.7.6 are used. The parameter, C_t, is 0.5 because the distance from the bottom of the beam to the top of the column is less than the depth of the column.

$$l_b = t_{bf} + 2w + 2t_p \tag{3-47}$$
$$= \tfrac{3}{8} \text{ in.} + 2(\tfrac{1}{4} \text{ in.}) + 2(\tfrac{5}{8} \text{ in.})$$
$$= 2.13 \text{ in.}$$

$$k_c = t_{cf} + t_{weld}$$
$$= \tfrac{3}{8} \text{ in.} + \tfrac{3}{16} \text{ in.}$$
$$= 0.563 \text{ in.}$$

$$R_{n,lwy} = (6C_t k_c + l_b) F_y t_{cw} \tag{3-46}$$
$$= \left[6(0.5)(0.563 \text{ in.}) + 2.13 \text{ in.}\right](50 \text{ ksi})(\tfrac{1}{4} \text{ in.})$$
$$= 47.7 \text{ kips}$$

The available column web local yielding strength is then calculated and compared to the required strength.

LRFD	ASD
$\phi R_{n,lwy} = 1.00(47.7 \text{ kips})$ $= 47.7 \text{ kips} \quad \le \quad P_u = 106 \text{ kips}$ **n.g.**	$\dfrac{R_{n,lwy}}{\Omega} = \dfrac{47.7 \text{ kips}}{1.50}$ $= 31.8 \text{ kips} \quad \le \quad P_a = 70.7 \text{ kips}$ **n.g.**

Column web stiffener plates are required.

Calculate the column web local crippling strength. The flange force applied from the bottom of the beam is located more than the half the column depth from the end of the column; therefore, use AISC *Specification* Equation J10-4 with $Q_f = 1.0$.

$$R_{n,lwc} = 0.80 t_{cw}^2 \left[1 + 3\left(\frac{l_b}{d_c}\right)\left(\frac{t_{cw}}{t_{cf}}\right)^{1.5}\right]\sqrt{\frac{EF_y t_{cf}}{t_{cw}}}\, Q_f \tag{*Spec.* Eq. J10-4}$$
$$= 0.80(\tfrac{1}{4} \text{ in.})^2 \left[1 + 3\left(\frac{2.13 \text{ in.}}{26 \text{ in.}}\right)\left(\frac{\frac{1}{4} \text{ in.}}{\frac{3}{8} \text{ in.}}\right)^{1.5}\right]\sqrt{\frac{(29{,}000 \text{ ksi})(50 \text{ ksi})(\frac{3}{8} \text{ in.})}{\frac{1}{4} \text{ in.}}}\,(1.0)$$
$$= 83.6 \text{ kips}$$

The available column web local crippling strength is calculated and compared to the required compression force.

LRFD	ASD
$\phi R_{n,lwc} = 0.75(83.6 \text{ kips})$ $= 62.7 \text{ kips} \quad \le \quad P_u = 106 \text{ kips}$ **n.g.**	$\dfrac{R_{n,lwc}}{\Omega} = \dfrac{83.6 \text{ kips}}{2.00}$ $= 41.8 \text{ kips} \quad \le \quad P_a = 70.7 \text{ kips}$ **n.g.**

The column web does not have sufficient strength for column web yielding and column web crippling. The strength of the column web stiffener plates, ⅜ in. × 3 in., shown in Figure 5-10 is now checked.

Check the geometric requirements in AISC *Specification* Section J10.8:

$$\min t_s = t_{bf}/2$$
$$= (⅜\text{ in.})/2$$
$$= 0.188\text{ in.} \quad \le \quad t_s = ⅜\text{ in.} \qquad \textbf{o.k.}$$

$$\min b_s = b_{bf}/3 - t_{cw}/2$$
$$= (8\text{ in.})/3 - (¼\text{ in.})/2$$
$$= 2.54\text{ in.} \quad \le \quad b_s = 3\text{ in.} \qquad \textbf{o.k.}$$

Check stiffener local buckling. From AISC *Specification* Table B4.1a, Case 2:

$$k_c = \frac{4}{\sqrt{h/t_{cw}}}$$
$$= \frac{4}{\sqrt{(24.5\text{ in.})/(¼\text{ in.})}}$$
$$= 0.404$$

$$\lambda_r = 0.64\sqrt{\frac{k_c E}{F_y}}$$
$$= 0.64\sqrt{\frac{0.404(29{,}000\text{ ksi})}{50\text{ ksi}}}$$
$$= 9.80$$

$$\frac{b_s}{t_s} = \frac{3\text{ in.}}{⅜\text{ in.}}$$
$$= 8.00 \le 9.80 \qquad \textbf{o.k.}$$

The required strength of the stiffener plates is the required compression force, P_r, minus the minimum of the available column web yielding strength and the available column web crippling strength. The required strength must be less than the available compression yield strength of the stiffener plates.

$$P_n = F_y A_s \qquad \text{(from } \textit{Spec.}\text{ Eq. J4-1)}$$
$$= (50\text{ ksi})\left[2(⅜\text{ in.})(3\text{ in.})\right]$$
$$= 113\text{ kips}$$

LRFD	ASD
$T_{u,stiff} = 112\text{ kips} - \min(47.7\text{ kips}, 62.7\text{ kips})$ $= 64.3\text{ kips}$	$T_{a,stiff} = 74.3\text{ kips} - \min(31.8\text{ kips}, 41.8\text{ kips})$ $= 42.5\text{ kips}$
$\phi R_n = 0.90(113\text{ kips})$ $= 102\text{ kips} \quad \ge \quad 64.3\text{ kips}$ **o.k.**	$\frac{R_n}{\Omega} = \frac{113\text{ kips}}{1.67}$ $= 67.7\text{ kips} \quad \ge \quad 42.5\text{ kips}$ **o.k.**

Check Stiffener to Column Flange Weld

The length of the stiffener to column flange weld is calculated as the stiffener width less a ¾ in. corner clip.

$$l_{wt} = b_s - clip$$
$$= 3 \text{ in.} - ¾ \text{ in.}$$
$$= 2.25 \text{ in.}$$

The stiffener to column flange weld is designed for the same required strength as calculated for the stiffener required axial strength. The nominal weld rupture strength for the double-sided ¼ in. fillet weld shown in Figure 5-10 is:

$$R_n = (4 \text{ welds}) 0.60 F_{EXX} \frac{t_{weld}}{\sqrt{2}} l_{wt} (1.0 + 0.5 \sin^{1.5} \theta) \quad \text{(from } \textit{Spec.} \text{ Eq. J2-4)}$$
$$= (4 \text{ welds})(0.60)(70 \text{ ksi}) \left(\frac{¼ \text{ in.}}{\sqrt{2}} \right) (2.25 \text{ in.})(1.0 + 0.5 \sin^{1.5} 90°)$$
$$= 100 \text{ kips}$$

LRFD	ASD
$\phi R_n = 0.75(100 \text{ kips})$ $= 75.0 \text{ kips} \quad \geq \quad T_{u,stiff} = 64.3 \text{ kips}$ **o.k.**	$\frac{R_n}{\Omega} = \frac{100 \text{ kips}}{2.00}$ $= 50.0 \text{ kips} \quad \geq \quad T_{a,stiff} = 42.5 \text{ kips}$ **o.k.**

Check Stiffener to Column Web Weld

The length of the stiffener to column web weld is calculated as the length of the full-depth stiffener, h = 24.5 in., less a ¾ in. corner clip on each end.

$$l_w = h - 2clip$$
$$= 24.5 \text{ in.} - 2(¾ \text{ in.})$$
$$= 23.0 \text{ in.}$$

The stiffener to column web weld is designed for the same required strength as calculated for the stiffener required axial strength. The nominal weld rupture strength for the double-sided 5/16 in. fillet weld shown in Figure 5-10 is:

$$R_n = (4 \text{ welds}) 0.60 F_{EXX} \frac{t_{weld}}{\sqrt{2}} l_w (1.0 + 0.5 \sin^{1.5} \theta) \quad \text{(from } \textit{Spec.} \text{ Eq. J2-4)}$$
$$= (4 \text{ welds})(0.60)(70 \text{ ksi}) \left(\frac{5/16 \text{ in.}}{\sqrt{2}} \right) (23.0 \text{ in.})(1.0 + 0.5 \sin^{1.5} 0°)$$
$$= 512 \text{ kips}$$

LRFD	ASD
$\phi R_n = 0.75(512 \text{ kips})$ $= 384 \text{ kips} \quad \geq \quad T_{u,stiff} = 64.3 \text{ kips}$ **o.k.**	$\frac{R_n}{\Omega} = \frac{512 \text{ kips}}{2.00}$ $= 256 \text{ kips} \quad \geq \quad T_{a,stiff} = 42.5 \text{ kips}$ **o.k.**

Check that the shear rupture strength of the column web at the stiffener welds using AISC *Specification* Equation J4-4 is sufficient. There are two shear rupture lines, one above and one below the stiffeners.

$$R_n = 0.60F_uA_{nv} \quad \text{(Spec. Eq. J4-4)}$$
$$= (2 \text{ lines})0.60F_u l_{wt} t_{cw}$$
$$= (2 \text{ lines})0.60(65 \text{ ksi})(24.5 \text{ in.})(¼ \text{ in.})$$
$$= 478 \text{ kips}$$

LRFD	ASD
$\phi R_n = 0.75(478 \text{ kips})$ $= 359 \text{ kips} \quad \geq \quad V_u = 64.3 \text{ kips}$ **o.k.**	$\frac{R_n}{\Omega} = \frac{478 \text{ kips}}{2.00}$ $= 239 \text{ kips} \quad \geq \quad V_a = 42.5 \text{ kips}$ **o.k.**

Because there are two ⅜ in. stiffeners, the shear rupture strength of the stiffeners is sufficient by inspection.

The stiffener to column web weld consisting of a double-sided 3⁄16 in. fillet weld is adequate.

Check Column Panel Zone Shear

Check the column panel zone for shear strength. The required shear strength is the beam flange force plus half the axial force.

LRFD	ASD
$V_u = \frac{M_u}{d - t_{bf}} + \frac{T_u}{2}$ $= \frac{2{,}510 \text{ kip-in.}}{24 \text{ in.} - ⅜ \text{ in.}} + \frac{11.0 \text{ kips}}{2}$ $= 112 \text{ kips}$	$V_a = \frac{M_a}{d - t_{bf}} + \frac{T_a}{2}$ $= \frac{1{,}670 \text{ kip-in.}}{24 \text{ in.} - ⅜ \text{ in.}} + \frac{7.30 \text{ kips}}{2}$ $= 74.3 \text{ kips}$

Calculate the panel zone shear yielding strength using AISC *Specification* Section J10.6. For the depth of the column, d_c, use the least column depth at the panel zone, which, for this example, occurs at the top of the panel zone.

$$d_c = a_v + t_{cf} + t_p$$
$$= 20⅝ \text{ in.} + ⅜ \text{ in.} + ⅝ \text{ in.}$$
$$= 21.6 \text{ in.}$$

Assuming the column required axial strength is less than $0.4P_y$ and the effect of inelastic panel-zone deformation on frame stability was not accounted for in the analysis, the nominal shear yielding strength of the panel zone is:

$$R_n = 0.60F_y d_c t_{cw} \quad \text{(Spec. Eq. J10-9)}$$
$$= 0.60(50 \text{ ksi})(21.6 \text{ in.})(¼ \text{ in.})$$
$$= 162 \text{ kips}$$

The panel zone is now checked for shear buckling and post-buckling strength. Because the moment is negative (see sign convention in Figure 3-16) and the column web stiffeners consist of full-depth stiffeners, a tension field can form. AISC *Specification* Section G2.2 is used to calculate the panel zone strength for shear buckling. First, the dimensions of the panel zone are determined, and the slenderness of the panel zone is checked against the limits given in AISC *Specification* Section G2.2.

$a = 24.5$ in. width of panel zone

$h = 23.3$ in. height of the panel zone

$$\frac{h}{t_{cw}} = \frac{23.3 \text{ in.}}{¼ \text{ in.}}$$
$$= 93.2$$

$$k_v = 5 + \frac{5}{(a/h)^2} \qquad \text{(Spec. Eq. G2-5)}$$
$$= 5 + \frac{5}{(24.5 \text{ in.}/23.3 \text{ in.})^2}$$
$$= 9.52$$

The slenderness limit for shear buckling is:

$$1.10\sqrt{\frac{k_v E}{F_y}} = 1.10\sqrt{\frac{9.52(29{,}000 \text{ ksi})}{50 \text{ ksi}}}$$
$$= 81.7$$

The slenderness limit for elastic shear buckling is:

$$1.37\sqrt{\frac{k_v E}{F_y}} = 1.37\sqrt{\frac{95.2(29{,}000 \text{ ksi})}{50 \text{ ksi}}}$$
$$= 102$$

Because the web slenderness is between $1.10\sqrt{k_v E/F_y}$ and $1.37\sqrt{k_v E/F_y}$, the web shear coefficient, C_{v2}, and post-buckling shear strength of the panel zone are:

$$C_{v2} = \frac{1.10\sqrt{k_v E/F_y}}{h/t_{cw}} \qquad \text{(Spec. Eq. G2-10)}$$
$$= \frac{81.7}{93.2}$$
$$= 0.877$$

Determine which equation from AISC *Specification* Section G2.2 to use for nominal strength by checking the following three inequalities, where the web area is taken in the width direction, $d_c t_{cw}$, for which panel zone shear is calculated, and the column flange next to the connection is the compression flange based on the direction of applied moment:

$$\frac{2A_w}{A_{fc} + A_{ft}} = \frac{2(21.6 \text{ in.})(¼ \text{ in.})}{(8 \text{ in.})(⅜ \text{ in.}) + (8 \text{ in.})(⅜ \text{ in.})}$$
$$= 1.08 \le 2.5 \quad \textbf{o.k.}$$

$$\frac{h}{b_{fc}} = \frac{23.3 \text{ in.}}{8 \text{ in.}}$$
$$= 2.91 \le 6.0 \quad \textbf{o.k.}$$

$$\frac{h}{b_{ft}} = \frac{23.3 \text{ in.}}{8 \text{ in.}}$$
$$= 2.91 \le 6.0 \quad \textbf{o.k.}$$

Because all three inequalities from AISC *Specification* Section G2.2(b)(1) are satisfied, AISC *Specification* Equation G2-7 is used to determine the panel zone nominal shear strength:

$$R_n = 0.60 d_c t_{cw} F_y \left[C_{v2} + \frac{1 - C_{v2}}{1.15\sqrt{1+(a/h)^2}} \right] \qquad \text{(from } \textit{Spec.} \text{ Eq. G2-7)}$$

$$= 0.60(21.6 \text{ in.})(¼ \text{ in.})(50 \text{ ksi}) \left\{ 0.877 + \frac{1 - 0.877}{1.15\sqrt{1+\left[(24.5 \text{ in.})/23.3 \text{ in.}\right]^2}} \right\}$$

$$= 154 \text{ kips}$$

The panel zone shear strength is the minimum of the shear yielding and post-buckling shear strengths.

$$R_n = \min(162 \text{ kips}, 154 \text{ kips})$$
$$= 154 \text{ kips}$$

Check that the design panel zone shear strength is greater than the required shear.

LRFD	ASD
$\phi R_n = 0.90(154 \text{ kips})$ $= 139 \text{ kips} \quad \geq \quad V_u = 112 \text{ kips}$ **o.k.**	$\frac{R_n}{\Omega} = \frac{154 \text{ kips}}{1.67}$ $= 92.2 \text{ kips} \quad \geq \quad V_a = 74.3 \text{ kips}$ **o.k.**

The column panel zone is sufficient to resist the required shear.

Summary

The connection shown in Figure 5-10 is adequate for the required moment and forces.

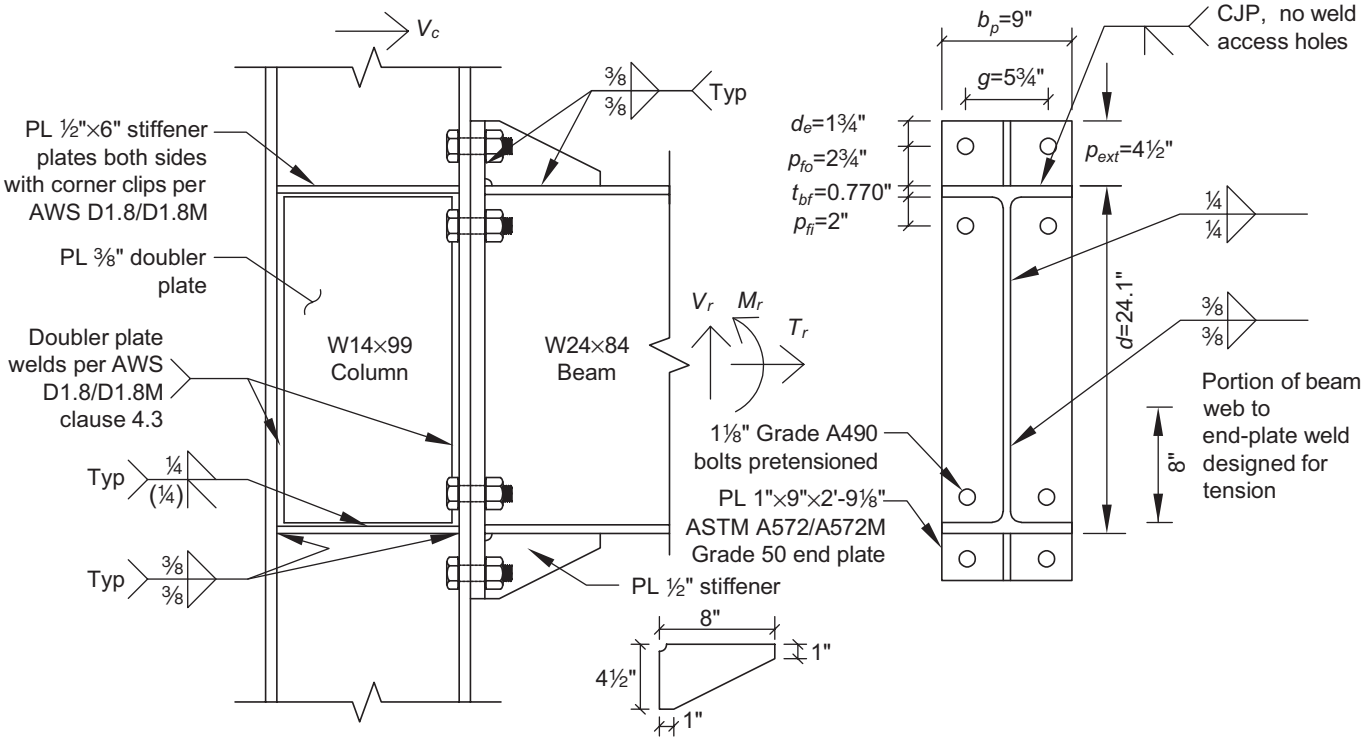

Fig. 5-11. Four-bolt stiffened end-plate configuration for Example 5.3-2.

EXAMPLE 5.3-2—Four-Bolt Extended Stiffened Thick End-Plate Example

Given:

The connection shown in Figure 5-11 is a four-bolt, extended, stiffened end-plate (4ES) connection for a W24×84 beam to a W14×99 column. The beam and column steel are ASTM A992/A992M, and plate steel is ASTM A572/A572M Grade 50. Bolts are ASTM F3125/F3125M Grade A490, pretensioned. Weld electrodes are E70XX. The connection, including column-side limits, is to be evaluated as a thick end-plate design for the following required moments and forces.

	LRFD ASD	ASD
Moment	M_u = 7,620 kip-in.	M_a = 5,080 kip-in.
Axial tension	T_u = 20.4 kips	T_a = 13.6 kips
Shear force	V_u = 45.8 kips	V_a = 30.5 kips
Column shear	V_{uc}=19.6 kips	V_{ac}=13.1 kips

Solution:

From AISC *Manual* Table 2-4, the material properties are as follows:

ASTM A992/A992M
F_y = 50 ksi
F_u = 65 ksi

ASTM A572/A572M Grade 50
F_y = 50 ksi
F_u = 65 ksi

From AISC *Specification* Table J3.2, the material properties of the bolts are as follows:

Group 150 ASTM F3125/F3125M 1⅛-in.-diameter Grade A490 pretensioned
F_{nt} = 113 ksi
F_{nv} = 68 ksi (Group 150 bolts with threads not excluded from the shear plane; thread condition N)

From AISC *Manual* Table 1-1, the geometric properties of the beam and column sections are as follows:

Beam: W24×84
d = 24.1 in. t_{bw} = 0.470 in.
b_{bf} = 9.02 in. t_{bf} = 0.770 in.

Column: W14×99
d_c = 14.2 in. t_{cw} = 0.485 in. b_{cf} = 14.6 in. t_{cf} = 0.780 in.
k_{des} = 1.38 in. $k_{det,c}$ = 2 1/16 in. $k_{1,c}$ = 1 7/16 in. h/t_{cw} = 23.5

End-plate geometric properties:
b_p = 9 in.
t_p = 1 in.
g = 5¾ in.
p_{ext} = 4½ in.
d_e = 1¾ in.
p_{fo} = 2¾ in.
p_{fi} = 2 in.
d_p = 33⅛ in.

The distances from the centerline of the compression flange to the bolt lines, h_1 and h_2, are depicted in Table 5-11 and computed as:

$$h_1 = d - \frac{t_{bf}}{2} + p_{fo}$$
$$= 24.1 \text{ in.} - \frac{0.770 \text{ in.}}{2} + 2¾ \text{ in.}$$
$$= 26.5 \text{ in.}$$

$$h_2 = d - \frac{3t_{bf}}{2} - p_{fi}$$
$$= 24.1 \text{ in.} - \frac{3(0.770 \text{ in.})}{2} - 2 \text{ in.}$$
$$= 20.9 \text{ in.}$$

$$b_{p,eff} \le b_{bf} + \max(t_p, 1 \text{ in.}) \quad (4\text{-}3)$$
$$\le 9.02 \text{ in.} + \max(1 \text{ in.}, 1 \text{ in.})$$
$$\le 10.0 \text{ in.}$$

$b_p = 9$ in. $\le$ 10.0 in. **o.k.**

$$b_{bf} \ge g \quad (4\text{-}1)$$

9.02 in. ≥ 5¾ in. **o.k.**

Beam flange to end-plate stiffener geometric properties:

$$h_{st} = p_{ext}$$
$$= 4½ \text{ in.}$$

$$L_{st} = \frac{h_{st}}{\tan 30°} \quad (4\text{-}4)$$
$$= \frac{4½ \text{ in.}}{\tan 30°}$$
$$= 7.79 \text{ in.} \le 8 \text{ in.} \quad \textbf{o.k.}$$

$$t_s \ge t_{bw}\left(\frac{F_{yb}}{F_{ys}}\right) \quad (3\text{-}36)$$
$$\ge (0.470 \text{ in.})\left(\frac{50 \text{ ksi}}{50 \text{ ksi}}\right)$$
$$\ge 0.470 \text{ in.}$$

$t_s = ½$ in. **o.k.**

$$\frac{h_{st}}{t_s} = \frac{4½ \text{ in.}}{½ \text{ in.}}$$
$$= 9.00$$

$$\frac{h_{st}}{t_s} \le 0.56\sqrt{\frac{E}{F_{ys}}} \quad (3\text{-}37)$$
$$\le 0.56\sqrt{\frac{29{,}000 \text{ ksi}}{50 \text{ ksi}}}$$
$$\le 13.5$$

$\frac{h_{st}}{t_s} = 9.00$ **o.k.**

A. End-Plate and Bolt Design Verification

Calculate the equivalent required moment considering the effect of the required tensile force using Equation 3-30.

LRFD	ASD
$M_{u,eq} = M_u + (T_u/2)(d - t_{bf})$ $= 7{,}620 \text{ kip-in.} + \left(\frac{20.4 \text{ kips}}{2}\right)(24.1 \text{ in.} - 0.770 \text{ in.})$ $M_{u,eq} = 7{,}860 \text{ kip-in.}$	$M_{a,eq} = M_a + (T_a/2)(d - t_{bf})$ $= 5{,}080 \text{ kip-in.} + \left(\frac{13.6 \text{ kips}}{2}\right)(24.1 \text{ in.} - 0.770 \text{ in.})$ $M_{a,eq} = 5{,}240 \text{ kip-in.}$

Determine if the specified 1 in. end-plate thickness and 1⅛ in. Grade A490 bolt diameter are sufficient using the thick end-plate/smaller bolt diameter procedure.

Solve for the required bolt diameter using Equations 5-3. For Grade A490 bolts, the nominal tensile stress is $F_{nt} = 113$ ksi.

$$\sum_i n_i h_i = (2 \text{ bolts})(26.5 \text{ in.}) + (2 \text{ bolts})(20.9 \text{ in.})$$
$$= 94.8 \text{ in.}$$

LRFD	ASD
$d_{b,reqd} = \sqrt{\frac{4M_{u,eq}}{\pi\phi F_{nt}\left(\sum_i n_i h_i\right)}}$ $= \sqrt{\frac{4(7{,}860 \text{ kip-in.})}{\pi(0.75)(113 \text{ ksi})(94.8 \text{ in.})}}$ $= 1.12 \text{ in.} \quad \le \quad d_b = 1⅛ \text{ in.} \quad$ **o.k.**	$d_{b,reqd} = \sqrt{\frac{4M_{a,eq}}{\frac{\pi F_{nt}}{\Omega}\left(\sum_i n_i h_i\right)}}$ $= \sqrt{\frac{4(5{,}240 \text{ kip-in.})}{\frac{\pi(113 \text{ ksi})}{2.00}(94.8 \text{ in.})}}$ $= 1.12 \text{ in.} \quad \le \quad d_b = 1⅛ \text{ in.} \quad$ **o.k.**

Solve for the required end-plate thickness using Equations 5-4. First solve for the distance, s, and yield line parameter, Y_p, using Table 5-11.

$$s = \frac{\sqrt{b_p g}}{2}$$
$$= \frac{\sqrt{(9 \text{ in.})(5¾ \text{ in.})}}{2}$$
$$= 3.60 \text{ in.}$$

Because $s > d_e = 1¾$ in., Y_p in Table 5-11 is applicable, and because $s \ge p_{fo} = 2¾$ in. and $p_{fi} = 2$ in., the dimensions p_{fo} and p_{fi} are used in the equation for the yield line parameter.

$$Y_p = \frac{b_p}{2}\left[h_1\left(\frac{1}{p_{fo}} + \frac{1}{2d_e}\right) + h_2\left(\frac{1}{p_{fi}} + \frac{1}{s}\right)\right] + \frac{2}{g}\left[h_1(p_{fo} + d_e) + h_2(p_{fi} + s)\right]$$
$$= \left(\frac{9 \text{ in.}}{2}\right)\left[(26.5 \text{ in.})\left(\frac{1}{2¾ \text{ in.}} + \frac{1}{2(1¾ \text{ in.})}\right) + (20.9 \text{ in.})\left(\frac{1}{2 \text{ in.}} + \frac{1}{3.60 \text{ in.}}\right)\right]$$
$$+ \left(\frac{2}{5¾ \text{ in.}}\right)\left[(26.5 \text{ in.})(2¾ \text{ in.} + 1¾ \text{ in.}) + (20.9 \text{ in.})(2 \text{ in.} + 3.60 \text{ in.})\right]$$
$$= 233 \text{ in.}$$

Determine the required end-plate thickness using Equations 5-4. For extended end-plate configurations, $\gamma_r = 1.0$.

LRFD	ASD
$t_{p,reqd} = \sqrt{\dfrac{1.10M_{u,eq}}{\gamma_r \phi_b F_y Y_p}}$ $= \sqrt{\dfrac{1.10(7{,}860 \text{ kip-in.})}{1.0(0.90)(50 \text{ ksi})(233 \text{ in.})}}$ $= 0.908 \text{ in.} \quad \leq \quad 1 \text{ in.} \quad$ **o.k.**	$t_{p,reqd} = \sqrt{\dfrac{1.10M_{a,eq}}{\gamma_r F_y Y_p / \Omega_b}}$ $= \sqrt{\dfrac{1.10(5{,}240 \text{ kip-in.})}{1.0(50 \text{ ksi})(233 \text{ in.})/1.67}}$ $= 0.909 \text{ in.} \quad \leq \quad 1 \text{ in.} \quad$ **o.k.**

Therefore, a 1-in.-thick end plate is sufficient.

Check Shear Yielding/Shear Rupture of the Extended Portion of the End Plate

For extended end-plate moment connections that are stiffened, shear yielding and shear rupture of the extended portion of the end plate are not limit states.

Check Shear Transfer at the Top Bolt Holes

Shear at the faying surface, V_u, is assumed to be resisted only by the four compression side bolts. The shear transfer strength at each bolt hole is the minimum of the end-plate bearing/tearout strength, the bolt shear rupture strength, and the column flange bearing/tearout strength. See the User Note in AISC *Specification* Section J3.7.

The nominal unthreaded body area of a 1⅛ in. bolt is $A_b = 0.994 \text{ in.}^2$ The nominal shear strength of a 1⅛-in.-diameter Grade A490 bolt is:

$$R_{n,bt} = F_{nv} A_b \qquad \text{(from } \textit{Spec.} \text{ Eq. J3-1)}$$
$$= (68 \text{ ksi})(0.994 \text{ in.}^2)$$
$$= 67.6 \text{ kips}$$

The nominal bearing/tearout strength is given by AISC *Specification* Section J3.11. The bolt shear force acting on the end plate is down toward the middle of the end plate, and therefore, tearout will not control. Likewise, tearout will not control at the column flange, and only bolt bearing needs to be checked. The column flange thickness, 0.780 in., is less than the end-plate thickness, 1 in.; therefore, the controlling nominal bearing strength at a bolt hole is:

$$R_{n,brg} = 2.4 d_b t_p F_{up} \qquad \text{(from } \textit{Spec.} \text{ Eq. J3-6a)}$$
$$= 2.4(1⅛ \text{ in.})(0.780 \text{ in.})(65 \text{ ksi})$$
$$= 137 \text{ kips}$$

The shear transfer strength is then the minimum of the column flange bearing strength, the bolt shear rupture strength, and the end-plate bearing strength, which results in $R_n = 67.6$ kips.

Therefore, the nominal shear transfer strength at the four top bolt holes is:

$$V_n = (4 \text{ bolts}) R_n$$
$$= (4 \text{ bolts})(67.6 \text{ kips})$$
$$= 270 \text{ kips}$$

LRFD	ASD
$\phi V_n = 0.75(270 \text{ kips})$ $= 203 \text{ kips} \quad \geq \quad V_u = 45.8 \text{ kips} \quad$ **o.k.**	$\dfrac{V_n}{\Omega} = \dfrac{270 \text{ kips}}{2.00}$ $= 135 \text{ kips} \quad \geq \quad V_a = 30.5 \text{ kips} \quad$ **o.k.**

The specified ASTM A572/A572M Grade 50 1-in.-thick end plate and 1⅛-in.-diameter Grade A490 pretensioned bolts are sufficient.

B. Check Beam to End-Plate Welds

The minimum fillet weld size in AISC *Specification* Table J2.4 is determined from the material thickness of the thinner part joined. The weld sizes shown in Figure 5-11 satisfy the requirements in Table J2.4.

Check Beam Flange to End-Plate Weld

The weld from the beam flange to the end plate is shown in Figure 5-11 as a CJP groove weld with the bevel facing away from the center of the beam and without weld access holes. (Double-sided 5/16 in. fillet welds or a PJP groove weld are alternate options.)

Check Stiffener Welds

Check that the stiffener to beam flange and stiffener to end-plate welds shown in Figure 5-11 are sufficient to develop the yield strengths of the stiffener plate.

Calculate the required strength for the stiffener to beam flange weld, and determine if the double-sided ⅜ in. fillet weld shown is sufficient.

LRFD	ASD
$V_u = 0.60F_y t_s$ $= 0.60(50\text{ ksi})(½\text{ in.})$ $= 15.0\text{ kips/in.}$	$V_a = 0.40F_y t_s$ $= 0.40(50\text{ ksi})(½\text{ in.})$ $= 10.0\text{ kips/in.}$

$$V_{nw} = (2\text{ welds})0.60F_{EXX}\frac{t_{weld}}{\sqrt{2}}(1.0+0.5\sin^{1.5}\theta) \qquad \text{(from } \textit{Spec.} \text{ Eq. J2-4)}$$

$$= (2\text{ welds})(0.60)(70\text{ ksi})\left(\frac{⅜\text{ in.}}{\sqrt{2}}\right)(1.0+0.5\sin^{1.5}0°)$$

$$= 22.3\text{ kips/in.}$$

LRFD	ASD
$\phi V_{nw} = 0.75(22.3\text{ kips/in.})$ $= 16.7\text{ kips/in.} \quad \geq \quad 15.0\text{ kips/in.}$ **o.k.**	$\frac{V_{nw}}{\Omega} = \frac{22.3\text{ kips/in.}}{2.00}$ $= 11.2\text{ kips/in.} \quad \geq \quad 10.0\text{ kips/in.}$ **o.k.**

The shear rupture strength of the stiffener is greater than its shear yield strength and does not have to be checked. The shear rupture strength of the beam flange is sufficient by inspection.

Therefore, double-sided ⅜ in. fillet welds are sufficient.

Calculate the required strength for the stiffener to end-plate weld, and determine if the double-sided ⅜ in. fillet weld shown is sufficient.

LRFD	ASD
$T_u = F_y t_s$ $= (50\text{ ksi})(½\text{ in.})$ $= 25.0\text{ kips/in.}$	$T_a = \frac{F_y}{1.50}t_s$ $= \frac{50\text{ ksi}}{1.50}(½\text{ in.})$ $= 16.7\text{ kips/in.}$

$$T_{nw} = (2\text{ welds})0.60F_{EXX}\frac{t_{weld}}{\sqrt{2}}(1.0+0.5\sin^{1.5}\theta) \quad \text{(from } \textit{Spec.} \text{ Eq. J2-4)}$$

$$= (2\text{ welds})(0.60)(70\text{ ksi})\left(\frac{\frac{3}{8}\text{ in.}}{\sqrt{2}}\right)(1.0+0.5\sin^{1.5}90°)$$

$$= 33.4\text{ kips/in.}$$

LRFD	ASD
$\phi T_{nw} = 0.75(33.4\text{ kips/in.})$ $= 25.1\text{ kips/in.} \quad \geq \quad 25.0\text{ kips/in.} \quad$ **o.k.**	$\frac{T_{nw}}{\Omega} = \frac{33.4\text{ kips/in.}}{2.00}$ $= 16.7\text{ kips/in.} \quad \geq \quad 16.7\text{ kips/in.} \quad$ **o.k.**

Therefore, double-sided ⅜ in. fillet welds are sufficient.

Check Beam Web to End-Plate Weld

The beam web to end-plate welds as shown in Figure 5-11 are separately checked for (1) tension rupture in the region around the tension bolt holes (extending 6 in. to the inside of the tension bolt holes), and (2) the rest of the web to end-plate weld is checked for shear. If moment reversal is expected, the bottom of the beam web to end-plate weld would also need to be designed for tension. This example is not designed for moment reversal.

As explained in Section 3.7.5, the demand for the tension web area, T_{uw} (LRFD) or T_{aw} (ASD), for this connection is the number of tension bolts adjacent to the web, n_{trib}, divided by the total number of tension bolts, n, multiplied by the calculated beam flange force, $T_{u,calc}$ (LRFD) or $T_{a,calc}$ (ASD), from the beam flange to end-plate weld demand calculations. Using Equations 3-39 and 3-40:

LRFD	ASD
$T_{u,calc} = \frac{M_u}{d-t_{bf}} + \frac{T_u}{2}$ $= \frac{7{,}620\text{ kip-in.}}{24.1\text{ in.} - 0.770\text{ in.}} + \frac{20.4\text{ kips}}{2}$ $= 337\text{ kips}$	$T_{a,calc} = \frac{M_a}{d-t_{bf}} + \frac{T_a}{2}$ $= \frac{5{,}080\text{ kip-in.}}{24.1\text{ in.} - 0.770\text{ in.}} + \frac{13.6\text{ kips}}{2}$ $= 225\text{ kips}$
$T_{uw} = (n_{trib}/n)T_{u,calc}$ $= (2/4)(337\text{ kips})$ $= 169\text{ kips}$	$T_{aw} = (n_{trib}/n)T_{a,calc}$ $= (2/4)(225\text{ kips})$ $= 113\text{ kips}$

The length of the web tension region is measured from the inside of the beam flange to 6 in. inside the tension bolt row:

$$l_{wt} = p_{fi} + 6\text{ in.}$$
$$= 2\text{ in.} + 6\text{ in.}$$
$$= 8.00\text{ in.}$$

The nominal web yield strength in the tension region is:

$$T_{yw} = F_y A_g \quad \text{(from } \textit{Spec.} \text{ Eq. J4-1)}$$
$$= F_y t_{bw} l_{wt}$$
$$= (50\text{ ksi})(0.470\text{ in.})(8.00\text{ in.})$$
$$= 188\text{ kips}$$

Check that the design tensile yield strength of the web is sufficient.

LRFD	ASD
$\phi T_{yw} = 0.90(188 \text{ kips})$ $= 169 \text{ kips} \quad \geq \quad T_{uw} = 169 \text{ kips}$ **o.k.**	$\frac{T_{yw}}{\Omega} = \frac{188 \text{ kips}}{1.67}$ $= 113 \text{ kips} \quad \geq \quad T_{aw} = 113 \text{ kips}$ **o.k.**

Check that the required strength is at least 60% (LRFD) or 40% (ASD) of the web tensile strength from Equations 3-41.

LRFD	ASD
$0.60T_{yw} = 0.60(188 \text{ kips})$ $= 113 \text{ kips}$ $T_{uwd} = \max(T_{uw}, 0.60T_{yw})$ $= \max(169 \text{ kips}, 113 \text{ kips})$ $= 169 \text{ kips}$	$0.40T_{yw} = 0.40(188 \text{ kips})$ $= 75.2 \text{ kips}$ $T_{awd} = \max(T_{aw}, 0.40T_{yw})$ $= \max(113 \text{ kips}, 75.2 \text{ kips})$ $= 113 \text{ kips}$

Check the web to end-plate weld around the tension bolts. Because the weld is loaded perpendicular to its longitudinal axis, the angle of loading, θ, is 90°.

$$R_n = (2 \text{ welds})0.60F_{EXX}\frac{t_{weld}}{\sqrt{2}}l_{wt}(1.0 + 0.5\sin^{1.5}\theta) \qquad \text{(from } \textit{Spec.} \text{ Eq. J2-4)}$$

$$= (2 \text{ welds})(0.60)(70 \text{ ksi})\left(\frac{\frac{3}{8} \text{ in.}}{\sqrt{2}}\right)(8.00 \text{ in.})(1.0 + 0.5\sin^{1.5}90°)$$

$$= 267 \text{ kips}$$

LRFD	ASD
$\phi R_n = 0.75(267 \text{ kips})$ $= 200 \text{ kips} \quad \geq \quad T_{uwd} = 169 \text{ kips}$ **o.k.**	$\frac{R_n}{\Omega} = \frac{267 \text{ kips}}{2.00}$ $= 134 \text{ kips} \quad \geq \quad T_{awd} = 113 \text{ kips.}$ **o.k.**

The double-sided ⅜ in. fillet weld from the web to the end plate in the tension region is sufficient.

Check the web to end-plate weld away from the tension bolts. Only the web to end-plate weld between the end of the assumed web tension length and the inside face of the bottom beam compression flange or the weld between the mid-depth of the beam and the inside face of the beam compression flange, whichever is smaller, is considered effective in resisting the beam end shear. The shear strength of this weld is compared to the required shear applied to the connection.

$$l_t = (d - 2t_{bf}) - l_{wt}$$

$$= 24.1 \text{ in.} - 2(0.770 \text{ in.}) - 8.00 \text{ in.}$$

$$= 14.6 \text{ in.}$$

$$l_{0.5w} = d/2 - t_{bf}$$

$$= (24.1 \text{ in.})/2 - 0.770 \text{ in.}$$

$$= 11.3 \text{ in.}$$

$$l_{wv} = \min(l_t, l_{0.5w})$$

$$= \min(14.6 \text{ in.}, 11.3 \text{ in.})$$

$$= 11.3 \text{ in.}$$

$$R_n = (2 \text{ welds})0.60F_{EXX}\frac{t_{weld}}{\sqrt{2}}l_{wv}(1.0+0.5\sin^{1.5}\theta) \quad \text{(from } \textit{Spec.} \text{ Eq. J2-4)}$$

$$= (2 \text{ welds})(0.60)(70 \text{ ksi})\left(\frac{\frac{1}{4} \text{ in.}}{\sqrt{2}}\right)(11.3 \text{ in.})(1.0+0.5\sin^{1.5}0°)$$

$$= 168 \text{ kips}$$

LRFD	ASD
$\phi R_n = 0.75(168 \text{ kips})$ $= 126 \text{ kips} \quad \geq \quad V_u = 45.8 \text{ kips}$ **o.k.**	$\frac{R_n}{\Omega} = \frac{168 \text{ kips}}{2.00}$ $= 84.0 \text{ kips} \quad \geq \quad V_a = 30.5 \text{ kips}$ **o.k.**

Check that the shear rupture strength of the beam web at the weld using AISC *Specification* Equation J4-4 is sufficient.

$$V_{nw} = 0.60F_uA_{nv} \quad \text{(}\textit{Spec.}\text{ Eq. J4-4)}$$

$$= 0.60F_ul_{wv}t_{bw}$$

$$= 0.60(65 \text{ ksi})(11.3 \text{ in.})(0.470 \text{ in.})$$

$$= 207 \text{ kips}$$

LRFD	ASD
$\phi R_n = 0.75(207 \text{ kips})$ $= 155 \text{ kips} \quad \geq \quad V_u = 45.8 \text{ kips}$ **o.k.**	$\frac{R_n}{\Omega} = \frac{207 \text{ kips}}{2.00}$ $= 104 \text{ kips} \quad \geq \quad V_a = 30.5 \text{ kips}$ **o.k.**

The double-sided ¼ in. fillet welds shown in Figure 5-11 from the web to the end plate are sufficient.

C. Column-Side Limit State Checks

Figure 5-11 shows column web stiffeners opposite both beam flanges. The strength of the stiffener plates and associated welds are now checked.

Check Strength of Column Web Stiffeners

The required strength of the column web stiffeners is the maximum difference between the beam flange force and the minimum strength of the local column limit states at the beam flange location. For this example, the limit states at the bottom beam flange are column flange flexural yielding and column web local yielding. The limit states at the top flange are column web local yielding and column web local crippling. From Part B, the maximum force is at the bottom beam flange, 337 kips (LRFD) and 225 kips (ASD), and is used to check both the top and bottom stiffeners. For column flange flexure, the design strength is compared to 1.10 times the beam flange force to prevent prying action on the bolts.

Check local flange yielding to determine if stiffeners are required opposite the beam bottom flange. First, calculate the unstiffened column flange flexural strength using the column flange yield line parameter from Appendix A. The distance to the upper yield line, s, the distance between bolt rows, c, and the yield line parameter, Y_{cu}, are now calculated using Table A-2, Figure A-2(a).

$$s = \frac{\sqrt{b_{cf}g}}{2}$$

$$= \frac{\sqrt{(14.6 \text{ in.})(5\frac{3}{4} \text{ in.})}}{2}$$

$$= 4.58 \text{ in.}$$

Because $s \geq p_{fo} = 2\frac{3}{4}$ in. and $p_{fi} = 2$ in., the dimensions p_{fo} and p_{fi} are used in the equation for the yield line parameter.

$$c = p_{fo} + t_{bf} + p_{fi}$$
$$= 2¾ \text{ in.} + 0.770 \text{ in.} + 2 \text{ in.}$$
$$= 5.52 \text{ in.}$$

$$Y_{cu} = \frac{b_{cf}}{2}\left[h_1\left(\frac{1}{s}\right) + h_2\left(\frac{1}{s}\right)\right] + \frac{2}{g}\left[h_1\left(s + \frac{3}{4}c\right) + h_2\left(s + \frac{1}{4}c\right)\right] + \frac{g}{2}$$
$$= \left(\frac{14.6 \text{ in.}}{2}\right)\left[(26.5 \text{ in.})\left(\frac{1}{4.58 \text{ in.}}\right) + (20.9 \text{ in.})\left(\frac{1}{4.58 \text{ in.}}\right)\right]$$
$$+ \left(\frac{2}{5¾ \text{ in.}}\right)\left\{(26.5 \text{ in.})\left[4.58 \text{ in.} + \frac{3(5.52 \text{ in.})}{4}\right] + (20.9 \text{ in.})\left(4.58 \text{ in.} + \frac{5.52 \text{ in.}}{4}\right)\right\} + \frac{5¾ \text{ in.}}{2}$$
$$= 202 \text{ in.}$$

The nominal unstiffened column flange flexural strength is:

$$M_{cf,u} = F_y t_{cf}^2 Y_{cu} \quad (3\text{-}43)$$
$$= (50 \text{ ksi})(0.780 \text{ in.})^2 (202 \text{ in.})$$
$$= 6{,}140 \text{ kip-in.}$$

$$R_{n,cu} = \frac{M_{cf,u}}{(d - t_{bf})} \quad (3\text{-}42)$$
$$= \frac{6{,}140 \text{ kip-in.}}{(24.1 \text{ in.} - 0.770 \text{ in.})}$$
$$= 263 \text{ kips}$$

LRFD	ASD
$\phi R_{n,cu} = 0.90(263 \text{ kips})$ $= 237 \text{ kips} \quad \le \quad 1.10T_{u,calc} = 371 \text{ kips}$ **n.g.**	$\frac{R_{n,cu}}{\Omega} = \frac{263 \text{ kips}}{1.67}$ $= 157 \text{ kips} \quad \le \quad 1.10T_{a,calc} = 248 \text{ kips}$ **n.g.**

Column web stiffener plates are required for this check.

Check that the stiffened column flange is sufficient using the column flange yield line parameter, Y_{cs}, from Table A-2, Figure A-2(c). Noting that each stiffener width, b_s, is 6 in., the effective column flange width is:

$$b_{cf,eff} = 2b_s + t_{cw} + \max(t_{cf}, 1 \text{ in.}) \quad \text{(from Eq. 4-3)}$$
$$= 2(6 \text{ in.}) + 0.485 \text{ in.} + \max(0.780 \text{ in.}, 1 \text{ in.})$$
$$= 13.5 \text{ in.} \quad \le \quad b_{cf} = 14.6 \text{ in.}$$

$$s = \frac{\sqrt{b_{cf,eff}\, g}}{2}$$
$$= \frac{\sqrt{(13.5 \text{ in.})(5¾ \text{ in.})}}{2}$$
$$= 4.41 \text{ in.}$$

$$Y_{cs} = \frac{b_{cf,eff}}{2}\left[h_1\left(\frac{1}{s}+\frac{1}{p_{so}}\right)+h_2\left(\frac{1}{s}+\frac{1}{p_{si}}\right)\right]+\frac{2}{g}\left[h_1(s+p_{so})+h_2(s+p_{si})\right]$$

$$=\left(\frac{13.5\text{ in.}}{2}\right)\left[26.5\text{ in.}\left(\frac{1}{4.41\text{ in.}}+\frac{1}{2¾\text{ in.}}\right)+20.9\text{ in.}\left(\frac{1}{4.41\text{ in.}}+\frac{1}{2\text{ in.}}\right)\right]$$

$$+\left(\frac{2}{5¾\text{ in.}}\right)\left[(26.5\text{ in.})(4.41\text{ in.}+2¾\text{ in.})+(20.9\text{ in.})(4.41\text{ in.}+2\text{ in.})\right]$$

$$=321\text{ in.}$$

The nominal column flange flexural strength from Equations 3-42 and 3-43 is:

$$M_{cf,s} = F_y t_{cf}^2 Y_{cs} \qquad (3\text{-}43)$$

$$=(50\text{ ksi})(0.780\text{ in.})^2(321\text{ in.})$$

$$=9{,}760\text{ kip-in.}$$

$$R_{n,cs} = \frac{M_{cf,s}}{(d-t_{bf})} \qquad (3\text{-}42)$$

$$=\frac{9{,}760\text{ kip-in.}}{(24.1\text{ in.}-0.770\text{ in.})}$$

$$=418\text{ kips}$$

LRFD	ASD
$\phi R_{n,cs} = 0.90(418\text{ kips})$ $= 376\text{ kips} \quad \geq \quad 1.10T_{u,calc} = 371\text{ kips}$ **o.k.**	$\frac{R_{n,cs}}{\Omega} = \frac{418\text{ kips}}{1.67}$ $= 250\text{ kips} \quad \geq \quad 1.10T_{a,calc} = 248\text{ kips}$ **o.k.**

Local flange yielding strength is satisfactory if web stiffeners are provided as shown in Figure 5-11.

Check web yielding to determine if stiffeners are required for the column web opposite the beam flanges. The concentrated force delivered by the beam bottom flange to the column is slightly greater than corresponding force at the top flange because of the required tension force, T_u. The following check is therefore slightly conservative for the top flange force.

The nominal column web local yielding strength opposite the bottom flange of the beam is calculated using equations from Section 3.7.6. The parameter, C_t, is 1.0 because the distance from the bottom of the beam to the bottom of the column is more than the depth of the column.

$$l_b = t_{bf} + 2t_p \qquad \text{(from Eq. 3-47)}$$

$$=0.770\text{ in.}+2(1\text{ in.})$$

$$=2.77\text{ in.}$$

$$k_c = k_{des}$$

$$=1.38\text{ in.}$$

$$R_{n,lwy} = (6C_t k_c + l_b)F_y t_{cw} \qquad (3\text{-}46)$$

$$=\left[6(1.0)(1.38\text{ in.})+2.77\text{ in.}\right](50\text{ ksi})(0.485\text{ in.})$$

$$=268\text{ kips}$$

The available column web local yielding strength is then calculated and compared to the required strength.

LRFD	ASD
$\phi R_{n,lwy} = 1.00(268 \text{ kips})$ $= 268 \text{ kips} \quad \le \quad T_{u,calc} = 337 \text{ kips}$ **n.g.**	$\frac{R_{n,lwy}}{\Omega} = \frac{268 \text{ kips}}{1.50}$ $= 179 \text{ kips} \quad \le \quad T_{a,calc} = 225 \text{ kips}$ **n.g.**

The column web stiffener plates are required for this check.

Calculate the column web local crippling strength opposite the top flange of the beam. The flange force is applied more than half the column depth from the end of the column; therefore, use AISC *Specification* Equation J10-4 with $Q_f = 1.0$.

$$R_{n,lwc} = 0.80 t_{cw}^2 \left[1 + 3\left(\frac{l_b}{d_c}\right)\left(\frac{t_{cw}}{t_{cf}}\right)^{1.5}\right]\sqrt{\frac{EF_y t_{cf}}{t_{cw}}} Q_f \qquad \text{(from } \textit{Spec.} \text{ Eq. J10-4)}$$

$$= 0.80(0.485 \text{ in.})^2 \left[1 + 3\left(\frac{2.77 \text{ in.}}{14.2 \text{ in.}}\right)\left(\frac{0.485 \text{ in.}}{0.780 \text{ in.}}\right)^{1.5}\right]\sqrt{\frac{(29{,}000 \text{ ksi})(50 \text{ ksi})(0.780 \text{ in.})}{0.485 \text{ in.}}}(1.0)$$

$$= 370 \text{ kips}$$

The available column web local crippling strength is calculated and compared to the required compression force.

LRFD	ASD
$\phi R_{n,lwc} = 0.75(370 \text{ kips})$ $= 278 \text{ kips} \quad \le \quad T_{u,calc} = 337 \text{ kips}$ **n.g.**	$\frac{R_{n,lwc}}{\Omega} = \frac{370 \text{ kips}}{2.00}$ $= 185 \text{ kips} \quad \le \quad T_{a,calc} = 225 \text{ kips}$ **n.g.**

The column web stiffener plates are required for this check.

Calculate the required stiffener strengths at the top and bottom beam flange locations.

LRFD	ASD
At bottom beam flange (tension): $T_{u,stiff} = T_{u,calc} - \min(\phi R_{n,cu}, \phi R_{n,lwy})$ $= 337 \text{ kips} - \min(237 \text{ kips}, 268 \text{ kips})$ $= 100 \text{ kips}$ At top beam flange (compression): $C_{u,stiff} = T_{u,calc} - \min(\phi R_{n,lwy}, \phi R_{n,lwc})$ $= 337 \text{ kips} - \min(268 \text{ kips}, 278 \text{ kips})$ $= 69.0 \text{ kips}$	At bottom beam flange (tension): $T_{a,stiff} = T_{a,calc} - \min\left(\frac{R_{n,cu}}{\Omega}, \frac{R_{n,lwy}}{\Omega}\right)$ $= 225 \text{ kips} - \min(157 \text{ kips}, 179 \text{ kips})$ $= 68.0 \text{ kips}$ At top beam flange (compression): $C_{a,stiff} = T_{a,calc} - \min\left(\frac{R_{n,lwy}}{\Omega}, \frac{R_{n,lwc}}{\Omega}\right)$ $= 225 \text{ kips} - \min(179 \text{ kips}, 185 \text{ kips})$ $= 46.0 \text{ kips}$

The column web does not have sufficient strength for column web yielding, column flange yielding, and column web crippling. The strength of the column web stiffener plates, ½ in. × 6 in., shown in Figure 5-11 is now checked.

Check the geometric requirements in AISC *Specification* Section J10.8:

$$\min t_s = t_{bf}/2$$

$$= (0.770 \text{ in.})/2$$

$$= 0.385 \text{ in.} \quad \le \quad t_s = ½ \text{ in.} \quad \textbf{o.k.}$$

$$\min b_s = b_{bf}/3 - t_{cw}/2$$
$$= (9.02\text{ in.})/3 - (0.485\text{ in.})/2$$
$$= 2.76\text{ in.} \leq b_s = 6\text{ in.} \quad \textbf{o.k.}$$

Check stiffener local buckling. From AISC *Specification* Table B4.1a, Case 2:

$$\lambda_r = 0.64\sqrt{\frac{k_c E}{F_{ys}}}$$

$$h = d_c - 2k_{des}$$
$$= 14.2\text{ in.} - 2(1.38\text{ in.})$$
$$= 11.4\text{ in.}$$

$$k_c = \frac{4}{\sqrt{h/t_{cw}}}$$
$$= \frac{4}{\sqrt{(11.4\text{ in.})/0.485\text{ in.}}}$$
$$= 0.825 \geq 0.76$$

Because the computed value of k_c is greater than 0.76, use the value $k_c = 0.76$:

$$\lambda_r = 0.64\sqrt{\frac{k_c E}{F_{ys}}}$$
$$= 0.64\sqrt{\frac{0.76(29{,}000\text{ ksi})}{50\text{ ksi}}}$$
$$= 13.4$$

$$\frac{b_s}{t_s} = \frac{6\text{ in.}}{\frac{1}{2}\text{ in.}}$$
$$= 12.0 \leq 13.4 \quad \textbf{o.k.}$$

Check that the required stiffener plate strength is less than the available yield strength of the stiffener plates. Note that the available yield strength of a stiffener plate is the same for tension or compression because $\phi = 0.90$ and $\Omega = 1.67$ for both tension and compression.

The stiffener plate must be clipped because of the column flange-to-web fillet. To satisfy the requirements of AWS D1.8/D1.8M clause 4.1, the clip adjacent to the column flange, $clip_f$, must extend past the flange-to-web fillet, but not by more than ½ in. Therefore, a 1⅜ in. clip is used.

$$clip_{f,min} = k_{1,c} - t_w/2$$
$$= 1\tfrac{7}{16}\text{ in.} - (0.485\text{ in.})/2$$
$$= 1.20\text{ in.} < clip_f = 1\tfrac{3}{8}\text{ in.} \quad \textbf{o.k.}$$

$$clip_{f,max} = k_{1,c} - t_w/2 + \tfrac{1}{2}\text{ in.}$$
$$= 1\tfrac{7}{16}\text{ in.} - (0.485\text{ in.})/2 + \tfrac{1}{2}\text{ in.}$$
$$= 1.70\text{ in.} > clip_f = 1\tfrac{3}{8}\text{ in.} \quad \textbf{o.k.}$$

$$A_{net} = 2(b_s - clip)t_s$$
$$= 2(6\text{ in.} - 1\tfrac{3}{8}\text{ in.})(\tfrac{1}{2}\text{ in.})$$
$$= 4.63\text{ in.}^2$$

$$P_{n,stiff} = F_y A_{net} \quad \text{(from } \textit{Spec.} \text{ Eq. J4-1)}$$
$$= (50 \text{ ksi})(4.63 \text{ in.}^2)$$
$$= 232 \text{ kips}$$

LRFD	ASD
$\phi P_{n,stiff} = 0.90(232 \text{ kips})$ $= 209 \text{ kips} \geq 100 \text{ kips}$ **o.k.**	$\frac{P_{n,stiff}}{\Omega} = \frac{232 \text{ kips}}{1.67}$ $= 139 \text{ kips} \geq 68.0 \text{ kips}$ **o.k.**

The column web stiffener plates shown in Figure 5-11 are adequate.

Check Stiffener Plate Welds

It is recommended that the stiffener plate to flange weld resist the tensile yield strength of the net section. Check that the double-sided ⅜ in. fillet welds shown in Figure 5-11 are satisfactory.

$$l_{wt} = b_s - clip_f$$
$$= 6 \text{ in.} - 1⅜ \text{ in.}$$
$$= 4.63 \text{ in.}$$

$$R_n = (4 \text{ welds}) 0.60 F_{EXX} \frac{t_{weld}}{\sqrt{2}} l_{wt} (1.0 + 0.5 \sin^{1.5} \theta) \quad \text{(from } \textit{Spec.} \text{ Eq. J2-4)}$$
$$= (4 \text{ welds})(0.60)(70 \text{ ksi}) \left(\frac{⅜ \text{ in.}}{\sqrt{2}} \right) (4.63 \text{ in.})(1.0 + 0.5 \sin^{1.5} 90°)$$
$$= 309 \text{ kips}$$

LRFD	ASD
$\phi R_n = 0.75(309 \text{ kips})$ $= 232 \text{ kips} \geq P_{n,stiff} = 232 \text{ kips}$ **o.k.**	$\frac{R_n}{\Omega} = \frac{309 \text{ kips}}{2.00}$ $= 155 \text{ kips} \geq \frac{P_{n,stiff}}{1.50} = 155 \text{ kips}$ **o.k.**

Check that the ¼ in. stiffener plate-to-column web fillet welds and single-bevel-groove welds shown in Figure 5-11 are satisfactory. The required strength is 100 kips (LRFD) and 68 kips (ASD). The stiffener plate must be clipped because of the column flange-to-web fillet. To satisfy the requirements of AWS D1.8/D1.8M clause 4.1, the clip adjacent to the column web, $clip_w$, must extend 1½ in. past the k_{det} dimension. Therefore, a 2 13⁄16 in. clip is used.

$$clip_{w,min} = k_{det,c} - t_{cf} + 1½ \text{ in.}$$
$$= 2 1⁄16 \text{ in.} - 0.780 \text{ in.} + 1½ \text{ in.}$$
$$= 2.78 \text{ in.} < clip_w = 2 13⁄16 \text{ in.} \quad \textbf{o.k.}$$

$$l_{wv} = d_c - 2t_{cf} - 2clip_w$$
$$= 14.2 \text{ in.} - 2(0.780 \text{ in.}) - 2(2 13⁄16 \text{ in.})$$
$$= 7.02 \text{ in.}$$

$$R_n = (2\text{ welds})0.60F_{EXX}\frac{t_{weld}}{\sqrt{2}}l_{wv}(1.0+0.5\sin^{1.5}\theta)+(2\text{ welds})0.60F_{EXX}S_{PJP}l_{wv}$$

$$=(2\text{ welds})0.60(70\text{ ksi})\left(\frac{¼\text{ in.}}{\sqrt{2}}\right)(7.02\text{ in.})(1.0+0.5\sin^{1.5}0°) \quad \text{(from } \textit{Spec.} \text{ Eq. J2-4)}$$

$$+(2\text{ welds})0.60(70\text{ ksi})(¼\text{ in.})(7.02\text{ in.})$$

$$=252\text{ kips}$$

LRFD	ASD
$\phi R_n = 0.75(252\text{ kips})$ $= 189\text{ kips} \geq T_{u,stiff} = 100\text{ kips}$ **o.k.**	$\frac{R_n}{\Omega} = \frac{252\text{ kips}}{2.00}$ $= 126\text{ kips} \geq T_{a,stiff} = 68.0\text{ kips}$ **o.k.**

Check that the shear rupture strength of the ½ in. stiffeners at the welds using AISC *Specification* Equation J4-4 is sufficient.

$$V_{nw} = 0.60F_uA_{nv} \quad \text{(}\textit{Spec.}\text{ Eq. J4-4)}$$

$$=(2\text{ stiffeners})0.60F_ul_{wv}t_s$$

$$=(2\text{ stiffeners})0.60(65\text{ ksi})(7.02\text{ in.})(½\text{ in.})$$

$$=274\text{ kips}$$

LRFD	ASD
$\phi R_n = 0.75(274\text{ kips})$ $= 206\text{ kips} \geq T_{u,stiff} = 100\text{ kips}$ **o.k.**	$\frac{R_n}{\Omega} = \frac{274\text{ kips}}{2.00}$ $= 137\text{ kips} \geq T_{a,stiff} = 68.0\text{ kips}$ **o.k.**

Because there are two shear rupture lines, one above and one below each stiffener, at the column web and at the doubler plate, shear rupture of the column web and doubler plate is sufficient by inspection.

The stiffener plate to column flange and web welds shown in Figure 5-11 are satisfactory.

Check Column Panel Zone Shear

Figure 5-11 shows a ⅜ in. doubler plate reinforcement in the column panel zone. Check the column panel zone for shear strength using AISC *Specification* Section J10.6. The column panel zone strength is the sum of the column web strength and the doubler plate shear yielding strengths. The required shear strength is the beam flange force less one-half of the required axial force, less the column shear.

LRFD	ASD
$V_u = \frac{M_u}{d-t_{bf}} - \frac{T_u}{2} - V_{uc}$ $= \frac{7{,}620\text{ kip-in.}}{24.1\text{ in.}-0.770\text{ in.}} - \frac{20.4\text{ kips}}{2} - 19.6\text{ kips}$ $= 297\text{ kips}$	$V_a = \frac{M_a}{d-t_{bf}} - \frac{T_a}{2} - V_{ac}$ $= \frac{5{,}080\text{ kip-in.}}{24.1\text{ in.}-0.770\text{ in.}} - \frac{13.6\text{ kips}}{2} - 13.1\text{ kips}$ $= 198\text{ kips}$

Check the doubler plate slenderness using AISC *Specification* Section G2.1. The width of the doubler plate is:

$$h_{dp} = d_c - 2t_{cf}$$
$$= 14.2 \text{ in.} - 2(0.780 \text{ in.})$$
$$= 12.6 \text{ in.}$$

If the slenderness limit with $k_v = 5.34$ is satisfied, the nominal shear strength of the panel zone doubler plate is its nominal shear yield strength.

$$\frac{h_{dp}}{t_{dp}} \le 1.10\sqrt{\frac{k_v E}{F_y}}$$
$$= 1.10\sqrt{\frac{5.34(29{,}000 \text{ ksi})}{50 \text{ ksi}}}$$
$$= 61.2$$

$$\frac{h_{dp}}{t_{dp}} = \frac{12.6 \text{ in.}}{\frac{3}{8} \text{ in.}}$$
$$= 33.6 \quad \le \quad 61.2 \quad \textbf{o.k.}$$

Shear buckling does not control for the doubler plate.

$$\frac{h}{t_{cw}} = 23.5 \quad \le \quad 61.2 \quad \textbf{o.k.}$$

Shear buckling does not control for the column web.

Therefore,

$$C_{v1} = 1.0 \qquad \text{(}\textit{Spec}\text{. Eq. G2-3)}$$

Assuming the column required axial strength is less than $0.4P_y$ and the effect of inelastic panel zone deformation on frame stability was not accounted for in the analysis, the nominal shear yielding strength of the panel zone column web plus ⅜ in. doubler plate is:

$$R_n = 0.60F_y A_w C_{v1} \qquad \text{(}\textit{Spec}\text{. Eq. G2-1)}$$
$$= 0.60F_y d_c (t_{cw} + t_{dp}) C_{v1}$$
$$= 0.60(50 \text{ ksi})(14.2 \text{ in.})(0.485 \text{ in.} + \tfrac{3}{8} \text{ in.})(1.0)$$
$$= 366 \text{ kips}$$

LRFD	ASD
$\phi_v R_n = 0.90(366 \text{ kips})$ $= 329 \text{ kips} \quad \ge \quad V_u = 297 \text{ kips} \quad$ **o.k.**	$\frac{R_n}{\Omega_v} = \frac{366 \text{ kips}}{1.67}$ $= 219 \text{ kips} \quad \ge \quad V_a = 198 \text{ kips} \quad$ **o.k.**

This check for panel zone shear strength compares the total required shear strength (associated with beam flange force and column shear) to the total design shear strength (associated with the column web and doubler plate) instead of analyzing the column web and doubler plate separately. This was deemed reasonable for this example, where the column web and doubler plate thicknesses were similar and the column shear was relatively small compared to the beam flange force.

Panel Zone to Column Web Welds

The long side vertical welds are shown in Figure 5-11 in accordance with AWS D1.8/D1.8M, clause 4.3, which develops the doubler plate. The short side single-bevel-groove welds are closure welds.

The column panel zone reinforced with a ⅜ in. doubler plate is sufficient to resist the required shear. (Note, alternatively, the column size could be increased to eliminate the need for a doubler plate.)

Summary

The connection shown in Figure 5-11 is adequate for the required moment and forces.

EXAMPLE 5.3-3—Multiple-Row Extended 1/2 Unstiffened Thick End-Plate Example

Given:

The connection shown in Figure 5-12 is a multiple-row extended (MRE) 1/2 unstiffened end-plate moment connection for a built-up beam. The beam and end-plate material are ASTM A572/A572M Grade 50, and the bolts are Group 120 ASTM F3125/F3125M Grade A325 pretensioned. Weld electrodes are E70XX. The connection is to be evaluated as a thick end-plate design for the following required moments and shear forces.

	LRFD	ASD
Moment	M_u = 4,800 kip-in.	M_a = 3,200 kip-in.
Shear force	V_u = 45.0 kips	V_a = 30.0 kips

Solution:

From the AISC *Manual*, Table 2-4, the material properties are as follows:

ASTM A572/A572M Grade 50
F_y = 50 ksi
F_u = 65 ksi

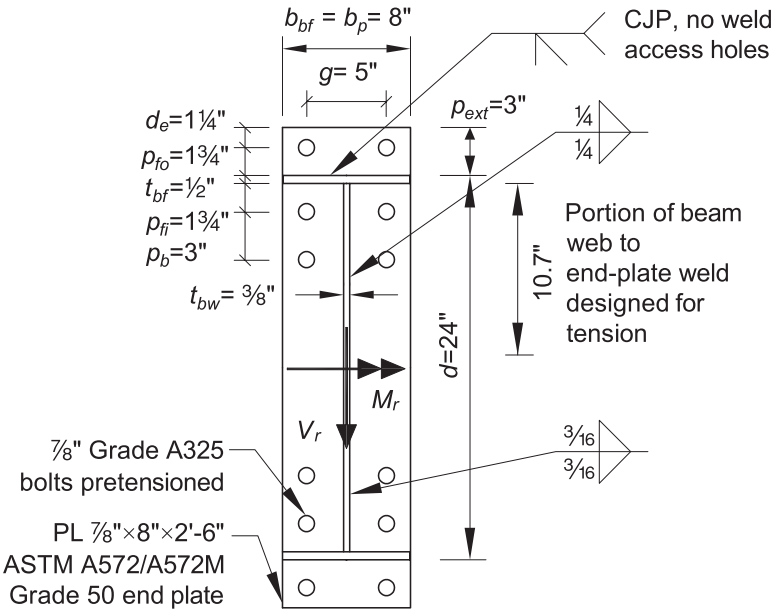

Fig. 5-12. MRE 1/2 unstiffened end-plate configuration for Example 5.3-3.

From AISC *Specification* Table J3.2, the material properties of the bolts are as follows:

Group 120 ASTM F3125/F3125M ⅞-in.-diameter Grade A325 pretensioned
F_{nt} = 90 ksi
F_{nv} = 54 ksi (Group 120 bolts with threads not excluded from the shear plane; thread condition N)

Beam
d = 24 in. t_{bw} = ⅜ in.
b_{bf} = 8 in. t_{bf} = ½ in.

End-plate geometric properties:
b_p = 8 in.
t_p = ⅞ in.
g = 5 in.
p_{ext} = 3 in.
d_e = 1¼ in.
p_{fo} = 1¾ in.
p_{fi} = 1¾ in.
p_b = 3 in.
d_p = 30 in.

The distances from the centerline of the compression flange to the bolt lines, h_1, h_2, and h_3, are depicted in Table 5-12 and computed as:

$$h_1 = d - \frac{t_{bf}}{2} + p_{fo}$$
$$= 24 \text{ in.} - \frac{½ \text{ in.}}{2} + 1¾ \text{ in.}$$
$$= 25.5 \text{ in.}$$

$$h_2 = d - \frac{3t_{bf}}{2} - p_{fi}$$
$$= 24 \text{ in.} - \frac{3(½ \text{ in.})}{2} - 1¾ \text{ in.}$$
$$= 21.5 \text{ in.}$$

$$h_3 = d - \frac{3t_{bf}}{2} - p_{fi} - p_b$$
$$= 24 \text{ in.} - \frac{3(½ \text{ in.})}{2} - 1¾ \text{ in.} - 3 \text{ in.}$$
$$= 18.5 \text{ in.}$$

$$b_{p,eff} \le b_{bf} + \max(t_p, 1 \text{ in.}) \quad (4\text{-}3)$$
$$\le 8 \text{ in.} + \max(⅞ \text{ in.}, 1 \text{ in.})$$
$$\le 9.00 \text{ in.}$$

b_p = 8 in. ≤ 9.00 in. **o.k.**

$$b_{bf} \ge g \quad (4\text{-}1)$$
8 in. ≥ 5 in. **o.k.**

A. End-Plate and Bolt Design Verification

Determine if the specified end-plate thickness, ⅞ in., and Grade A325 bolt diameter, ⅞ in., using the thick end-plate/smaller bolt diameter procedure are sufficient.

Solve for the required bolt diameter using Equations 5-3. For Grade A325 bolts, the nominal tensile stress is $F_{nt} = 90$ ksi.

$$\sum_i n_i h_i = 2(25.5 \text{ in.}) + 2(21.5 \text{ in.}) + 2(18.5 \text{ in.})$$
$$= 131 \text{ in.}$$

LRFD	ASD
$d_{b,reqd} = \sqrt{\dfrac{4M_u}{\pi\phi F_{nt}\left(\sum_i n_i h_i\right)}}$ $= \sqrt{\dfrac{4(4{,}800 \text{ kip-in.})}{\pi(0.75)(90 \text{ ksi})(131 \text{ in.})}}$ $= 0.831 \text{ in.} \quad \le \quad ⅞ \text{ in.} \quad$ **o.k.**	$d_{b,reqd} = \sqrt{\dfrac{4M_a}{\dfrac{\pi F_{nt}}{\Omega}\left(\sum_i n_i h_i\right)}}$ $= \sqrt{\dfrac{4(3{,}200 \text{ kip-in.})}{\dfrac{\pi(90 \text{ ksi})}{2.00}(131 \text{ in.})}}$ $= 0.831 \text{ in.} \quad \le \quad ⅞ \text{ in.} \quad$ **o.k.**

The specified ⅞-in.-diameter Grade A325 bolts are sufficient to resist the required moment.

Solve for the required end-plate thickness using Equations 5-4. First solve for the distance, s, and yield line parameter, Y_p, using Table 5-12.

$$s = \frac{\sqrt{b_p g}}{2}$$
$$= \frac{\sqrt{(8 \text{ in.})(5 \text{ in.})}}{2}$$
$$= 3.16 \text{ in.}$$

Because $s \ge p_{fi} = 1¾$ in., the dimension p_{fi} is used in the equation for the yield line parameter.

$$Y_p = \frac{b_p}{2}\left[h_1\left(\frac{1}{p_{fo}}\right) + h_2\left(\frac{1}{p_{fi}}\right) + h_3\left(\frac{1}{s}\right) - \frac{1}{2} + \frac{2}{g}\left[h_2(p_{fi} + 0.75p_b) + h_3(s + 0.25p_b)\right] + \frac{g}{2}\right.$$
$$= \left(\frac{8 \text{ in.}}{2}\right)\left[(25.5 \text{ in.})\left(\frac{1}{1¾ \text{ in.}}\right) + (21.5 \text{ in.})\left(\frac{1}{1¾ \text{ in.}}\right) + (18.5 \text{ in.})\left(\frac{1}{3.16 \text{ in.}}\right) - \frac{1}{2}\right]$$
$$+ \left(\frac{2}{5 \text{ in.}}\right)\left\{21.5 \text{ in.}\left[1¾ \text{ in.} + 0.75(3 \text{ in.})\right] + 18.5 \text{ in.}\left[3.16 \text{ in.} + 0.25(3 \text{ in.})\right]\right\} + \frac{5 \text{ in.}}{2}$$
$$= 195 \text{ in.}$$

Determine the required end-plate thickness using Equations 5-4. For extended end-plate configurations, $\gamma_r = 1.0$.

LRFD	ASD
$t_{p,reqd} = \sqrt{\dfrac{1.10M_u}{\gamma_r \phi_b F_y Y_p}}$ $= \sqrt{\dfrac{1.10(4{,}800 \text{ kip-in.})}{1.0(0.90)(50 \text{ ksi})(195 \text{ in.})}}$ $= 0.776 \text{ in.} \quad \le \quad ⅞ \text{ in.} \quad$ **o.k.**	$t_{p,reqd} = \sqrt{\dfrac{1.10M_a}{\gamma_r F_y Y_p / \Omega_b}}$ $= \sqrt{\dfrac{1.10(3{,}200 \text{ kip-in.})}{1.0(50 \text{ ksi})(195 \text{ in.})/1.67}}$ $= 0.776 \text{ in.} \quad \le \quad ⅞ \text{ in.} \quad$ **o.k.**

Check Shear Yielding/Shear Rupture of the Extended Portion of the End Plate

For extended end-plate moment connections that are unstiffened, potential limit states that must be checked are shear yielding and shear rupture of the extended portion of the end plate. For the MRE 1/2 connection, the shear demand is taken as one-third of the tension flange force because the exterior bolts represent one-third of the bolts. The shear strength is calculated in accordance with AISC *Specification* Section J4.2.

Calculate the shear demand on the extended portion of the end plate.

LRFD	ASD
$V_{up} = \frac{1}{3}\left(\frac{M_u}{d - t_{bf}}\right)$	$V_{ap} = \frac{1}{3}\left(\frac{M_a}{d - t_{bf}}\right)$
$= \frac{1}{3}\left(\frac{4{,}800 \text{ kip-in.}}{24 \text{ in.} - ½ \text{ in.}}\right)$	$= \frac{1}{3}\left(\frac{3{,}200 \text{ kip-in.}}{24 \text{ in.} - ½ \text{ in.}}\right)$
$= 68.1$ kips	$= 45.4$ kips

Calculate the nominal shear yielding strength.

$$R_n = 0.60F_yA_{gv} \qquad \text{(}\textit{Spec}\text{. Eq. J4-3)}$$
$$= 0.60F_yb_pt_p$$
$$= 0.60(50 \text{ ksi})(8 \text{ in.})(⅞ \text{ in.})$$
$$= 210 \text{ kips}$$

Compare the design shear yielding strength to the shear demand. According to AISC *Specification* Section J4.2 for yielding of elements in shear, the resistance factor is $\phi = 1.00$, and the safety factor is $\Omega = 1.50$.

LRFD	ASD
$\phi R_n = 1.00(210 \text{ kips})$	$\frac{R_n}{\Omega} = \frac{210 \text{ kips}}{1.50}$
$= 210 \text{ kips} \quad \geq \quad V_{up} = 68.1 \text{ kips}$ **o.k.**	$= 140 \text{ kips} \quad \geq \quad V_{ap} = 45.4 \text{ kips}$ **o.k.**

Calculate the nominal shear rupture strength. The width of the extended portion of the end plate for use in the net section area is the width minus two effective hole diameters. The effective hole diameter is the hole diameter from AISC *Specification* Table J3.3 plus 1⁄16 in. The additional 1⁄16 in. accounts for damage around the hole caused by drilling, punching, or thermal cutting. For ⅞-in.-diameter bolts, the standard hole diameter, d_h, is 15⁄16 in.

$$A_{nv} = \left[b_p - 2(d_h + 1⁄16 \text{ in.})\right]t_p$$
$$= \left[8 \text{ in.} - 2(15⁄16 \text{ in.} + 1⁄16 \text{ in.})\right](⅞ \text{ in.})$$
$$= 5.25 \text{ in.}^2$$
$$R_n = 0.60F_uA_{nv} \qquad \text{(}\textit{Spec}\text{. Eq. J4-4)}$$
$$= 0.60(65 \text{ ksi})(5.25 \text{ in.}^2)$$
$$= 205 \text{ kips}$$

Compare the design shear rupture strength to the shear demand. Using AISC *Specification* Section J4.2 for rupture of elements in shear, the resistance factor is $\phi = 0.75$, and the safety factor is $\Omega = 2.00$.

LRFD	ASD
$\phi R_n = 0.75(205 \text{ kips})$ $= 154 \text{ kips} \quad \geq \quad V_{up} = 68.1 \text{ kips}$ **o.k.**	$\frac{R_n}{\Omega} = \frac{205 \text{ kips}}{2.00}$ $= 103 \text{ kips} \quad \geq \quad V_{ap} = 45.4 \text{ kips}$ **o.k.**

The extended portion of the ⅞-in.-thick end plate has sufficient resistance to shear yielding and shear rupture.

Check Shear Transfer at Bolt Holes

See Example 5.3-1 or 5.3-2 for calculation procedures.

B. Check Beam to End-Plate Welds

The minimum weld size in AISC *Specification* Table J2.4 is determined from the material thickness of the thinner part joined. The fillet weld sizes shown in Figure 5-12 satisfy the requirements in Table J2.4.

Check Beam Flange to End-Plate Weld

The weld from the beam flange to the end plate is shown in Figure 5-12 as a CJP groove weld with the bevel facing away from the center of the beam and without weld access holes. (Double-sided 7/16 in. fillet welds or a PJP groove weld are alternate options.)

Check Beam Web to End-Plate Weld

The beam web to end-plate welds shown in Figure 5-12 are separately checked for (1) tension rupture in the region around the tension bolts (extending 6 in. to the inside of the tension bolts), and (2) the remainder of the web to end-plate weld is checked for shear.

As explained in Section 3.7.5, the demand for the tension web area, T_{uw} (LRFD) or T_{aw} (ASD), for this connection is the number of tension bolts adjacent to the web, n_{trib}, divided by the total number of tension bolts, n, multiplied by the calculated beam flange force, $T_{u,calc}$ (LRFD) or $T_{a,calc}$ (ASD).

LRFD	ASD
$T_{u,calc} = \frac{M_u}{d - t_{bf}}$ $= \frac{4{,}800 \text{ kip-in.}}{24 \text{ in.} - ½ \text{ in.}}$ $= 204 \text{ kips}$	$T_{a,calc} = \frac{M_a}{d - t_{bf}}$ $= \frac{3{,}200 \text{ kip-in.}}{24 \text{ in.} - ½ \text{ in.}}$ $= 136 \text{ kips}$
$T_{uw} = (n_{trib}/n)T_{u,calc}$ $= (4/6)(204 \text{ kips})$ $= 136 \text{ kips}$	$T_{aw} = (n_{trib}/n)T_{a,calc}$ $= (4/6)(136 \text{ kips})$ $= 90.7 \text{ kips}$

The length of the web tension region is measured from the inside of the beam flange to 6 in. inside the tension bolt row:

$l_{wt} = p_{fi} + p_b + 6 \text{ in.}$
$= 1¾ \text{ in.} + 3 \text{ in.} + 6 \text{ in.}$
$= 10.8 \text{ in.}$

The nominal web yield strength in the tension region is:

$$T_{yw} = F_y A_g \qquad \text{(from } \textit{Spec}\text{. Eq. J4-1)}$$
$$= F_y t_{bw} l_{wt}$$
$$= (50 \text{ ksi})(⅜ \text{ in.})(10.8 \text{ in.})$$
$$= 203 \text{ kips}$$

Check that the web design tensile yield strength is sufficient.

LRFD	ASD
$\phi T_{yw} = 0.90(203 \text{ kips})$ $= 183 \text{ kips} \quad \geq \quad T_{uw} = 136 \text{ kips}$ **o.k.**	$\frac{T_{yw}}{\Omega} = \frac{203 \text{ kips}}{1.67}$ $= 122 \text{ kips} \quad \geq \quad T_{aw} = 90.7 \text{ kips}$ **o.k.**

Check that the required strength is at least 60% (LRFD) or 40% (ASD) of the web tensile strength from Equations 3-41.

LRFD	ASD
$0.60T_{yw} = 0.60(203 \text{ kips})$ $= 122 \text{ kips}$ $T_{uwd} = \max(T_{uw}, 0.60T_{yw})$ $= \max(136 \text{ kips}, 122 \text{ kips})$ $= 136 \text{ kips}$	$0.40T_{yw} = 0.40(203 \text{ kips})$ $= 81.2 \text{ kips}$ $T_{awd} = \max(T_{aw}, 0.40T_{yw})$ $= \max(90.7 \text{ kips}, 81.2 \text{ kips})$ $= 90.7 \text{ kips}$

Check the web to end-plate weld around the tension bolts. Because the weld is loaded perpendicular to its longitudinal axis, the angle of loading, θ, is 90°.

$$R_n = (2 \text{ welds})0.60F_{EXX}\frac{t_{weld}}{\sqrt{2}} l_{wt}(1.0 + 0.5\sin^{1.5}\theta) \qquad \text{(from } \textit{Spec}\text{. Eq. J2-4)}$$
$$= (2 \text{ welds})(0.60)(70 \text{ ksi})\left(\frac{¼ \text{ in.}}{\sqrt{2}}\right)(10.8 \text{ in.})(1.0 + 0.5\sin^{1.5} 90°)$$
$$= 241 \text{ kips}$$

LRFD	ASD
$\phi R_n = 0.75(241 \text{ kips})$ $= 181 \text{ kips} \quad \geq \quad T_{uwd} = 136 \text{ kips}$ **o.k.**	$\frac{R_n}{\Omega} = \frac{241 \text{ kips}}{2.00}$ $= 121 \text{ kips} \quad \geq \quad T_{awd} = 90.7 \text{ kips}$ **o.k.**

Check the web to end-plate weld away from the tension bolts. Only the web to end-plate weld between the end of the assumed web tension length and the inside face of the bottom beam compression flange or the weld between the mid-depth of the beam and the inside face of the beam compression flange, whichever is smaller, is considered effective in resisting the beam end shear. The shear strength of this weld is compared to the required shear applied to the connection.

$$l_t = d - 2t_{bf} - l_{wt}$$
$$= 24 \text{ in.} - 2(½ \text{ in.}) - 10.8 \text{ in.}$$
$$= 12.2 \text{ in.}$$

$$l_{0.5w} = d/2 - t_{bf}$$
$$= (24 \text{ in.})/2 - ½ \text{ in.}$$
$$= 11.5 \text{ in.}$$

$$l_{wv} = \min(l_t, l_{0.5w})$$
$$= \min(12.2 \text{ in.}, 11.5 \text{ in.})$$
$$= 11.5 \text{ in.}$$

$$R_n = (2 \text{ welds}) 0.60 F_{EXX} \frac{t_{weld}}{\sqrt{2}} l_{wv} (1.0 + 0.5 \sin^{1.5} \theta) \quad \text{(from } Spec. \text{ Eq. J2-4)}$$
$$= (2 \text{ welds})(0.60)(70 \text{ ksi}) \left(\frac{3/16 \text{ in.}}{\sqrt{2}} \right) (11.5 \text{ in.})(1.0 + 0.5 \sin^{1.5} 0°)$$
$$= 128 \text{ kips}$$

LRFD	ASD
$\phi R_n = 0.75(128 \text{ kips})$ $= 96.0 \text{ kips} \quad \geq \quad V_u = 45.0 \text{ kips}$ **o.k.**	$\frac{R_n}{\Omega} = \frac{128 \text{ kips}}{2.00}$ $= 64.0 \text{ kips} \quad \geq \quad V_a = 30.0 \text{ kips}$ **o.k.**

Check that the shear rupture strength of the beam web at the weld using AISC *Specification* Equation J4-4 is sufficient.

$$V_{nw} = 0.60 F_u A_{nv} \quad \text{(} Spec. \text{ Eq. J4-4)}$$
$$= 0.60 F_u l_{wv} t_{bw}$$
$$= 0.60(65 \text{ ksi})(11.5 \text{ in.})(3/8 \text{ in.})$$
$$= 168 \text{ kips}$$

LRFD	ASD
$\phi R_n = 0.75(168 \text{ kips})$ $= 126 \text{ kips} \quad \geq \quad V_u = 45.0 \text{ kips}$ **o.k.**	$\frac{R_n}{\Omega} = \frac{168 \text{ kips}}{2.00}$ $= 84.0 \text{ kips} \quad \geq \quad V_a = 30.0 \text{ kips}$ **o.k.**

The double-sided fillet welds shown in Figure 5-12 from the web to the end plate are sufficient.

C. Column-Side Limit State Checks

See Example 5.3-1 or 5.3-2 for example column-side limit state check calculations.

Summary

The design shown in Figure 5-12 is satisfactory for the required moment and shear force shown.

EXAMPLE 5.3-4—Multiple-Row Extended 1/3 Unstiffened Thick End-Plate Example

Given:

The connection shown in Figure 5-13 is a multiple-row extended (MRE) 1/3 unstiffened end-plate moment connection for a built-up beam. The beam and end plate material are ASTM A572/A572M Grade 50, and the bolts are Group 120 ASTM F3125/F3125M Grade A325 pretensioned. Weld electrodes are E70XX. The connection is to be evaluated as a thick end-plate design for the following required moments and shear forces.

	LRFD	ASD
Moment	M_u = 8,000 kip-in.	M_a = 5,330 kip-in.
Shear force	V_u = 60.0 kips	V_a = 40.0 kips

Solution:

From AISC *Manual* Table 2-4, the material properties are as follows:

ASTM A572/A572M Grade 50
F_y = 50 ksi
F_u = 65 ksi

From AISC *Specification* Table J3.2, the material properties of the bolts are as follows:

Group 120 ASTM F3125/F3125M ⅞-in.-diameter Grade A325 pretensioned
F_{nt} = 90 ksi
F_{nv} = 54 ksi (Group 120 bolts with threads not excluded from the shear plane; thread condition N)

Beam
d = 36 in. t_{bw} = ⅜ in.
b_{bf} = 8 in. t_{bf} = ½ in.

End-plate geometric properties:
b_p = 8 in.

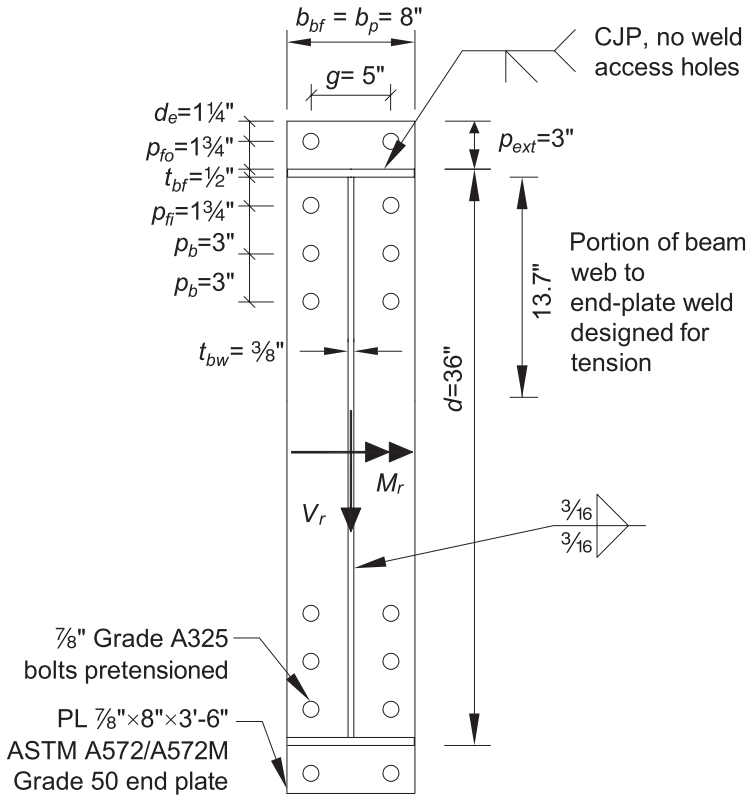

Fig. 5-13. MRE 1/3 unstiffened end-plate configuration for Example 5.3-4.

t_p = 7/8 in.
g = 5 in.
p_{ext} = 3 in.
d_e = 1¼ in.
p_{fo} = 1¾ in.
p_{fi} = 1¾ in.
p_b = 3 in.
d_p = 42 in.

The distances from the centerline of the compression flange to the bolt lines, h_1, h_2, h_3, and h_4, are depicted in Table 5-13 and computed as:

$$h_1 = d - \frac{t_{bf}}{2} + p_{fo}$$
$$= 36 \text{ in.} - \frac{½ \text{ in.}}{2} + 1¾ \text{ in.}$$
$$= 37.5 \text{ in.}$$

$$h_2 = d - \frac{3t_{bf}}{2} - p_{fi}$$
$$= 36 \text{ in.} - \frac{3(½ \text{ in.})}{2} - 1¾ \text{ in.}$$
$$= 33.5 \text{ in.}$$

$$h_3 = d - \frac{3t_{bf}}{2} - p_{fi} - p_b$$
$$= 36 \text{ in.} - \frac{3(½ \text{ in.})}{2} - 1¾ \text{ in.} - 3 \text{ in.}$$
$$= 30.5 \text{ in.}$$

$$h_4 = d - \frac{3t_{bf}}{2} - p_{fi} - 2p_b$$
$$= 36 \text{ in.} - \frac{3(½ \text{ in.})}{2} - 1¾ \text{ in.} - 2(3 \text{ in.})$$
$$= 27.5 \text{ in.}$$

$$b_{p,eff} \le b_{bf} + \max(t_p, 1 \text{ in.}) \quad (4\text{-}3)$$
$$\le 8 \text{ in.} + \max(7/8 \text{ in.}, 1 \text{ in.})$$
$$\le 9.00 \text{ in.}$$

$b_p = 8 \text{ in.} \le 9.00 \text{ in.}$ **o.k.**

$$b_{bf} \ge g \quad (4\text{-}1)$$
8 in. ≥ 5 in. **o.k.**

A. End-Plate and Bolt Design Verification

Determine if the specified end-plate thickness, 7/8 in., and 7/8-in.-diameter Grade A325 bolts are sufficient using the thick end-plate/smaller bolt diameter procedure.

Solve for the required bolt diameter using Equations 5-3. For Grade A325 bolts, the nominal tensile stress is F_{nt} = 90 ksi.

$$\sum_i n_i h_i = 2(37.5 \text{ in.}) + 2(33.5 \text{ in.}) + 2(30.5 \text{ in.}) + 2(27.5 \text{ in.})$$
$$= 258 \text{ in.}$$

LRFD	ASD
$d_{b,reqd} = \sqrt{\dfrac{4M_u}{\pi\phi F_{nt}\left(\sum_i n_i h_i\right)}}$	$d_{b,reqd} = \sqrt{\dfrac{4M_a}{\dfrac{\pi F_{nt}}{\Omega}\left(\sum_i n_i h_i\right)}}$
$= \sqrt{\dfrac{4(8{,}000 \text{ kip-in.})}{\pi(0.75)(90 \text{ ksi})(258 \text{ in.})}}$	$= \sqrt{\dfrac{4(5{,}330 \text{ kip-in.})}{\dfrac{\pi(90 \text{ ksi})}{2.00}(258 \text{ in.})}}$
$= 0.765 \text{ in.} \quad \le \quad ⅞ \text{ in.} \quad$ **o.k.**	$= 0.765 \text{ in.} \quad \le \quad ⅞ \text{ in.} \quad$ **o.k.**

The specified ⅞-in.-diameter Grade A325 bolts are sufficient to resist the required moment.

Solve for the required end-plate thickness using Equations 5-4. First solve for the distance, s, and yield line parameter, Y_p, using Table 5-13.

$$s = \frac{\sqrt{b_p g}}{2}$$
$$= \frac{\sqrt{(8 \text{ in.})(5 \text{ in.})}}{2}$$
$$= 3.16 \text{ in.}$$

Because $s \ge p_{fi} = 1¾$ in., the dimension p_{fi} is used in the equation for the yield line parameter.

$$Y_p = \frac{b_p}{2}\left[h_1\left(\frac{1}{p_{fo}}\right) + h_2\left(\frac{1}{p_{fi}}\right) + h_4\left(\frac{1}{s}\right) - \frac{1}{2}\right] + \frac{2}{g}\left[h_2(p_{fi} + 1.5p_b) + h_4(s + 0.5p_b)\right] + \frac{g}{2}$$
$$= \left(\frac{8 \text{ in.}}{2}\right)\left[(37.5 \text{ in.})\left(\frac{1}{1¾ \text{ in.}}\right) + (33.5 \text{ in.})\left(\frac{1}{1¾ \text{ in.}}\right) + (27.5 \text{ in.})\left(\frac{1}{3.16 \text{ in.}}\right) - \frac{1}{2}\right]$$
$$+ \left(\frac{2}{5 \text{ in.}}\right)\left\{(33.5 \text{ in.})\left[1¾ \text{ in.} + 1.5(3 \text{ in.})\right] + (27.5 \text{ in.})\left[3.16 \text{ in.} + 0.5(3 \text{ in.})\right]\right\} + \frac{5 \text{ in.}}{2}$$
$$= 333 \text{ in.}$$

Determine the required end-plate thickness using Equations 5-4. For extended end-plate configurations, $\gamma_r = 1.0$.

LRFD	ASD
$t_{p,reqd} = \sqrt{\dfrac{1.10M_u}{\gamma_r \phi_b F_y Y_p}}$	$t_{p,reqd} = \sqrt{\dfrac{1.10M_a}{\gamma_r F_y Y_p / \Omega_b}}$
$= \sqrt{\dfrac{1.10(8{,}000 \text{ kip-in.})}{1.0(0.90)(50 \text{ ksi})(333 \text{ in.})}}$	$= \sqrt{\dfrac{1.10(5{,}330 \text{ kip-in.})}{1.0(50 \text{ ksi})(333 \text{ in.})/1.67}}$
$= 0.766 \text{ in.} \quad \le \quad ⅞ \text{ in.} \quad$ **o.k.**	$= 0.767 \text{ in.} \quad \le \quad ⅞ \text{ in.} \quad$ **o.k.**

Check Shear Yielding/Shear Rupture of the Extended Portion of the End Plate

For extended end-plate moment connections that are unstiffened, potential limit states that must be checked are shear yielding and shear rupture of the extended portion of the end plate. For the MRE 1/3 connection, the shear demand is taken as one-fourth of the tension flange force because the exterior bolts represent one-fourth of the bolts. The shear strength is calculated in accordance with AISC *Specification* Section J4.2.

Calculate the shear demand on the extended portion of the end plate.

LRFD	ASD
$V_{up} = \frac{1}{4}\left(\frac{M_u}{d - t_{bf}}\right)$ $= \frac{1}{4}\left(\frac{8{,}000 \text{ kip-in.}}{36 \text{ in.} - ½ \text{ in.}}\right)$ $= 56.3 \text{ kips}$	$V_{ap} = \frac{1}{4}\left(\frac{M_a}{d - t_{bf}}\right)$ $= \frac{1}{4}\left(\frac{5{,}330 \text{ kip-in.}}{36 \text{ in.} - ½ \text{ in.}}\right)$ $= 37.5 \text{ kips}$

Calculate the nominal shear yielding strength:

$$R_n = 0.60F_yA_{gv} \qquad \text{(}\textit{Spec}\text{. Eq. J4-3)}$$
$$= 0.60F_yb_pt_p$$
$$= 0.60(50 \text{ ksi})(8 \text{ in.})(⅞ \text{ in.})$$
$$= 210 \text{ kips}$$

Compare the design shear yielding strength to the shear demand. According to AISC *Specification* Section J4.2 for yielding of elements in shear, the resistance factor is $\phi = 1.00$, and the safety factor is $\Omega = 1.50$.

LRFD	ASD
$\phi R_n = 1.00(210 \text{ kips})$ $= 210 \text{ kips} \geq V_{up} = 56.3 \text{ kips}$ **o.k.**	$\frac{R_n}{\Omega} = \frac{210 \text{ kips}}{1.50}$ $= 140 \text{ kips} \geq V_{ap} = 37.5 \text{ kips}$ **o.k.**

Calculate the nominal shear rupture strength. The width of the extended portion of the end plate for use in the net section area is the width minus two effective hole diameters. The effective hole diameter is the hole diameter from AISC *Specification* Table J3.3 plus 1⁄16 in. The additional 1⁄16 in. accounts for damage around the hole caused by drilling, punching, or thermal cutting. For ⅞-in.-diameter bolts, the standard hole diameter, d_h, is 15⁄16 in.

$$A_{nv} = \left[b_p - 2(d_h + 1⁄16)\right]t_p$$
$$= \left[8 \text{ in.} - 2(15⁄16 \text{ in.} + 1⁄16 \text{ in.})\right](⅞ \text{ in.})$$
$$= 5.25 \text{ in.}^2$$
$$R_n = 0.60F_uA_{nv} \qquad \text{(}\textit{Spec}\text{. Eq. J4-4)}$$
$$= 0.60(65 \text{ ksi})(5.25 \text{ in.}^2)$$
$$= 205 \text{ kips}$$

Compare the design shear rupture strength to the shear demand. Using AISC *Specification* Section J4.2 for rupture of elements in shear, the resistance factor is $\phi = 0.75$, and the safety factor is $\Omega = 2.00$.

LRFD	ASD
$\phi R_n = 0.75(205 \text{ kips})$ $= 154 \text{ kips} \geq V_{up} = 56.3 \text{ kips}$ **o.k.**	$\frac{R_n}{\Omega} = \frac{205 \text{ kips}}{2.00}$ $= 103 \text{ kips} \geq V_{ap} = 37.5 \text{ kips}$ **o.k.**

The extended portion of the ⅞-in.-thick end plate has sufficient resistance to shear yielding and shear rupture.

Check Shear Transfer at Bolt Holes

See Example 5.3-1 or 5.3-2 for calculation procedures.

B. Check Beam to End-Plate Welds

The minimum weld size in AISC *Specification* Table J2.4 is determined from the material thickness of the thinner part joined. The fillet weld sizes shown in Figure 5-13 satisfy the requirements in Table J2.4.

Check Beam Flange to End-Plate Weld

The weld from the beam flange to the end plate is shown in Figure 5-13 as a CJP groove weld with the bevel facing away from the center of the beam and without weld access holes. (Double-sided 7/16 in. fillet welds or a PJP groove weld are alternate options.)

Check Beam Web to End-Plate Weld

The beam web to end-plate welds shown in Figure 5-13 are separately checked for (1) tension rupture in the region around the tension bolts (extending 6 in. to the inside of the tension bolts), and (2) the remainder of the web to end-plate weld is checked for shear. As explained in Section 3.7.5, the demand for the tension web area, T_{uw} (LRFD) or T_{aw} (ASD), for this connection is the number of tension bolts adjacent to the web, n_{trib}, divided by the total number of tension bolts, n, multiplied by the calculated beam flange force, $T_{u,calc}$ (LRFD) or $T_{a,calc}$ (ASD).

LRFD	ASD
$T_{u,calc} = \dfrac{M_u}{d - t_{bf}}$	$T_{a,calc} = \dfrac{M_a}{d - t_{bf}}$
$= \dfrac{8{,}000 \text{ kip-in.}}{36 \text{ in.} - ½ \text{ in.}}$	$= \dfrac{5{,}330 \text{ kip-in.}}{36 \text{ in.} - ½ \text{ in.}}$
$= 225$ kips	$= 150$ kips
$T_{uw} = (n_{trib}/n)T_{u,calc}$	$T_{aw} = (n_{trib}/n)T_{a,calc}$
$= (6/8)(225 \text{ kips})$	$= (6/8)(150 \text{ kips})$
$= 169$ kips	$= 113$ kips

The length of the web tension region is measured from the inside of the beam flange to 6 in. inside the tension bolt row:

$$l_{wt} = p_{fi} + 2p_b + 6 \text{ in.}$$
$$= 1¾ \text{ in.} + 2(3 \text{ in.}) + 6 \text{ in.}$$
$$= 13.8 \text{ in.}$$

The nominal web yield strength in the tension region is

$$T_{yw} = F_y A_g \qquad \text{(from } \textit{Spec}\text{. Eq. J4-1)}$$
$$= F_y t_{bw} l_{wt}$$
$$= (50 \text{ ksi})(⅜ \text{ in.})(13.8 \text{ in.})$$
$$= 259 \text{ kips}$$

Check that the web design tensile yield strength is sufficient.

LRFD	ASD
$\phi T_{yw} = 0.90(259 \text{ kips})$	$\dfrac{T_{yw}}{\Omega} = \dfrac{259 \text{ kips}}{1.67}$
$= 233 \text{ kips} \quad \geq \quad T_{uw} = 169 \text{ kips}$ **o.k.**	$= 155 \text{ kips} \quad \geq \quad T_{aw} = 113 \text{ kips}$ **o.k.**

Check that the required strength is at least 60% (LRFD) or 40% (ASD) of the web tensile strength from Equations 3-41.

LRFD	ASD
$0.60T_{yw} = 0.60(259 \text{ kips})$ $= 155 \text{ kips}$ $T_{uwd} = \max(T_{uw}, 0.60T_{yw})$ $= \max(169 \text{ kips}, 155 \text{ kips})$ $= 169 \text{ kips}$	$0.40T_{yw} = 0.40(259 \text{ kips})$ $= 104 \text{ kips}$ $T_{awd} = \max(T_{aw}, 0.40T_{yw})$ $= \max(113 \text{ kips}, 104 \text{ kips})$ $= 113 \text{ kips}$

Check the web to end-plate weld around the tension bolts. Because the weld is loaded perpendicular to its longitudinal axis, the angle of loading, θ, is 90°.

$$R_n = (2 \text{ welds})0.60F_{EXX}\frac{t_{weld}}{\sqrt{2}}l_{wt}(1.0 + 0.5\sin^{1.5}\theta) \quad \text{(from } \textit{Spec.} \text{ Eq. J2-4)}$$

$$= (2 \text{ welds})(0.60)(70 \text{ ksi})\left(\frac{3/16 \text{ in.}}{\sqrt{2}}\right)(13.8 \text{ in.})(1.0 + 0.5\sin^{1.5} 90°)$$

$$= 231 \text{ kips}$$

LRFD	ASD
$\phi R_n = 0.75(231 \text{ kips})$ $= 173 \text{ kips} \quad \geq \quad T_{uwd} = 169 \text{ kips}$ **o.k.**	$\frac{R_n}{\Omega} = \frac{231 \text{ kips}}{2.00}$ $= 116 \text{ kips} \quad \geq \quad T_{awd} = 113 \text{ kips}$ **o.k.**

Check the web to end-plate weld away from the tension bolts. Only the web to end-plate weld between the end of the assumed web tension length and the inside face of the bottom beam compression flange or the weld between the mid-depth of the beam and the inside face of the beam compression flange, whichever is smaller, is considered effective in resisting the beam end shear. The shear strength of this weld is compared to the required shear applied to the connection.

$$l_t = d - 2t_{bf} - l_{wt}$$

$$= 36 \text{ in.} - 2(½ \text{ in.}) - 13.8 \text{ in.}$$

$$= 21.2 \text{ in.}$$

$$l_{0.5w} = d/2 - t_{bf}$$

$$= (36 \text{ in.})/2 - ½ \text{ in.}$$

$$= 17.5 \text{ in.}$$

$$l_{wv} = \min(l_t, l_{0.5w})$$

$$= \min(21.2 \text{ in.}, 17.5 \text{ in.})$$

$$= 17.5 \text{ in.}$$

$$R_n = (2 \text{ welds})0.60F_{EXX}\frac{t_{weld}}{\sqrt{2}}l_{wv}(1.0 + 0.5\sin^{1.5}\theta) \quad \text{(from } \textit{Spec.} \text{ Eq. J2-4)}$$

$$= (2 \text{ welds})(0.60)(70 \text{ ksi})\left(\frac{3/16 \text{ in.}}{\sqrt{2}}\right)(17.5 \text{ in.})(1.0 + 0.5\sin^{1.5} 0°)$$

$$= 195 \text{ kips}$$

LRFD	ASD
$\phi R_n = 0.75(195 \text{ kips})$ $= 146 \text{ kips} \quad \geq \quad V_u = 60.0 \text{ kips}$ **o.k.**	$\frac{R_n}{\Omega} = \frac{195 \text{ kips}}{2.00}$ $= 97.5 \text{ kips} \quad \geq \quad V_a = 40.0 \text{ kips}$ **o.k.**

Check that the shear rupture strength of the beam web at the weld using AISC *Specification* Equation J4-4 is sufficient.

$V_{nw} = 0.60 F_u A_{nv}$ (*Spec.* Eq. J4-4)

$= 0.60 F_u l_{wv} t_{bw}$

$= 0.60(65 \text{ ksi})(17.5 \text{ in.})(\frac{3}{8} \text{ in.})$

$= 256 \text{ kips}$

LRFD	ASD
$\phi R_n = 0.75(256 \text{ kips})$ $= 192 \text{ kips} \quad \geq \quad V_u = 60.0 \text{ kips}$ **o.k.**	$\frac{R_n}{\Omega} = \frac{256 \text{ kips}}{2.00}$ $= 128 \text{ kips} \quad \geq \quad V_a = 40.0 \text{ kips}$ **o.k.**

The double-sided 3⁄16 in. fillet welds shown in Figure 5-13 from the web to the end plate are sufficient.

C. Column-Side Limit State Checks

See Example 5.3-1 or 5.3-2 for example column-side limit state check calculations.

Summary

The design shown in Figure 5-13 is satisfactory for the required moment and shear force shown.

EXAMPLE 5.3-5—Multiple-Row Extended 1/3 Stiffened Thick End-Plate Example

Given:

The connection shown in Figure 5-14 is a multiple-row extended (MRE) 1/3 stiffened end-plate moment connection for a built-up beam. The beam and all plate material are ASTM A572/A572M Grade 50, and the bolts are Group 120 ASTM F3125/F3125M Grade A325 pretensioned. Weld electrodes are E70XX. The connection is to be evaluated as a thick end-plate design for the following required moments and shear forces.

	LRFD	ASD
Moment	$M_u = 10{,}300$ kip-in.	$M_a = 6{,}870$ kip-in.
Shear force	$V_u = 60.0$ kips	$V_a = 40.0$ kips

Solution:

From AISC *Manual* Table 2-4, the material properties are as follows:

ASTM A572/A572M Grade 50
$F_y = 50$ ksi
$F_u = 65$ ksi

From AISC *Specification* Table J3.2, the material properties of the bolts are as follows:

Group 120 ASTM F3125/F3125M 7⁄8-in.-diameter Grade A325 pretensioned
$F_{nt} = 90$ ksi

F_{nv} = 54 ksi (Group 120 bolts with threads not excluded from the shear plane; thread condition N)

Beam
d = 36 in. t_{bw} = ⅜ in.
b_{bf} = 8 in. t_{bf} = ½ in.

End-plate geometric properties:
b_p = 8 in.
t_p = ⅞ in.
g = 5 in.
p_{ext} = 3 in.
d_e = 1¼ in.
p_{fo} = 1¾ in.
p_{fi} = 1¾ in.
p_b = 3 in.
d_p = 42 in.

The distances from the centerline of the compression flange to the bolt lines, h_1, h_2, h_3, and h_4, are depicted in Table 5-14 and computed as:

$$h_1 = d - \frac{t_{bf}}{2} + p_{fo}$$
$$= 36 \text{ in.} - \frac{½ \text{ in.}}{2} + 1¾ \text{ in.}$$
$$= 37.5 \text{ in.}$$

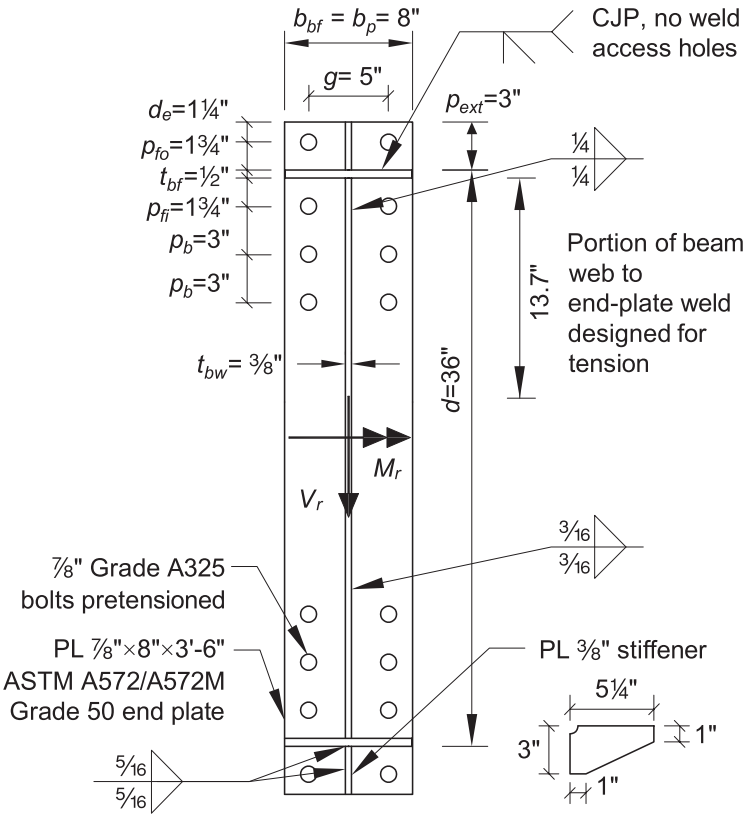

Fig. 5-14. MRE 1/3 stiffened end-plate configuration for Example 5.3-5.

$$h_2 = d - \frac{3t_{bf}}{2} - p_{fi}$$
$$= 36\text{ in.} - \frac{3(½\text{ in.})}{2} - 1¾\text{ in.}$$
$$= 33.5\text{ in.}$$

$$h_3 = d - \frac{3t_{bf}}{2} - p_{fi} - p_b$$
$$= 36\text{ in.} - \frac{3(½\text{ in.})}{2} - 1¾\text{ in.} - 3\text{ in.}$$
$$= 30.5\text{ in.}$$

$$h_4 = d - \frac{3t_{bf}}{2} - p_{fi} - 2p_b$$
$$= 36\text{ in.} - \frac{3(½\text{ in.})}{2} - 1¾\text{ in.} - 2(3\text{ in.})$$
$$= 27.5\text{ in.}$$

$$b_{p,eff} \le b_{bf} + \max(t_p, 1\text{ in.}) \quad (4\text{-}3)$$
$$\le 8\text{ in.} + \max(⅞\text{ in.}, 1\text{ in.})$$
$$\le 9.00\text{ in.}$$

$b_p = 8\text{ in.} \le 9.00\text{ in.}$ **o.k.**

$$b_{bf} \ge g \quad (4\text{-}1)$$

$8\text{ in.} \ge 5\text{ in.}$ **o.k.**

Beam flange to end-plate stiffener geometric properties:

$$h_{st} = p_{fi} + d_e$$
$$= 1¾\text{ in.} + 1¼\text{ in.}$$
$$= 3\text{ in.}$$

$$L_{st} = \frac{h_{st}}{\tan 30°} \quad (4\text{-}4)$$
$$= \frac{3\text{ in.}}{\tan 30°}$$
$$= 5.20\text{ in.} \le 5¼\text{ in.}$$ **o.k.**

$$t_s \ge t_{bw}\left(\frac{F_{yb}}{F_{ys}}\right) \quad (3\text{-}36)$$
$$\ge (⅜\text{ in.})\left(\frac{50\text{ ksi}}{50\text{ ksi}}\right)$$
$$\ge ⅜\text{ in.}$$

$t_s = ⅜\text{ in.}$ **o.k.**

$$\frac{h_{st}}{t_s} = \frac{3\text{ in.}}{⅜\text{ in.}}$$
$$= 8.00$$

$$\frac{h_{st}}{t_s} \le 0.56\sqrt{\frac{E}{F_{ys}}} \tag{3-37}$$

$$\le 0.56\sqrt{\frac{29{,}000\,\text{ksi}}{50\,\text{ksi}}}$$

$$\le 13.5$$

$$\frac{h_{st}}{t_s} = 8.00 \quad \textbf{o.k.}$$

A. End-Plate and Bolt Design Verification

Determine if the specified end-plate thickness, ⅞ in., and ⅞-in.-diameter Grade A325 bolts are sufficient using the thick end-plate/smaller bolt diameter procedure.

Solve for the required bolt diameter using Equations 5-3. For Grade A325 bolts, the nominal tensile stress is $F_{nt} = 90$ ksi.

$$\sum_i n_i h_i = 2(37.5\text{ in.}) + 2(33.5\text{ in.}) + 2(30.5\text{ in.}) + 2(27.5\text{ in.})$$

$$= 258\text{ in.}$$

LRFD	ASD
$d_{b,reqd} = \sqrt{\frac{4M_u}{\pi\phi F_{nt}\left(\sum_i n_i h_i\right)}}$	$d_{b,reqd} = \sqrt{\frac{4M_a}{\frac{\pi F_{nt}}{\Omega}\left(\sum_i n_i h_i\right)}}$
$= \sqrt{\frac{4(10{,}300\text{ kip-in.})}{\pi(0.75)(90\text{ ksi})(258\text{ in.})}}$	$= \sqrt{\frac{4(6{,}870\text{ kip-in.})}{\frac{\pi(90\text{ ksi})}{2.00}(258\text{ in.})}}$
$= 0.868\text{ in.} \le ⅞\text{ in.}$ **o.k.**	$= 0.868\text{ in.} \le ⅞\text{ in.}$ **o.k.**

The specified ⅞-in.-diameter Grade A325 bolts are sufficient to resist the required moment.

Solve for the required end-plate thickness using Equations 5-4. First solve for the distance, s, and yield line parameter, Y_p, using Table 5-14.

$$s = \frac{\sqrt{b_p g}}{2}$$

$$= \frac{\sqrt{(8\text{ in.})(5\text{ in.})}}{2}$$

$$= 3.16\text{ in.}$$

Because $s > d_e = 1¼$ in., Y_p in Table 5-14 is applicable, and because $s \ge p_{fo} = 1¾$ in. and $p_{fi} = 1¾$ in., the dimensions p_{fo} and p_{fi} are used in the equation for the yield line parameter.

$$Y_p = \frac{b_p}{2}\left[h_1\left(\frac{1}{p_{fo}}+\frac{1}{2d_e}\right)+h_2\left(\frac{1}{p_{fi}}\right)+h_4\left(\frac{1}{s}\right)\right]+\frac{2}{g}\left[h_1(p_{fo}+d_e)+h_2(p_{fi}+1.5p_b)+h_4(s+0.5p_b)\right]+\frac{g}{2}$$

$$= \left(\frac{8\text{ in.}}{2}\right)\left\{(37.5\text{ in.})\left[\frac{1}{1¾\text{ in.}}+\frac{1}{2(1¼\text{ in.})}\right]+(33.5\text{ in.})\left(\frac{1}{1¾\text{ in.}}\right)+(27.5\text{ in.})\left(\frac{1}{3.16\text{ in.}}\right)\right\}$$

$$+\left(\frac{2}{5\text{ in.}}\right)\left\{\begin{matrix}(37.5\text{ in.})(1¾\text{ in.}+1¼\text{ in.})+(33.5\text{ in.})\left[1¾\text{ in.}+1.5(3\text{ in.})\right]\\+(27.5\text{ in.})\left[3.16\text{ in.}+0.5(3\text{ in.})\right]\end{matrix}\right\}+\frac{5\text{ in.}}{2}$$

$$= 440\text{ in.}$$

Determine the required end-plate thickness using Equations 5-4. For extended end-plate configurations, $\gamma_r = 1.0$.

LRFD	ASD
$t_{p,reqd} = \sqrt{\dfrac{1.10M_u}{\gamma_r\phi_b F_y Y_p}}$	$t_{p,reqd} = \sqrt{\dfrac{1.10M_a}{\gamma_r F_y Y_p/\Omega_b}}$
$= \sqrt{\dfrac{1.10(10{,}300\text{ kip-in.})}{1.0(0.90)(50\text{ ksi})(440\text{ in.})}}$	$= \sqrt{\dfrac{1.10(6{,}870\text{ kip-in.})}{1.0(50\text{ ksi})(440\text{ in.})/1.67}}$
$= 0.756\text{ in.} \le ⅞\text{ in.}$ **o.k.**	$= 0.757\text{ in.} \le ⅞\text{ in.}$ **o.k.**

Check Shear Yielding/Shear Rupture of the Extended Portion of the End Plate

For extended end-plate moment connections that are stiffened, shear yielding and shear rupture of the extended portion of the end plate are not limit states.

Check Shear Transfer at Bolt Holes

See Example 5.3-1 or 5.3-2 for calculation procedures.

B. Check Beam to End-Plate Welds

The minimum weld size in AISC *Specification* Table J2.4 is determined from the material thickness of the thinner part joined. The fillet weld sizes shown in Figure 5-14 satisfy the requirements in Table J2.4.

Check Beam Flange to End-Plate Weld

The weld from the beam flange to the end plate is shown in Figure 5-14 as a CJP groove weld with the bevel facing away from the center of the beam and without weld access holes. (Double-sided 9⁄16 in. fillet welds or a PJP groove weld are alternate options.)

Check Stiffener Welds

Check that the stiffener to flange welds shown in Figure 5-14 are sufficient to develop the shear yield strength of the stiffener plate.

Calculate the required strength for the stiffener to beam flange weld, and determine if the 5⁄16 in. double-sided fillet weld shown is sufficient.

LRFD	ASD
$V_{uw} = 0.60F_y t_s$	$V_{aw} = 0.40F_y t_s$
$= 0.60(50\text{ ksi})(⅜\text{ in.})$	$= 0.40(50\text{ ksi})(⅜\text{ in.})$
$= 11.3\text{ kips/in.}$	$= 7.50\text{ kips/in.}$

$$V_{nw} = (2 \text{ welds})0.60F_{EXX}\frac{t_{weld}}{\sqrt{2}}(1.0+0.5\sin^{1.5}\theta) \quad \text{(from } \textit{Spec}\text{. Eq. J2-4)}$$

$$= (2 \text{ welds})(0.60)(70 \text{ ksi})\left(\frac{5/16 \text{ in.}}{\sqrt{2}}\right)(1.0+0.5\sin^{1.5}0°)$$

$$= 18.6 \text{ kips/in.}$$

LRFD	ASD
$\phi V_{nw} = 0.75(18.6 \text{ kips/in.})$ $= 14.0 \text{ kips/in} \geq V_{uw} = 11.3 \text{ kips/in.}$ **o.k.**	$\frac{V_{nw}}{\Omega} = \frac{18.6 \text{ kips/in.}}{2.00}$ $= 9.30 \text{ kips/in.} \geq V_{aw} = 7.50 \text{ kips/in.}$ **o.k.**

The shear rupture strength of the stiffener is greater than its shear yield strength and does not have to be checked. The shear rupture strength of the beam flange is sufficient by inspection.

Therefore, the double-sided 5/16 in. fillet weld is sufficient.

Calculate the required strength for the stiffener to end-plate weld, and determine if the 5/16 in. double-sided fillet weld shown is sufficient.

LRFD	ASD
$T_{uw} = F_y t_s$ $= (50 \text{ ksi})(3/8 \text{ in.})$ $= 18.8 \text{ kips/in.}$	$T_{aw} = \frac{F_y}{1.50}t_s$ $= \left(\frac{50 \text{ ksi}}{1.50}\right)(3/8 \text{ in.})$ $= 12.5 \text{ kips/in.}$

$$T_{nw} = (2 \text{ welds})0.60F_{EXX}\frac{t_{weld}}{\sqrt{2}}(1.0+0.5\sin^{1.5}\theta) \quad \text{(from } \textit{Spec}\text{. Eq. J2-4)}$$

$$= (2 \text{ welds})(0.60)(70 \text{ ksi})\left(\frac{5/16 \text{ in.}}{\sqrt{2}}\right)(1.0+0.5\sin^{1.5}90°)$$

$$= 27.8 \text{ kips/in.}$$

LRFD	ASD
$\phi T_{nw} = 0.75(27.8 \text{ kips/in.})$ $= 20.9 \text{ kips/in.} \geq T_{uw} = 18.8 \text{ kips/in.}$ **o.k.**	$\frac{T_{nw}}{\Omega} = \frac{27.8 \text{ kips/in.}}{2.00}$ $= 13.9 \text{ kips/in.} \geq T_{aw} = 12.5 \text{ kips/in.}$ **o.k.**

Therefore, the double-sided 5/16 in. fillet welds are sufficient.

Check Beam Web to End-Plate Weld

The beam web to end-plate welds shown in Figure 5-14 are separately checked for (1) tension rupture in the region around the tension bolts (extending 6 in. to the inside of the tension bolts), and (2) the remainder of the web to end-plate weld is checked for shear. As explained in Section 3.7.5, the demand for the tension web area, T_{uw} (LRFD) or T_{aw} (ASD), for this connection is the number of tension bolts adjacent to the web, n_{trib}, divided by the total number of tension bolts, n, multiplied by the calculated beam flange force, $T_{u,calc}$ (LRFD) or $T_{a,calc}$ (ASD).

LRFD	ASD
$T_{u,calc} = \dfrac{M_u}{d - t_{bf}}$ $= \dfrac{10{,}300 \text{ kip-in.}}{36 \text{ in.} - ½ \text{ in.}}$ $= 290 \text{ kips}$ $T_{uw} = (n_{trib}/n)T_{u,calc}$ $= (6/8)(290 \text{ kips})$ $= 218 \text{ kips}$	$T_{a,calc} = \dfrac{M_a}{d - t_{bf}}$ $= \dfrac{6{,}870 \text{ kip-in.}}{36 \text{ in.} - ½ \text{ in.}}$ $= 194 \text{ kips}$ $T_{aw} = (n_{trib}/n)T_{a,calc}$ $= (6/8)(194 \text{ kips})$ $= 146 \text{ kips}$

The length of the web tension region is measured from the inside of the beam flange to 6 in. inside the tension bolt row:

$l_{wt} = p_{fi} + 2p_b + 6 \text{ in.}$
$= 1¾ \text{ in.} + 2(3 \text{ in.}) + 6 \text{ in.}$
$= 13.8 \text{ in.}$

The nominal web yield strength in the tension region is:

$T_{yw} = F_y A_g$ (from *Spec.* Eq. J4-1)
$= F_y t_{bw} l_{wt}$
$= (50 \text{ ksi})(⅜ \text{ in.})(13.8 \text{ in.})$
$= 259 \text{ kips}$

Check that the web design tensile yield strength is sufficient.

LRFD	ASD
$\phi T_{yw} = 0.90(259 \text{ kips})$ $= 233 \text{ kips} \quad \geq \quad T_{uw} = 218 \text{ kips}$ **o.k.**	$\dfrac{T_{yw}}{\Omega} = \dfrac{259 \text{ kips}}{1.67}$ $= 155 \text{ kips} \quad \geq \quad T_{aw} = 146 \text{ kips}$ **o.k.**

Check that the required strength is at least 60% (LRFD) or 40% (ASD) of the web tensile strength from Equations 3-41.

LRFD	ASD
$0.60T_{yw} = 0.60(259 \text{ kips})$ $= 155 \text{ kips}$ $T_{uwd} = \max(T_{uw}, 0.60T_{yw})$ $= \max(218 \text{ kips}, 155 \text{ kips})$ $= 218 \text{ kips}$	$0.40T_{yw} = 0.40(259 \text{ kips})$ $= 104 \text{ kips}$ $T_{awd} = \max(T_{aw}, 0.40T_{yw})$ $= \max(146 \text{ kips}, 104 \text{ kips})$ $= 146 \text{ kips}$

Check the web to end-plate weld around the tension bolts. Because the weld is loaded perpendicular to its longitudinal axis, the angle of loading, θ, is 90°.

$$R_n = (2\text{ welds})0.60F_{EXX}\frac{t_{weld}}{\sqrt{2}}l_{wt}(1.0+0.5\sin^{1.5}\theta) \qquad \text{(from } \textit{Spec.} \text{ Eq. J2-4)}$$

$$= (2\text{ welds})(0.60)(70\text{ ksi})\left(\frac{¼\text{ in.}}{\sqrt{2}}\right)(13.8\text{ in.})(1.0+0.5\sin^{1.5}90°)$$

$$= 307\text{ kips}$$

LRFD	ASD
$\phi R_n = 0.75(307\text{ kips})$ $= 230\text{ kips} \quad \geq \quad T_{uwd} = 218\text{ kips}$ **o.k.**	$\frac{R_n}{\Omega} = \frac{307\text{ kips}}{2.00}$ $= 154\text{ kips} \quad \geq \quad T_{awd} = 146\text{ kips}$ **o.k.**

Check the web to end-plate weld away from the tension bolts. Only the web to end-plate weld between the end of the assumed web tension length and the inside face of the bottom beam compression flange or the weld between the mid-depth of the beam and the inside face of the beam compression flange, whichever is smaller, is considered effective in resisting the beam end shear. The shear strength of this weld is compared to the required shear applied to the connection.

$$l_t = d - 2t_{bf} - l_{wt}$$

$$= 36\text{ in.} - 2(½\text{ in.}) - 13.8\text{ in.}$$

$$= 21.2\text{ in.}$$

$$l_{0.5w} = d/2 - t_{bf}$$

$$= (36\text{ in.})/2 - ½\text{ in.}$$

$$= 17.5\text{ in.}$$

$$l_{wv} = \min(l_t, l_{0.5w})$$

$$= \min(21.2\text{ in.}, 17.5\text{ in.})$$

$$= 17.5\text{ in.}$$

$$R_n = (2\text{ welds})0.60F_{EXX}\frac{t_{weld}}{\sqrt{2}}l_{wv}(1.0+0.5\sin^{1.5}\theta) \qquad \text{(from } \textit{Spec.} \text{ Eq. J2-4)}$$

$$= (2\text{ welds})(0.60)(70\text{ ksi})\left(\frac{3⁄16\text{ in.}}{\sqrt{2}}\right)(17.5\text{ in.})(1.0+0.5\sin^{1.5}0°)$$

$$= 195\text{ kips}$$

LRFD	ASD
$\phi R_n = 0.75(195\text{ kips})$ $= 146\text{ kips} \quad \geq \quad V_u = 60.0\text{ kips}$ **o.k.**	$\frac{R_n}{\Omega} = \frac{195\text{ kips}}{2.00}$ $= 97.5\text{ kips} \quad \geq \quad V_a = 40.0\text{ kips}$ **o.k.**

Check that the shear rupture strength of the beam web at the weld using AISC *Specification* Equation J4-4 is sufficient.

$$V_{nw} = 0.60F_uA_{nv} \qquad \text{(}\textit{Spec.}\text{ Eq. J4-4)}$$

$$= 0.60F_ul_{wv}t_{bw}$$

$$= 0.60(65\text{ ksi})(17.5\text{ in.})(0.375\text{ in.})$$

$$= 256\text{ kips}$$

LRFD	ASD
$\phi R_n = 0.75(256 \text{ kips})$ $= 192 \text{ kips} \quad \geq \quad V_u = 60.0 \text{ kips}$ **o.k.**	$\frac{R_n}{\Omega} = \frac{256 \text{ kips}}{2.00}$ $= 128 \text{ kips} \quad \geq \quad V_a = 40.0 \text{ kips}$ **o.k.**

The double-sided fillet welds shown in Figure 5-14 from the web to the end plate are sufficient.

C. Column-Side Limit State Checks

See Example 5.3-1 or 5.3-2 for example column-side limit state check calculations.

Summary

The design shown in Figure 5-14 is satisfactory for the required moment and shear force shown.

EXAMPLE 5.3-6—Eight-Bolt Extended Four-Wide Unstiffened Thick End-Plate Example

Given:

The connection shown in Figure 5-15 is an eight-bolt extended four-wide unstiffened end-plate moment connection for a built-up beam. The beam and end plate material are ASTM A572/A572M Grade 50, and the bolts are Group 120 ASTM F3125/F3125M Grade A325 pretensioned. Weld electrodes are E70XX. The connection is to be evaluated as a thick end-plate design for the following required moments and shear forces.

	LRFD	ASD
Moment	$M_u = 8{,}500$ kip-in.	$M_a = 5{,}670$ kip-in.
Shear force	$V_u = 60.0$ kips	$V_a = 40.0$ kips

Solution:

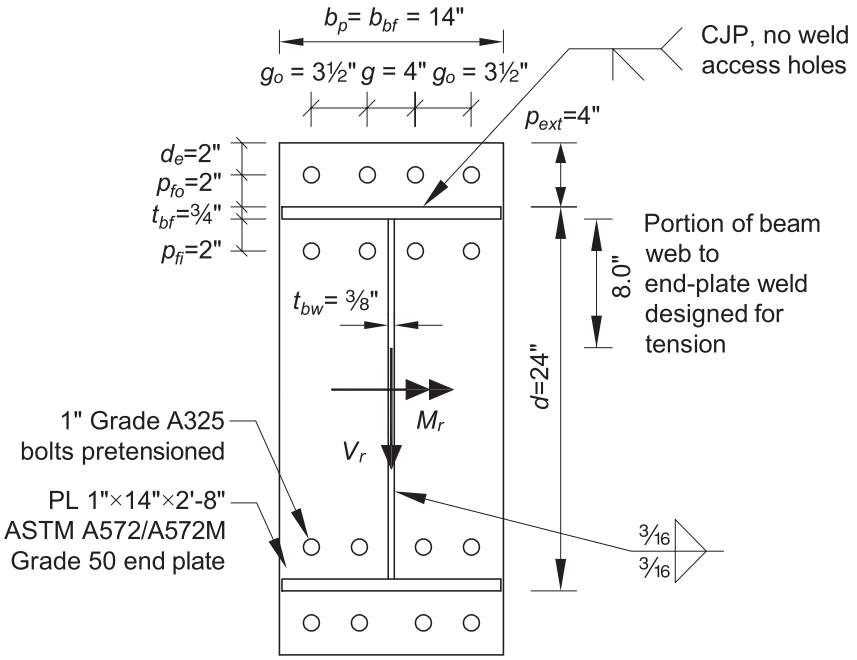

Fig. 5-15. Eight-bolt extended four-wide unstiffened connection thick end-plate configuration for Example 5.3-6.

From AISC *Manual* Table 2-4, the material properties are as follows:

ASTM A572/A572M Grade 50
$F_y = 50$ ksi
$F_u = 65$ ksi

From AISC *Specification* Table J3.2, the material properties of the bolts are as follows:

Group 120 ASTM F3125/F3125M 1-in.-diameter Grade A325 pretensioned
$F_{nt} = 90$ ksi
$F_{nv} = 54$ ksi (Group 120 bolts with threads not excluded from the shear plane; thread condition N)

Beam
$d = 24$ in. $\quad t_{bw} = ⅜$ in.
$b_{bf} = 14$ in. $\quad t_{bf} = ¾$ in.

End-plate geometric properties:
$b_p = 14$ in.
$t_p = 1$ in.
$g = 4$ in.
$p_{ext} = 4$ in.
$d_e = 2$ in.
$g_o = 3½$ in.
$p_{fo} = 2$ in.
$p_{fi} = 2$ in.
$d_p = 32$ in.

The distances from the centerline of the compression flange to the bolt lines, h_1 and h_2, are depicted in Table 5-15 and computed as:

$$h_1 = d - \frac{t_{bf}}{2} + p_{fo}$$
$$= 24 \text{ in.} - \frac{¾ \text{ in.}}{2} + 2 \text{ in.}$$
$$= 25.6 \text{ in.}$$

$$h_2 = d - \frac{3t_{bf}}{2} - p_{fi}$$
$$= 24 \text{ in.} - \frac{3(¾ \text{ in.})}{2} - 2 \text{ in.}$$
$$= 20.9 \text{ in.}$$

$$b_{p,eff} \le b_{bf} + \max(t_p, 1 \text{ in.}) \qquad (4\text{-}3)$$
$$\le 14 \text{ in.} + \max(1 \text{ in.}, 1 \text{ in.})$$
$$\le 15.0 \text{ in.}$$

$b_p = 14$ in. $\le$ 15.0 in. **o.k.**

$$b_{bf} \ge g + 2g_o \qquad (4\text{-}2)$$
$$14 \text{ in.} \ge 4 \text{ in.} + 2(3½ \text{ in.})$$
$$14 \text{ in.} \ge 11.0 \text{ in.} \quad \textbf{o.k.}$$

A. End-Plate and Bolt Design Verification

Determine if the specified end-plate thickness, 1 in., and 1-in.-diameter Grade A325 bolts are sufficient using the thick end-plate/smaller bolt diameter procedure.

Solve for the required bolt diameter using Equations 5-3. For Grade A325 bolts, the nominal tensile stress is $F_{nt} = 90$ ksi.

$$\sum_i n_i h_i = 4(25.6 \text{ in.}) + 4(20.9 \text{ in.})$$
$$= 186 \text{ in.}$$

LRFD	ASD
$d_{b,reqd} = \sqrt{\dfrac{4M_u}{\pi\phi F_{nt}\left(\sum_i n_i h_i\right)}}$	$d_{b,reqd} = \sqrt{\dfrac{4M_a}{\dfrac{\pi F_{nt}}{\Omega}\left(\sum_i n_i h_i\right)}}$
$= \sqrt{\dfrac{4(8{,}500 \text{ kip-in.})}{\pi(0.75)(90 \text{ ksi})(186 \text{ in.})}}$	$= \sqrt{\dfrac{4(5{,}670 \text{ kip-in.})}{\dfrac{\pi(90 \text{ ksi})}{2.00}(186 \text{ in.})}}$
$= 0.928 \text{ in.} \quad \le \quad 1 \text{ in.}$ **o.k.**	$= 0.928 \text{ in.} \quad \le \quad 1 \text{ in.}$ **o.k.**

The specified 1-in.-diameter Grade A325 bolts are sufficient to resist the required moment.

Solve for the required end-plate thickness using Equations 5-4. First solve for the distance, s, and yield line parameter, Y_p, using Table 5-15.

$$s = \frac{\sqrt{b_p g}}{2}$$
$$= \frac{\sqrt{(14 \text{ in.})(4 \text{ in.})}}{2}$$
$$= 3.74 \text{ in.}$$

Because $s \ge p_{fi} = 2$ in., the dimension p_{fi} is used in the equation for the yield line parameter.

$$Y_p = \frac{b_p}{2}\left[h_1\left(\frac{1}{p_{fo}}\right) + h_2\left(\frac{1}{p_{fi}} + \frac{1}{s}\right) - \frac{1}{2}\right] + \frac{2}{g}\left[h_2(p_{fi} + s)\right]$$
$$= \left(\frac{14 \text{ in.}}{2}\right)\left[(25.6 \text{ in.})\left(\frac{1}{2 \text{ in.}}\right) + (20.9 \text{ in.})\left(\frac{1}{2 \text{ in.}} + \frac{1}{3.74 \text{ in.}}\right) - \frac{1}{2}\right]$$
$$+ \left(\frac{2}{4 \text{ in.}}\right)\left[(20.9 \text{ in.})(2 \text{ in.} + 3.74 \text{ in.})\right]$$
$$= 258 \text{ in.}$$

Determine the required end-plate thickness using Equations 5-4. For extended end-plate configurations, $\gamma_r = 1.0$.

LRFD	ASD
$t_{p,reqd} = \sqrt{\dfrac{1.10M_u}{\gamma_r \phi_b F_y Y_p}}$	$t_{p,reqd} = \sqrt{\dfrac{1.10M_a}{\gamma_r F_y Y_p / \Omega_b}}$
$= \sqrt{\dfrac{1.10(8{,}500 \text{ kip-in.})}{1.0(0.90)(50 \text{ ksi})(258 \text{ in.})}}$	$= \sqrt{\dfrac{1.10(5{,}670 \text{ kip-in.})}{1.0(50 \text{ ksi})(258 \text{ in.})/1.67}}$
$= 0.897 \text{ in.} \quad \le \quad 1 \text{ in.}$ **o.k.**	$= 0.899 \text{ in.} \quad \le \quad 1 \text{ in.}$ **o.k.**

Check Shear Yielding/Shear Rupture of the Extended Portion of the End Plate

For extended end-plate moment connections that are unstiffened, potential limit states that must be checked are shear yielding and shear rupture of the extended portion of the end plate. For the eight-bolt extended four-wide unstiffened connection, the shear demand is taken as one-half of the tension flange force because the exterior bolts represent one-half of the bolts. The shear strength is calculated in accordance with AISC *Specification* Section J4.2.

Calculate the shear demand on the extended portion of the end plate.

LRFD	ASD
$V_{up} = \frac{1}{2}\left(\frac{M_u}{d - t_{bf}}\right)$	$V_{ap} = \frac{1}{2}\left(\frac{M_a}{d - t_{bf}}\right)$
$= \frac{1}{2}\left(\frac{8{,}500 \text{ kip-in.}}{24 \text{ in.} - ¾ \text{ in.}}\right)$	$= \frac{1}{2}\left(\frac{5{,}670 \text{ kip-in.}}{24 \text{ in.} - ¾ \text{ in.}}\right)$
$= 183$ kips	$= 122$ kips

Calculate the nominal shear yielding strength.

$$R_n = 0.60 F_y A_{gv} \qquad \text{(Spec. Eq. J4-3)}$$
$$= 0.60 F_y b_p t_p$$
$$= 0.60(50 \text{ ksi})(14 \text{ in.})(1 \text{ in.})$$
$$= 420 \text{ kips}$$

Compare the design shear yielding strength to the shear demand. According to AISC *Specification* Section J4.2 for yielding of elements in shear, the resistance factor is $\phi = 1.00$, and the safety factor is $\Omega = 1.50$.

LRFD	ASD
$\phi R_n = 1.00(420 \text{ kips})$	$\frac{R_n}{\Omega} = \frac{420 \text{ kips}}{1.50}$
$= 420 \text{ kips} \geq V_{up} = 183 \text{ kips}$ **o.k.**	$= 280 \text{ kips} \geq V_{ap} = 122 \text{ kips}$ **o.k.**

Calculate the nominal shear rupture strength. The width of the extended portion of the end plate for use in the net section area is the width minus four effective hole diameters. The effective hole diameter is the hole diameter from AISC *Specification* Table J3.3 plus ⅛6 in. The additional ⅛6 in. accounts for damage around the hole caused by drilling, punching, or thermal cutting. For 1-in.-diameter bolts, the standard hole diameter, d_h, is 1⅛ in.

$$A_{nv} = \left[b_p - 4(d_h + ⅛6 \text{ in.})\right] t_p$$
$$= \left[14 \text{ in.} - 4(1⅛ \text{ in.} + ⅛6 \text{ in.})\right](1 \text{ in.})$$
$$= 9.25 \text{ in.}^2$$
$$R_n = 0.60 F_u A_{nv} \qquad \text{(Spec. Eq. J4-4)}$$
$$= 0.60(65 \text{ ksi})(9.25 \text{ in.}^2)$$
$$= 361 \text{ kips}$$

Compare the design shear rupture strength to the shear demand. Using AISC *Specification* Section J4.2 for rupture of elements in shear, the resistance factor is $\phi = 0.75$, and the safety factor is $\Omega = 2.00$.

LRFD	ASD
$\phi R_n = 0.75(361 \text{ kips})$ $= 271 \text{ kips} \quad \geq \quad V_{up} = 182 \text{ kips}$ **o.k.**	$\frac{R_n}{\Omega} = \frac{361 \text{ kips}}{2.00}$ $= 181 \text{ kips} \quad \geq \quad V_{ap} = 122 \text{ kips}$ **o.k.**

The extended portion of the 1-in.-thick end plate has sufficient resistance to shear yielding and shear rupture.

Check Shear Transfer at Bolt Holes

See Example 5.3-1 or 5.3-2 for calculation procedures.

B. Check Beam to End-Plate Welds

The minimum weld size in AISC *Specification* Table J2.4 is determined from the material thickness of the thinner part joined. The fillet weld sizes shown in Figure 5-15 satisfy the requirements in Table J2.4.

Check Beam Flange to End-Plate Weld

The weld from the beam flange to the end plate is shown in Figure 5-15 as a CJP groove weld with the bevel facing away from the center of the beam and without weld access holes. (Double-sided 7⁄16 in. fillet welds or a PJP groove weld are alternate options.)

Check Beam Web to End-Plate Weld

The beam web to end-plate welds shown in Figure 5-15 are separately checked for (1) tension rupture in the region around the tension bolts (extending 6 in. to the inside of the tension bolts), and (2) the remainder of the web to end-plate weld is checked for shear. As explained in Section 3.7.5, the demand for the tension web area, T_{uw} (LRFD) or T_{aw} (ASD), for this connection is the number of tension bolts adjacent to the web, n_{trib}, divided by the total number of tension bolts, n, multiplied by the calculated beam flange force, $T_{u,calc}$ (LRFD) or $T_{a,calc}$ (ASD).

LRFD	ASD
$T_{u,calc} = \frac{M_u}{d - t_{bf}}$ $= \frac{8{,}500 \text{ kip-in.}}{24 \text{ in.} - 3/4 \text{ in.}}$ $= 366 \text{ kips}$	$T_{a,calc} = \frac{M_a}{d - t_{bf}}$ $= \frac{5{,}670 \text{ kip-in.}}{24 \text{ in.} - 3/4 \text{ in.}}$ $= 244 \text{ kips}$
$T_{uw} = (n_{trib}/n)T_{u,calc}$ $= (2/8)(366 \text{ kips})$ $= 91.5 \text{ kips}$	$T_{aw} = (n_{trib}/n)T_{a,calc}$ $= (2/8)(244 \text{ kips})$ $= 61.0 \text{ kips}$

The length of the web tension region is measured from the inside of the beam flange to 6 in. inside the tension bolt row:

$l_{wt} = p_{fi} + 6 \text{ in.}$
$= 2 \text{ in.} + 6 \text{ in.}$
$= 8.00 \text{ in.}$

The nominal web yield strength in the tension region is:

$T_{yw} = F_y A_g$ (from *Spec.* Eq. J4-1)
$= F_y t_{bw} l_{wt}$
$= (50 \text{ ksi})(3/8 \text{ in.})(8.00 \text{ in.})$
$= 150 \text{ kips}$

Check that the web design tensile yield strength is sufficient.

LRFD	ASD
$\phi T_{yw} = 0.90(150 \text{ kips})$ $= 135 \text{ kips} \quad \geq \quad T_{uw} = 91.5 \text{ kips}$ **o.k.**	$\frac{T_{yw}}{\Omega} = \frac{150 \text{ kips}}{1.67}$ $= 89.8 \text{ kips} \quad \geq \quad T_{aw} = 61.0 \text{ kips}$ **o.k.**

Check that the required strength is at least 60% (LRFD) or 40% (ASD) of the web tensile strength from Equations 3-41.

LRFD	ASD
$0.60T_{yw} = 0.60(150 \text{ kips})$ $= 90.0 \text{ kips}$ $T_{uwd} = \max(T_{uw}, 0.60T_{yw})$ $= \max(91.5 \text{ kips}, 90.0 \text{ kips})$ $= 91.5 \text{ kips}$	$0.40T_{yw} = 0.40(150 \text{ kips})$ $= 60.0 \text{ kips}$ $T_{awd} = \max(T_{aw}, 0.40T_{yw})$ $= \max(61.0 \text{ kips}, 60.0 \text{ kips})$ $= 61.0 \text{ kips}$

Check the web to end-plate weld around the tension bolts. Because the weld is loaded perpendicular to its longitudinal axis, the angle of loading, θ, is 90°.

$$R_n = (2 \text{ welds}) 0.60 F_{EXX} \frac{t_{weld}}{\sqrt{2}} l_{wt} (1.0 + 0.5 \sin^{1.5} \theta) \qquad \text{(from } \textit{Spec.} \text{ Eq. J2-4)}$$

$$= (2 \text{ welds})(0.60)(70 \text{ ksi}) \left(\frac{3/16 \text{ in.}}{\sqrt{2}} \right) (8.00 \text{ in.})(1.0 + 0.5 \sin^{1.5} 90°)$$

$$= 134 \text{ kips}$$

LRFD	ASD
$\phi R_n = 0.75(134 \text{ kips})$ $= 101 \text{ kips} \quad \geq \quad T_{uwd} = 91.5 \text{ kips}$ **o.k.**	$\frac{R_n}{\Omega} = \frac{134 \text{ kips}}{2.00}$ $= 67.0 \text{ kips} \quad \geq \quad T_{awd} = 61.0 \text{ kips}$ **o.k.**

Check the web to end-plate weld away from the tension bolts. Only the web to end-plate weld between the end of the assumed web tension length and the inside face of the bottom beam compression flange or the weld between the mid-depth of the beam and the inside face of the beam compression flange, whichever is smaller, is considered effective in resisting the beam end shear. The shear strength of this weld is compared to the required shear applied to the connection.

$$l_t = d - 2t_{bf} - l_{wt}$$

$$= 24 \text{ in.} - 2(3/4 \text{ in.}) - 8.00 \text{ in.}$$

$$= 14.5 \text{ in.}$$

$$l_{0.5w} = d/2 - t_{bf}$$

$$= (24 \text{ in.})/2 - 3/4 \text{ in.}$$

$$= 11.3 \text{ in.}$$

$$l_{wv} = \min(l_t, l_{0.5w})$$

$$= \min(14.5 \text{ in.}, 11.3 \text{ in.})$$

$$= 11.3 \text{ in.}$$

$$R_n = (2 \text{ welds})0.60F_{EXX}\frac{t_{weld}}{\sqrt{2}}l_{wv}(1.0+0.5\sin^{1.5}\theta) \quad \text{(from } \textit{Spec.} \text{ Eq. J2-4)}$$

$$= (2 \text{ welds})(0.60)(70 \text{ ksi})\left(\frac{3/16 \text{ in.}}{\sqrt{2}}\right)(11.3 \text{ in.})(1.0+0.5\sin^{1.5}0°)$$

$$= 126 \text{ kips}$$

LRFD	ASD
$\phi R_n = 0.75(126 \text{ kips})$ $= 94.5 \text{ kips} \geq V_u = 60.0 \text{ kips}$ **o.k.**	$\frac{R_n}{\Omega} = \frac{126 \text{ kips}}{2.00}$ $= 63.0 \text{ kips} \geq V_a = 40.0 \text{ kips}$ **o.k.**

Check that the shear rupture strength of the beam web at the weld using AISC *Specification* Equation J4-4 is sufficient.

$$V_{nw} = 0.60F_uA_{nv} \quad \text{(}\textit{Spec.}\text{ Eq. J4-4)}$$

$$= 0.60F_ul_{wv}t_{bw}$$

$$= 0.60(65 \text{ ksi})(11.3 \text{ in.})(3/8 \text{ in.})$$

$$= 165 \text{ kips}$$

LRFD	ASD
$\phi R_n = 0.75(165 \text{ kips})$ $= 124 \text{ kips} \geq V_u = 60.0 \text{ kips}$ **o.k.**	$\frac{R_n}{\Omega} = \frac{165 \text{ kips}}{2.00}$ $= 82.5 \text{ kips} \geq V_a = 40.0 \text{ kips}$ **o.k.**

The double-sided 3/16 in. fillet welds shown in Figure 5-15 from the web to the end plate are sufficient.

C. Column-Side Limit State Checks

See Example 5.3-1 or 5.3-2 for example column-side limit state check calculations.

Summary

The design shown in Figure 5-15 is satisfactory for the required moment and shear force shown.

EXAMPLE 5.3-7—Eight-Bolt Extended Stiffened Thick End-Plate Example

Given:

The connection shown in Figure 5-16 is an eight-bolt extended stiffened (8ES) end-plate moment connection for a built-up beam. All plate material is ASTM A572/A572M Grade 50, and the beam is ASTM A992/A992M material. The bolts are Group 120 ASTM F3125/F3125M Grade A325 pretensioned. Weld electrodes are E70XX. The connection is to be evaluated as a thick end-plate design for the following required moments and shear forces.

	LRFD	ASD
Moment	$M_u = 23{,}100$ kip-in.	$M_a = 15{,}400$ kip-in.
Shear force	$V_u = 90.0$ kips	$V_a = 60.0$ kips

Solution:

From AISC *Manual* Table 2-4, the material properties are as follows:

ASTM A992/A992M
F_y = 50 ksi
F_u = 65 ksi

ASTM A572/A572M Grade 50
F_y = 50 ksi
F_u = 65 ksi

From AISC *Specification* Table J3.2, the material properties of the bolts are as follows:

Group 120 ASTM F3125/F3125M 1¼-in.-diameter Grade A325 pretensioned
F_{nt} = 90 ksi
F_{nv} = 54 ksi (Group 120 bolts with threads not excluded from the shear plane; thread condition N)

From AISC *Manual* Table 1-1, the geometric properties of the beam section are as follows:

Beam: W36×150
d = 35.9 in. t_{bw} = 0.625 in.
b_{bf} = 12.0 in. t_{bf} = 0.940 in.

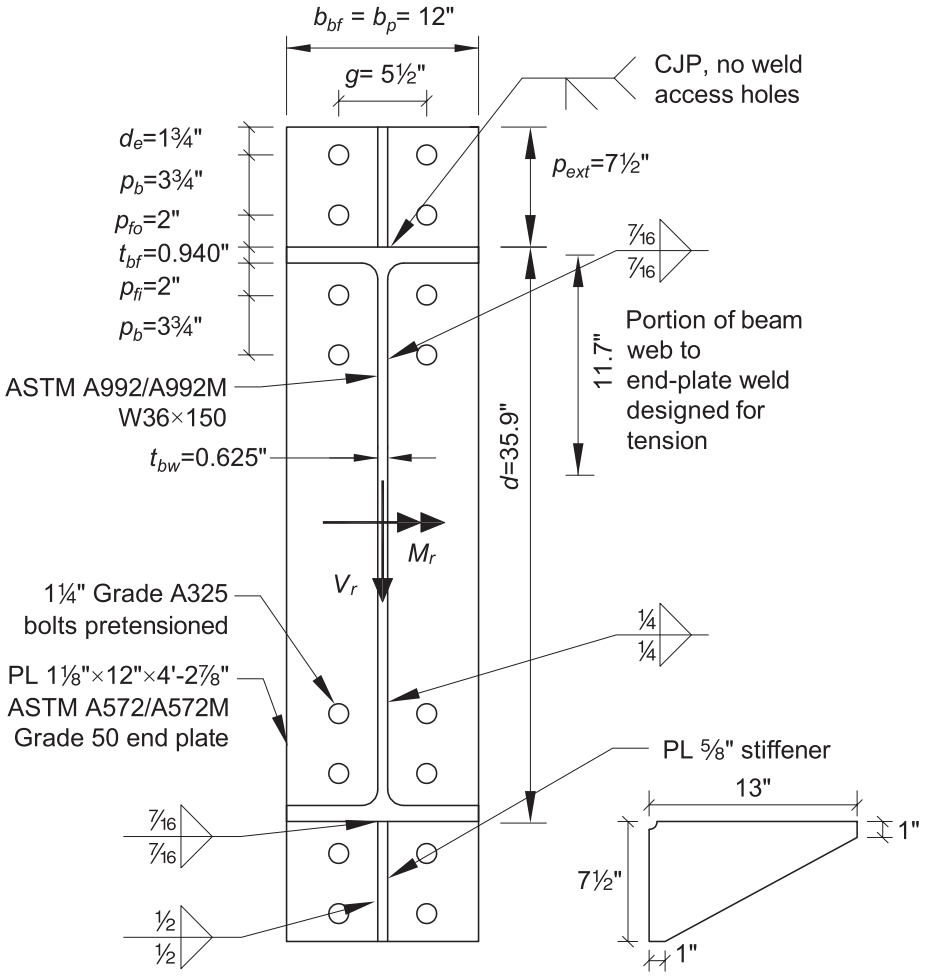

Fig. 5-16. Eight-bolt extended stiffened end-plate configuration for Example 5.3-7.

End-plate geometric properties:

b_p = 12 in.
t_p = 1⅛ in.
g = 5½ in.
p_{ext} = 7½ in.
d_e = 1¾ in.
p_{fi} = 2 in.
p_{fo} = 2 in.
p_b = 3¾ in.
d_p = 50⅞ in.

The distances from the centerline of the compression flange to the bolt lines, h_1, h_2, h_3, and h_4, are depicted in Table 5-16 and computed as:

$$h_1 = d - \frac{t_{bf}}{2} + p_{fo} + p_b$$
$$= 35.9 \text{ in.} - \frac{0.940 \text{ in.}}{2} + 2 \text{ in.} + 3¾ \text{ in.}$$
$$= 41.2 \text{ in.}$$

$$h_2 = d - \frac{t_{bf}}{2} + p_{fo}$$
$$= 35.9 \text{ in.} - \frac{0.940 \text{ in.}}{2} + 2 \text{ in.}$$
$$= 37.4 \text{ in.}$$

$$h_3 = d - \frac{3t_{bf}}{2} - p_{fi}$$
$$= 35.9 \text{ in.} - \frac{3(0.940 \text{ in.})}{2} - 2 \text{ in.}$$
$$= 32.5 \text{ in.}$$

$$h_4 = d - \frac{3t_{bf}}{2} - p_{fi} - p_b$$
$$= 35.9 \text{ in.} - \frac{3(0.940 \text{ in.})}{2} - 2 \text{ in.} - 3¾ \text{ in.}$$
$$= 28.7 \text{ in.}$$

$$b_{p,eff} \le b_{bf} + \max(t_p, 1 \text{ in.}) \quad (4\text{-}3)$$
$$\le 12.0 \text{ in.} + \max(1⅛ \text{ in.}, 1 \text{ in.})$$
$$\le 13.1 \text{ in.}$$

b_p = 12 in. ≤ 13.1 in. **o.k.**

$$b_{bf} \ge g \quad (4\text{-}1)$$

12.0 in. ≥ 5½ in. **o.k.**

Beam flange to end-plate stiffener geometric properties:

$$h_{st} = p_{fo} + p_b + d_e$$
$$= 2 \text{ in.} + 3¾ \text{ in.} + 1¾ \text{ in.}$$
$$= 7½ \text{ in.}$$

$$L_{st} = \frac{h_{st}}{\tan 30°} \tag{4-4}$$
$$= \frac{7½ \text{ in.}}{\tan 30°}$$
$$= 13.0 \text{ in.} \quad \leq \quad 13 \text{ in.} \quad \textbf{o.k.}$$

$$t_s \geq t_{bw}\left(\frac{F_{yb}}{F_{ys}}\right) \tag{3-36}$$
$$\geq (0.625 \text{ in.})\left(\frac{50 \text{ ksi}}{50 \text{ ksi}}\right)$$
$$\geq 0.625 \text{ in.}$$
$t_s = ⅝$ in. **o.k.**

$$\frac{h_{st}}{t_s} = \frac{7½ \text{ in.}}{⅝ \text{ in.}}$$
$$= 12.0$$

$$\frac{h_{st}}{t_s} \leq 0.56\sqrt{\frac{E}{F_{ys}}} \tag{3-37}$$
$$\leq 0.56\sqrt{\frac{29{,}000 \text{ ksi}}{50 \text{ ksi}}}$$
$$\leq 13.5$$
$$\frac{h_{st}}{t_s} = 12.0 \quad \textbf{o.k.}$$

A. End-Plate and Bolt Design Verification

Determine if the specified end-plate thickness, 1⅛ in., and 1¼-in.-diameter Grade A325 bolts are sufficient using the thick end-plate/smaller bolt diameter procedure.

Solve for the required bolt diameter using Equations 5-3. For Grade A325 bolts, the nominal tensile stress is $F_{nt} = 90$ ksi.

$$\sum_i n_i h_i = 2(41.2 \text{ in.}) + 2(37.4 \text{ in.}) + 2(32.5 \text{ in.}) + 2(28.7 \text{ in.})$$
$$= 280 \text{ in.}$$

LRFD	ASD
$d_{b,reqd} = \sqrt{\frac{4M_u}{\pi\phi F_{nt}\left(\sum_i n_i h_i\right)}}$	$d_{b,reqd} = \sqrt{\frac{4M_a}{\frac{\pi F_{nt}}{\Omega}\left(\sum_i n_i h_i\right)}}$
$= \sqrt{\frac{4(23{,}100 \text{ kip-in.})}{\pi(0.75)(90 \text{ ksi})(280 \text{ in.})}}$	$= \sqrt{\frac{4(15{,}400 \text{ kip-in.})}{\frac{\pi(90 \text{ ksi})}{2.00}(280 \text{ in.})}}$
$= 1.25 \text{ in.} \quad \leq \quad 1¼ \text{ in.}$ **o.k.**	$= 1.25 \text{ in.} \quad \leq \quad 1¼ \text{ in.}$ **o.k.**

The specified 1¼-in.-diameter Grade A325 bolts are sufficient to resist the required moment.

Solve for the required end-plate thickness using Equations 5-4. First solve for the distance, s, and yield line parameter, Y_p, using Table 5-16.

$$s = \frac{\sqrt{b_p g}}{2}$$
$$= \frac{\sqrt{(12\text{ in.})(5\frac{1}{2}\text{ in.})}}{2}$$
$$= 4.06\text{ in.}$$

Because $s > d_e = 1\frac{3}{4}$ in., Y_p in Table 5-16 is applicable, and because $s \geq p_{fo} = 2$ in. and $p_{fi} = 2$ in., the dimensions p_{fo} and p_{fi} are used in the equation for the yield line parameter.

$$Y_p = \frac{b_p}{2}\left[h_1\left(\frac{1}{2d_e}\right) + h_2\left(\frac{1}{p_{fo}}\right) + h_3\left(\frac{1}{p_{fi}}\right) + h_4\left(\frac{1}{s}\right)\right]$$
$$+ \frac{2}{g}\left[h_1(d_e + 0.75p_b) + h_2(p_{fo} + 0.25p_b) + h_3(p_{fi} + 0.75p_b) + h_4(s + 0.25p_b)\right] + g$$
$$= \left(\frac{12\text{ in.}}{2}\right)\left\{(41.2\text{ in.})\left[\frac{1}{2(1\frac{3}{4}\text{ in.})}\right] + (37.4\text{ in.})\left(\frac{1}{2\text{ in.}}\right) + (32.5\text{ in.})\left(\frac{1}{2\text{ in.}}\right) + (28.7\text{ in.})\left(\frac{1}{4.06\text{ in.}}\right)\right\}$$
$$+ \left(\frac{2}{5\frac{1}{2}\text{ in.}}\right)\left\{\begin{array}{l}(41.2\text{ in.})\left[1\frac{3}{4}\text{ in.} + 0.75(3\frac{3}{4}\text{ in.})\right] + (37.4\text{ in.})\left[2\text{ in.} + 0.25(3\frac{3}{4}\text{ in.})\right] \\ + (32.5\text{ in.})\left[2\text{ in.} + 0.75(3\frac{3}{4}\text{ in.})\right] + (28.7\text{ in.})\left[4.06\text{ in.} + 0.25(3\frac{3}{4}\text{ in.})\right]\end{array}\right\} + 5\frac{1}{2}\text{ in.}$$
$$= 546\text{ in.}$$

Determine the required end-plate thickness using Equations 5-4. For extended end-plate configurations, $\gamma_r = 1.0$.

LRFD	ASD
$t_{p,reqd} = \sqrt{\frac{1.10M_u}{\gamma_r \phi_b F_y Y_p}}$	$t_{p,reqd} = \sqrt{\frac{1.10M_a}{\gamma_r F_y Y_p / \Omega_b}}$
$= \sqrt{\frac{1.10(23{,}100\text{ kip-in.})}{1.0(0.90)(50\text{ ksi})(546\text{ in.})}}$	$= \sqrt{\frac{1.10(15{,}400\text{ kip-in.})}{1.0(50\text{ ksi})(546\text{ in.})/1.67}}$
$= 1.02\text{ in.} \leq 1\frac{1}{8}\text{ in.}$ **o.k.**	$= 1.02\text{ in.} \leq 1\frac{1}{8}\text{ in.}$ **o.k.**

Check Shear Yielding/Shear Rupture of the Extended Portion of the End Plate

For extended end-plate moment connections that are stiffened, shear yielding and shear rupture of the extended portion of the end plate are not limit states.

Therefore, a 1⅛-in.-thick end plate is sufficient.

Check Shear Transfer at Bolt Holes

See Example 5.3-1 or 5.3-2 for calculation procedures.

B. Check Beam to End-Plate Welds

The minimum weld size in AISC *Specification* Table J2.4 is determined from the material thickness of the thinner part joined. The fillet weld sizes shown in Figure 5-16 satisfy the requirements in Table J2.4.

Check Beam Flange to End-Plate Weld

The weld from the beam flange to the end plate is shown in Figure 5-16 as a CJP groove weld with the bevel facing away from the center of the beam and without weld access holes. (A PJP groove weld is an alternate option.)

Check Stiffener Welds

Check that the stiffener welds shown in Figure 5-16 are sufficient to develop the yield strengths of the stiffener plate.

Calculate the required strength for the stiffener to beam flange weld, and determine if the double-sided 7/16 in. fillet weld shown is sufficient.

LRFD	ASD
$V_{uw} = 0.60F_y t_s$ $= 0.60(50\text{ ksi})(5/8\text{ in.})$ $= 18.8\text{ kips/in.}$	$V_{aw} = 0.40F_y t_s$ $= 0.40(50\text{ ksi})(5/8\text{ in.})$ $= 12.5\text{ kips/in.}$

$$V_{nw} = (2\text{ welds})0.60F_{EXX}\frac{t_{weld}}{\sqrt{2}}(1.0+0.5\sin^{1.5}\theta) \quad \text{(from } \textit{Spec.} \text{ Eq. J2-4)}$$

$$= (2\text{ welds})(0.60)(70\text{ ksi})\left(\frac{7/16\text{ in.}}{\sqrt{2}}\right)(1.0+0.5\sin^{1.5}0°)$$

$$= 26.0\text{ kips/in.}$$

LRFD	ASD
$\phi V_{nw} = 0.75(26.0\text{ kips/in.})$ $= 19.5\text{ kips/in.} \geq V_{uw} = 18.8\text{ kips/in.}$ **o.k.**	$\frac{V_{nw}}{\Omega} = \frac{26.0\text{ kips/in.}}{2.00}$ $= 13.0\text{ kips/in.} \geq V_{aw} = 12.5\text{ kips/in.}$ **o.k.**

The shear rupture strength of the stiffener is greater than its shear yield strength and does not have to be checked. The shear rupture strength of the beam flange is sufficient by inspection.

Therefore, double-sided 7/16 in. fillet welds are sufficient. (Alternatively, a CJP groove weld could be used.)

Calculate the required strength for the stiffener to end-plate weld, and determine if the double-sided 1/2 in. fillet weld shown is sufficient.

LRFD	ASD
$T_{uw} = F_y t_s$ $= (50\text{ ksi})(5/8\text{ in.})$ $= 31.3\text{ kips/in.}$	$T_{aw} = \frac{F_y}{1.50}t_s$ $= \left(\frac{50\text{ ksi}}{1.50}\right)(5/8\text{ in.})$ $= 20.8\text{ kips/in.}$

$$T_{nw} = (2\text{ welds})0.60F_{EXX}\frac{t_{weld}}{\sqrt{2}}(1.0+0.5\sin^{1.5}\theta) \quad \text{(from } \textit{Spec.} \text{ Eq. J2-4)}$$

$$= (2\text{ welds})(0.60)(70\text{ ksi})\left(\frac{1/2\text{ in.}}{\sqrt{2}}\right)(1.0+0.5\sin^{1.5}90°)$$

$$= 44.5\text{ kips/in.}$$

LRFD	ASD
$\phi T_{nw} = 0.75(44.5\text{ kips/in.})$ $= 33.4\text{ kips/in.} \geq T_{uw} = 31.3\text{ kips/in.}$ **o.k.**	$\frac{T_{nw}}{\Omega} = \frac{44.5\text{ kips/in.}}{2.00}$ $= 22.3\text{ kips/in.} \geq T_{aw} = 20.8\text{ kips/in.}$ **o.k.**

Double-sided 1/2 in. fillet welds are sufficient. Alternatively, a CJP groove weld could be used.

Check Beam Web to End-Plate Weld

The beam web to end-plate welds shown in Figure 5-16 are separately checked for (1) tension rupture in the region around the tension bolts (extending 6 in. to the inside of the tension bolts), and (2) the remainder of the web to end-plate weld is checked for shear. As explained in Section 3.7.5, the demand for the tension web area, T_{uw} (LRFD) or T_{aw} (ASD), for this connection is the number of tension bolts adjacent to the web, n_{trib}, divided by the total number of tension bolts, n, multiplied by the calculated beam flange force, $T_{u,calc}$ (LRFD) or $T_{a,calc}$ (ASD).

LRFD	ASD
$T_{u,calc} = \dfrac{M_u}{d - t_{bf}}$ $= \dfrac{23{,}100 \text{ kip-in.}}{35.9 \text{ in.} - 0.940 \text{ in.}}$ $= 661 \text{ kips}$ $T_{uw} = (n_{trib}/n)T_{u,calc}$ $= (4/8)(661 \text{ kips})$ $= 331 \text{ kips}$	$T_{a,calc} = \dfrac{M_a}{d - t_{bf}}$ $= \dfrac{15{,}400 \text{ kip-in.}}{35.9 \text{ in.} - 0.940 \text{ in.}}$ $= 441 \text{ kips}$ $T_{aw} = (n_{trib}/n)T_{a,calc}$ $= (4/8)(441 \text{ kips})$ $= 221 \text{ kips}$

The length of the web tension region is measured from the inside of the beam flange to 6 in. inside the tension bolt row:

$l_{wt} = p_{fi} + p_b + 6 \text{ in.}$
$= 2 \text{ in.} + 3¾ \text{ in.} + 6 \text{ in.}$
$= 11.8 \text{ in.}$

The nominal web yield strength in the tension region is:

$T_{yw} = F_y A_g$ (from *Spec.* Eq. J4-1)
$= F_y t_{bw} l_{wt}$
$= (50 \text{ ksi})(0.625 \text{ in.})(11.8 \text{ in.})$
$= 369 \text{ kips}$

Check that the web design tensile yield strength is sufficient.

LRFD	ASD
$\phi T_{yw} = 0.90(369 \text{ kips})$ $= 332 \text{ kips} \quad \geq \quad T_{uw} = 331 \text{ kips}$ **o.k.**	$\dfrac{T_{yw}}{\Omega} = \dfrac{369 \text{ kips}}{1.67}$ $= 221 \text{ kips} \quad \geq \quad T_{aw} = 221 \text{ kips}$ **o.k.**

Check that the required strength is at least 60% (LRFD) or 40% (ASD) of the web tensile strength from Equations 3-41.

LRFD	ASD
$0.60T_{yw} = 0.60(369 \text{ kips})$ $= 221 \text{ kips}$ $T_{uwd} = \max(T_{uw}, 0.60T_{yw})$ $= \max(331 \text{ kips}, 221 \text{ kips})$ $= 331 \text{ kips}$	$0.40T_{yw} = 0.40(369 \text{ kips})$ $= 148 \text{ kips}$ $T_{awd} = \max(T_{aw}, 0.40T_{yw})$ $= \max(221 \text{ kips}, 148 \text{ kips})$ $= 221 \text{ kips}$

Check the web to end-plate weld around the tension bolts. Because the weld is loaded perpendicular to its longitudinal axis, the angle of loading, θ, is 90°.

$$R_n = (2\text{ welds})0.60F_{EXX}\frac{t_{weld}}{\sqrt{2}}l_{wt}(1.0+0.5\sin^{1.5}\theta) \quad \text{(from } \textit{Spec.} \text{ Eq. J2-4)}$$

$$= (2\text{ welds})(0.60)(70\text{ ksi})\left(\frac{7/16\text{ in.}}{\sqrt{2}}\right)(11.8\text{ in.})(1.0+0.5\sin^{1.5}90°)$$

$$= 460\text{ kips}$$

LRFD	ASD
$\phi R_n = 0.75(460\text{ kips})$ $= 345\text{ kips} \quad \geq \quad T_{uwd} = 331\text{ kips}$ **o.k.**	$\frac{R_n}{\Omega} = \frac{460\text{ kips}}{2.00}$ $= 230\text{ kips} \quad \geq \quad T_{awd} = 221\text{ kips}$ **o.k.**

Double-sided 7/16 in. fillet welds are sufficient. Alternatively, a CJP groove weld could be used.

Check the web to end-plate weld away from the tension bolts. Only the web to end-plate weld between the end of the assumed web tension length and the inside face of the bottom beam compression flange or the weld between the mid-depth of the beam and the inside face of the beam compression flange, whichever is smaller, is considered effective in resisting the beam end shear. The shear strength of this weld is compared to the required shear applied to the connection.

$$l_t = d - 2t_{bf} - l_{wt}$$

$$= 35.9\text{ in.} - 2(0.940\text{ in.}) - 11.8\text{ in.}$$

$$= 22.2\text{ in.}$$

$$l_{0.5w} = d/2 - t_{bf}$$

$$= (35.9\text{ in.})/2 - 0.940\text{ in.}$$

$$= 17.0\text{ in.}$$

$$l_{wv} = \min(l_t, l_{0.5w})$$

$$= \min(22.2\text{ in.}, 17.0\text{ in.})$$

$$= 17.0\text{ in.}$$

$$R_n = (2\text{ welds})0.60F_{EXX}\frac{t_{weld}}{\sqrt{2}}l_{wv}(1.0+0.5\sin^{1.5}\theta) \quad \text{(from } \textit{Spec.} \text{ Eq. J2-4)}$$

$$= (2\text{ welds})(0.60)(70\text{ ksi})\left(\frac{1/4\text{ in.}}{\sqrt{2}}\right)(17.0\text{ in.})(1.0+0.5\sin^{1.5}0°)$$

$$= 252\text{ kips}$$

LRFD	ASD
$\phi R_n = 0.75(252\text{ kips})$ $= 189\text{ kips} \quad \geq \quad V_u = 90.0\text{ kips}$ **o.k.**	$\frac{R_n}{\Omega} = \frac{252\text{ kips}}{2.00}$ $= 126\text{ kips} \quad \geq \quad V_a = 60.0\text{ kips}$ **o.k.**

Check that the shear rupture strength of the beam web at the weld using AISC *Specification* Equation J4-4 is sufficient.

$$V_{nw} = 0.60F_u A_{nv} \quad \text{(Spec. Eq. J4-4)}$$
$$= 0.60F_u l_{wt} t_{bw}$$
$$= 0.60(65 \text{ ksi})(17.0 \text{ in.})(0.625 \text{ in.})$$
$$= 414 \text{ kips}$$

LRFD	ASD
$\phi R_n = 0.75(414 \text{ kips})$ $= 311 \text{ kips} \geq V_u = 90.0 \text{ kips}$ **o.k.**	$\frac{R_n}{\Omega} = \frac{414 \text{ kips}}{2.00}$ $= 207 \text{ kips} \geq V_a = 60.0 \text{ kips}$ **o.k.**

The double-sided ¼ in. fillet welds shown in Figure 5-16 from the web to the end plate are sufficient.

C. Column-Side Limit State Checks

See Example 5.3-1 or 5.3-2 for example column-side limit state check calculations.

Summary

The design shown in Figure 5-16 is satisfactory for the required moment and shear force shown.

EXAMPLE 5.3-8—12-Bolt Multiple-Row Extended 1/3 Four-Wide/Two-Wide Unstiffened Thick End-Plate Example

Given:

The connection shown in Figure 5-17 is a 12-bolt, multiple-row extended (MRE) 1/3 four-wide/two-wide, extended unstiffened end-plate moment connection for a built-up beam. The beam and end-plate material are ASTM A572/A572M Grade 50, and the bolts are Group 120 ASTM F3125/F3125M Grade A325 pretensioned. Weld electrodes are E70XX. The connection is to be evaluated as a thick end-plate design for the following required moments and shear forces.

	LRFD	ASD
Moment	$M_u = 20{,}100$ kip-in.	$M_a = 13{,}400$ kip-in.
Shear force	$V_u = 90.0$ kips	$V_a = 60.0$ kips

Solution:

From AISC *Manual* Table 2-4, the material properties are as follows:

ASTM A572/A572M Grade 50
$F_y = 50$ ksi
$F_u = 65$ ksi

From AISC *Specification* Table J3.2, the material properties of the bolts are as follows:

Group 120 ASTM F3125/F3125M 1-in.-diameter Grade A325 pretensioned
$F_{nt} = 90$ ksi
$F_{nv} = 54$ ksi (Group 120 bolts with threads not excluded from the shear plane; thread condition N)

Beam
$d = 36$ in. $\quad t_{bw} = ½$ in.
$b_{bf} = 15$ in. $\quad t_{bf} = ¾$ in.

End-plate geometric properties:
$b_p = 15$ in.
$t_p = 1⅛$ in.
$g = 4$ in.

$p_{ext} = 5¼$ in.
$d_e = 1¾$ in.
$g_o = 3¾$ in.
$p_{fo} = 2½$ in.
$p_{fi} = 2½$ in.
$p_b = 3¾$ in.
$d_p = 44½$ in.

The distances from the centerline of the compression flange to the bolt lines, h_1, h_2, h_3, and h_4, are depicted in Table 5-17 and computed as:

$$h_1 = d - \frac{t_{bf}}{2} + p_{fo}$$
$$= 36 \text{ in.} - \frac{¾ \text{ in.}}{2} + 2½ \text{ in.}$$
$$= 38.1 \text{ in.}$$

$$h_2 = d - \frac{3t_{bf}}{2} - p_{fi}$$
$$= 36 \text{ in.} - \frac{3(¾ \text{ in.})}{2} - 2½ \text{ in.}$$
$$= 32.4 \text{ in.}$$

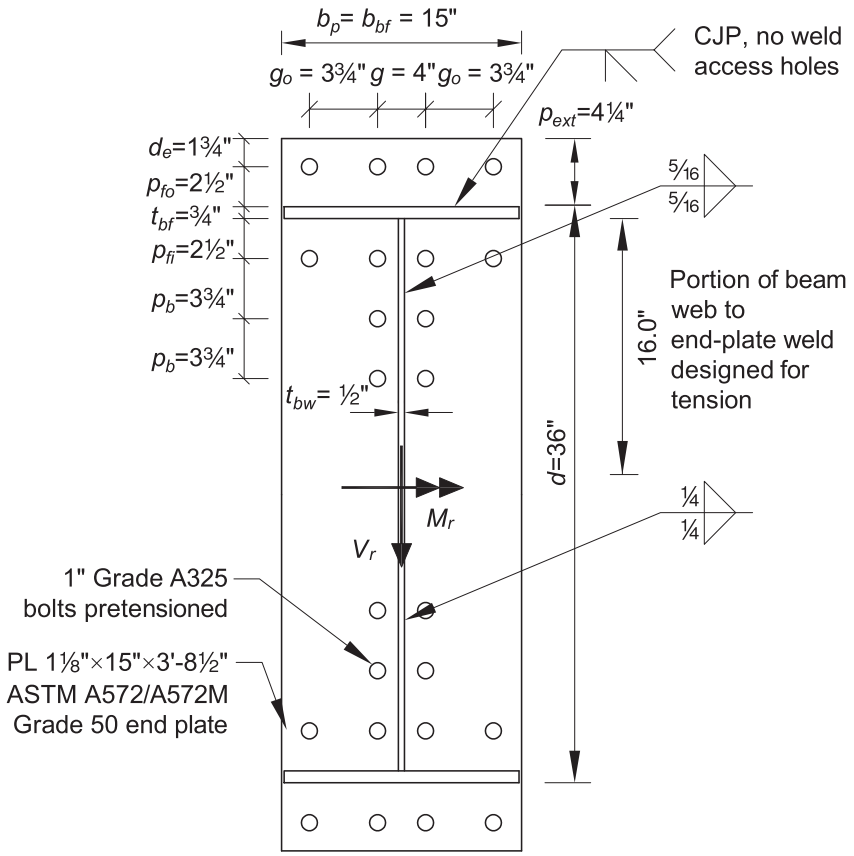

Fig. 5-17. 12-bolt multiple-row extended 1/3 four-wide/two-wide unstiffened end-plate configuration for Example 5.3-8.

$$h_3 = d - \frac{3t_{bf}}{2} - p_{fi} - p_b$$

$$= 36 \text{ in.} - \frac{3(¾ \text{ in.})}{2} - 2½ \text{ in.} - 3¾ \text{ in.}$$

$$= 28.6 \text{ in.}$$

$$h_4 = d - \frac{3t_{bf}}{2} - p_{fi} - 2p_b$$

$$= 36 \text{ in.} - \frac{3(¾ \text{ in.})}{2} - 2½ \text{ in.} - 2(3¾ \text{ in.})$$

$$= 24.9 \text{ in.}$$

$$b_{p,eff} \le b_{bf} + \max(t_p, 1 \text{ in.}) \quad (4\text{-}3)$$

$$= 15 \text{ in.} + \max(1⅛ \text{ in.}, 1 \text{ in.})$$

$$= 16.1 \text{ in.}$$

$b_p = 15$ in. $\le$ 16.1 in. **o.k.**

$$b_{bf} \ge g + 2g_o \quad (4\text{-}2)$$

15 in. $\ge$ 4 in. + 2(3¾ in.)

15 in. $\ge$ 11.5 in. **o.k.**

A. End-Plate and Bolt Design Verification

Determine if the specified end-plate thickness, 1⅛ in., and 1-in.-diameter Grade A325 bolts are sufficient using the thick end-plate/smaller bolt diameter procedure.

Solve for the required bolt diameter using Equations 5-3. For Grade A325 bolts, the nominal tensile stress is $F_{nt} = 90$ ksi.

$$\sum_i n_i h_i = 4(38.1 \text{ in.}) + 4(32.4 \text{ in.}) + 2(28.6 \text{ in.}) + 2(24.9 \text{ in.})$$

$$= 389 \text{ in.}$$

LRFD	ASD
$d_{b,reqd} = \sqrt{\frac{4M_u}{\pi\phi F_{nt}\left(\sum_i n_i h_i\right)}}$	$d_{b,reqd} = \sqrt{\frac{4M_a}{\frac{\pi F_{nt}}{\Omega}\left(\sum_i n_i h_i\right)}}$
$= \sqrt{\frac{4(20{,}100 \text{ kip-in.})}{\pi(0.75)(90 \text{ ksi})(389 \text{ in.})}}$	$= \sqrt{\frac{4(13{,}400 \text{ kip-in.})}{\frac{\pi(90 \text{ ksi})}{2.00}(389 \text{ in.})}}$
$= 0.987 \text{ in.} \le 1 \text{ in.}$ **o.k.**	$= 0.987 \text{ in.} \le 1 \text{ in.}$ **o.k.**

The specified 1-in.-diameter Grade A325 bolts are sufficient to resist the required moment.

Solve for the required end-plate thickness using Equations 5-4. First solve for the distance, s, and yield line parameter, Y_p, using Table 5-17.

$$s = \frac{\sqrt{b_p g}}{2}$$
$$= \frac{\sqrt{(15\text{ in.})(4\text{ in.})}}{2}$$
$$= 3.87\text{ in.}$$

Because $s \geq p_{fi} = 2\frac{1}{2}$ in., the dimension p_{fi} is used in the equation for the yield line parameter.

$$Y_p = \frac{b_p}{2}\left[h_1\left(\frac{1}{p_{fo}}\right) + h_2\left(\frac{1}{p_{fi}}\right) + h_4\left(\frac{1}{s}\right) - \frac{1}{2}\right] + \frac{2}{g}\left[h_2(p_{fi} + 1.5p_b) + h_4(s + 0.5p_b)\right] + \frac{g}{2}$$
$$= \left(\frac{15\text{ in.}}{2}\right)\left[(38.1\text{ in.})\left(\frac{1}{2\frac{1}{2}\text{ in.}}\right) + (32.4\text{ in.})\left(\frac{1}{2\frac{1}{2}\text{ in.}}\right) + (28.6\text{ in.})\left(\frac{1}{3.87\text{ in.}}\right) - \frac{1}{2}\right]$$
$$+ \left(\frac{2}{4\text{ in.}}\right)\left\{(32.4\text{ in.})\left[2\frac{1}{2}\text{ in.} + 1.5(3\frac{3}{4}\text{ in.})\right] + (24.9\text{ in.})\left[3.87\text{ in.} + 0.5(3\frac{3}{4}\text{ in.})\right]\right\} + \frac{4\text{ in.}}{2}$$
$$= 461\text{ in.}$$

Determine the required end-plate thickness using Equations 5-4. For extended end-plate configurations, $\gamma_r = 1.0$.

LRFD	ASD
$t_{p,reqd} = \sqrt{\frac{1.10M_u}{\gamma_r \phi_b F_y Y_p}}$	$t_{p,reqd} = \sqrt{\frac{1.10M_a}{\gamma_r F_y Y_p / \Omega_b}}$
$= \sqrt{\frac{1.10(20{,}100\text{ kip-in.})}{1.0(0.90)(50\text{ ksi})(461\text{ in.})}}$	$= \sqrt{\frac{1.10(13{,}400\text{ kip-in.})}{1.0(50\text{ ksi})(461\text{ in.})/1.67}}$
$= 1.03\text{ in.} \leq 1\frac{1}{8}\text{ in.}$ **o.k.**	$= 1.03\text{ in.} \leq 1\frac{1}{8}\text{ in.}$ **o.k.**

Check Shear Yielding/Shear Rupture of the Extended Portion of the End Plate

For extended end-plate moment connections that are unstiffened, potential limit states that must be checked are shear yielding and shear rupture of the extended portion of the end plate. For the 12-bolt MRE 1/3 four-wide/two-wide unstiffened connection, the shear demand is taken as one-third of the tension flange force because the exterior bolts represent one-third of the bolts. The shear strength is calculated in accordance with AISC *Specification* Section J4.2.

Calculate the shear demand on the extended portion of the end plate.

LRFD	ASD
$V_{up} = \frac{1}{3}\left(\frac{M_u}{d - t_{bf}}\right)$	$V_{ap} = \frac{1}{3}\left(\frac{M_a}{d - t_{bf}}\right)$
$= \frac{1}{3}\left(\frac{20{,}100\text{ kip-in.}}{36\text{ in.} - \frac{3}{4}\text{ in.}}\right)$	$= \frac{1}{3}\left(\frac{13{,}400\text{ kip-in.}}{36\text{ in.} - \frac{3}{4}\text{ in.}}\right)$
$= 190\text{ kips}$	$= 127\text{ kips}$

Calculate the nominal shear yielding strength of the 1⅛-in.-thick end plate:

$$R_n = 0.60F_yA_{gv} \quad \text{(Spec. Eq. J4-3)}$$
$$= 0.60F_yb_pt_p$$
$$= 0.60(50\text{ ksi})(15\text{ in.})(1\text{⅛ in.})$$
$$= 506\text{ kips}$$

Compare the design shear yielding strength to the shear demand. According to AISC *Specification* Section J4.2 for yielding of elements in shear, the resistance factor is $\phi = 1.00$, and the safety factor is $\Omega = 1.50$.

LRFD	ASD
$\phi R_n = 1.00(506\text{ kips})$ $= 506\text{ kips} \geq V_{up} = 190\text{ kips}$ **o.k.**	$\frac{R_n}{\Omega} = \frac{506\text{ kips}}{1.50}$ $= 337\text{ kips} \geq V_{ap} = 127\text{ kips}$ **o.k.**

Calculate the nominal shear rupture strength. The width of the extended portion of the end plate for use in the net section area is the width minus four effective hole diameters. The effective hole diameter is the hole diameter from AISC *Specification* Table J3.3 plus ⅛ in. The additional ⅛ in. accounts for damage around the hole caused by drilling, punching, or thermal cutting. For 1-in.-diameter bolts, the standard hole diameter, d_h, is 1⅛ in.

$$A_{nv} = \left[b_p - 4(d_h + \text{⅛ in.})\right]t_p$$
$$= \left[15\text{ in.} - 4(1\text{⅛ in.} + \text{⅛ in.})\right](1\text{⅛ in.})$$
$$= 11.5\text{ in.}^2$$
$$R_n = 0.60F_uA_{nv} \quad \text{(Spec. Eq. J4-4)}$$
$$= 0.60(65\text{ ksi})(11.5\text{ in.}^2)$$
$$= 449\text{ kips}$$

Compare the design shear rupture strength to the shear demand. Using AISC *Specification* Section J4.2 for rupture of elements in shear, the resistance factor is $\phi = 0.75$, and the safety factor is $\Omega = 2.00$.

LRFD	ASD
$\phi R_n = 0.75(449\text{ kips})$ $= 337\text{ kips} \geq V_{up} = 190\text{ kips}$ **o.k.**	$\frac{R_n}{\Omega} = \frac{449\text{ kips}}{2.00}$ $= 225\text{ kips} \geq V_{ap} = 127\text{ kips}$ **o.k.**

The extended portion of the 1⅛-in.-thick end plate has sufficient resistance to shear yielding and shear rupture.

Check Shear Transfer at Bolt Holes

See Example 5.3-1 or 5.3-2 for calculation procedures.

B. Check Beam to End-Plate Welds

The minimum weld size in AISC *Specification* Table J2.4 is determined from the material thickness of the thinner part joined. The fillet weld sizes shown in Figure 5-17 satisfy the requirements in Table J2.4.

Check Beam Flange to End-Plate Weld

The weld from the beam flange to the end plate is shown in Figure 5-17 as a CJP groove weld with the bevel facing away from the center of the beam and without weld access holes. (Double-sided ⅝ in. fillet welds or a PJP groove weld are alternate options.)

Check Beam Web to End-Plate Weld

The beam web to end-plate welds shown in Figure 5-17 are separately checked for (1) tension rupture in the region around the tension bolts (extending 6 in. to the inside of the tension bolts), and (2) the remainder of the web to end-plate weld is checked for shear. As explained in Section 3.7.5, the demand for the tension web area, T_{uw} (LRFD) or T_{aw} (ASD), for this connection is the number of tension bolts adjacent to the web, n_{trib}, divided by the total number of tension bolts, n, multiplied by the calculated beam flange force, $T_{u,calc}$ (LRFD) or $T_{a,calc}$ (ASD).

LRFD	ASD
$T_{u,calc} = \dfrac{M_u}{d - t_{bf}}$ $= \dfrac{20{,}100 \text{ kip-in.}}{36 \text{ in.} - ¾ \text{ in.}}$ $= 570 \text{ kips}$ $T_{uw} = (n_{trib}/n)T_{u,calc}$ $= (6/12)(570 \text{ kips})$ $= 285 \text{ kips}$	$T_{a,calc} = \dfrac{M_a}{d - t_{bf}}$ $= \dfrac{13{,}400 \text{ kip-in.}}{36 \text{ in.} - ¾ \text{ in.}}$ $= 380 \text{ kips}$ $T_{aw} = (n_{trib}/n)T_{a,calc}$ $= (6/12)(380 \text{ kips})$ $= 190 \text{ kips}$

The length of the web tension region is measured from the inside of the beam flange to 6 in. inside the tension bolt row:

$l_{wt} = p_{fi} + 2p_b + 6 \text{ in.}$
$= 2½ \text{ in.} + 2(3¾ \text{ in.}) + 6 \text{ in.}$
$= 16.0 \text{ in.}$

The nominal web yield strength in the tension region is:

$T_{yw} = F_y A_g$ (from *Spec*. Eq. J4-1)
$= F_y t_{bw} l_{wt}$
$= (50 \text{ ksi})(½ \text{ in.})(16.0 \text{ in.})$
$= 400 \text{ kips}$

Check that the web design tensile yield strength is sufficient.

LRFD	ASD
$\phi T_{yw} = 0.90(400 \text{ kips})$ $= 360 \text{ kips} \geq T_{uw} = 285 \text{ kips}$ **o.k.**	$\dfrac{T_{yw}}{\Omega} = \dfrac{400 \text{ kips}}{1.67}$ $= 240 \text{ kips} \geq T_{aw} = 190 \text{ kips}$ **o.k.**

Check that the required strength is at least 60% (LRFD) or 40% (ASD) of the web tensile strength from Equations 3-41.

LRFD	ASD
$0.60T_{yw} = 0.60(400 \text{ kips})$ $= 240 \text{ kips}$ $T_{uwd} = \max(T_{uw}, 0.60T_{yw})$ $= \max(285 \text{ kips}, 240 \text{ kips})$ $= 285 \text{ kips}$	$0.40T_{yw} = 0.40(400 \text{ kips})$ $= 160 \text{ kips}$ $T_{awd} = \max(T_{aw}, 0.40T_{yw})$ $= \max(190 \text{ kips}, 160 \text{ kips})$ $= 190 \text{ kips}$

Check the web to end-plate weld around the tension bolts. Because the weld is loaded perpendicular to its longitudinal axis, the angle of loading, θ, is 90°.

$$R_n = (2\text{ welds})0.60F_{EXX}\frac{t_{weld}}{\sqrt{2}}l_{wt}(1.0+0.5\sin^{1.5}\theta) \quad \text{(from } \textit{Spec.} \text{ Eq. J2-4)}$$

$$= (2\text{ welds})(0.60)(70\text{ ksi})\left(\frac{5/16\text{ in.}}{\sqrt{2}}\right)(16.0\text{ in.})(1.0+0.5\sin^{1.5}90°)$$

$$= 445\text{ kips}$$

LRFD	ASD
$\phi R_n = 0.75(445\text{ kips})$ $= 334\text{ kips} \quad \geq \quad T_{uwd} = 285\text{ kips}$ **o.k.**	$\frac{R_n}{\Omega} = \frac{445\text{ kips}}{2.00}$ $= 223\text{ kips} \quad \geq \quad T_{awd} = 190\text{ kips.}$ **o.k.**

Double-sided 5⁄16 in. fillet welds are sufficient.

Check the web to end-plate weld away from the tension bolts. Only the web to end-plate weld between the end of the assumed web tension length and the inside face of the bottom beam compression flange or the weld between the mid-depth of the beam and the inside face of the beam compression flange, whichever is smaller, is considered effective in resisting the beam end shear. The shear strength of this weld is compared to the required shear applied to the connection.

$$l_t = d - 2t_{bf} - l_{wt}$$

$$= 36\text{ in.} - 2(3/4\text{ in.}) - 16.0\text{ in.}$$

$$= 18.5\text{ in.}$$

$$l_{0.5w} = d/2 - t_{bf}$$

$$= (36\text{ in.})/2 - 3/4\text{ in.}$$

$$= 17.3\text{ in.}$$

$$l_{wv} = \min(l_t, l_{0.5w})$$

$$= \min(18.5\text{ in.}, 17.3\text{ in.})$$

$$= 17.3\text{ in.}$$

$$R_n = (2\text{ welds})0.60F_{EXX}\frac{t_{weld}}{\sqrt{2}}l_{wv}(1.0+0.5\sin^{1.5}\theta) \quad \text{(from } \textit{Spec.} \text{ Eq. J2-4)}$$

$$= (2\text{ welds})(0.60)(70\text{ ksi})\left(\frac{1/4\text{ in.}}{\sqrt{2}}\right)(17.3\text{ in.})(1.0+0.5\sin^{1.5}0°)$$

$$= 257\text{ kips}$$

LRFD	ASD
$\phi R_n = 0.75(257\text{ kips})$ $= 193\text{ kips} \quad \geq \quad V_u = 90.0\text{ kips}$ **o.k.**	$\frac{R_n}{\Omega} = \frac{257\text{ kips}}{2.00}$ $= 129\text{ kips} \quad \geq \quad V_a = 60.0\text{ kips}$ **o.k.**

Check that the shear rupture strength of the beam web at the weld using AISC *Specification* Equation J4-4 is sufficient.

$$V_{nw} = 0.60F_u A_{nv} \quad \text{(Spec. Eq. J4-4)}$$
$$= 0.60F_u l_{wv} t_{bw}$$
$$= 0.60(65 \text{ ksi})(17.3 \text{ in.})(\tfrac{1}{2} \text{ in.})$$
$$= 337 \text{ kips}$$

LRFD	ASD
$\phi R_n = 0.75(337 \text{ kips})$ $= 253 \text{ kips} \quad \geq \quad V_u = 90.0 \text{ kips}$ **o.k.**	$\frac{R_n}{\Omega} = \frac{337 \text{ kips}}{2.00}$ $= 169 \text{ kips} \quad \geq \quad V_a = 60.0 \text{ kips}$ **o.k.**

The double-sided ¼ in. fillet welds shown in Figure 5-17 from the web to the end plate are sufficient.

C. Column-Side Limit State Checks

See Example 5.3-1 or 5.3-2 for example column-side limit state check calculations.

Summary

The design shown in Figure 5-17 is satisfactory for the required moment and shear force shown.

EXAMPLE 5.3-9—12-Bolt Extended Stiffened Thick End-Plate Example

Given:

The connection shown in Figure 5-18 is a 12-bolt extended stiffened (12ES) end-plate moment connection example for a built-up beam. The beam and plate material are ASTM A572/A572M Grade 50. The bolts are Group 120 ASTM F3125/F3125M Grade A325 pretensioned. Weld electrodes are E70XX. The connection is to be evaluated as a thick end-plate design for the following required moments and shear forces.

	LRFD	ASD
Moment	$M_u = 20{,}100$ kip-in.	$M_a = 13{,}400$ kip-in.
Shear force	$V_u = 90.0$ kips	$V_a = 60.0$ kips

Solution:

From AISC *Manual* Table 2-4, the material properties are as follows:

ASTM A572/A572M Grade 50
$F_y = 50$ ksi
$F_u = 65$ ksi

From AISC *Specification* Table J3.2, the material properties of the bolts are as follows:

Group 120 ASTM F3125/F3125M 1-in.-diameter Grade A325 pretensioned
$F_{nt} = 90$ ksi
$F_{nv} = 54$ ksi (Group 120 bolts with threads not excluded from the shear plane; thread condition N)

Beam
$d = 36$ in. $\quad t_{bw} = \frac{3}{8}$ in.
$b_{bf} = 15$ in. $\quad t_{bf} = \frac{3}{4}$ in.

End-plate geometric properties:
b_p = 15 in.
t_p = 1 in.
g = 4 in.
p_{ext} = 8 in.
d_e = 1¾ in.
g_o = 3¾ in.
p_{fi} = 2½ in.
p_{fo} = 2½ in.
p_b = 3¾ in.
d_p = 52 in.

The distances from the centerline of the compression flange to the bolt lines, h_1, h_2, h_3, and h_4, are depicted in Table 5-18 and computed as:

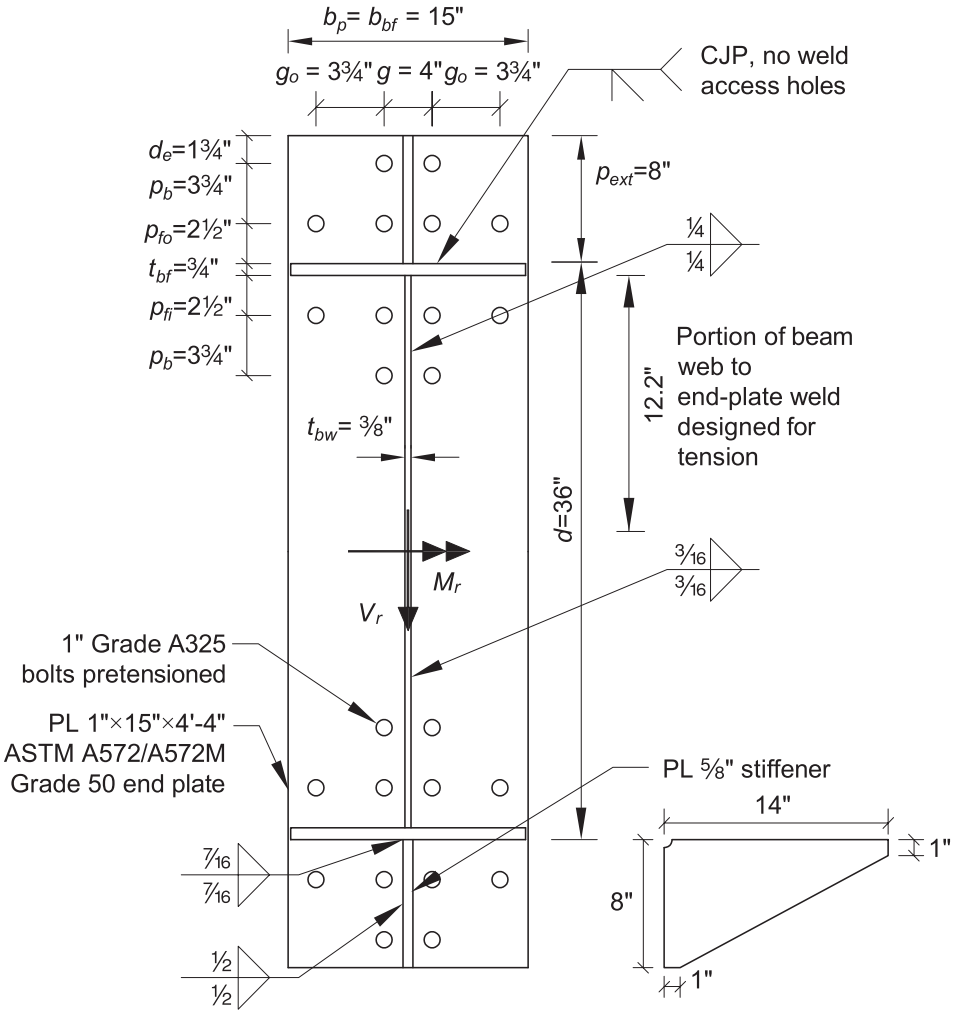

Fig. 5-18. 12ES end-plate configuration for Example 5.3-9.

$$h_1 = d - \frac{t_{bf}}{2} + p_{fo} + p_b$$
$$= 36 \text{ in.} - \frac{¾ \text{ in.}}{2} + 2½ \text{ in.} + 3¾ \text{ in.}$$
$$= 41.9 \text{ in.}$$

$$h_2 = d - \frac{t_{bf}}{2} + p_{fo}$$
$$= 36 \text{ in.} - \frac{¾ \text{ in.}}{2} + 2½ \text{ in.}$$
$$= 38.1 \text{ in.}$$

$$h_3 = d - \frac{3t_{bf}}{2} - p_{fi}$$
$$= 36 \text{ in.} - \frac{3(¾ \text{ in.})}{2} - 2½ \text{ in.}$$
$$= 32.4 \text{ in.}$$

$$h_4 = d - \frac{3t_{bf}}{2} - p_{fi} - p_b$$
$$= 36 \text{ in.} - \frac{3(¾ \text{ in.})}{2} - 2½ \text{ in.} - 3¾ \text{ in.}$$
$$= 28.6 \text{ in.}$$

$$b_{p,eff} \le b_{bf} + \max(t_p, 1 \text{ in.}) \quad (4\text{-}3)$$
$$\le 15 \text{ in.} + \max(1 \text{ in.}, 1 \text{ in.})$$
$$\le 16.0 \text{ in.}$$

$b_p = 15 \text{ in.} \le 16.0 \text{ in.}$ **o.k.**

$$b_{bf} \ge g + 2g_o \quad (4\text{-}2)$$
$15 \text{ in.} \ge 4 \text{ in.} + 2(3¾ \text{ in.})$
$15 \text{ in.} \ge 11.5 \text{ in.}$ **o.k.**

Beam flange to end-plate stiffener geometric properties:

$$h_{st} = p_{fo} + p_b + d_e$$
$$= 2½ \text{ in.} + 3¾ \text{ in.} + 1¾ \text{ in.}$$
$$= 8.00 \text{ in.}$$

$$L_{st} = \frac{h_{st}}{\tan 30°} \quad (4\text{-}4)$$
$$= \frac{8.00 \text{ in.}}{\tan 30°}$$
$$= 13.9 \text{ in.} \le 14 \text{ in.}$$ **o.k.**

$$t_s \geq t_{bw}\left(\frac{F_{yb}}{F_{ys}}\right) \tag{3-36}$$

$$\geq (⅜\text{ in.})\left(\frac{50\text{ ksi}}{50\text{ ksi}}\right)$$

$$\geq ⅜\text{ in.}$$

$t_s = ⅝$ in. **o.k.**

$$\frac{h_{st}}{t_s} = \frac{8.00\text{ in.}}{⅝\text{ in.}}$$

$$= 12.8$$

$$\frac{h_{st}}{t_s} \leq 0.56\sqrt{\frac{E}{F_{ys}}} \tag{3-37}$$

$$\leq 0.56\sqrt{\frac{29{,}000\text{ ksi}}{50\text{ ksi}}}$$

$$\leq 13.5$$

$\frac{h_{st}}{t_s} = 12.8$ **o.k.**

A. End-Plate and Bolt Design Verification

Determine if the specified end-plate thickness, 1 in., and 1-in.-diameter Grade A325 bolts are sufficient using the thick end-plate/smaller bolt diameter procedure.

Solve for the required bolt diameter using Equations 5-3. For Grade A325 bolts, the nominal tensile stress is $F_{nt} = 90$ ksi.

$$\sum_i n_i h_i = 2(41.9\text{ in.}) + 4(38.1\text{ in.}) + 4(32.4\text{ in.}) + 2(28.6\text{ in.})$$

$$= 423\text{ in.}$$

LRFD	ASD
$d_{b,reqd} = \sqrt{\frac{4M_u}{\pi\phi F_{nt}\left(\sum_i n_i h_i\right)}}$	$d_{b,reqd} = \sqrt{\frac{4M_a}{\frac{\pi F_{nt}}{\Omega}\left(\sum_i n_i h_i\right)}}$
$= \sqrt{\frac{4(20{,}100\text{ kip-in.})}{\pi(0.75)(90\text{ ksi})(423\text{ in.})}}$	$= \sqrt{\frac{4(13{,}400\text{ kip-in.})}{\frac{\pi(90\text{ ksi})}{2.00}(423\text{ in.})}}$
$= 0.947\text{ in.} \leq 1\text{ in.}$ **o.k.**	$= 0.947\text{ in.} \leq 1\text{ in.}$ **o.k.**

The specified 1-in.-diameter Grade A325 bolts are sufficient to resist the required moments.

Solve for the required end-plate thickness using Equations 5-4. First solve for the distance, s, and yield line parameter, Y_p, using Table 5-18.

$$s = \frac{\sqrt{b_p g}}{2}$$

$$= \frac{\sqrt{(15\text{ in.})(4\text{ in.})}}{2}$$

$$= 3.87\text{ in.}$$

Because $s \geq p_{fo} = 2\frac{1}{2}$ in., $p_{fi} = 2\frac{1}{2}$ in., and $d_e = 1\frac{3}{4}$ in., the dimensions p_{fo}, p_{fi}, and d_e are used in the equation for the yield line parameter.

$$Y_p = \frac{b_p}{2}\left[h_2\left(\frac{1}{p_{fo}}\right) + h_3\left(\frac{1}{p_{fi}}\right) + h_4\left(\frac{1}{s}\right) - \frac{1}{2}\right] +$$

$$\frac{2}{g}\left[h_1(d_e + 0.75p_b) + h_2(p_{fo} + 0.25p_b) + h_3(p_{fi} + 0.75p_b) + h_4(s + 0.25p_b)\right] + \frac{5g}{4}$$

$$= \left(\frac{15\text{ in.}}{2}\right)\left[\frac{38.1\text{ in.}}{2\frac{1}{2}\text{ in.}} + \frac{32.4\text{ in.}}{2\frac{1}{2}\text{ in.}} + \frac{28.6\text{ in.}}{3.87\text{ in.}} - \frac{1}{2}\right] +$$

$$\left(\frac{2}{4\text{ in.}}\right)\left\{\begin{array}{l}(41.9\text{ in.})\left[1\frac{3}{4}\text{ in.} + 0.75(3\frac{3}{4}\text{ in.})\right] + \\ (38.1\text{ in.})\left[2\frac{1}{2}\text{ in.} + 0.25(3\frac{3}{4}\text{ in.})\right] + \\ (32.4\text{ in.})\left[2\frac{1}{2}\text{ in.} + 0.75(3\frac{3}{4}\text{ in.})\right] + \\ (28.6\text{ in.})\left[3.87\text{ in.} + 0.25(3\frac{3}{4}\text{ in.})\right]\end{array}\right\} + \frac{5(4\text{ in.})}{4}$$

$$= 584\text{ in.}$$

Determine the required end-plate thickness using Equations 5-4. For extended end-plate configurations, $\gamma_r = 1.0$.

LRFD	ASD
$t_{p,reqd} = \sqrt{\frac{1.10M_u}{\gamma_r\phi_b F_y Y_p}}$	$t_{p,reqd} = \sqrt{\frac{1.10M_a}{\gamma_r F_y Y_p/\Omega_b}}$
$= \sqrt{\frac{1.10(20{,}100\text{ kip-in.})}{1.0(0.90)(50\text{ ksi})(584\text{ in.})}}$	$= \sqrt{\frac{1.10(13{,}400\text{ kip-in.})}{1.0(50\text{ ksi})(584\text{ in.})/1.67}}$
$= 0.917\text{ in.} \leq 1\text{ in.}$ **o.k.**	$= 0.918\text{ in.} \leq 1\text{ in.}$ **o.k.**

Check Shear Yielding/Shear Rupture of the Extended Portion of the End Plate

For extended end-plate moment connections that are stiffened, shear yielding and shear rupture of the extended portion of the end plate are not limit states.

Therefore, a 1-in.-thick end plate is sufficient.

Check Shear Transfer at Bolt Holes

See Example 5.3-1 or 5.3-2 for calculation procedures.

B. Check Beam to End-Plate Welds

The minimum weld size in AISC *Specification* Table J2.4 is determined from the material thickness of the thinner part joined. The fillet weld sizes shown in Figure 5-18 satisfy the requirements in Table J2.4.

Check Beam Flange to End-Plate Weld

The weld from the beam flange to the end plate is shown in Figure 5-18 as a CJP groove weld with the bevel facing away from the center of the beam and without weld access holes. (Double-sided $\frac{5}{8}$ in. fillet welds or a PJP groove weld are alternate options.)

Check Stiffener Welds

Check that the stiffener welds shown in Figure 5-18 are sufficient to develop the yield strengths of the stiffener plate.

Calculate the required strength for the stiffener to beam flange weld, and determine if the double-sided 7/16 in. fillet weld shown is sufficient.

LRFD	ASD
$V_{uw} = 0.60F_y t_s$ $= 0.60(50 \text{ ksi})(5/8 \text{ in.})$ $= 18.8 \text{ kips/in.}$	$V_{aw} = 0.40F_y t_s$ $= 0.40(50 \text{ ksi})(5/8 \text{ in.})$ $= 12.5 \text{ kips/in.}$

$$V_{nw} = (2 \text{ welds})0.60F_{EXX}\frac{t_{weld}}{\sqrt{2}}(1.0 + 0.5\sin^{1.5}\theta) \quad \text{(from } \textit{Spec.} \text{ Eq. J2-4)}$$

$$= (2 \text{ welds})(0.60)(70 \text{ ksi})\left(\frac{7/16 \text{ in.}}{\sqrt{2}}\right)(1.0 + 0.5\sin^{1.5} 0°)$$

$$= 26.0 \text{ kips/in.}$$

LRFD	ASD
$\phi V_{nw} = 0.75(26.0 \text{ kips/in.})$ $= 19.5 \text{ kips/in.} \geq V_{uw} = 18.8 \text{ kips/in.}$ **o.k.**	$\frac{V_{nw}}{\Omega} = \frac{26.0 \text{ kips/in.}}{2.00}$ $= 13.0 \text{ kips/in.} \geq V_{aw} = 12.5 \text{ kips/in.}$ **o.k.**

The shear rupture strength of the stiffener is greater than its shear yield strength and does not have to be checked. The shear rupture strength of the beam flange is sufficient by inspection.

Therefore, double-sided 7/16 in. fillet welds are sufficient.

Calculate the required strength for the stiffener to end-plate weld, and determine if the double-sided 1/2 in. fillet weld shown is sufficient.

LRFD	ASD
$T_{uw} = F_y t_s$ $= (50 \text{ ksi})(5/8 \text{ in.})$ $= 31.3 \text{ kips/in.}$	$T_{aw} = \frac{F_y}{1.50} t_s$ $= \left(\frac{50 \text{ ksi}}{1.50}\right)(5/8 \text{ in.})$ $= 20.8 \text{ kips/in.}$

$$T_{nw} = (2 \text{ welds})0.60F_{EXX}\frac{t_{weld}}{\sqrt{2}}(1.0 + 0.5\sin^{1.5}\theta) \quad \text{(from } \textit{Spec.} \text{ Eq. J2-4)}$$

$$= (2 \text{ welds})(0.60)(70 \text{ ksi})\left(\frac{1/2 \text{ in.}}{\sqrt{2}}\right)(1.0 + 0.5\sin^{1.5} 90°)$$

$$= 44.5 \text{ kips/in.}$$

LRFD	ASD
$\phi T_{nw} = 0.75(44.5 \text{ kips/in.})$ $= 33.4 \text{ kips/in.} \geq T_{uw} = 31.3 \text{ kips/in.}$ **o.k.**	$\frac{T_{nw}}{\Omega} = \frac{44.5 \text{ kips/in.}}{2.00}$ $= 22.3 \text{ kips/in.} \geq T_{aw} = 20.8 \text{ kips/in.}$ **o.k.**

Therefore, double-sided 1/2 in. fillet welds are sufficient.

Check Beam Web to End-Plate Weld

The beam web to end-plate welds shown in Figure 5-18 are separately checked for (1) tension rupture in the region around the tension bolts (extending 6 in. to the inside of the tension bolts), and (2) the remainder of the web to end-plate weld is checked for shear. As explained in Section 3.7.5, the demand for the tension web area, T_{uw} (LRFD) or T_{aw} (ASD), for this connection is the number of tension bolts adjacent to the web, n_{trib}, divided by the total number of tension bolts, n, multiplied by the calculated beam flange force, $T_{u,calc}$ (LRFD) or $T_{a,calc}$ (ASD).

LRFD	ASD
$T_{u,calc} = \dfrac{M_u}{d - t_{bf}}$ $= \dfrac{20{,}100 \text{ kip-in.}}{36 \text{ in.} - 3/4 \text{ in.}}$ $= 570 \text{ kips}$ $T_{uw} = (n_{trib}/n)T_{u,calc}$ $= (4/12)(570 \text{ kips})$ $= 190 \text{ kips}$	$T_{a,calc} = \dfrac{M_a}{d - t_{bf}}$ $= \dfrac{13{,}400 \text{ kip-in.}}{36 \text{ in.} - 3/4 \text{ in.}}$ $= 380 \text{ kips}$ $T_{aw} = (n_{trib}/n)T_{a,calc}$ $= (4/12)(380 \text{ kips})$ $= 127 \text{ kips}$

The length of the web tension region is measured from the inside of the beam flange to 6 in. inside the tension bolt row:

$l_{wt} = p_{fi} + p_b + 6 \text{ in.}$
$= 2\frac{1}{2} \text{ in.} + 3\frac{3}{4} \text{ in.} + 6 \text{ in.}$
$= 12.3 \text{ in.}$

The nominal web yield strength in the tension region is:

$T_{yw} = F_y A_g$ (from *Spec.* Eq. J4-1)
$= F_y t_{bw} l_{wt}$
$= (50 \text{ ksi})(3/8 \text{ in.})(12.3 \text{ in.})$
$= 231 \text{ kips}$

Check that the web design tensile yield strength is sufficient.

LRFD	ASD
$\phi T_{yw} = 0.90(231 \text{ kips})$ $= 208 \text{ kips} \quad \geq \quad T_{uw} = 190 \text{ kips}$ **o.k.**	$\dfrac{T_{yw}}{\Omega} = \dfrac{231 \text{ kips}}{1.67}$ $= 138 \text{ kips} \quad \geq \quad T_{aw} = 127 \text{ kips}$ **o.k.**

Check that the required strength is at least 60% (LRFD) or 40% (ASD) of the web tensile strength from Equation 3-41.

LRFD	ASD
$0.60T_{yw} = 0.60(231 \text{ kips})$ $= 139 \text{ kips}$ $T_{uwd} = \max(T_{uw}, 0.60T_{yw})$ $= \max(190 \text{ kips}, 139 \text{ kips})$ $= 190 \text{ kips}$	$0.40T_{yw} = 0.40(231 \text{ kips})$ $= 92.4 \text{ kips}$ $T_{awd} = \max(T_{aw}, 0.40T_{yw})$ $= \max(127 \text{ kips}, 92.4 \text{ kips})$ $= 127 \text{ kips}$

Check the web to end-plate weld around the tension bolts. Because the weld is loaded perpendicular to its longitudinal axis, the angle of loading, θ, is 90°.

$$R_n = (2 \text{ welds})0.60F_{EXX}\frac{t_{weld}}{\sqrt{2}}l_{wt}(1.0+0.5\sin^{1.5}\theta) \quad \text{(from } \textit{Spec.} \text{ Eq. J2-4)}$$

$$= (2 \text{ welds})(0.60)(70 \text{ ksi})\left(\frac{\frac{1}{4} \text{ in.}}{\sqrt{2}}\right)(12.3 \text{ in.})(1.0+0.5\sin^{1.5}90°)$$

$$= 274 \text{ kips}$$

LRFD	ASD
$\phi R_n = 0.75(274 \text{ kips})$ $= 206 \text{ kips} \quad \geq \quad T_{uwd} = 190 \text{ kips}$ **o.k.**	$\frac{R_n}{\Omega} = \frac{274 \text{ kips}}{2.00}$ $= 137 \text{ kips} \quad \geq \quad T_{awd} = 127 \text{ kips}$ **o.k.**

Double-sided ¼ in. fillet welds are sufficient.

Check the web to end-plate weld away from the tension bolts. Only the web to end-plate weld between the end of the assumed web tension length and the inside face of the bottom beam compression flange or the weld between the mid-depth of the beam and the inside face of the beam compression flange, whichever is smaller, is considered effective in resisting the beam end shear. The shear strength of this weld is compared to the required shear applied to the connection.

$$l_t = d - 2t_{bf} - l_{wt}$$

$$= 36 \text{ in.} - 2(\tfrac{3}{4} \text{ in.}) - 12.3 \text{ in.}$$

$$= 22.2 \text{ in.}$$

$$l_{0.5w} = d/2 - t_{bf}$$

$$= (36 \text{ in.})/2 - \tfrac{3}{4} \text{ in.}$$

$$= 17.3 \text{ in.}$$

$$l_{wv} = \min(l_t, l_{0.5w})$$

$$= \min(22.2 \text{ in.}, 17.3 \text{ in.})$$

$$= 17.3 \text{ in.}$$

$$R_n = (2 \text{ welds})0.60F_{EXX}\frac{t_{weld}}{\sqrt{2}}l_{wv}(1.0+0.5\sin^{1.5}\theta) \quad \text{(from } \textit{Spec.} \text{ Eq. J2-4)}$$

$$= (2 \text{ welds})(0.60)(70 \text{ ksi})\left(\frac{\frac{3}{16} \text{ in.}}{\sqrt{2}}\right)(17.3 \text{ in.})(1.0+0.5\sin^{1.5}0°)$$

$$= 193 \text{ kips}$$

LRFD	ASD
$\phi R_n = 0.75(193 \text{ kips})$ $= 145 \text{ kips} \quad \geq \quad V_u = 90.0 \text{ kips}$ **o.k.**	$\frac{R_n}{\Omega} = \frac{193 \text{ kips}}{2.00}$ $= 96.5 \text{ kips} \quad \geq \quad V_a = 60.0 \text{ kips}$ **o.k.**

Check that the shear rupture strength of the beam web at the weld using AISC *Specification* Equation J4-4 is sufficient.

$$V_{nw} = 0.60F_u A_{nv} \quad \text{(Spec. Eq. J4-4)}$$
$$= 0.60F_u l_{wv} t_{bw}$$
$$= 0.60(65 \text{ ksi})(17.3 \text{ in.})(\tfrac{3}{8} \text{ in.})$$
$$= 253 \text{ kips}$$

LRFD	ASD
$\phi R_n = 0.75(253 \text{ kips})$ $= 190 \text{ kips} \quad \geq \quad V_u = 90.0 \text{ kips}$ **o.k.**	$\frac{R_n}{\Omega} = \frac{253 \text{ kips}}{2.00}$ $= 127 \text{ kips} \quad \geq \quad V_a = 60.0 \text{ kips}$ **o.k.**

The double-sided 3⁄16 in. fillet welds shown in Figure 5-18 from the web to the end plate are sufficient.

C. Column-Side Limit State Checks

See Example 5.3-1 or 5.3-2 for example column-side limit state check calculations.

Summary

The design shown in Figure 5-18 is satisfactory for the required moment and shear force shown.

Chapter 6
High-Seismic-Ductility Design

6.1 INTRODUCTION AND DESIGN APPROACH

The steel SMF is capable of significant inelastic story drift because of deformations in the beam plastic hinge and limited inelasticity in the column panel zone. Plastic hinges form in the beam near the face of the end plate for unstiffened end-plate connections or at the end of the stiffeners for stiffened end-plate connections. The beam flanges experience local buckling at large rotations, but the connections should not exhibit substantial flexural strength degradation before reaching 0.04 rad of story drift angle. The end plate, bolts, column flange, and welds are designed and detailed to delay significant fracture or failure until after this level of story drift. To date, there has been sufficient previous testing of three end-plate moment connections for them to be considered prequalified as SMF connections and are included in AISC *Prequalified Connections*. If a connection is designed according to the requirements in AISC *Prequalified Connections*, then it is expected that the connection will exhibit the ductile behavior described in this paragraph.

End-plate moment connections can also be designed for steel IMF. The requirements for IMF as described in the AISC *Seismic Provisions* are relaxed as compared to SMF, including the use of moderately ductile beam and column sections instead of highly ductile, larger unbraced lengths are allowed, a relaxed clear span-to-depth ratio requirement, the strong-column/weak-beam check is not required, and loads used to design panel zone and continuity plates are smaller. IMF are expected to have some inelastic deformation capacity with connections capable of 0.02 rad of rotation capacity without significant loss of flexural strength. The end-plate moment connection design requirements described in AISC *Prequalified Connections* can be applied for IMF or SMF. The examples included in this chapter follow SMF criteria.

The design process for most moment frames starts with sizing the beams and columns for drift. At the same time, it is necessary for beams and columns to satisfy highly ductile section criteria and strong-column/weak-beam requirements (for SMF). In selecting column sizes, it is also necessary to check that the column flange bending strength will be sufficient and it may be desirable for economy to size the column to eliminate continuity plates and doubler plates. After the beam and column sections have been selected, the maximum expected beam moment that can be produced at the face of the column is calculated and used in connection design. One of three end-plate configuration options in AISC *Prequalified Connections* is selected—the four-bolt unstiffened (4E), the four-bolt stiffened (4ES), or the eight-bolt stiffened (8ES). It is necessary to keep the geometry of the connection (e.g., beam size, end-plate size, and bolt hole locations) within the geometry that has been previously tested. Limit states that are checked on the end-plate side include bolt tension rupture, end-plate yielding, shear yielding, shear rupture of unstiffened end plates, end-plate stiffener local buckling, bolt shear, and bolt bearing/tearout. The end plate is designed not to yield in flexure (i.e., thick plate behavior), and thus bolt tension demands are calculated assuming no prying action. Limit states on the column side include flange flexural yielding, column web yielding, column web crippling, and panel zone shear. To finish the design, the connection is detailed including welds.

It is useful to know where to find information during the design process. The requirements for SMF and IMF are given in the AISC *Seismic Provisions*. The LRFD design procedure and related requirements for the end-plate connection design are included in AISC *Prequalified Connections*. Some of the calculations including welds, continuity plate, and panel zone shear design rely on the AISC *Specification*. All three of these documents have valuable supporting information in their Commentary sections. Some of the key testing programs that supported the prequalification of end-plate moment connections include Meng and Murray (1996), Ryan and Murray (1999), and Sumner et al. (2000).

The following section describes the high-seismic-ductility design requirements. The next section includes design examples for the four-bolt unstiffened (4E), four-bolt stiffened (4ES), and eight-bolt stiffened (8ES) end-plate connection configurations. The objective is to demonstrate the complete connection design procedure.

6.2 DESIGN REQUIREMENTS

6.2.1 General

The requirements for design of end-plate moment connections for use in SMF are given in AISC *Prequalified Connections*. Connections designed in accordance with this standard are considered prequalified for SMF, and no additional testing or data is required to demonstrate that the connection conforms to SMF requirements in the AISC *Seismic Provisions*.

Calculations of design strength in AISC *Prequalified Connections* use different resistance factors than the AISC *Specification*. The resistance factors for nonductile limit states (e.g., bolt rupture), and ductile limit states (e.g., end-plate yielding) are:

For nonductile limit states

$$\phi_n = 0.90 \quad (6\text{-}1)$$

For ductile limit states

$$\phi_d = 1.00 \quad (6\text{-}2)$$

The materials, workmanship, and quality assurance requirements for SMF connections are more controlled than for typical structural steel, and the demands are believed to be conservative, thus allowing larger resistance factors than the AISC *Specification.* For design strengths calculated according to the AISC *Specification* (e.g., weld strength), the resistance factors from that specification are used.

The specified minimum yield stress of the connected members, end plates, stiffeners, and continuity plates must be 50 ksi or less, with the exception that columns can have a specified minimum yield stress up to 70 ksi. Only Group 120 or Group 150 high-strength bolts of a diameter not greater than 1½ in. are permitted.

The region at the end of the beam where inelastic deformations occur is defined as the protected zone. In the protected zone, the AISC *Seismic Provisions* prohibit all welded, bolted, screwed, or shot-in attachments, except decking attachments made with arc spot welds or power actuated fasteners up to 0.18 in. diameter. The dimensions of the protected zone are shown in Figure 6-1. In addition to protected zone requirements, there are prequalification limits in AISC *Prequalified Connections* requiring that concrete structural slab shear connectors not be located within a distance equal to 1.5 times the beam depth from the face of the column and that the nominal beam depth be not less than 24 in. when a concrete structural slab is present. Decking attachments, such as those allowed in the protected zone, are permitted in the region without shear connectors.

Beams in SMF need to be laterally braced according to the AISC *Seismic Provisions* as specified for highly ductile members. It is also necessary to provide special bracing at the plastic hinge locations. The special bracing must be designed to have sufficient strength and stiffness as specified in the AISC *Seismic Provisions* and, according to AISC *Prequalified Connections*, be located between the end of the protected zone and a distance of $d/2$ from the end of the protected zone. Special bracing is not permitted in the protected zone.

6.2.2 Geometric Limitations for Beams, Columns, Bolts, and End Plates

There are limitations in AISC *Prequalified Connections* on bolt size, bolt locations, end-plate geometry, and which steel sections can be used for the beams and columns. The limitations on beam and column sizes will be described first, then the limitations on bolts and end plates.

Table 6-1 summarizes the limitations for beam and column size, not including requirements for strength or drift. The first three rows are related to the limits on prequalification and represent the range of beam flange thickness, t_{bf}, beam flange width, b_{bf}, and beam depth, d, that have been tested in full-scale subassemblage testing programs. Significant changes in the geometry could affect the mechanism configuration and thus the predicted strength. Therefore, the design equations in this chapter apply only for the tested parameter ranges given in Table 6-1 with a variation of ±10%, which is consistent with the qualification testing requirements for IMF and SMF given in AISC *Seismic Provisions* Section K2.3b.

The last five rows in Table 6-1 are additional limitations for the beam depth, d, beam flange slenderness, $b_{bf}/2t_{bf}$,

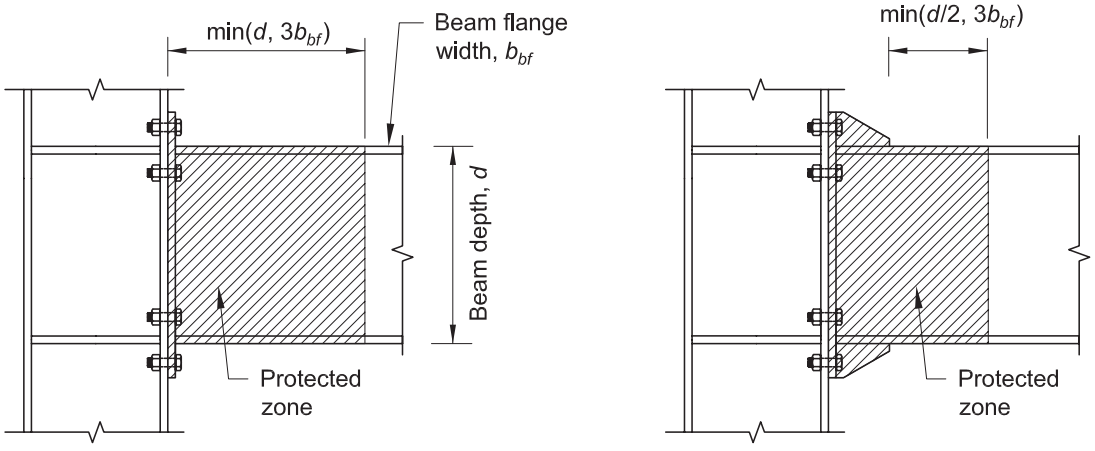

(a) Unstiffened connection *(b) Stiffened connection*

Fig. 6-1. Extents of the protected zones.

Table 6-1. Summary of Limitations on Beam and Column Size						
	Four-Bolt Unstiffened		Four-Bolt Stiffened		Eight-Bolt Stiffened	
Parameter	Maximum	Minimum	Maximum	Minimum	Maximum	Minimum
t_{bf} (in.)	¾	⅜	¾	⅜	1	9⁄16
b_{bf} (in.)	9¼	6	9	6	12¼	7½
d (in.)	24	13¾	24	13¾	36	18
d (in.)	Beam no shallower than W24 if there is a composite slab					
$b_{bf}/2t_{bf}$, h_b/t_{bw}	Beam must satisfy compactness limits for highly ductile member					
$b_{cf}/2t_{cf}$, h_c/t_{cw}	Column must satisfy compactness limits for highly ductile member					
d_c (in.)	Column cannot be larger than a W36					
d (in.)	Beam clear span-to-depth ratio not less than 7 for SMF and not less than 5 for IMF					

Table 6-2. Summary of Section Sizes Satisfying Parametric Limitations for Beams and Highly Ductile Section Criteria for F_{yb} = 50 ksi

Section Size	4E	4ES	8ES	$P_{u\,max}$ for Highly Ductile Web (kips)	Section Size	4E	4ES	8ES	$P_{u\,max}$ for Highly Ductile Web (kips)
W36×150			X	105	W21×62*	X	X	X	84.7
W33×141			X	141	W21×57*	X	X		82.0
W33×130			X	93.7	W21×50*	X	X		51.1
W30×124			X	181	W18×106*			X	474
W30×116			X	144	W18×97*			X	385
W30×108			X	107	W18×71*	X	X	X	253
W27×114			X	226	W18×65*	X	X	X	196
W27×102			X	136	W18×60*	X	X	X	153
W27×94			X	94.7	W18×55*	X	X	X	120
W24×103			X	255	W18×50*	X	X		79.8
W24×94			X	195	W18×46*	X	X		77.2
W24×84			X	126	W18×40*	X	X		33.1
W24×76	X	X	X	82.0	W16×57*	X	X		198
W24×62	X	X		57.5	W16×50*	X	X		137
W21×93*			X	332	W16×45*	X	X		98.9
W21×83*			X	241	W14×53*	X	X		203
W21×73*	X	X	X	159	W14×48*	X	X		161
W21×68*	X	X	X	124	W14×38*	X	X		91.8

* Sections smaller than W24 are not prequalified for beams supporting concrete slabs.

beam web slenderness, h_b/t_{bw}, and column depth, d_c. The limits on beam flange and web slenderness to satisfy highly ductile member requirements are included in the AISC *Seismic Provisions*.

Table 6-2 shows the wide-flange sections that satisfy the parametric limitations on prequalification in AISC *Prequalified Connections* and the highly ductile member criteria in the AISC *Seismic Provisions*. For each of the four-bolt extended unstiffened, 4E, four-bolt extended stiffened, 4ES, and eight-bolt extended stiffened, 8ES, connection types, an "X" means that the section satisfies the parametric limitations on prequalification and the highly ductile

Table 6-3. Summary of Limitations on End-Plate Geometry						
	Four-Bolt Unstiffened		Four-Bolt Stiffened		Eight-Bolt Stiffened	
Parameter	Maximum	Minimum	Maximum	Minimum	Maximum	Minimum
t_p (in.)	2¼	½	1½	½	2½	¾
b_p (in.)	10¾	7	10¾	7	15	9
g (in.)	6	4	6	3¼	6	5
p_{fi}, p_{fo} (in.)	4½	1½	5½	1¾	2	1⅝
p_b (in.)	—	—	—	—	3¾	3½
g (in.)	Bolt gage cannot be larger than the beam flange width, $g < b_{bf}$					
p_{fi}, p_{fo}, p_{si}, p_{so} (in.)	Recommendation: Greater than (d_b + ½ in.) for $d_b \le 1$ in., greater than (d_b + ¾ in.) for $d_b > 1$ in.					
p_b (in.)	$p_b \ge 2.67d_b$ per AISC *Specification* Section J3.4; User Note: $3d_b$ preferred					
b_p (in.)	$b_p \ge b_{bf}$ b_p must not be taken as larger than the beam flange width plus 1 in.					

member limit on flange slenderness, assuming a yield stress of $F_{yb} = 50$ ksi and an expected yield stress factor of $R_y = 1.1$. If the required axial strength, P_u, is less than the maximum value shown in Table 6-2, then the section also satisfies the highly ductile member limit for web slenderness, assuming a yield stress of $F_{yb} = 50$ ksi and an expected yield stress factor of $R_y = 1.1$. $P_{u\ max}$ is calculated for a section by setting the web width-to-thickness ratio, h/t_w, equal to the highly ductile web limiting width-to-thickness ratio from AISC *Seismic Provisions* Table D1.1b and solving for P_r.

Beyond Table 6-2, AISC *Prequalified Connections* also allows built-up sections if they satisfy the requirements in Table 6-1. Welds between the flange and web are discussed in Section 6.2.7. It is noted that the experimental programs that supported prequalification were conducted exclusively with rolled beam shapes and that recent testing suggests there may be potential for fracture at the toe of the stiffener in extended stiffened end-plate connections with built-up beams (Szabo et al., 2017; Zarat Basir et al., 2020). Until research is able to show that extended stiffened moment connections with built-up beams are capable of satisfying qualification criteria, these configurations are not recommended for IMF or SMF applications.

There are also parametric limitations on the end-plate and bolt hole location geometry that have been defined based on the geometry of specimens that have been tested in full-scale experiments. Table 6-3 summarizes the limitations for end-plate geometry, bolt size, and bolt locations. Figure 6-2 shows the definition of the variables.

6.2.3 Design Requirements for Bolts

AISC *Prequalified Connections* includes procedures for end-plate/bolt design and column-side design. First, it is necessary to calculate the moment at the face of the column, M_f, associated with plastic hinging of the beam that will be used as the required strength (demand) for the bolts (and end plate). The probable maximum moment at the plastic hinge, M_{pr}, is given by:

$$M_{pr} = C_{pr} R_y F_{yb} Z_e \qquad \text{(}\textit{Preq. Conn.}\text{ Eq. 2.4-1)}$$

where

C_{pr} = factor to account for peak connection strength, including strain hardening

$$C_{pr} = \frac{F_{yb} + F_{ub}}{2F_{yb}} \le 1.2 \qquad \text{(}\textit{Preq. Conn.}\text{ Eq. 2.4-2)}$$

F_{ub} = specified minimum tensile strength of beam material, ksi

F_{yb} = specified minimum yield stress of beam material, ksi

R_y = ratio of expected yield stress to specified minimum yield stress as given in the AISC *Seismic Provisions*

Z_e = effective plastic section modulus of the beam, for end-plate connections this is equal to the nominal plastic section modulus of the beam, Z_b, in.^{3}

The moment at the plastic hinge is an intermediate step in calculating the moment at the face of the column, which is used to design the connection. The moment at the face of the column, M_f, is given by the following and is demonstrated graphically in Figure 6-3(a):

$$M_f = M_{pr} + V_h S_h \qquad \text{(}\textit{Preq. Conn.}\text{ Eq. 2.4-4)}$$

where

S_h = assumed distance from column face to plastic hinge, in.

$$= \begin{bmatrix} \min\left(\frac{d}{2}, 3b_{bf}\right) & \text{for 4E} \\ L_{st} + t_p & \text{for 4ES and 8ES} \end{bmatrix} \begin{matrix} \text{(Preq. Conn. Eq. 6.7-1)} \\ \text{(Preq. Conn. Eq. 6.7-2)} \end{matrix}$$

L_{st} = length of stiffener in extended end-plate connections, see Section 6.2.5, in.

and

$$V_h = \frac{2M_{pr}}{L_h} + V_{gravity}$$

(*Preq. Conn.* Eq. 2.4-3)

where

L_h = distance between beam plastic hinge locations, in.

$V_{gravity}$ = factored beam shear resulting from the load combination $1.2D + f_1L + 0.15S$, where f_1 is determined from the applicable building code, but not less than 0.5, kips.

The bolt diameter is then determined as described in Step 6 of the AISC *Prequalified Connections* design procedure. The required bolt diameter, $d_{b,req}$, is determined using AISC *Prequalified Connections* Equation 6.7-3 or 6.7-4. It is noted that these equations assume that there is no significant beam axial tension. If the beam axial tension force is large, the bolt design equations are incorrect, and the connections are not prequalified for SMF because those conditions have not been tested. See Section 3.5 for guidance about the magnitude of axial force that is considered large.

For 4E and 4ES

$$d_{b,req} = \sqrt{\frac{2M_f}{\pi\phi_n F_{nt}(h_1 + h_2)}}$$

(*Preq. Conn.* Eq. 6.7-3)

For 8ES

$$d_{b,req} = \sqrt{\frac{2M_f}{\pi\phi_n F_{nt}(h_1 + h_2 + h_3 + h_4)}}$$

(*Preq. Conn.* Eq. 6.7-4)

where

F_{nt} = nominal tensile strength of bolt from the AISC *Specification*, ksi

h_i = distance from center of the beam compression flange to the *i*th load-carrying bolt line, in.; see Figures 6-4 and 6-5

The selected bolt diameter must satisfy:

$$d_b \geq d_{b,req} \tag{6-3}$$

Two other design checks related to the bolts are associated with resisting the required shear force—bolt shear and bearing/tearout. As shown in Figure 6-3(b), a simplified model is assumed wherein the required shear force, V_u, is resisted by the bolts at the compression flange. The required shear strength is given by AISC *Prequalified Connections* Equation 2.4-3. The bolt design shear strength is:

$$\phi R_n = \phi_n n_b F_{nv} A_b$$

(from *Preq. Conn.* Eq. 6.7-11)

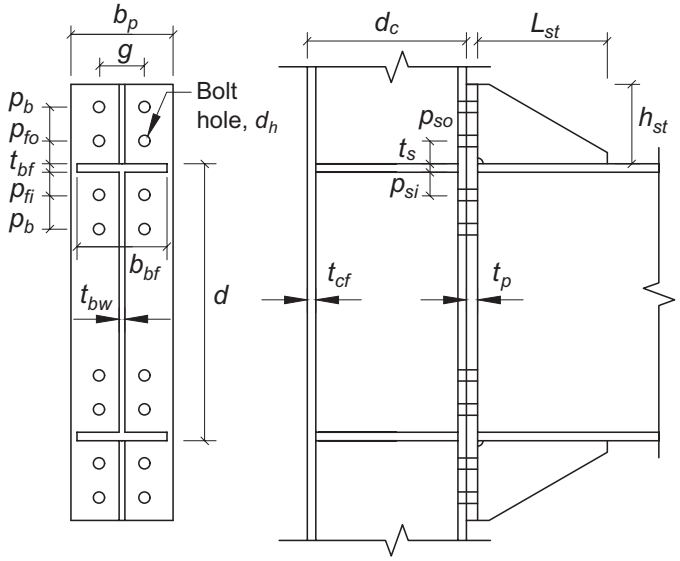

Fig. 6-2. Definition of variables associated with end plate, bolt hole locations, and member limitations.

where

A_b = nominal gross area of bolt, in.^{2}

F_{nv} = nominal shear strength of bolt from the AISC *Specification*, ksi

n_b = number of bolts at the compression flange (4 for 4E and 4ES, 8 for 8ES)

Similarly, the end plate and column flange at the beam compression flange need to be checked for bearing/tearout failure using Equation 6.4, which is based on AISC *Prequalified Connections* Equation 6.7-12.

$$\phi R_n = \phi_n \sum_k r_{nk} \tag{6.4}$$

where

$r_{nk} = 1.2 l_c t F_u \le 2.4 d_b t F_u$ (bearing/tearout strength at bolt k, adopted from AISC *Specification* Section J3.11), kips

d_b = diameter of bolt, in.

l_c = clear distance, in the direction of force, between edge of hole and edge of the adjacent hole or edge of material, in.

t = end-plate or column flange thickness, in.

Note: The User Note in AISC *Specification* Section J3.7 recommends that the effective strength of an individual bolt be taken as the lesser of the bolt shear strength, bearing strength, or tearout strength at the bolt hole. The individual strengths are then summed to determine the connection strength.

Finger shims can be used between the end plate and the column flange, as necessary. Finger shims can aid erection by allowing for some tolerance and adjustability between columns in frames. See Chapter 4 for additional discussion of finger shims.

6.2.4 Design Requirements for End Plates

The design checks for the end-plate thickness are end-plate flexure and end-plate shear if unstiffened. For both checks, the end-plate width, b_p, is taken as no larger than the beam flange width plus 1 in. This applies to all equations in this section.

The end-plate thickness, t_p, must be greater than the required thickness, $t_{p,req}$,

$$t_p \ge t_{p,req} \tag{6-5}$$

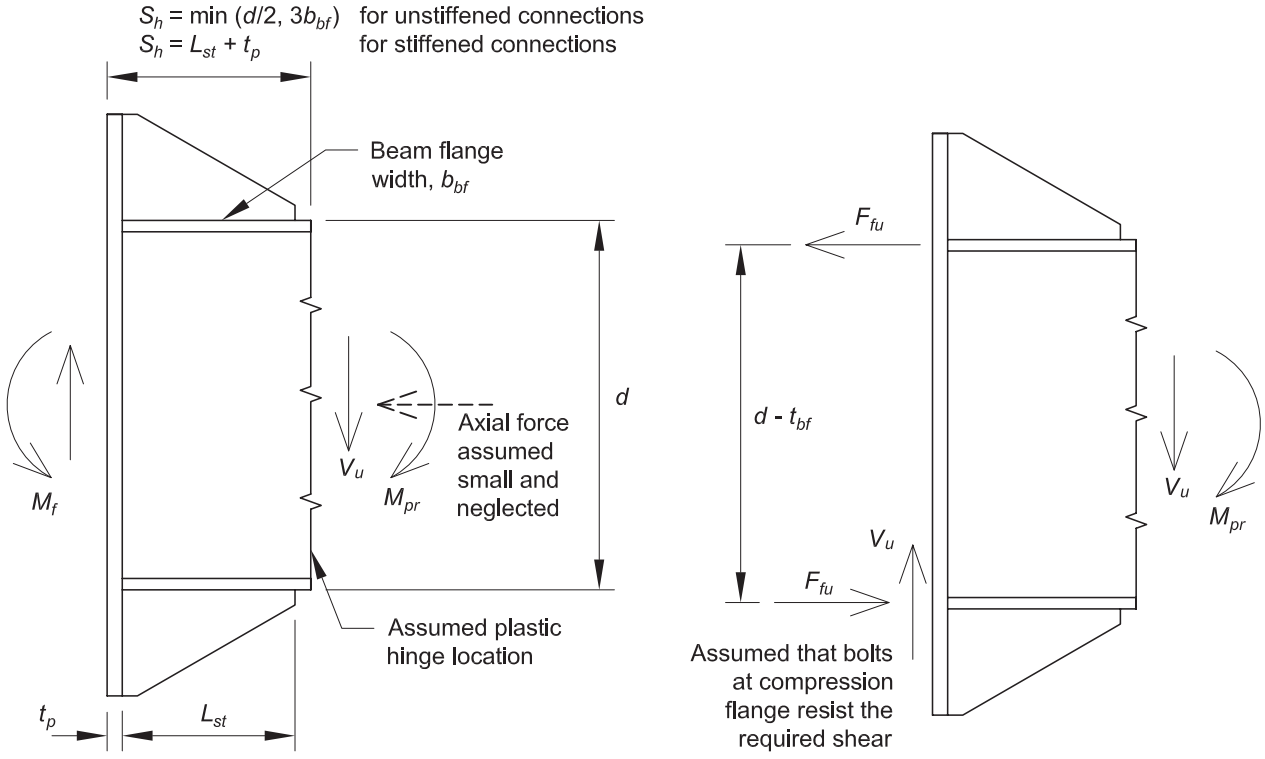

(a) Calculation of moment at column face, M_f *(b) Calculation of flange force,* F_{fu}

Fig. 6-3. Definition of variables associated with end-plate, bolt, and member limitations.

where

$$t_{p,req} = \sqrt{\frac{1.11M_f}{\phi_d F_{yp} Y_p}} \qquad \text{(Preq. Conn. Eq. 6.7-5)}$$

F_{yp} = specified minimum yield stress of end-plate material, ksi

Y_p = end-plate yield line mechanism parameter, in.

The required end-plate thickness is determined by requiring the design strength associated with end-plate yielding (M_{pl} such as given in Equation 3-15) to be greater than the probable maximum moment at face of column, M_f. The 1.11 factor is applied for the same reason as the 1.10 factor in Equation 3-18 (similar but with different rounding) to ensure thick end-plate behavior and that the bolts will not be subject to significant prying forces.

The end-plate yield line parameters, Y_p, are given for the different end-plate configurations in AISC *Prequalified Connections* and included in the following. For all of the end-plate yield line parameters, the distance from the bolt line to an adjacent yield line, s, is:

$$s = \frac{\sqrt{b_p g}}{2} \qquad (6\text{-}6)$$

For the four-bolt extended unstiffened connection configuration, 4E, the yield line mechanism is shown in Figure 6-4(a) and the yield line parameter is:

$$Y_p = \frac{b_p}{2}\left[h_1\left(\frac{1}{p_{fo}}\right) + h_2\left(\frac{1}{p_{fi}} + \frac{1}{s}\right) - \frac{1}{2}\right] + \frac{2}{g}\left[h_2(s + p_{fi})\right] \qquad (6\text{-}7)$$

If p_{fi} is greater than s, p_{fi} is set equal to s. All other geometric parameters are defined in Figure 6-4.

For the four-bolt extended stiffened connection configuration, 4ES, two cases of the yield line mechanism are considered as shown in Figures 6-4(b) and 6-4(c) with yield line parameters:

Case 1 for $d_e \le s$

$$Y_p = \frac{b_p}{2}\left[h_2\left(\frac{1}{p_{fi}} + \frac{1}{s}\right) + h_1\left(\frac{1}{p_{fo}} + \frac{1}{2d_e}\right)\right] + \frac{2}{g}\left[h_2(p_{fi} + s) + h_1(d_e + p_{fo})\right] \qquad (6\text{-}8)$$

Case 2 for $d_e > s$

$$Y_p = \frac{b_p}{2}\left[h_2\left(\frac{1}{p_{fi}} + \frac{1}{s}\right) + h_1\left(\frac{1}{p_{fo}} + \frac{1}{s}\right)\right] + \frac{2}{g}\left[h_2(p_{fi} + s) + h_1(s + p_{fo})\right] \qquad (6\text{-}9)$$

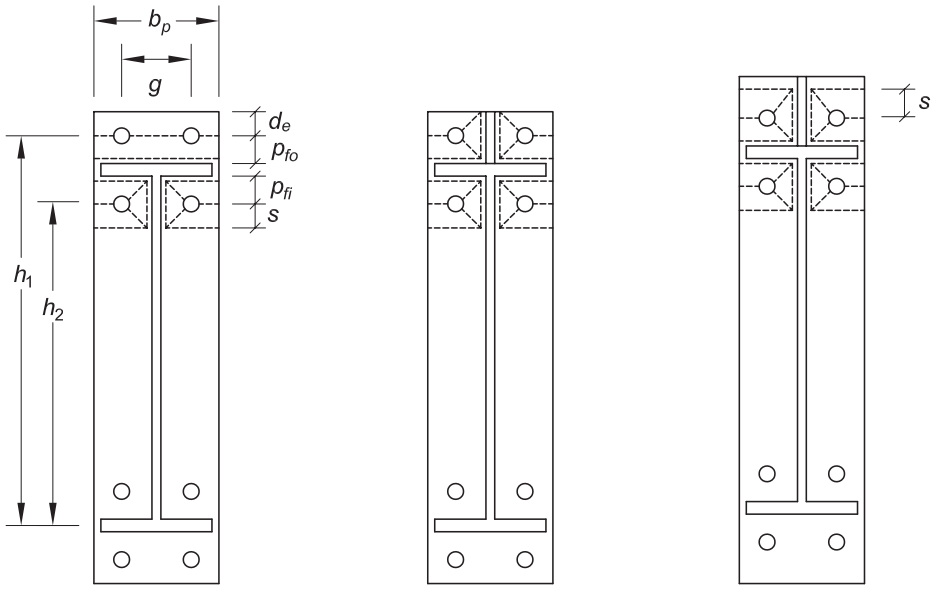

(a) 4E *(b) 4ES, Case 1,* $d_e < s$ *(c) 4ES, Case 2,* $d_e > s$

Fig. 6-4. End-plate yield line mechanisms for 4E and 4ES configurations.

For the eight-bolt extended stiffened end plate, 8ES, there are also two possible yield line mechanisms shown in Figures 6-5(a) and 6-5(b).

The 8ES yield line parameters are:

Case 1 for $d_e \le s$

$$Y_p = \frac{b_p}{2}\left[h_1\left(\frac{1}{2d_e}\right)+h_2\left(\frac{1}{p_{fo}}\right)+h_3\left(\frac{1}{p_{fi}}\right)+h_4\left(\frac{1}{s}\right)\right] + \frac{2}{g}\left[\begin{matrix}h_1\left(d_e+\frac{3}{4}p_b\right)+h_2\left(p_{fo}+\frac{1}{4}p_b\right)\\ +h_3\left(p_{fi}+\frac{3}{4}p_b\right)+h_4\left(s+\frac{1}{4}p_b\right)\end{matrix}\right]+g \tag{6-10}$$

Case 2 for $d_e > s$

$$Y_p = \frac{b_p}{2}\left[h_1\left(\frac{1}{s}\right)+h_2\left(\frac{1}{p_{fo}}\right)+h_3\left(\frac{1}{p_{fi}}\right)+h_4\left(\frac{1}{s}\right)\right] + \frac{2}{g}\left[\begin{matrix}h_1\left(s+\frac{1}{4}p_b\right)+h_2\left(p_{fo}+\frac{3}{4}p_b\right)\\ +h_3\left(p_{fi}+\frac{1}{4}p_b\right)+h_4\left(s+\frac{3}{4}p_b\right)\end{matrix}\right]+g \tag{6-11}$$

The extended portion of an unstiffened end plate must have adequate flexural and shear strength to transfer one-half of the flange force to the outside bolts. The previous check ensures adequate flexural strength. The required shear strength, R_u, is:

$$R_u = \frac{F_{fu}}{2} \tag{6-12}$$

where

$$F_{fu} = \frac{M_f}{d - t_{bf}} \text{ [see Figure 6-3(b)]} \quad (\textit{Preq. Conn.} \text{ Eq. 6.7-6})$$

d = depth of beam, in.

t_{bf} = beam flange thickness, in.

The design shear strengths for the limit states of shear yielding and shear rupture are, respectively:

$$\phi R_n = \phi_d (0.6) F_{yp} b_p t_p \quad (\text{from } \textit{Preq. Conn.} \text{ Eq. 6.7-7})$$

$$\phi R_n = \phi_n (0.6) F_{up} A_n \quad (\text{from } \textit{Preq. Conn.} \text{ Eq. 6.7-8})$$

where

A_n = net area of end plate, in.^{2}

F_{up} = specified minimum ultimate stress of end-plate material, ksi

F_{yp} = specified minimum yield stress of end plate, ksi

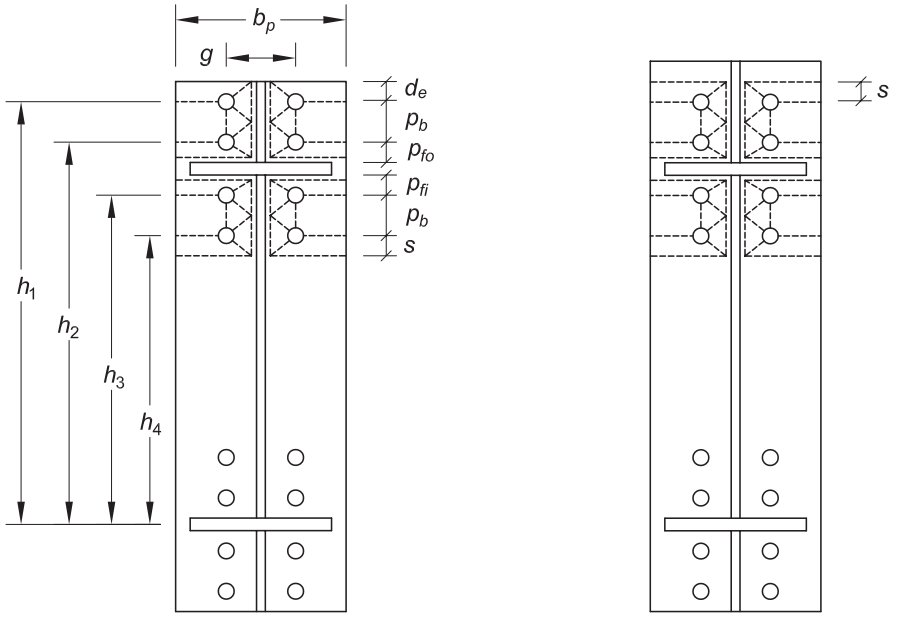

(a) 8ES, Case 1, $d_e \le s$ *(b) 8ES, Case 2,* $d_e > s$

Fig. 6-5. End-plate yield line mechanisms for 8ES.

6.2.5 Design Requirements for End-Plate Stiffeners

This section is an overview of stiffener detailing for 4ES and 8ES configurations. Stiffener geometry and detailing are a key part of producing a ductile moment resisting connection. Because the plastic hinge forms just outside the stiffener, there are large inelastic strains in the flange at the end of the stiffener.

The height of the stiffener, h_{st}, is equal to the extension of the end plate above the top of the beam flange. The length of the stiffener, L_{st}, is determined by extending a 30° line from the top corner of the end plate down to the beam flange as shown in Figure 6-6. The stiffener length is then:

$$L_{st} = \frac{h_{st}}{\tan 30°}$$

(*Preq. Conn.* Eq. 6.6-1)

The stiffener thickness is determined based on the beam web and a local buckling criterion. The stiffener strength should be greater than or equal to that of the beam web. If the beam web and stiffener have the same specified minimum yield stress, the minimum required thickness of the stiffener is the beam web thickness. If the beam web and stiffener have different yield stresses, the minimum stiffener thickness is:

$$t_s \geq t_{bw}\left(\frac{F_{yb}}{F_{ys}}\right)$$

(*Preq. Conn.* Eq. 6.7-9)

where

F_{yb} = specified minimum yield stress of beam, ksi

F_{ys} = specified minimum yield stress of stiffener, ksi

t_{bw} = thickness of beam web, in.

t_s = thickness of stiffener, in.

The stiffener is detailed to have 1 in. landings at the top edge and the end as shown in Figure 6-6. The landings serve two purposes. First, the landings encourage higher-quality weld terminations. Because the starts and stops of the weld are generally low-quality weld material, the landings provide a taller tee joint to allow cleaner starts and stops at this location than if the stiffener extended to a point. Second, the landings allow more accurate cutting of the stiffener to the specified height and length than if the stiffener extended to a sharp point.

6.2.6 Detailing of Composite Slabs at End-Plate Connections

Detailing requirements for composite slabs around the end-plate moment connection are summarized in Figure 6-7. A specimen tested by Sumner and Murray (2002) showed that if steel headed stud anchors are located on the beam close to the column and there is no gap between the concrete slab and the column, the added strength and shift in the neutral axis can cause larger demands at the bottom flange, resulting in bolt fracture. The detailing requirements given in AISC *Prequalified Connections* and summarized in Figure 6-7 were shown by Seek and Murray (2008) to mitigate the problem.

6.2.7 Weld Design and Detailing Requirements

There are a number of requirements for how the beam and stiffener are welded to the end plate, some of which are summarized in Figure 6-8. The flanges of the beam must be CJP groove welded to the end plate. Because weld access holes are not permitted, the weld over the web is considered a PJP groove weld because it is not possible to backgouge the root and place a reinforcing fillet on the back side. These flange to end-plate CJP groove welds have to be made with the single groove facing outward and no web access holes. Both the CJP groove weld and fillet weld on the back side are demand-critical welds and need to satisfy the associated requirements in the AISC *Seismic Provisions* and AWS D1.8/D1.8M.

The web to end-plate weld in the vicinity of the tension bolts can be either a CJP groove weld or double fillet weld

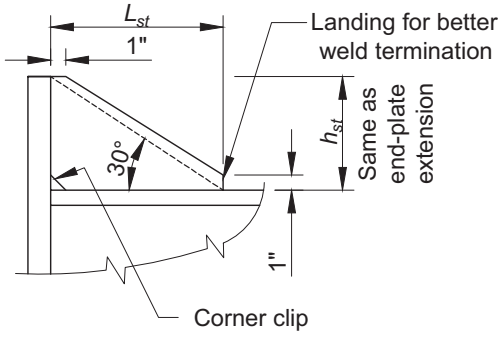

Fig. 6-6. Stiffener geometry.

that develops the tension strength of the web. This zone of larger weld extends to 6 in. inside the innermost tension bolt. As shown in Figure 6-8(a), the rest of the web to the end-plate weld outside this zone and in the vicinity of the compression bolts is used to resist the required shear force. Typically, the shear strength of the web to end-plate weld at the compression side (the weld in the vicinity of the tension bolts during load reversal) is sufficient, and the weld in between the tension zones can be minimum double fillet welds.

For the 4ES and 8ES configurations, the stiffener is installed after the flange welds are finished and inspected. The stiffener is welded to the end plate using a CJP groove weld, unless the stiffener thickness is less than or equal to ⅜ in., in which case, double-sided fillet welds that develop the nominal tensile strength of the stiffener are allowed. The stiffener to beam flange weld can be a CJP groove weld or double-sided fillet that develops the nominal shear rupture strength of the stiffener.

Similarly, AISC *Prequalified Connections* Section 6.4 states that continuity plates less than or equal to ⅜ in. thick can be welded to the flanges with double fillet welds that develop the nominal tensile strength of the continuity plates over their contact area with the column flange. Clip geometry requirements for continuity plates welded to hot-rolled sections are given in AWS D1.8/D1.8M, clause 4.1. AWS does not have provisions for clip geometry of continuity plates welded to built-up sections. For built-up sections, the authors of this Design Guide recommend a minimum diagonal clip dimension of ¾ in. or a radiused cut with a minimum radius of ½ in.

The web to flange interface in built-up members is subjected to large demands in the connection region as the beam plastic hinge forms and the beam flanges undergo local buckling. Within a distance that is at least the lesser of the depth of the beam, d, or three times the beam flange width, b_{bf}, the web has to be CJP groove welded to the flange or have double fillet welds with thickness at least 75% of the beam web thickness, $0.75t_{bw}$, or ¼ in., whichever is larger, as shown graphically in Figure 6-8(b).

6.2.8 Column-Side Limit States

The design procedure in AISC *Prequalified Connections* includes seven steps for column-side design. The design check for column flange flexure can affect the choice of column section because if the loads are large, some column flanges will not be sufficient, even if they are stiffened by continuity plates. Along with column flange flexure, the checks for local column web yielding and unstiffened column web crippling determine if continuity plates are required and their size. AISC *Prequalified Connections* does not include a check for web buckling because that limit state only applies when there is a pair of compressive concentrated forces acting on opposing sides of the column, which is not the case for moment frames subjected to lateral loading where opposing beam flange forces are tension and compression.

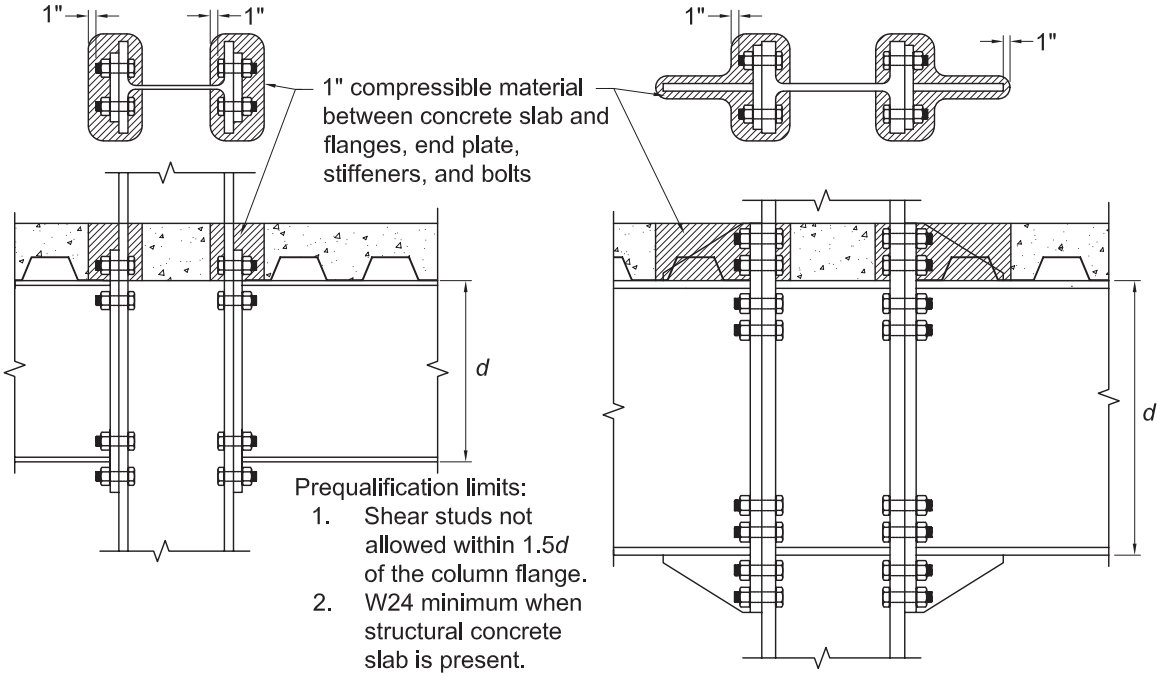

Fig. 6-7. Detailing for composite slabs.

Other column-side limit states include panel zone yielding; bearing and tearout at holes, which was discussed in Section 6.2.3; and the AISC *Seismic Provisions* strong-column/weak-beam requirements.

The column flange flexure check is similar to the check for end-plate yielding. Column flange yield line parameters are presented in AISC *Prequalified Connections* for cases without continuity plates (unstiffened column flange) and with continuity plates (stiffened column flange). Both are given for connections that are sufficiently far away from the top of the column that the yield line pattern is not affected. The yield line parameters for additional configurations, including those where the connection is relatively close to the top of the column, are given in Appendix A. The equation for

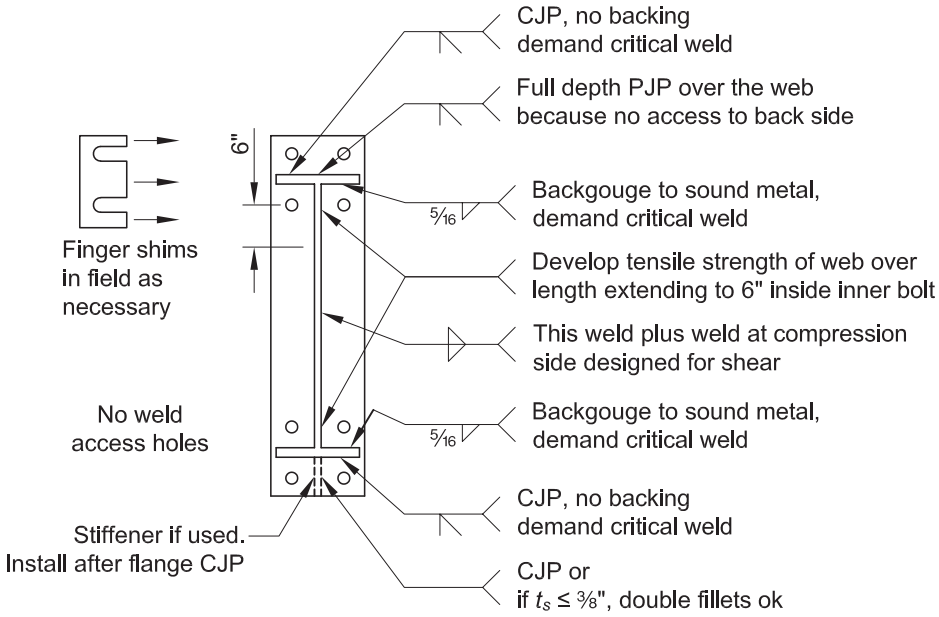

(a) Welds to the end plate

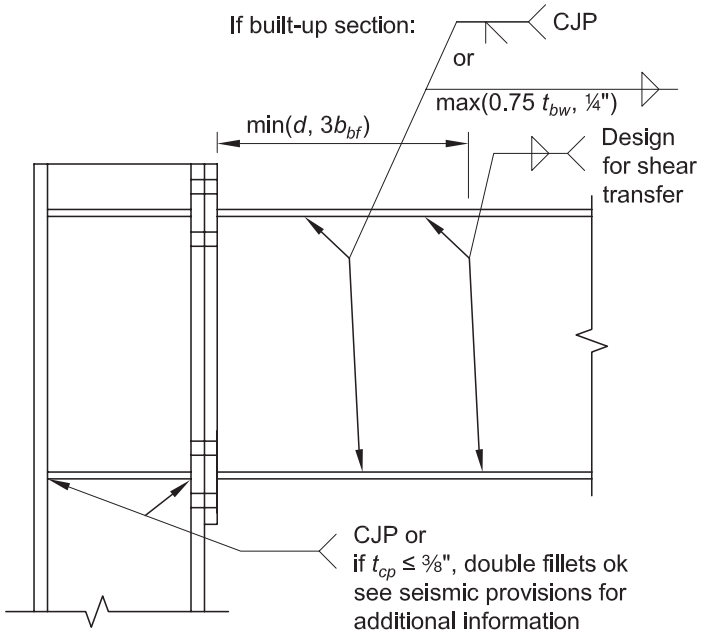

(b) Additional weld requirements

Fig. 6-8. Detailing of welds.

minimum column flange thickness, $t_{cf,req}$, is given by AISC *Prequalified Connections* Equation 6.7-13. The required column flange thickness is:

$$t_{cf,req} = \sqrt{\frac{1.11M_f}{\phi_d F_{yc} Y_c}}$$

(from *Preq. Conn.* Eq. 6.7-13)

where

F_{yc} = specified minimum yield stress of column flange material, ksi

Y_c = column flange yield line mechanism parameter given as follows, in.

The column flange thickness must satisfy:

$$t_{cf} \geq t_{cf,req} \tag{6-13}$$

The column flange yield line parameter, Y_c, is given for the different bolt configurations with and without continuity plates in AISC *Prequalified Connections* Tables 6.5 and 6.6 and included in the following. For all column flange yield line parameters:

$$s = \frac{\sqrt{b_{cf} g}}{2} \tag{6-14}$$

For four-bolt connection configurations, the yield line mechanisms are shown in Figure 6-9(a) and Figure 6-9(b) and the yield line parameters are:

Unstiffened column flange

$$Y_{cu} = \frac{b_{cf}}{2}\left[h_1\left(\frac{1}{s}\right) + h_2\left(\frac{1}{s}\right)\right] + \frac{2}{g}\left[h_1\left(s + \frac{c}{4}\right) + h_2\left(s + \frac{3c}{4}\right) + \frac{c^2}{2}\right] + \frac{g}{2} \tag{6-15}$$

Stiffened column flange

$$Y_{cs} = \frac{b_{cf}}{2}\left[h_1\left(\frac{1}{s} + \frac{1}{p_{so}}\right) + h_2\left(\frac{1}{s} + \frac{1}{p_{si}}\right)\right] + \frac{2}{g}\left[h_1(s + p_{so}) + h_2(s + p_{si})\right] \tag{6-16}$$

All other geometric parameters are defined in Figure 6-9. For end-plate connections at the top of the column, the column flange yield line parameters are given in Appendix A.

For the eight-bolt connection configuration, the yield line pattern for unstiffened and stiffened column flanges (without and with continuity plates) are shown in Figures 6-9(c) and 6-9(d), respectively, with yield line parameters:

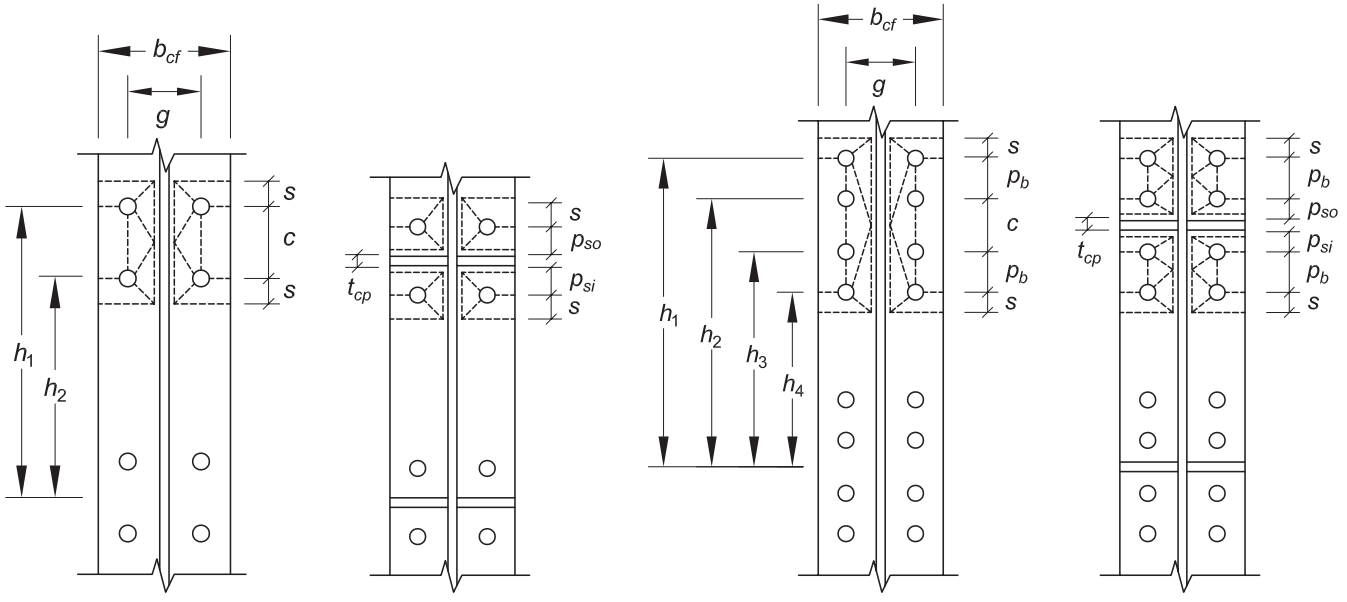

(a) Four-bolt unstiffened column flange

(b) Four-bolt stiffened column flange

(c) Eight-bolt unstiffened column flange

(d) Eight-bolt stiffened column flange

Fig. 6-9. Column flange yield line mechanisms.

Eight-bolt unstiffened column flange

$$Y_{cu} = \frac{b_{cf}}{2}\left[h_1\left(\frac{1}{s}\right) + h_4\left(\frac{1}{s}\right)\right] + \frac{2}{g}\begin{bmatrix} h_1\left(p_b + \frac{1}{2}c + s\right) + h_2\left(\frac{1}{2}p_b + \frac{1}{4}c\right) + \\ h_3\left(\frac{1}{2}p_b + \frac{1}{2}c\right) + h_4(s) \end{bmatrix} + \frac{g}{2} \quad (6\text{-}17)$$

Eight-bolt stiffened column flange

$$Y_{cs} = \frac{b_{cf}}{2}\left[h_1\left(\frac{1}{s}\right) + h_2\left(\frac{1}{p_{so}}\right) + h_3\left(\frac{1}{p_{si}}\right) + h_4\left(\frac{1}{s}\right)\right] + \frac{2}{g}\begin{bmatrix} h_1\left(s + \frac{1}{4}p_b\right) + h_2\left(p_{so} + \frac{3}{4}p_b\right) + \\ h_3\left(p_{si} + \frac{1}{4}p_b\right) + h_4\left(s + \frac{3}{4}p_b\right) + p_b^2 \end{bmatrix} + g \quad (6\text{-}18)$$

All other geometric parameters are defined in Figure 6-9. For end-plate connections at the top of the column, the column flange yield line parameters are given in Appendix A.

The column web is checked for two limit states to determine if continuity plates are required and, if they are required, the associated demand for the continuity plates. The resistance of the web to local column web yielding is given by AISC *Prequalified Connections* Equations 6.7-16 and 6.7-17, using $\phi_d = 1.00$ from AISC *Prequalified Connections*. The load is assumed to be applied over a width equal to the beam flange thickness that then spreads out at a 1:1 slope in the end plate and a 3:1 slope in the column flange. At the top of a column, the web yielding zone may extend above the top of the column. Therefore, the resistance, R_n, is multiplied by $C_t = 0.5$ if the distance from the beam top flange to top of column is less than the depth of the column. If the computed design strength, ϕR_n, is less than the flange force, F_{fu}, then continuity plates are required, and the demand for the continuity plates is the difference between the two.

$$F_{fu} \le \phi_d R_n \quad (\textit{Preq. Conn.} \text{ Eq. 6.7-16})$$

where

$$R_n = (6C_t k_c + l_b)F_{yc}t_{cw} \quad (\textit{Preq. Conn.} \text{ Eq. 6.7-17})$$

where

C_t = 0.5 if distance from beam top flange to top of column is less than the column depth, C_t = 1.0 otherwise.
F_{yc} = specified minimum yield stress of column flange material, ksi
k_c = distance from the outer face of the column flange to the web toe of fillet (k_{des} for rolled shapes) or to the inside of the fillet weld if welded built-up section, in.
l_b = length of bearing, $t_{bf} + 2w + 2t_p$, in.
t_{bf} = thickness of beam flange, in.
t_{cw} = thickness of the column web, in.
t_p = thickness of end plate, in.
w = leg size of optional double-sided fillet weld if used in the beam flange-to-end-plate weld, in.

AISC *Prequalified Connections* Equations 6.7-18 through 6.7-21 are used to check for crippling of the unstiffened column web, with $\phi = 0.75$ from AISC *Prequalified Connections*. Just like the previous two column web checks, if the computed design strength, ϕR_n, is less than the flange force, F_{fu}, then continuity plates are required, and the demand for the continuity plates is the difference between the two. The continuity plate design is discussed next.

$$F_{fu} \le \phi R_n \quad (\textit{Preq. Conn.} \text{ Eq. 6.7-18})$$

For F_{fu} applied at least $d_c/2$ from the end of the column:

$$R_n = 0.80t_{cw}^2\left[1 + 3\left(\frac{l_b}{d_c}\right)\left(\frac{t_{cw}}{t_{cf}}\right)^{1.5}\right]\sqrt{\frac{EF_{yc}t_{cf}}{t_{cw}}} \quad (\textit{Preq. Conn.} \text{ Eq. 6.7-19})$$

For F_{fu} applied within $d_c/2$ from the end of the column and $l_b/d_c \le 0.2$:

$$R_n = 0.40t_{cw}^2\left[1 + 3\left(\frac{l_b}{d_c}\right)\left(\frac{t_{cw}}{t_{cf}}\right)^{1.5}\right]\sqrt{\frac{EF_{yc}t_{cf}}{t_{cw}}} \quad (\textit{Preq. Conn.} \text{ Eq. 6.7-20})$$

For F_{fu} applied within $d_c/2$ from the end of the column and $l_b/d_c > 0.2$:

$$R_n = 0.40t_{cw}^2\left[1 + \left(\frac{4l_b}{d_c} - 0.2\right)\left(\frac{t_{cw}}{t_{cf}}\right)^{1.5}\right]\sqrt{\frac{EF_{yc}t_{cf}}{t_{cw}}} \quad (\textit{Preq. Conn.} \text{ Eq. 6.7-21})$$

where

F_{yc} = specified minimum yield stress of column flange material, ksi
d_c = depth of the column, in.
l_b = $t_{bf} + 2w + 2t_p$, in.
t_{bf} = thickness of the beam flange, in.
t_{cf} = thickness of the column flange, in.
t_{cw} = thickness of the column web, in.
t_p = end-plate thickness, in.
w = size of fillet weld or groove weld reinforcement at beam flange to end-plate weld, in.
ϕ = 0.75

If the stiffened column yield line parameter (as opposed to the unstiffened parameter) was required to provide sufficient

column flange flexural design strength, or if any of the previous two checks for an unstiffened web (unstiffened column web local yielding, unstiffened column web crippling) were found to have insufficient strength, then continuity plates are required. The force demand on the continuity plates is given in AISC *Prequalified Connections* Equation 6.7-22 as the difference between the flange force, F_{fu}, and the minimum resistance, $\phi_d R_n$, from the four limit states. Once the force demand is obtained, the continuity plates can be designed according to AISC *Seismic Provisions* Section E3.6f, AISC *Prequalified Connections* Section 3.6, and AISC *Specification* Section J10.8.

$$F_{su} = F_{fu} - \min \begin{bmatrix} (\phi_d R_n)_{flange\ flexure} \\ (\phi_d R_n)_{web\ yielding} \\ (\phi R_n)_{web\ crippling} \end{bmatrix}$$

(from *Preq. Conn.* Eq. 6.7-22)

where

$$(\phi_d R_n)_{flange\ flexure} = \frac{\phi_d M_{cf}}{d - t_{bf}} \qquad (Preq.\ Conn.\ \text{Eq. 6.7-15})$$

$$\phi_d M_{cf} = \phi_d F_{yc} Y_c t_{cf}^2 \qquad (Preq.\ Conn.\ \text{Eq. 6.7-14})$$

Y_c = unstiffened column yield line mechanism parameter for this calculation

$(\phi_d R_n)_{web\ yielding}$ and $(\phi R_n)_{web\ crippling}$ are the ϕR_n for each limit state

The column panel zone needs to be checked for shear strength. The calculations for column panel zone design strength are in AISC *Specification* Section J10.6, and additional requirements for the panel zone and doubler plates in SMF connections are given in AISC *Seismic Provisions* Section E3.6e. These checks are demonstrated in the following design examples but are not repeated here.

Finally, the column must also satisfy the strong-column/weak-beam criterion, which is given as the moment ratio in AISC *Seismic Provisions* Section E3.4a. As stated in the exceptions, the strong-column/weak-beam check is not required in one-story buildings or at the top story of a multistory building. In other cases, this check can control the size of the column section and is best conducted at the beginning of the column design. The strong-column/weak-beam criterion is checked in the following design examples.

6.3 DESIGN EXAMPLES

Examples are provided for the three end-plate configurations currently included in AISC *Prequalified Connections*. The examples include all the steps and attempt to be as complete as possible. For each example, it is assumed that the beams and columns have been sized so that drift limits are satisfied. It is noted that ASD calculations are not provided because AISC *Prequalified Connections* is written in LRFD format only.

EXAMPLE 6.3-1—Four-Bolt Extended Unstiffened End-Plate Example

Given:

Figure 6-10 shows a portal frame knee 4E end-plate moment connection with built-up beam and column sections. This connection is part of an SMF with a column centerline to column centerline distance of 50 ft and a height from top of foundation to beam centerline at eave of 20 ft. All steel, including beam, column, and plate material, is ASTM A529/A529M (2019c) Grade 50. The connection is subjected to the following LRFD factored loads:

Beam axial tension/compression	P_{ub}	= 35.0 kips
Vertical beam shear	$V_{gravity}$	= 20.0 kips

Because almost all qualification testing has been conducted on specimens representing an intermediate story, top of column connections, including end-plate connections, are not in AISC *Prequalified Connections.* However, it is stated in the corresponding Commentary Section 2.6 that a top of column detail similar to that shown in Figure 6-10, "is believed to be capable of providing reliable performance." On this basis, the authors developed the design for this example. This example is a portal frame knee connection; identical design steps apply to top of column connections in multistory frames.

Solution:

From AISC *Manual* Table 2-4, the material properties are as follows:

ASTM A529/A529M Grade 50
F_y = 50 ksi
F_u = 65 ksi

From AISC *Specification* Table J3.2, the material properties of the bolts are as follows:

Group 150 ASTM F3125/F3125M Grade A490 pretensioned
F_{nt} = 113 ksi
F_{nv} = 68 ksi (Group 150 bolts with threads not excluded from the shear plane; thread condition N)

Beam
A_b = 13.1 in.^{2} d = 20 in. t_{bw} = ⅜ in.
b_{bf} = 6 in. t_{bf} = ½ in. Z_b = 92.3 in.^{3}

Column
A_c = 25.0 in.^{2} d_c = 20 in. t_{cw} = ½ in.
b_{cf} = 8 in. t_{cf} = 1 in.

End-plate geometric properties:
b_p = 8 in.
g = 4 in.
p_{ext} = 3 in.
d_e = 1¼ in.
p_{fo} = 1¾ in.
p_{fi} = 1¾ in.
d_p = 26 in.

Follow the design procedure given in AISC *Prequalified Connections*.

Part 1. End-Plate and Bolt Design

Step 1.1–Compute Probable Maximum Moment, M_{pr}

The member sizes are built-up sections with properties given in Figure 6-10. Check that the beam flange satisfies the highly ductile section criteria in AISC *Seismic Provisions* Table D1.1b, using R_y = 1.1 from Table A3.2.

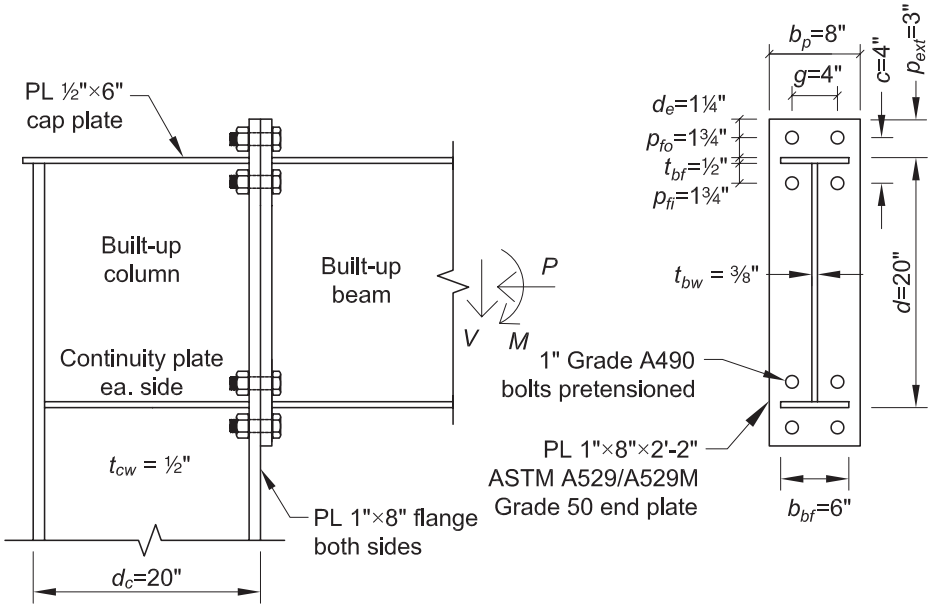

Fig. 6-10. 4E seismic end-plate configuration for Example 6.3-1.

$$\lambda_{hd} = 0.30\sqrt{\frac{E}{R_y F_y}} \qquad \text{(}\textit{Prov.}\text{ Table D1.1b)}$$

$$= 0.30\sqrt{\frac{29{,}000 \text{ ksi}}{1.1(50 \text{ ksi})}}$$

$$= 6.89$$

$$\lambda = \frac{b_{bf}}{2t_{bf}}$$

$$= \frac{6 \text{ in.}}{2(½ \text{ in.})}$$

$$= 6.00 \quad \leq \quad \lambda_{hd} = 6.89 \quad \textbf{o.k.}$$

Check that the beam web satisfies the highly ductile section criteria in AISC *Seismic Provisions* Table D1.1b.

$$\alpha_s = 1.0$$

$$C_a = \frac{\alpha_s P_r}{R_y F_{yb} A_{gb}} \qquad \text{(}\textit{Prov.}\text{ Table D1.1b)}$$

$$= \frac{1.0(35 \text{ kips})}{1.1(50 \text{ ksi})(13.1 \text{ in.}^2)}$$

$$= 0.0486$$

$$\lambda_{hd} = 2.5(1 - C_a)^{2.3}\sqrt{\frac{E}{R_y F_y}} \qquad \text{(}\textit{Prov.}\text{ Table D1.1b)}$$

$$= 2.5(1 - 0.0486)^{2.3}\sqrt{\frac{29{,}000 \text{ ksi}}{1.1(50 \text{ ksi})}}$$

$$= 51.2$$

$$\lambda = \frac{h}{t_{bw}}$$

$$= \frac{d - 2t_{bf}}{t_{bw}}$$

$$= \frac{20 \text{ in.} - 2(½ \text{ in.})}{⅜ \text{ in.}}$$

$$= 50.7 \quad \leq \quad \lambda_{hd} = 51.2 \quad \textbf{o.k.}$$

The column flange and column web were checked in the same way and found to satisfy highly ductile section criteria. Now check that the beam flange thickness, t_{bf}, flange width, b_{bf}, and depth, d, satisfy the parametric limitations on prequalification given in Table 6-1 of this Design Guide and AISC *Prequalified Connections* Table 6.1:

$⅜ \text{ in.} \leq t_{bf} \leq ¾ \text{ in.}$

$t_{bf} = ½ \text{ in.}$ **o.k.**

$6 \text{ in.} \leq b_{bf} \leq 9¼ \text{ in.}$

$b_{bf} = 6 \text{ in.}$ **o.k.**

$13¾ \text{ in.} \leq d \leq 24 \text{ in.}$

$d = 20 \text{ in.}$ **o.k.**

It is also necessary to check that the clear span-to-depth ratio of the beam is greater than or equal to 7:

$$\frac{L_c}{d} = \frac{L - d_c}{d}$$

$$= \frac{(50.0 \text{ ft})(12 \text{ in./ft}) - 20 \text{ in.}}{20 \text{ in.}}$$

$$= 29.0 \geq 7 \quad \textbf{o.k.}$$

Calculate the moment at the plastic hinge, M_{pr}. The beam plastic section modulus is calculated based on section geometry to be $Z_b = 92.3 \text{ in.}^3$

$$C_{pr} = \frac{F_{yb} + F_{ub}}{2F_{yb}} \leq 1.2 \qquad \text{(}\textit{Preq. Conn.}\text{ Eq. 2.4-2)}$$

$$= \frac{50 \text{ ksi} + 65 \text{ ksi}}{2(50 \text{ ksi})}$$

$$= 1.15 \leq 1.2$$

$$M_{pr} = C_{pr} R_y F_{yb} Z_b \qquad \text{(}\textit{Preq. Conn.}\text{ Eq. 2.4-1)}$$

$$= 1.15(1.1)(50 \text{ ksi})(92.3 \text{ in.}^3)$$

$$= 5{,}840 \text{ kip-in.}$$

Step 1.2—Determine Dimension, S_h

The distance from the column face to the plastic hinge, S_h, and the distance between plastic hinges, L_h, from AISC *Prequalified Connections* Section 6.7.1 are:

$$S_h = \min\left(\frac{d}{2}, 3b_{bf}\right) \qquad \text{(}\textit{Preq. Conn.}\text{ Eq. 6.7-1)}$$

$$= \min\left[\frac{20 \text{ in.}}{2}, 3(6 \text{ in.})\right]$$

$$= 10.0 \text{ in.}$$

$$L_h = L - d_c - 2S_h$$

$$= (50.0 \text{ ft})(12 \text{ in./ft}) - 20 \text{ in.} - 2(10.0 \text{ in.})$$

$$= 560 \text{ in.}$$

Step 1.3—Compute the Shear Force at the Plastic Hinge, V_h

The shear force at the plastic hinge, V_h, can then be calculated as:

$$V_h = \frac{2M_{pr}}{L_h} + V_{gravity} \qquad \text{(}\textit{Preq. Conn.}\text{ Eq. 2.4-3)}$$

$$= \frac{2(5{,}840 \text{ kip-in.})}{560 \text{ in.}} + 20.0 \text{ kips}$$

$$= 40.9 \text{ kips}$$

Step 1.4—Compute the Probable Maximum Moment at the Column Face, M_f

The moment at the face of the column, M_f, can then be calculated as:

$$M_f = M_{pr} + V_h S_h \qquad \text{(Preq. Conn. Eq. 2.4-4)}$$
$$= 5{,}840 \text{ kip-in.} + (40.9 \text{ kips})(10.0 \text{ in.})$$
$$= 6{,}250 \text{ kip-in.}$$

The value of the moment at the face of the column will be used in later steps as the demand for the design of elements of the connection.

Step 1.5—Select Connection Configuration and Establish Geometry

A four-bolt extended unstiffened moment end-plate connection (4E) configuration is selected. The bolt locations are defined with the following parameters:

$g = 4$ in.
$p_{fo} = 1¾$ in.
$p_{fi} = 1¾$ in.

The distances from the centerline of the compression flange to the two bolt lines, h_1 and h_2, are depicted in Figure 6-4 and are computed as:

$$h_1 = d - \frac{t_{bf}}{2} + p_{fo}$$
$$= 20 \text{ in.} - \frac{½ \text{ in.}}{2} + 1¾ \text{ in.}$$
$$= 21.5 \text{ in.}$$

$$h_2 = d - \frac{3t_{bf}}{2} - p_{fi}$$
$$= 20 \text{ in.} - \frac{3(½ \text{ in.})}{2} - 1¾ \text{ in.}$$
$$= 17.5 \text{ in.}$$

Check that the gage, g, and spacings, p_{fi} and p_{fo}, satisfy the parametric limitations given in Table 6-3 of this Design Guide and AISC *Prequalified Connections* Table 6.1:

4 in. $\le g \le$ 6 in.
$g = 4$ in. **o.k.**

1½ in. $\le p_{fo} \le$ 4½ in.
$p_{fo} = 1¾$ in. **o.k.**

1½ in. $\le p_{fi} \le$ 4½ in.
$p_{fi} = 1¾$ in. **o.k.**

Step 1.6—Determine Required Bolt Diameter

For a four-bolt extended unstiffened connection, use AISC *Prequalified Connections* Equation 6.7-3 to calculate the minimum required bolt diameter. Try Grade A490 bolts with nominal tensile strength $F_{nt} = 113$ ksi. The resistance factor for nonductile limit states is given in AISC *Prequalified Connections* as $\phi_n = 0.90$.

$$d_{b,req} = \sqrt{\frac{2M_f}{\pi\phi_n F_{nt}(h_1 + h_2)}} \qquad \text{(Preq. Conn. Eq. 6.7-3)}$$

$$= \sqrt{\frac{2(6{,}250 \text{ kip-in.})}{\pi(0.90)(113 \text{ ksi})(21.5 \text{ in.} + 17.5 \text{ in.})}}$$

$$= 1.00 \text{ in.}$$

Step 1.7—Select Bolt Diameter

Select 1-in.-diameter Grade A490 bolts.

$$d_b = 1 \text{ in.} \quad \geq \quad d_{b,req} = 1.00 \text{ in.} \quad \textbf{o.k.} \qquad (6\text{-}3)$$

Step 1.8—Determine Required End-Plate Thickness

Calculate the dimension, s, using Equation 6-6 and the yield line parameter, Y_p, for this bolt configuration and dimensions using Equation 6-7. The end-plate width, b_p, must not be taken as larger than the width of the beam flange plus 1.0 in. Because the beam flange width is $b_{bf} = 6$ in., an end-plate width equal to 7.00 in. is used in the following calculations instead of the full width of the end plate, $b_p = 8$ in.

$$b_{p,eff} \leq b_{bf} + 1 \text{ in.} \qquad (4\text{-}3)$$

$$\leq 6 \text{ in.} + 1 \text{ in.}$$

$$\leq 7.00 \text{ in.}$$

Because the upper limit for $b_{p,eff} = 7.00$ in. is less than the end plate width, $b_p = 8.00$ in., use $b_p = b_{p,eff} = 7.00$ in.

$$s = \frac{\sqrt{b_p g}}{2} \qquad (6\text{-}6)$$

$$= \frac{\sqrt{(7.00 \text{ in.})(4 \text{ in.})}}{2}$$

$$= 2.65 \text{ in.} \quad \geq \quad p_{fi} = 1¾ \text{ in.}$$

Because p_{fi} is less than s, it can be used directly in Equation 6-7.

$$Y_p = \frac{b_p}{2}\left[h_2\left(\frac{1}{p_{fi}} + \frac{1}{s}\right) + h_1\left(\frac{1}{p_{fo}}\right) - \frac{1}{2}\right] + \frac{2}{g}\left[h_2(p_{fi} + s)\right] \qquad (6\text{-}7)$$

$$= \left(\frac{7.00 \text{ in.}}{2}\right)\left[(17.5 \text{ in.})\left(\frac{1}{1¾ \text{ in.}} + \frac{1}{2.65 \text{ in.}}\right) + (21.5 \text{ in.})\left(\frac{1}{1¾ \text{ in.}}\right) - \frac{1}{2}\right]$$

$$+ \left(\frac{2}{4 \text{ in.}}\right)\left[(21.5 \text{ in.})(1¾ \text{ in.} + 2.65 \text{ in.})\right]$$

$$= 138 \text{ in.}$$

Compute the required end-plate thickness using AISC *Prequalified Connections* Equation 6.7-5. The resistance factor for ductile limit states is given in AISC *Prequalified Connections* as $\phi_d = 1.00$.

$$t_{p,req} = \sqrt{\frac{1.11M_f}{\phi_d F_{yp} Y_p}} \qquad \text{(Preq. Conn. Eq. 6.7-5)}$$

$$= \sqrt{\frac{1.11(6{,}250 \text{ kip-in.})}{1.00(50 \text{ ksi})(138 \text{ in.})}}$$

$$= 1.00 \text{ in.}$$

Step 1.9—Select End-Plate Thickness

Select an end-plate thickness $t_p = 1$ in.

$$t_p = 1 \text{ in.} \quad \geq \quad t_{p,req} = 1.00 \text{ in.} \quad \textbf{o.k.} \tag{6-5}$$

Now that the end-plate thickness, t_p, and width, b_p, have been established, it is necessary to check that they fall within the parametric limitations listed in Table 6-3 of this Design Guide and AISC *Prequalified Connections* Table 6.1.

$$½ \text{ in.} \leq t_p \leq 2¼ \text{ in.}$$

$$t_p = 1 \text{ in.} \quad \textbf{o.k.}$$

$$7 \text{ in.} \leq b_p \leq 10¾ \text{ in.}$$

$$b_p = 8 \text{ in.} \quad \textbf{o.k.}$$

Step 1.10—Calculate the Beam Flange Force

Use AISC *Prequalified Connections* Equation 6.7-6 to calculate the factored beam flange force, F_{fu}.

$$F_{fu} = \frac{M_f}{d - t_{bf}} \tag{*Preq. Conn.* Eq. 6.7-6}$$

$$= \frac{6{,}250 \text{ kip-in.}}{20 \text{ in.} - ½ \text{ in.}}$$

$$= 321 \text{ kips}$$

Step 1.11—Check Shear Yielding of Extended Portion of End Plate

The demand, V_u, is taken as one-half the beam flange force, F_{fu}. The design strength, $\phi_d R_n$, is given in AISC *Prequalified Connections* Equation 6.7-7. The effective end-plate width, $b_{p,eff} = 7.00$ in., is used to check the shear yield strength of the extended portion of the end plate.

$$\frac{F_{fu}}{2} = \frac{321 \text{ kips}}{2}$$

$$= 161 \text{ kips}$$

$$\phi_d R_n = \phi_d (0.6) F_{yp} b_p t_p$$

$$= (1.00)(0.6)(50 \text{ ksi})(7.00 \text{ in.})(1 \text{ in.})$$

$$= 210 \text{ kips}$$

$$\frac{F_{fu}}{2} = 161 \text{ kips} \quad \leq \quad \phi_d R_n = 210 \text{ kips} \quad \textbf{o.k.} \tag{from *Preq. Conn.* Eq. 6.7-7}$$

Step 1.12—Check Shear Rupture of Extended Portion of End Plate

The shear rupture demand is the same as for shear yielding. The design strength, $\phi_n R_n$, is given in AISC *Prequalified Connections* Equation 6.7-8. Similar to shear yielding, an effective end-plate width, $b_{p,eff} = 7.00$ in., is used. Standard size holes are used.

$$\phi_n R_n = \phi_n (0.6) F_{up} \left[b_p - 2(d_b + ⅛ \text{ in.}) \right] t_p$$

$$= (0.90)(0.6)(65 \text{ ksi}) \left[7.00 \text{ in.} - 2(1 \text{ in.} + ⅛ \text{ in.}) \right] (1 \text{ in.})$$

$$= 167 \text{ kips}$$

$$\frac{F_{fu}}{2} = 161 \text{ kips} \quad \leq \quad \phi_n R_n = 167 \text{ kips} \quad \textbf{o.k.} \tag{from *Preq. Conn.* Eq. 6.7-8}$$

Step 1.13—Define the Stiffener Geometry

This step is applicable only for stiffened end-plate connections.

Step 1.14—Check Beam Shear Strength

The required shear strength for the beam was calculated in Step 1.3 as $V_u = 40.9$ kips. Calculate the design shear strength of the beam using AISC *Specification* Section G2.1(b):

$$\frac{h}{t_w} = \frac{d - 2t_{bf}}{t_{bw}}$$
$$= \frac{20 \text{ in.} - 2(½ \text{ in.})}{⅜ \text{ in.}}$$
$$= 50.7$$

Because the web has no transverse stiffeners, the web plate shear buckling coefficient is $k_v = 5.34$. The slenderness limit for shear buckling is:

$$1.10\sqrt{\frac{k_v E}{F_y}} = 1.10\sqrt{\frac{5.34(29{,}000 \text{ ksi})}{50 \text{ ksi}}}$$
$$= 61.2$$

Because the web slenderness is less than $1.10\sqrt{k_v E/F_y}$, the web shear coefficient is $C_{v1} = 1.0$. The design shear strength is given as:

$$V_n = 0.6F_y A_w C_{v1} \qquad \text{(}\textit{Spec.}\text{ Eq. G2-1)}$$
$$= 0.6F_y d t_{bw} C_{v1}$$
$$= 0.6(50 \text{ ksi})(20 \text{ in.})(⅜ \text{ in.})(1.0)$$
$$= 225 \text{ kips}$$

From AISC *Specification* Section G1, $\phi_v = 0.90$.

$$\phi_v V_n = 0.90(225 \text{ kips})$$
$$= 203 \text{ kips}$$

$V_u = 40.9$ kips $\leq$ $\phi_v V_n = 203$ kips **o.k.**

Step 1.15—Determine the Required Shear Strength, V_u

The vertical shear demand at the end-plate connection was calculated in Step 1.3, $V_u = 40.9$ kips.

Step 1.16—Bolt Shear Rupture Strength

The design shear strength, $\phi_n R_n$, is given by AISC *Prequalified Connections* Equation 6.7-11 as the shear strength of the four bolts at the compression flange. The nominal shear strength of Grade A490 bolts is $F_{nv} = 68$ ksi. The area of a 1-in.-diameter bolt is 0.785 in.^{2}

$$\phi_n R_n = \phi_n n_b F_{nv} A_b$$
$$= 0.90(4 \text{ bolts})(68 \text{ ksi})(0.785 \text{ in.}^2)$$
$$= 192 \text{ kips}$$

$V_u = 40.9$ kips $\leq$ $\phi_n R_n = 192$ kips **o.k.** (from *Preq. Conn.* Eq. 6.7-11)

Step 1.17—Bearing/Tearout Failure of End Plate and Column Flange

Similar to the previous step, the vertical shear demand at the end-plate connection is $V_u = 40.9$ kips. The design bearing/tearout strength, $\phi_n R_n$, is given by AISC *Prequalified Connections* Equation 6.7-12. Because vertical shear is assumed to be resisted only by the compression side bolts, bearing/tearout is checked at the bottom bolt hole locations for the shear loading shown in Figure 6-10. By inspection, tearout will not control at the end plate, and therefore, only bolt bearing needs to be checked for this example. The same is true at the column flange if continuity plates are used. If not, tearout must be checked between the top and bottom bolt holes. As found later in the example, continuity plates are required. Because the column flange thickness, 1 in., is the same as the end-plate thickness, 1 in., the check is done for a 1 in. plate thickness.

The bearing strength at one bolt hole is:

$$r_n = 2.4 d_b t_{cf} F_{uc} \qquad \text{(from } \textit{Spec.} \text{ Eq. J3-6a)}$$
$$= 2.4(1 \text{ in.})(1 \text{ in.})(65 \text{ ksi})$$
$$= 156 \text{ kips}$$

The bearing strength at the top and bottom bolt holes is then:

$$\phi_n R_n = \phi_n n r_n$$
$$= 0.90(4 \text{ bolts})(156 \text{ kips})$$
$$= 562 \text{ kips}$$

$V_u = 40.9$ kips $\leq$ $\phi_n R_n = 562$ kips **o.k.** (from *Preq. Conn.* Eq. 6.7-12)

Note: The User Note in the AISC *Specification* Section J3.7 recommends that the effective strength of an individual bolt be taken as the lesser of the bolt shear strength, bearing strength, or tearout strength at the bolt hole. For this example, the effective shear strength of the top or bottom bolts is the shear strength of four bolts, 192 kips.

Step 1.18—Design the Welds

The beam web to beam flange welds need to be larger in the connection region per AISC *Prequalified Connections* Section 6.3.1(1). Over a region from the end plate to a distance equal to the lesser of d or $3b_{bf}$, the web to flange must be either CJP groove welded or fillet welded with a pair of fillet welds at least 75% of the beam web thickness, but not less than ¼ in. Try double-sided fillet welds 5⁄16 in. by 18 in. long

$$t_{weld,req} = 0.75 t_{bw}$$
$$= 0.75(3⁄8 \text{ in.})$$
$$= 0.281 \text{ in.}$$

$t_{weld} = 5⁄16$ in. $\geq$ $t_{weld,req} = 0.281$ in. **o.k.**

$$L_{weld,req} = \min(d, 3b_{bf})$$
$$= \min\left[20 \text{ in.}, 3(6 \text{ in.})\right]$$
$$= 18.0 \text{ in.}$$

$L_{weld} = 18.0$ in. $\geq$ $L_{weld,req} = 18.0$ in. **o.k.**

The same weld requirements apply to the column web to column flange welds, which would result in double-sided 3⁄8 in. fillet welds.

In accordance with AISC *Prequalified Connections* Section 6.6.6(2), the beam flange to end plate and cap plate to column flange welds are made using a CJP groove weld (bevel facing away from the center of the beam) without weld access holes and without back-up bars. The inside face of the flange will have a 5⁄16 in. reinforcing fillet weld. This CJP groove weld and reinforcing weld are the only welds that need to be demand critical.

The beam web to end-plate weld is designed in two parts. The web weld from the point nearest the top or bottom flange to a point 6 in. beyond the most interior bolt row is either a CJP groove weld or fillet welds that can develop the full yield strength of the web in tension. Try double-sided 5⁄16 in. fillet welds:

$$R_u = F_y t_{bw} \quad \text{(from } Spec. \text{ Eq. J4-1)}$$
$$= (50 \text{ ksi})(3/8 \text{ in.})$$
$$= 18.8 \text{ kips/in.}$$

$$R_n = (2 \text{ welds})(0.60F_{EXX})\left(\frac{t_{weld}}{\sqrt{2}}\right)(1.0 + 0.5\sin^{1.5}\theta) \quad \text{(from } Spec. \text{ Eq. J2-4)}$$
$$= (2 \text{ welds})(0.60)(70 \text{ ksi})\left(\frac{5/16 \text{ in.}}{\sqrt{2}}\right)(1.0 + 0.5\sin^{1.5} 90°)$$
$$= 27.8 \text{ kips/in.}$$

$$\phi R_n = 0.75(27.8 \text{ kips/in.})$$
$$= 20.9 \text{ kips/in.}$$

$R_u = 18.8$ kips/in. $\leq$ $\phi R_n = 20.9$ kips/in. **o.k.**

The beam web to end-plate weld outside the tension zone is designed for the shear demand and is typically smaller. From Step 1.3, the shear demand is 40.9 kips. By inspection, the weld strength provided by the 5⁄16 in. doubled-sided fillet weld required to develop the yield strength of the weld at the top and bottom bolts is more than sufficient to resist this shear demand.

Use double-sided 5⁄16 in. fillet welds the full depth of the beam web.

Part 2. Column-Side Design

The top of the column uses similar detailing as the beam side, including a cap plate that is at least as thick as the beam flange, the cap plate to column flange weld is the same as the beam flange to end-plate weld, and the column web to column flange weld follows the same rules as the beam web to end-plate weld as described in Step 1.18. Because these aspects of the top of column are selected as equal to or greater than the beam side, they are sufficient by inspection.

Step 2.1—Column Flange Flexural Yielding

For the portal frame connection shown in Figure 6-10, when the moment is such that that beam top flange is in tension, the column flange yield line mechanism is identical to the mechanism for the unstiffened end plate used in Step 1.8, assuming the cap plate is equivalent to the beam flange. Therefore, use the end-plate yield line parameter Equation 6-7 with the width of the column flange (and cap plate), b_{cf}, substituted for the end-plate width, b_p, and assuming s is greater than p_{si}. Because the cap plate thickness is the same as the beam top flange thickness, the distances from the face of the cap plate to the bolt line on the inside and outside of the flange are, $p_{si} = p_{fi}$ and $p_{so} = p_{fo}$, respectively.

$$s = \frac{\sqrt{b_{cf} g}}{2} \quad (6\text{-}14)$$
$$= \frac{\sqrt{(8 \text{ in.})(4 \text{ in.})}}{2}$$
$$= 2.83 \text{ in.}$$

Because $s \geq p_{si} = 1¾$ in., the dimension p_{si} is used in the equation for the yield line parameter.

$$Y_c = \frac{b_{cf}}{2}\left[h_2\left(\frac{1}{p_{si}}+\frac{1}{s}\right)+h_1\left(\frac{1}{p_{so}}\right)-\frac{1}{2}\right]+\frac{2}{g}\left[h_2\left(p_{si}+s\right)\right] \quad \text{(from Eq. 6-7)}$$

$$= \left(\frac{8\text{ in.}}{2}\right)\left[(17.5\text{ in.})\left(\frac{1}{1¾\text{ in.}}+\frac{1}{2.83\text{ in.}}\right)+(21.5\text{ in.})\left(\frac{1}{1¾\text{ in.}}\right)-\frac{1}{2}\right]$$

$$+\left(\frac{2}{4\text{ in.}}\right)\left[(21.5\text{ in.})(1¾\text{ in.}+2.83\text{ in.})\right]$$

$$= 152\text{ in.}$$

$$t_{cf,req} = \sqrt{\frac{1.11M_f}{\phi_d F_{yc} Y_c}} \quad \text{(from } \textit{Preq. Conn.} \text{ Eq. 6.7-13)}$$

$$= \sqrt{\frac{1.11(6{,}250\text{ kip-in.})}{(1.00)(50\text{ ksi})(152\text{ in.})}}$$

$$= 0.955\text{ in.}$$

$$t_{cf} = 1\text{ in.} \quad \geq \quad t_{cf,req} = 0.955\text{ in.} \quad \textbf{o.k.} \qquad (6\text{-}13)$$

When the connection is subjected to moment such that the beam bottom flange is in tension, then the yield line parameters shown in AISC *Prequalified Connections* Table 6.5 or Appendix A are appropriate. The required column flange thickness is first determined using the yield-line parameter for an unstiffened column flange from Equation 6-13 or from AISC *Prequalified Connections* Table 6.5.

$$c = p_{fi} + t_{bf} + p_{fo}$$

$$= 1¾\text{ in.} + ½\text{ in.} + 1¾\text{ in.}$$

$$= 4.00\text{ in.}$$

$$s = \frac{\sqrt{b_{cf} g}}{2} \qquad (6\text{-}14)$$

$$= \frac{\sqrt{(8\text{ in.})(4\text{ in.})}}{2}$$

$$= 2.83\text{ in.}$$

$$Y_{cu} = \frac{b_{cf}}{2}\left[h_2\left(\frac{1}{s}\right)+h_1\left(\frac{1}{s}\right)\right]+\frac{2}{g}\left[h_2\left(s+\frac{3c}{4}\right)+h_1\left(s+\frac{c}{4}\right)+\frac{c^2}{2}\right]+\frac{g}{2} \qquad (6\text{-}15)$$

$$= \left(\frac{8\text{ in.}}{2}\right)\left[(17.5\text{ in.})\left(\frac{1}{2.83\text{ in.}}\right)+(21.5\text{ in.})\left(\frac{1}{2.83\text{ in.}}\right)\right]$$

$$+\left(\frac{2}{4\text{ in.}}\right)\left\{(17.5\text{ in.})\left[2.83\text{ in.}+\frac{3(4.00\text{ in.})}{4}\right]+(21.5\text{ in.})\left(2.83\text{ in.}+\frac{4.00\text{ in.}}{4}\right)+\frac{(4.00\text{ in.})^2}{2}\right\}+\frac{4\text{ in.}}{2}$$

$$= 153\text{ in.}$$

$$t_{cf,req} = \sqrt{\frac{1.11M_f}{\phi_d F_{yc} Y_{cu}}} \quad \text{(from } \textit{Preq. Conn.} \text{ Eq. 6.7-13)}$$

$$= \sqrt{\frac{1.11(6{,}250\text{ kip-in.})}{(1.00)(50\text{ ksi})(153\text{ in.})}}$$

$$= 0.952\text{ in.}$$

$$t_{cf} = 1\text{ in.} \quad \geq \quad t_{cf,req} = 0.952\text{ in.} \quad \textbf{o.k.} \qquad (6\text{-}13)$$

Step 2.2—Column Flange Available Flexural Strength for Continuity Plate Demand

As shown in Step 2.1, the flexural strength of the column flange opposite the beam bottom flange is sufficient and continuity plates are not needed for this limit state.

Step 2.3—Local Column Web Yielding

Check the local column web yielding design strength opposite the bottom beam flange against the calculated beam flange force from Step 1.10 using AISC *Prequalified Connections* Equation 6.7-17 with $\phi_d = 1.00$. This calculation is performed assuming no continuity plates exist. If a check is satisfied, then no continuity plates are necessary at that location. If the check is not satisfied, then the difference between the required strength and the unstiffened column available strength is used in Step 2.5 to find the required strength for the continuity plates.

For the distance from the outer face of the column flange to the toe of the fillet weld, k_c, the weld of the column web to column flange is 5⁄16 in., and thus, the value of k_c is:

$$\begin{aligned} k_c &= t_{cf} + t_w \\ &= 1 \text{ in.} + 5/16 \text{ in.} \\ &= 1.31 \text{ in.} \end{aligned}$$

Because the distance from the column top to the top face of the beam flange is less than the depth of the column, $C_t = 0.5$. The effective width of bearing, l_b, includes the size of the reinforcing fillet, w, from the beam flange to end-plate CJP groove weld. Because there is only one reinforcing fillet weld at the CJP groove weld and assuming a 5⁄16 in. fillet weld,

$$\begin{aligned} l_b &= t_{bf} + w + 2t_p \\ &= 1/2 \text{ in.} + 5/16 \text{ in.} + 2(1 \text{ in.}) \\ &= 2.81 \text{ in.} \end{aligned}$$

$$\begin{aligned} R_n &= (6C_t k_c + l_b) F_{yc} t_{cw} \qquad \text{(Preq. Conn. Eq. 6 .7-17)} \\ &= \left[6(0.5)(1.31 \text{ in.}) + 2.81 \text{ in.}\right](50 \text{ ksi})(1/2 \text{ in.}) \\ &= 169 \text{ kips} \end{aligned}$$

$$\begin{aligned} \phi_d R_n &= 1.00(169 \text{ kips}) \\ &= 169 \text{ kips} \end{aligned}$$

$$\phi_d R_n = 169 \text{ kips} \quad < \quad F_{fu} = 321 \text{ kips} \qquad \text{(Preq. Conn. Eq. 6.7-16)}$$

Because $\phi_d R_n < F_{fu}$, continuity plates are required.

Step 2.4—Column Web Crippling

As was done in Step 2.3, the column web crippling available strength is evaluated assuming no continuity plates exist. If a check fails, then continuity plates are required. AISC *Prequalified Connections* Equations 6.7-19 through 6.7-21 are used to compute the web crippling available strength with $\phi = 0.75$. First calculate l_b/d_c:

$$\begin{aligned} \frac{l_b}{d_c} &= \frac{2.81 \text{ in.}}{20.0 \text{ in.}} \\ &= 0.141 \end{aligned}$$

Because the beam bottom flange force is applied at a distance greater than $d_c/2$ from the top of the column, use AISC *Prequalified Connections* Equation 6.7-19 with $\phi = 0.75$ to calculate the available strength of the column web for resisting web crippling.

$$R_n = 0.80 t_{cw}^2 \left[1 + 3\left(\frac{l_b}{d_c}\right)\left(\frac{t_{cw}}{t_{cf}}\right)^{1.5}\right]\sqrt{\frac{EF_{yc}t_{cf}}{t_{cw}}} \qquad \text{(Preq. Conn. Eq. 6.7-19)}$$

$$= 0.80(\tfrac{1}{2}\text{ in.})^2\left[1 + 3(0.141)\left(\frac{\tfrac{1}{2}\text{ in.}}{1\text{ in.}}\right)^{1.5}\right]\sqrt{\frac{(29{,}000\text{ ksi})(50\text{ ksi})(1\text{ in.})}{\tfrac{1}{2}\text{ in.}}}$$

$$= 392 \text{ kips}$$

$$\phi R_n = 0.75(392 \text{ kips})$$

$$= 294 \text{ kips}$$

$$\phi R_n = 294 \text{ kips} \quad < \quad F_{fu} = 321 \text{ kips} \qquad \text{(Preq. Conn. Eq. 6.7-18)}$$

Because $\phi R_n < F_{fu}$, continuity plates are required.

Step 2.5—Continuity Plates and Welds

Steps 2.3 and 2.4 showed that continuity plates are necessary opposite the bottom flange of the beam. Determine the required strength of the continuity plates, F_{fsu}, as the difference between the beam flange force, F_{fu}, and the minimum available strength computed from Steps 2.3 and 2.4.

$$F_{fsu} = F_{fu} - \min\left[(\phi_d R_n)_{step\ 2.3}, (\phi R_n)_{step\ 2.4}\right] \qquad \text{(from Preq. Conn. Eq. 6.7-22)}$$

$$= 321 \text{ kips} - \min(169 \text{ kips}, 294 \text{ kips})$$

$$= 152 \text{ kips}$$

Try ½ in. × 3¾ in. continuity plates. First, check that this thickness is greater than the minimum plate thickness given in the AISC *Seismic Provisions* Section E3.6f.2(b):

$$t_{cp,req} = \frac{t_{bf}}{2}$$

$$= \frac{\tfrac{1}{2}\text{ in.}}{2}$$

$$= 0.250 \text{ in.}$$

$$t_{cp} = \tfrac{1}{2}\text{ in.} \quad \geq \quad t_{cp,req} = 0.250 \text{ in.} \quad \textbf{o.k.}$$

According to AISC *Specification* Section J10.8, design the continuity plates for compression per AISC *Specification* Section J4.4. It can be shown that the continuity plate slenderness, l/r, is less than 25, therefore with $\phi = 0.90$ from the AISC *Specification*:

$$A_{gcp} = 2t_{cp}w_{cp}$$

$$= 2(\tfrac{1}{2}\text{ in.})(3\tfrac{3}{4}\text{ in.})$$

$$= 3.75 \text{ in.}^2$$

$$P_n = F_y A_{gcp} \qquad \text{(Spec. Eq. J4-6)}$$

$$= (50 \text{ ksi})(3.75 \text{ in.}^2)$$

$$= 188 \text{ kips}$$

$$\phi P_n = 0.90(188 \text{ kips})$$

$$= 169 \text{ kips}$$

$$\phi P_n = 169 \text{ kips} \quad \geq \quad F_{fsu} = 153 \text{ kips} \quad \textbf{o.k.}$$

The weld from the continuity plates to the column flange is required to be a CJP groove weld per the AISC *Seismic Provisions* Section E3.6f.2(c). The same section states that the required strength for the weld from the continuity plates to the column web must be the lesser of (1) the nominal tensile strength of the continuity plates contact area with the column flange, (2) the nominal shear strength of the continuity plates contact area with the column web, or (3) the nominal shear strength of the column web (panel zone).

To determine the required strength of the continuity plates to column web welds, the contact lengths between the continuity plates and column flange, l_{cpf}, and between the continuity plates and the column web, l_{cpw} (shown in Figure 6-11), must first be determined. AWS D1.8/D1.8M clause 4.1 has requirements for the size of clips when the column is a hot-rolled section but does not provide requirements for built-up column sections. The weld size at the column web to column flange is 5⁄16 in., and in the authors' judgment, a ¾ in. clip is sufficient. As shown in Figure 6-11, the continuity plates are detailed to extend to the edges of the column flange, making their width w_{cp} = 3¾ in. The contact lengths at the column web and flange are then:

$$l_{cpw} = d_c - 2t_{cf} - 2(clip)$$
$$= 20 \text{ in.} - 2(1 \text{ in.}) - 2(¾ \text{ in.})$$
$$= 16.5 \text{ in.}$$

$$l_{cpf} = w_{cp} - 1(clip)$$
$$= 3¾ \text{ in.} - 1(¾ \text{ in.})$$
$$= 3.00 \text{ in.}$$

The nominal tensile strength of the continuity plates is:

$$R_{u1} = F_y 2 l_{cpf} t_{cp} \qquad \text{(from } Spec. \text{ Eq. J4-1)}$$
$$= (50 \text{ ksi})(2)(3.00 \text{ in.})(½ \text{ in.})$$
$$= 150 \text{ kips}$$

The nominal shear yield strength of the continuity plates is:

$$R_{u2} = 0.60 F_{ycp} 2 l_{cpw} t_{cp} \qquad \text{(from } Spec. \text{ Eq. J4-3)}$$
$$= 0.60(50 \text{ ksi})(2)(16.5 \text{ in.})(½ \text{ in.})$$
$$= 495 \text{ kips}$$

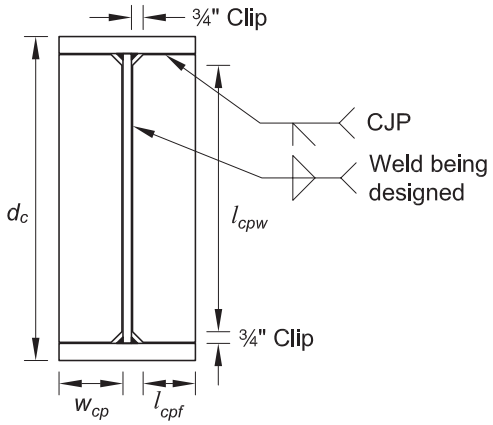

Fig. 6-11. Calculating weld lengths for continuity plates.

The nominal shear yield strength of the panel zone is calculated according to AISC *Specification* Section J10.6. First find the column required axial strength, P_u, and the ratio of this required axial strength to the axial yield strength of the column, P_y.

$$P_{uc} = V_u$$
$$= 40.9 \text{ kips}$$

Note that this is the same as the required beam shear from Step 1.3.

$$P_y = F_{yc} A_c$$
$$= (50 \text{ ksi})(25.0 \text{ in.}^2)$$
$$= 1{,}250 \text{ kips}$$

$$\frac{P_{uc}}{P_y} = \frac{40.9 \text{ kips}}{1{,}250 \text{ kips}}$$
$$= 0.0327$$

Assuming that frame stability was assessed including plastic panel zone deformation with the ratio P_{uc}/P_y equal to 0.0327, which is less than 0.75, then use AISC *Specification* Equation J10-11 for panel zone available strength.

$$R_{u3} = 0.60 F_{yc} d_c t_{cw} \left(1 + \frac{3 b_{cf} t_{cf}^2}{d d_c t_{cw}}\right) \quad \text{(from } \textit{Spec.} \text{ Eq. J10-11)}$$
$$= 0.60(50 \text{ ksi})(20 \text{ in.})(\tfrac{1}{2} \text{ in.}) \left[1 + \frac{3(8 \text{ in.})(1 \text{ in.})^2}{(20 \text{ in.})(20 \text{ in.})(\tfrac{1}{2} \text{ in.})}\right]$$
$$= 336 \text{ kips}$$

$$R_u = \min(R_{u1}, R_{u2}, R_{u3})$$
$$= \min(150 \text{ kips}, 495 \text{ kips}, 336 \text{ kips})$$
$$= 150 \text{ kips}$$

The minimum size welds per AISC *Specification* Table J2.4 is 3⁄16 in. Try double-sided 3⁄16 in. welds between the continuity plates and the column web.

$$R_n = (4 \text{ welds}) \left(0.60 F_{EXX} \frac{t_{weld}}{\sqrt{2}} l_{cpw}\right)(1.0 + 0.5 \sin^{1.5} \theta) \quad \text{(from } \textit{Spec.} \text{ Eq. J2-4)}$$
$$= (4 \text{ welds})(0.60)(70 \text{ ksi}) \left(\frac{\tfrac{3}{16} \text{ in.}}{\sqrt{2}}\right)(16.5 \text{ in.})(1.0 + 0.5 \sin^{1.5} 0^\circ)$$
$$= 368 \text{ kips}$$

$$\phi R_n = 0.75(368 \text{ kips})$$
$$= 276 \text{ kips}$$

$$\phi R_n = 276 \text{ kips} \quad \geq \quad R_u = 150 \text{ kips} \quad \textbf{o.k.}$$

Check that the shear rupture strength of the column web at the stiffener welds using AISC *Specification* Equation J4-4 is sufficient. There are two shear rupture lines, one above and one below the stiffeners.

$$R_n = 0.60F_uA_{nv} \qquad \text{(Spec. Eq. J4-4)}$$

$$= (2 \text{ lines})0.60F_u l_{cpw} t_{cw}$$

$$= (2 \text{ lines})(0.60)(65 \text{ ksi})(16.5 \text{ in.})(½ \text{ in.})$$

$$= 644 \text{ kips}$$

$$\phi R_n = 0.75(644 \text{ kips})$$

$$= 483 \text{ kips}$$

$$\phi R_n = 483 \text{ kips} \quad \geq \quad R_u = 150 \text{ kips} \quad \textbf{o.k.}$$

Step 2.6—Panel Zone Shear

The panel zone is checked in accordance with AISC *Seismic Provisions* Section E3.6e(1). The panel zone shear is similar to that shown in Figure 3.15(d). The panel zone required shear strength is the flange force, F_{fu}, less one-half the axial force, P_{ub}.

$$V_{upz} = F_{fu} - \frac{P_{ub}}{2}$$

$$= 321 \text{ kips} - \frac{35 \text{ kips}}{2}$$

$$= 304 \text{ kips}$$

The panel zone design strength is calculated according to AISC *Specification* Section J10.6, using a resistance factor $\phi_d = 1.00$ according to AISC *Seismic Provisions* Section E3.6e(1). The nominal yield strength of the panel zone was calculated in Step 2.5 as $R_n = 336$ kips.

$$\phi_d R_n = 1.00(336 \text{ kips})$$

$$= 336 \text{ kips}$$

$$\phi_d R_n = 336 \text{ kips} \quad \geq \quad V_{upz} = 304 \text{ kips} \quad \textbf{o.k.}$$

Additionally, check that the column web satisfies the minimum panel zone thickness given in AISC *Seismic Provisions* Section E3.6e(2), Equation E3-6.

$$d_z = d - 2t_{bf}$$

$$= 20 \text{ in.} - 2(½ \text{ in.})$$

$$= 19.0 \text{ in.}$$

$$w_z = d_c - 2t_{cf}$$

$$= 20 \text{ in.} - 2(1 \text{ in.})$$

$$= 18.0 \text{ in.}$$

$$t_{cw,req} = \frac{d_z + w_z}{90} \qquad \text{(from Prov. Eq. E3-6)}$$

$$= \frac{19.0 \text{ in.} + 18.0 \text{ in.}}{90}$$

$$= 0.411 \text{ in.}$$

$$t_{cw} = ½ \text{ in.} \quad \geq \quad t_{cw,req} = 0.411 \text{ in.} \quad \textbf{o.k.}$$

Step 2.7—Strong-Column/Weak-Beam Check

Evaluate whether the strong-column/weak-beam moment ratio requirements of AISC *Seismic Provisions* Section E3.4a are satisfied. That section states that if the ratio of the required column axial strength to the axial yield strength is less than 0.3 and

the column is for a one-story building, then the moment ratio does not apply. In Step 2.5, the ratio of the required column axial strength was shown to be less than 0.3 times the axial yield strength of the column, and therefore the requirement does not apply for this example.

Summary of the Design

The final design of the connection is shown in Figure 6-12.

EXAMPLE 6.3-2—Four-Bolt Extended Stiffened End-Plate Example

Given:

The seismic example shown in Figure 6-13 is a four-bolt extended stiffened (4ES) end-plate connection for a W24×62 beam in a bay that is 30 ft centerline to centerline of W14×159 columns. The moment connection is single sided (i.e., beam on one side only), and the column extends above the connection. The beam and column are ASTM A992/A992M steel, and the plate is ASTM A572/A572M Grade 50 steel. The connection is subjected to the following forces:

Beam axial tension/compression	P_{ub}	= 28.0 kips
Vertical beam shear due to factored gravity loads	$V_{gravity}$	= 31.0 kips
Column compression due to gravity loads	P_{uc}	= 10.0 kips
Column shear above connection	V_{uc}	= 69.0 kips

Solution:

From AISC *Manual* Table 2-4, the material properties are as follows:

ASTM A992/A992M
F_y = 50 ksi
F_u = 65 ksi

ASTM A572/A572M Grade 50
F_y = 50 ksi
F_u = 65 ksi

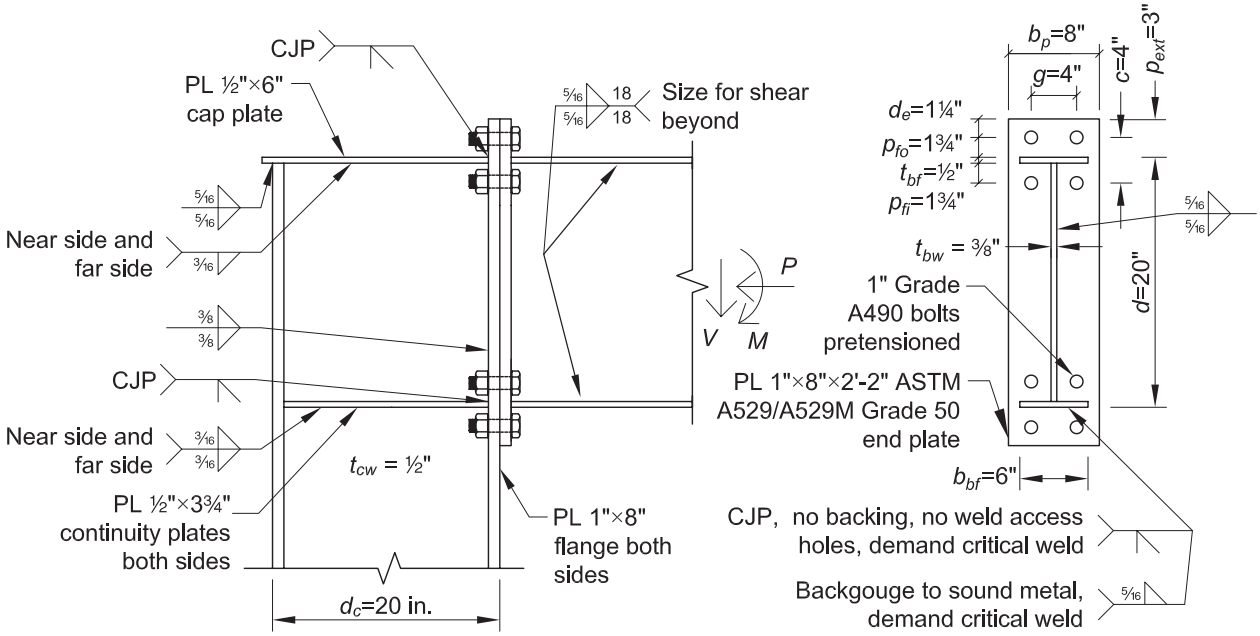

Fig. 6-12. Summary of final design for 4E seismic end-plate configuration.

From AISC *Specification* Table J3.2, the material properties of the bolts are as follows:

Group 150 ASTM F3125/F3125M Grade A490 pretensioned
F_{nt} = 113 ksi
F_{nv} = 68 ksi (Group 150 bolts with threads not excluded from the shear plane; thread condition N)

From AISC *Manual* Table 1-1, the geometric properties are as follows:

Beam: W24×62
A_b = 18.2 in.^{2} d = 23.7 in. t_{bw} = 0.430 in.
b_{bf} = 7.04 in. t_{bf} = 0.590 in. Z_b = 153 in.^{3}

Column: W14×159
A_c = 46.7 in.^{2} d_c = 15.0 in. t_{cw} = 0.745 in. b_{cf} = 15.6 in.
t_{cf} = 1.19 in. k_c = 1.79 in. Z_{cx} = 287 in.^{3}

End-plate geometric properties:
b_p = 9 in.
g = 5½ in.
p_{ext} = 3⅝ in.
d_e = 1⅝ in.
p_{fo} = 2 in.
p_{fi} = 2 in.
d_p = 31 in.

This section follows the Design Procedure given in AISC *Prequalified Connections*. The design is split into two parts: Part 1 is End-Plate and Bolt Design, and Part 2 is Column-Side Design.

Part 1. End-Plate and Bolt Design

Step 1.1—Compute Probable Maximum Moment, M_{pr}

The beam and column are given as ASTM A992/A992M W24×62 and W14×159, respectively. Because the beam section is listed in Table 6-2, the flange of the section satisfies highly ductile section compactness. For the web to satisfy highly ductile section

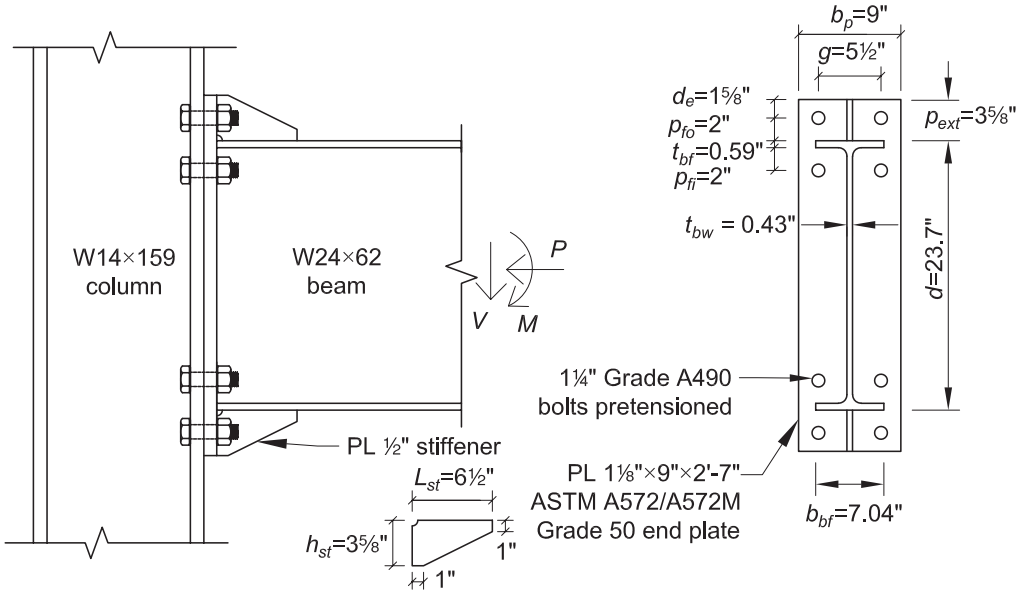

Fig. 6-13. 4ES seismic end-plate configuration for Example 6.3-2.

criteria, the required axial force in the beam has to be less than $P_{u,max}$, listed in Table 6-2. Determine whether the beam web satisfies highly ductile section compactness:

$P_{u,max}$ = 57.5 for W24×62 from Table 6-2

P_{ub} = 28.0 kips < $P_{u\,max}$ **o.k.**

The W14×159 column flange and column web were checked using the procedure shown for the beam in Example 6.3-1 and found to satisfy highly ductile section criteria.

Now check that the beam flange thickness, t_{bf}, flange width, b_{bf}, and depth, d, satisfy the parametric limitations on prequalification given in Table 6-1 of this Design Guide and AISC *Prequalified Connections* Table 6.1:

⅜ in. ≤ t_{bf} ≤ ¾ in.

t_{bf} = 0.590 in. **o.k.**

6 in. ≤ b_{bf} ≤ 9 in.

b_{bf} = 7.04 in. **o.k.**

13¾ in. ≤ d ≤ 24 in.

d = 23.7 in. **o.k.**

It is also necessary to check that the clear span-to-depth ratio of the beam is greater than or equal to 7:

$$\frac{L_c}{d} = \frac{L - d_c}{d}$$

$$= \frac{(30\text{ ft})(12\text{ in./ft}) - 15.0\text{ in.}}{23.7\text{ in.}}$$

$$= 14.6 \geq 7 \quad \textbf{o.k.}$$

Calculate the probable maximum moment at the plastic hinge, M_{pr}. From AISC *Seismic Provisions* Table A3.2, R_y = 1.1.

$$C_{pr} = \frac{F_{yb} + F_{ub}}{2F_{yb}} \leq 1.2 \qquad \text{(}\textit{Preq. Conn.}\text{ Eq. 2.4-2)}$$

$$= \frac{50\text{ ksi} + 65\text{ ksi}}{2(50\text{ ksi})}$$

$$= 1.15 \leq 1.2$$

$$M_{pr} = C_{pr}R_yF_{yb}Z_b \qquad \text{(from }\textit{Preq. Conn.}\text{ Eq. 2.4-1)}$$

$$= 1.15(1.1)(50\text{ ksi})(153\text{ in.}^3)$$

$$= 9{,}680\text{ kip-in.}$$

Step 1.2—Determine Dimension, S_h

Next calculate the distance from the column face to the plastic hinge, S_h, and the distance between plastic hinges, L_h. The height of the stiffener is the same as the height of the end plate above the beam flange, which is shown in Figure 6-13 as h_{st} = 3⅝ in. The length of the stiffener, L_{st}, is calculated using AISC *Prequalified Connections* Equation 6.6-1. For the calculation of the plastic hinge location, assume the end-plate thickness is t_p = 1⅛ in. Later in the design process, this assumption will be checked.

$$L_{st} = \frac{h_{st}}{\tan 30°} \qquad \text{(}\textit{Preq. Conn.}\text{ Eq. 6.6-1)}$$

$$= \frac{3⅝\text{ in.}}{\tan 30°}$$

$$= 6.28\text{ in.} \leq 6½\text{ in.} \quad \textbf{o.k.}$$

$$S_h = L_{st} + t_p \qquad \text{(Preq. Conn. Eq. 6.7-2)}$$
$$= 6\tfrac{1}{2} \text{ in.} + 1\tfrac{1}{8} \text{ in.}$$
$$= 7.63 \text{ in.}$$

$$L_h = L - d_c - 2S_h$$
$$= (30 \text{ ft})(12 \text{ in./ft}) - 15.0 \text{ in.} - 2(7.63 \text{ in.})$$
$$= 330 \text{ in.}$$

Step 1.3—Compute the Shear Force at the Plastic Hinge, V_h

The shear force at the plastic hinge, V_h, can then be calculated as:

$$V_h = \frac{2M_{pr}}{L_h} + V_{gravity} \qquad \text{(Preq. Conn. Eq. 2.4-3)}$$
$$= \frac{2(9{,}680 \text{ kip-in.})}{330 \text{ in.}} + 30.0 \text{ kips}$$
$$= 89.7 \text{ kips}$$

Step 1.4—Compute the Probable Maximum Moment at the Column Face, M_f

The probable maximum moment at the face of the column, M_f, can then be calculated as:

$$M_f = M_{pr} + V_h S_h \qquad \text{(Preq. Conn. Eq. 2.4-4)}$$
$$= 9{,}680 \text{ kip-in.} + (89.7 \text{ kips})(7.63 \text{ in.})$$
$$= 10{,}400 \text{ kip-in.}$$

The value of the probable maximum moment at the face of the column will be used in later steps as the demand for the design of elements of the connection.

Step 1.5—Select Connection Configuration and Establish Geometry

A four-bolt extended stiffened end-plate connection (4ES) configuration is selected. The bolt locations are shown in Figure 6-13 with:

$g = 5\tfrac{1}{2}$ in.
$p_{fo} = 2$ in.
$p_{fi} = 2$ in.

The distances from the centerline of the compression flange to the two bolt lines, h_1 and h_2, are depicted in Figure 6-4 and are computed as:

$$h_1 = d - \frac{t_{bf}}{2} + p_{fo}$$
$$= 23.7 \text{ in.} - \frac{0.590 \text{ in.}}{2} + 2 \text{ in.}$$
$$= 25.4 \text{ in.}$$

$$h_2 = d - \frac{3t_{bf}}{2} - p_{fi}$$
$$= 23.7 \text{ in.} - \frac{3(0.590 \text{ in.})}{2} - 2 \text{ in.}$$
$$= 20.8 \text{ in.}$$

Check that the gage, g, and spacings, p_{fi} and p_{fo}, satisfy the parametric limitations given in Table 6-3 of this Design Guide or AISC *Prequalified Connections* Table 6.1:

3¼ in. ≤ g ≤ 6 in.

g = 5½ in. **o.k.**

1¾ in. ≤ p_{fo} ≤ 5½ in.

p_{fo} = 2 in. **o.k.**

1¾ in. ≤ p_{fi} ≤ 5½ in.

p_{fi} = 2 in. **o.k.**

Step 1.6—Determine Required Bolt Diameter

For a four-bolt extended stiffened connection, use AISC *Prequalified Connections* Equation 6.7-3 to calculate the minimum required bolt diameter. Try Grade A490 bolts with nominal tensile strength F_{nt} = 113 ksi. The resistance factor for nonductile limit states is given in AISC *Prequalified Connections* as $\phi_n = 0.90$.

$$d_{b,req} = \sqrt{\frac{2M_f}{\pi\phi_n F_{nt}(h_1 + h_2)}} \qquad \text{(}\textit{Preq. Conn.}\text{ Eq. 6.7-3)}$$

$$= \sqrt{\frac{2(10{,}400 \text{ kip-in.})}{\pi(0.90)(113 \text{ ksi})(25.4 \text{ in.} + 20.8 \text{ in.})}}$$

$$= 1.19 \text{ in.}$$

Step 1.7—Select Bolt Diameter

Select 1¼-in.-diameter Grade A490 bolts.

d_b = 1¼ in. ≥ $d_{b,req}$ = 1.19 in. **o.k.** (6-3)

Step 1.8—Determine Required End-Plate Thickness

Calculate the dimension, s, using Equation 6-6 and the yield line parameter, Y_p, for this bolt configuration and dimensions. The end-plate width, b_p, must not be taken as larger than the width of the beam flange plus 1.0 in. Because the beam flange width is b_f = 7.04 in., an end-plate width equal to 8.04 in. is used in the following calculations instead of the full width of the end plate, b_p = 9 in. First determine the distance, s, then select the appropriate case from Figure 6-4.

$b_{p,eff} \le b_{bf} + 1$ in. (from Eq. 4-3)

$\le$ 7.04 in. + 1 in.

$\le$ 8.04 in.

Because the upper limit for $b_{p,eff}$ = 8.04 in. is less than the end plate width, b_p = 9 in., use $b_p = b_{p,eff}$ = 8.04 in.

$$s = \frac{\sqrt{b_p g}}{2} \qquad (6\text{-}6)$$

$$= \frac{\sqrt{(8.04 \text{ in.})(5.50 \text{ in.})}}{2}$$

$$= 3.32 \text{ in.}$$

Because d_e = 1⅝ in. is less than s, Case 1 in Figure 6-4(b) applies, and Y_p is determined using Equation 6-8.

$$Y_p = \frac{b_p}{2}\left[h_2\left(\frac{1}{p_{fi}}+\frac{1}{s}\right)+h_1\left(\frac{1}{p_{fo}}+\frac{1}{2d_e}\right)\right]+\frac{2}{g}\left[h_2(p_{fi}+s)+h_1(p_{fo}+d_e)\right] \quad (6\text{-}8)$$

$$=\left(\frac{8.04\text{ in.}}{2}\right)\left\{(20.8\text{ in.})\left(\frac{1}{2\text{ in.}}+\frac{1}{3.32\text{ in.}}\right)+(25.4\text{ in.})\left[\frac{1}{2\text{ in.}}+\frac{1}{2(1⅝\text{ in.})}\right]\right\}$$

$$+\left(\frac{2}{5½\text{ in.}}\right)\left[(20.8\text{ in.})(2\text{ in.}+3.32\text{ in.})+(25.4\text{ in.})(2\text{ in.}+1⅝\text{ in.})\right]$$

$$=223\text{ in.}$$

Compute the required end-plate thickness using AISC *Prequalified Connections* Equation 6.7-5. The resistance factor for ductile limit states is given in AISC *Prequalified Connections* as $\phi_d = 1.00$, and the yield stress of the end plate is given as $F_{yp} = 50$ ksi.

$$t_{p,req} = \sqrt{\frac{1.11M_f}{\phi_d F_{yp} Y_p}} \quad (\textit{Preq. Conn.}\text{ Eq. 6.7-5})$$

$$=\sqrt{\frac{1.11(10{,}400\text{ kip-in.})}{1.00(50\text{ ksi})(223\text{ in.})}}$$

$$=1.02\text{ in.}$$

Step 1.9—Select End-Plate Thickness

Select an end-plate thickness, $t_p = 1⅛$ in., and width, $b_p = 9$ in.

$$t_p = 1⅛\text{ in.} \quad \geq \quad t_{p,req} = 1.02\text{ in.} \quad \textbf{o.k.} \quad (6\text{-}5)$$

Now that the end-plate thickness, t_p, and width, b_p, have been established, it is necessary to check that they fall within the parametric limitations listed in Table 6-3 of this Design Guide and AISC *Prequalified Connections* Table 6.1.

$½\text{ in.} \leq t_p \leq 1½\text{ in.}$

$t_p = 1⅛\text{ in.}$ **o.k.**

$7\text{ in.} \leq b_p \leq 10¾\text{ in.}$

$b_p = 9\text{ in.}$ **o.k.**

Step 1.10—Calculate the Beam Flange Force

Use AISC *Prequalified Connections* Equation 6.7-6 to calculate the factored beam flange force, F_{fu}.

$$F_{fu} = \frac{M_f}{d - t_{bf}} \quad (\textit{Preq. Conn.}\text{ Eq. 6.7-6})$$

$$=\frac{10{,}400\text{ kip-in.}}{23.7\text{ in.} - 0.590\text{ in.}}$$

$$=450\text{ kips}$$

Step 1.11—Check Shear Yielding of Extended Portion of End Plate

Step 1.11 is related to shear failure of the extended portion of the end plate. Because the end plate is stiffened, this limit state does not apply.

Step 1.12—Check Shear Rupture of Extended Portion of End Plate

Similarly, this step is also related to shear failure of the extended portion of the end plate and thus does not apply for stiffened end plates.

Step 1.13—Select Stiffener Thickness and Design Stiffener Welds

Calculate the minimum stiffener thickness using AISC *Prequalified Connections* Equation 6.7-9.

$$t_{s,req} = t_{bw}\left(\frac{F_{yb}}{F_{ys}}\right) \qquad \text{(from } \textit{Preq. Conn.} \text{ Eq. 6.7-9)}$$

$$= (0.430 \text{ in.})\left(\frac{50 \text{ ksi}}{50 \text{ ksi}}\right)$$

$$= 0.430 \text{ in.}$$

Select a ½-in.-thick stiffener.

$t_s = ½$ in. $\geq$ $t_{s,req} = 0.430$ in. **o.k.**

Check that the stiffener geometry satisfies the local buckling check in AISC *Prequalified Connections* Equation 6.7-10. The height of the stiffener is shown in Figure 6-13 as $h_{st} = 3⅝$ in.

$$\frac{h_{st}}{t_s} = \frac{3⅝ \text{ in.}}{½ \text{ in.}}$$

$$= 7.25$$

$$0.56\sqrt{\frac{E}{F_{ys}}} = 0.56\sqrt{\frac{29{,}000 \text{ ksi}}{50 \text{ ksi}}}$$

$$= 13.5$$

$$\frac{h_{st}}{t_s} = 7.25 \leq 0.56\sqrt{\frac{E}{F_{ys}}} = 13.5 \quad \textbf{o.k.} \qquad \text{(}\textit{Preq. Conn.}\text{ Eq. 6.7-10)}$$

AISC *Prequalified Connections* states that if the stiffener is thicker than ⅜ in., then CJP groove welds are required between the stiffener and end plate. CJP groove welds are therefore required between the stiffener and end plate. Fillet welds are acceptable for the weld of the stiffener to the beam flange and must be designed to develop the stiffener plate in shear. The demand, R_u, is calculated in terms of shear force per unit length as follows.

$$R_u = 0.60F_{ys}t_s \qquad \text{(from } \textit{Spec.} \text{ Eq. J4-3)}$$

$$= 0.60(50 \text{ ksi})(½ \text{ in.})$$

$$= 15.0 \text{ kips/in.}$$

Use a double-sided ⅜ in. fillet weld from the stiffener to the beam flange.

$$R_n = (2 \text{ welds})(0.60F_{EXX})\left(\frac{t_{ws}}{\sqrt{2}}\right)(1.0 + 0.5\sin^{1.5}\theta) \qquad \text{(from } \textit{Spec.} \text{ Eq. J2-4)}$$

$$= (2 \text{ welds})(0.60)(70 \text{ ksi})\left(\frac{⅜ \text{ in.}}{\sqrt{2}}\right)(1.0 + 0.5\sin^{1.5} 0°)$$

$$= 22.3 \text{ kips/in.}$$

$$\phi R_n = 0.75(22.3 \text{ kips/in.})$$

$$= 16.7 \text{ kips/in.}$$

$\phi R_n = 16.7$ kips/in. $\geq$ $R_u = 15.0$ kips/in. **o.k.**

Step 1.14—Check Beam Shear Strength

The required shear strength for the beam was calculated in Step 1.3 as $V_u = 89.7$ kips. Calculate the design shear strength of the beam using AISC *Specification* G2.1(a). Because the W24×62 is not included in the list in the User Note, the section meets the criteria for G2.1(a) for $F_y = 50$ ksi, and thus, $\phi_v = 1.00$ and $C_{v1} = 1.0$. The design shear strength is given as:

$$V_n = 0.6F_yA_wC_{v1} \qquad \text{(Spec. Eq. G2-1)}$$
$$= 0.6F_ydt_{bw}C_{v1}$$
$$= 0.6(50 \text{ ksi})(23.7 \text{ in.})(0.430 \text{ in.})(1.0)$$
$$= 306 \text{ kips}$$

$$\phi_vV_n = 1.00(306 \text{ kips})$$
$$= 306 \text{ kips}$$

$$V_u = 89.7 \text{ kips} \quad \leq \quad \phi_vV_n = 306 \text{ kips} \quad \textbf{o.k.}$$

Step 1.15—Determine the Required Shear Strength, V_u

The vertical shear demand at the end-plate connection was calculated in Step 1.3 to be $V_u = 89.7$ kips.

Step 1.16—Bolt Shear Rupture Strength

The vertical shear demand at the end-plate connection, V_u, was calculated in Step 1.3. The design shear strength, ϕ_nR_n, is given by AISC *Prequalified Connections* Equation 6.7-11 as the shear strength of the four bolts at the compression flange. The nominal shear strength of Grade A490 bolts is $F_{nv} = 68$ ksi. The area of a 1¼-in.-diameter bolt is 1.23 in.^{2}

$$\phi_nR_n = \phi_nn_bF_{nv}A_b \qquad \text{(from Preq. Conn. Eq. 6.7-11)}$$
$$= 0.90(4 \text{ bolts})(68 \text{ ksi})(1.23 \text{ in.}^2)$$
$$= 301 \text{ kips}$$

$$V_u = 89.7 \text{ kips} \quad \leq \quad \phi_nR_n = 301 \text{ kips} \quad \textbf{o.k.}$$

Step 1.17—Bearing/Tearout Failure of End Plate and Column Flange

Similar to the previous step, the vertical shear demand at the end-plate connection, V_u, was calculated in Step 1.3. The design bearing/tearout strength, ϕ_nR_n, is given by AISC *Prequalified Connections* Equation 6.7-12. Because vertical shear is assumed to be resisted only by the compression side bolts, bearing/tearout is checked at the bottom bolt hole locations for the shear loading shown in Figure 6-13. By inspection, tearout will not control at the end plate, and therefore, only bolt bearing needs to be checked in the example. The same is true at the column flange if a continuity plate is used. If not, tearout must be checked between the bottom bolt holes. As found later in the example, continuity plates are not required. Because the end-plate thickness, 1⅛ in., is less than the column flange thickness, 1.19 in., bearing must be checked at the end plate and bearing/tearout checked at the column flange.

At the end plate:

$$r_n = 2.4d_bt_pF_{up} \qquad \text{(from Spec. Eq. J3-6a)}$$
$$= 2.4(1¼ \text{ in.})(1⅛ \text{ in.})(65 \text{ ksi})$$
$$= 219 \text{ kips}$$

$$\phi_nR_n = \phi_nnr_n \qquad \text{(from Preq. Conn. Eq. 6.7-12)}$$
$$= 0.90(4 \text{ bolts})(219 \text{ kips})$$
$$= 788 \text{ kips}$$

$$V_u = 89.7 \text{ kips} \quad \leq \quad \phi_nR_n = 788 \text{ kips} \quad \textbf{o.k.}$$

At column flange between bottom bolt holes where the nominal strength is the minimum of the nominal tearout and bearing strengths:

$$l_{ci} = p_{fo} + t_{bf} + p_{fi} - (d_b + \text{⅛ in.})$$
$$= 2 \text{ in.} + 0.590 \text{ in.} + 2 \text{ in.} - (1\text{¼ in.} + \text{⅛ in.})$$
$$= 3.22 \text{ in.}$$

$$r_{ni} = \min(1.2 l_{ci} t_{cf} F_{uc}, 2.4 d_b t_{cf} F_{uc})$$
$$= \min\left[1.2(3.22 \text{ in.})(1.19 \text{ in.})(65 \text{ ksi}),\ 2.4(1\text{¼ in.})(1.19 \text{ in.})(65 \text{ ksi})\right]$$
$$= \min(299 \text{ kips}, 232 \text{ kips})$$
$$= 232 \text{ kips}$$

At column flange bottom bolt holes:

$$r_{no} = 2.4 d_b t_{cf} F_{uc} \qquad \text{(from } \textit{Spec.} \text{ Eq. J3-6a)}$$
$$= 2.4(1\text{¼ in.})(1.19 \text{ in.})(65 \text{ ksi})$$
$$= 232 \text{ kips}$$

$$\phi_n R_n = \phi_n n_i r_{ni} + \phi_n n_o r_{no}$$
$$= 0.90(2 \text{ bolts})(232 \text{ kips}) + 0.90(2 \text{ bolts})(232 \text{ kips})$$
$$= 835 \text{ kips}$$

$R_u = 89.7 \text{ kips} \quad \le \quad \phi_n R_n = 835 \text{ kips}$ **o.k.** (from *Preq. Conn.* Eq.6.7-12)

Note: The User Note in AISC *Specification* Section J3.7 recommends that the effective strength of an individual bolt be taken as the lesser of the bolt shear strength, bearing strength, or tearout strength at the bolt hole. For this example, the effective shear strength of the top or bottom bolts is the design shear strength of four bolts, 301 kips.

Step 1.18—Design the Welds

In this step, design the welds of the beam to the end plate. In accordance with AISC *Prequalified Connections* Section 6.6.6(2), the beam flange to end-plate welds are made using a CJP groove weld (bevel facing away from the center of the beam) without weld access holes and without back-up bars. The inside face of the flange will have a 5⁄16 in. reinforcing fillet weld. These welds are the only welds that need to be considered demand critical.

The beam web to end-plate weld is designed in two parts. The web weld from the point nearest the flange to a point 6 in. beyond the most interior bolt row should either be CJP groove welds or fillet welds that develop the full strength of the web in tension. Try double-sided ⅜ in. fillet welds with $\phi = 0.75$:

$$R_u = F_{yb} t_{bw} \qquad \text{(from } \textit{Spec.} \text{ Eq. J4-1)}$$
$$= (50 \text{ ksi})(0.430 \text{ in.})$$
$$= 21.5 \text{ kips/in.}$$

$$R_n = (2 \text{ welds})(0.60 F_{EXX})\left(\frac{t_{weld}}{\sqrt{2}}\right)(1.0 + 0.5 \sin^{1.5}\theta) \qquad \text{(from } \textit{Spec.} \text{ Eq. J2-4)}$$
$$= (2 \text{ welds})(0.60)(70 \text{ ksi})\left(\frac{\text{⅜ in.}}{\sqrt{2}}\right)(1.0 + 0.5 \sin^{1.5} 90°)$$
$$= 33.4 \text{ kips/in.}$$

$$\phi R_n = 0.75(33.4 \text{ kips/in.})$$
$$= 25.1 \text{ kips/in.}$$

$R_u = 21.5 \text{ kips/in.} \quad \le \quad \phi R_n = 25.1 \text{ kips/in.}$ **o.k.**

The beam web to end-plate weld outside the tension zone is designed for the shear demand and is typically smaller. From Step 1.3, the shear demand is 89.7 kips. By inspection, the weld strength provided by the ⅜ in. doubled-sided weld required to develop the yield strength of the weld at the top and bottom bolts is more than sufficient to resist this shear demand.

Use double-sided ⅜ in. fillet welds the full depth of the beam web.

Part 2. Column-Side Design

Step 2.1—Column Flange Flexural Yielding

The beam and end-plate checks are complete. The following is the column-side design. First, check the column flange for flexural yielding. Preliminary calculations (not shown here) determined that a W14×109 column would be sufficient if continuity plates and doubler plates are used. Similar preliminary calculations showed that a W14×159 column would be sufficient without any continuity plates or doubler plates. The expense of cutting, installing, welding, and inspecting continuity plates and doubler plates may outweigh the 46% increase in column weight. Some fabricators have reported that a 50% increase in column size is more economical than the use of continuity plates and doubler plates. Designing the most economical moment frames should consider the connection expense, and beam and column sizes should be selected accordingly. For this example, select a W14×159 column and use the unstiffened column flange yield line parameter, Equation 6-15, to determine if the W14×159 column flange thickness is sufficient.

$$s = \frac{\sqrt{b_{cf}\, g}}{2} \tag{6-14}$$

$$= \frac{\sqrt{(15.6\text{ in.})(5\tfrac{1}{2}\text{ in.})}}{2}$$

$$= 4.63\text{ in.}$$

$$c = p_{fi} + t_{bf} + p_{fo}$$

$$= 2\text{ in.} + 0.590\text{ in.} + 2\text{ in.}$$

$$= 4.59\text{ in.}$$

$$Y_{cu} = \frac{b_{cf}}{2}\left[h_2\left(\frac{1}{s}\right) + h_1\left(\frac{1}{s}\right)\right] + \frac{2}{g}\left[h_2\left(s + \frac{3c}{4}\right) + h_1\left(s + \frac{c}{4}\right) + \frac{c^2}{2}\right] + \frac{g}{2} \tag{6-15}$$

$$= \left(\frac{15.6\text{ in.}}{2}\right)\left[(20.8\text{ in.})\left(\frac{1}{4.63\text{ in.}}\right) + (25.4\text{ in.})\left(\frac{1}{4.63\text{ in.}}\right)\right]$$

$$+ \left(\frac{2}{5\tfrac{1}{2}\text{ in.}}\right)\left\{(20.8\text{ in.})\left[4.63\text{ in.} + \frac{3(4.59\text{ in.})}{4}\right] + (25.4\text{ in.})\left(4.63\text{ in.} + \frac{4.59\text{ in.}}{4}\right) + \frac{(4.59\text{ in.})^2}{2}\right\} + \frac{5\tfrac{1}{2}\text{ in.}}{2}$$

$$= 199\text{ in.}$$

$$t_{cf,req} = \sqrt{\frac{1.11 M_f}{\phi_d F_{yc} Y_{cu}}} \qquad \text{(from } \textit{Preq. Conn.} \text{ Eq. 6.7-13)}$$

$$= \sqrt{\frac{1.11(10{,}400\text{ kip-in.})}{(1.00)(50\text{ ksi})(199\text{ in.})}}$$

$$= 1.08\text{ in.}$$

$$t_{cf} = 1.19\text{ in.} \quad \geq \quad t_{cf,req} = 1.08\text{ in.} \tag{6-13}$$

Column flange stiffeners are not required for this limit state.

Step 2.2—Column Flange Available Strength for Continuity Plate Demand

The column flange yield line parameter is used to compute the beam flange force that is associated with column flange flexural yielding. If the column flange flexural yielding strength is not sufficient, this force is used later in Step 2.5 to determine the

continuity plates required strength. From Step 2.1, continuity plates are not required for this example. The following calculations are shown to demonstrate how the force is calculated if continuity plates are required for a connection.

Calculate the available strength of the column flange using AISC *Prequalified Connections* Equations 6.7-14 and 6.7-15.

$$\phi_d M_{cf} = \phi_d F_{yc} Y_c t_{cf}^2 \qquad \text{(Preq. Conn. Eq. 6.7-14)}$$

$$= 1.00(50 \text{ ksi})(199 \text{ in.})(1.19 \text{ in.})^2$$

$$= 14{,}100 \text{ kip-in.}$$

$$\phi_d R_n = \frac{\phi_d M_{cf}}{(d - t_{bf})} \qquad \text{(Preq. Conn. Eq. 6.7-15)}$$

$$= \frac{14{,}100 \text{ kip-in.}}{(23.7 \text{ in.} - 0.590 \text{ in.})}$$

$$= 610 \text{ kips}$$

$$\phi_d R_n = 610 \text{ kips} > F_{fu} = 450 \text{ kips}$$

Because $\phi_d R_n > F_{fu}$, continuity plates are not required.

Step 2.3—Local Column Web Yielding

Check the local column web yielding design strength against the calculated flange force from Step 1.10, F_{fu} = 450 kips, using AISC *Prequalified Connections* Equations 6.7-16 and 6.7-17. This calculation is performed assuming no continuity plates exist. If the check is satisfied, then continuity plates are not necessary. If the check is not satisfied, then the difference between the required strength and the unstiffened column available strength will be used in Step 2.5 to find the required strength for the continuity plates. Because the distance from the top of the beam flange to the top of the column is greater than the depth of the beam, a value of $C_t = 1.0$ is used. The effective width of bearing, l_b, includes the size of the reinforcing fillet, w, from the beam flange to end-plate CJP groove weld.

$$l_b = t_{bf} + w + 2t_p$$

$$= 0.590 \text{ in.} + 5/16 \text{ in.} + 2(1\,1/8 \text{ in.})$$

$$= 3.15 \text{ in.}$$

$$R_n = (6C_t k_c + l_b) F_{yc} t_{cw} \qquad \text{(Preq. Conn. Eq. 6.7-17)}$$

$$= \left[6(1.0)(1.79 \text{ in.}) + 3.15 \text{ in.}\right](50 \text{ ksi})(0.745 \text{ in.})$$

$$= 517 \text{ kips}$$

$$\phi_d R_n = 1.00(517 \text{ kips})$$

$$= 517 \text{ kips}$$

$$\phi_d R_n = 517 \text{ kips} \geq F_{fu} = 450 \text{ kips} \qquad \text{(Preq. Conn. Eq. 6.7-16)}$$

Because $\phi_d R_n > F_{fu}$, continuity plates are not required.

Step 2.4—Column Web Crippling

As was done in Step 2.3, the column web crippling available strength is evaluated assuming no continuity plates. If the check is satisfied, then continuity plates are not required. AISC *Prequalified Connections* Equation 6.7-19 is used to compute web crippling available strength.

$$R_n = 0.80 t_{cw}^2 \left[1 + 3\left(\frac{l_b}{d_c}\right)\left(\frac{t_{cw}}{t_{cf}}\right)^{1.5}\right]\sqrt{\frac{EF_{yc}t_{cf}}{t_{cw}}} \qquad \text{(Preq. Conn. Eq. 6.7-19)}$$

$$= 0.80(0.745 \text{ in.})^2 \left[1 + 3\left(\frac{3.15 \text{ in.}}{15.0 \text{ in.}}\right)\left(\frac{0.745 \text{ in.}}{1.19 \text{ in.}}\right)^{1.5}\right]\sqrt{\frac{(29{,}000 \text{ ksi})(50 \text{ ksi})(1.19 \text{ in.})}{0.745 \text{ in.}}}$$

$$= 887 \text{ kips}$$

$$\phi R_n = 0.75(887 \text{ kips})$$

$$= 665 \text{ kips}$$

$$\phi R_n = 665 \text{ kips} > F_{fu} = 450 \text{ kips} \qquad \text{(Preq. Conn. Eq. 6.7-18)}$$

Because $\phi R_n > F_{fu}$, continuity plates are not required.

Step 2.5—Continuity Plate Design

Steps 2.1 through 2.4 indicate that continuity plates are not required.

Step 2.6—Panel Zone Shear

The panel zone is checked in accordance with AISC *Seismic Provisions* Section E3.6e(1). The panel zone shear is similar to that shown in Figure 3.15(b). The panel zone required shear strength is the flange force, F_{fu}, less the column shear, V_{uc}, and half the axial force, P_{ub}.

$$V_{upz} = F_{fu} - V_{uc} - \frac{P_{ub}}{2}$$

$$= 450 \text{ kips} - 69.0 \text{ kips} - \frac{28.0 \text{ kips}}{2}$$

$$= 367 \text{ kips}$$

The panel zone design strength is calculated according to AISC *Specification* Section J10.6, but using a resistance factor, ϕ_d = 1.00, according to the AISC *Seismic Provisions* Section E3.6e(1). First, find the column required axial strength, P_u, and the ratio of this required axial strength to the column axial yield strength of the column, P_y.

$$P_{uc,total} = P_{uc} + V_{ub}$$

$$= 10.0 \text{ kips} + 89.7 \text{ kips}$$

$$= 99.7 \text{ kips}$$

$$P_y = F_{yc} A_{gc}$$

$$= (50 \text{ ksi})(46.7 \text{ in.}^2)$$

$$= 2{,}340 \text{ kips}$$

$$\frac{P_{uc,total}}{P_y} = \frac{99.7 \text{ kips}}{2{,}340 \text{ kips}}$$

$$= 0.0426$$

Because it is assumed that frame stability was assessed including plastic panel zone deformation, and that the ratio P_{uc}/P_y is equal to 0.0426, which is less than 0.75, then AISC *Specification* Equation J10-11 is used to determine the panel zone nominal strength.

$$R_n = 0.60F_{yc}d_c t_{cw}\left(1+\frac{3b_{cf}t_{cf}^2}{dd_c t_{cw}}\right) \quad \text{(Spec. Eq. J10-11)}$$

$$= 0.60(50\text{ ksi})(15.0\text{ in.})(0.745\text{ in.})\left[1+\frac{3(15.6\text{ in.})(1.19\text{ in.})^2}{(23.7\text{ in.})(15.0\text{ in.})(0.745\text{ in.})}\right]$$

$$= 419\text{ kips}$$

$$\phi_d R_n = 1.00(419\text{ kips})$$

$$= 419\text{ kips}$$

$V_{upz} = 367\text{ kips} \quad \leq \quad \phi_d R_n = 419\text{ kips}$ **o.k.**

Additionally, check that the column web satisfies the minimum panel zone thickness given in AISC *Seismic Provisions* Section E3.6e(2).

$$d_z = d - 2t_{bf}$$

$$= 23.7\text{ in.} - 2(0.590\text{ in.})$$

$$= 22.5\text{ in.}$$

$$w_z = d_c - 2t_{cf}$$

$$= 15.0\text{ in.} - 2(1.19\text{ in.})$$

$$= 12.6\text{ in.}$$

$$t_{cw,req} = \frac{d_z + w_z}{90}$$

$$= \frac{22.5\text{ in.} + 12.6\text{ in.}}{90}$$

$$= 0.390\text{ in.}$$

$t_{cw} = 0.745\text{ in.} \quad \geq \quad t_{cw,req} = 0.390\text{ in.}$ **o.k.** (from *Prov.* Eq. E3-6)

Step 2.7—Strong-Column/Weak-Beam Check

Evaluate whether the strong-column/weak-beam moment ratio requirement of AISC *Seismic Provisions* Section E3.4a is satisfied.

From Step 2.6:

$$P_{uc,total} = 99.7\text{ kips}$$

$$\sum M_{pc}^* = \sum Z_c\left(F_{yc} - \alpha_s\frac{P_{uc,total}}{A_{gc}}\right) \quad \text{(from Prov. Eq. E3-2)}$$

$$= 2(287\text{ in.}^3)\left[50\text{ ksi} - 1.0\left(\frac{99.7\text{ kips}}{46.7\text{ in.}^2}\right)\right]$$

$$= 27{,}500\text{ kip-in.}$$

$$M_v = V_u\left(S_h + \frac{d_c}{2}\right)$$

$$= (89.7\text{ kips})\left(7.63\text{ in.} + \frac{15.0\text{ in.}}{2}\right)$$

$$= 1{,}360\text{ kip-in.}$$

$$\sum M_{be}^{*} = \sum (M_{pr} + \alpha_s M_v) \qquad \text{(Prov. Eq. E3-3)}$$

$$= 9{,}680 \text{ kip-in.} + 1.0(1{,}360 \text{ kip-in.})$$

$$= 11{,}000 \text{ kip-in.}$$

$$\frac{M_{pc}^{*}}{M_{be}^{*}} = \frac{27{,}500 \text{ kip-in.}}{11{,}000 \text{ kip-in.}} \geq 1.0 \qquad \text{(Prov. Eq. E3-1)}$$

$$= 2.50 \quad \geq \quad 1.0 \quad \textbf{o.k.}$$

Summary

The final design of the connection is shown in Figure 6-14.

EXAMPLE 6.3-3—Eight-Bolt Extended Stiffened End-Plate Example

Given:

The seismic example shown in Figure 6-15 is an eight-bolt extended stiffened (8ES) end-plate connection for a W36×150 beam in a bay that is 40 ft centerline to centerline of W18×258 columns. The moment connection is single sided, and the column extends above the connection. The beam and column are ASTM A992/A992M steel and the plate is ASTM A572/A572M Grade 50 steel. The connection is subjected to the following forces:

Beam axial tension/compression	P_{ub}	= 40.0 kips
Vertical beam shear due to factored gravity loads	$V_{gravity}$	= 30.0 kips
Column compression due to gravity loads	P_{uc}	= 50.0 kips
Column shear above connection	V_{uc}	= 540 kips

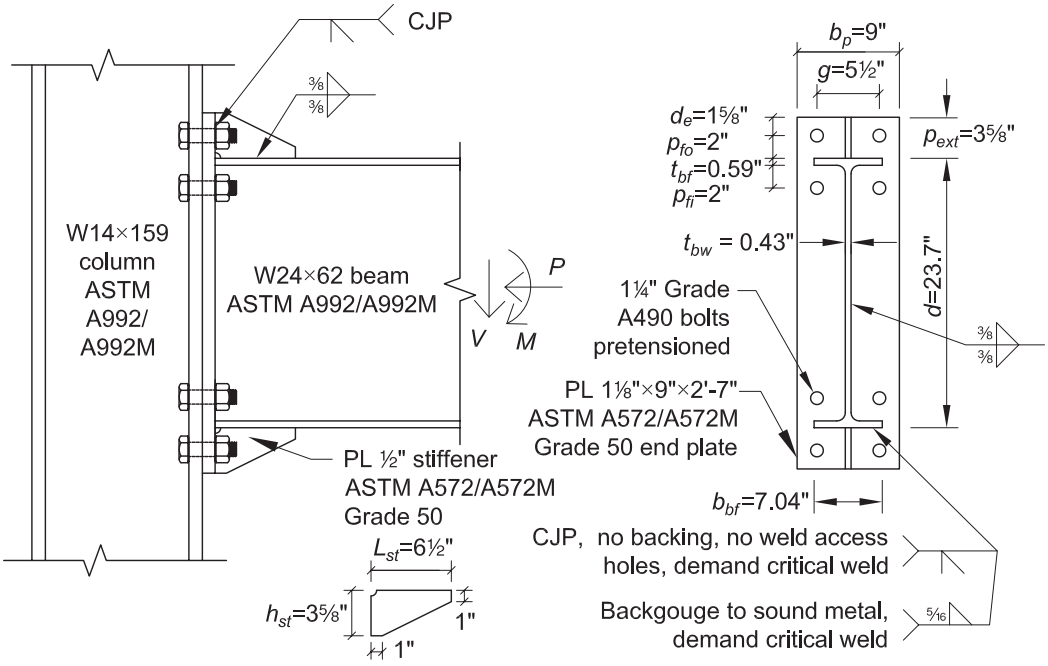

Fig. 6-14. Summary of final design for 4ES seismic end-plate configuration.

Solution:

From AISC *Manual* Table 2-4, the material properties are as follows:

ASTM A992/A992M
$F_y = 50$ ksi
$F_u = 65$ ksi

ASTM A572/A572M Grade 50
$F_y = 50$ ksi
$F_u = 65$ ksi

From AISC *Specification* Table J3.2, the material properties of the bolts are as follows:

Group 150 ASTM F3125/F3125M Grade A490 pretensioned
$F_{nt} = 113$ ksi
$F_{nv} = 68$ ksi (Group 150 bolts with threads not excluded from the shear plane; thread condition N)

From AISC *Manual* Table 1-1, the geometric properties are as follows:

Beam: W36×150
$A_b = 44.3$ in.^{2} $d = 35.9$ in. $t_{bw} = 0.625$ in. $b_{bf} = 12.0$ in.
$t_{bf} = 0.940$ in. $Z_b = 581$ in.^{3}

Column: W18×258
$A_c = 76.0$ in.^{2} $d_c = 21.5$ in. $t_{cw} = 1.28$ in. $b_{cf} = 11.8$ in.
$t_{cf} = 2.30$ in. $k_{des} = 2.70$ in. $Z_c = 611$ in.^{3}

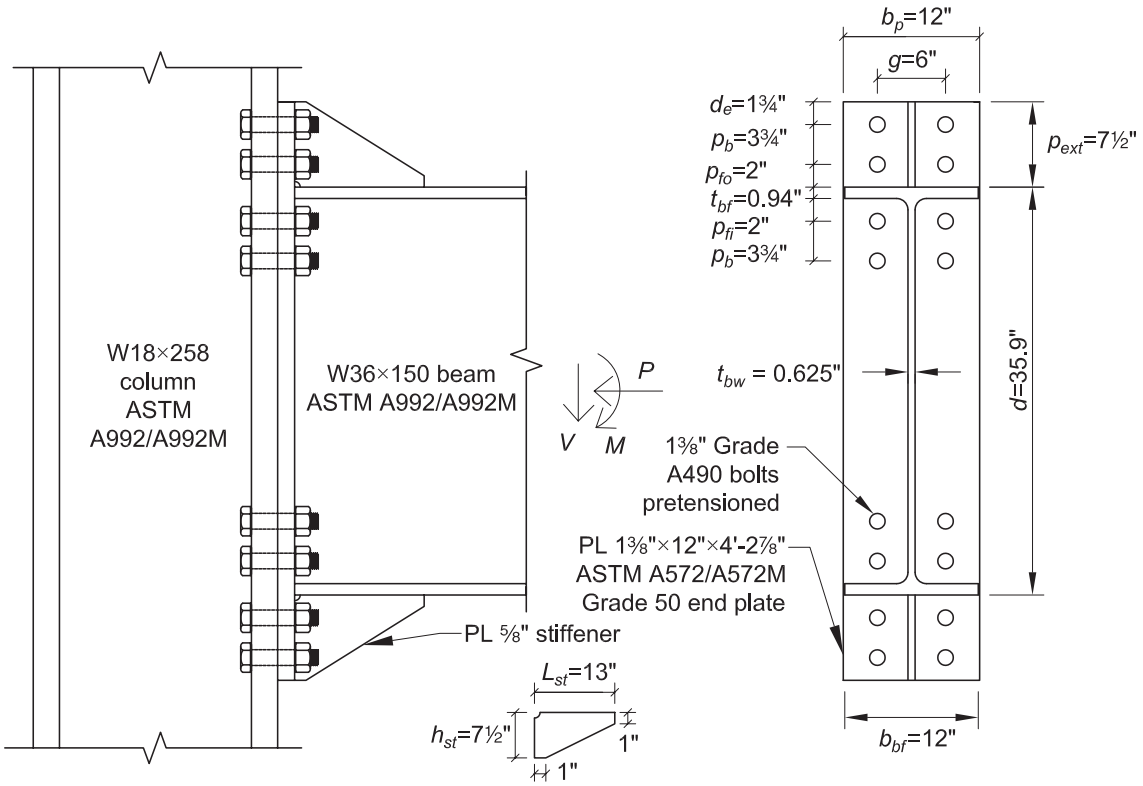

Fig. 6-15. 8ES seismic end-plate configuration for Example 6.3-3.

End-plate geometric properties:

b_p = 12 in.
g = 6 in.
p_{ext} = 7½ in.
d_e = 1¾ in.
p_{fo} = 2 in.
p_{fi} = 2 in.
p_b = 3¾ in.
d_p = 50⅞ in.

This example follows the Design Procedure given in AISC *Prequalified Connections*. The design is split into two parts: Part 1 is End-Plate and Bolt Design, and Part 2 is Column-Side Design.

Part 1. End-Plate and Bolt Design

Step 1.1—Compute Probable Maximum Moment, M_{pr}

The beam and column are given as ASTM A992/A992M W36×150 and W18×258, respectively. Because the beam section is listed in Table 6-2, the flange of the section satisfies highly ductile section compactness. For the web to satisfy highly ductile section criteria, the required axial force in the beam has to be less than $P_{u,max}$, listed in Table 6-2. Determine whether the beam web satisfies highly ductile section compactness:

$P_{u\,max}$ = 105 kips for W36×150 from Table 6-2

P_{ub} = 40 kips < $P_{u\,max}$ **o.k.**

The W18×258 column flange and column web were checked using the procedure shown for the beam in Example 6.3-1 and found to satisfy highly ductile section criteria.

Now check that the beam flange thickness, t_{bf}, flange width, b_{bf}, and depth, d, satisfy the parametric limitations on prequalification given in Table 6-1 of this Design Guide and AISC *Prequalified Connections* Table 6.1:

⅜ in. ≤ t_{bf} ≤ 1 in.
t_{bf} = 0.940 in. **o.k.**

7½ in. ≤ b_{bf} ≤ 12¼ in.
b_{bf} = 12.0 in. **o.k.**

18 in. ≤ d ≤ 36 in.
d = 35.9 in. **o.k.**

It is also necessary to check that the clear span-to-depth ratio of the beam is greater than or equal to 7:

$$\frac{L_c}{d} = \frac{L - d_c}{d}$$
$$= \frac{40\text{ ft}(12\text{ in./ft}) - 21.5\text{ in.}}{35.9\text{ in.}}$$
$$= 12.8 \geq 7 \quad \textbf{o.k.}$$

Calculate the probable moment at the plastic hinge, M_{pr}. From AISC *Seismic Provisions* Table A3.2, R_y = 1.1.

$$C_{pr} = \frac{F_{yb} + F_{ub}}{2F_{yb}} \leq 1.2 \qquad \text{(}\textit{Preq. Conn.}\text{ Eq. 2.4-2)}$$
$$= \frac{50\text{ ksi} + 65\text{ ksi}}{2(50\text{ ksi})}$$
$$= 1.15 \leq 1.2$$

$$M_{pr} = C_{pr} R_y F_{yb} Z_b \quad \text{(from } \textit{Preq. Conn.} \text{ Eq. 2.4-1)}$$
$$= 1.15(1.1)(50 \text{ ksi})(581 \text{ in.}^3)$$
$$= 36{,}700 \text{ kip-in.}$$

Step 1.2—Determine Dimension, S_h

Next calculate the distance from the column face to the plastic hinge, S_h, and the distance between plastic hinges, L_h. The height of the stiffener is the same as the height of the end plate above the beam flange, which is shown in Figure 6-15 as $h_{st} = 7\frac{1}{2}$ in. The length of the stiffener, L_{st}, is calculated using AISC *Prequalified Connections* Equation 6.6-1. For the calculation of the plastic hinge location, assume the end-plate thickness is $t_p = 1\frac{3}{8}$ in. Later in the design process, this assumption will be checked.

$$L_{st} = \frac{h_{st}}{\tan 30°} \quad \text{(}\textit{Preq. Conn.} \text{ Eq. 6.6-1)}$$
$$= \frac{7\frac{1}{2} \text{ in.}}{\tan 30°}$$
$$= 13.0 \text{ in.} \quad \leq \quad 13 \text{ in.} \quad \textbf{o.k.}$$

$$S_h = L_{st} + t_p \quad \text{(}\textit{Preq. Conn.} \text{ Eq. 6.7-2)}$$
$$= 13 \text{ in.} + 1\frac{3}{8} \text{ in.}$$
$$= 14.4 \text{ in.}$$

$$L_h = L - d_c - 2S_h$$
$$= 40 \text{ ft}(12 \text{ in./ft}) - 21.5 \text{ in.} - 2(14.4 \text{ in.})$$
$$= 430 \text{ in.}$$

Step 1.3—Compute the Shear Force at the Plastic Hinge, V_h

The shear force at the plastic hinge, V_h, can then be calculated as:

$$V_h = \frac{2M_{pr}}{L_h} + V_{gravity} \quad \text{(}\textit{Preq. Conn.} \text{ Eq. 2.4-3)}$$
$$= \frac{2(36{,}700 \text{ kip-in.})}{430 \text{ in.}} + 30.0 \text{ kips}$$
$$= 201 \text{ kips}$$

Step 1.4—Compute the Probable Maximum Moment at the Column Face, M_f

The probable maximum moment at the face of the column, M_f, can then be calculated as:

$$M_f = M_{pr} + V_h S_h \quad \text{(}\textit{Preq. Conn.} \text{ Eq. 2.4-4)}$$
$$= 36{,}700 \text{ kip-in.} + (201 \text{ kips})(14.4 \text{ in.})$$
$$= 39{,}600 \text{ kip-in.}$$

The value of the probable maximum moment at the face of the column will be used in later steps as the demand for the design of elements of the connection.

Step 1.5—Select Connection Configuration and Establish Geometry

An eight-bolt extended stiffened end-plate connection (8ES) configuration is selected. The bolt locations are shown in Figure 6-15 with:

g = 6 in.
p_{fo} = 2 in.
p_{fi} = 2 in.
p_b = 3¾ in.

The distances from the centerline of the compression flange to the four bolt lines, h_1, h_2, h_3, and h_4, are depicted in Figure 6-5 and are computed as:

$$h_1 = d - \frac{t_{bf}}{2} + p_{fo} + p_b$$
$$= 35.9 \text{ in.} - \frac{0.940 \text{ in.}}{2} + 2 \text{ in.} + 3¾ \text{ in.}$$
$$= 41.2 \text{ in.}$$

$$h_2 = d - \frac{t_{bf}}{2} + p_{fo}$$
$$= 35.9 \text{ in.} - \frac{0.940 \text{ in.}}{2} + 2 \text{ in.}$$
$$= 37.4 \text{ in.}$$

$$h_3 = d - \frac{3t_{bf}}{2} - p_{fi}$$
$$= 35.9 \text{ in.} - \frac{3(0.940 \text{ in.})}{2} - 2 \text{ in.}$$
$$= 32.5 \text{ in.}$$

$$h_4 = d - \frac{3t_f}{2} - p_{fi} - p_b$$
$$= 35.9 \text{ in.} - \frac{3(0.940 \text{ in.})}{2} - 2 \text{ in.} - 3¾ \text{ in.}$$
$$= 28.7 \text{ in.}$$

Check that the gage, g, and spacings, p_{fi}, p_{fo}, and p_b, satisfy the parametric limitations given in Table 6-3 of this Design Guide and AISC *Prequalified Connections* Table 6.1:

5 in. ≤ g ≤ 6 in.
g = 6 in. **o.k.**

1⅝ in. ≤ p_{fo} ≤ 2 in.
p_{fo} = 2 in. **o.k.**

1⅝ in. ≤ p_{fi} ≤ 2 in.
p_{fi} = 2 in. **o.k.**

3½ in. ≤ p_{fi} ≤ 3¾ in.
p_{fi} = 3¾ in. **o.k.**

Step 1.6—Determine Required Bolt Diameter

For an eight-bolt extended stiffened connection, use AISC *Prequalified Connections* Equation 6.7-4 to calculate the minimum required bolt diameter. Try Grade A490 bolts with nominal tensile strength F_{nt} = 113 ksi. The resistance factor for nonductile limit states is given in AISC *Prequalified Connections* as ϕ_n = 0.90.

$$d_{b,req} = \sqrt{\frac{2M_f}{\pi\phi_n F_{nt}(h_1+h_2+h_3+h_4)}} \qquad \text{(}\textit{Preq. Conn.}\text{ Eq. 6.7-4)}$$

$$= \sqrt{\frac{2(39{,}600 \text{ kip-in.})}{\pi(0.90)(113 \text{ ksi})(41.2 \text{ in.}+37.4 \text{ in.}+32.5 \text{ in.}+28.7 \text{ in.})}}$$

$$= 1.33 \text{ in.}$$

Step 1.7—Select Bolt Diameter

Select 1⅜-in.-diameter Grade A490 bolts.

$$d_b = 1⅜ \text{ in.} \quad \geq \quad d_{b,req} = 1.33 \text{ in.} \quad \textbf{o.k.} \qquad (6\text{-}3)$$

Step 1.8—Determine Required End-Plate Thickness

Calculate the dimension, s, using Equation 6-6 and the yield line parameter, Y_p, for this bolt configuration and dimensions. First determine the distance, s, then select the appropriate case from Figure 6-5.

$$b_{p,eff} \leq b_{bf} + 1 \text{ in.} \qquad (4\text{-}3)$$

$$\leq 12.0 \text{ in.} + 1 \text{ in.}$$

$$\leq 13.0 \text{ in.}$$

Because the upper limit of $b_{p,eff} = 13.0$ in. is greater than the end plate width, $b_p = 12$ in., use $b_p = 12$ in.

$$s = \frac{\sqrt{b_p g}}{2} \qquad (6\text{-}6)$$

$$= \frac{\sqrt{(12 \text{ in.})(6 \text{ in.})}}{2}$$

$$= 4.24 \text{ in.}$$

Because $d_e = 1¾$ in. is less than s, Case 1 in Figure 6-5(a) applies, and Y_p is determined using Equation 6-10.

$$Y_p = \frac{b_p}{2}\left[h_1\left(\frac{1}{2d_e}\right)+h_2\left(\frac{1}{p_{fo}}\right)+h_3\left(\frac{1}{p_{fi}}\right)+h_4\left(\frac{1}{s}\right)\right] \qquad (6\text{-}10)$$

$$+\frac{2}{g}\left[h_1\left(d_e+\frac{3p_b}{4}\right)+h_2\left(p_{fo}+\frac{p_b}{4}\right)+h_3\left(p_{fi}+\frac{3p_b}{4}\right)+h_4\left(s+\frac{p_b}{4}\right)\right]+g$$

$$= \left(\frac{12 \text{ in.}}{2}\right)\left[41.4 \text{ in.}\left(\frac{1}{2(1¾ \text{ in.})}\right)+37.4 \text{ in.}\left(\frac{1}{2 \text{ in.}}\right)+32.5 \text{ in.}\left(\frac{1}{2 \text{ in.}}\right)+28.5 \text{ in.}\left(\frac{1}{4.24 \text{ in.}}\right)\right]$$

$$+\left(\frac{2}{6 \text{ in.}}\right)\left[\begin{array}{l}41.4 \text{ in.}\left(1¾ \text{ in.}+\dfrac{3(3¾ \text{ in.})}{4}\right)+37.4 \text{ in.}\left(2.00 \text{ in.}+\dfrac{3¾ \text{ in.}}{4}\right)\\ +32.5 \text{ in.}\left(2 \text{ in.}+\dfrac{3(3¾ \text{ in.})}{4}\right)+28.5 \text{ in.}\left(4.24 \text{ in.}+\dfrac{3¾ \text{ in.}}{4}\right)\end{array}\right]+6 \text{ in.}$$

$$= 528 \text{ in.}$$

Compute the required end-plate thickness using AISC *Prequalified Connections* Equation 6.7-5. The resistance factor for ductile limit states is given in AISC *Prequalified Connections* as $\phi_d = 1.00$. The yield stress of the end plate is given as $F_{yp} = 50$ ksi.

$$t_{p,req} = \sqrt{\frac{1.11 M_f}{\phi_d F_{yp} Y_p}} \qquad \text{(Preq. Conn. Eq. 6.7-5)}$$

$$= \sqrt{\frac{1.11(39{,}600 \text{ kip-in.})}{1.00(50 \text{ ksi})(528 \text{ in.})}}$$

$$= 1.29 \text{ in.}$$

Step 1.9—Select End-Plate Thickness

Select an end-plate thickness, $t_p = 1\frac{3}{8}$ in., and width, $b_p = 12$ in.

$$t_p = 1\frac{3}{8} \text{ in.} \quad \geq \quad t_{p,req} = 1.29 \text{ in.} \quad \textbf{o.k.} \qquad (6\text{-}5)$$

Now that the end-plate thickness, t_p, and width, b_p, have been established, it is necessary to check that they fall within the parametric limitations listed in Table 6-3 of this Design Guide and AISC *Prequalified Connections* Table 6.1.

$\frac{3}{4}$ in. $\leq t_p \leq 2\frac{1}{2}$ in.

$t_p = 1\frac{3}{8}$ in. **o.k.**

9 in. $\leq b_p \leq 15$ in.

$b_p = 12$ in. **o.k.**

Step 1.10—Calculate the Beam Flange Force

Use AISC *Prequalified Connections* Equation 6.7-6 to calculate the factored beam flange force, F_{fu}.

$$F_{fu} = \frac{M_f}{d - t_{bf}} \qquad \text{(Preq. Conn. Eq. 6.7-6)}$$

$$= \frac{39{,}600 \text{ kip-in.}}{35.9 \text{ in.} - 0.940 \text{ in.}}$$

$$= 1{,}130 \text{ kips}$$

Step 1.11—Check Shear Yielding of Extended Portion of End Plate

Step 1.11 is related to shear failure of the extended portion of the end plate. Because the end plate is stiffened, this limit state does not apply.

Step 1.12—Check Shear Rupture of Extended Portion of End Plate

Similarly, this step is also related to shear failure of the extended portion of the end plate and does not apply for stiffened end plates.

Step 1.13—Select Stiffener Thickness and Design Stiffener Welds

Calculate the minimum stiffener thickness using AISC *Prequalified Connections* Equation 6.7-9.

$$t_{s,req} = t_{bw}\left(\frac{F_{yb}}{F_{ys}}\right) \qquad \text{(from Preq. Conn. Eq. 6.7-9)}$$

$$= (0.625 \text{ in.})\left(\frac{50 \text{ ksi}}{50 \text{ ksi}}\right)$$

$$= 0.625 \text{ in.}$$

Select a $\frac{5}{8}$-in.-thick stiffener.

$$t_s = \tfrac{5}{8} \text{ in.} \quad \geq \quad t_{s,req} = 0.625 \text{ in.} \quad \textbf{o.k.}$$

Check that the stiffener geometry satisfies the local buckling check in AISC *Prequalified Connections* Equation 6.7-10. The height of the stiffener is shown in Figure 6-11 as $h_{st} = 7\frac{1}{2}$ in.

$$\frac{h_{st}}{t_s} = \frac{7\frac{1}{2} \text{ in.}}{\frac{5}{8} \text{ in.}}$$
$$= 12.0$$

$$0.56\sqrt{\frac{E}{F_{ys}}} = 0.56\sqrt{\frac{29{,}000 \text{ ksi}}{50 \text{ ksi}}}$$
$$= 13.5$$

$$\frac{h_{st}}{t_s} = 12.0 \quad \leq \quad 0.56\sqrt{\frac{E}{F_{ys}}} = 13.5 \quad \textbf{o.k.} \qquad \text{(}\textit{Preq. Conn.}\text{ Eq. 6.7-10)}$$

Design the stiffener welds. In Step 13, AISC *Prequalified Connections* states that if the stiffener is thicker than $\frac{3}{8}$ in., then CJP groove welds are required between the stiffener and end plate. CJP groove welds are therefore used between the stiffener and end plate. Fillet welds are acceptable for the weld of the stiffener to the beam flange and must be designed to develop the stiffener plate in shear. The demand, R_u, is calculated in terms of shear force per unit length as follows.

$$R_u = 0.60F_{ys}t_s \qquad \text{(from } \textit{Spec.}\text{ Eq. J4-3)}$$
$$= 0.60(50 \text{ ksi})(\tfrac{5}{8} \text{ in.})$$
$$= 18.8 \text{ kips/in.}$$

Use a double-sided $\frac{7}{16}$ in. fillet weld from the stiffener to the beam flange. (Minimum size of fillet welds from AISC *Specification* Table J2.4 is $\frac{1}{4}$ in.)

$$R_n = (2 \text{ welds})(0.60F_{EXX})\left(\frac{t_{weld}}{\sqrt{2}}\right)(1.0 + 0.5\sin^{1.5}\theta) \qquad \text{(from } \textit{Spec.}\text{ Eq. J2-4)}$$
$$= (2 \text{ welds})(0.60)(70 \text{ ksi})\left(\frac{\frac{7}{16} \text{ in.}}{\sqrt{2}}\right)(1.0 + 0.5\sin^{1.5} 0°)$$
$$= 26.0 \text{ kips/in.}$$

$$\phi R_n = 0.75(26.0 \text{ kips/in.})$$
$$= 19.5 \text{ kips/in.}$$

$$\phi R_n = 19.5 \text{ kips/in.} \quad \geq \quad R_u = 18.8 \text{ kips/in.} \quad \textbf{o.k.}$$

Step 1.14—Check Beam Shear Strength

The required shear strength for the beam was calculated in Step 1.3 as $V_u = 201$ kips. Calculate the design shear strength of the beam using AISC *Specification* G2.1(a). Because the W36×150 is not included in the list in the User Note, the section meets the criteria for G2.1(a) for $F_y = 50$ ksi, and thus $\phi_v = 1.00$ and $C_{v1} = 1.0$. The design shear strength is given as:

$$V_n = 0.60F_yA_wC_{v1} \qquad \text{(}\textit{Spec.}\text{ Eq. G2-1)}$$
$$= 0.60F_ydt_{bw}C_{v1}$$
$$= 0.60(50 \text{ ksi})(35.9 \text{ in.})(0.625 \text{ in.})(1.0)$$
$$= 673 \text{ kips}$$

$$\phi_v V_n = 1.00(673 \text{ kips})$$
$$= 673 \text{ kips}$$

$$V_u = 201 \text{ kips} \quad \leq \quad \phi_v V_n = 673 \text{ kips} \quad \textbf{o.k.}$$

Step 1.15—Determine the Required Shear Strength, V_u

The vertical shear demand at the end-plate connection was calculated in Step 1.3 to be $V_u = 201$ kips.

Step 1.16—Bolt Shear Rupture Strength

The vertical shear demand at the end-plate connection, V_u, was calculated in Step 1.3. The design shear strength, $\phi_n R_n$, is given by AISC *Prequalified Connections* Equation 6.7-11 as the shear strength of the eight bolts at the compression flange. The nominal shear strength of Grade A490 bolts is $F_{nv} = 68$ ksi. The area of a 1⅜-in.-diameter bolt is 1.48 in.^{2}

$$\phi_n R_n = \phi_n n_b F_{nv} A_b$$
$$= 0.90(8 \text{ bolts})(68 \text{ ksi})(1.48 \text{ in.}^2)$$
$$= 725 \text{ kips}$$

$V_u = 201$ kips $\leq$ $\phi_n R_n = 725$ kips **o.k.** (from *Preq. Conn.* Eq. 6.7-11)

Step 1.17—Bearing/Tearout Failure of End-Plate Column Flange

Similar to the previous step, the vertical shear demand at the end-plate connection, V_u, was calculated in Step 1.3. The design bearing/tearout strength, $\phi_n R_n$, is given by AISC *Prequalified Connections* Equation 6.7-12. Because vertical shear is assumed to be resisted only by the compression side bolts, bearing/tearout is checked at the bottom bolt hole locations for the shear loading shown in Figure 6-15. By inspection, tearout will not control at the end plate, and therefore, only bolt bearing needs to be checked in this example. The same is true at the column flange if a continuity plate is used. If not, tearout must be checked between the bottom bolt holes. As found later in the example, continuity plates are not required. Because the end-plate thickness, 1⅜ in., is less than the column flange thickness, 2.30 in., bearing must be checked at the end plate and bearing/tearout checked at the column flange.

At the end plate:

$$r_n = 2.4 d_b t_p F_{up}$$ (from *Spec.* Eq. J3-6a)
$$= 2.4(1\tfrac{3}{8} \text{ in.})(1\tfrac{3}{8} \text{ in.})(65 \text{ ksi})$$
$$= 295 \text{ kips}$$

$$\phi_n R_n = \phi_n n r_n$$ (from *Preq. Conn.* Eq. 6.7-12)
$$= 0.90(8 \text{ bolts})(295 \text{ kips})$$
$$= 2{,}120 \text{ kips}$$

$V_u = 201$ kips $\leq$ $\phi_n R_n = 2{,}120$ kips **o.k.**

By inspection, bearing or tearout at the bolt hole of the 2.30-in.-thick column flange will not be the controlling limit states.

Note: The User Note in AISC *Specification* Section J3.7 recommends that the effective strength of an individual bolt be taken as the lesser of the bolt shear strength, bearing strength, or tearout strength at the bolt hole. For this example, the effective shear strength of the top or bottom bolts is the shear strength of eight bolts, 725 kips.

Step 1.18—Design the Welds

In this step, design the welds of the beam to the end plate. In accordance with AISC *Prequalified Connections* Section 6.6.6(2), the beam flange to end-plate welds are made using a CJP groove weld (bevel facing away from the center of the beam) without weld access holes and without back-up bars. The inside face of the flange will have a 5⁄16 in. reinforcing fillet weld. These welds are the only welds that need to be considered demand critical.

The beam web to end-plate weld is designed in two parts. The web weld from the point nearest the flange to a point 6 in. beyond the most interior bolt row will either be CJP groove welds or fillet welds that develop the full strength of the web in tension. Try double-sided ½ in. fillet welds:

$$R_u = F_{yb} t_{bw} \quad \text{(from } Spec. \text{ Eq. J4-1)}$$
$$= (50 \text{ ksi})(0.625 \text{ in.})$$
$$= 31.3 \text{ kips/in.}$$

$$R_n = (2 \text{ welds})(0.60 F_{EXX}) \left(\frac{t_{weld}}{\sqrt{2}} \right) (1.0 + 0.5 \sin^{1.5} \theta) \quad \text{(from } Spec. \text{ Eq. J2-4)}$$
$$= (2 \text{ welds})(0.60)(70 \text{ ksi}) \left(\frac{\frac{1}{2} \text{ in.}}{\sqrt{2}} \right) (1.0 + 0.5 \sin^{1.5} 90°)$$
$$= 44.5 \text{ kips/in.}$$

$$\phi R_n = 0.75(44.5 \text{ kips/in.})$$
$$= 33.4 \text{ kips/in.}$$

$R_u = 31.3$ kips/in. $\leq \phi R_n = 33.4$ kips/in. **o.k.**

From Step 1.3, the shear demand is 201 kips. The following calculations shows that the ½ in. double-sided fillet weld at the compression side has sufficient strength to resist the shear and that the web to end-plate weld between the tension zones can be the minimum fillet weld size. The length of each tension region weld is:

$$l_{wt} = p_{fi} + p_b + 6 \text{ in.}$$
$$= 2 \text{ in.} + 3¾ \text{ in.} + 6 \text{ in.}$$
$$= 11.8 \text{ in.}$$

The available vertical shear strength of the double-sided ½ in. fillet weld is:

$$R_n = (2 \text{ welds})(0.60 F_{EXX}) \left(\frac{t_{weld}}{\sqrt{2}} l_{wt} \right) (1.0 + 0.5 \sin^{1.5} \theta) \quad \text{(from } Spec. \text{ Eq. J2-4)}$$
$$= (2 \text{ welds})(0.60)(70 \text{ ksi}) \left(\frac{\frac{1}{2} \text{ in.}}{\sqrt{2}} \right) (11.8 \text{ in.})(1.0 + 0.5 \sin^{1.5} 0°)$$
$$= 350 \text{ kips}$$

$$\phi R_n = 0.75(350 \text{ kips})$$
$$= 263 \text{ kips}$$

$V_u = 201$ kips $\leq \phi R_n = 263$ kips **o.k.**

Use ½ in. double-sided fillet welds in web tension regions and ¼ in. double-sided fillet welds (minimum weld size from AISC *Specification* Table J2.4) between tension regions.

Part 2. Column-Side Design

Step 2.1—Column Flange Flexural Yielding

The beam and end-plate checks are complete. The following is the column-side design. Preliminary calculations (not shown here) determined that the minimum W18 column section that satisfies the strong-column/weak-beam moment ratio requirement is W18×211, but a W18×258 would eliminate the need for continuity or doubler plates. Use a W18×258 column.

First, check the column flange for flexural yielding. It is assumed that no column continuity plates will be required, which will be verified in later steps. Use the unstiffened column flange yield line parameter, Equation 6-17.

$$s = \frac{\sqrt{b_{cf}\, g}}{2} \tag{6-14}$$
$$= \frac{\sqrt{(11.8\text{ in.})(6\text{ in.})}}{2}$$
$$= 4.21\text{ in.}$$

$$c = p_{fi} + t_{bf} + p_{fo}$$
$$= 2\text{ in.} + 0.940\text{ in.} + 2\text{ in.}$$
$$= 4.94\text{ in.}$$

$$Y_c = \frac{b_{cf}}{2}\left[h_1\left(\frac{1}{s}\right) + h_4\left(\frac{1}{s}\right)\right] + \frac{2}{g}\left[h_1\left(p_b + \frac{c}{2} + s\right) + h_2\left(\frac{p_b}{2} + \frac{c}{4}\right) + h_3\left(\frac{p_b}{2} + \frac{c}{2}\right) + h_4(s)\right] + \frac{g}{2} \tag{6-17}$$
$$= \left(\frac{11.8\text{ in.}}{2}\right)\left[(41.4\text{ in.})\left(\frac{1}{4.21\text{ in.}}\right) + (28.5\text{ in.})\left(\frac{1}{4.21\text{ in.}}\right)\right]$$
$$+ \left(\frac{2}{6\text{ in.}}\right)\left[\begin{array}{l}(41.4\text{ in.})\left(3\tfrac{3}{4}\text{ in.} + \dfrac{4.94\text{ in.}}{2} + 4.21\text{ in.}\right) + (37.4\text{ in.})\left(\dfrac{3\tfrac{3}{4}\text{ in.}}{2} + \dfrac{4.94\text{ in.}}{4}\right) \\ + (32.5\text{ in.})\left(\dfrac{3\tfrac{3}{4}\text{ in.}}{2} + \dfrac{4.94\text{ in.}}{2}\right) + (28.5\text{ in.})(4.21\text{ in.})\end{array}\right] + \frac{6\text{ in.}}{2}$$
$$= 370\text{ in.}$$

$$t_{cf,req} = \sqrt{\frac{1.11 M_f}{\phi_d F_{yc} Y_c}} \qquad \text{(from } \textit{Preq. Conn.} \text{ Eq. 6.7-13)}$$
$$= \sqrt{\frac{1.11(39{,}600\text{ kip-in.})}{(1.00)(50\text{ ksi})(370\text{ in.})}}$$
$$= 1.54\text{ in.}$$

$$t_{cf} = 2.30\text{ in.} \quad \geq \quad t_{cf,req} = 1.54\text{ in.} \tag{6-13}$$

Column flange stiffeners are not required for this limit state.

Step 2.2—Column Flange Available Strength for Continuity Plate Demand

The column flange yield line parameter is used to compute the beam flange force associated with column flange flexural yielding. If insufficient, the required column flange thickness will be used later in Step 2.5 to determine the continuity plate required strength.

Calculate the available strength of the column flange using AISC *Prequalified Connections* Equations 6.7-14 and 6.7-15.

$$\phi_d M_{cf} = \phi_d F_{yc} Y_c t_{cf}^2 \qquad \text{(}\textit{Preq. Conn.}\text{ Eq. 6.7-14)}$$
$$= 1.00(50\text{ ksi})(370\text{ in.})(2.30\text{ in.})^2$$
$$= 97{,}900\text{ kip-in.}$$

$$\phi_d R_n = \frac{\phi_d M_{cf}}{(d - t_{bf})} \qquad \text{(}\textit{Preq. Conn.}\text{ Eq. 6.7-15)}$$
$$= \frac{97{,}900\text{ kip-in.}}{(35.9\text{ in.} - 0.940\text{ in.})}$$
$$= 2{,}800\text{ kips}$$

$$\phi_d R_n = 2{,}800\text{ kips} \quad > \quad F_{fu} = 1{,}130\text{ kips}$$

Because $\phi_d R_n > F_{fu}$, continuity plates are not required.

Step 2.3—Local Column Web Yielding

Check the local column web yielding design strength against the calculated flange force from Step 1.10, F_{fu} = 1,130 kips, using AISC *Prequalified Connections* Equations 6.7-16 and 6.7-17. This calculation is performed assuming no continuity plates exist. If the check is satisfied, then continuity plates are not necessary. If the check is not satisfied, then the difference between the required strength and the unstiffened column available strength will be used in Step 2.5 to find the required strength for the continuity plates. Because the distance from the top of beam flange to top of column is greater than the depth of the beam, a value of $C_t = 1.0$ is used. The effective width of bearing, l_b, includes the size of the reinforcing fillet, w, from the beam flange to end-plate CJP groove weld.

$$l_b = t_{bf} + w + 2t_p$$
$$= 0.940 \text{ in.} + 5/16 \text{ in.} + 2(1\tfrac{3}{8} \text{ in.})$$
$$= 4.00 \text{ in.}$$

$$R_n = (6C_t k_c + l_b) F_{yc} t_{cw}$$
$$= \left[6(1.0)(2.70 \text{ in.}) + 4.00 \text{ in.}\right](50 \text{ ksi})(1.28 \text{ in.})$$
$$= 1{,}290 \text{ kips}$$

$$\phi_d R_n = 1.00(1{,}290 \text{ kips}) \qquad \text{(}\textit{Preq. Conn.}\text{ Eq. 6.7-17)}$$
$$= 1{,}290 \text{ kips}$$

$$\phi_d R_n = 1{,}290 \text{ kips} \quad > \quad F_{fu} = 1{,}130 \text{ kips} \qquad \text{(}\textit{Preq. Conn.}\text{ Eq. 6.7-16)}$$

Because $\phi_d R_n > F_{fu}$, continuity plates are not required.

Step 2.4—Column Web Crippling

As was done in the previous steps, the column web crippling available strength is evaluated assuming no continuity plates. If the check is satisfied, then continuity plates are not required. AISC *Prequalified Connections* Equation 6.7-18 is used to compute web crippling available strength.

$$R_n = 0.80 t_{cw}^2 \left[1 + 3\left(\frac{l_b}{d_c}\right)\left(\frac{t_{cw}}{t_{cf}}\right)^{1.5}\right]\sqrt{\frac{EF_{yc}t_{cf}}{t_{cw}}} \qquad \text{(}\textit{Preq. Conn.}\text{ Eq. 6.7-19)}$$
$$= 0.80(1.28 \text{ in.})^2 \left[1 + 3\left(\frac{4.00 \text{ in.}}{21.5 \text{ in.}}\right)\left(\frac{1.28 \text{ in.}}{2.30 \text{ in.}}\right)^{1.5}\right]\sqrt{\frac{(29{,}000 \text{ ksi})(50 \text{ ksi})(2.30 \text{ in.})}{1.28 \text{ in.}}}$$
$$= 2{,}610 \text{ kips}$$

$$\phi R_n = 0.75(2{,}610 \text{ kips})$$
$$= 1{,}960 \text{ kips}$$

$$\phi R_n = 1{,}960 \text{ kips} \; > \; F_{fu} = 1{,}130 \text{ kips} \qquad \text{(}\textit{Preq. Conn.}\text{ Eq. 6.7-18)}$$

Because $\phi R_n > F_{fu}$, continuity plates are not required.

Step 2.5—Continuity Plate Design

Steps 2.1 through 2.4 indicate that continuity plates are not required.

Step 2.6—Panel Zone Shear

The panel zone is checked in accordance with the AISC *Seismic Provisions* Section E3.6e(1). The panel zone shear is similar to that shown in Figure 3.15(b). The panel zone required shear strength is the flange force, F_{fu}, less the column shear, $V_{uc,}$, and half the axial force, P_{ub}.

$$V_{upz} = F_{fu} - V_{uc} - \frac{P_{ub}}{2}$$
$$= 1{,}130 \text{ kips} - 540 \text{ kips} - \frac{40.0 \text{ kips}}{2}$$
$$= 570 \text{ kips}$$

The panel zone design strength is calculated according to AISC *Specification* Section J10.6, but using a resistance factor ϕ_d = 1.00, according to AISC *Seismic Provisions* Section E3.6e(1). First, find the column required axial strength, P_u, and the ratio of this required axial strength to the axial yield strength of the column, P_y.

$$P_{uc,total} = P_{uc} + V_{ub}$$
$$= 50.0 \text{ kips} + 201 \text{ kips}$$
$$= 251 \text{ kips}$$

$$P_y = F_{yc} A_{cg}$$
$$= (50 \text{ ksi})(76.0 \text{ in.}^2)$$
$$= 3{,}800 \text{ kips}$$

$$\frac{P_{uc,total}}{P_y} = \frac{251 \text{ kips}}{3{,}800 \text{ kips}}$$
$$= 0.0661$$

Because it is assumed that frame stability was assessed including plastic panel zone deformation, and that the ratio P_{uc}/P_y is equal to 0.0661, which is less than 0.75, then AISC *Specification* Equation J10-11 is used to determine the panel zone nominal strength.

$$R_n = 0.60 F_{yc} d_c t_{cw} \left(1 + \frac{3 b_{cf} t_{cf}^2}{d\, d_c\, t_{cw}} \right) \qquad \text{(Spec. Eq. J10-11)}$$
$$= 0.60(50 \text{ ksi})(21.5 \text{ in.})(1.28 \text{ in.}) \left[1 + \frac{3(11.8 \text{ in.})(2.30 \text{ in.})^2}{(35.9 \text{ in.})(21.5 \text{ in.})(1.28 \text{ in.})} \right]$$
$$= 982 \text{ kips}$$

$$\phi_d R_n = 1.00(982 \text{ kips})$$
$$= 982 \text{ kips}$$

$$V_{upz} = 570 \text{ kips} \quad \leq \quad \phi_d R_n = 982 \text{ kips} \quad \textbf{o.k.}$$

Additionally, check that the column web satisfies the minimum panel zone thickness given in AISC *Seismic Provisions* Section E3.6e(2).

$$d_z = d - 2t_{bf}$$
$$= 35.9 \text{ in.} - 2(0.940 \text{ in.})$$
$$= 34.0 \text{ in.}$$

$$w_z = d_c - 2t_{cf}$$
$$= 21.5 \text{ in.} - 2(2.30 \text{ in.})$$
$$= 16.9 \text{ in.}$$

$$t_{cw,req} = \frac{d_z + w_z}{90}$$
$$= \frac{34.0 \text{ in.} + 16.9 \text{ in.}}{90}$$
$$= 0.566 \text{ in.}$$

$t_{cw} = 1.28$ in. $\geq$ $t_{cw,req} = 0.566$ in. **o.k.** (from *Prov.* Eq. E3-6)

Step 2.7—Strong-Column/Weak-Beam Check

Evaluate whether the strong-column/weak-beam moment ratio requirement of AISC *Seismic Provisions* Section E3.4a is satisfied.

From Step 2.6:

$P_{uc,total} = 251$ kips

$$\sum M_{pc}^{*} = \sum Z_c \left(F_{yc} - \alpha_s \frac{P_{uc,total}}{A_{gc}} \right)$$ (from *Prov.* Eq. E3-2)
$$= 2(611 \text{ in.}^3) \left[50 \text{ ksi} - 1.0 \left(\frac{251 \text{ kips}}{76.0 \text{ in.}^2} \right) \right]$$
$$= 57{,}100 \text{ kip-in.}$$

$$M_v = V_u \left(S_h + \frac{d_c}{2} \right)$$
$$= (201 \text{ kips}) \left(14.4 \text{ in.} + \frac{21.5 \text{ in.}}{2} \right)$$
$$= 5{,}060 \text{ kip-in.}$$

$$\sum M_{be}^{*} = \sum (M_{pr} + \alpha_s M_v)$$ (*Prov.* Eq. E3-3)
$$= 36{,}700 \text{ kip-in.} + 1.0(5{,}060 \text{ kip-in.})$$
$$= 41{,}800 \text{ kip-in.}$$

$$\frac{M_{pc}^{*}}{M_{be}^{*}} = \frac{57{,}100 \text{ kip-in.}}{41{,}800 \text{ kip-in.}}$$ (*Prov.* Eq. E3-1)
$$= 1.37 \geq 1.0 \quad \textbf{o.k.}$$

Summary

The final design of the connection is shown in Figure 6-16.

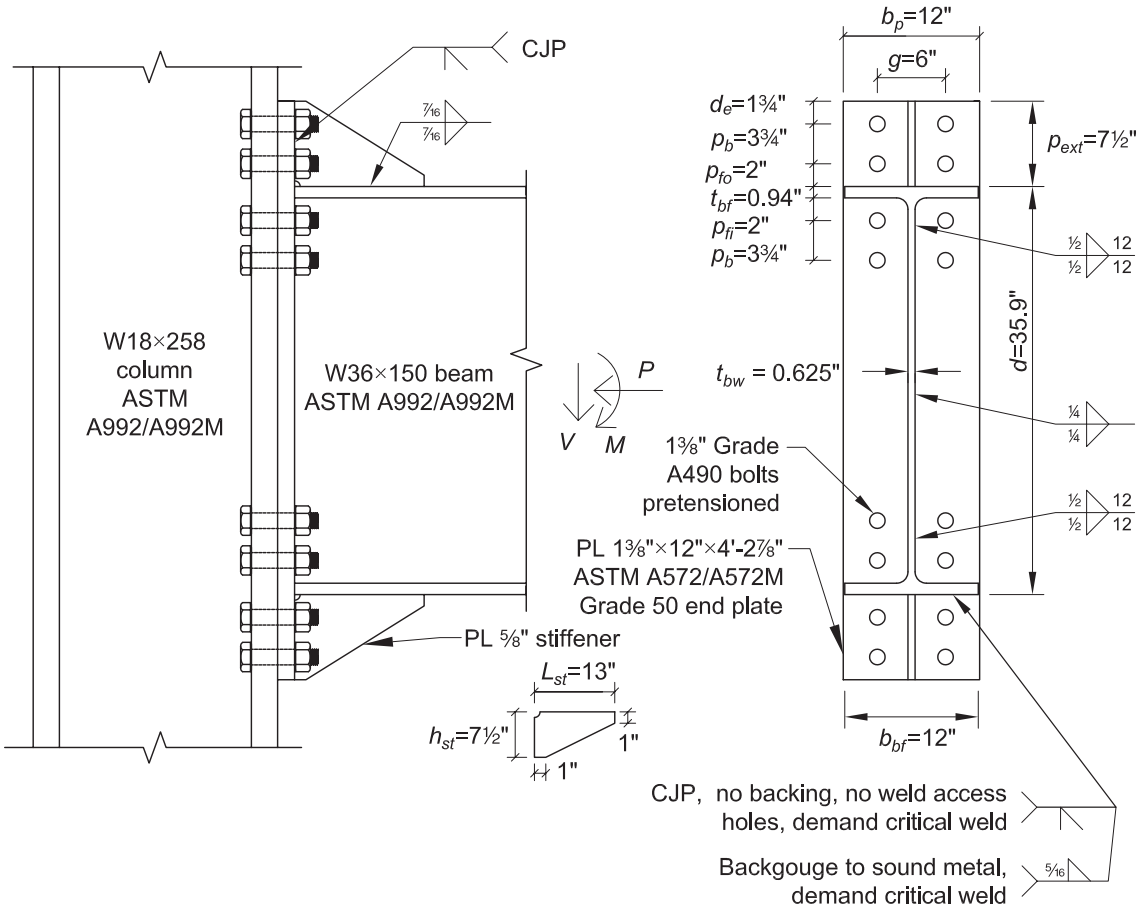

Fig. 6-16. Summary of final design for 8ES seismic end-plate configuration.

APPENDIX A
Column-Side Yield Line Parameters

This appendix contains the yield line parameters for end-plate connections to a column flange. Derivations for all yield line parameters are provided in Eatherton et al. (2021).

Table A-1. Column-Side Yield Line Parameters for Two-Bolt Configurations

Configuration	Yield Line Parameter
Continuous unstiffened column [Fig. A-1(a)]	$Y_c = \frac{b_{cf} h_1}{s} + \frac{4 h_1 s}{g}$
Continuous stiffened column [Fig. A-1(b)]	$Y_c = \frac{b_{cf}}{2}\left[h_1\left(\frac{1}{p_{si}} + \frac{1}{s}\right)\right] + \frac{2}{g}\left[h_1(p_{si} + s)\right]$ Note: Use $p_{si} = s$ if $p_{si} > s$
Top of column, unstiffened [Fig. A-1(c)]	$Y_c = \left\{\frac{b_{cf}}{2}\left[h_1\left(\frac{1}{s}\right) - \frac{1}{2}\right] + \frac{2}{g}\left[h_1(s + d_e)\right] + \frac{g}{4}\right\}$
Top of column with cap plate [Fig. A-1(d)]	$Y_c = \frac{b_{cf}}{2}\left[h_1\left(\frac{1}{p_{cp}} + \frac{1}{s}\right)\right] + \frac{2}{g}\left[h_1(p_{cp} + s)\right]$ Note: Use $p_{cp} = s$ if $p_{cp} > s$

In Tables A-1 through A-8, $s = \frac{\sqrt{b_{cf} g}}{2}$

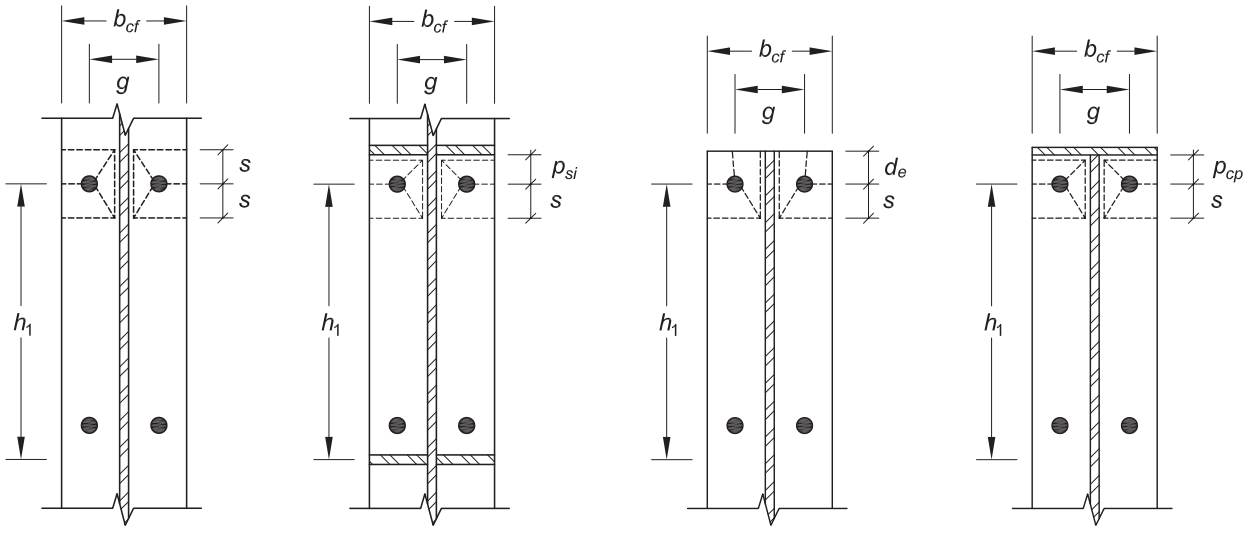

(a) Continuous column unstiffened

(b) Continuous column stiffened

(c) Top of column unstiffened

(d) Top of column with cap plate

Fig. A-1. Yield line patterns for two-bolt configurations.

Table A-2. Column-Side Yield Line Parameters for Four-Bolt Configurations	
Configuration	**Yield Line Parameter**
Continuous unstiffened column [Fig. A-2(a)]	$Y_c = \frac{b_{cf}}{2}\left[h_1\left(\frac{1}{s}\right)+h_2\left(\frac{1}{s}\right)\right.+\frac{2}{g}\left[h_1\left(s+\frac{3}{4}c\right)+h_2\left(s+\frac{1}{4}c\right)\right]+\frac{g}{2}$
Continuous column stiffened above the bolts [Fig. A-2(b)]	$Y_c = \frac{b_{cf}}{2}\left[h_1\left(\frac{1}{p_{si}}\right)+h_2\left(\frac{1}{s}\right)\right]+\frac{2}{g}\left[h_1\left(p_{si}+\frac{3}{4}c\right)+h_2\left(s+\frac{1}{4}c\right)\right]+\frac{g}{2}$ Note: Use $p_{si} = s$ if $p_{si} > s$
Continuous column stiffened between the bolts [Fig. A-2(c)]	$Y_c = \frac{b_{cf}}{2}\left[h_1\left(\frac{1}{s}+\frac{1}{p_{so}}\right)+h_2\left(\frac{1}{p_{si}}+\frac{1}{s}\right)\right]+\frac{2}{g}\left[h_1(s+p_{so})+h_2(p_{si}+s)\right]$ Note: Use $p_{si} = s$ if $p_{si} > s$ Use $p_{so} = s$ if $p_{so} > s$
Top of column, unstiffened [Fig. A-2(d)]	$Y_c = \frac{b_{cf}}{2}\left[h_2\left(\frac{1}{s}\right)-\frac{1}{2}\right]+\frac{2}{g}\left[h_1\left(d_e+\frac{3}{4}c\right)+h_2\left(s+\frac{1}{4}c\right)\right]+\frac{3g}{4}$
Top of column with cap plate [Fig. A-2(e)]	$Y_c = \frac{b_{cf}}{2}\left[h_1\left(\frac{1}{p_{cp}}\right)+h_2\left(\frac{1}{s}\right)\right]+\frac{2}{g}\left[h_1\left(p_{cp}+\frac{3}{4}c\right)+h_2\left(s+\frac{1}{4}c\right)\right]+\frac{g}{2}$ Note: Use $p_{cp} = s$ if $p_{cp} > s$
Top of column stiffened between the bolts [Fig. A-2(f)]	$Y_c = \frac{b_{cf}}{2}\left[h_1\left(\frac{1}{p_{so}}\right)+h_2\left(\frac{1}{p_{si}}+\frac{1}{s}\right)-\frac{1}{2}\right]+\frac{2}{g}\left[h_1(d_{ce}+p_{so})+h_2(s+p_{si})\right]+\frac{g}{4}$ Note: Use $p_{si} = s$ if $p_{si} > s$ Use $p_{so} = s$ if $p_{so} > s$

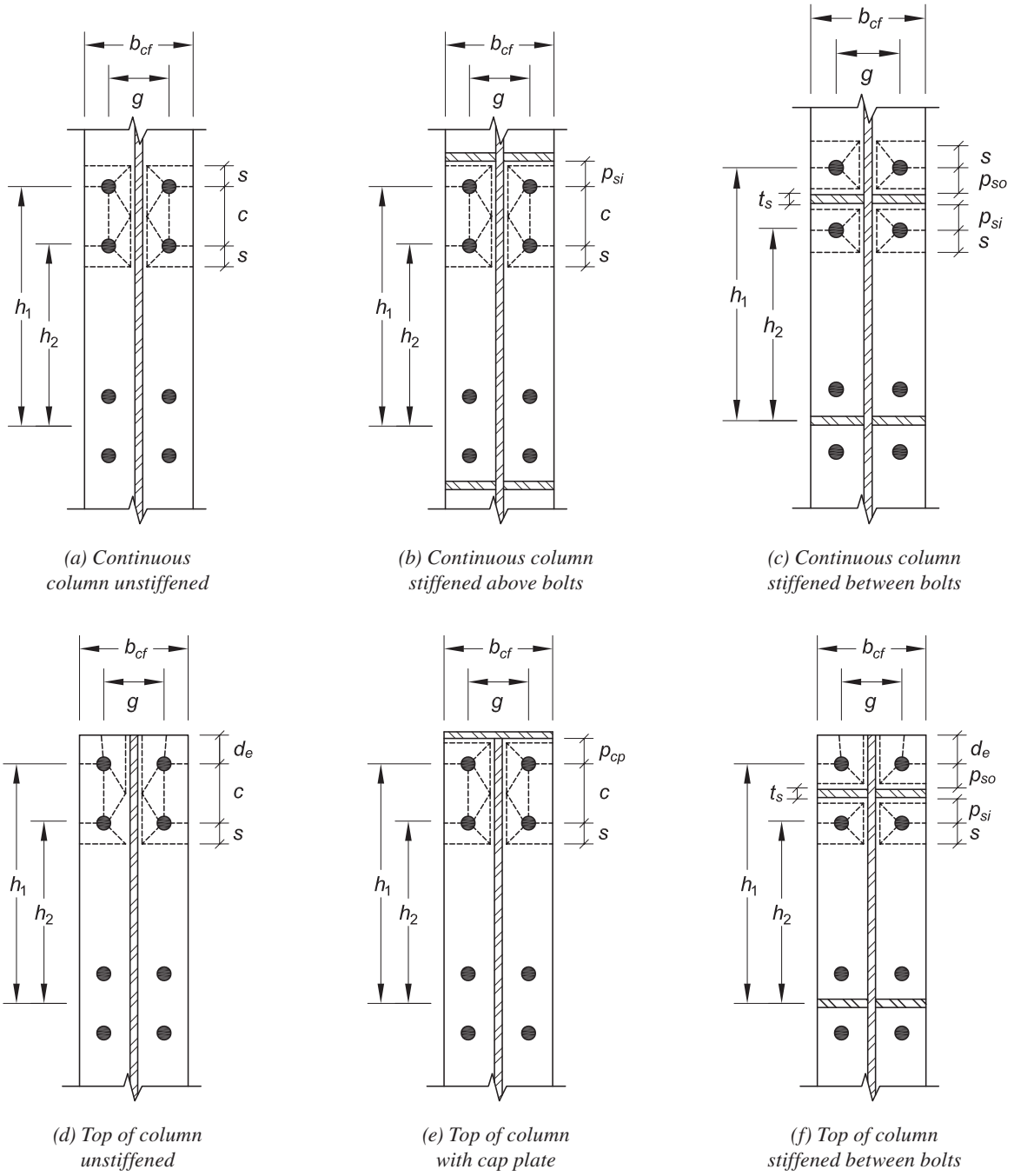

(a) Continuous column unstiffened

(b) Continuous column stiffened above bolts

(c) Continuous column stiffened between bolts

(d) Top of column unstiffened

(e) Top of column with cap plate

(f) Top of column stiffened between bolts

Fig. A-2. Yield line pattern for four-bolt configurations.

Table A-3. Column-Side Yield Line Parameters for Six-Bolt, 4W/2W Configurations	
Configuration	**Yield Line Parameter**
Continuous unstiffened column [Fig. A-3(a)]	$Y_c = \frac{b_{cf}}{2}\left[h_1\left(\frac{1}{s}\right)+h_2\left(\frac{1}{s}\right)\right]+\frac{2}{g}\left[h_1\left(s+\frac{3}{4}c\right)+h_2\left(s+\frac{1}{4}c\right)\right]+\frac{g}{2}$
Continuous column stiffened above the bolts [Fig. A-3(b)]	$Y_c = \frac{b_{cf}}{2}\left[h_1\left(\frac{1}{p_{si}}\right)+h_2\left(\frac{1}{s}\right)\right]+\frac{2}{g}\left[h_1\left(p_{si}+\frac{3}{4}c\right)+h_2\left(s+\frac{1}{4}c\right)\right]+\frac{g}{2}$ Note: Use $p_{si} = s$ if $p_{si} > s$
Top of column, unstiffened [Fig. A-3(c)]	$Y_c = \frac{b_{cf}}{2}\left[h_2\left(\frac{1}{s}\right)-\frac{1}{2}\right]+\frac{2}{g}\left[h_1\left(d_e+\frac{3}{4}c\right)+h_2\left(s+\frac{1}{4}c\right)\right]+\frac{3g}{4}$
Top of column with cap plate [Fig. A-3(d)]	$Y_c = \frac{b_{cf}}{2}\left[h_1\left(\frac{1}{p_{cp}}\right)+h_2\left(\frac{1}{s}\right)\right]+\frac{2}{g}\left[h_1\left(p_{cp}+\frac{3}{4}c\right)+h_2\left(s+\frac{1}{4}c\right)\right]+\frac{g}{2}$ Note: Use $p_{cp} = s$ if $p_{cp} > s$

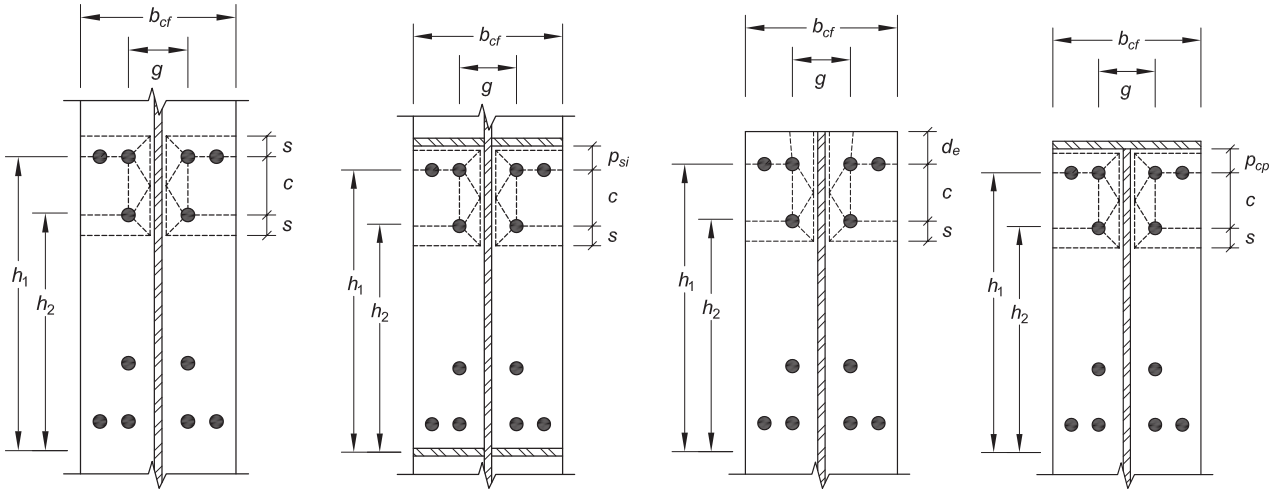

(a) Continuous column unstiffened

(b) Continuous column stiffened above bolts

(c) Top of column unstiffened

(d) Top of column with cap plate

Fig. A-3. Yield line pattern for six-bolt, 4W/2W configurations.

Table A-4. Column-Side Yield Line Parameters for Six-Bolt, Three-Row Configurations	
Configuration	**Yield Line Parameter**
Continuous unstiffened column [Fig. A-4(a)]	$Y_c = \frac{b_{cf}}{2}\left[h_1\left(\frac{1}{s}\right)+h_3\left(\frac{1}{s}\right)\right]+\frac{2}{g}\left[h_1\left(s+\frac{3}{4}p_b+\frac{3}{4}c\right)+h_3\left(s+\frac{1}{4}p_b+\frac{1}{4}c)\right)\right]+\frac{g}{2}$
Continuous column stiffened between the bolts [Fig. A-4(b)]	$Y_c = \frac{b_{cf}}{2}\left[h_1\left(\frac{1}{p_{so}}+\frac{1}{s}\right)+h_2\left(\frac{1}{p_{si}}\right)+h_3\left(\frac{1}{s}\right)\right]$ $+\frac{2}{g}\left[h_1(p_{so}+s)+h_2\left(p_{si}+\frac{3}{4}p_b\right)+h_3\left(s+\frac{1}{4}p_b\right)\right]+\frac{g}{2}$ Note: Use $p_{si}=s$ if $p_{si}>s$ Use $p_{so}=s$ if $p_{so}>s$
Top of column, unstiffened [Fig. A-4(c)]	$Y_c = \frac{b_{cf}}{2}\left[h_3\left(\frac{1}{s}\right)-\frac{1}{2}\right]+\frac{2}{g}\left[h_1\left(d_e+\frac{3}{4}p_b+\frac{3}{4}c\right)+h_3\left(s+\frac{1}{4}p_b+\frac{1}{4}c\right)\right]+\frac{3g}{4}$
Top of column with cap plate [Fig. A-4(d)]	$Y_c = \frac{b_{cf}}{2}\left[h_1\left(\frac{1}{p_{cp}}\right)+h_3\left(\frac{1}{s}\right)\right]+\frac{2}{g}\left[h_1\left(p_{cp}+\frac{3}{4}p_b+\frac{3}{4}c\right)+h_3\left(s+\frac{1}{4}p_b+\frac{1}{4}c\right)\right]+\frac{g}{2}$ Note: Use $p_{cp}=s$ if $p_{cp}>s$
Top of column stiffened between the bolts [Fig. A-4(e)]	$Y_c = \frac{b_{cf}}{2}\left[h_1\left(\frac{1}{p_{so}}\right)+h_2\left(\frac{1}{p_{si}}\right)+h_3\left(\frac{1}{s}\right)-\frac{1}{2}\right]$ $+\frac{2}{g}\left[h_1(p_{so}+d_e)+h_2\left(p_{si}+\frac{3}{4}p_b\right)+h_3\left(\frac{1}{4}p_b+s\right)\right]+\frac{3g}{4}$ Note: Use $p_{si}=s$ if $p_{si}>s$ Use $p_{so}=s$ if $p_{so}>s$

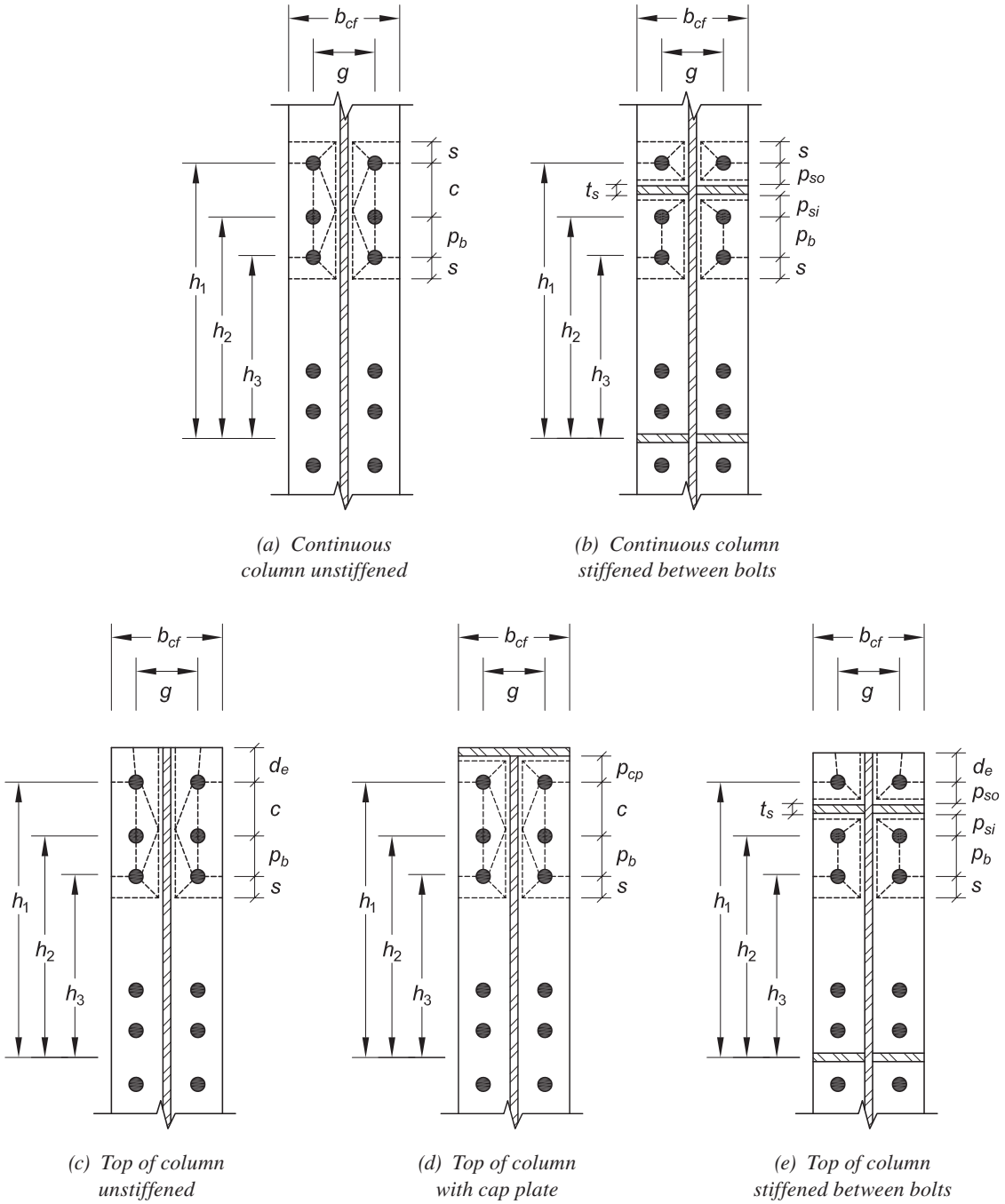

(a) Continuous column unstiffened

(b) Continuous column stiffened between bolts

(c) Top of column unstiffened

(d) Top of column with cap plate

(e) Top of column stiffened between bolts

Fig. A-4. Yield line pattern for six-bolt, three-row configurations.

Table A-5. Column-Side Yield Line Parameters for Eight-Bolt, Four-Row Configurations	
Configuration	**Yield Line Parameter**
Continuous unstiffened column [Fig. A-5(a)]	$Y_c = \frac{b_{cf}}{2}\left[h_1\left(\frac{1}{s}\right)+h_4\left(\frac{1}{s}\right)\right] + \frac{2}{g}\left[h_1\left(p_b+\frac{c}{2}+s\right)+h_2\left(\frac{p_b}{2}+\frac{c}{4}\right)+h_3\left(\frac{p_b}{2}+\frac{c}{2}\right)+h_4(s)\right]+\frac{g}{2}$
Continuous column stiffened below the first bolt line [Fig. A-5(b)]	$Y_c = \frac{b_{cf}}{2}\left[h_1\left(\frac{1}{p_{so}}+\frac{1}{s}\right)+h_2\left(\frac{1}{p_{si}}\right)+h_4\left(\frac{1}{s}\right)\right] + \frac{2}{g}\left[h_1(p_{so}+s)+h_2\left(p_{si}+\frac{3}{2}p_b\right)+h_4\left(s+\frac{1}{2}p_b\right)\right]+\frac{g}{2}$ Note: Use $p_{si} = s$ if $p_{si} > s$ Use $p_{so} = s$ if $p_{so} > s$
Continuous column stiffened below the second bolt line [Fig. A-5(c)]	$Y_c = \frac{b_{cf}}{2}\left[h_1\left(\frac{1}{s}\right)+h_2\left(\frac{1}{p_{so}}\right)+h_3\left(\frac{1}{p_{si}}\right)+h_4\left(\frac{1}{s}\right)\right] + \frac{2}{g}\left[h_1\left(\frac{3p_b}{4}+s\right)+h_2\left(\frac{p_b}{4}+p_{so}\right)+h_3\left(\frac{3p_b}{4}+p_{si}\right)+h_4\left(s+\frac{p_b}{4}\right)\right]+g$ Note: Use $p_{si} = s$ if $p_{si} > s$ Use $p_{so} = s$ if $p_{so} > s$
Top of column unstiffened [Fig. A-5(d)]	$Y_c = \frac{b_{cf}}{2}\left[h_4\left(\frac{1}{s}\right)-\frac{1}{2}\right]+\frac{2}{g}\left[h_1\left(d_e+\frac{3}{4}(2p_b+c)\right)+h_4\left(s+\frac{1}{4}(2p_b+c)\right)\right]+\frac{3g}{4}$
Top of column with cap plate [Fig. A-5(e)]	$Y_c = \frac{b_{cf}}{2}\left[h_1\left(\frac{1}{p_{cp}}\right)+h_4\left(\frac{1}{s}\right)\right]+\frac{2}{g}\left[h_1\left(p_{cp}+\frac{3}{4}(2p_b+c)\right)+h_4\left(s+\frac{1}{4}(2p_b+c)\right)\right]+\frac{g}{2}$ Note: Use $p_{cp} = s$ if $p_{cp} > s$
Top of column stiffened below the first bolt line [Fig. A-5(f)]	$Y_c = \frac{b_{cf}}{2}\left[h_1\left(\frac{1}{p_{so}}\right)+h_2\left(\frac{1}{p_{si}}\right)+h_4\left(\frac{1}{s}\right)-\frac{1}{2}\right] + \frac{2}{g}\left[h_1(p_{so}+d_e)+h_2\left(p_{si}+\frac{3}{2}p_b\right)+h_4\left(\frac{1}{2}p_b+s\right)\right]+\frac{3g}{4}$ Note: Use $p_{si} = s$ if $p_{si} > s$ Use $p_{so} = s$ if $p_{so} > s$
Top of column stiffened below the second bolt line [Fig. A-5(g)]	$Y_c = \frac{b_{cf}}{2}\left[h_2\left(\frac{1}{p_{so}}\right)+h_3\left(\frac{1}{p_{si}}\right)+h_4\left(\frac{1}{s}\right)-\frac{1}{2}\right] + \frac{2}{g}\left[h_1\left(\frac{3p_b}{4}+d_e\right)+h_2\left(\frac{p_b}{4}+p_{so}\right)+h_3\left(\frac{3p_b}{4}+p_{si}\right)+h_4\left(s+\frac{p_b}{4}\right)\right]+\frac{5g}{4}$ Note: Use $p_{si} = s$ if $p_{si} > s$ Use $p_{so} = s$ if $p_{so} > s$

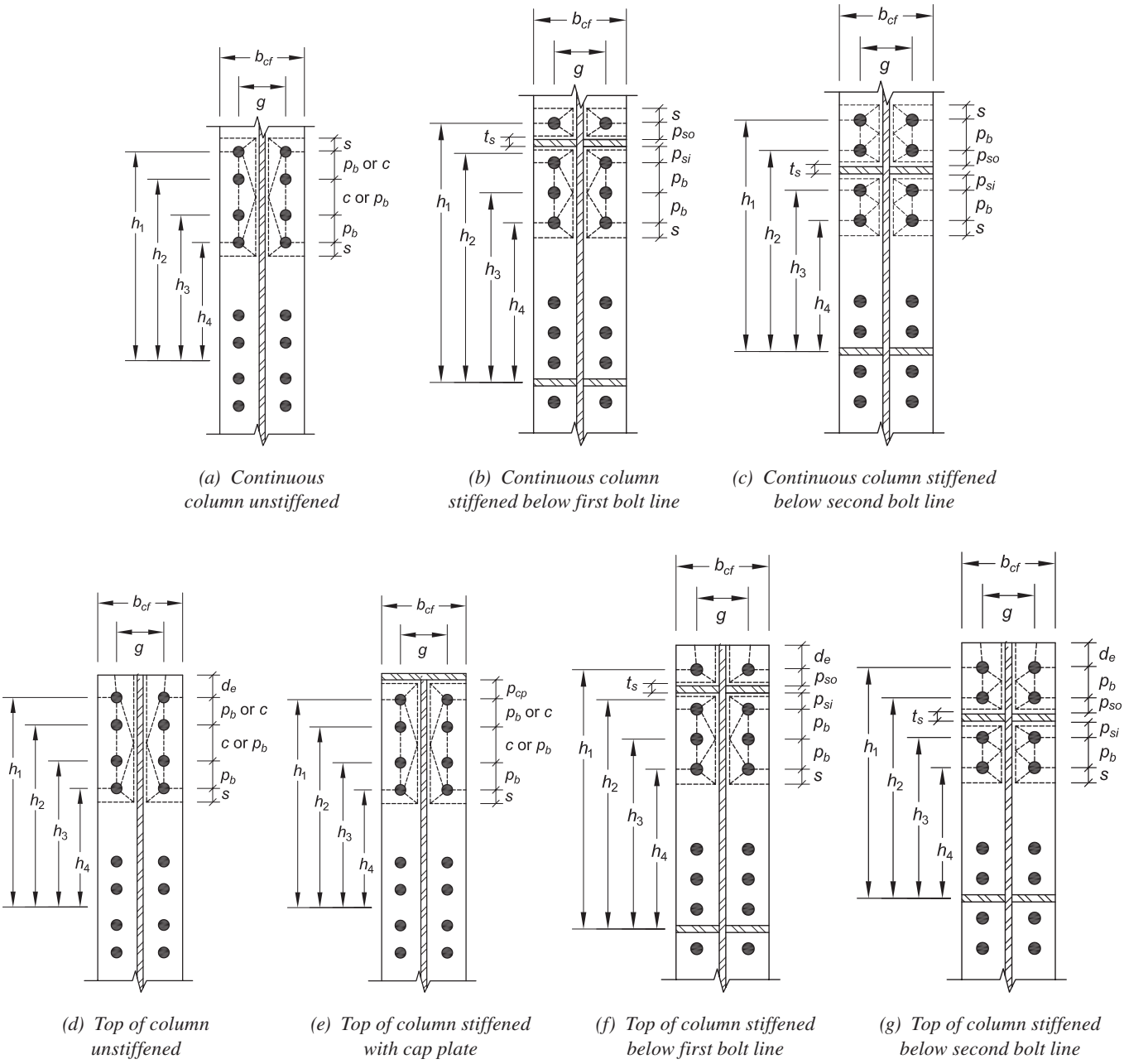

(a) Continuous column unstiffened

(b) Continuous column stiffened below first bolt line

(c) Continuous column stiffened below second bolt line

(d) Top of column unstiffened

(e) Top of column stiffened with cap plate

(f) Top of column stiffened below first bolt line

(g) Top of column stiffened below second bolt line

Fig. A-5. Yield line pattern for eight-bolt, four-row configurations.

Table A-6. Column-Side Yield Line Parameters for Eight-Bolt, Four-Wide Configurations	
Configuration	**Yield Line Parameter**
Continuous unstiffened column [Fig. A-6(a)]	$Y_c = \frac{b_{cf}}{2}\left[h_1\left(\frac{1}{s}\right)+h_2\left(\frac{1}{s}\right)\right]+\frac{2}{g}\left[h_1\left(s+\frac{3}{4}c\right)+h_2\left(s+\frac{1}{4}c\right)\right]+\frac{g}{2}$
Continuous column stiffened between the bolts [Fig. A-6(b)]	$Y_c = \frac{b_{cf}}{2}\left[h_1\left(\frac{1}{s}+\frac{1}{p_{so}}\right)+h_2\left(\frac{1}{p_{si}}+\frac{1}{s}\right)\right]+\frac{2}{g}\left[h_1(s+p_{so})+h_2(p_{si}+s)\right]$ Note: Use $p_{si}=s$ if $p_{si}>s$ Use $p_{so}=s$ if $p_{so}>s$
Top of column unstiffened [Fig. A-6(c)]	$Y_c = \frac{b_{cf}}{2}\left[h_2\left(\frac{1}{s}\right)-\frac{1}{2}\right]+\frac{2}{g}\left[h_1\left(d_e+\frac{3}{4}c\right)+h_2\left(s+\frac{1}{4}c\right)\right]+\frac{3g}{4}$
Top of column with cap plate [Fig. A-6(d)]	$Y_c = \frac{b_{cf}}{2}\left[h_1\left(\frac{1}{p_{cp}}\right)+h_2\left(\frac{1}{s}\right)\right]+\frac{2}{g}\left[h_1\left(p_{cp}+\frac{3}{4}c\right)+h_2\left(s+\frac{1}{4}c\right)\right]+\frac{g}{2}$ Note: Use $p_{cp}=s$ if $p_{cp}>s$
Top of column stiffened between the bolts [Fig. A-6(e)]	$Y_c = \frac{b_{cf}}{2}\left[h_1\left(\frac{1}{p_{so}}\right)+h_2\left(\frac{1}{p_{si}}+\frac{1}{s}\right)-\frac{1}{2}\right]+\frac{2}{g}\left[h_1(p_{so}+d_e)+h_2(p_{si}+s)\right]+\frac{g}{4}$ Note: Use $p_{si}=s$ if $p_{si}>s$ Use $p_{so}=s$ if $p_{so}>s$

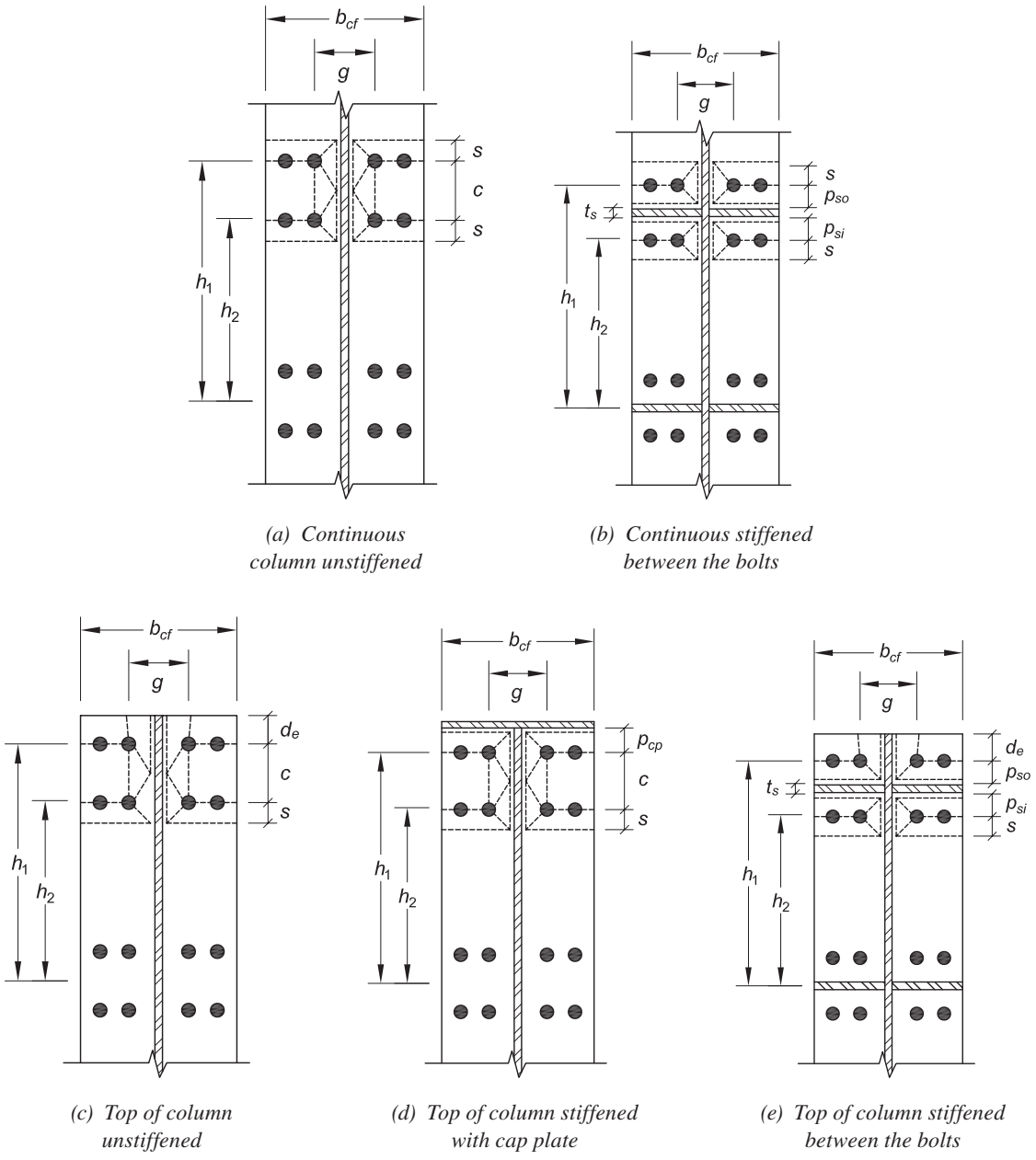

(a) Continuous column unstiffened

(b) Continuous stiffened between the bolts

(c) Top of column unstiffened

(d) Top of column stiffened with cap plate

(e) Top of column stiffened between the bolts

Fig. A-6. Yield line pattern for eight-bolt, four-wide configurations.

Table A-7. Column-Side Yield Line Parameters for 12-Bolt, 4W×2/2W×2 Configurations	
Configuration	**Yield Line Parameter**
Continuous unstiffened column [Fig. A-7(a)]	$Y_c = \frac{b_{cf}}{2}\left[h_1\left(\frac{1}{s}\right)+h_4\left(\frac{1}{s}\right)\right]+\frac{2}{g}\left[h_1\left(s+\frac{3}{2}p_b+\frac{3}{4}c\right)+h_4\left(s+\frac{1}{2}p_b+\frac{1}{4}c\right)\right]+\frac{g}{2}$
Continuous column stiffened below the first bolt line [Fig. A-7(b)]	$Y_c = \frac{b_{cf}}{2}\left[h_1\left(\frac{1}{p_{so}}+\frac{1}{s}\right)+h_2\left(\frac{1}{p_{si}}\right)+h_4\left(\frac{1}{s}\right)\right]$ $+\frac{2}{g}\left[h_1(p_{so}+s)+h_2\left(p_{si}+\frac{3}{2}p_b\right)+h_4\left(s+\frac{1}{2}p_b\right)\right]+\frac{g}{2}$ Note: Use $p_{si}=s$ if $p_{si}>s$ Use $p_{so}=s$ if $p_{so}>s$
Top of column unstiffened [Fig. A-7(c)]	$Y_c = \frac{b_{cf}}{2}\left[h_4\left(\frac{1}{s}\right)-\frac{1}{2}\right]+\frac{2}{g}\left[h_1\left(d_e+\frac{3}{2}p_b+\frac{3}{4}c\right)+h_4\left(s+\frac{1}{2}p_b+\frac{1}{4}c\right)\right]+\frac{3g}{4}$
Top of column with cap plate [Fig. A-7(d)]	$Y_c = \frac{b_{cf}}{2}\left[h_1\left(\frac{1}{p_{cp}}\right)+h_4\left(\frac{1}{s}\right)\right]+\frac{2}{g}\left[h_1\left(p_{cp}+\frac{3}{2}p_b+\frac{3}{4}c\right)+h_4\left(s+\frac{1}{2}p_b+\frac{1}{4}c\right)\right]+\frac{g}{2}$ Note: Use $p_{cp}=s$ if $p_{cp}>s$
Top of column stiffened below the first bolt line [Fig. A-7(e)]	$Y_c = \frac{b_{cf}}{2}\left[h_1\left(\frac{1}{p_{so}}\right)+h_2\left(\frac{1}{p_{si}}\right)+h_4\left(\frac{1}{s}\right)-\frac{1}{2}\right]$ $+\frac{2}{g}\left[h_1(p_{so}+d_e)+h_2\left(p_{si}+\frac{3}{2}p_b\right)+h_4\left(s+\frac{1}{2}p_b\right)\right]+\frac{3g}{4}$ Note: Use $p_{si}=s$ if $p_{si}>s$ Use $p_{so}=s$ if $p_{so}>s$

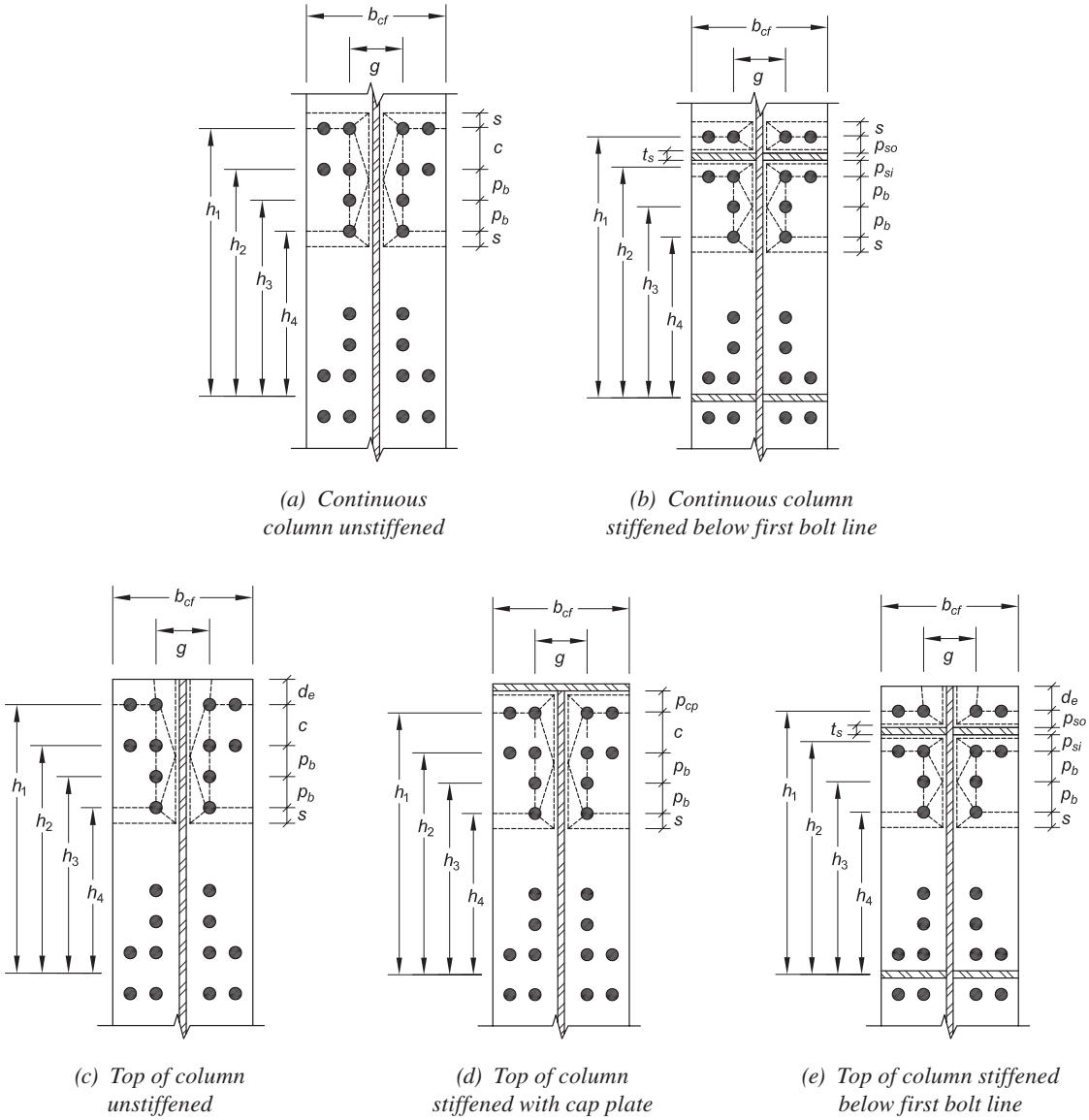

(a) Continuous column unstiffened

(b) Continuous column stiffened below first bolt line

(c) Top of column unstiffened

(d) Top of column stiffened with cap plate

(e) Top of column stiffened below first bolt line

Fig. A-7. Yield line pattern for 12-bolt, 4W×2/2W×2 configurations.

Table A-8. Column-Side Yield Line Parameters for 12-Bolt, 2W/4W×2/2W Configurations	
Configuration	**Yield Line Parameter**
Continuous unstiffened column [Fig. A-8(a)]	$Y_c = \frac{b_{cf}}{2}\left[h_1\left(\frac{1}{s}\right)+h_4\left(\frac{1}{s}\right)\right]+\frac{2}{g}\left[h_1\left(s+\frac{3}{2}p_b+\frac{3}{4}c\right)+h_4\left(s+\frac{1}{2}p_b+\frac{1}{4}c\right)\right]+\frac{g}{2}$
Continuous column stiffened below the second bolt line [Fig. A-8(b)]	$Y_c = \frac{b_{cf}}{2}\left[h_1\left(\frac{1}{s}\right)+h_2\left(\frac{1}{p_{so}}\right)+h_3\left(\frac{1}{p_{si}}\right)+h_4\left(\frac{1}{s}\right)\right]$ $+\frac{2}{g}\left[h_1\left(\frac{3p_b}{4}+s\right)+h_2\left(\frac{p_b}{4}+p_{so}\right)+h_3\left(\frac{3p_b}{4}+p_{si}\right)+h_4\left(\frac{p_b}{4}+s\right)\right]+g$ Note: Use $p_{si}=s$ if $p_{si}>s$ Use $p_{so}=s$ if $p_{so}>s$
Top of column unstiffened [Fig. A-8(c)]	$Y_c = \frac{b_{cf}}{2}\left[h_4\left(\frac{1}{s}\right)-\frac{1}{2}\right]+\frac{2}{g}\left[h_1\left(d_e+\frac{3}{2}p_b+\frac{3}{4}c\right)+h_4\left(s+\frac{1}{2}p_b+\frac{1}{4}c\right)\right]+\frac{3g}{4}$
Top of column with cap Plate [Fig. A-8(d)]	$Y_c = \frac{b_{cf}}{2}\left[h_1\left(\frac{1}{p_{cp}}\right)+h_4\left(\frac{1}{s}\right)\right]+\frac{2}{g}\left[h_1\left(p_{cp}+\frac{3}{2}p_b+\frac{3}{4}c\right)+h_4\left(s+\frac{1}{2}p_b+\frac{1}{4}c\right)\right]+\frac{g}{2}$ Note: Use $p_{cp}=s$ if $p_{cp}>s$
Top of column stiffened below the second bolt line [Fig. A-8(e)]	$Y = \frac{b_{cf}}{2}\left[h_2\left(\frac{1}{p_{so}}\right)+h_3\left(\frac{1}{p_{si}}\right)+h_4\left(\frac{1}{s}\right)-\frac{1}{2}\right]$ $+\frac{2}{g}\left[h_1\left(\frac{3p_b}{4}+d_e\right)+h_2\left(\frac{p_b}{4}+p_{so}\right)+h_3\left(\frac{3p_b}{4}+p_{si}\right)+h_4\left(s+\frac{p_b}{4}\right)\right]+\frac{5g}{4}$ Note: Use $p_{si}=s$ if $p_{si}>s$ Use $p_{so}=s$ if $p_{so}>s$

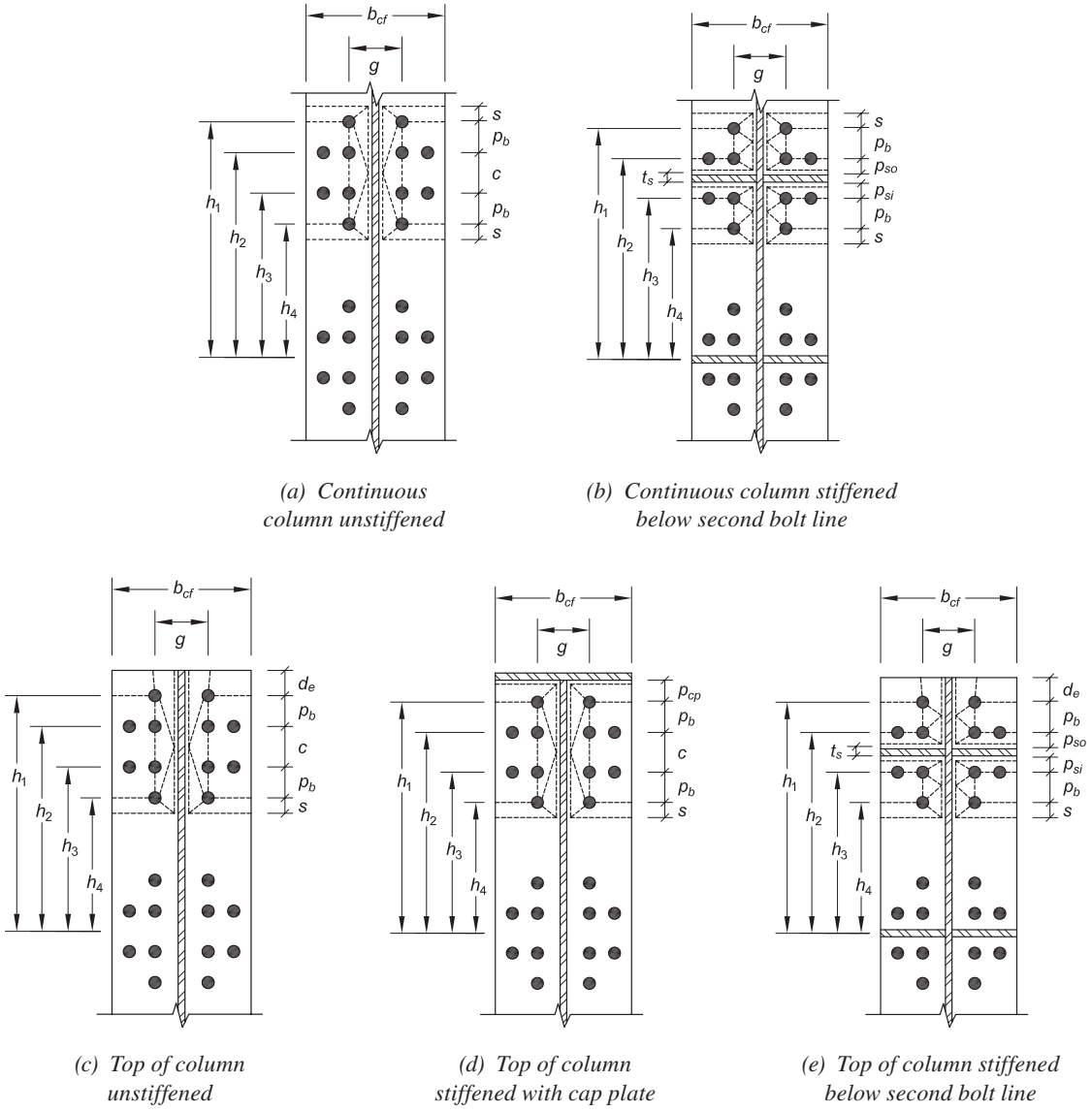

(a) Continuous column unstiffened

(b) Continuous column stiffened below second bolt line

(c) Top of column unstiffened

(d) Top of column stiffened with cap plate

(e) Top of column stiffened below second bolt line

Fig. A-8. Yield line pattern for 12-bolt, 2W/4W×2/2W configurations.

APPENDIX B
Gravity, Wind, and Low-Seismic-Ductility Thin End-Plate Design Examples

This appendix contains flush and extended thin end-plate design examples.

B.1 CONNECTION EXAMPLES

The connection design data for each connection is the same as for the corresponding thick end-plate design examples in Section 5.2.3 Flush End-Plate Connections and Section 5.3.3 Extended End-Plate Connections, with one exception. The exception is Example B.3-7, where a built-up beam section is specified for the 8ES connection instead of the hot-rolled section used in Example 5.3-7.

B.2 FLUSH THIN END-PLATE CONNECTIONS

EXAMPLE B.2-1—Two-Bolt Flush Unstiffened Thin End-Plate Example

Given:

The connection shown in Figure B-1 is a two-bolt flush end-plate connection for a W18×35 beam to the top of a W12×35 column. The beam and column are ASTM A992/A992M steel, and the plate steel is ASTM A572/A572M Grade 50. Bolts are Group 120 ASTM F3125/F3125M Grade A325, snug-tightened. Weld electrodes are E70XX. Note that the end-plate width is greater than the beam flange width. The connection is to be evaluated as a thin end-plate design for the following required moments and forces:

	LRFD	ASD
Moment	M_u = 800 kip-in.	M_a = 533 kip-in.
Axial tension	T_u = 3.3 kips	T_a = 2.2 kips
Shear force	V_u = 25.8 kips	V_a = 17.2 kips

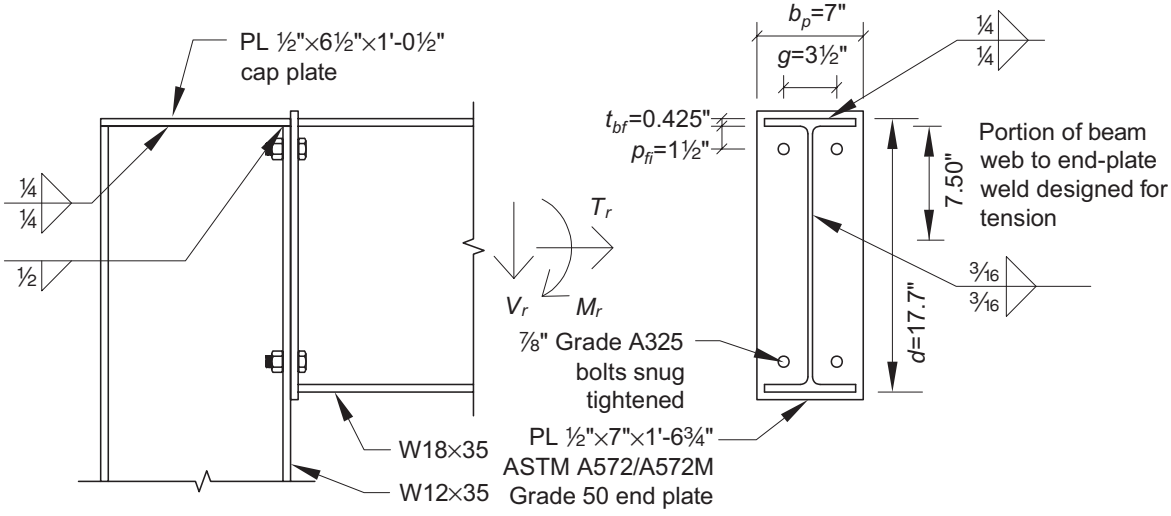

Fig. B-1. Two-bolt unstiffened thin end-plate configuration for Example B.2-1.

Solution:

From AISC *Manual* Table 2-4, the material properties are as follows:

ASTM A992/A992M
$F_y = 50$ ksi
$F_u = 65$ ksi

ASTM A572/A572M Grade 50
$F_y = 50$ ksi
$F_u = 65$ ksi

From AISC *Specification* Table J3.2, the material properties of the bolts are as follows:

Group 120 ASTM F3125/F3125M ⅞-in.-diameter Grade A325 bolts snug-tightened
$F_{nt} = 90$ ksi
$F_{nv} = 54$ ksi (Group 120 bolts with threads not excluded from the shear plane; thread condition N)

From AISC *Manual* Table 1-1, the geometric properties are as follows:

Beam: W18×35
$d = 17.7$ in. $t_{bw} = 0.300$ in.
$b_{bf} = 6.00$ in. $t_{bf} = 0.425$ in.

Column: W12×35
$d_c = 12.5$ in. $t_{cw} = 0.300$ in.
$b_{cf} = 6.56$ in. $t_{cf} = 0.520$ in.
$k_{des} = 0.820$ in. $k_1 = ¾$ in.

End-plate geometric properties:
$b_p = 7$ in.
$t_p = ½$ in.
$g = 3½$ in.
$p_{fi} = 1½$ in.
$d_p = 18¾$ in.

The distance from the centerline of the compression flange to the bolt line, h_1, is depicted in Table 5-2 and computed as:

$$h_1 = d - \frac{3}{2}t_{bf} - p_{fi}$$
$$= 17.7 \text{ in.} - \frac{3(0.425 \text{ in.})}{2} - 1½ \text{ in.}$$
$$= 15.6 \text{ in.}$$

$$b_{p,eff} \le b_{bf} + \max(t_p, 1 \text{ in.}) \quad (4\text{-}3)$$
$$\le 6.00 \text{ in.} + \max(½ \text{ in.}, 1 \text{ in.})$$
$$\le 7.00 \text{ in.}$$

$b_p = 7$ in. $\le$ 7.00 in. **o.k.**

$$b_{bf} \ge g \quad (4\text{-}1)$$
6.00 in. ≥ 3½ in. **o.k.**

A. End-Plate and Bolt Design Verification

Calculate the equivalent required moment considering the effect of the required tension force using Equation 3-30.

LRFD	ASD
$M_{u,eq} = M_u + (T_u/2)(d - t_{bf})$ $= 800 \text{ kip-in.} + (3.3 \text{ kips}/2)(17.7 \text{ in.} - 0.425 \text{ in.})$ $= 829 \text{ kip-in.}$	$M_{a,eq} = M_a + (T_a/2)(d - t_{bf})$ $= 533 \text{ kip-in.} + (2.2 \text{ kips}/2)(17.7 \text{ in.} - 0.425 \text{ in.})$ $= 552 \text{ kip-in.}$

Determine the required end-plate thickness using Equations 5-5. First solve for the distance, s, and yield line parameter, Y_p, using Table 5-2.

$$s = \frac{\sqrt{b_p g}}{2}$$
$$= \frac{\sqrt{(7 \text{ in.})(3\frac{1}{2} \text{ in.})}}{2}$$
$$= 2.47 \text{ in.}$$

Because $s \geq p_{fi} = 1\frac{1}{2}$ in., the dimension p_{fi} is used in the equation for the yield line parameter.

$$Y_p = \frac{b_p}{2}\left[h_1\left(\frac{1}{p_{fi}} + \frac{1}{s}\right)\right] + \frac{2}{g}\left[h_1(p_{fi} + s)\right]$$
$$= \left(\frac{7 \text{ in.}}{2}\right)\left[(15.6 \text{ in.})\left(\frac{1}{1\frac{1}{2} \text{ in.}} + \frac{1}{2.47 \text{ in.}}\right)\right] + \left(\frac{2}{3\frac{1}{2} \text{ in.}}\right)\left[(15.6 \text{ in.})(1\frac{1}{2} \text{ in.} + 2.47 \text{ in.})\right]$$
$$= 93.9 \text{ in.}$$

Determine the required end-plate thickness using Equations 5-5. For flush end-plate configurations, $\gamma_r = 0.80$.

LRFD	ASD
$t_{p,reqd} = \sqrt{\frac{M_{u,eq}}{\gamma_r \phi_b F_y Y_p}}$ $= \sqrt{\frac{829 \text{ kip-in.}}{0.80(0.90)(50 \text{ ksi})(93.9 \text{ in.})}}$ $= 0.495 \text{ in.} \quad \leq \quad ½ \text{ in.} \quad$ **o.k.**	$t_{p,reqd} = \sqrt{\frac{\Omega_b M_{a,eq}}{\gamma_r F_y Y_p}}$ $= \sqrt{\frac{1.67(552 \text{ kip-in.})}{0.80(50 \text{ ksi})(93.9 \text{ in.})}}$ $= 0.495 \text{ in.} \quad \leq \quad ½ \text{ in.} \quad$ **o.k.**

The specified ½-in.-thick ASTM A572/A572M Grade 50 end plate is sufficient.

Determine if the specified ⅞-in.-diameter Grade A325 snug-tightened bolts are sufficient. First calculate the geometry of the effective tee stub; then calculate the related forces, F_i, Q_{max}, and P_{qi}; finally, calculate the required bolt diameter and compare with the specified diameter.

The bolts are specified to be snug-tightened according to Figure B-1. According to Table 3-3, the snug-tightened bolt pretension for a ⅞-in.-diameter Grade A325 bolt is approximately 38% of the full pretension, or $T_b = 14.6$ kips. The nominal unthreaded body area of a ⅞ in. bolt is $A_b = 0.601 \text{ in.}^2$, and the nominal tensile stress for a Grade A325 bolt is $F_{nt} = 90$ ksi. The resulting nominal tensile strength of a ⅞-in.-diameter Grade A325 bolt is:

$$P_t = F_{nt} A_b \qquad \text{(from } \textit{Spec.} \text{ Eq. J3-1)}$$
$$= (90 \text{ ksi})(0.601 \text{ in.}^2)$$
$$= 54.1 \text{ kips}$$

Calculate the geometry of the effective tee stub, including the distance from the bolt to the prying reaction force, a_1, the width of the effective tee stub, w_1, the net effective width, w_1', and the distance from the effective tee stem to the bolt hole, b_1.

$$a_1 = 3.62\left(\frac{t_p}{d_b}\right)^3 - 0.085 \tag{3-24}$$

$$= 3.62\left(\frac{½ \text{ in.}}{⅞ \text{ in.}}\right)^3 - 0.085$$

$$= 0.590 \text{ in.}$$

$$w_1 = \frac{b_p}{2}$$

$$= \frac{7 \text{ in.}}{2}$$

$$= 3.50 \text{ in.}$$

$$w_1' = w_1 - (d_b + 1/16 \text{ in.}) \tag{5-7}$$

$$= 3.50 \text{ in.} - (⅞ \text{ in.} + 1/16 \text{ in.})$$

$$= 2.56 \text{ in.}$$

$$b_1 = p_{fi}$$

$$= 1½ \text{ in.}$$

Find the forces related to prying, including the force, F_1', the prying force, $Q_{max,1}$, and the bolt tension contributing to flexural strength, P_{q1}.

$$F_1' = \frac{1}{b_1}\left[\frac{t_p^2 F_y}{4}(0.85w_1 + 0.8w_1') + \frac{\pi d_b^2 F_{nt}}{32}\right] \tag{3-26}$$

$$= \left(\frac{1}{1½ \text{ in.}}\right)\left\{\left[\frac{(½ \text{ in.})^2 (50 \text{ ksi})}{4}\right]\left[0.85(3.50 \text{ in.}) + 0.8(2.56 \text{ in.})\right] + \frac{\pi(⅞ \text{ in.})^3 (90 \text{ ksi})}{32}\right\}$$

$$= 14.4 \text{ kips}$$

$$Q_{max,1} = \frac{w_1' t_p^2}{4a_1}\sqrt{F_y^2 - 3\left(\frac{F_1'}{w_1' t_p}\right)^2} \tag{3-23}$$

$$= \frac{(2.56 \text{ in.})(½ \text{ in.})^2}{4(0.590 \text{ in.})}\sqrt{(50 \text{ ksi})^2 - 3\left[\frac{14.4 \text{ kips}}{(2.56 \text{ in.})(½ \text{ in.})}\right]^2}$$

$$= 12.5 \text{ kips}$$

$$P_{q1} = \max(P_t - Q_{max,1}, T_b) \tag{3-27}$$

$$= \max(54.1 \text{ kips} - 12.5 \text{ kips}, 14.6 \text{ kips})$$

$$= 41.6 \text{ kips}$$

Calculate the flexural strength for bolt rupture with prying action, M_q, using Equation 3-28. Then the available flexural strength is compared to the required flexural strength.

$$M_q = \sum_i \alpha_i P_{qi} n_i h_i \tag{3-28}$$

$$= 1.0(41.6 \text{ kips})(2 \text{ bolts})(15.6 \text{ in.})$$

$$= 1{,}300 \text{ kip-in.}$$

LRFD	ASD
$\phi M_q = 0.75(1{,}300 \text{ kip-in.})$ $= 975 \text{ kip-in.} \quad \geq \quad M_u = 800 \text{ kip-in.}$ **o.k.**	$\frac{M_q}{\Omega} = \frac{1{,}300 \text{ kip-in.}}{2.00}$ $= 650 \text{ kip-in.} \quad \geq \quad M_a = 533 \text{ kip-in.}$ **o.k.**

Check Shear Transfer at the Bottom Holes

Shear at the faying surface, V_u, is assumed to be resisted only by the two compression side bolts. The shear transfer strength at each bolt hole is the minimum of the end-plate bearing/tearout strength, the bolt shear rupture strength, and the column flange bearing/tearout strength. See the User Note in AISC *Specification* Section J3.7.

The nominal unthreaded body area of a ⅞ in. bolt is $A_b = 0.601 \text{ in.}^2$ The resulting nominal shear strength of a ⅞-in.-diameter Grade A325 bolt is:

$R_{n,bt} = F_{nv} A_b$ (from *Spec.* Eq. J3-1)

$= (54 \text{ ksi})(0.601 \text{ in.}^2)$

$= 32.5 \text{ kips}$

The nominal bearing/tearout strength is given in AISC *Specification* Section J3.11. The bolt shear force acting on the end plate is up toward the middle of the end plate, and therefore, tearout will not control. The bolt shear force acting on the column flange is down, and again, tearout will not control. The end plate is ½ in. thick and the column flange is 0.520 in. thick, so the end plate will control the bearing/tearout strength at the bottom bolt holes. The bearing strength at a bolt hole is:

$R_{n,brg} = 2.4 d_b t_p F_u$ (from *Spec.* Eq. J3-6a)

$= 2.4(⅞ \text{ in.})(½ \text{ in.})(65 \text{ ksi})$

$= 68.3 \text{ kips}$

The shear transfer strength is then the minimum of the column flange bearing strength and the bolt shear rupture strength; hence, $R_n = 32.5$ kips.

Therefore, the nominal shear transfer strength at the two bottom bolt holes is:

$V_n = (2 \text{ bolts}) R_n$

$= (2 \text{ bolts})(32.5 \text{ kips})$

$= 65.0 \text{ kips}$

LRFD	ASD
$\phi V_n = 0.75(65.0 \text{ kips})$ $= 48.8 \text{ kips} \quad \geq \quad V_u = 25.8 \text{ kips}$ **o.k.**	$\frac{V_n}{\Omega} = \frac{65.0 \text{ kips}}{2.00}$ $= 32.5 \text{ kips} \quad \geq \quad V_a = 17.2 \text{ kips}$ **o.k.**

The specified ASTM A572/A572M Grade 50 ½-in.-thick end plate and ⅞-in.-diameter Grade A325 snug-tightened bolts are sufficient.

B. Check Beam to End-Plate Welds

Weld strength calculations for this thin end-plate design are the same as for the thick end-plate design in Example 5.2-1.

C. Check Column-Side Limit States

Calculations to verify the strength of the column-side limit states for the connection shown in Figure B-1 are identical to those for the thick end-plate design in Example 5.2-1, except for the column web local yielding check. For this check, the end-plate thickness is ½ in. instead of 9/16 in. for the thick plate design. The difference has no effect on the design shown in Figure B-1.

Summary

The connection shown in Figure B-1 is adequate for the required moment and tensile and shear forces.

EXAMPLE B.2-2—Four-Bolt Flush Unstiffened Thin End-Plate Example

Given:

The connection shown in Figure B-2 is a four-bolt flush unstiffened end-plate moment connection for a W18×35 beam. The W18×35 beam is ASTM A992/A992M material, and the end-plate material is ASTM A572/A572M Grade 50. Bolts are Group 120 ASTM F3125/F3125M Grade A325 snug tightened. Weld electrodes are E70XX. The connection is to be evaluated as a thin end-plate design for the following required moments and shear forces.

	LRFD	ASD
Moment	M_u = 1,500 kip-in.	M_a = 1,000 kip-in.
Shear force	V_u = 25.8 kips	V_a = 17.2 kips

Solution:

From AISC *Manual* Table 2-4, the material properties are as follows:

ASTM A992/A992M
F_y = 50 ksi
F_u = 65 ksi

ASTM A572/A572M Grade 50
F_y = 50 ksi
F_u = 65 ksi

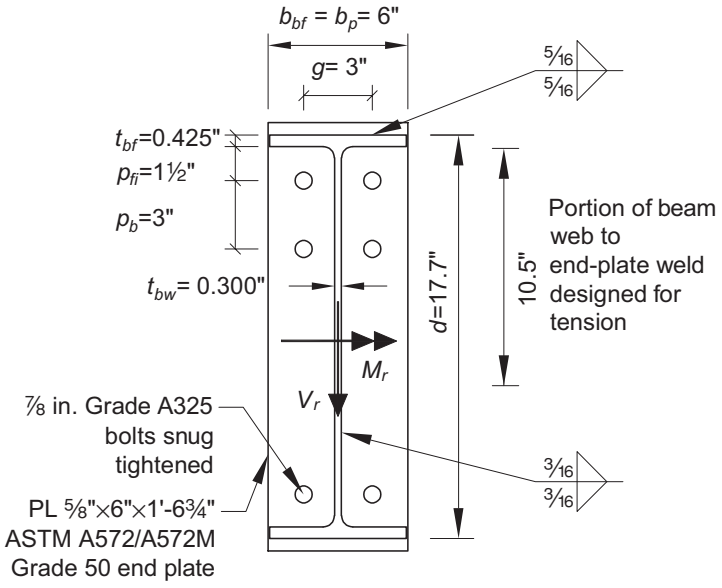

Fig. B-2. Four-bolt unstiffened thin end-plate configuration for Example B.2-2.

From AISC *Specification* Table J3.2, the material properties of the bolts are as follows:

Group 120 ASTM F3125/F3125M ⅞-in.-diameter Grade 325 bolts snug-tightened
$F_{nt} = 90$ ksi
$F_{nv} = 54$ ksi (Group 120 bolts with threads not excluded from the shear plane; thread condition N)

From AISC *Manual* Table 1-1, the geometric properties are as follows:

Beam: W18×35
$d = 17.7$ in. $t_{bw} = 0.300$ in.
$b_{bf} = 6.00$ in. $t_{bf} = 0.425$ in.

End-plate geometric properties:
$b_p = 6$ in.
$t_p = ⅝$ in.
$g = 3$ in.
$p_{fi} = 1½$ in.
$p_b = 3$ in.
$d_p = 18¾$ in.

The distances from the centerline of the compression flange to the bolt lines, h_1 and h_2, are depicted in Table 5-3 and computed as:

$$h_1 = d - \frac{3}{2}t_{bf} - p_{fi}$$
$$= 17.7 \text{ in.} - \frac{3(0.425 \text{ in.})}{2} - 1½ \text{ in.}$$
$$= 15.6 \text{ in.}$$

$$h_2 = d - \frac{3}{2}t_{bf} - p_{fi} - p_b$$
$$= 17.7 \text{ in.} - \frac{3(0.425 \text{ in.})}{2} - 1½ \text{ in.} - 3 \text{ in.}$$
$$= 12.6 \text{ in.}$$

$$b_{p,eff} \le b_{bf} + \max(t_p, 1 \text{ in.}) \quad (4\text{-}3)$$
$$\le 6.00 \text{ in.} + \max(⅝ \text{ in.}, 1 \text{ in.})$$
$$\le 7.00 \text{ in.}$$

$b_p = 6$ in. $\le$ 7.00 in. **o.k.**

$$b_{bf} \ge g \quad (4\text{-}1)$$
6.00 in. ≥ 3 in. **o.k.**

A. End-Plate and Bolt Design Verification

Determine the required end-plate thickness using Equations 5-5. First solve for the distance, s, and yield line parameter, Y_p, using Table 5-3.

$$s = \frac{\sqrt{b_p g}}{2}$$
$$= \frac{\sqrt{(6 \text{ in.})(3 \text{ in.})}}{2}$$
$$= 2.12 \text{ in.}$$

Because $s \geq p_{fi} = 1\frac{1}{2}$ in., the dimension p_{fi} is used in the equation for the yield line parameter.

$$Y_p = \frac{b_p}{2}\left[h_1\left(\frac{1}{p_{fi}}\right) + h_2\left(\frac{1}{s}\right)\right] + \frac{2}{g}\left[h_1(p_{fi} + 0.75p_b) + h_2(s + 0.25p_b)\right] + \frac{g}{2}$$

$$= \left(\frac{6 \text{ in.}}{2}\right)\left[(15.6 \text{ in.})\left(\frac{1}{1\frac{1}{2} \text{ in.}}\right) + (12.6 \text{ in.})\left(\frac{1}{2.12 \text{ in.}}\right)\right]$$

$$+ \left(\frac{2}{3 \text{ in.}}\right)\left\{(15.6 \text{ in.})\left[1\frac{1}{2} \text{ in.} + 0.75(3 \text{ in.})\right] + (12.6 \text{ in.})\left[2.12 \text{ in.} + 0.25(3 \text{ in.})\right]\right\} + \frac{3 \text{ in.}}{2}$$

$$= 114 \text{ in.}$$

Determine the required end-plate thickness using Equations 5-5. For flush end-plate configurations, $\gamma_r = 0.80$.

LRFD	ASD
$t_{p,reqd} = \sqrt{\frac{M_u}{\gamma_r \phi_b F_y Y_p}}$	$t_{p,reqd} = \sqrt{\frac{\Omega_b M_a}{\gamma_r F_y Y_p}}$
$= \sqrt{\frac{1{,}500 \text{ kip-in.}}{0.80(0.90)(50 \text{ ksi})(114 \text{ in.})}}$	$= \sqrt{\frac{1.67(1{,}000 \text{ kip-in.})}{0.80(50 \text{ ksi})(114 \text{ in.})}}$
$= 0.605 \text{ in.} \leq \frac{5}{8} \text{ in.}$ **o.k.**	$= 0.605 \text{ in.} \leq \frac{5}{8} \text{ in.}$ **o.k.**

The specified 5/8-in.-thick ASTM A572/A572M Grade 50 end plate is sufficient.

Determine if the specified 7/8-in.-diameter Grade A325 snug-tightened bolts are sufficient. Solve for the flexural strength for bolt rupture with prying action, and check that the bolt size is sufficient. Because the effective tee stub associated with the two bolt positions is unique, it is necessary to calculate the prying action for each bolt position separately. Figure B-3 shows effective tee-stub geometry for the two bolt positions, wherein the strategy presented in Section 5.1.2 is used to determine the orientation of each effective tee stub.

The selected bolts are given to be snug-tightened according to Figure B-2. According to Table 3-3, the snug-tightened bolt pretension for a 7/8 in. Grade A325 bolt is approximately 38% of the full pretension, or $T_b = 14.6$ kips. The nominal unthreaded body area of a 7/8 in. bolt is $A_b = 0.601$ in.^{2}, and the nominal tensile stress for a Grade A325 bolt is $F_{nt} = 90$ ksi. The resulting nominal tensile strength of a 7/8-in.-diameter Grade A325 bolt is:

$$P_t = F_{nt} A_b \qquad \text{(from } \textit{Spec.} \text{ Eq. J3-1)}$$

$$= (90 \text{ ksi})(0.601 \text{ in.}^2)$$

$$= 54.1 \text{ kips}$$

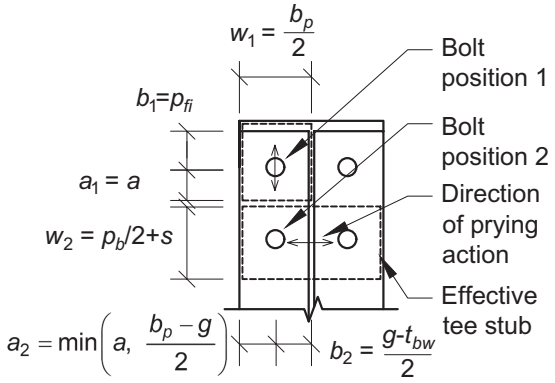

Fig. B-3. Effective tee-stub geometry for the four-bolt flush configuration.

Calculate the bolt distance from the bolt to the edge of the effective tee stub:

$$a = 3.62\left(\frac{t_p}{d_b}\right)^3 - 0.085 \text{ in.} \tag{3-24}$$

$$= 3.62\left(\frac{\text{⅝ in.}}{\text{⅞ in.}}\right)^3 - 0.085 \text{ in.}$$

$$= 1.23 \text{ in.}$$

Bolt Position 1—Top Bolt

For bolt position 1 (see Figure B-3), calculate the geometry of the effective tee stub, including the width of the effective tee stub, w_1, the net effective width, w_1', and distance from effective tee stem to the bolt, b_1.

$$w_1 = \frac{b_p}{2}$$

$$= \frac{6 \text{ in.}}{2}$$

$$= 3.00 \text{ in.}$$

$$w_1' = w_1 - (d_b + \text{1⁄16 in.}) \tag{5-7}$$

$$= 3.00 \text{ in.} - (\text{⅞ in.} + \text{1⁄16 in.})$$

$$= 2.06 \text{ in.}$$

$$a_1 = a$$

$$= 1.23 \text{ in.}$$

$$b_1 = p_{fi}$$

$$= 1\text{½ in.}$$

Find the forces related to prying, including the force, F_1', the prying force, $Q_{max,1}$, and the bolt tension contributing to flexural strength, P_{q1}.

$$F_1' = \frac{1}{b_1}\left[\frac{t_p^2 F_y}{4}(0.85w_1 + 0.8w_1') + \frac{\pi d_b^3 F_{nt}}{32}\right] \tag{3-26}$$

$$= \left(\frac{1}{1\text{½ in.}}\right)\left\{\left[\frac{(\text{⅝ in.})^2(50 \text{ ksi})}{4}\right]\left[0.85(3.00 \text{ in.}) + 0.8(2.06 \text{ in.})\right] + \frac{\pi(\text{⅞ in.})^3(90 \text{ ksi})}{32}\right\}$$

$$= 17.6 \text{ kips}$$

$$Q_{max,1} = \frac{w_1' t_p^2}{4a_1}\sqrt{F_y^2 - 3\left(\frac{F_1'}{w_1' t_p}\right)^2} \tag{3-23}$$

$$= \frac{(2.06 \text{ in.})(\text{⅝ in.})^2}{4(1.23 \text{ in.})}\sqrt{(50 \text{ ksi})^2 - 3\left[\frac{17.6 \text{ kips}}{(2.06 \text{ in.})(\text{⅝ in.})}\right]^2}$$

$$= 7.20 \text{ kips}$$

$$P_{q1} = \max(P_t - Q_{max,1},\ T_b) \tag{3-27}$$

$$= \max(54.1 \text{ kips} - 7.19 \text{ kips},\ 14.6 \text{ kips})$$

$$= 46.9 \text{ kips}$$

Table B-1. Prying Action for the Four-Bolt Unstiffened Example		
Parameter	**Bolt Position 1**	**Bolt Position 2**
w_i (in.)	3.00	3.62
w_i' (in.)	2.06	2.68
a_i (in.)	1.23	1.23
b_i (in.)	1.50	1.35
F_i' (kips)	17.6	23.3
$Q_{max,i}$ (kips)	7.19	9.32
P_{qi} (kips)	46.9	44.8
α_i	1.0	1.0

Prying forces for bolt position 2 are calculated in a similar way using the effective tee-stub geometry shown in Figure B-3. Table B-1 gives the geometric parameters, the related prying force, the usable strength for each bolt position, and the reduction in bolt contribution factor, α_i.

Calculate the flexural strength for bolt rupture with prying action, M_q, using Equation 3-28. Then the design flexural strength is compared to the required flexural strength.

$$M_q = \sum_i \alpha_i P_{qi} n_i h_i \tag{3-28}$$

$$= 1.0(46.9 \text{ kips})(2 \text{ bolts})(15.6 \text{ in.}) + 1.0(44.8 \text{ kips})(2 \text{ bolts})(12.6 \text{ in.})$$

$$= 2{,}590 \text{ kip-in.}$$

LRFD	ASD
$\phi M_q = 0.75(2{,}590 \text{ kip-in.})$ $= 1{,}940 \text{ kip-in.} \quad \geq \quad M_u = 1{,}500 \text{ kip-in.}$ **o.k.**	$\frac{M_q}{\Omega} = \frac{2{,}590 \text{ kip-in.}}{2.00}$ $= 1{,}300 \text{ kip-in.} \quad \geq \quad M_a = 1{,}000 \text{ kip-in.}$ **o.k.**

Therefore ⅞-in.-diameter Grade A325 snug-tightened bolts are sufficient.

Check Shear Transfer Strength at the Bottom Holes

See Example B.2-1 for calculation procedures.

B. Check Beam to End-Plate Welds

Weld strength calculations for this thin end-plate design are the same as for the thick end-plate design in Example 5.2-2.

C. Check Column-Side Limit States

See Example 5.2-1 for example column-side limit state check calculations.

Summary

The connection shown in Figure B-2 is adequate for the required moment and shear force.

EXAMPLE B.2-3—Four-Bolt Flush Stiffened with Web Stiffener between the Tension Bolts Thin End-Plate Example

Given:

The connection shown in Figure B-4 is a four-bolt flush, stiffened between the tension bolts, end-plate moment connection with a built-up beam. The beam and all plates are ASTM A572/A572M Grade 50 material. The bolts are Group 120 ASTM F3125/F3125M Grade A325 snug-tightened. Weld electrodes are E70XX. The connection is to be evaluated as a thin end-plate design for the following required moments and shear forces.

	LRFD	ASD
Moment	M_u = 2,500 kip-in.	M_a = 1,670 kip-in.
Shear force	V_u = 25.8 kips	V_a = 17.2 kips

Solution:

From AISC *Manual* Table 2-4, the material properties are as follows:

ASTM A572/A572M Grade 50
F_y = 50 ksi
F_u = 65 ksi

From AISC *Specification* Table J3.2, the material properties of the bolts are as follows:

Group 120 ASTM F3125/F3125M 1-in.-diameter Grade A325 bolts snug-tightened
F_{nt} = 90 ksi
F_{nv} = 54 ksi (Group 120 bolts with threads not excluded from the shear plane; thread condition N)

Beam
d = 20 in. t_{bw} = ¼ in.
b_{bf} = 6 in. t_{bf} = ½ in.

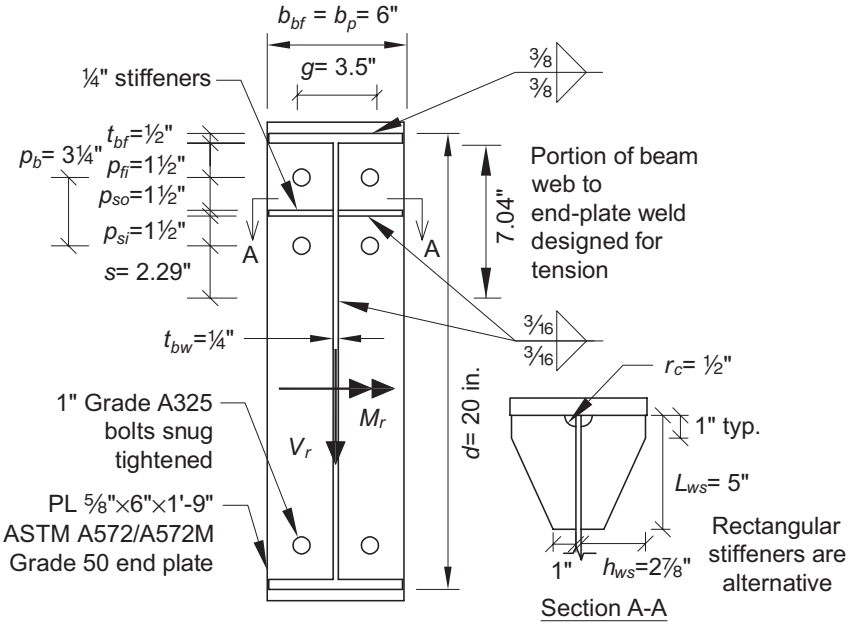

Fig. B-4. Four-bolt stiffened with web stiffener between the tension bolts thin end-plate configuration for Example B.2-3.

End-plate geometric properties:

b_p = 6 in.
t_p = ⅝ in.
g = 3½ in.
p_{fi} = 1½ in.
p_{so} = 1½ in.
p_{si} = 1½ in.
p_b = 3¼ in.
d_p = 21 in.

The distances from the centerline of the compression flange to the bolt lines, h_1 and h_2, are depicted in Table 5-4 and computed as:

$$h_1 = d - \frac{3}{2}t_{bf} - p_{fi}$$
$$= 20 \text{ in.} - \frac{3(½ \text{ in.})}{2} - 1½ \text{ in.}$$
$$= 17.8 \text{ in.}$$

$$h_2 = d - \frac{3}{2}t_{bf} - p_{fi} - p_b$$
$$= 20 \text{ in.} - \frac{3(½ \text{ in.})}{2} - 1½ \text{ in.} - 3¼ \text{ in.}$$
$$= 14.5 \text{ in.}$$

$$b_{p,eff} \le b_{bf} + \max(t_p, 1 \text{ in.}) \quad (4\text{-}3)$$
$$\le 6 \text{ in.} + \max(⅝ \text{ in.}, 1 \text{ in.})$$
$$\le 7.00 \text{ in.}$$

$b_p = 6 \text{ in.} \le 7.00 \text{ in.}$ **o.k.**

$$b_{bf} \ge g \quad (4\text{-}1)$$

6 in. ≥ 3½ in. **o.k.**

Beam web stiffener geometric properties:

$$h_{ws} = (b_p - t_{bw})/2$$
$$= (6 \text{ in.} - ¼ \text{ in.})/2$$
$$= 2⅞ \text{ in.}$$

$$L_{ws} = h_{ws}/\tan 30° \quad (4\text{-}4)$$
$$= (2⅞ \text{ in.})/\tan 30°$$
$$= 4.99 \text{ in.} \le 5 \text{ in.}$$ **o.k.**

A. End-Plate and Bolt Design Verification

Determine if the specified end-plate thickness, ⅝ in., and bolt diameter, 1 in., are sufficient using the thin end-plate/smaller bolt diameter procedure.

Solve for the required end-plate thickness using Equations 5-5. First solve for the distance, s, and check limits. Then calculate the yield line parameter, Y_p, using Table 5-4.

$$s = \frac{\sqrt{b_p g}}{2}$$
$$= \frac{\sqrt{(6\text{ in.})(3\text{½ in.})}}{2}$$
$$= 2.29\text{ in.}$$

Because $s \geq p_{fi} = 1\text{½}$ in., $p_{so} = 1\text{½}$ in., and $p_{si} = 1\text{½}$ in., the dimensions p_{fi}, p_{so}, and p_{si} are used in the equation for the yield line parameter.

$$Y_p = \frac{b_p}{2}\left[h_1\left(\frac{1}{p_{fi}} + \frac{1}{p_{so}}\right) + h_2\left(\frac{1}{s} + \frac{1}{p_{si}}\right)\right] + \frac{2}{g}\left[h_1(p_{fi} + p_{so}) + h_2(s + p_{si})\right]$$
$$= \left(\frac{6\text{ in.}}{2}\right)\left[(17.8\text{ in.})\left(\frac{1}{1\text{½ in.}} + \frac{1}{1\text{½ in.}}\right) + (14.5\text{ in.})\left(\frac{1}{2.29\text{ in.}} + \frac{1}{1\text{½ in.}}\right)\right]$$
$$+ \left(\frac{2}{3\text{½ in.}}\right)\left[(17.8\text{ in.})(1\text{½ in.} + 1\text{½ in.}) + (14.5\text{ in.})(2.29\text{ in.} + 1\text{½ in.})\right]$$
$$= 181\text{ in.}$$

Determine the required end-plate thickness using Equations 5-5. For flush end-plate configurations, $\gamma_r = 0.80$.

LRFD	ASD
$t_{p,reqd} = \sqrt{\dfrac{M_u}{\gamma_r \phi_b F_y Y_p}}$	$t_{p,reqd} = \sqrt{\dfrac{\Omega_b M_a}{\gamma_r F_y Y_p}}$
$= \sqrt{\dfrac{2{,}500\text{ kip-in.}}{0.80(0.90)(50\text{ ksi})(181\text{ in.})}}$	$= \sqrt{\dfrac{1.67(1{,}670\text{ kip-in.})}{0.80(50\text{ ksi})(181\text{ in.})}}$
$= 0.619\text{ in.} \leq$ ⅝ in. **o.k.**	$= 0.621\text{ in.} \leq$ ⅝ in. **o.k.**

The specified ⅝-in.-thick ASTM A572/A572M Grade 50 end plate is sufficient.

Determine if the specified 1-in.-diameter Grade A325 snug-tightened bolts are sufficient. Solve for the flexural strength for bolt rupture with prying action, and check that the bolt size is sufficient. Because the effective tee stub associated with the two bolt positions is unique, it is necessary to calculate the prying action for each bolt position separately. Figure B-5 shows the effective tee-stub geometry for the two bolt positions, wherein the strategy presented in Section 5.1.2 is used to determine the orientation of each effective tee stub.

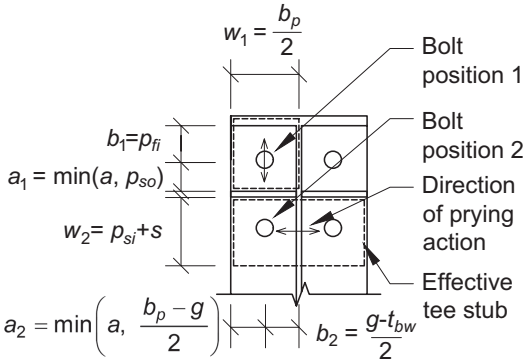

Fig. B-5. Effective tee-stub geometry for the four-bolt with web stiffeners between tension bolts configuration.

The bolts are specified to be snug tightened according to Figure B-4. According to Table 3-3, the snug-tightened bolt pretension for a 1-in.-diameter Grade A325 bolt is approximately $T_b = 12.8$ kips. The nominal unthreaded body area of a 1 in. bolt is $A_b = 0.785$ in.^{2}, and the nominal tensile stress for a Grade A325 bolt is $F_{nt} = 90$ ksi. The resulting nominal tensile strength of a 1-in.-diameter Grade A325 bolt is:

$$P_t = F_{nt} A_b \qquad \text{(from } \textit{Spec.} \text{ Eq. J3-1)}$$
$$= (90 \text{ ksi})(0.785 \text{ in.}^2)$$
$$= 70.7 \text{ kips}$$

Calculate the bolt distance from the bolt to the edge of the effective tee stub:

$$a = 3.62\left(\frac{t_p}{d_b}\right)^3 - 0.085 \text{ in.} \qquad (3\text{-}24)$$
$$= 3.62\left(\frac{⅝ \text{ in.}}{1 \text{ in.}}\right)^3 - 0.085 \text{ in.}$$
$$= 0.799 \text{ in.}$$

Bolt Position 1—Top Bolt

For bolt position 1 (see Figure B-5), calculate the geometry of the effective tee stub, including the width of the effective tee stub, w_1, the net effective width, w_1', and the distance from the effective tee stem to the bolt, b_1.

$$w_1 = \frac{b_p}{2}$$
$$= \frac{6 \text{ in.}}{2}$$
$$= 3.00 \text{ in.}$$

$$w_1' = w_1 - (d_b + ⅛ \text{ in.}) \qquad (5\text{-}7)$$
$$= 3.00 \text{ in.} - (1 \text{ in.} + ⅛ \text{ in.})$$
$$= 1.88 \text{ in.}$$

$$a_1 = \min(a, p_{so})$$
$$= \min(0.799, 1½)$$
$$= 0.799 \text{ in.}$$

$$b_1 = p_{fi}$$
$$= 1½ \text{ in.}$$

Find the forces related to prying, including the force, F_1', the prying force, $Q_{max,1}$, and the bolt tension contributing to flexural strength, P_{q1}.

$$F_1' = \frac{1}{b}\left[\frac{t_p^2 F_y}{4}(0.85w_1 + 0.8w_1') + \frac{\pi d_b^3 F_{nt}}{32}\right] \qquad (3\text{-}26)$$
$$= \left(\frac{1}{1½ \text{ in.}}\right)\left\{\left[\frac{(⅝ \text{ in.})^2 (50 \text{ ksi})}{4}\right]\left[0.85(3.00 \text{ in.}) + 0.8(1.88 \text{ in.})\right] + \frac{\pi(1 \text{ in.})^3 (90 \text{ ksi})}{32}\right\}$$
$$= 19.1 \text{ kips}$$

Table B-2. Prying Action for the Four-Bolt with Web Stiffener between Example		
Parameter	**Bolt Position 1**	**Bolt Position 2**
w_i (in.)	3.00	3.79
w_i' (in.)	1.88	2.67
a_i (in.)	0.799	0.799
b_i (in.)	1.50	1.63
F_i' (kips)	19.1	21.5
$Q_{max,i}$ (kips)	9.49	14.6
P_{qi} (kips)	61.2	56.1
α_i	1.0	1.0

$$Q_{max,1} = \frac{w_1' t_p^2}{4a_1}\sqrt{F_y^2 - 3\left(\frac{F_1'}{w_1' t_p}\right)^2} \tag{3-23}$$

$$= \frac{(1.88\text{ in.})(⅝\text{ in.})^2}{4(0.799\text{ in.})}\sqrt{(50\text{ ksi})^2 - 3\left[\frac{19.1\text{ kips}}{(1.88\text{ in.})(⅝\text{ in.})}\right]^2}$$

$$= 9.49\text{ kips}$$

$$P_{q1} = \max(P_t - Q_{max,1},\ T_b) \tag{3-27}$$

$$= \max(70.7\text{ kips} - 9.49\text{ kips},\ 12.8\text{ kips})$$

$$= 61.2\text{ kips}$$

Prying forces for bolt position 2 are calculated in a similar way using the effective tee-stub geometry shown in Figure B-5. Table B-2 gives the geometric parameters, the related prying force, the usable strength for each bolt position, and the reduction in bolt contribution factor, α_i.

Calculate the flexural strength for bolt rupture with prying action, M_q, using Equation 3-28. Then the design flexural strength is compared to the required flexural strength.

$$M_q = \sum_i \alpha_i P_{qi}\, n_i\, h_i \tag{3-28}$$

$$= 1.0(61.2\text{ kips})(2\text{ bolts})(17.8\text{ in.}) + 1.0(56.1\text{ kips})(2\text{ bolts})(14.5\text{ in.})$$

$$= 3{,}810\text{ kip-in.}$$

LRFD	ASD
$\phi M_q = 0.75(3{,}810\text{ kip-in.})$ $= 2{,}860\text{ kip-in.} \geq M_u = 2{,}500\text{ kip-in.}$ **o.k.**	$\frac{M_q}{\Omega} = \frac{3{,}810\text{ kip-in.}}{2.00}$ $= 1{,}910\text{ kip-in.} \geq M_a = 1{,}670\text{ kip-in.}$ **o.k.**

The specified 1-in.-diameter Grade A325 snug-tightened bolts are sufficient.

Check Shear Transfer Strength at the Bottom Holes

See Example B.2-1 for calculation procedures.

B. Check Beam to End-Plate Welds

Weld strength calculations for this thin end-plate design are the same as for the thick end-plate design in Example 5.2-3.

C. Check Column-Side Limit States

See Example 5.2-1 for example column-side limit state check calculations.

Summary

The connection shown in Figure B-4 is adequate for the required moment and shear force.

EXAMPLE B.2-4—Four-Bolt Flush Stiffened with Web Stiffener below the Tension Bolts Thin End-Plate Example

Given:

The connection shown in Figure B-6 is a four-bolt flush, stiffened below the tension bolts, end-plate moment connection with a built-up beam. The beam and all plates are ASTM A572/A572M Grade 50 material. Bolts are Group 120 ASTM F3125/F3125M Grade A325 snug-tightened. Weld electrodes are E70XX. The connection is to be evaluated as a thin end-plate design for the following required moments and shear forces.

	LRFD	ASD
Moment	M_u = 2,500 kip-in.	M_a = 1,670 kip-in.
Shear force	V_u = 25.8 kips	V_a = 17.2 kips

Solution:

From AISC *Manual* Table 2-4, the material properties are as follows:

ASTM A572/A572M Grade 50
F_y = 50 ksi
F_u = 65 ksi

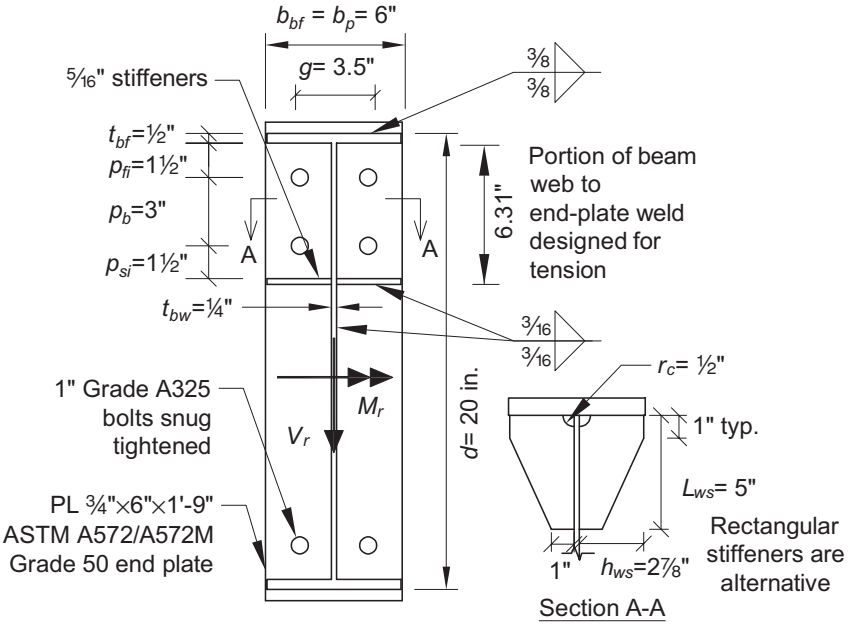

Fig. B-6. Four-bolt stiffened with web stiffeners below the tension bolts thin end-plate configuration for Example B.2-4.

From AISC *Specification* Table J3.2, the material properties of the bolts are as follows:

Group 120 ASTM F3125/F3125M 1-in.-diameter Grade A325 bolts snug-tightened
$F_{nt} = 90$ ksi
$F_{nv} = 54$ ksi (Group 120 bolts with threads not excluded from the shear plane; thread condition N)

Beam
$d = 20$ in. $\quad t_{bw} = ¼$ in.
$b_{bf} = 6$ in. $\quad t_{bf} = ½$ in.

End-plate geometric properties:
$b_p = 6$ in.
$t_p = ¾$ in.
$g = 3½$ in.
$p_{fi} = 1½$ in.
$p_b = 3$ in.
$p_s = 1½$ in.
$d_p = 21$ in.

The distances from the centerline of the compression flange to the bolt lines, h_1 and h_2, are depicted in Table 5-5 and computed as:

$$h_1 = d - \frac{3}{2}t_{bf} - p_{fi}$$
$$= 20 \text{ in.} - \frac{3(½ \text{ in.})}{2} - 1½ \text{ in.}$$
$$= 17.8 \text{ in.}$$

$$h_2 = d - \frac{3}{2}t_{bf} - p_{fi} - p_b$$
$$= 20 \text{ in.} - \frac{3(½ \text{ in.})}{2} - 1½ \text{ in.} - 3 \text{ in.}$$
$$= 14.8 \text{ in.}$$

$$b_{p,eff} \le b_{bf} + \max(t_p, 1 \text{ in.}) \qquad (4\text{-}3)$$
$$\le 6 \text{ in.} + \max(¾ \text{ in.}, 1 \text{ in.})$$
$$\le 7.00 \text{ in.}$$

$b_p = 6$ in. $\le$ 7.00 in. **o.k.**

$$b_{bf} \ge g \qquad (4\text{-}1)$$
6 in. $\ge$ 3½ in. **o.k.**

Beam flange to beam web stiffener geometric properties:

$$h_{ws} = (b_p - t_{bw})/2$$
$$= (6 \text{ in.} - ¼ \text{ in.})/2$$
$$= 2⅞ \text{ in.}$$

$$L_{ws} = h_{ws}/\tan 30° \qquad (4\text{-}4)$$
$$= (2⅞ \text{ in.})/\tan 30°$$
$$= 4.98 \text{ in.} \le 5 \text{ in.} \quad \textbf{o.k.}$$

A. End-Plate and Bolt Design Verification

Determine if the specified end-plate thickness, ¾ in., and bolt diameter, 1 in., are sufficient using the thin end-plate/smaller bolt diameter procedure.

Solve for the required end-plate thickness using Equations 5-5. First solve for the distance, s, and yield line parameter, Y_p, using Table 5-5.

$$s = \frac{\sqrt{b_p g}}{2}$$
$$= \frac{\sqrt{(6\text{ in.})(3\text{½ in.})}}{2}$$
$$= 2.29\text{ in.}$$

Because $s \geq p_{fi} = 1\text{½}$ in., $p_{so} = 1\text{½}$ in., and $p_{si} = 1\text{½}$ in., the dimensions p_{fi}, p_{so}, and p_{si} are used in the equation for the yield line parameter.

$$Y_p = \frac{b_p}{2}\left[h_1\left(\frac{1}{p_{fi}}\right) + h_2\left(\frac{1}{p_{si}}\right)\right] + \frac{2}{g}\left[h_1(p_{fi} + 0.75p_b) + h_2(p_{si} + 0.25p_b)\right] + \frac{g}{2}$$
$$= \left(\frac{6\text{ in.}}{2}\right)\left[(17.8\text{ in.})\left(\frac{1}{1\text{½ in.}}\right) + (14.8\text{ in.})\left(\frac{1}{1\text{½ in.}}\right)\right]$$
$$+ \left(\frac{2}{3\text{½ in.}}\right)\left\{(17.8\text{ in.})\left[1\text{½ in.} + 0.75(3\text{ in.})\right] + (14.8\text{ in.})\left[1\text{½ in.} + 0.25(3\text{ in.})\right]\right\} + \frac{3\text{½ in.}}{2}$$
$$= 124\text{ in.}$$

Determine the required end-plate thickness using Equations 5-5. For flush end-plate configurations, $\gamma_r = 0.80$.

LRFD	ASD
$t_{p,reqd} = \sqrt{\frac{M_u}{\gamma_r \phi_b F_y Y_p}}$	$t_{p,reqd} = \sqrt{\frac{\Omega_b M_a}{\gamma_r F_y Y_p}}$
$= \sqrt{\frac{2{,}500\text{ kip-in.}}{0.80(0.90)(50\text{ ksi})(124\text{ in.})}}$	$= \sqrt{\frac{1.67(1{,}670\text{ kip-in.})}{0.80(50\text{ ksi})(124\text{ in.})}}$
$= 0.748\text{ in.} \quad \leq \quad$ ¾ in. **o.k.**	$= 0.750\text{ in.} \quad \leq \quad$ ¾ in. **o.k.**

The specified ¾-in.-thick ASTM A572/A572M Grade 50 end plate is sufficient.

The snug-tightened bolts are 1-in.-diameter Grade A325. Solve for the flexural strength for bolt rupture with prying action, and check that the bolt size is sufficient. Because the effective tee stub associated with the two bolt positions is unique, it is necessary to calculate the prying action for each bolt position separately. Figure B-7 shows effective tee-stub geometry for the two bolt positions, wherein the strategy presented in Section 5.1.2 is used to determine the orientation of each effective tee stub.

The bolts are given to be snug-tightened according to Figure B-6. According to Table 3-3, the snug-tightened bolt pretension for a 1-in.-diameter Grade A325 bolt is approximately 25% of full pretension, or $T_b = 12.8$ kips. The nominal unthreaded body area of a 1 in. bolt is $A_b = 0.785\text{ in.}^2$, and the nominal tensile stress for a Grade A325 bolt is $F_{nt} = 90$ ksi. The resulting nominal tensile strength of a 1-in.-diameter Grade A325 bolt is:

$$P_t = F_{nt} A_b \qquad \text{(from } \textit{Spec.}\text{ Eq. J3-1)}$$
$$= (90\text{ ksi})(0.785\text{ in.}^2)$$
$$= 70.7\text{ kips}$$

Calculate the bolt distance from the bolt to the edge of the effective tee stub:

$$a = 3.62\left(\frac{t_p}{d_b}\right)^3 - 0.085 \text{ in.} \tag{3-24}$$
$$= 3.62\left(\frac{¾ \text{ in.}}{1 \text{ in.}}\right)^3 - 0.085 \text{ in.}$$
$$= 1.44 \text{ in.}$$

Bolt Position 1—Top Bolt

For bolt position 1 (see Figure B-7), calculate the geometry of the effective tee stub, including the width of the effective tee stub, w_1, the net effective width, w_1', and distance from effective tee stem to the bolt, b_1.

$$w_1 = \frac{b_p}{2}$$
$$= \frac{6 \text{ in.}}{2}$$
$$= 3.00 \text{ in.}$$

$$w_1' = w_1 - (d_b + ⅛ \text{ in.}) \tag{5-7}$$
$$= 3.00 \text{ in.} - (1 \text{ in.} + ⅛ \text{ in.})$$
$$= 1.88 \text{ in.}$$

$$a_1 = a$$
$$= 1.44 \text{ in.}$$

$$b_1 = p_{fi}$$
$$= 1½ \text{ in.}$$

Find forces related to prying, including the force, F_1', the prying force, $Q_{max,1}$, and the bolt tension contributing to flexural strength, P_{q1}.

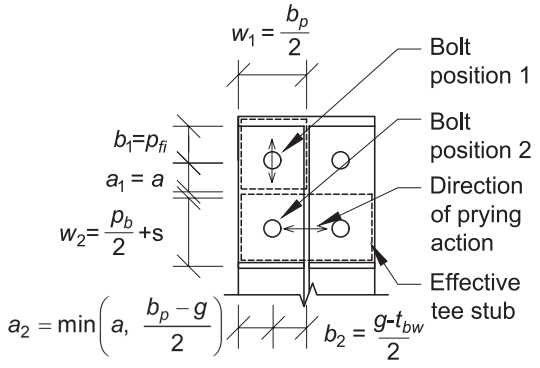

Fig. B-7. Effective tee-stub geometry for the four-bolt with web stiffeners below tension bolts configuration.

Table B-3. Prying Action for the Four-Bolt with Web Stiffener below Example		
Parameter	**Bolt Position 1**	**Bolt Position 2**
w_i (in.)	3.00	3.79
w_i' (in.)	1.88	2.67
a_i (in.)	1.44	1.25
b_i (in.)	1.50	1.63
F_i' (kips)	24.9	28.5
$Q_{max,i}$ (kips)	7.22	13.1
P_{qi} (kips)	63.4	57.6
α_i	1.0	1.0

$$F_1' = \frac{1}{b_1}\left[\frac{t_p^2 F_{py}}{4}(0.85w_1 + 0.8w_1') + \frac{\pi d_b^3 F_{nt}}{32}\right] \quad (3\text{-}26)$$

$$= \left(\frac{1}{1\text{½ in.}}\right)\left\{\left[\frac{(\text{¾ in.})^2(50\text{ ksi})}{4}\right]\left[0.85(3.00\text{ in.}) + 0.8(1.88\text{ in.})\right] + \frac{\pi(1\text{ in.})^3(90\text{ ksi})}{32}\right\}$$

$$= 24.9 \text{ kips}$$

$$Q_{max,1} = \frac{w_1' t_p^2}{4a_1}\sqrt{F_{py}^2 - 3\left(\frac{F_1'}{w_1' t_p}\right)^2} \quad (3\text{-}23)$$

$$= \frac{(1.88\text{ in.})(\text{¾ in.})^2}{4(1.44\text{ in.})}\sqrt{(50\text{ ksi})^2 - 3\left[\frac{24.9\text{ kips}}{(1.88\text{ in.})(\text{¾ in.})}\right]^2}$$

$$= 7.26 \text{ kips}$$

$$P_{q1} = \max(P_t - Q_{max,1}, T_b) \quad (3\text{-}27)$$

$$= \max(70.7\text{ kips} - 7.26\text{ kips}, 12.8\text{ kips})$$

$$= 63.4 \text{ kips}$$

Prying forces for bolt position 2 are calculated in a similar way using the effective tee-stub geometry shown in Figure B-7. Table B-3 gives the geometric parameters, the related prying force, the usable strength for each bolt position, and the reduction in bolt contribution factor, α_i.

Calculate the flexural strength for bolt rupture with prying action, M_q, using Equation 3-28. Then the design flexural strength is compared to the required flexural strength.

$$M_q = \sum_i \alpha_i P_{qi} n_i h_i \quad (3\text{-}28)$$

$$= 1.0(63.4\text{ kips})(2\text{ bolts})(17.8\text{ in.}) + 1.0(57.6\text{ kips})(2\text{ bolts})(14.8\text{ in.})$$

$$= 9{,}960 \text{ kip-in.}$$

LRFD	ASD
$\phi M_q = 0.75(3{,}960\text{ kip-in.})$ $= 2{,}970\text{ kip-in.} \geq M_u = 2{,}500\text{ kip-in.}$ **o.k.**	$\frac{M_q}{\Omega} = \frac{3{,}960\text{ kip-in.}}{2.00}$ $= 1{,}980\text{ kip-in.} \geq M_a = 1{,}670\text{ kip-in.}$ **o.k.**

The specified 1-in.-diameter Grade A325 snug-tightened bolts are sufficient.

Check Shear Transfer Strength at the Bottom Holes

See Example B.2-1 for calculation procedures.

B. Check Beam to End-Plate Welds

Weld strength calculations for this thin end-plate design are the same as for the thick end-plate design in Example 5.2-4.

C. Check Column-Side Limit States

See Example 5.2-1 for example column-side limit state check calculations.

Summary

The connection shown in Figure B-6 is adequate for the required moment and shear force.

EXAMPLE B.2-5—Six-Bolt Flush Unstiffened Thin End-Plate Example

Given:

The connection shown in Figure B-8 is a six-bolt flush unstiffened end-plate moment connection with a built-up beam. The beam and end plate are ASTM A572/A572M Grade 50 material. Bolts are ASTM F3125/F3125M Grade A490 pretensioned. Weld electrodes are E70XX. The connection is to be evaluated as a thin end-plate design for the following required moments and shear forces.

	LRFD	ASD
Moment	$M_u = 14{,}000$ kip-in.	$M_a = 9{,}330$ kip-in.
Shear force	$V_u = 80.0$ kips	$V_a = 53.3$ kips

Solution:

From AISC *Manual* Table 2-4, the material properties are as follows:

ASTM A572/A572M Grade 50
$F_y = 50$ ksi
$F_u = 65$ ksi

From AISC *Specification* Table J3.2, the material properties of the bolts are as follows:

Group 150 ASTM F3125/F3125M 1⅛-in.-diameter Grade A490 Grade bolts pretensioned
$F_{nt} = 113$ ksi
$F_{nv} = 68$ ksi (Group 150 bolts with threads not excluded from the shear plane; thread contention N)

Beam
$d = 48$ in. $t_{bw} = ½$ in.
$b_{bf} = 10$ in. $t_{bf} = 1$ in.

End-plate geometric properties:
$b_p = 11$ in.
$t_p = 1$ in.
$g = 5$ in.
$p_{fi} = 2$ in.
$p_b = 3½$ in.
$d_p = 50$ in.

The distances from the centerline of the compression flange to the bolt lines, h_1, h_2, and h_3, are depicted in Table 5-6 and computed as:

$$h_1 = d - \frac{3t_{bf}}{2} - p_{fi}$$
$$= 48 \text{ in.} - \frac{3(1 \text{ in.})}{2} - 2 \text{ in.}$$
$$= 44.5 \text{ in.}$$

$$h_2 = d - \frac{3t_{bf}}{2} - p_{fi} - p_b$$
$$= 48 \text{ in.} - \frac{3(1 \text{ in.})}{2} - 2 \text{ in.} - 3\text{½ in.}$$
$$= 41.0 \text{ in.}$$

$$h_3 = d - \frac{3t_{bf}}{2} - p_{fi} - 2p_b$$
$$= 48 \text{ in.} - \frac{3(1 \text{ in.})}{2} - 2 \text{ in.} - 2(3\text{½ in.})$$
$$= 37.5 \text{ in.}$$

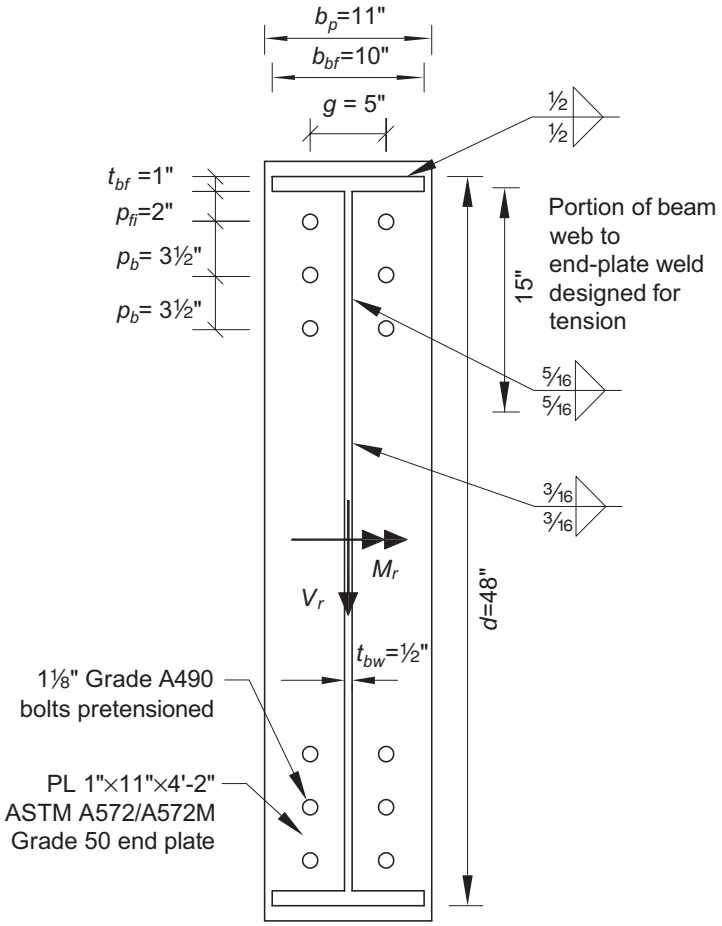

Fig. B-8. Six-bolt unstiffened flush thin end-plate configuration for Example B.2-5.

$$b_{p,eff} \le b_{bf} + \max(t_p, 1 \text{ in.}) \quad (4\text{-}3)$$
$$\le 10 \text{ in.} + \max(1 \text{ in.}, 1 \text{ in.})$$
$$\le 11.0 \text{ in.}$$

$b_p = 11$ in. $\le$ 11.0 in. **o.k.**

$$b_{bf} \ge g \quad (4\text{-}1)$$

10 in. $\ge$ 5 in. **o.k.**

A. End-Plate and Bolt Design Verification

Determine if the specified 1⅛ in. bolt diameter and 1 in. end-plate thickness are sufficient using the thin end-plate/larger bolt diameter procedure.

Solve for the required end-plate thickness using Equations 5-5. First solve for the distance, s, and yield line parameter, Y_p, using Table 5-6.

$$s = \frac{\sqrt{b_p g}}{2}$$
$$= \frac{\sqrt{(11 \text{ in.})(5 \text{ in.})}}{2}$$
$$= 3.71 \text{ in.}$$

Because $s \ge p_{fi} = 2$, the dimension p_{fi} is used in the equation for the yield line parameter.

$$Y_p = \frac{b_p}{2}\left[h_1\left(\frac{1}{p_{fi}}\right) + h_3\left(\frac{1}{s}\right)\right] + \frac{2}{g}\left[h_1(p_{fi} + 1.50p_b) + h_3(s + 0.50p_b)\right] + \frac{g}{2}$$
$$= \left(\frac{11 \text{ in.}}{2}\right)\left[(44.5 \text{ in.})\left(\frac{1}{2 \text{ in.}}\right) + (37.5 \text{ in.})\left(\frac{1}{3.71 \text{ in.}}\right)\right]$$
$$+ \left(\frac{2}{5 \text{ in.}}\right)\left\{(44.5 \text{ in.})\left[2 \text{ in.} + 1.50(3\text{½ in.})\right] + (37.5 \text{ in.})\left[3.71 \text{ in.} + 0.50(3\text{½ in.})\right]\right\} + \frac{5 \text{ in.}}{2}$$
$$= 391 \text{ in.}$$

Determine the required end-plate thickness using Equations 5-5. For flush end-plate configurations, $\gamma_r = 0.80$.

LRFD	ASD
$t_{p,reqd} = \sqrt{\frac{M_u}{\gamma_r \phi_b F_y Y_p}}$	$t_{p,reqd} = \sqrt{\frac{\Omega_b M_a}{\gamma_r F_y Y_p}}$
$= \sqrt{\frac{14{,}000 \text{ kip-in.}}{0.80(0.90)(50 \text{ ksi})(391 \text{ in.})}}$	$= \sqrt{\frac{1.67(9{,}330 \text{ kip-in.})}{0.80(50 \text{ ksi})(391 \text{ in.})}}$
$= 0.997 \text{ in.} \le 1 \text{ in.}$ **o.k.**	$= 0.998 \text{ in.} \le 1 \text{ in.}$ **o.k.**

The specified 1-in.-thick ASTM A572/A572M Grade 50 end plate is sufficient.

Determine if the specified 1⅛ in. Grade A490 pretensioned bolts are sufficient. Solve for the flexural strength for bolt rupture with prying action, and check that the bolt size is sufficient. Because the effective tee stub associated with each of the three bolt positions is unique, it is necessary to calculate the prying action for each bolt position separately. Figure B-9 shows the effective tee-stub geometry for each bolt position, wherein the strategy presented in Section 5.1.2 is used to determine the orientation of each effective tee stub.

The bolts are specified to be pretensioned. AISC *Specification* Table J3.1 gives the minimum bolt pretension as T_b = 80 kips. The nominal unthreaded body area of a 1⅛ in. bolt is A_b = 0.994 in.^{2}, and the nominal tensile stress for a Grade A490 bolt is F_{nt} =113 ksi. The resulting nominal tensile strength of a 1⅛-in.-diameter Grade A490 bolt is:

$$P_t = F_{nt} A_b \qquad \text{(from } \textit{Spec.} \text{ Eq. J3-1)}$$
$$= (113 \text{ ksi})(0.994 \text{ in.}^2)$$
$$= 112 \text{ kips}$$

Calculate the bolt distance from bolt to edge of effective tee stub:

$$a = 3.62\left(\frac{t_p}{d_b}\right)^3 - 0.085 \text{ in.} \qquad (3\text{-}24)$$
$$= 3.62\left(\frac{1 \text{ in.}}{1⅛ \text{ in.}}\right)^3 - 0.085 \text{ in.}$$
$$= 2.46 \text{ in.}$$

Bolt Position 1—Top Bolt

For bolt position 1 (see Figure B-9), calculate the geometry of the effective tee stub, including the width of the effective tee stub, w_1, the net effective width, w_1', and the distance from the effective tee stem to the bolt, b_1.

$$w_1 = \frac{b_p}{2}$$
$$= \frac{11 \text{ in.}}{2}$$
$$= 5.50 \text{ in.}$$

$$w_1' = w_1 - (d_b + ⅛ \text{in.}) \qquad (5\text{-}7)$$
$$= 5.50 \text{ in.} - (1⅛ \text{ in.} + ⅛ \text{ in.})$$
$$= 4.25 \text{ in.}$$

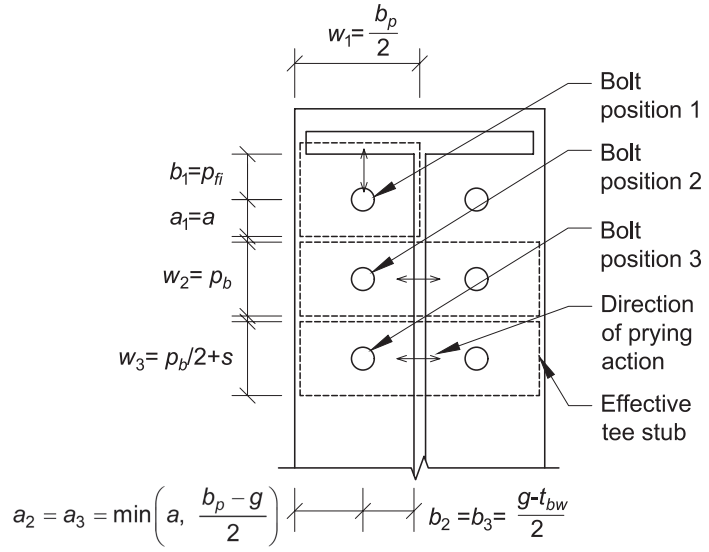

Fig. B-9. Effective tee-stub geometry for six-bolt unstiffened configuration.

$$b_1 = p_{fi}$$
$$= 2 \text{ in.}$$

Find forces related to prying, including the force, F_1', the prying force, $Q_{max,1}$, and the bolt tension contributing to flexural strength, P_{q1}.

$$F_1' = \frac{1}{b_1}\left[\frac{t_p^2 F_y}{4}(0.85w_1 + 0.8w_1') + \frac{\pi d_b^3 F_{nt}}{32}\right] \quad (3\text{-}26)$$

$$= \left(\frac{1}{2 \text{ in.}}\right)\left\{\left[\frac{(1 \text{ in.})^2(50 \text{ ksi})}{4}\right]\left[0.85(5.50 \text{ in.}) + 0.8(4.25 \text{ in.})\right] + \frac{\pi(1\text{⅛ in.})^3(113 \text{ ksi})}{32}\right\}$$

$$= 58.4 \text{ kips}$$

$$Q_{max,1} = \frac{w_1' t_p^2}{4a_1}\sqrt{F_y^2 - 3\left(\frac{F_1'}{w_1' t_p}\right)^2} \quad (3\text{-}23)$$

$$= \frac{(4.25 \text{ in.})(1 \text{ in.})^2}{4(2.46 \text{ in.})}\sqrt{(50 \text{ ksi})^2 - 3\left[\frac{58.4 \text{ kips}}{(4.25 \text{ in.})(1 \text{ in.})}\right]^2}$$

$$= 19.0 \text{ kips}$$

$$P_{q1} = \max(P_t - Q_{max,1}, T_b) \quad (3\text{-}27)$$

$$= \max(112 \text{ kips} - 19.0 \text{ kips}, 80.0 \text{ kips})$$

$$= 93.0 \text{ kips}$$

Prying forces for bolt positions 2 and 3 are calculated in a similar way using the effective tee-stub geometry shown in Figure B-9. Table B-4 gives the geometric parameters, related prying force, the usable strength for each bolt position, and reduction in bolt contribution factor, α_i. Then the design flexural strength is compared to the required flexural strength.

Calculate the flexural strength for bolt rupture with prying action, M_q, using Equation 3-28.

$$M_q = \sum_i \alpha_i P_{qi} n_i h_i \quad (3\text{-}28)$$

$$= 1.0(93.0 \text{ kips})(2 \text{ bolts})(44.5 \text{ in.}) + 1.0(80.0 \text{ kips})(2 \text{ bolts})(41.0 \text{ in.})$$
$$+ 1.0(92.6 \text{ kips})(2 \text{ bolts})(37.5 \text{ in.})$$

$$= 21{,}800 \text{ kip-in.}$$

LRFD	ASD
$\phi M_q = 0.75(21{,}800 \text{ kip-in.})$ $= 16{,}400 \text{ kip-in.} \geq M_u = 14{,}000 \text{ kip-in.}$ **o.k.**	$\frac{M_q}{\Omega} = \frac{21{,}800 \text{ kip-in.}}{2.00}$ $= 10{,}900 \text{ kip-in.} \geq M_a = 9{,}330 \text{ kip-in.}$ **o.k.**

The specified 1⅛-in.-diameter Grade A490 pretensioned bolts are sufficient.

Check Shear Transfer Strength at the Bottom Holes

See Example B.2-1 for calculation procedures.

B. Check Beam to End-Plate Welds

Weld strength calculations for this thin end-plate design are the same as for the thick end-plate design in Example 5.2-5.

Table B-4. Prying Action for the Six-Bolt Unstiffened Flush Example			
Parameter	**Bolt Position 1**	**Bolt Position 2**	**Bolt Position 3**
w_i (in.)	5.50	*NO PRYING*	5.46
w'_i (in.)	4.25		4.21
a_i (in.)	2.46		2.46
b_i (in.)	2.00		2.25
F'_i (kips)	58.4		51.5
$Q_{max,i}$ (kips)	19.0	0.0	19.4
P_{qi} (kips)	93.0	80.0	92.6
α_i	1.0	1.0	1.0

C. Check Column-Side Limit States

See Example 5.2-1 for example column-side limit state check calculations.

Summary

The connection shown in Figure B-8 is adequate for the required moment and shear force.

EXAMPLE B.2-6—Six-Bolt Flush Four-Wide/Two-Wide Unstiffened Thin End-Plate Example

Given:

The connection shown in Figure B-10 is a six-bolt flush, four-wide/two-wide, unstiffened end-plate moment connection with a built-up beam. The beam and end plate are ASTM A572/A572M Grade 50 material. Bolts are Group 150 ASTM F3125/F3125M Grade A490 pretensioned. Weld electrodes are E70XX. The connection is to be evaluated as a thin end-plate design for the following required moments and shear forces.

	LRFD	ASD
Moment	$M_u = 15{,}000$ kip-in.	$M_a = 10{,}000$ kip-in.
Shear force	$V_u = 87.9$ kips	$V_a = 58.6$ kips

Solution:

From AISC *Manual* Table 2-4, the material properties are as follows:

ASTM A572/A572M Grade 50
$F_y = 50$ ksi
$F_u = 65$ ksi

From AISC *Specification* Table J3.2, the material properties of the bolts are as follows:

Group 150 ASTM F3125/F3125M 1⅛-in.-diameter Grade A490 Grade bolts pretensioned
$F_{nt} = 113$ ksi
$F_{nv} = 68$ ksi (Group 150 bolts with threads not excluded from the shear plane; thread condition N)

Beam
$d = 48$ in. $t_{bw} = ½$ in.
$b_{bf} = 13$ in. $t_{bf} = ¾$ in.

End-plate geometric properties:
$b_p = 14$ in.
$t_p = 1$ in.
$g = 4$ in.
$g_o = 3½$ in.
$p_{fi} = 2$ in.
$p_b = 3½$ in.
$d_p = 49$ in.

The distances from the centerline of the compression flange to the bolt lines, h_1 and h_2, are depicted in Table 5-7 and computed as:

$$h_1 = d - \frac{3}{2}t_{bf} - p_{fi}$$
$$= 48 \text{ in.} - \frac{3(¾ \text{ in.})}{2} - 2 \text{ in.}$$
$$= 44.9 \text{ in.}$$

$$h_2 = d - \frac{3}{2}t_{bf} - p_{fi} - p_b$$
$$= 48 \text{ in.} - \frac{3(¾ \text{ in.})}{2} - 2 \text{ in.} - 3½ \text{ in.}$$
$$= 41.4 \text{ in.}$$

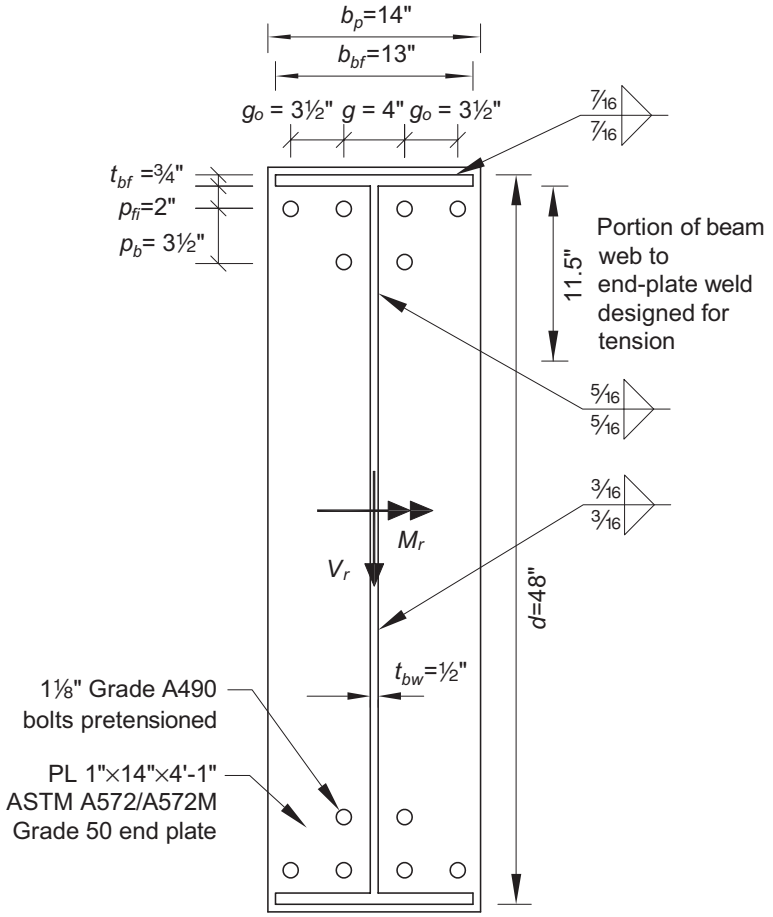

Fig. B-10. Six-bolt four-wide/two-wide unstiffened flush thin end-plate configuration for Example 5.2-6.

$$b_{p,eff} \le b_{bf} + \max(t_p, 1 \text{ in.}) \quad (4\text{-}3)$$
$$\le 13 \text{ in.} + \max(1 \text{ in.}, 1 \text{ in.})$$
$$\le 14.0 \text{ in.}$$

$b_p = 14$ in. $\le$ 14.0 in. **o.k.**

$$b_{bf} \ge g + 2g_o \quad (4\text{-}2)$$

13 in. ≥ 4 in. $+ 2(3\frac{1}{2}$ in.)

13 in. ≥ 11 in. **o.k.**

A. End-Plate and Bolt Design Verification

Determine if the specified bolt diameter, 1⅛ in., and end-plate thickness, 1 in., are sufficient using the thin end-plate/larger bolt diameter procedure.

Solve for the required end-plate thickness using Equations 5-5. First solve for the distance, s, and yield line parameter, Y_p, using Table 5-7.

$$s = \frac{\sqrt{b_p g}}{2}$$
$$= \frac{\sqrt{(14 \text{ in.})(4 \text{ in.})}}{2}$$
$$= 3.74 \text{ in.}$$

Because $s \ge p_{fi} = 2$, the dimension p_{fi} is used in the equation for the yield line parameter.

$$Y_p = \frac{b_p}{2}\left[h_1\left(\frac{1}{p_{fi}}\right) + h_2\left(\frac{1}{s}\right)\right] + \frac{2}{g}\left[h_1(p_{fi} + 0.75p_b) + h_2(s + 0.25p_b)\right] + \frac{g}{2}$$
$$= \left(\frac{14 \text{ in.}}{2}\right)\left[(44.9 \text{ in.})\left(\frac{1}{2 \text{ in.}}\right) + (41.4 \text{ in.})\left(\frac{1}{3.74 \text{ in.}}\right)\right]$$
$$+ \left(\frac{2}{4 \text{ in.}}\right)\left\{(44.9 \text{ in.})\left[2 \text{ in.} + 0.75(3\frac{1}{2} \text{ in.})\right] + (41.4 \text{ in.})\left[3.74 \text{ in.} + 0.25(3\frac{1}{2} \text{ in.})\right]\right\} + \frac{4 \text{ in.}}{2}$$
$$= 436 \text{ in.}$$

Determine the required end-plate thickness using Equations 5-5. For flush end-plate configurations, $\gamma_r = 0.80$.

LRFD	ASD
$t_{p,reqd} = \sqrt{\frac{M_u}{\gamma_r \phi_b F_y Y_p}}$	$t_{p,reqd} = \sqrt{\frac{\Omega_b M_a}{\gamma_r F_y Y_p}}$
$= \sqrt{\frac{15{,}000 \text{ kip-in.}}{0.80(0.90)(50 \text{ ksi})(436 \text{ in.})}}$	$= \sqrt{\frac{1.67(10{,}000 \text{ kip-in.})}{0.80(50 \text{ ksi})(436 \text{ in.})}}$
$= 0.978$ in. $\le$ 1 in. **o.k.**	$= 0.979$ in. $\le$ 1 in. **o.k.**

The specified 1-in.-thick ASTM A572/A572M Grade 50 end plate is sufficient.

Determine if the specified 1⅛ in. Grade A490 pretensioned bolts are sufficient. Solve for the flexural strength for bolt rupture with prying action, and check that the bolt size is sufficient. Because the effective tee stub associated with each of the three bolt positions is unique, it is necessary to calculate the prying action for each bolt position separately. Figure B-11 shows effective

tee-stub geometry for each bolt position, wherein the strategy presented in Section 5.1.2 is used to determine the orientation of each effective tee stub.

The bolts are specified to be pretensioned. AISC *Specification* Table J3.1 gives the minimum bolt pretension as T_b = 80 kips. The nominal unthreaded body area of a 1⅛ in. bolt is A_b = 0.994 in.^{2}, and the nominal tensile stress for a Grade A490 bolt is F_{nt} =113 ksi. The resulting nominal tensile strength of a 1⅛-in.-diameter Grade A490 bolt is:

$$P_t = F_{nt} A_b \qquad \text{(from } \textit{Spec.}\text{ Eq. J3-1)}$$
$$= (113 \text{ ksi})(0.994 \text{ in.}^2)$$
$$= 112 \text{ kips}$$

Calculate the bolt distance from bolt to edge of effective tee stub:

$$a = 3.62\left(\frac{t_p}{d_b}\right)^3 - 0.085 \text{ in.} \qquad (3\text{-}24)$$
$$= 3.62\left(\frac{1 \text{ in.}}{1⅛ \text{ in.}}\right)^3 - 0.085 \text{ in.}$$
$$= 2.46 \text{ in.}$$

Bolt Position 1—Outer Bolt

For bolt position 1 (see Figure B-11), calculate the geometry of the effective tee stub, including the width of the effective tee stub, w_1, the net effective width, w_1', and distance from effective tee stem to the bolt, b_1.

$$w_1 = \frac{b_p - g - g_o}{2}$$
$$= \frac{14 \text{ in.} - 4 \text{ in.} - 3½ \text{ in.}}{2}$$
$$= 3.25 \text{ in.}$$

$$w_1' = w_1 - (d_b + ⅛ \text{in.}) \qquad (5\text{-}7)$$
$$= 3.25 \text{ in.} - (1⅛ \text{ in.} + ⅛ \text{ in.})$$
$$= 2.00 \text{ in.}$$

$$b_1 = p_{fi}$$
$$= 2 \text{ in.}$$

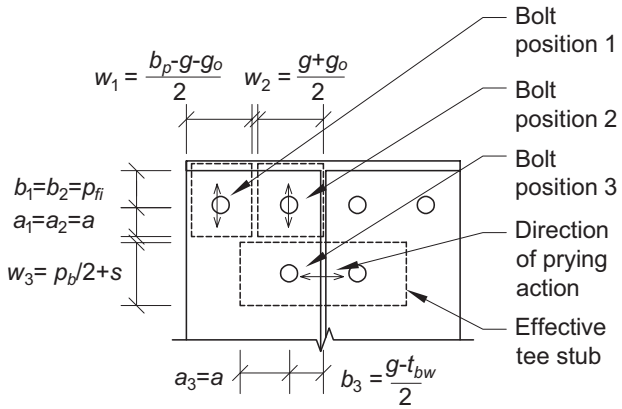

Fig. B-11. Effective tee-stub geometry for six-bolt four-wide/two-wide unstiffened configuration.

Find forces related to prying, including the force, F_1', the prying force, $Q_{max,1}$, and the bolt tension contributing to flexural strength, P_{q1}.

$$F_1' = \frac{1}{b_1}\left[\frac{t_p^2 F_y}{4}(0.85w_1 + 0.8w_1') + \frac{\pi d_b^3 F_{nt}}{32}\right] \tag{3-26}$$

$$= \left(\frac{1}{2\text{ in.}}\right)\left\{\left[\frac{(1\text{ in.})^2(50\text{ ksi})}{4}\right]\left[0.85(3.25\text{ in.}) + 0.8(2.00\text{ in.})\right] + \frac{\pi(1\text{⅛ in.})^3(113\text{ ksi})}{32}\right\}$$

$$= 35.2\text{ kips}$$

$$Q_{max,1} = \frac{w_1' t_p^2}{4a_1}\sqrt{F_y^2 - 3\left(\frac{F_1'}{w_1' t_p}\right)^2} \tag{3-23}$$

$$= \frac{(2.00\text{ in.})(2\text{ in.})^2}{4(2.46\text{ in.})}\sqrt{(50\text{ ksi})^2 - 3\left[\frac{35.2\text{ kips}}{(2.00\text{ in.})(1\text{ in.})}\right]^2}$$

$$= 8.06\text{ kips}$$

$$P_{q1} = \max(P_t - Q_{max,1},\ T_b) \tag{3-27}$$

$$= \max(112\text{ kips} - 8.06\text{ kips},\ 80.0\text{ kips})$$

$$= 104\text{ kips}$$

Prying forces for bolt positions 2 and 3 are calculated in a similar way using the effective tee-stub geometry shown in Figure B-11. Table B-5 gives the geometric parameters, related prying force, the usable strength for each bolt position, and reduction in bolt contribution factor, α_i. The reduction factors for bolt locations that do not fully realize their bolt rupture strength before the first bolt fractures are $\alpha_1 = \alpha_3 = 0.75$. The factor for bolt location 2 is $\alpha_2 = 1.0$.

Calculate the flexural strength for bolt rupture with prying action, M_q, using Equation 3-28, and then compare the design flexural strength to the required flexural strength.

$$M_q = \sum_i \alpha_i P_{qi} n_i h_i \tag{3-28}$$

$$= 0.75(104\text{ kips})(2\text{ bolts})(44.9\text{ in.}) + 1.0(102\text{ kips})(2\text{ bolts})(44.9\text{ in.}) + 0.75(93.9\text{ kips})(2\text{ bolts})(41.4\text{ in.})$$

$$= 22{,}000\text{ kip-in.}$$

LRFD	ASD
$\phi M_q = 0.75(22{,}000\text{ kip-in.})$ $= 16{,}500\text{ kip-in.} \geq M_u = 15{,}000\text{ kip-in.}$ **o.k.**	$\frac{M_q}{\Omega} = \frac{22{,}000\text{ kip-in.}}{2.00}$ $= 11{,}000\text{ kip-in.} \geq M_a = 10{,}000\text{ kip-in.}$ **o.k.**

The specified 1⅛-in.-diameter Grade A490 pretensioned bolts are sufficient.

Check Shear Transfer Strength at the Bottom Holes

See Example B.2-1 for calculation procedures.

B. Check Beam to End-Plate Welds

Weld strength calculations for this thin end-plate design are the same as for the thick end-plate design in Example 5.2-5.

Table B-5. Prying Action for the Six-Bolt Unstiffened Flush Example			
Parameter	**Bolt Position 1**	**Bolt Position 2**	**Bolt Position 3**
w_i (in.)	3.25	3.75	5.49
w'_i (in.)	2.00	2.50	4.24
a_i (in.)	2.46	2.46	2.46
b_i (in.)	2.00	2.00	1.75
F'_i (kips)	35.2	40.3	66.6
$Q_{max,i}$ (kips)	8.06	10.5	18.1
P_{qi} (kips)	104	102	93.9
α_i	0.75	1.0	0.75

C. Check Column-Side Limit States

See Example 5.2-1 for example column-side limit state check calculations.

Summary

The connection shown in Figure B-10 is adequate for the required moment and shear force.

B.3 EXTENDED THIN END-PLATE CONNECTIONS

EXAMPLE B.3-1—Four-Bolt Extended Unstiffened Thin End-Plate Example

Given:

The connection shown in Figure B-12 is a four-bolt unstiffened extended (4E) gable frame connection of a built-up rafter and a built-up column. All plate steel is ASTM A572/A572M Grade 50. Bolts are Group 120 ASTM F3125/F3125M Grade A325, snug-tightened. Weld electrodes are E70XX. The connection is to be evaluated as a thin end-plate design for the following required moments and forces:

	LRFD	ASD
Moment	M_u = 2,510 kip-in.	M_a = 1,670 kip-in.
Axial tension	T_u = 11.0 kips	T_a = 7.30 kips
Shear force	V_u = 33.8 kips	V_a = 22.5 kips

Solution:

From AISC *Manual* Table 2-4, the material properties are as follows:

ASTM A572/A572M Grade 50
F_y = 50 ksi
F_u = 65 ksi

From AISC *Specification* Table J3.2, the material properties of the bolts are as follows:

Group 120 ASTM F3125/F3125M ⅞-in.-diameter Grade A325 snug tightened
F_{nt} = 90 ksi
F_{nv} = 54 ksi (Group 120 bolts with threads not excluded from the shear plane; thread condition N)

Beam
d = 24 in. t_{bw} = ¼ in.
b_{bf} = 8 in. t_{bf} = ⅜ in.

Column

$d_c = 26$ in. $\quad t_{cw} = 1/4$ in.

$b_{cf} = 8$ in. $\quad t_{cf} = 3/8$ in.

End-plate geometric properties:

$b_p = 8$ in.

$t_p = 9/16$ in.

$g = 3$ in.

$p_{ext} = 5$ in.

$d_e = 2\frac{1}{2}$ in.

$p_{fi} = 1\frac{3}{4}$ in.

$p_{fo} = 2\frac{1}{2}$ in.

$d_p = 34$ in.

The distances from the centerline of the compression flange to the bolt lines, h_1 and h_2, are depicted in Table 5-10 and computed as:

$$h_1 = d - \frac{t_{bf}}{2} + p_{fo}$$

$$= 24 \text{ in.} - \frac{3/8 \text{ in.}}{2} + 2\frac{1}{2} \text{ in.}$$

$$= 26.3 \text{ in.}$$

$$h_2 = d - \frac{3t_{bf}}{2} - p_{fi}$$

$$= 24 \text{ in.} - \frac{3(3/8 \text{ in.})}{2} - 1\frac{3}{4} \text{ in.}$$

$$= 21.7 \text{ in.}$$

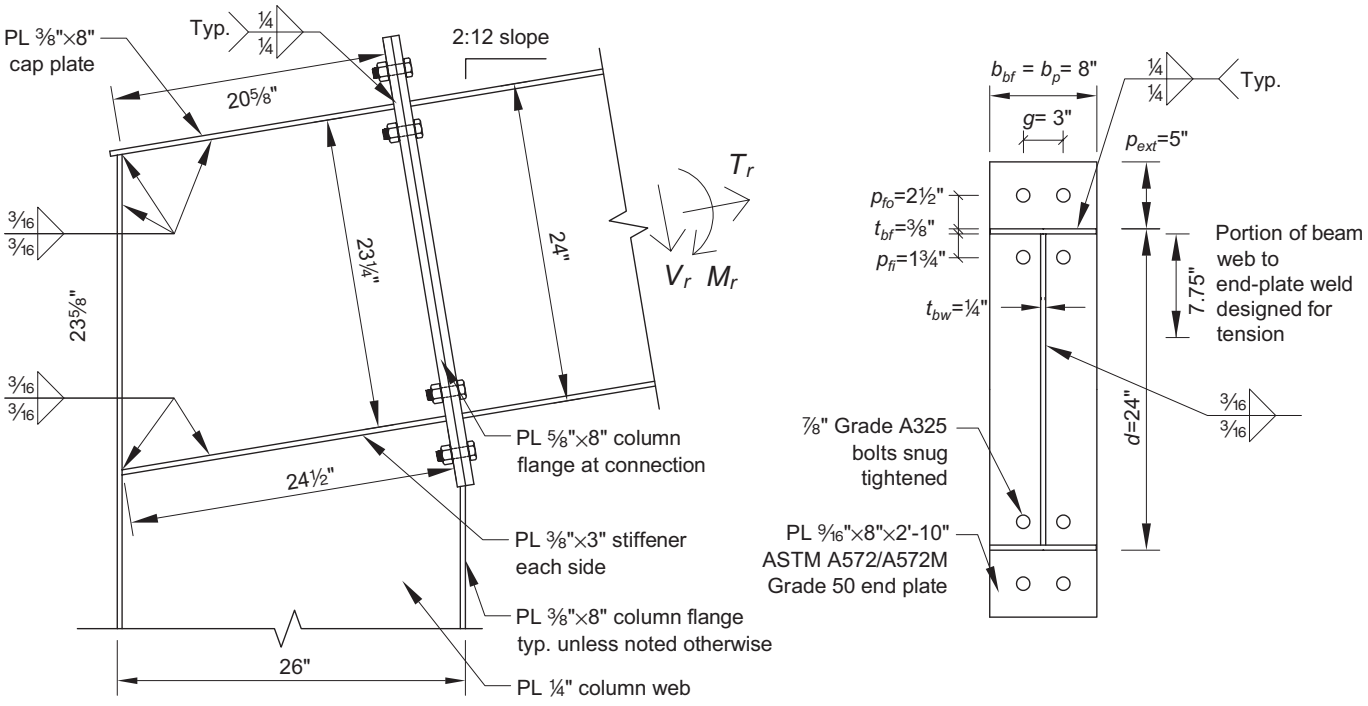

Fig. B-12. Four-bolt unstiffened thin end-plate configuration for Example B.3-1.

$$b_{p,eff} \le b_{bf} + \max(t_p, 1 \text{ in.}) \quad (4\text{-}3)$$
$$\le 8 \text{ in.} + \max(9/16 \text{ in.}, 1 \text{ in.})$$
$$\le 9.00 \text{ in.}$$

$b_p = 8$ in. $\le$ 9.00 in. **o.k.**

$$b_{bf} \ge g \quad (4\text{-}1)$$

8 in. $\ge$ 3 in. **o.k.**

A. End-Plate and Bolt Design Verification

Calculate the equivalent required moment considering the effect of the required tensile force using Equation 3-30.

LRFD	ASD
$M_{u,eq} = M_u + (T_u/2)(d - t_{bf})$	$M_{a,eq} = M_a + (T_a/2)(d - t_{bf})$
$= 2{,}510 \text{ kip-in.} + \left(\frac{11.0 \text{ kips}}{2}\right)(24 \text{ in.} - 3/8 \text{ in.})$	$= 1{,}670 \text{ kip-in.} + \left(\frac{7.30 \text{ kips}}{2}\right)(24 \text{ in.} - 3/8 \text{ in.})$
$= 2{,}640$ kip-in.	$= 1{,}760$ kip-in.

Determine if the specified end-plate thickness, 9/16 in., and bolt diameter, 7/8 in., are sufficient using the thin end-plate/larger bolt diameter procedure.

Solve for the required end-plate thickness using Equations 5-5. First solve for the distance, s, and yield line parameter, Y_p, using Table 5-10.

$$s = \frac{\sqrt{b_p g}}{2}$$
$$= \frac{\sqrt{(8 \text{ in.})(3 \text{ in.})}}{2}$$
$$= 2.45 \text{ in.}$$

Because $s \ge p_{fi} = 1\frac{3}{4}$ in., the dimension p_{fi} is used in the equation for the yield line parameter.

$$Y_p = \frac{b_p}{2}\left[h_1\left(\frac{1}{p_{fo}}\right) + h_2\left(\frac{1}{p_{fi}} + \frac{1}{s}\right) - \frac{1}{2}\right] + \frac{2}{g}\left[h_2(s + p_{fi})\right]$$
$$= \left(\frac{8 \text{ in.}}{2}\right)\left[(26.3 \text{ in.})\left(\frac{1}{2\frac{1}{2} \text{ in.}}\right) + (21.7 \text{ in.})\left(\frac{1}{1\frac{3}{4} \text{ in.}} + \frac{1}{2.45 \text{ in.}}\right) - \frac{1}{2}\right] + \left(\frac{2}{3 \text{ in.}}\right)\left[(21.7 \text{ in.})(2.45 \text{ in.} + 1\frac{3}{4} \text{ in.})\right]$$
$$= 186 \text{ in.}$$

Determine the required end-plate thickness using Equations 5-5. For extended end-plate configurations, $\gamma_r = 1.0$.

LRFD	ASD
$t_{p,reqd} = \sqrt{\frac{M_{u,eq}}{\gamma_r \phi_b F_y Y_p}}$	$t_{p,reqd} = \sqrt{\frac{\Omega_b M_{a,eq}}{\gamma_r F_y Y_p}}$
$= \sqrt{\frac{2{,}640 \text{ kip-in.}}{1.0(0.90)(50 \text{ ksi})(186 \text{ in.})}}$	$= \sqrt{\frac{1.67(1{,}760 \text{ kip-in.})}{1.0(50 \text{ ksi})(186 \text{ in.})}}$
$= 0.562 \text{ in.} \le 9/16 \text{ in.}$ **o.k.**	$= 0.562 \text{ in.} \le 9/16 \text{ in.}$ **o.k.**

Therefore, a 9⁄16-in.-thick end-plate is sufficient.

Determine if the specified Grade A325 7⁄8 in. bolt diameter is sufficient. First calculate the geometry of the effective tee stub; then calculate the related forces, F_i, Q_{max}, and P_{qi}; finally, calculate the flexural strength for bolt rupture with prying action, M_q, and compare with the required flexural strength.

The bolts are specified as snug-tightened. According to Table 3-3, the snug-tightened bolt pretension for a 7⁄8 in. Grade A325 bolt is approximately $T_b = 14.6$ kips. The nominal unthreaded body area of a 7⁄8 in. bolt is $A_b = 0.601$ in.^{2}, and the nominal tensile stress for a Grade A325 bolt is $F_{nt} = 90$ ksi. The resulting nominal tensile strength of a 7⁄8-in.-diameter Grade A325 bolt is:

$$P_t = F_{nt} A_b \qquad \text{(from } Spec. \text{ Eq. J3-1)}$$
$$= (90 \text{ ksi})(0.601 \text{ in.}^2)$$
$$= 54.1 \text{ kips}$$

There are two unique bolt locations as labeled in Figure B-13. The orientation of the effective tee stubs are defined using the rules given in Section 5.1.2 and are shown in Figure B-13.

Calculate the distance from the bolt line to the prying force when not at the edge of the end plate:

$$a = 3.62\left(\frac{t_p}{d_b}\right)^3 - 0.085 \text{ in.} \qquad (3\text{-}24)$$
$$= 3.62\left(\frac{9/16 \text{ in.}}{7/8 \text{ in.}}\right)^3 - 0.085 \text{ in.}$$
$$= 0.877 \text{ in.}$$

Bolt Position 1—Outside Bolt

For the bolts outside the flange, calculate the geometry of the effective tee stub, including the width of the effective tee stub, w_1, the net effective width, w_1', and distance from effective tee stem to the bolt, b_1.

$$w_1 = \frac{b_p}{2}$$
$$= \frac{8 \text{ in.}}{2}$$
$$= 4.00 \text{ in.}$$

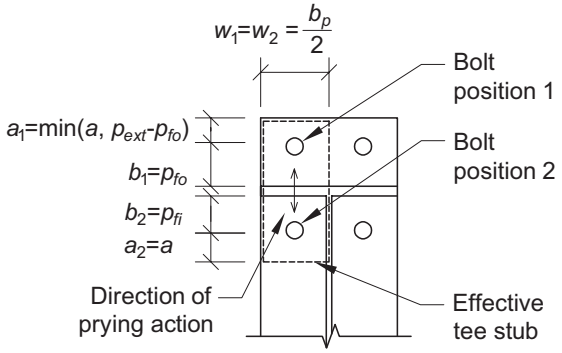

Fig. B-13. Effective tee-stub geometry for the four-bolt extended unstiffened configuration.

$$w_1' = w_1 - (d_b + 1/16 \text{ in.}) \tag{5-7}$$
$$= 4.00 \text{ in.} - (7/8 \text{ in.} + 1/16 \text{ in.})$$
$$= 3.06 \text{ in.}$$

$$a_1 = \min(a, p_{ext} - p_{fo})$$
$$= \min(0.877 \text{ in.}, 5 \text{ in.} - 2\frac{1}{2} \text{ in.})$$
$$= 0.877 \text{ in.}$$

$$b_1 = p_{fo}$$
$$= 2\frac{1}{2} \text{ in.}$$

Find forces related to prying, including the force, F_1', the prying force, $Q_{max,1}$, and the bolt tension contributing to flexural strength, P_{q1}.

$$F_1' = \frac{1}{b_1}\left[\frac{t_p^2 F_y}{4}(0.85w_1 + 0.8w_1') + \frac{\pi d_b^3 F_{nt}}{32}\right] \tag{3-26}$$
$$= \left(\frac{1}{2\frac{1}{2} \text{ in.}}\right)\left\{\left[\frac{(9/16 \text{ in.})^2 (50 \text{ ksi})}{4}\right]\left[0.85(4.00 \text{ in.}) + 0.8(3.06 \text{ in.})\right] + \frac{\pi(7/8 \text{ in.})^3 (90 \text{ ksi})}{32}\right\}$$
$$= 11.6 \text{ kips}$$

$$Q_{max,1} = \frac{w_1' t_p^2}{4a_1}\sqrt{F_y^2 - 3\left(\frac{F_1'}{w_1' t_p}\right)^2} \tag{3-23}$$
$$= \frac{(3.06 \text{ in.})(9/16 \text{ in.})^2}{4(0.877 \text{ in.})}\sqrt{(50 \text{ ksi})^2 - 3\left[\frac{11.6 \text{ kips}}{(3.06 \text{ in.})(9/16 \text{ in.})}\right]^2}$$
$$= 13.4 \text{ kips}$$

$$P_{q1} = \max(P_t - Q_{max,1}, T_b) \tag{3-27}$$
$$= \max(54.1 \text{ kips} - 13.4 \text{ kips}, 14.6 \text{ kips})$$
$$= 40.7 \text{ kips}$$

Bolt position 2 is the interior bolt, which also experiences prying about the flange. Prying forces for bolt position 2 are calculated in a similar way as bolt position 1. Table B-6 gives the geometric parameters, related prying force, the usable strength for each bolt position, and reduction in bolt contribution factor, α_i.

Calculate the flexural strength for bolt rupture with prying action, M_q, using Equation 3-28. Then the design flexural strength is compared to the required flexural strength.

$$M_q = \sum_i \alpha_i P_{qi} n_i h_i \tag{3-28}$$
$$= 1.0(40.7 \text{ kips})(2 \text{ bolts})(26.3 \text{ in.}) + 1.0(41.1 \text{ kips})(2 \text{ bolts})(21.7 \text{ in.})$$
$$= 3{,}920 \text{ kip-in.}$$

LRFD	ASD
$\phi M_q = 0.75(3{,}920 \text{ kip-in.})$ $= 2{,}940 \text{ kip-in.} \geq M_{u,eq} = 2{,}640 \text{ kip-in.}$ **o.k.**	$\frac{M_q}{\Omega} = \frac{3{,}920 \text{ kip-in.}}{2.00}$ $= 1{,}960 \text{ kip-in.} \geq M_{eq} = 1{,}760 \text{ kip-in.}$ **o.k.**

Table B-6. Prying Action for the Four-Bolt Extended Unstiffened Example		
Parameter	**Bolt Position 1**	**Bolt Position 2**
w_i (in.)	4.00	4.00
w_i' (in.)	3.06	3.06
a_i (in.)	0.887	0.887
b_i (in.)	2.50	1.75
F_i' (kips)	11.6	16.6
$Q_{max,i}$ (kips)	13.4	13.0
P_{qi} (kips)	40.7	41.1
α_i	1.0	1.0

Therefore, Grade A325 ⅞-in.-diameter bolts are sufficient.

Check Shear Yielding and Shear Rupture of the Extended Portion of the End Plate

For extended end-plate moment connections that are unstiffened, potential limit states that must be checked are shear yielding and shear rupture of the extended portion of the end plate. For the 4E connection, the shear demand is taken as one-half of the tension flange force because this is the force that is transferred through the extended portion of the end plate to the exterior bolts. The shear strength is calculated in accordance with AISC *Specification* Section J4.2.

Calculate the shear demand on the extended portion of the end plate.

LRFD	ASD
$V_{up} = \frac{1}{2}\left(\frac{M_u}{d - t_{bf}} + \frac{T_u}{2}\right)$	$V_{ap} = \frac{1}{2}\left(\frac{M_a}{d - t_{bf}} + \frac{T_a}{2}\right)$
$= \frac{1}{2}\left(\frac{2{,}510 \text{ kip-in.}}{24 \text{ in.} - ⅜ \text{ in.}} + \frac{11.0 \text{ kips}}{2}\right)$	$= \frac{1}{2}\left(\frac{1{,}670 \text{ kip-in.}}{24 \text{ in.} - ⅜ \text{ in.}} + \frac{7.30 \text{ kips}}{2}\right)$
$= 55.9$ kips	$= 37.2$ kips

Calculate the nominal shear yielding strength.

$$R_n = 0.60F_yA_{gv} \qquad \text{(Spec. Eq. J4-3)}$$
$$= 0.60F_yb_pt_p$$
$$= 0.60(50 \text{ ksi})(8 \text{ in.})(\tfrac{9}{16} \text{ in.})$$
$$= 135 \text{ kips}$$

Compare the available shear yielding strength to the shear demand. According to AISC *Specification* Section J4.2, for yielding of elements in shear, the resistance factor is $\phi = 1.00$, and the safety factor is $\Omega = 1.50$.

LRFD	ASD
$\phi R_n = 1.00(135 \text{ kips})$	$\frac{R_n}{\Omega} = \frac{135 \text{ kips}}{1.50}$
$= 135 \text{ kips} \geq V_{up} = 55.9 \text{ kips}$ **o.k.**	$= 90.0 \text{ kips} \geq V_{ap} = 37.2 \text{ kips}$ **o.k.**

Calculate the nominal shear rupture strength. The net area subject to shear, A_{nv}, is the width of the end plate minus two effective hole diameters multiplied by the end-plate thickness. The effective hole diameter is the standard hole diameter, d_h, from AISC *Specification* Table J3.3 plus 1/16 in. For 7/8-in.-diameter bolts, the standard hole diameter is 15/16 in.

$$A_{nv} = \left[b_p - 2(d_h + 1/16) \right] t_p$$
$$= \left[8 \text{ in.} - 2(15/16 \text{ in.} + 1/16 \text{ in.}) \right] (9/16 \text{ in.})$$
$$= 3.38 \text{ in.}^2$$

$$R_n = 0.60 F_u A_{nv} \qquad \text{(}Spec.\text{ Eq. J4-4)}$$
$$= 0.60(65 \text{ ksi})(3.38 \text{ in.}^2)$$
$$= 132 \text{ kips}$$

Compare the available shear rupture strength to the shear demand. Using AISC *Specification* Section J4.2 for rupture of elements in shear, the resistance factor is $\phi = 0.75$, and the safety factor is $\Omega = 2.00$.

LRFD	ASD
$\phi R_n = 0.75(132 \text{ kips})$ $= 99.0 \text{ kips} \quad \geq \quad V_{up} = 55.9 \text{ kips}$ **o.k.**	$\frac{R_n}{\Omega} = \frac{132 \text{ kips}}{2.00}$ $= 66.0 \text{ kips} \quad \geq \quad V_{ap} = 37.2 \text{ kips}$ **o.k.**

The extended portion of the 9/16-in.-thick end plate has sufficient resistance to shear yield and shear rupture.

Check Shear Transfer at the Bottom Holes

Shear at the faying surface, V_u, is assumed to be resisted only by the four compression side bolts. The shear transfer strength at each bolt hole is the minimum of the end-plate bearing/tearout strength, the bolt shear rupture strength, and the column flange bearing/tearout strength. See the User Note in AISC *Specification* Section J3.7.

The nominal unthreaded body area of a 7/8 in. bolt is $A_b = 0.601 \text{ in.}^2$, and the nominal shear strength in bearing-type connections with threads not excluded from the shear planes is $F_{nt} = 54$ ksi. The resulting nominal shear strength of a 7/8-in.-diameter Grade A325 bolt is:

$$R_{n,bt} = F_{nv} A_b \qquad \text{(from } Spec.\text{ Eq. J3-1)}$$
$$= (54 \text{ ksi})(0.601 \text{ in.}^2)$$
$$= 32.5 \text{ kips}$$

The nominal bearing/tearout strength is given by AISC *Specification* Section J3.11. The bolt shear force acting on the end plate is up toward the middle of the end plate, and therefore, tearout will not control. The bolt shear force acting on the column flange is down. Conservatively, the bottom of the sloping column flange is checked for both bearing and tearout. Because both the end plate and column flange are 9/16 in. thick, the column flange will be checked for bearing/tearout strength. The bearing strength at a bolt hole is:

$$R_{n,brg} = 2.4 d_b t_p F_u \qquad \text{(from } Spec.\text{ Eq. J3-6a)}$$
$$= 2.4(7/8 \text{ in.})(9/16 \text{ in.})(65 \text{ ksi})$$
$$= 76.8 \text{ kips}$$

The tearout strength at a bottom column flange bolt using the edge distance 2½ in. is:

$$R_{n,to} = 1.2 l_c t_p F_u \qquad \text{(from } Spec.\text{ Eq. J3-6c)}$$
$$= 1.2\left[2½ \text{ in.} - (7/8 \text{ in.} + 1/16 \text{ in.})/2 \right](9/16 \text{ in.})(65 \text{ ksi})$$
$$= 89.1 \text{ kips}$$

Because the tearout strength is greater than the bearing strength, bearing controls at the column flange. The shear transfer strength is then the minimum of the column flange bearing strength, the bolt shear rupture strength, and the end-plate bearing strength, which results in $R_n = 32.5$ kips.

Therefore, the nominal shear transfer strength at the four bottom bolt holes is:

$$V_n = (4 \text{ bolts}) R_n$$
$$= (4 \text{ bolts})(32.5 \text{ kips})$$
$$= 130 \text{ kips}$$

LRFD	ASD
$\phi V_n = 0.75(130 \text{ kips})$ $= 97.5 \text{ kips} \geq V_u = 33.8 \text{ kips}$ **o.k.**	$\frac{V_n}{\Omega} = \frac{130 \text{ kips}}{2.00}$ $= 65.0 \text{ kips} \geq V_a = 22.5 \text{ kips}$ **o.k.**

The specified ASTM A572/A572M Grade 50 9⁄16-in.-thick end plate and 7⁄8-in.-diameter Grade A325 snug-tightened bolts are sufficient.

B. Check Beam to End-Plate Welds

Weld strength calculations for this thin end-plate design are the same as for the thick end-plate design in Example 5.3-1.

C. Check Column-Side Limit States

Calculations to verify the strength of the column-side limit states for the connection shown in Figure B-12 are identical to those for the thick end-plate design in Example 5.3-1, except for the column web local yielding check. For this check, the end-plate thickness is 9⁄16 in. instead of 5⁄8 in. The difference has no effect on the design shown in Figure B-12.

Summary

The connection shown in Figure B-12 is adequate for the required moment and tension and shear forces.

EXAMPLE B.3-2—Four-Bolt Extended Stiffened Thin End-Plate Example

Given:

The connection shown in Figure B-14 is a four-bolt extended stiffened end-plate (4ES) connection for a W24×84 beam to a W14×99 column. The beam and column steel is ASTM A992/A992M, and plate steel is ASTM A572/A572M Grade 50. Bolts are Group 150 ASTM F3125/F3125M Grade A490, pretensioned. Weld electrodes are E70XX. The connection is to be evaluated as a thin end-plate design for the following required moments and forces:

	LRFD	ASD
Moment	$M_u = 7{,}620$ kip-in.	$M_a = 5{,}080$ kip-in.
Axial tension	$T_u = 20.4$ kips	$T_a = 13.6$ kips
Shear force	$V_u = 45.8$ kips	$V_a = 30.5$ kips
Column shear	$V_{uc} = 19.6$ kips	$V_{ac} = 13.1$ kips

Solution:

From AISC *Manual* Table 2-4, the material properties are as follows:

ASTM A992/A992M
$F_y = 50$ ksi
$F_u = 65$ ksi

ASTM A572/A572M Grade 50
$F_y = 50$ ksi
$F_u = 65$ ksi

From AISC *Specification* Table J3.2, the material properties of the bolts are as follows:

Group 150 ASTM F3125/F3125M 1¼-in.-diameter Grade A490 pretensioned
$F_{nt} = 113$ ksi
$F_{nv} = 68$ ksi (Group 150 bolts with threads not excluded from the shear plane; thread condition N)

From AISC *Manual* Table 1-1, the geometric properties of the beam and column sections are as follows:

Beam: W24×84
$d = 24.1$ in. $t_{bw} = 0.470$ in.
$b_{bf} = 9.02$ in. $t_{bf} = 0.770$ in.

Column: W14×99
$d_c = 14.2$ in. $t_{cw} = 0.485$ in. $b_{cf} = 14.6$ in.
$t_{cf} = 0.780$ in. $k_{des} = 1.38$ in.

End-plate geometric properties:
$b_p = 9$ in.
$t_p = ⅞$ in.
$g = 5¾$ in.
$p_{ext} = 4½$ in.
$d_e = 1¾$ in.
$p_{fo} = 2¾$ in.
$p_{fi} = 2$ in.
$d_p = 33⅛$ in.

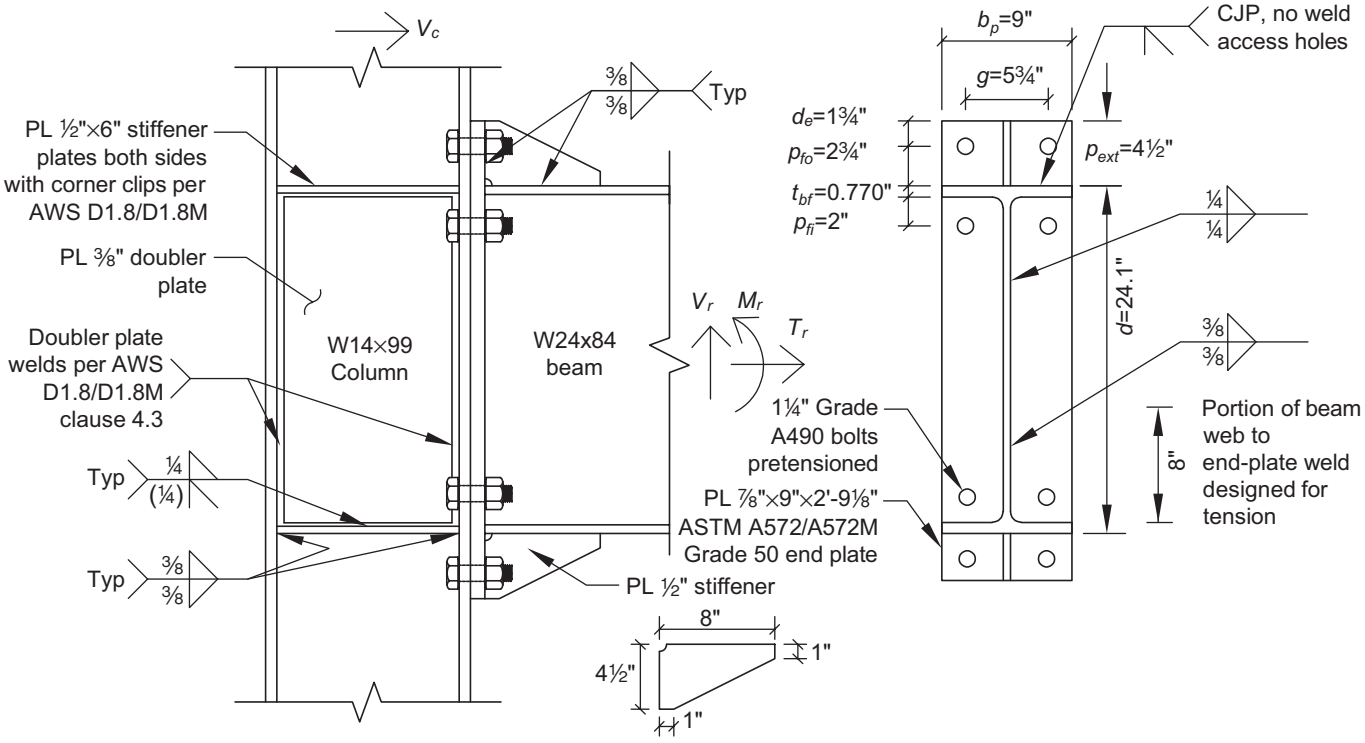

Fig. B-14. Four-bolt extended stiffened thin end-plate configuration for Example B.3-2.

The distances from the centerline of the compression flange to the bolt lines, h_1 and h_2, are depicted in Table 5-11 and computed as:

$$h_1 = d - \frac{t_{bf}}{2} + p_{fo}$$
$$= 24.1 \text{ in.} - \frac{0.770 \text{ in.}}{2} + 2\frac{3}{4} \text{ in.}$$
$$= 26.5 \text{ in.}$$

$$h_2 = d - \frac{3t_{bf}}{2} - p_{fi}$$
$$= 24.1 \text{ in.} - \frac{3(0.770 \text{ in.})}{2} - 2 \text{ in.}$$
$$= 20.9 \text{ in.}$$

$$b_{p,eff} \le b_{bf} + \max(t_p, 1 \text{ in.}) \quad (4\text{-}3)$$
$$\le 9.02 \text{ in.} + \max(\tfrac{7}{8} \text{ in.}, 1 \text{ in.})$$
$$\le 10.0 \text{ in.}$$

$b_p = 9 \text{ in.} \le 10.0 \text{ in.}$ **o.k.**

$$b_{bf} \ge g \quad (4\text{-}1)$$

$9.02 \text{ in.} \ge 5\frac{3}{4} \text{ in.}$ **o.k.**

Beam flange to end-plate stiffener geometric properties:

$$h_{st} = p_{ext}$$
$$= 4\tfrac{1}{2} \text{ in.}$$

$$L_{st} = \frac{h_{st}}{\tan 30^\circ} \quad (4\text{-}4)$$
$$= \frac{4\tfrac{1}{2} \text{ in.}}{\tan 30^\circ}$$
$$= 7.79 \text{ in.} \le 8 \text{ in.}$$ **o.k.**

$$t_s \ge t_{bw}\left(\frac{F_{yb}}{F_{ys}}\right) \quad (3\text{-}36)$$
$$\ge (0.470 \text{ in.})\left(\frac{50 \text{ ksi}}{50 \text{ ksi}}\right)$$
$$\ge 0.470 \text{ in.}$$

$t_s = \tfrac{1}{2} \text{ in.}$ **o.k.**

$$\frac{h_{st}}{t_s} = \frac{4\tfrac{1}{2} \text{ in.}}{\tfrac{1}{2} \text{ in.}}$$
$$= 9.00$$

$$\frac{h_{st}}{t_s} \le 0.56\sqrt{\frac{E}{F_{ys}}} \tag{3-37}$$

$$\le 0.56\sqrt{\frac{29{,}000 \text{ ksi}}{50 \text{ ksi}}}$$

$$\le 13.5$$

$$\frac{h_{st}}{t_s} = 9.00 \quad \textbf{o.k.}$$

A. End-Plate and Bolt Design Verification

Calculate the equivalent required moment considering the effect of the required tensile force using Equation 3-30.

LRFD	ASD
$M_{u,eq} = M_u + (T_u/2)(d - t_{bf})$ $= 7{,}620 \text{ kip-in.} + \left(\frac{20.4 \text{ kips}}{2}\right)(24.1 \text{ in.} - 0.770 \text{ in.})$ $= 7{,}860 \text{ kip-in.}$	$M_{a,eq} = M_a + (T_a/2)(d - t_{bf})$ $= 5{,}080 \text{ kip-in.} + \left(\frac{13.6 \text{ kips}}{2}\right)(24.1 \text{ in.} - 0.770 \text{ in.})$ $= 5{,}240 \text{ kip-in.}$

Determine if the specified end-plate thickness, ⅞ in., and Grade A490 bolt diameter, 1¼ in., are sufficient using the thin end-plate/larger bolt diameter procedure.

Solve for the required end-plate thickness using Equations 5-5. First solve for the distance, s, and yield line parameter, Y_p, using Table 5-11.

$$s = \frac{\sqrt{b_p g}}{2}$$

$$= \frac{\sqrt{(9 \text{ in.})(5¾ \text{ in.})}}{2}$$

$$= 3.60 \text{ in.}$$

Because $s > d_e = 1¾$ in., Y_p in Table 5-11 is applicable, and because $s \ge p_{fo} = 2¾$ in. and $p_{fi} = 2$ in., the dimensions p_{fo} and p_{fi} are used in the equation for the yield line parameter.

$$Y_p = \frac{b_p}{2}\left[h_1\left(\frac{1}{p_{fo}} + \frac{1}{2d_e}\right) + h_2\left(\frac{1}{p_{fi}} + \frac{1}{s}\right)\right] + \frac{2}{g}\left[h_1(p_{fo} + d_e) + h_2(p_{fi} + s)\right]$$

$$= \left(\frac{9 \text{ in.}}{2}\right)\left\{(26.5 \text{ in.})\left[\frac{1}{2¾ \text{ in.}} + \frac{1}{2(1¾ \text{ in.})}\right] + (20.9 \text{ in.})\left(\frac{1}{2 \text{ in.}} + \frac{1}{3.60 \text{ in.}}\right)\right\}$$

$$+ \left(\frac{2}{5¾ \text{ in.}}\right)\left[(26.5 \text{ in.})(2¾ \text{ in.} + 1¾ \text{ in.}) + (20.9 \text{ in.})(2 \text{ in.} + 3.60 \text{ in.})\right]$$

$$= 233 \text{ in.}$$

Determine the required end-plate thickness using Equations 5-5. For extended end-plate configurations, $\gamma_r = 1.0$.

LRFD	ASD
$t_{p,reqd} = \sqrt{\dfrac{M_{u,eq}}{\gamma_r \phi_b F_y Y_p}}$ $= \sqrt{\dfrac{7{,}860 \text{ kip-in.}}{1.0(0.90)(50 \text{ ksi})(233 \text{ in.})}}$ $= 0.866 \text{ in.} \quad \le \quad ⅞ \text{ in.} \quad$ **o.k.**	$t_{p,reqd} = \sqrt{\dfrac{\Omega_b M_{a,eq}}{\gamma_r F_y Y_p}}$ $= \sqrt{\dfrac{1.67(5{,}240 \text{ kip-in.})}{1.0(50 \text{ ksi})(233 \text{ in.})}}$ $= 0.867 \text{ in.} \quad \le \quad ⅞ \text{ in.} \quad$ **o.k.**

Therefore, a ⅞-in.-thick end plate is sufficient.

Determine if the specified Grade A490, 1¼-in.-diameter bolts are sufficient. First calculate the geometry of the effective tee stub; then calculate the related forces, F_i, Q_{max}, and P_{qi}; finally, calculate the required bolt diameter and compare with the specified bolt diameter.

The bolts are specified as pretensioned. From AISC *Specification* Table J3.1, the pretension force for a 1¼-in.-diameter, Grade A490 bolt is $T_b = 102$ kips. The nominal unthreaded body area of a 1¼ in. bolt is $A_b = 1.23 \text{ in.}^2$, and the nominal tensile stress for a Grade A490 bolt is $F_{nt} = 113$ ksi. The resulting nominal tensile strength of a 1¼-in.-diameter Grade A490 bolt is:

$$P_t = F_{nt} A_b \qquad \text{(from } \textit{Spec.} \text{ Eq. J3-1)}$$
$$= (113 \text{ ksi})(1.23 \text{ in.}^2)$$
$$= 139 \text{ kips}$$

There are two unique bolt locations as labeled in Figure B-15. The orientation of the effective tee stubs are defined using the rules given in Section 5.1.2 and are shown in Figure B-15.

Calculate the bolt distance from bolt to edge of effective tee stub:

$$a = 3.62\left(\frac{t_p}{d_b}\right)^3 - 0.085 \text{ in} \qquad (3\text{-}24)$$
$$= 3.62\left(\frac{⅞ \text{ in.}}{1¼ \text{ in.}}\right)^3 - 0.085 \text{ in.}$$
$$= 1.16 \text{ in.}$$

Bolt Position 1—Outside Bolt

For the bolts outside the flange, calculate the geometry of the effective tee stub, including the width of the effective tee stub, w_1, the net effective width, w_1', and distance from effective tee stem to the bolt, b_1.

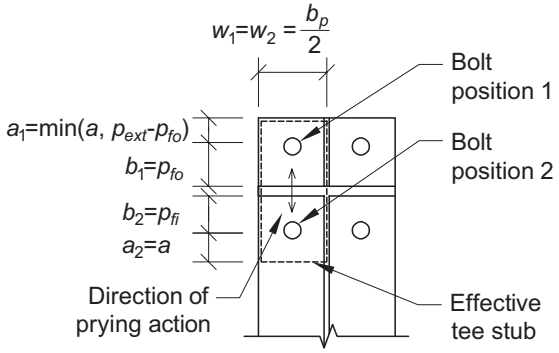

Fig. B-15. Effective tee-stub geometry for the four-bolt extended stiffened configuration.

$$w_1 = \frac{b_p}{2}$$
$$= \frac{9 \text{ in.}}{2}$$
$$= 4.50 \text{ in.}$$

$$w_1' = w_1 - (d_b + \tfrac{1}{8} \text{ in.}) \quad (5\text{-}7)$$
$$= 4.50 \text{ in.} - (1\tfrac{1}{4} \text{ in.} + \tfrac{1}{8} \text{ in.})$$
$$= 3.13 \text{ in.}$$

$$a_1 = \min(a, d_e)$$
$$= \min(1.16 \text{ in.}, 1\tfrac{3}{4} \text{ in.})$$
$$= 1.16 \text{ in.}$$

$$b_1 = p_{fo}$$
$$= 2\tfrac{3}{4} \text{ in.}$$

Find forces related to prying, including the force, F_1', the prying force, $Q_{max,1}$, and the bolt tension contributing to flexural strength, P_{q1}.

$$F_1' = \frac{1}{b_1}\left[\frac{t_p^2 F_y}{4}(0.85w_1 + 0.8w_1') + \frac{\pi d_b^3 F_{nt}}{32}\right] \quad (3\text{-}26)$$
$$= \left(\frac{1}{2\tfrac{3}{4} \text{ in.}}\right)\left\{\left[\frac{(\tfrac{7}{8} \text{ in.})^2 (50 \text{ ksi})}{4}\right]\left[0.85(4.50 \text{ in.}) + 0.8(3.13 \text{ in.})\right] + \frac{\pi(1\tfrac{1}{4} \text{ in.})^3 (113 \text{ ksi})}{32}\right\}$$
$$= 29.9 \text{ kips}$$

$$Q_{max,1} = \frac{w_1' t_p^2}{4a_1}\sqrt{F_y^2 - 3\left(\frac{F_1'}{w_1' t_p}\right)^2} \quad (3\text{-}23)$$
$$= \frac{(3.13 \text{ in.})(\tfrac{7}{8} \text{ in.})^2}{4(1.16 \text{ in.})}\sqrt{(50 \text{ ksi})^2 - 3\left[\frac{29.9 \text{ kips}}{(3.13 \text{ in.})(\tfrac{7}{8} \text{ in.})}\right]^2}$$
$$= 23.9 \text{ kips}$$

$$P_{q1} = \max(P_t - Q_{max,1}, T_b) \quad (3\text{-}27)$$
$$= \max(139 \text{ kips} - 23.9 \text{ kips}, 102 \text{ kips})$$
$$= 115 \text{ kips}$$

Bolt position 2 is the interior bolt, which also experiences prying about the flange. Prying forces for bolt position 2 are calculated in a similar way as bolt position 1. Table B-7 gives the geometric parameters, related prying force, the usable strength for each bolt position, and reduction in bolt contribution factor, α_i.

Calculate the flexural strength for bolt rupture with prying action, M_q, using Equation 3-28. Then the design flexural strength is compared to the required flexural strength.

$$M_q = \sum_i \alpha_i P_{qi} n_i h_i \quad (3\text{-}28)$$
$$= 1.0(115 \text{ kips})(2 \text{ bolts})(26.5 \text{ in.}) + 1.0(117 \text{ kips})(2 \text{ bolts})(20.9 \text{ in.})$$
$$= 11{,}000 \text{ kip-in.}$$

Table B-7. Prying Action for the Four-Bolt Extended Stiffened Example		
Parameter	**Bolt Position 1**	**Bolt Position 2**
w_i (in.)	4.50	4.50
w_i' (in.)	3.13	3.13
a_i (in.)	1.16	1.16
b_i (in.)	2.75	2.00
F_i' (kips)	29.9	41.1
$Q_{max,i}$ (kips)	23.9	22.1
P_{qi} (kips)	115	117
α_i	1.0	1.0

LRFD	ASD
$\phi M_q = 0.75(11{,}000 \text{ kip-in.})$ $= 8{,}250 \text{ kip-in.} \quad \geq \quad M_{u,eq} = 7{,}860 \text{ kip-in.}$ **o.k.**	$\frac{M_q}{\Omega} = \frac{11{,}000 \text{ kip-in.}}{2.00}$ $= 5{,}500 \text{ kip-in.} \quad \geq \quad M_{a,eq} = 5{,}240 \text{ kip-in.}$ **o.k.**

Therefore, 1¼-in.-diameter Grade A490 bolts are sufficient.

Check Shear Yielding and Shear Rupture of the Extended Portion of the End Plate

For extended end-plate moment connections that are stiffened, shear yielding and shear rupture of the extended portion of the end plate are not limit states.

Check Shear Transfer at the Top Bolt Holes

Shear at the faying surface, V_u, is assumed to be resisted only by the four compression side bolts. The shear transfer strength at each bolt hole is the minimum of the end-plate bearing/tearout strength, the bolt shear rupture strength, and the column flange bearing/tearout strength. See the User Note in AISC *Specification* Section J3.7.

The nominal unthreaded body area of a 1¼ in. bolt is $A_b = 1.23 \text{ in.}^2$, and the nominal shear strength in bearing-type connections with threads not excluded from the shear planes is $F_{nt} = 68$ ksi. The resulting nominal shear strength of a 1¼-in-diameter Grade A490 bolt is:

$$R_{n,bt} = F_{nv} A_b \qquad \text{(from } \textit{Spec.} \text{ Eq. J3-1)}$$
$$= (68 \text{ ksi})(1.23 \text{ in.}^2)$$
$$= 83.6 \text{ kips}$$

The nominal bearing/tearout strength is given by AISC *Specification* Section J3.11. The bolt force acting on the end plate is down toward the middle of the end plate, and therefore, tearout will not control. Likewise, tearout will not control at the column flange, and only bolt bearing needs to be checked. The column flange thickness, 0.780 in., is less than the end-plate thickness, ⅞ in.; therefore, the controlling nominal bearing strength at a bolt hole is:

$$R_{n,brg} = 2.4 d_b t_{cf} F_{up} \qquad \text{(from } \textit{Spec.} \text{ Eq. J3-6a)}$$
$$= 2.4(1¼ \text{ in.})(0.780 \text{ in.})(65 \text{ ksi})$$
$$= 152 \text{ kips}$$

The shear transfer strength is then the minimum of the column flange bearing strength, the bolt shear rupture strength, and the end-plate bearing strength, which results in $R_n = 83.6$ kips.

Therefore, the nominal shear transfer strength at the four top bolt holes is:

$V_n = (4 \text{ bolts}) R_n$

$= (4 \text{ bolts})(83.6 \text{ kips})$

$= 334 \text{ kips}$

LRFD	ASD
$\phi V_n = 0.75(334 \text{ kips})$ $= 251 \text{ kips} \geq V_u = 45.8 \text{ kips}$ **o.k.**	$\frac{V_n}{\Omega} = \frac{334 \text{ kips}}{2.00}$ $= 167 \text{ kips} \geq V_a = 30.5 \text{ kips}$ **o.k.**

The specified ASTM A572/A572M Grade 50 ⅞-in.-thick end plate and 1¼-in.-diameter Grade A490 pretensioned bolts are sufficient.

B. Check Beam to End-Plate Welds

Weld strength calculations for this thin plate design are the same as for the thick plate design in Example 5.3-2.

C. Check Column-Side Limit States

Calculations to verify the strength of the column-side limit states for the connection shown in Figure B-14 are identical to those for the thick plate design in Example 5.3-2, except for the web local yielding. For this check, the end-plate thickness is ⅞ in. instead of 1 in. This difference has no effect on the design shown in Figure B-14.

Summary

The connection shown in Figure B-14 is adequate for the required moment and tension and shear forces.

EXAMPLE B.3-3—Multiple-Row Extended 1/2 Unstiffened Thin End-Plate Example

Given:

The connection shown in Figure B-16 is a multiple-row extended (MRE) 1/2 unstiffened end-plate moment connection for a built-up beam. The beam and end plate are ASTM A572/A572M Grade 50 material, and the bolts are Group 120 ASTM F3125/F3125M Grade A325 pretensioned. Weld electrodes are E70XX. The connection is to be evaluated as a thin end-plate design for the following required moments and shear forces:

	LRFD	ASD
Moment	$M_u = 4{,}800$ kip-in.	$M_a = 3{,}200$ kip-in.
Shear force	$V_u = 45.0$ kips	$V_a = 30.0$ kips

Solution:

From AISC *Manual* Table 2-4, the material properties are as follows:

ASTM A572/A572M Grade 50
$F_y = 50$ ksi
$F_u = 65$ ksi

From AISC *Specification* Table J3.2, the material properties of the bolts are as follows:

Group 120 ASTM F3125/F3125M 1-in.-diameter Grade A325 pretensioned
$F_{nt} = 90$ ksi
$F_{nv} = 54$ ksi (Group 120 bolts with threads not excluded from the shear plane; thread condition N)

Beam

$d = 24$ in. $\quad t_{bw} = 3/8$ in.

$b_{bf} = 8$ in. $\quad t_{bf} = 1/2$ in.

End-plate geometric properties:

$b_p = 8$ in.

$t_p = 3/4$ in.

$g = 5$ in.

$p_{ext} = 3$ in.

$d_e = 1\frac{1}{4}$ in.

$p_{fo} = 1\frac{3}{4}$ in.

$p_{fi} = 1\frac{3}{4}$ in.

$p_b = 3$ in.

$d_p = 30$ in.

The distances from the centerline of the compression flange to the bolt lines, h_1, h_2, and h_3, are depicted in Table 5-12 and computed as:

$$h_1 = d - \frac{t_{bf}}{2} + p_{fo}$$

$$= 24 \text{ in.} - \frac{1/2 \text{ in.}}{2} + 1\frac{3}{4} \text{ in.}$$

$$= 25.5 \text{ in.}$$

$$h_2 = d - \frac{3t_{bf}}{2} - p_{fi}$$

$$= 24 \text{ in.} - \frac{3(1/2 \text{ in.})}{2} - 1\frac{3}{4} \text{ in.}$$

$$= 21.5 \text{ in.}$$

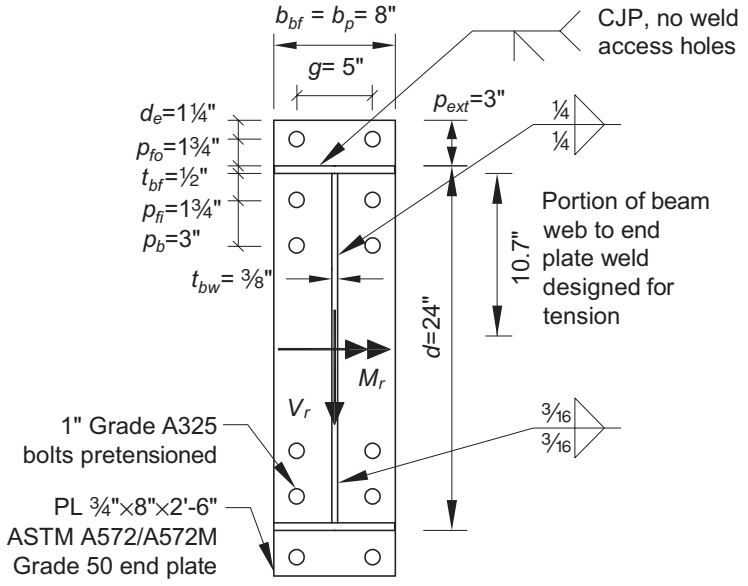

Fig. B-16. MRE 1/2 unstiffened thin end-plate configuration for Example B.3-3.

$$h_3 = d - \frac{3t_{bf}}{2} - p_{fi} - p_b$$
$$= 24 \text{ in.} - \frac{3(\text{½ in.})}{2} - 1\text{¾ in.} - 3 \text{ in.}$$
$$= 18.5 \text{ in.}$$

$$b_{p,eff} \le b_{bf} + \max(t_p, 1 \text{ in.}) \quad (4\text{-}3)$$
$$\le 8 \text{ in.} + \max(\text{¾ in.}, 1 \text{ in.})$$
$$\le 9.00 \text{ in.}$$

$b_p = 8 \text{ in.} \le 9.00 \text{ in.}$ **o.k.**

$$b_{bf} \ge g \quad (4\text{-}1)$$
$8 \text{ in.} \ge 5 \text{ in.}$ **o.k.**

A. End-Plate and Bolt Design Verification

Determine if the specified end-plate thickness, ¾ in., and bolt diameter, 1 in., are sufficient using the thin end-plate/larger bolt diameter procedure are sufficient.

Solve for the required end-plate thickness using Equations 5-5. First solve for the distance, s, and yield line parameter, Y_p, using Table 5-12.

$$s = \frac{\sqrt{b_p g}}{2}$$
$$= \frac{\sqrt{(8 \text{ in.})(5 \text{ in.})}}{2}$$
$$= 3.16 \text{ in.}$$

Because $s \ge p_{fi} = 1\text{¾}$ in., the dimension p_{fi} is used in the equation for the yield line parameter.

$$Y_p = \frac{b_p}{2}\left[h_1\left(\frac{1}{p_{fo}}\right) + h_2\left(\frac{1}{p_{fi}}\right) + h_3\left(\frac{1}{s}\right) - \frac{1}{2}\right] + \frac{2}{g}\left[h_2(p_{fi} + 0.75p_b) + h_3(s + 0.25p_b)\right] + \frac{g}{2}$$
$$= \left(\frac{8 \text{ in.}}{2}\right)\left[(25.5 \text{ in.})\left(\frac{1}{1\text{¾ in.}}\right) + (21.5 \text{ in.})\left(\frac{1}{1\text{¾ in.}}\right) + (18.5 \text{ in.})\left(\frac{1}{3.16 \text{ in.}}\right) - \frac{1}{2}\right]$$
$$+ \left(\frac{2}{5 \text{ in.}}\right)\left\{(21.5 \text{ in.})\left[1\text{¾ in.} + 0.75(3 \text{ in.})\right] + (18.5 \text{ in.})\left[3.16 \text{ in.} + 0.25(3 \text{ in.})\right]\right\} + \frac{5 \text{ in.}}{2}$$
$$= 195 \text{ in.}$$

Determine the required end-plate thickness using Equations 5-5. For extended end-plate configurations, $\gamma_r = 1.0$.

LRFD	ASD
$t_{p,reqd} = \sqrt{\dfrac{M_u}{\gamma_r \phi_b F_y Y_p}}$	$t_{p,reqd} = \sqrt{\dfrac{\Omega_b M_a}{\gamma_r F_y Y_p}}$
$= \sqrt{\dfrac{4{,}800 \text{ kip-in.}}{1.0(0.90)(50 \text{ ksi})(195 \text{ in.})}}$	$= \sqrt{\dfrac{1.67(3{,}200 \text{ kip-in.})}{1.0(50 \text{ ksi})(195 \text{ in.})}}$
$= 0.740 \text{ in.} \le$ ¾ in. **o.k.**	$= 0.740 \text{ in.} \le$ ¾ in. **o.k.**

Therefore, a ¾-in.-thick end plate is sufficient.

Determine if the specified 1-in.-diameter Grade A325 bolts are sufficient. First calculate the geometry of the effective tee stub; then calculate the related forces, F_i, Q_{max}, and P_{qi}; finally, calculate the required bolt diameter.

The bolts are specified as pretensioned. The minimum bolt pretension for a 1-in.-diameter Grade A325 bolt is $T_b = 51$ kips. The nominal unthreaded body area of a 1 in. bolt is $A_b = 0.785$ in.^{2}, and the nominal tensile stress for a Grade A325 bolt is $F_{nt} = 90$ ksi. The resulting nominal tensile strength of a 1-in.-diameter Grade A325 bolt is:

$$P_t = F_{nt}A_b \qquad \text{(from } Spec. \text{ Eq. J3-1)}$$
$$= (90 \text{ ksi})(0.785 \text{ in.}^2)$$
$$= 70.7 \text{ kips}$$

There are three unique bolt locations as labeled in Figure B-17. The orientation of the effective tee stubs are defined using the rules given in Section 5.1.2 and are shown in Figure B-17.

Calculate the distance from bolt line to edge of effective tee stub:

$$a = 3.62\left(\frac{t_p}{d_b}\right)^3 - 0.085 \text{ in.} \qquad (3\text{-}24)$$
$$= 3.62\left(\frac{¾ \text{ in.}}{1 \text{ in.}}\right)^3 - 0.085 \text{ in.}$$
$$= 1.44 \text{ in.}$$

Bolt Position 1—Outside Bolt

For bolt position 1 (see Figure B-17), calculate the geometry of the effective tee stub, including the width of the effective tee stub, w_1, the net effective width, w_1', and distance from effective tee stem to the bolt line, b_1.

$$w_1 = \frac{b_p}{2}$$
$$= \frac{8 \text{ in.}}{2}$$
$$= 4.00 \text{ in.}$$

$$w_1' = w_1 - (d_b + ⅛ \text{ in.}) \qquad (5\text{-}7)$$
$$= 4.00 \text{ in.} - (1 \text{ in.} + ⅛ \text{ in.})$$
$$= 2.88 \text{ in.}$$

$$a_1 = \min(a, p_{ext} - p_{fo})$$
$$= \min(1.44 \text{ in.},\ 3 \text{ in.} - 1¾ \text{ in.})$$
$$= 1.25 \text{ in.}$$

$$b_1 = p_{fo}$$
$$= 1¾ \text{ in.}$$

Find forces related to prying, including the force, F_1', the prying force, $Q_{max,1}$, and the bolt tension contributing to flexural strength, P_{q1}.

$$F_1' = \frac{1}{b_1}\left[\frac{t_p^2 F_y}{4}(0.85w_1 + 0.8w_1') + \frac{\pi d_b^3 F_{nt}}{32}\right] \quad (3\text{-}26)$$

$$= \left(\frac{1}{1¾\text{ in.}}\right)\left\{\left[\frac{(¾\text{ in.})^2(50\text{ ksi})}{4}\right]\left[0.85(4.00\text{ in.}) + 0.8(2.88\text{ in.})\right] + \frac{\pi(1\text{ in.})^3(90\text{ ksi})}{32}\right\}$$

$$= 28.0\text{ kips}$$

$$Q_{max,1} = \frac{w_1' t_p^2}{4a_1}\sqrt{F_p^2 - 3\left(\frac{F_1'}{w_1' t_p}\right)^2} \quad (3\text{-}23)$$

$$= \frac{(2.88\text{ in.})(¾\text{ in.})^2}{4(1.25\text{ in.})}\sqrt{(50\text{ ksi})^2 - 3\left[\frac{28.0\text{ kips}}{(2.88\text{ in.})(¾\text{ in.})}\right]^2}$$

$$= 14.5\text{ kips}$$

$$P_{q1} = \max(P_t - Q_{max,1},\ T_b) \quad (3\text{-}27)$$

$$= \max(70.7\text{ kips} - 14.5\text{ kips},\ 51.0\text{ kips})$$

$$= 56.2\text{ kips}$$

Prying forces for bolt positions 2 and 3 are calculated in a similar way using the effective tee-stub geometry shown in Figure B-17. Table B-8 gives the geometric parameters, related prying force, the usable strength for each bolt position, and reduction in bolt contribution factor, α_i.

Calculate the flexural strength for bolt rupture with prying action, M_q, using Equation 3-28. Then the design flexural strength is compared to the required flexural strength.

$$M_q = \sum_i \alpha_i P_{qi} n_i h_i \quad (3\text{-}28)$$

$$= 1.0(56.2\text{ kips})(2\text{ bolts})(25.5\text{ in.}) + 1.0(58.1\text{ kips})(2\text{ bolts})(21.5\text{ in.})$$

$$+ 1.0(54.3\text{ kips})(2\text{ bolts})(18.5\text{ in.})$$

$$= 7{,}370\text{ kip-in.}$$

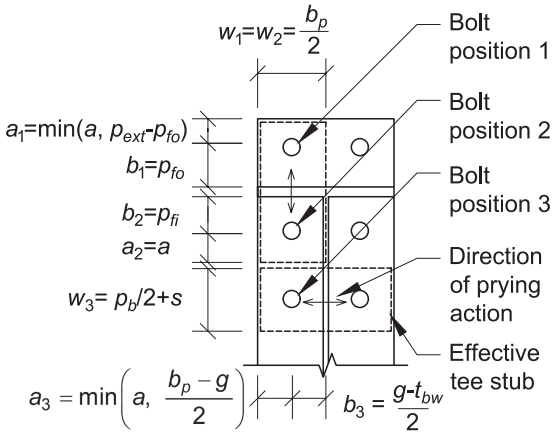

Fig. B-17. Effective tee-stub geometry for the MRE 1/2 unstiffened configuration.

Table B-8. Prying Action for the MRE 1/2 Unstiffened Example			
Parameter	**Bolt Position 1**	**Bolt Position 2**	**Bolt Position 3**
w_i (in.)	4.00	4.00	4.66
w_i' (in.)	2.88	2.88	3.54
a_i (in.)	1.25	1.44	1.44
b_i (in.)	1.75	1.75	2.31
F_i' (kips)	28.0	28.0	24.5
$Q_{max,i}$ (kips)	14.5	12.6	16.4
P_{qi} (kips)	56.2	58.1	54.3
α_i	1.0	1.0	1.0

LRFD	ASD
$\phi M_q = 0.75(7{,}370 \text{ kip-in.})$ $= 5{,}530 \text{ kip-in.} \quad \geq \quad M_u = 4{,}800 \text{ kip-in.}$ **o.k.**	$\frac{M_q}{\Omega} = \frac{7{,}370 \text{ kip-in.}}{2.00}$ $= 3{,}690 \text{ kip-in.} \quad \geq \quad M_a = 3{,}200 \text{ kip-in.}$ **o.k.**

Therefore, 1-in.-diameter bolts are sufficient.

Check Shear Yielding and Shear Rupture of the Extended Portion of the End Plate

For extended end-plate moment connections that are unstiffened, potential limit states that must be checked are shear yielding and shear rupture of the extended portion of the end plate. For the MRE 1/2 connection, the shear demand is taken as one-third of the tension flange force because the exterior bolts represent one-third of the bolts. The shear strength is calculated in accordance with AISC *Specification* Section J4.2.

Calculate the shear demand on the extended portion of the end plate.

LRFD	ASD
$V_{up} = \frac{1}{3}\left(\frac{M_u}{d - t_{bf}}\right)$ $= \frac{1}{3}\left(\frac{4{,}800 \text{ kip-in.}}{24 \text{ in.} - ½ \text{ in.}}\right)$ $= 68.1 \text{ kips}$	$V_{ap} = \frac{1}{3}\left(\frac{M_a}{d - t_{bf}}\right)$ $= \frac{1}{3}\left(\frac{3{,}200 \text{ kip-in.}}{24 \text{ in.} - ½ \text{ in.}}\right)$ $= 45.4 \text{ kips}$

Calculate the nominal shear yielding strength.

$$R_n = 0.60F_yA_{gv} \qquad \text{(Spec. Eq. J4-3)}$$
$$= 0.60F_yb_pt_p$$
$$= 0.60(50 \text{ ksi})(8 \text{ in.})(¾ \text{ in.})$$
$$= 180 \text{ kips}$$

Compare the design shear yielding strength to the shear demand. According to AISC *Specification* Section J4.2 for yielding of elements in shear, the resistance factor is $\phi = 1.00$, and the safety factor is $\Omega = 1.50$.

LRFD	ASD
$\phi R_n = 1.00(180 \text{ kips})$ $= 180 \text{ kips} \quad \geq \quad V_{up} = 68.0 \text{ kips}$ **o.k.**	$\frac{R_n}{\Omega} = \frac{180 \text{ kips}}{1.50}$ $= 120 \text{ kips} \quad \geq \quad V_{ap} = 45.4 \text{ kips}$ **o.k.**

Calculate the nominal shear rupture strength. The width of the extended portion of the end plate for use in the net section area is the width minus two effective hole diameters. The effective hole diameter is the hole diameter from AISC *Specification* Table J3.3 plus ⅛6 in. The additional ⅛6 in. accounts for damage around the hole caused by drilling, punching, or thermal cutting. For 1-in.-diameter bolts, the standard hole diameter, d_h, is 1⅛ in.

$$A_{nv} = \left[b_p - 2(d_h + ⅛6)\right] t_p$$
$$= \left[8 \text{ in.} - 2(1⅛ \text{ in.} + ⅛6 \text{ in.})\right](¾ \text{ in.})$$
$$= 4.22 \text{ in.}^2$$

$$R_n = 0.60 F_u A_{nv} \qquad \text{(}\textit{Spec}\text{. Eq. J4-4)}$$
$$= 0.60(65 \text{ ksi})(4.22 \text{ in.}^2)$$
$$= 165 \text{ kips}$$

Compare the design shear rupture strength to the shear demand. Using AISC *Specification* Section J4.2 for rupture of elements in shear, the resistance factor is $\phi = 0.75$, and the safety factor is $\Omega = 2.00$.

LRFD	ASD
$\phi R_n = 0.75(165 \text{ kips})$ $= 124 \text{ kips} \quad \geq \quad V_{up} = 68.0 \text{ kips}$ **o.k.**	$\frac{R_n}{\Omega} = \frac{165 \text{ kips}}{2.00}$ $= 82.5 \text{ kips} \quad \geq \quad V_{ap} = 45.4 \text{ kips}$ **o.k.**

The extended portion of the ¾-in.-thick end plate has sufficient resistance to shear yielding and shear rupture.

Check Shear Transfer at Bolt Holes

See Example 5.3-1 or 5.3-2 for calculation procedures.

The specified ASTM A572/A572M Grade 50 ¾-in.-thick end plate and 1-in.-diameter Grade A325 pretensioned bolts are sufficient.

B. Check Beam to End-Plate Welds

The beam to end-plate welds shown in Figure B-16 are the same as shown in Figure 5-12. See Example 5.3-3 for weld strength checks.

The design shown in Figure B-16 is satisfactory for the required moment and shear force shown.

C. Column-Side Limit State Checks

See Example 5.3-1 or 5.3-2 for example column-side limit state check calculations.

Summary

The connection shown in Figure B-16 is adequate for the required moment and shear force.

EXAMPLE B.3-4—Multiple-Row Extended 1/3 Unstiffened Thin End-Plate Example

Given:

The connection shown in Figure B-18 is a multiple-row extended (MRE) 1/3 unstiffened end-plate moment connection for a built-up beam. The beam and end plate are ASTM A572/A572M Grade 50 material, and the bolts are Group 120 ASTM F3125/F3125M Grade A325 pretensioned. Weld electrodes are E70XX. The connection is to be evaluated as a thin end-plate design for the following required moments and shear forces:

	LRFD	ASD
Moment	$M_u = 8{,}000$ kip-in.	$M_a = 5{,}330$ kip-in.
Shear force	$V_u = 60.0$ kips	$V_a = 40.0$ kips

Solution:

From AISC *Manual* Table 2-4, the material properties are as follows:

ASTM A572/A572M Grade 50
$F_y = 50$ ksi
$F_u = 65$ ksi

From AISC *Specification* Table J3.2, the material properties of the bolts are as follows:

Group 120 ASTM F3125/F3125M 1-in.-diameter Grade A325 bolts pretensioned
$F_{nt} = 90$ ksi
$F_{nv} = 54$ ksi (Group 120 with threads included in the shear plane.)

Beam
$d = 36$ in. $\quad t_{bw} = ⅜$ in.
$b_{bf} = 8$ in. $\quad t_{bf} = ½$ in.

End-plate geometric properties:
$b_p = 8$ in.
$t_p = ¾$ in.
$g = 5$ in.
$p_{ext} = 3$ in.
$d_e = 1¼$ in.
$p_{fo} = 1¾$ in.
$p_{fi} = 1¾$ in.
$p_b = 3$ in.
$d_p = 42$ in.

The distances from the centerline of the compression flange to the bolt lines, h_1, h_2, h_3, and h_4, are depicted in Table 5-13 and computed as:

$$h_1 = d - \frac{t_{bf}}{2} + p_{fo}$$
$$= 36 \text{ in.} - \frac{½ \text{ in.}}{2} + 1¾ \text{ in.}$$
$$= 37.5 \text{ in.}$$

$$h_2 = d - \frac{3t_{bf}}{2} - p_{fi}$$
$$= 36 \text{ in.} - \frac{3(½ \text{ in.})}{2} - 1¾ \text{ in.}$$
$$= 33.5 \text{ in.}$$

$$h_3 = d - \frac{3t_{bf}}{2} - p_{fi} - p_b$$

$$= 36 \text{ in.} - \frac{3(½ \text{ in.})}{2} - 1¾ \text{ in.} - 3 \text{ in.}$$

$$= 30.5 \text{ in.}$$

$$h_4 = d - \frac{3t_{bf}}{2} - p_{fi} - 2p_b$$

$$= 36 \text{ in.} - \frac{3(½ \text{ in.})}{2} - 1¾ \text{ in.} - 2(3 \text{ in.})$$

$$= 27.5 \text{ in.}$$

$$b_{p,eff} \le b_{bf} + \max(t_p, 1 \text{ in.}) \qquad (4\text{-}3)$$

$$\le 8 \text{ in.} + \max(¾ \text{ in.}, 1 \text{ in.})$$

$$\le 9.00 \text{ in.}$$

$b_p = 8.00$ in. $\le$ 9.00 in. **o.k.**

$$b_{bf} \ge g \qquad (4\text{-}1)$$

8 in. $\ge$ 5 in. **o.k.**

A. End-Plate and Bolt Design Verification

Determine if the specified end-plate thickness, ¾ in., and bolt diameter, 1-in.-diameter Grade A325 bolts, are sufficient using the thin end-plate/larger bolt diameter procedure.

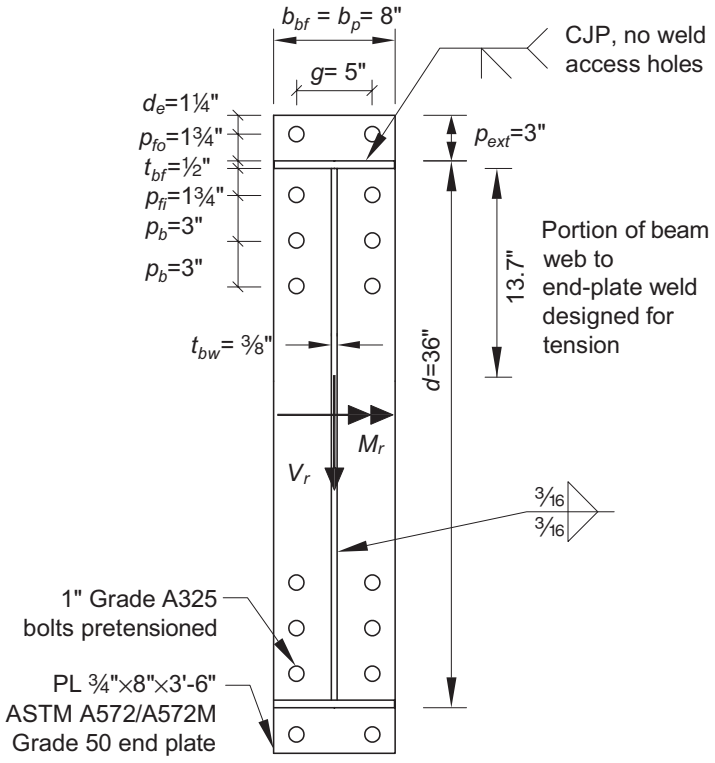

Fig. B-18. MRE 1/3 unstiffened thin end-plate configuration for Example B.3-4.

Solve for the required end-plate thickness using Equations 5-5. First solve for the distance, s, and yield line parameter, Y_p., using Table 5-13.

$$s = \frac{\sqrt{b_p g}}{2}$$
$$= \frac{\sqrt{(8\text{ in.})(5\text{ in.})}}{2}$$
$$= 3.16\text{ in.}$$

Because $s \geq p_{fi} = 1¾$ in., the dimension p_{fi} is used in the equation for the yield line parameter.

$$Y_p = \frac{b_p}{2}\left[h_1\left(\frac{1}{p_{fo}}\right) + h_2\left(\frac{1}{p_{fi}}\right) + h_4\left(\frac{1}{s}\right) - \frac{1}{2}\right] + \frac{2}{g}\left[h_2(p_{fi} + 1.5p_b) + h_4(s + 0.5p_b)\right] + \frac{g}{2}$$
$$= \left(\frac{8\text{ in.}}{2}\right)\left[(37.5\text{ in.})\left(\frac{1}{1¾\text{ in.}}\right) + (33.5\text{ in.})\left(\frac{1}{1¾\text{ in.}}\right) + (27.5\text{ in.})\left(\frac{1}{3.16\text{ in.}}\right) - \frac{1}{2}\right]$$
$$+ \left(\frac{2}{5\text{ in.}}\right)\left\{(33.5\text{ in.})\left[1¾\text{ in.} + 1.5(3\text{ in.})\right] + (27.5\text{ in.})\left[3.16\text{ in.} + 0.5(3\text{ in.})\right]\right\} + \frac{5\text{ in.}}{2}$$
$$= 333\text{ in.}$$

Determine the required end-plate thickness using Equations 5-5. For extended end-plate configurations, $\gamma_r = 1.0$.

LRFD	ASD
$t_{p,reqd} = \sqrt{\frac{M_u}{\gamma_r \phi_b F_y Y_p}}$	$t_{p,reqd} = \sqrt{\frac{\Omega_b M_a}{\gamma_r F_y Y_p}}$
$= \sqrt{\frac{8{,}000\text{ kip-in.}}{1.0(0.90)(50\text{ ksi})(333\text{ in.})}}$	$= \sqrt{\frac{1.67(5{,}330\text{ kip-in.})}{1.0(50\text{ ksi})(333\text{ in.})}}$
$= 0.731\text{ in.} \leq ¾\text{ in.}$ **o.k.**	$= 0.731\text{ in.} \leq ¾\text{ in.}$ **o.k.**

Therefore, a ¾-in.-thick end plate is sufficient.

Determine if the specified 1-in.-diameter Grade A325 bolts are sufficient. First calculate the geometry of the effective tee stub; then calculate the related forces, F_i, Q_{max}, and P_{qi}; finally, calculate the required bolt diameter.

The bolts are specified as pretensioned. The minimum bolt pretension for a 1 in. Grade A325 bolt is $T_b = 51$ kips. The nominal unthreaded body area of a 1 in. bolt is $A_b = 0.785\text{ in.}^2$, and the nominal tensile stress for a Grade A325 bolt is $F_{nt} = 90$ ksi. The resulting nominal tensile strength of a 1-in.-diameter Grade A325 bolt is:

$$P_t = F_{nt} A_b \qquad \text{(from } \textit{Spec.}\text{ Eq. J3-1)}$$
$$= (90\text{ ksi})(0.785\text{ in.}^2)$$
$$= 70.7\text{ kips}$$

There are four unique bolt locations as labeled in Figure B-19. The orientation of the effective tee stubs are defined using the rules given in Section 5.1.2 and are shown in Figure B-19.

Calculate the distance from bolt line to edge of effective tee stub:

$$a = 3.62\left(\frac{t_p}{d_b}\right)^3 - 0.085 \text{ in.} \tag{3-24}$$
$$= 3.62\left(\frac{¾ \text{ in.}}{1 \text{ in.}}\right)^3 - 0.085 \text{ in.}$$
$$= 1.44 \text{ in.}$$

Bolt Position 1—Outside Bolt

For bolt position 1 (see Figure B-19), calculate the geometry of the effective tee stub, including the width of the effective tee stub, w_1, the net effective width, w_1', and distance from effective tee stem to the bolt line, b_1.

$$w_1 = \frac{b_p}{2}$$
$$= \frac{8 \text{ in.}}{2}$$
$$= 4.00 \text{ in.}$$

$$w_1' = w_1 - (d_b + ⅛ \text{ in.}) \tag{5-7}$$
$$= 4.00 \text{ in.} - (1 \text{ in.} + ⅛ \text{ in.})$$
$$= 2.88 \text{ in.}$$

$$a_1 = \min(a, p_{ext} - p_{fo})$$
$$= \min(1.44 \text{ in.}, 3 \text{ in.} - 1¾ \text{ in.})$$
$$= 1.25 \text{ in.}$$

$$b_1 = p_{fo}$$
$$= 1¾ \text{ in.}$$

Find forces related to prying, including the force, F_1', the prying force, $Q_{max,1}$, and the bolt tension contributing to flexural strength, P_{q1}.

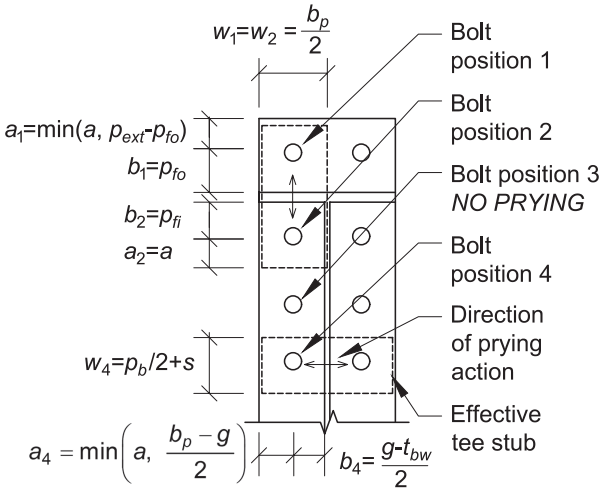

Fig. B-19. Effective tee-stub geometry for the MRE 1/3 unstiffened configuration.

$$F_1' = \frac{1}{b_1}\left[\frac{t_p^2 F_y}{4}(0.85w_1 + 0.8w_1') + \frac{\pi d_b^3 F_{nt}}{32}\right] \quad (3\text{-}26)$$

$$= \left(\frac{1}{1\frac{3}{4}\text{ in.}}\right)\left\{\left[\frac{\left(\frac{3}{8}\text{ in.}\right)^2(50\text{ ksi})}{4}\right]\left[0.85(4.00\text{ in.}) + 0.8(2.88\text{ in.})\right] + \frac{\pi(1\text{ in.})^3(90\text{ ksi})}{32}\right\}$$

$$= 28.0\text{ kips}$$

$$Q_{max,1} = \frac{w_1' t_p^2}{4a_1}\sqrt{F_y^2 - 3\left(\frac{F_1'}{w_1' t_p}\right)^2} \quad (3\text{-}23)$$

$$= \frac{(2.88\text{ in.})\left(\frac{3}{4}\text{ in.}\right)^2}{4(1.25\text{ in.})}\sqrt{(50\text{ ksi})^2 - 3\left[\frac{28.0\text{ kips}}{(2.88\text{ in.})\left(\frac{3}{4}\text{ in.}\right)}\right]^2}$$

$$= 14.5\text{ kips}$$

$$P_{q1} = \max\left(P_t - Q_{max,1}, T_b\right) \quad (3\text{-}27)$$

$$= \max(70.7\text{ kips} - 14.4\text{ kips}, 51.0\text{ kips})$$

$$= 56.2\text{ kips}$$

Prying forces for bolt positions 2 and 4 are calculated in a similar way using the effective tee-stub geometry shown in Figure B-19. Table B-9 gives the geometric parameters, related prying force, the usable strength for each bolt position, and reduction in bolt contribution factor, α_i. As described in Section 5.1.2, experiments have shown that bolts in the second interior row of configurations with three or more interior rows do not experience prying forces. However, they may not reach their full tensile strength. The bolt strength is taken equal to the bolt pretension for bolt position 3.

Calculate the flexural strength for bolt rupture with prying action, M_q, using Equation 3-28. Then the design flexural strength is compared to the required flexural strength.

$$M_q = \sum_i \alpha_i P_{qi} n_i h_i \quad (3\text{-}28)$$

$$= 1.0(56.2\text{ kips})(2\text{ bolts})(37.5\text{ in.}) + 1.0(58.1\text{ kips})(2\text{ bolts})(33.5\text{ in.})$$

$$+ 1.0(51.0\text{ kips})(2\text{ bolts})(30.5\text{ in.}) + 1.0(54.3\text{ kips})(2\text{ bolts})(27.5\text{ in.})$$

$$= 14{,}200\text{ kip-in.}$$

LRFD	ASD
$\phi M_q = 0.75(14{,}200\text{ kip-in.})$ $= 10{,}700\text{ kip-in.} \geq M_u = 8{,}000\text{ kip-in.}$ **o.k.**	$\frac{M_q}{\Omega} = \frac{14{,}200\text{ kip-in.}}{2.00}$ $= 7{,}100\text{ kip-in.} \geq M_a = 5{,}330\text{ kip-in.}$ **o.k.**

Therefore, 1-in.-diameter Grade A325 bolts are sufficient.

Check Shear Yielding and Shear Rupture of the Extended Portion of the End Plate

For extended end-plate moment connections that are unstiffened, potential limit states that must be checked are shear yielding and shear rupture of the extended portion of the end plate. For the MRE 1/3 connection, the shear demand is taken as one-fourth of the tension flange force because the exterior bolts represent one-fourth of the bolts. The shear strength is calculated in accordance with AISC *Specification* Section J4.2.

Calculate the shear demand on the extended portion of the end plate.

Table B-9. Prying Action for the MRE 1/3 Unstiffened Example				
Parameter	**Bolt Position 1**	**Bolt Position 2**	**Bolt Position 3**	**Bolt Position 4**
w_i (in.)	4.00	4.00	*NO PRYING*	4.66
w'_i (in.)	2.88	2.88		3.54
a_i (in.)	1.25	1.44		1.44
b_i (in.)	1.75	1.75		2.31
F'_i (kips)	28.0	28.0		24.5
$Q_{max,i}$ (kips)	14.5	12.6	0.0	16.4
P_{qi} (kips)	56.2	58.1	51.0	54.3
α_i	1.0	1.0	1.0	1.0

LRFD	ASD
$V_{up} = \frac{1}{4}\left(\frac{M_u}{d - t_{bf}}\right)$	$V_{ap} = \frac{1}{4}\left(\frac{M_a}{d - t_{bf}}\right)$
$= \frac{1}{4}\left(\frac{8{,}000 \text{ kip-in.}}{36 \text{ in.} - ½ \text{ in.}}\right)$	$= \frac{1}{4}\left(\frac{5{,}330 \text{ kip-in.}}{36 \text{ in.} - ½ \text{ in.}}\right)$
$= 56.3$ kips	$= 37.5$ kips

Calculate the nominal shear yielding strength.

$$R_n = 0.60F_yA_{gv} \qquad \text{(}Spec\text{. Eq. J4-3)}$$
$$= 0.60F_yb_pt_p$$
$$= 0.60(50 \text{ ksi})(8 \text{ in.})(¾ \text{ in.})$$
$$= 180 \text{ kips}$$

Compare the design shear yielding strength to the shear demand. According to AISC *Specification* Section J4.2 for yielding of elements in shear, the resistance factor is $\phi = 1.00$, and the safety factor is $\Omega = 1.50$.

LRFD	ASD
$\phi R_n = 1.00(180 \text{ kips})$	$\frac{R_n}{\Omega} = \frac{180 \text{ kips}}{1.50}$
$= 180 \text{ kips} \geq V_{up} = 56.3 \text{ kips}$ **o.k.**	$= 120 \text{ kips} \geq V_{ap} = 37.5 \text{ kips}$ **o.k.**

Calculate the nominal shear rupture strength. The width of the extended portion of the end plate for use in the net section area is the width minus two effective hole diameters. The effective hole diameter is the hole diameter from AISC *Specification* Table J3.3 plus 1⁄16 in. The additional 1⁄16 in. accounts for damage around the hole caused by drilling, punching, or thermal cutting. For 1-in.-diameter bolts, the standard hole diameter, d_h, is 1⅛ in.

$$A_{nv} = \left[b_p - 2(d_h + 1⁄16 \text{ in.})\right]t_p$$
$$= \left[8 \text{ in.} - 2(1⅛ \text{ in.} + 1⁄16 \text{ in.})\right](¾ \text{ in.})$$
$$= 4.22 \text{ in.}^2$$

$$R_n = 0.60F_uA_{nv} \qquad \text{(Spec. Eq. J4-4)}$$
$$= 0.60(65 \text{ ksi})(4.22 \text{ in.}^2)$$
$$= 165 \text{ kips}$$

Compare the design shear rupture strength to the shear demand. Using AISC *Specification* Section J4.2 for rupture of elements in shear, the resistance factor is $\phi = 0.75$, and the safety factor is $\Omega = 2.00$.

LRFD	ASD
$\phi R_n = 0.75(165 \text{ kips})$ $= 124 \text{ kips} \geq V_{up} = 56.3 \text{ kips}$ **o.k.**	$\frac{R_n}{\Omega} = \frac{165 \text{ kips}}{2.00}$ $= 82.5 \text{ kips} \geq V_{ap} = 37.5 \text{ kips}$ **o.k.**

The extended portion of the ¾-in.-thick end plate has sufficient resistance to shear yielding and shear rupture.

Check Shear Transfer at Bolt Holes

See Example 5.3-1 or 5.3-2 for calculation procedures.

The specified ASTM A572/A572M Grade 50 ¾-in.-thick end plate and 1-in.-diameter Grade A325 pretensioned bolts are sufficient.

B. Check Beam to End-Plate Welds

The beam to end-plate welds shown in Figure B-18 are the same as shown in Figure 5-13. See Example 5.3-4 for weld strength checks.

The design shown in Figure B-18 is satisfactory for the required moment and shear force shown.

C. Column-Side Limit State Checks

See Example 5.3-1 or 5.3-2 for example column-side limit state check calculations.

Summary

The connection shown in Figure B-18 is adequate for the required moment and shear force.

EXAMPLE B.3-5—Multiple-Row Extended 1/3 Stiffened Thin End-Plate Example

Given:

The connection shown in Figure B-20 is a multiple-row extended 1/3 stiffened end-plate moment connection for a built-up beam. The beam and plates are ASTM A572/A572M Grade 50 material, and the bolts are Group 120 ASTM F3125/F3125M Grade A325 pretensioned. Weld electrodes are E70XX. The connection is to be evaluated as a thin end-plate design for the following required moments and shear forces:

	LRFD	ASD
Moment	M_u =10,300 kip-in.	M_a = 6,870 kip-in.
Shear force	V_u = 60.0 kips	V_a = 40.0 kips

Solution:

From AISC *Manual* Table 2-4, the material properties are as follows:

ASTM A572/A572M Grade 50
$F_y = 50$ ksi
$F_u = 65$ ksi

From AISC *Specification* Table J3.2, the material properties of the bolts are as follows:

Group 120 ASTM F3125/F3125M 1-in.-diameter Grade A325 pretensioned
F_{nt} = 90 ksi
F_{nv} = 54 ksi (Group 120 bolts with threads not excluded from the shear plane; thread condition N)

Beam
d = 36 in. t_{bw} = ⅜ in.
b_{bf} = 8 in. t_{bf} = ½ in.

End-plate geometric properties:
b_p = 8 in.
t_p = ¾ in.
g = 5 in.
p_{ext} = 3 in.
d_e = 1¼ in.
p_{fo} = 1¾ in.
p_{fi} = 1¾ in.
p_b = 3 in.
d_p = 42 in.

The distances from the centerline of the compression flange to the bolt lines, h_1, h_2, h_3, and h_4, are depicted in Table 5-14 and computed as:

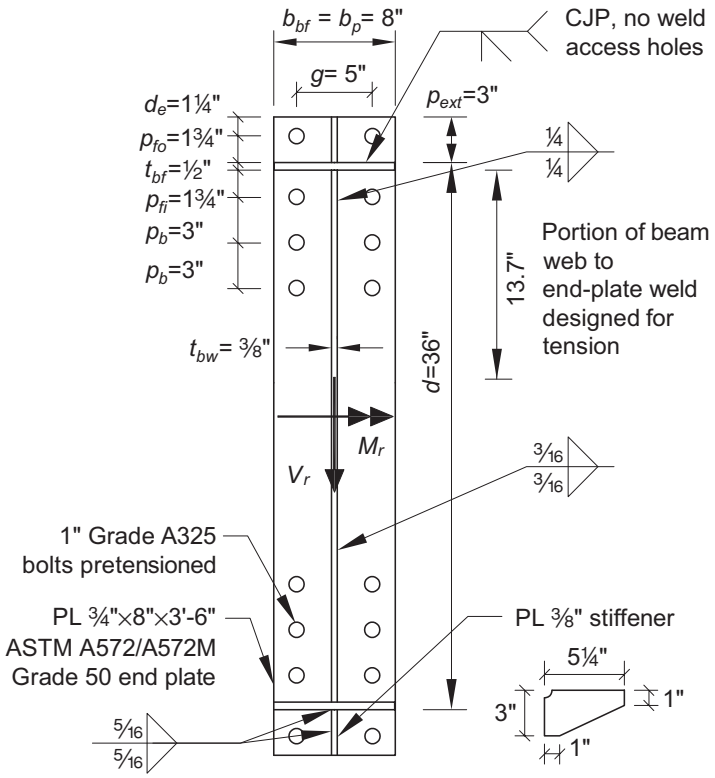

Fig. B-20. MRE 1/3 stiffened thin end-plate configuration for Example B.3-5.

$$h_1 = d - \frac{t_{bf}}{2} + p_{fo}$$
$$= 36 \text{ in.} - \frac{½ \text{ in.}}{2} + 1¾ \text{ in.}$$
$$= 37.5 \text{ in.}$$

$$h_2 = d - \frac{3t_{bf}}{2} - p_{fi}$$
$$= 36 \text{ in.} - \frac{3(½ \text{ in.})}{2} - 1¾ \text{ in.}$$
$$= 33.5 \text{ in.}$$

$$h_3 = d - \frac{3t_{bf}}{2} - p_{fi} - p_b$$
$$= 36 \text{ in.} - \frac{3(½ \text{ in.})}{2} - 1¾ \text{ in.} - 3 \text{ in.}$$
$$= 30.5 \text{ in.}$$

$$h_4 = d - \frac{3t_{bf}}{2} - p_{fi} - 2p_b$$
$$= 36 \text{ in.} - \frac{3(½ \text{ in.})}{2} - 1¾ \text{ in.} - 2(3 \text{ in.})$$
$$= 27.5 \text{ in.}$$

$$b_{p,eff} \le b_{bf} + \max(t_p, 1 \text{ in.}) \quad (4\text{-}3)$$
$$\le 8 \text{ in.} + \max(¾ \text{ in.}, 1 \text{ in.})$$
$$\le 9.00 \text{ in.}$$

$b_p = 8 \text{ in.} \le 9.00 \text{ in.}$ **o.k.**

$$b_{bf} \ge g \quad (4\text{-}1)$$

$8 \text{ in.} \ge 5 \text{ in.}$ **o.k.**

Beam flange to end-plate stiffener geometric properties:

$$h_{st} = p_{fi} + d_e$$
$$= 1¾ \text{ in.} + 1¼ \text{ in.}$$
$$= 3.00 \text{ in.}$$

$$L_{st} = \frac{h_{st}}{\tan 30°} \quad (4\text{-}4)$$
$$= \frac{3 \text{ in.}}{\tan 30°}$$
$$= 5.20 \text{ in.} \le 5¼ \text{ in.}$$ **o.k.**

$$t_s \ge t_{bw}\left(\frac{F_{yb}}{F_{ys}}\right) \quad (3\text{-}36)$$
$$\ge (⅜ \text{ in.})\left(\frac{50 \text{ ksi}}{50 \text{ ksi}}\right)$$
$$\ge ⅜ \text{ in.}$$

$t_s = ⅜ \text{ in.}$ **o.k.**

$$\frac{h_{st}}{t_s} = \frac{3 \text{ in.}}{⅜ \text{ in.}}$$
$$= 8.00$$

$$\frac{h_{st}}{t_s} \le 0.56\sqrt{\frac{E}{F_{ys}}} \tag{3-37}$$
$$\le 0.56\sqrt{\frac{29{,}000 \text{ ksi}}{50 \text{ ksi}}}$$
$$\le 13.5$$

$$\frac{h_{st}}{t_s} = 8.00 \quad \textbf{o.k.}$$

A. End-Plate and Bolt Design Verification

Determine if the specified end-plate thickness, ¾ in., and 1-in.-diameter Grade A325 bolts are sufficient using the thin end-plate/larger bolt diameter procedure.

Solve for the required end-plate thickness using Equations 5-5. First solve for the distance, s, and yield line parameter, Y_p, using Table 5-14.

$$s = \frac{\sqrt{b_p g}}{2}$$
$$= \frac{\sqrt{(8 \text{ in.})(5 \text{ in.})}}{2}$$
$$= 3.16 \text{ in.}$$

Because $s > d_e = 1¼$ in., Y_p in Table 5-14 is applicable, and because $s \ge p_{fo} = 1¾$ in. and $p_{fi} = 1¾$ in., the dimensions p_{fo} and p_{fi} are used in the equation for the yield line parameter.

$$Y_p = \frac{b_p}{2}\left[h_1\left(\frac{1}{p_{fo}} + \frac{1}{2d_e}\right) + h_2\left(\frac{1}{p_{fi}}\right) + h_4\left(\frac{1}{s}\right)\right] + \frac{2}{g}\left[h_1(p_{fo} + d_e) + h_2(p_{fi} + 1.5p_b) + h_4(s + 0.5p_b)\right] + \frac{g}{2}$$
$$= \left(\frac{8 \text{ in.}}{2}\right)\left[(37.5 \text{ in.})\left(\frac{1}{1¾ \text{ in.}} + \frac{1}{2(1¼ \text{ in.})}\right) + (33.5 \text{ in.})\left(\frac{1}{1¾ \text{ in.}}\right) + (27.5 \text{ in.})\left(\frac{1}{3.16 \text{ in.}}\right)\right]$$
$$+ \left(\frac{2}{5 \text{ in.}}\right)\left\{\begin{matrix}(37.5 \text{ in.})(1¾ \text{ in.} + 1¼ \text{ in.}) + (33.5 \text{ in.})\left[1¾ \text{ in.} + 1.5(3 \text{ in.})\right] \\ + (27.5 \text{ in.})\left[3.16 \text{ in.} + 0.5(3 \text{ in.})\right]\end{matrix}\right\} + \frac{5 \text{ in.}}{2}$$
$$= 440 \text{ in.}$$

Determine the required end-plate thickness using Equations 5-5. For extended end-plate configurations, $\gamma_r = 1.0$.

LRFD	ASD
$t_{p,reqd} = \sqrt{\frac{M_u}{\gamma_r \phi_b F_y Y_p}}$	$t_{p,reqd} = \sqrt{\frac{\Omega_b M_a}{\gamma_r F_y Y_p}}$
$= \sqrt{\frac{10{,}300 \text{ kip-in.}}{1.0(0.90)(50 \text{ ksi})(440 \text{ in.})}}$	$= \sqrt{\frac{1.67(6{,}870 \text{ kip-in.})}{1.0(50 \text{ ksi})(440 \text{ in.})}}$
$= 0.721 \text{ in.} \le ¾ \text{ in.}$ **o.k.**	$= 0.722 \text{ in.} \le ¾ \text{ in.}$ **o.k.**

Therefore, a ¾-in.-thick end plate is sufficient.

Determine if the specified 1-in.-diameter Grade A325 bolts are sufficient. First calculate geometry of the effective tee stub; then calculate the related forces, F_i, Q_{max}, and P_{qi}; finally, calculate the required bolt diameter.

The bolts are specified as pretensioned. The minimum bolt pretension for a 1 in. Grade A325 bolt is $T_b = 51$ kips. The nominal unthreaded body area of a 1 in. bolt is $A_b = 0.785$ in.^{2}, and the nominal tensile stress for a Grade A325 bolt is $F_{nt} = 90$ ksi. The resulting nominal tensile strength of a 1-in.-diameter Grade A325 bolt is:

$$P_t = F_{nt} A_b \qquad \text{(from } Spec. \text{ Eq. J3-1)}$$
$$= (90 \text{ ksi})(0.785 \text{ in.}^2)$$
$$= 70.7 \text{ kips}$$

There are four unique bolt locations as labeled in Figure B-21. The orientation of the effective tee stubs are defined using the rules given in Section 5.1.2 and are shown in Figure B-21.

Calculate the distance from bolt line to edge of effective tee stub:

$$a = 3.62\left(\frac{t_p}{d_b}\right)^3 - 0.085 \text{ in.} \qquad (3\text{-}24)$$
$$= 3.62\left(\frac{¾ \text{ in.}}{1 \text{ in.}}\right)^3 - 0.085 \text{ in.}$$
$$= 1.44 \text{ in.}$$

Bolt Position 1—Outside Bolt

For bolt position 1 (see Figure B-21), calculate the geometry of the effective tee stub, including the width of the effective tee stub, w_1, the net effective width, w_1', and distance from effective tee stem to the bolt, b_1.

$$w_1 = \frac{b_p}{2}$$
$$= \frac{8 \text{ in.}}{2}$$
$$= 4.00 \text{ in.}$$

$$w_1' = w_1 - (d_b + ⅛ \text{ in.}) \qquad (5\text{-}7)$$
$$= 4.00 \text{ in.} - (1 \text{ in.} + ⅛ \text{ in.})$$
$$= 2.88 \text{ in.}$$

$$a_1 = \min(a, p_{ext} - p_{fo})$$
$$= \min(1.44 \text{ in.},\ 3 \text{ in.} - 1¾ \text{ in.})$$
$$= 1.25 \text{ in.}$$

$$b_1 = p_{fo}$$
$$= 1¾ \text{ in.}$$

Find forces related to prying, including the force, F_1', the prying force, $Q_{max,1}$, and the bolt tension contributing to flexural strength, P_{q1}.

$$F_1' = \frac{1}{b_1}\left[\frac{t_p^2 F_y}{4}(0.85w_1 + 0.8w_1') + \frac{\pi d_b^3 F_{nt}}{32}\right] \quad (3\text{-}26)$$

$$= \left(\frac{1}{1¾\text{ in.}}\right)\left\{\left[\frac{(¾\text{ in.})^2(50\text{ ksi})}{4}\right]\left[0.85(4.00\text{ in.}) + 0.8(2.88\text{ in.})\right] + \frac{\pi(1\text{ in.})^3(90\text{ ksi})}{32}\right\}$$

$$= 28.0\text{ kips}$$

$$Q_{max,1} = \frac{w_1' t_p^2}{4a_1}\sqrt{F_y^2 - 3\left(\frac{F_1'}{w_1' t_p}\right)^2} \quad (3\text{-}23)$$

$$= \frac{(2.88\text{ in.})(¾\text{ in.})^2}{4(1.25\text{ in.})}\sqrt{(50\text{ ksi})^2 - 3\left[\frac{28.0\text{ kips}}{(2.88\text{ in.})(¾\text{ in.})}\right]^2}$$

$$= 14.5\text{ kips}$$

$$P_{q1} = \max(P_t - Q_{max,1},\ T_b) \quad (3\text{-}27)$$

$$= \max(70.7\text{ kips} - 14.5\text{ kips},\ 51.0\text{ kips})$$

$$= 56.2\text{ kips}$$

Prying forces for bolt positions 2 and 4 are calculated in a similar way using the effective tee-stub geometry shown in Figure B-21. Table B-10 gives the geometric parameters, related prying force, the usable strength for each bolt position, and reduction in bolt contribution factor, α_i. As described in Section 5.1.2, experiments have shown that bolts in the second interior row of configurations with three or more interior rows do not experience prying forces. However, they may not reach their full tensile strength. The bolt strength is taken equal to the bolt pretension for bolt position 3.

Calculate the flexural strength for bolt rupture with prying action, M_q, using Equation 3-28. Then the design flexural strength is compared to the required flexural strength.

$$M_q = \sum_i \alpha_i P_{qi} n_i h_i \quad (3\text{-}28)$$

$$= 1.0(56.2\text{ kips})(2\text{ bolts})(37.5\text{ in.}) + 1.0(58.1\text{ kips})(2\text{ bolts})(33.5\text{ in.})$$

$$+ 1.0(51.0\text{ kips})(2\text{ bolts})(30.5\text{ in.}) + 1.0(54.3\text{ kips})(2\text{ bolts})(27.5\text{ in.})$$

$$= 14{,}200\text{ kip-in.}$$

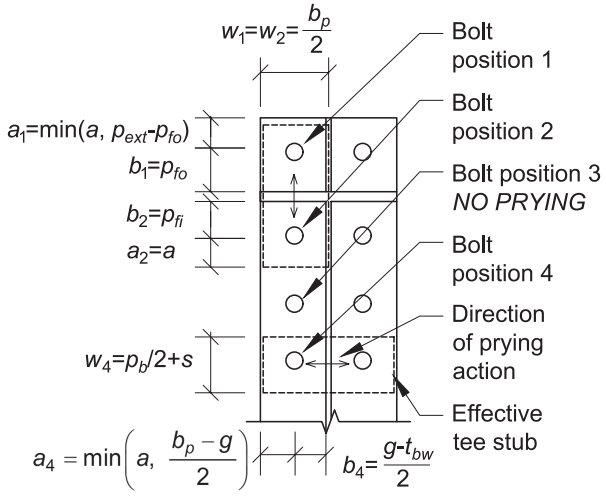

Fig. B-21. Effective tee-stub geometry for the MRE 1/3 stiffened configuration.

Table B-10. Prying Action for the MRE 1/3 Stiffened Example				
Parameter	**Bolt Position 1**	**Bolt Position 2**	**Bolt Position 3**	**Bolt Position 4**
w_i (in.)	4.00	4.00	*NO PRYING*	4.66
w'_i (in.)	2.88	2.88		3.54
a_i (in.)	1.25	1.44		1.44
b_i (in.)	1.75	1.75		2.31
F'_i (kips)	28.0	28.0		24.5
$Q_{max,i}$ (kips)	14.5	12.6	0.0	16.4
P_{qi} (kips)	56.2	58.1	51.0	54.3
α_i	1.0	1.0	1.0	1.0

LRFD	ASD
$\phi M_q = 0.75(14{,}200 \text{ kip-in.})$ $= 10{,}700 \text{ kip-in.} \quad \geq \quad M_u = 10{,}300 \text{ kip-in.}$ **o.k.**	$\frac{M_q}{\Omega} = \frac{14{,}200 \text{ kip-in.}}{2.00}$ $= 7{,}100 \text{ kip-in.} \quad \geq \quad M_a = 6{,}870 \text{ kip-in.}$ **o.k.**

Therefore, 1-in.-diameter Grade A325 bolts are sufficient.

Check Shear Yielding and Shear Rupture of the Extended Portion of the End Plate

For extended end-plate moment connections that are stiffened, shear yielding and shear rupture of the extended portion of the end plate are not limit states.

Check Shear Transfer at Bolt Holes

See Example 5.3-1 or 5.3-2 for calculation procedures.

B. Check Beam to End-Plate Welds

The beam to end-plate welds shown in Figure B-20 are the same as shown in Figure 5-14. See Example 5.3-5 for weld strength checks.

The design shown in Figure B-20 is satisfactory for the required moment and shear force shown.

C. Column-Side Limit State Checks

See Example 5.3-1 or 5.3-2 for example column-side limit state check calculations.

Summary

The connection shown in Figure B-20 is adequate for the required moment and shear force.

EXAMPLE B.3-6—Eight-Bolt Extended Four-Wide Unstiffened Thin End-Plate Example

Given:

The connection shown in Figure B-22 is an eight-bolt extended four-wide unstiffened end-plate moment connection for a built-up beam. The beam and end plate are ASTM A572/A572M Grade 50 material, and the bolts are Group 120 ASTM F3125/F3125M Grade A325 pretensioned. Weld electrodes are E70XX. The connection is to be evaluated as a thin end-plate design for the following required moments and shear forces:

	LRFD	ASD
Moment	M_u = 8,500 kip-in.	M_a = 5,670 kip-in.
Shear force	V_u = 60.0 kips	V_a = 40.0 kips

Solution:

From AISC *Manual* Table 2-4, the material properties are as follows:

ASTM A572/A572M Grade 50
F_y = 50 ksi
F_u = 65 ksi

From AISC *Specification* Table J3.2, the material properties of the bolts are as follows:

Group 120 ASTM F3125/F3125M 1⅛-in.-diameter Grade A325 bolts pretensioned
F_{nt} = 90 ksi
F_{nv} = 54 ksi (Group 120 bolts with threads not excluded from the shear plane; thread condition N)

Beam
d = 24 in. t_{bw} = ⅜ in.
b_{bf} = 14 in. t_{bf} = ¾ in.

End-plate geometric properties:
b_p = 14 in.
t_p = ⅞ in.
g = 4 in.
g_o = 3½ in.
p_{ext} = 4 in.
d_e = 2 in.
p_{fo} = 2 in.
p_{fi} = 2 in.
d_p = 32 in.

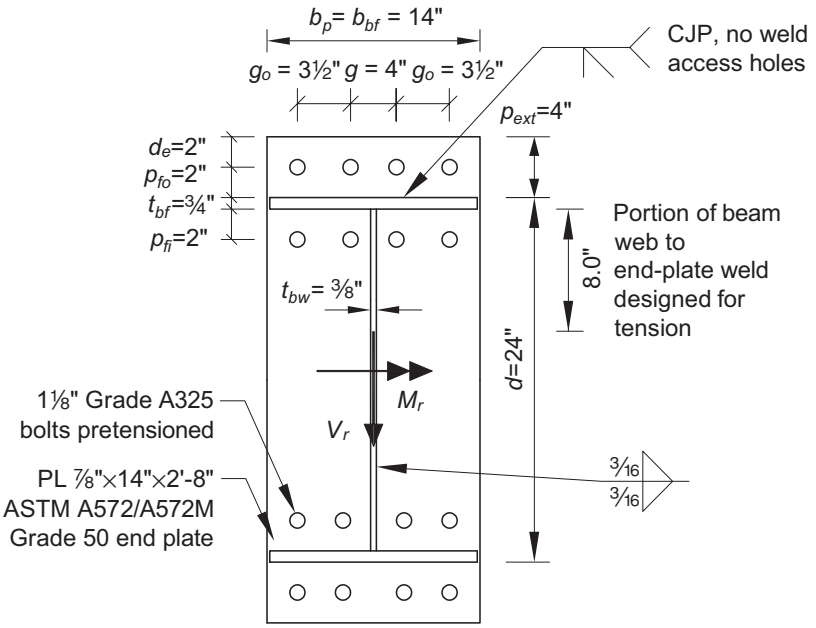

Fig. B-22. Eight-bolt extended four-wide unstiffened thin end-plate configuration for Example B.3-6.

The distances from the centerline of the compression flange to the bolt lines, h_1 and h_2, are depicted in Table 5-15 and computed as:

$$h_1 = d - \frac{t_{bf}}{2} + p_{fo}$$
$$= 24 \text{ in.} - \frac{¾ \text{ in.}}{2} + 2 \text{ in.}$$
$$= 25.6 \text{ in.}$$

$$h_2 = d - \frac{3t_{bf}}{2} - p_{fi}$$
$$= 24 \text{ in.} - \frac{3(¾ \text{ in.})}{2} - 2 \text{ in.}$$
$$= 20.9 \text{ in.}$$

$$b_{p,eff} \le b_{bf} + \max(t_p, 1 \text{ in.}) \quad (4\text{-}3)$$
$$\le 14 \text{ in.} + \max(⅞ \text{ in.}, 1 \text{ in.})$$
$$\le 15.0 \text{ in.}$$

$b_p = 14$ in. $\le$ 15.0 in. **o.k.**

$$b_{bf} \ge g + 2g_o \quad (4\text{-}2)$$
$$14 \text{ in.} \ge 4 \text{ in.} + 2(3½ \text{ in.})$$
$$14 \text{ in.} \ge 11.0 \text{ in.} \quad \textbf{o.k.}$$

A. End-Plate and Bolt Design Verification

Determine if the specified end-plate thickness, ⅞ in., and 1⅛-in.-diameter Grade A325 bolts are sufficient using the thin end-plate/larger bolt diameter procedure.

Solve for the required end-plate thickness using Equations 5-5. First solve for the distance, s, and yield line parameter, Y_p, using Table 5-15.

$$s = \frac{\sqrt{b_p g}}{2}$$
$$= \frac{\sqrt{(14 \text{ in.})(4 \text{ in.})}}{2}$$
$$= 3.74 \text{ in.}$$

Because $s \ge p_{fi} = 2$ in., the dimension p_{fi} is used in the equation for the yield line parameter.

$$Y_p = \frac{b_p}{2}\left[h_1\left(\frac{1}{p_{fo}}\right) + h_2\left(\frac{1}{p_{fi}} + \frac{1}{s}\right) - \frac{1}{2}\right] + \frac{2}{g}\left[h_2(p_{fi} + s)\right]$$
$$= \left(\frac{14 \text{ in.}}{2}\right)\left[(25.6 \text{ in.})\left(\frac{1}{2 \text{ in.}}\right) + (20.9 \text{ in.})\left(\frac{1}{2 \text{ in.}} + \frac{1}{3.74 \text{ in.}}\right) - \frac{1}{2}\right]$$
$$+ \left(\frac{2}{4 \text{ in.}}\right)\left[(20.9 \text{ in.})(2 \text{ in.} + 3.74 \text{ in.})\right]$$
$$= 258 \text{ in.}$$

Determine the required end-plate thickness using Equations 5-5. For extended end-plate configurations, $\gamma_r = 1.0$.

LRFD	ASD
$t_{p,reqd} = \sqrt{\dfrac{M_u}{\gamma_r \phi_b F_y Y_p}}$ $= \sqrt{\dfrac{8{,}500 \text{ kip-in.}}{1.0(0.90)(50 \text{ ksi})(258 \text{ in.})}}$ $= 0.856 \text{ in.} \le \frac{7}{8} \text{ in.}$ **o.k.**	$t_{p,reqd} = \sqrt{\dfrac{\Omega_b M_a}{\gamma_r F_y Y_p}}$ $= \sqrt{\dfrac{1.67(5{,}670 \text{ kip-in.})}{1.0(50 \text{ ksi})(258 \text{ in.})}}$ $= 0.857 \text{ in.} \le \frac{7}{8} \text{ in.}$ **o.k.**

Therefore, a ⅞-in.-thick end plate is sufficient.

Determine if the specified 1⅛-in.-diameter Grade A325 bolts are sufficient. First, calculate the geometry of the effective tee stub; then calculate the related forces, F_i, Q_{max}, and P_{qi}; finally, calculate the required bolt diameter

The bolts are specified as pretensioned. The minimum bolt pretension for a 1⅛ in. Grade A325 bolt is $T_b = 64$ kips. The nominal unthreaded body area of a 1⅛ in. bolt is $A_b = 0.994 \text{ in.}^2$, and the nominal tensile stress for a Grade A325 bolt is $F_{nt} = 90$ ksi. The resulting nominal tensile strength of a 1⅛-in.-diameter Grade A325 bolt is:

$$P_t = F_{nt} A_b \qquad \text{(from } \textit{Spec.} \text{ Eq. J3-1)}$$
$$= (90 \text{ ksi})(0.994 \text{ in.}^2)$$
$$= 89.5 \text{ kips}$$

There are four unique bolt locations as labeled in Figure B-23. The orientation of the effective tee stubs are defined using the rules given in Section 5.1.2 and are shown in Figure B-23.

Calculate the bolt distance from bolt to edge of effective tee stub:

$$a = 3.62\left(\frac{t_p}{d_b}\right)^3 - 0.085 \text{ in.} \qquad (3\text{-}24)$$
$$= 3.62\left(\frac{\frac{7}{8} \text{ in.}}{1\frac{1}{8} \text{ in.}}\right)^3 - 0.085 \text{ in.}$$
$$= 1.62 \text{ in.}$$

Bolt Position 1—Outside Corner Bolt

For bolt position 1 (see Figure B-23), calculate the geometry of the effective tee stub, including the width of the effective tee stub, w_1, the net effective width, w_1', and distance from effective tee stem to the bolt, b_1.

$$w_1 = \frac{b_p - g - g_o}{2}$$
$$= \frac{14 \text{ in.} - 4 \text{ in.} - 3\frac{1}{2} \text{ in.}}{2}$$
$$= 3.25 \text{ in.}$$

$$w_1' = w_1 - (d_b + \tfrac{1}{8} \text{ in.}) \qquad (5\text{-}7)$$
$$= 3.25 \text{ in.} - (1\tfrac{1}{8} \text{ in.} + \tfrac{1}{8} \text{ in.})$$
$$= 2.00 \text{ in.}$$

$$a_1 = \min(a_{calc}, p_{ext} - p_{fo})$$
$$= \min(1.62 \text{ in.}, 4 \text{ in.} - 2 \text{ in.})$$
$$= 1.62 \text{ in.}$$

$$b_1 = p_{fo}$$
$$= 2 \text{ in.}$$

Find forces related to prying, including the force, F_1', the prying force, $Q_{max,1}$, and the bolt tension contributing to flexural strength, P_{q1}.

$$F_1' = \frac{1}{b_1}\left[\frac{t_p^2 F_y}{4}(0.85w_1 + 0.8w_1') + \frac{\pi d_b^3 F_{nt}}{32}\right] \quad (3\text{-}26)$$
$$= \left(\frac{1}{2 \text{ in.}}\right)\left\{\left[\frac{(⅞ \text{ in.})^2 (50 \text{ ksi})}{4}\right]\left[0.85(3.25 \text{ in.}) + 0.8(2.00 \text{ in.})\right] + \frac{\pi (1⅛ \text{ in.})^3 (90 \text{ ksi})}{32}\right\}$$
$$= 27.2 \text{ kips}$$

$$Q_{max,1} = \frac{w_1' t_p^2}{4a_1}\sqrt{F_y^2 - 3\left(\frac{F_1'}{w_1' t_p}\right)^2} \quad (3\text{-}23)$$
$$= \frac{(2.00 \text{ in.})(⅞ \text{ in.})^2}{4(1.62 \text{ in.})}\sqrt{(50 \text{ ksi})^2 - 3\left[\frac{27.2 \text{ kips}}{(2.00 \text{ in.})(⅞ \text{ in.})}\right]^2}$$
$$= 9.96 \text{ kips}$$

$$P_{q1} = \max(P_t - Q_{max,1}, T_b) \quad (3\text{-}27)$$
$$= \max(89.5 \text{ kips} - 9.96 \text{ kips},\ 64.0 \text{ kips})$$
$$= 79.5 \text{ kips}$$

Prying forces for bolt positions 2, 3, and 4 are calculated in a similar way using the effective tee-stub geometry shown in Figure B-23. Table B-11 gives the geometric parameters, related prying force, the usable strength for each bolt position, and reduction in bolt contribution factor, α_i.

Calculate the flexural strength for bolt rupture with prying action, M_q, using Equation 3-28. Then the design flexural strength is compared to the required flexural strength.

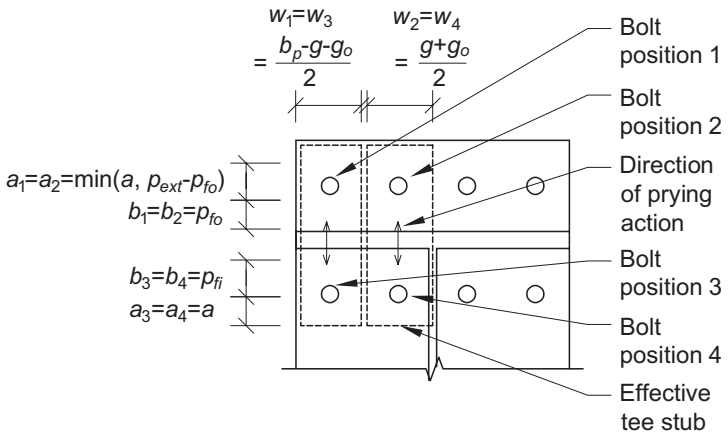

Fig. B-23. Effective tee-stub geometry for the eight-bolt extended four-wide unstiffened configuration.

$$M_q = \sum_i \alpha_i P_{qi}\, n_i\, h_i \tag{3-28}$$
$$= 0.5(79.5 \text{ kips})(2 \text{ bolts})(25.6 \text{ in.}) + 1.0(76.6 \text{ kips})(2 \text{ bolts})(25.6 \text{ in.})$$
$$+ 0.75(79.5 \text{ kips})(2 \text{ bolts})(20.9 \text{ in.}) + 1.0(76.6 \text{ kips})(2 \text{ bolts})(20.9 \text{ in.})$$
$$= 11{,}700 \text{ kip-in.}$$

LRFD	ASD
$\phi M_q = 0.75(11{,}700 \text{ kip-in.})$ $= 8{,}780 \text{ kip-in.} \geq M_u = 8{,}500 \text{ kip-in.}$ **o.k.**	$\frac{M_q}{\Omega} = \frac{11{,}700 \text{ kip-in.}}{2.00}$ $= 5{,}850 \text{ kip-in.} \geq M_a = 5{,}670 \text{ kip-in.}$ **o.k.**

Therefore, 1⅛-in.-diameter Grade A325 bolts are sufficient.

Check Shear Yielding and Shear Rupture of the Extended Portion of the End Plate

For extended end-plate moment connections that are unstiffened, potential limit states that must be checked are shear yielding and shear rupture of the extended portion of the end plate. For the eight-bolt extended four-wide unstiffened connection, the shear demand is taken as one-half of the tension flange force because the exterior bolts represent one-half the bolts. The shear strength is calculated in accordance with AISC *Specification* Section J4.2.

Calculate the shear demand on the extended portion of the end plate.

LRFD	ASD
$V_{up} = \frac{1}{2}\left(\frac{M_u}{d - t_{bf}}\right)$ $= \frac{1}{2}\left(\frac{8{,}500 \text{ kip-in.}}{24 \text{ in.} - ¾ \text{ in.}}\right)$ $= 183 \text{ kips}$	$V_{ap} = \frac{1}{2}\left(\frac{M_a}{d - t_{bf}}\right)$ $= \frac{1}{2}\left(\frac{5{,}670 \text{ kip-in.}}{24 \text{ in.} - ¾ \text{ in.}}\right)$ $= 122 \text{ kips}$

Calculate the nominal shear yielding strength.

$$R_n = 0.60 F_y A_{gv} \tag{*Spec.* Eq. J4-3}$$
$$= 0.60 F_y b_p t_p$$
$$= 0.60(50 \text{ ksi})(14 \text{ in.})(⅞ \text{ in.})$$
$$= 368 \text{ kips}$$

Compare the design shear yielding strength to the shear demand. According to AISC *Specification* Section J4.2 for yielding of elements in shear, the resistance factor is $\phi = 1.00$, and the safety factor is $\Omega = 1.50$.

LRFD	ASD
$\phi R_n = 1.00(368 \text{ kips})$ $= 368 \text{ kips} \geq V_{up} = 183 \text{ kips}$ **o.k.**	$\frac{R_n}{\Omega} = \frac{368 \text{ kips}}{1.50}$ $= 245 \text{ kips} \geq V_{ap} = 122 \text{ kips}$ **o.k.**

Calculate the nominal shear rupture strength. The width of the extended portion of the end plate for use in the net section area is the width minus four effective hole diameters. The effective hole diameter is the hole diameter from AISC *Specification* Table J3.3 plus 1/16 in. The additional 1/16 in. accounts for damage around the hole caused by drilling, punching, or thermal cutting. For 1⅛-in.-diameter bolts, the standard hole diameter, d_h, is 1¼ in.

Table B-11. Prying Action for the Eight-Bolt Extended Four-Wide Unstiffened Example				
Parameter	**Bolt Position 1**	**Bolt Position 2**	**Bolt Position 3**	**Bolt Position 4**
w_i (in.)	3.25	3.75	3.25	3.75
w_i' (in.)	2.00	2.50	2.00	2.50
a_i (in.)	1.62	1.62	1.62	1.62
b_i (in.)	2.00	2.00	2.00	2.00
F_i' (kips)	27.2	31.1	27.2	31.1
$Q_{max,i}$ (kips)	9.96	12.9	9.96	12.9
P_{qi} (kips)	79.5	76.6	79.5	76.6
α_i	0.5	1.0	0.75	1.0

$$A_{nv} = \left[b_p - 4\left(d_h + \tfrac{1}{16}\right)\right]t_p$$
$$= \left[14\text{ in.} - 4\left(1\tfrac{1}{4}\text{ in.} + \tfrac{1}{16}\text{ in.}\right)\right]\left(\tfrac{7}{8}\text{ in.}\right)$$
$$= 7.66\text{ in.}^2$$

$$R_n = 0.60F_uA_{nv} \qquad \text{(}Spec\text{. Eq. J4-4)}$$
$$= 0.60(65\text{ ksi})(7.66\text{ in.}^2)$$
$$= 299\text{ kips}$$

Compare the design shear rupture strength to the shear demand. Using AISC *Specification* Section J4.2 for rupture of elements in shear, the resistance factor is $\phi = 0.75$, and the safety factor is $\Omega = 2.00$.

LRFD	ASD
$\phi R_n = 0.75(299\text{ kips})$ $= 224\text{ kips} \quad \geq \quad V_{up} = 183\text{ kips}$ **o.k.**	$\frac{R_n}{\Omega} = \frac{299\text{ kips}}{2.00}$ $= 150\text{ kips} \quad \geq \quad V_{ap} = 122\text{ kips}$ **o.k.**

The extended portion of the ⅞-in.-thick end plate has sufficient resistance to shear yielding and shear rupture.

Check Shear Transfer at Bolt Holes

See Example 5.3-1 or 5.3-2 for calculation procedures.

B. Check Beam to End-Plate Welds

The beam to end-plate welds shown in Figure B-22 are the same as shown in Figure 5-15. See Example 5.3-6 for weld strength checks.

The connection shown in Figure B-22 is adequate for the required moment and shear force shown.

C. Check Column-Side Limit States

See Example 5.3-1 or 5.3-2 for example column-side limit state check calculations.

Summary

The connection shown in Figure B-22 is adequate for the required moment and shear force.

EXAMPLE B.3-7—Eight-Bolt Extended Stiffened Thin End-Plate Example

Given:

The connection shown in Figure B-24 is an eight-bolt extended stiffened (8ES) end-plate moment connection for a built-up beam. The beam and all plates are ASTM A572/A572M Grade 50 material, and the bolts are Group 120 ASTM F3125/F3125M Grade A325 pretensioned. Weld electrodes are E70XX. The connection is to be evaluated as a thin end-plate design for the following required moments and shear forces.

	LRFD	ASD
Moment	M_u = 9,000 kip-in.	M_a = 6,000 kip-in.
Shear force	V_u = 60.0 kips	V_a = 40.0 kips

Solution:

From AISC *Manual* Table 2-4, the material properties are as follows:

ASTM A572/A572M Grade 50
F_y = 50 ksi
F_u = 65 ksi

From AISC *Specification* Table J3.2, the material properties of the bolts are as follows:

Group 120 ASTM F3125/F3125M 1-in.-diameter Grade A325 pretensioned
F_{nt} = 90 ksi
F_{nv} = 54 ksi (Group 120 bolts with threads not excluded from the shear plane; thread condition N)

Beam
d = 36 in. t_{bw} = ⅜ in.
b_{bf} = 8 in. t_{bf} = ½ in.

End-plate geometric properties:
b_p = 8 in.
t_p = ¾ in.
g = 5½ in.
p_{ext} = 6¾ in.
d_e = 1¾ in.
p_{fo} = 2 in.
p_{fi} = 2 in.
p_b = 3 in.
d_p = 49½ in.

The distances from the centerline of the compression flange to the bolt lines, h_1, h_2, h_3, and h_4, are depicted in Table 5-16 and computed as:

$$h_1 = d - \frac{t_{bf}}{2} + p_{fo} + p_b$$
$$= 36 \text{ in.} - \frac{½ \text{ in.}}{2} + 2 \text{ in.} + 3 \text{ in.}$$
$$= 40.8 \text{ in.}$$

$$h_2 = d - \frac{t_{bf}}{2} + p_{fo}$$
$$= 36 \text{ in.} - \frac{½ \text{ in.}}{2} + 2 \text{ in.}$$
$$= 37.8 \text{ in.}$$

$$h_3 = d - \frac{3t_{bf}}{2} - p_{fi}$$

$$= 36 \text{ in.} - \frac{3(½ \text{ in.})}{2} - 2 \text{ in.}$$

$$= 33.3 \text{ in.}$$

$$h_4 = d - \frac{3t_{bf}}{2} - p_{fi} - p_b$$

$$= 36 \text{ in.} - \frac{3(½ \text{ in.})}{2} - 2 \text{ in.} - 3 \text{ in.}$$

$$= 30.3 \text{ in.}$$

$$b_{p,eff} \le b_{bf} + \max(t_p, 1 \text{ in.}) \quad (4\text{-}3)$$

$$\le 8 \text{ in.} + \max(¾ \text{ in.}, 1 \text{ in.})$$

$$\le 9.00 \text{ in.}$$

$b_p = 8$ in. $\le$ 9.00 in. **o.k.**

$$b_{bf} \ge g \quad (4\text{-}1)$$

8 in. ≥ 5½ in. **o.k.**

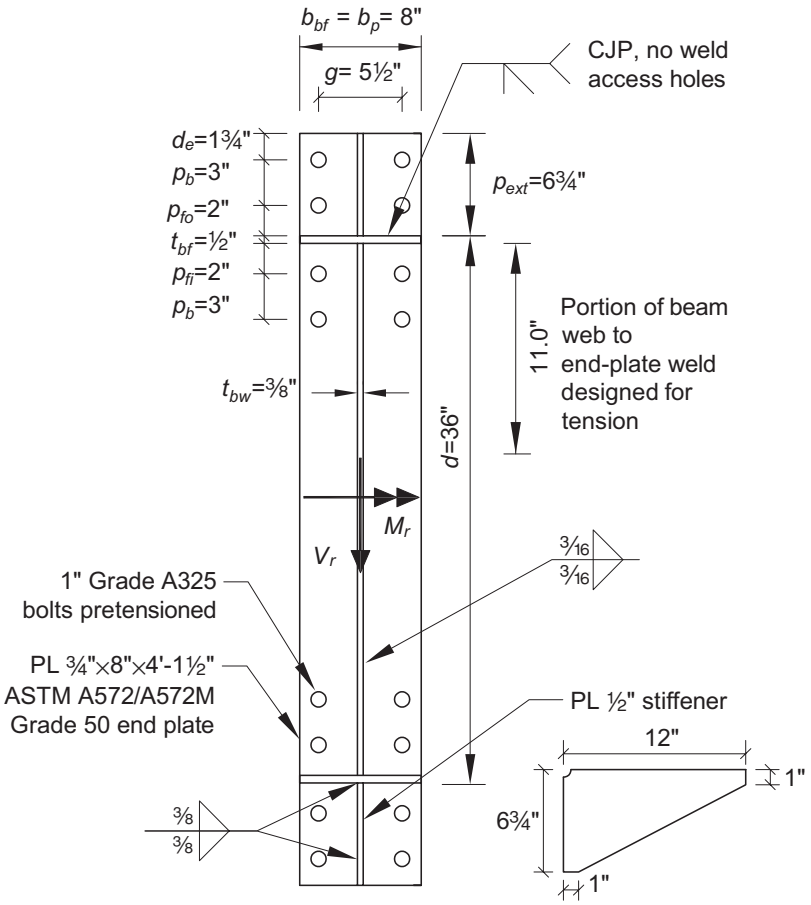

Fig. B-24. Eight-bolt extended stiffened thin end-plate configuration for Example B.3-7.

Beam flange to end-plate stiffener geometric properties:

$$h_{st} = p_{fo} + p_b + d_e$$
$$= 2 \text{ in.} + 3 \text{ in.} + 1¾ \text{ in.}$$
$$= 6¾ \text{ in.}$$

$$L_{st} = \frac{h_{st}}{\tan 30°} \tag{4-4}$$
$$= \frac{6¾ \text{ in.}}{\tan 30°}$$
$$= 11.7 \text{ in.} \quad \leq \quad 12 \text{ in.} \quad \textbf{o.k.}$$

$$t_s \geq t_{bw}\left(\frac{F_{yb}}{F_{ys}}\right) \tag{3-36}$$
$$\geq (⅜ \text{ in.})\left(\frac{50 \text{ ksi}}{50 \text{ ksi}}\right)$$
$$\geq ⅜ \text{ in.}$$
$$t_s = ½ \text{ in.} \quad \textbf{o.k.}$$

$$\frac{h_{st}}{t_s} = \frac{6¾ \text{ in.}}{½ \text{ in.}}$$
$$= 13.5$$

$$\frac{h_{st}}{t_s} \leq 0.56\sqrt{\frac{E}{F_{ys}}} \tag{3-37}$$
$$\leq 0.56\sqrt{\frac{29{,}000 \text{ ksi}}{50 \text{ ksi}}}$$
$$\leq 13.5$$
$$\frac{h_{st}}{t_s} = 13.5 \quad \textbf{o.k.}$$

A. End-Plate and Bolt Design Verification

Determine if the specified end-plate thickness, ¾ in., and 1-in.-diameter Grade A325 bolts are sufficient using the thin end-plate/larger bolt diameter procedure.

Solve for the required end-plate thickness using Equations 5-5. First solve for the distance, s, and yield line parameter, Y_p, using Table 5-16.

$$s = \frac{\sqrt{b_p g}}{2}$$
$$= \frac{\sqrt{(8 \text{ in.})(5½ \text{ in.})}}{2}$$
$$= 3.32 \text{ in.}$$

Because $s > d_e = 1¾$ in., Y_p in Table 5-16 is applicable, and because $s \geq p_{fo} = 2$ in. and $p_{fi} = 2$ in., the dimensions p_{fo} and p_{fi} are used in the equation for the yield line parameter.

$$Y_p = \frac{b_p}{2}\left[h_1\left(\frac{1}{2d_e}\right)+h_2\left(\frac{1}{p_{fo}}\right)+h_3\left(\frac{1}{p_{fi}}\right)+h_4\left(\frac{1}{s}\right)\right]$$
$$+\frac{2}{g}\left[h_1(d_e+0.75p_b)+h_2(p_{fo}+0.25p_b)+h_3(p_{fi}+0.75p_b)+h_4(s+0.25p_b)\right]+g$$
$$=\left(\frac{8\text{ in.}}{2}\right)\left\{(40.8\text{ in.})\left[\frac{1}{2(1¾\text{ in.})}\right]+(37.8\text{ in.})\left(\frac{1}{2\text{ in.}}\right)+(33.3\text{ in.})\left(\frac{1}{2\text{ in.}}\right)+(30.3\text{ in.})\left(\frac{1}{3.32\text{ in.}}\right)\right\}$$
$$+\left(\frac{2}{5½\text{ in.}}\right)\left\{\begin{matrix}(40.8\text{ in.})\left[1¾\text{ in.}+0.75(3\text{ in.})\right]+(37.8\text{ in.})\left[2\text{ in.}+0.25(3\text{ in.})\right]\\+(33.3\text{ in.})\left[2\text{ in.}+0.75(3\text{ in.})\right]+(30.3\text{ in.})\left[3.32\text{ in.}+0.25(3\text{ in.})\right]\end{matrix}\right\}+5½\text{ in.}$$
$$=424\text{ in.}$$

Determine the required end-plate thickness using Equations 5-5. For extended end-plate configurations, $\gamma_r = 1.0$.

LRFD	ASD
$t_{p,reqd} = \sqrt{\frac{M_u}{\gamma_r \phi_b F_y Y_p}}$ $= \sqrt{\frac{9{,}000\text{ kip-in.}}{1.0(0.90)(50\text{ ksi})(424\text{ in.})}}$ $= 0.687\text{ in.} \le ¾\text{ in.}$ **o.k.**	$t_{p,reqd} = \sqrt{\frac{\Omega_b M_a}{\gamma_r F_y Y_p}}$ $= \sqrt{\frac{1.67(6{,}000\text{ kip-in.})}{1.0(50\text{ ksi})(424\text{ in.})}}$ $= 0.687\text{ in.} \le ¾\text{ in.}$ **o.k.**

Therefore, a ¾-in.-thick end plate is sufficient.

Determine if the specified 1-in.-diameter Grade A325 bolts are sufficient. First, calculate geometry of the effective tee stub; then calculate the related forces, F_i, Q_{max}, and P_{qi}; finally, calculate the required bolt diameter.

The bolts are specified as pretensioned. The minimum bolt pretension for a 1 in. Grade A325 bolt is $T_b = 51$ kips. The nominal unthreaded body area of a 1 in. bolt is $A_b = 0.785\text{ in.}^2$, and the nominal tensile stress for a Grade A325 bolt is $F_{nt} = 90$ ksi. The resulting nominal tensile strength of a 1-in.-diameter Grade A325 bolt is:

$$P_t = F_{nt}A_b \qquad \text{(from } \textit{Spec.}\text{ Eq. J3-1)}$$
$$=(90\text{ ksi})(0.785\text{ in.}^2)$$
$$=70.7\text{ kips}$$

There are four unique bolt locations as labeled in Figure B-25. The orientation of the effective tee stubs is defined using the rules given in Section 5.1.2 and are shown in Figure B-25.

Calculate the bolt distance from bolt to edge of effective tee stub.

$$a = 3.62\left(\frac{t_p}{d_b}\right)^3 - 0.085\text{ in.} \qquad (3\text{-}24)$$
$$=3.62\left(\frac{¾\text{ in.}}{1\text{ in.}}\right)^3 - 0.085\text{ in.}$$
$$=1.44\text{ in.}$$

Bolt Position 1—Most Exterior Bolt

For bolt position 1 (see Figure B-25), calculate the geometry of the effective tee stub, including the width of the effective tee stub, w_1, the net effective width, w_1', and distance from effective tee stem to the bolt, b_1.

$$w_1 = d_e + \frac{p_b}{2}$$
$$= 1¾ \text{ in.} + \frac{3 \text{ in.}}{2}$$
$$= 3.25 \text{ in.}$$

$$w_1' = w_1 - (d_b + ⅛ \text{ in.}) \quad (5\text{-}7)$$
$$= 3.25 \text{ in.} - (1 \text{ in.} + ⅛ \text{ in.})$$
$$= 2.13 \text{ in.}$$

$$a_1 = \min\left(a, \frac{b_p - g}{2}\right)$$
$$= \min\left(1.44 \text{ in.}, \frac{8 \text{ in.} - 5½ \text{ in.}}{2}\right)$$
$$= 1.25 \text{ in.}$$

$$b_1 = \frac{g - t_{bw}}{2}$$
$$= \frac{5½ \text{ in.} - ⅜ \text{ in.}}{2}$$
$$= 2.56 \text{ in.}$$

Find forces related to prying, including the force, F_1', the prying force, $Q_{max,1}$, and the bolt tension contributing to flexural strength, P_{q1}.

$$F_1' = \frac{1}{b_1}\left[\frac{t_p^2 F_y}{4}(0.85w_1 + 0.80w_1') + \frac{\pi d_b^3 F_{nt}}{32}\right] \quad (3\text{-}26)$$
$$= \left(\frac{1}{2.56 \text{ in.}}\right)\left\{\left[\frac{(¾ \text{ in.})^2 (50 \text{ ksi})}{4}\right]\left[0.85(3.25 \text{ in.}) + 0.80(2.13 \text{ in.})\right] + \frac{\pi (1 \text{ in.})^3 (90 \text{ ksi})}{32}\right\}$$
$$= 15.7 \text{ kips}$$

$$Q_{max,1} = \frac{w_1' t_p^2}{4a_1}\sqrt{F_y^2 - 3\left(\frac{F_1'}{w_1' t_p}\right)^2} \quad (3\text{-}23)$$
$$= \frac{(2.13 \text{ in.})(¾ \text{ in.})^2}{4(1.25 \text{ in.})}\sqrt{(50 \text{ ksi})^2 - 3\left[\frac{15.7 \text{ kips}}{(2.13 \text{ in.})(¾ \text{ in.})}\right]^2}$$
$$= 11.3 \text{ kips}$$

$$P_{q1} = \max(P_t - Q_{max,1},\ T_b) \quad (3\text{-}27)$$
$$= \max(70.7 \text{ kips} - 11.2 \text{ kips},\ 51.0 \text{ kips})$$
$$= 59.4 \text{ kips}$$

Prying forces for bolt positions 2, 3, and 4 are calculated in a similar way using the effective tee-stub geometry shown in Figure B-25. Table B-12 gives the geometric parameters, related prying force, the usable strength for each bolt position, and reduction in bolt contribution factor, α_i.

Calculate the flexural strength for bolt rupture with prying action, M_q, using Equation 3-28. Then the design flexural strength is compared to the required flexural strength.

$$M_q = \sum_i \alpha_i P_{qi}\, n_i\, h_i \tag{3-28}$$

$$= 1.0(59.4 \text{ kips})(2 \text{ bolts})(40.8 \text{ in.}) + 1.0(57.8 \text{ kips})(2 \text{ bolts})(37.8 \text{ in.})$$
$$+ 1.0(57.8 \text{ kips})(2 \text{ bolts})(33.3 \text{ in.}) + 1.0(51.0 \text{ kips})(2 \text{ bolts})(30.3 \text{ in.})$$
$$= 16{,}200 \text{ kip-in.}$$

LRFD	ASD
$\phi M_q = 0.75(16{,}200 \text{ kip-in.})$ $= 12{,}200 \text{ kip-in.} \quad \geq \quad M_u = 9{,}000 \text{ kip-in.}$ **o.k.**	$\frac{M_q}{\Omega} = \frac{16{,}200 \text{ kip-in.}}{2.00}$ $= 8{,}100 \text{ kip-in.} \quad \geq \quad M_a = 6{,}000 \text{ kip-in.}$ **o.k.**

Therefore 1-in.-diameter Grade A325 bolts are sufficient.

Check Shear Yielding/Shear Rupture of the Extended Portion of the End Plate

For extended end-plate moment connections that are stiffened, shear yielding and shear rupture of the extended portion of the end plate are not limit states.

Therefore, a ¾-in.-thick end plate is sufficient.

Check Shear Transfer at Bolt Holes

See Examples 5.3-1 or 5.3-2 for calculation procedures.

B. Check Beam to End-Plate Welds

The minimum weld size in the AISC *Specification* Table J2.4 is determined from material thickness of the thinner part joined. The fillet weld sizes shown in Figure B-24 satisfy the requirements in Table J2.4.

Check Beam Flange to End-Plate Weld

The weld from the beam flange to the end plate is shown in Figure B-24 as a CJP groove weld with the bevel facing away from the center of the beam and without weld access holes. A PJP groove weld is an alternate option.

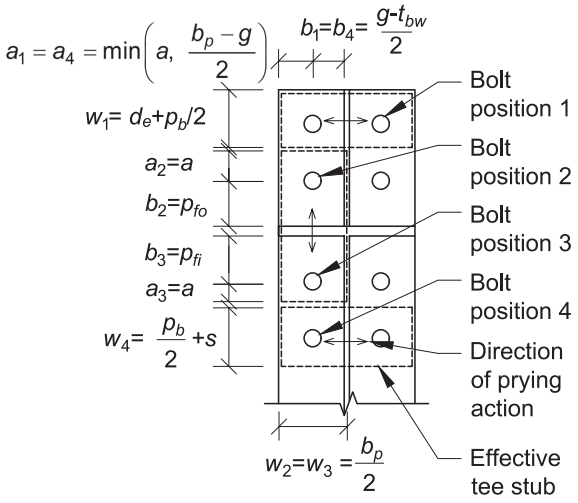

Fig. B-25. Effective tee-stub geometry for the eight-bolt extended stiffened configuration.

Table B-12. Prying Action for the Eight-Bolt Extended Stiffened Example				
Parameter	**Bolt Position 1**	**Bolt Position 2**	**Bolt Position 3**	**Bolt Position 4**
w_i (in.)	3.25	4.00	4.00	4.82
w_i' (in.)	2.13	2.88	2.88	3.70
a_i (in.)	1.25	1.44	1.44	1.25
b_i (in.)	2.56	2.00	2.00	2.56
F_i' (kips)	15.7	24.5	24.5	22.8
$Q_{max,i}$ (kips)	11.3	12.9	12.9	20.0
P_{qi} (kips)	59.4	57.8	57.8	51.0
α_i	1.0	1.0	1.0	1.0

Check Stiffener Welds

Check that the stiffener welds shown in Figure B-24 are sufficient to develop the yield strengths of the stiffener plate.

Calculate the required strength for the stiffener to beam flange weld, and determine if the double-sided ⅜ in. fillet weld shown is sufficient.

LRFD	ASD
$V_{uw} = 0.60F_y t_s$ $= 0.60(50 \text{ ksi})(½ \text{ in.})$ $= 15.0 \text{ kips/in.}$	$V_{aw} = 0.40F_y t_s$ $= 0.40(50 \text{ ksi})(½ \text{ in.})$ $= 10.0 \text{ kips/in.}$

$$V_{nw} = (2 \text{ welds})0.60F_{EXX}\frac{t_{weld}}{\sqrt{2}}(1.0 + 0.5\sin^{1.5}\theta) \quad \text{(from } \textit{Spec.} \text{ Eq. J2-4)}$$

$$= (2 \text{ welds})(0.60)(70 \text{ ksi})\left(\frac{⅜ \text{ in.}}{\sqrt{2}}\right)(1.0 + 0.5\sin^{1.5} 0°)$$

$$= 22.3 \text{ kips/in.}$$

LRFD	ASD
$\phi V_{nw} = 0.75(22.3 \text{ kips/in.})$ $= 16.7 \text{ kips/in.} \geq V_{uw} = 15.0 \text{ kips/in.}$ **o.k.**	$\frac{V_{nw}}{\Omega} = \frac{22.3 \text{ kips/in.}}{2.00}$ $= 11.2 \text{ kips/in.} \geq V_{aw} = 10.0 \text{ kips/in.}$ **o.k.**

The shear rupture strength of the stiffener is greater than its shear yield strength and does have to be checked. The shear rupture strength of the beam is sufficient by inspection.

Therefore, the double-sided ⅜ in. fillet welds are sufficient.

Calculate the required strength for the stiffener to end-plate weld and determine if the double-sided ⅜ in. fillet welds shown are sufficient.

LRFD	ASD
$T_{uw} = F_y t_s$ $= (50 \text{ ksi})(½ \text{ in.})$ $= 25.0 \text{ kips/in.}$	$T_{aw} = \frac{F_y}{1.50} t_s$ $= \left(\frac{50 \text{ ksi}}{1.50}\right)(½ \text{ in.})$ $= 16.7 \text{ kips/in.}$

$$T_{nw} = (2 \text{ welds}) 0.60 F_{EXX} \frac{t_{weld}}{\sqrt{2}} (1.0 + 0.5 \sin^{1.5} \theta) \qquad \text{(from } \textit{Spec}\text{. Eq. J2-4)}$$

$$= (2 \text{ welds})(0.60)(70 \text{ ksi}) \left(\frac{⅜ \text{ in.}}{\sqrt{2}}\right)(1.0 + 0.5 \sin^{1.5} 90°)$$

$$= 33.4 \text{ kips/in.}$$

LRFD	ASD
$\phi T_{nw} = 0.75(33.4 \text{ kips/in.})$ $= 25.1 \text{ kips/in.} \geq T_{uw} = 25.0 \text{ kips/in.}$ **o.k.**	$\frac{T_{nw}}{\Omega} = \frac{33.4 \text{ kips/in.}}{2.00}$ $= 16.7 \text{ kips/in.} \geq T_{aw} = 16.7 \text{ kips/in.}$ **o.k.**

Double-sided ⅜ in. fillet welds are sufficient.

Check Beam Web to End-Plate Weld

The beam web to end-plate welds shown in Figure B-24 are separately checked for (1) tension rupture in the region around the tension bolts (extending 6 in. to the inside of the tension bolts), and (2) the remainder of the web to end-plate weld is checked for shear. As explained in Section 3.7.5, the demand for the tension web area, T_{uw} (LRFD) or T_{aw} (ASD), for this connection is the number of tension bolts adjacent to the web, n_{trib}, divided by the total number of tension bolts, n, multiplied by the calculated beam flange force, $T_{u,calc}$ (LRFD) or $T_{a,calc}$ (ASD).

LRFD	ASD
$T_{u,calc} = \frac{M_u}{d - t_{bf}}$ $= \frac{9{,}000 \text{ kip-in.}}{36 \text{ in.} - ½ \text{ in.}}$ $= 254 \text{ kips}$ $T_{uw} = (n_{trib}/n) T_{u,calc}$ $= (4/8)(254 \text{ kips})$ $= 127 \text{ kips}$	$T_{a,calc} = \frac{M_a}{d - t_{bf}}$ $= \frac{6{,}000 \text{ kip-in.}}{36 \text{ in.} - ½ \text{ in.}}$ $= 169 \text{ kips}$ $T_{aw} = (n_{trib}/n) T_{a,calc}$ $= (4/8)(169 \text{ kips})$ $= 84.5 \text{ kips}$

The length of the web tension region is measured from the inside of the beam flange to 6 in. inside the tension bolt row:

$$l_{wt} = p_{fi} + p_b + 6 \text{ in.}$$
$$= 2 \text{ in.} + 3 \text{ in.} + 6 \text{ in.}$$
$$= 11.0 \text{ in.}$$

The nominal web yield strength is:

$$T_{yw} = F_y A_g \qquad \text{(from } \textit{Spec.} \text{ Eq. J4-1)}$$
$$= F_y t_{bw} l_{wt}$$
$$= (50 \text{ ksi})(⅜ \text{ in.})(11.0 \text{ in.})$$
$$= 206 \text{ kips}$$

Check that the web design tension yield strength is sufficient.

LRFD	ASD
$\phi T_{yw} = 0.90(206 \text{ kips})$ $= 185 \text{ kips} \quad \geq \quad T_{uw} = 127 \text{ kips}$ **o.k.**	$\frac{T_{yw}}{\Omega} = \frac{206 \text{ kips}}{1.67}$ $= 123 \text{ kips} \quad \geq \quad T_{aw} = 84.5 \text{ kips}$ **o.k.**

Check that the required strength must be at least 60% (LRFD) or 40% (ASD) of the web tension strength from Equations 3-41.

LRFD	ASD
$0.60T_{yw} = 0.60(206 \text{ kips})$ $= 124 \text{ kips}$ $T_{uwd} = \max(T_{uw}, 0.60T_{yw})$ $= \max(127 \text{ kips}, 124 \text{ kips})$ $= 127 \text{ kips}$	$0.40T_{yw} = 0.40(206 \text{ kips})$ $= 82.4 \text{ kips}$ $T_{awd} = \max(T_{aw}, 0.40T_{yw})$ $= \max(84.5 \text{ kips}, 82.4 \text{ kips})$ $= 84.5 \text{ kips}$

Check the web to end-plate weld around the tension bolts. Because the weld is loaded perpendicular to its longitudinal axis, the angle of loading, θ, is 90°.

$$R_n = (2 \text{ welds}) 0.60 F_{EXX} \frac{t_{weld}}{\sqrt{2}} l_{wt} (1.0 + 0.5 \sin^{1.5} \theta) \qquad \text{(from } \textit{Spec.} \text{ Eq. J2-4)}$$
$$= (2 \text{ welds})(0.60)(70 \text{ ksi}) \left(\frac{3/16 \text{ in.}}{\sqrt{2}} \right) (11.0 \text{ in.})(1.0 + 0.5 \sin^{1.5} 90°)$$
$$= 184 \text{ kips}$$

LRFD	ASD
$\phi R_n = 0.75(184 \text{ kips})$ $= 138 \text{ kips} \quad \geq \quad T_{uwd} = 127 \text{ kips}$ **o.k.**	$\frac{R_n}{\Omega} = \frac{184 \text{ kips}}{2.00}$ $= 92.0 \text{ kips} \quad \geq \quad T_{awd} = 84.5 \text{ kips}$ **o.k.**

Double-sided 3⁄16 in. fillet welds are sufficient.

Check the web to end-plate weld away from the tension bolts. Only the web to end-plate weld between the end of the assumed web tension length and the inside face of the bottom beam compression flange or the weld between the mid-depth of the beam and the inside face of the beam compression flange, whichever is smaller, is considered effective in resisting the beam end shear. The shear strength of this weld is compared to the required shear applied to the connection.

$$l_t = d - 2t_{fb} - l_{wt}$$
$$= 36 \text{ in.} - 2(½ \text{ in.}) - 11.0 \text{ in.}$$
$$= 24.0 \text{ in.}$$

$$l_{0.5w} = d/2 - t_{bf}$$
$$= (36 \text{ in.})/2 - ½ \text{ in.}$$
$$= 17.5 \text{ in.}$$

$$l_{wv} = \min(l_t, l_{0.5w})$$
$$= \min(24.0 \text{ in.}, 17.5 \text{ in.})$$
$$= 17.5 \text{ in.}$$

$$R_n = (2 \text{ welds}) 0.60 F_{EXX} \frac{t_{weld}}{\sqrt{2}} l_{wv} (1.0 + 0.5 \sin^{1.5} \theta) \quad \text{(from } \textit{Spec.} \text{ Eq. J2-4)}$$
$$= (2 \text{ welds})(0.60)(70 \text{ ksi}) \left(\frac{3/16 \text{ in.}}{\sqrt{2}} \right) (17.5 \text{ in.})(1.0 + 0.5 \sin^{1.5} 0°)$$
$$= 195 \text{ kips}$$

LRFD	ASD
$\phi R_n = 0.75(195 \text{ kips})$ $= 146 \text{ kips} \quad \geq \quad V_u = 60.0 \text{ kips}$ **o.k.**	$\frac{R_n}{\Omega} = \frac{195 \text{ kips}}{2.00}$ $= 97.5 \text{ kips} \quad \geq \quad V_a = 40.0 \text{ kips}$ **o.k.**

Check that the shear rupture strength of the beam web at the weld using AISC *Specification* Equation J4-4 is sufficient.

$$R_n = 0.60 F_u A_{nv} \quad \text{(}\textit{Spec.}\text{ Eq. J4-4)}$$
$$= 0.60 F_u l_{wv} t_{bw}$$
$$= 0.60(65 \text{ ksi})(17.5 \text{ in.})(3/8 \text{ in.})$$
$$= 256 \text{ kips}$$

LRFD	ASD
$\phi R_n = 0.75(256 \text{ kips})$ $= 192 \text{ kips} \quad \geq \quad V_u = 60.0 \text{ kips}$ **o.k.**	$\frac{R_n}{\Omega} = \frac{256 \text{ kips}}{2.00}$ $= 128 \text{ kips} \quad \geq \quad V_a = 40.0 \text{ kips}$ **o.k.**

The double-sided 3/16 in. fillet welds shown in Figure B-24 from the web to the end plate are sufficient.

Summary

The connection shown in Figure B-24 is adequate for the required moment and shear force shown.

C. Column-Side Limit State Checks

See Example 5.3-1 or 5.3-2 for example column-side limit state check calculations.

Summary

The connection shown in Figure B-24 is adequate for the required moment and shear force.

EXAMPLE B.3-8—12-Bolt Multiple-Row Extended 1/3 Four-Wide/Two-Wide Unstiffened Thin End-Plate Example

Given:

The connection shown in Figure B-26 is a 12-bolt multiple-row extended (MRE) 1/3 four-wide/two-wide unstiffened end-plate moment connection for a built-up beam. The beam and end plate are ASTM A572/A572M Grade 50 material, and the bolts are Group 120 ASTM F3125/F3125M Grade A325 pretensioned. Weld electrodes are E70XX. The connection is to be evaluated as a thin end-plate design for the following required moments and shear forces.

	LRFD	ASD
Moment	$M_u = 20{,}100$ kip-in.	$M_a = 13{,}400$ kip-in.
Shear force	$V_u = 90.0$ kips	$V_a = 60.0$ kips

Solution:

From AISC *Manual* Table 2-4, the material properties are as follows:

ASTM A572/A572M Grade 50
$F_y = 50$ ksi
$F_u = 65$ ksi

From AISC *Specification* Table J3.2, the material properties of the bolts are as follows:

Group 120 ASTM F3125/F3125M 1¼-in.-diameter Grade A325 pretensioned
$F_{nt} = 90$ ksi
$F_{nv} = 54$ ksi (Group 120 bolts with threads not excluded from the shear plane; thread condition N)

Beam
$d = 36$ in. $\quad t_{bw} = ½$ in.
$b_{bf} = 15$ in. $\quad t_{bf} = ¾$ in.

End-plate geometric properties:
$b_p = 15$ in.
$t_p = 1$ in.
$g = 4$ in.
$g_o = 3¾$ in.
$p_{ext} = 4¼$ in.
$d_e = 1¾$ in.
$p_{fo} = 2½$ in.
$p_{fi} = 2½$ in.
$p_b = 3¾$ in.
$d_p = 44½$ in.

The distances from the centerline of the compression flange to the bolt lines, h_1, h_2, h_3, and h_4, are depicted in Table 5-17 and computed as:

$$h_1 = d - \frac{t_{bf}}{2} + p_{fo}$$
$$= 36 \text{ in.} - \frac{¾ \text{ in.}}{2} + 2½ \text{ in.}$$
$$= 38.1 \text{ in.}$$

$$h_2 = d - \frac{3t_{bf}}{2} - p_{fi}$$
$$= 36 \text{ in.} - \frac{3(¾ \text{ in.})}{2} - 2½ \text{ in.}$$
$$= 32.4 \text{ in.}$$

$$h_3 = d - \frac{3t_{bf}}{2} - p_{fi} - p_b$$

$$= 36 \text{ in.} - \frac{3(¾ \text{ in.})}{2} - 2½ \text{ in.} - 3¾ \text{ in.}$$

$$= 28.6 \text{ in.}$$

$$h_4 = d - \frac{3t_{bf}}{2} - p_{fi} - 2p_b$$

$$= 36 \text{ in.} - \frac{3(¾ \text{ in.})}{2} - 2½ \text{ in.} - 2(3¾ \text{ in.})$$

$$= 24.9 \text{ in.}$$

$$b_{p,eff} \le b_{bf} + \max(t_p, 1 \text{ in.}) \quad (4\text{-}3)$$

$$= 15 \text{ in.} + \max(1 \text{ in.}, 1 \text{ in.})$$

$$= 16.0 \text{ in.}$$

$b_p = 15 \text{ in.} \le 16.0 \text{ in.}$ **o.k.**

$$b_{bf} \ge g + 2g_o \quad (4\text{-}2)$$

$15 \text{ in.} \ge 4 \text{ in.} + 2(3¾ \text{ in.})$

$15 \text{ in.} \ge 11.5 \text{ in.}$ **o.k.**

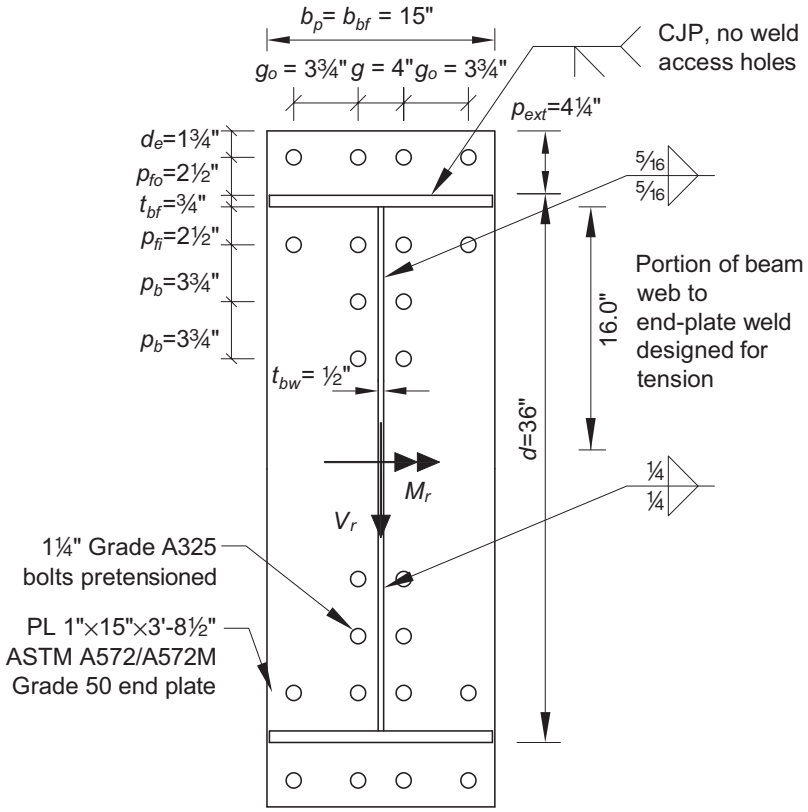

Fig. B-26. 12-bolt MRE 1/3 four-wide/two-wide unstiffened thin end-plate configuration for Example B.3-8.

A. End-Plate and Bolt Design Verification

Determine if the specified end-plate thickness, 1 in., and 1¼-in.-diameter Grade A325 bolts are sufficient using the thin end-plate/larger bolt diameter procedure.

Solve for the required end-plate thickness using Equations 5-5. First solve for the distance, s, and yield line parameter, Y_p, using Table 5-17.

$$s = \frac{\sqrt{b_p g}}{2}$$
$$= \frac{\sqrt{(15\text{ in.})(4\text{ in.})}}{2}$$
$$= 3.87\text{ in.}$$

Because $s \geq p_{fi} = 2\text{½}$ in., the dimension p_{fi} is used in the equation for the yield line parameter.

$$Y_p = \frac{b_p}{2}\left[h_1\left(\frac{1}{p_{fo}}\right) + h_2\left(\frac{1}{p_{fi}}\right) + h_4\left(\frac{1}{s}\right) - \frac{1}{2}\right] + \frac{2}{g}\left[h_2(p_{fi} + 1.5p_b) + h_4(s + 0.5p_b)\right] + \frac{g}{2}$$
$$= \left(\frac{15\text{ in.}}{2}\right)\left[(38.1\text{ in.})\left(\frac{1}{2\text{½ in.}}\right) + (32.4\text{ in.})\left(\frac{1}{2\text{½ in.}}\right) + (24.9\text{ in.})\left(\frac{1}{3.87\text{ in.}}\right) - \frac{1}{2}\right]$$
$$+ \left(\frac{2}{4\text{ in.}}\right)\left\{(32.4\text{ in.})\left[2\text{½ in.} + 1.5(3\text{¾ in.})\right] + (24.9\text{ in.})\left[3.87\text{ in.} + 0.5(3\text{¾ in.})\right]\right\} + \frac{4\text{ in.}}{2}$$
$$= 461\text{ in.}$$

Determine the required end-plate thickness using Equations 5-5. For extended end-plate configurations, $\gamma_r = 1.0$.

LRFD	ASD
$t_{p,reqd} = \sqrt{\dfrac{M_u}{\gamma_r \phi_b F_y Y_p}}$ $= \sqrt{\dfrac{20{,}100\text{ kip-in.}}{1.0(0.90)(50\text{ ksi})(461\text{ in.})}}$ $= 0.984\text{ in.} \quad \leq \quad 1\text{ in.} \quad$ **o.k.**	$t_{p,reqd} = \sqrt{\dfrac{\Omega_b M_a}{\gamma_r F_y Y_p}}$ $= \sqrt{\dfrac{1.67(13{,}400\text{ kip-in.})}{1.0(50\text{ ksi})(461\text{ in.})}}$ $= 0.985\text{ in.} \quad \leq \quad 1\text{ in.} \quad$ **o.k.**

Therefore, a 1-in.-thick end plate is sufficient.

Determine if the specified 1¼-in.-diameter Grade A325 bolts are sufficient. First, calculate geometry of the effective tee stub; then calculate the related forces, F_i, Q_{max}, and P_{qi}; finally, calculate the required bolt diameter.

The bolts are specified as pretensioned. The minimum bolt pretension for a 1¼-in.-diameter Grade A325 bolt is $T_b = 81$ kips. The nominal unthreaded body area of a 1¼ in. bolt is $A_b = 1.23\text{ in.}^2$, and the nominal tensile stress for a Grade A325 bolt is $F_{nt} = 90$ ksi. The resulting nominal tensile strength of a 1¼-in.-diameter Grade A325 bolt is:

$$P_t = F_{nt} A_b \qquad \text{(from } \textit{Spec.}\text{ Eq. J3-1)}$$
$$= (90\text{ ksi})(1.23\text{ in.}^2)$$
$$= 111\text{ kips}$$

There are six unique bolt locations as labeled in Figure B-27. The orientation of the effective tee stubs are defined using the rules given in Section 5.1.2 and are shown in Figure B-27.

Calculate the bolt distance from bolt to edge of effective tee stub:

$$a = 3.62\left(\frac{t_p}{d_b}\right)^3 - 0.085 \tag{3-24}$$

$$= 3.62\left(\frac{1 \text{ in.}}{1¼ \text{ in.}}\right)^3 - 0.085$$

$$= 1.77 \text{ in.}$$

Bolt Position 1—Outside Corner Bolt

For bolt position 1 (see Figure B-27), calculate the geometry of the effective tee stub, including the width of the effective tee stub, w_1, the net effective width, w_1', and distance from effective tee stem to the bolt, b_1.

$$w_1 = \frac{b_p - g - g_o}{2}$$

$$= \frac{15 \text{ in.} - 4 \text{ in.} - 3¾ \text{ in.}}{2}$$

$$= 3.63 \text{ in.}$$

$$w_1' = w_1 - (d_b + ⅛ \text{ in.}) \tag{5-7}$$

$$= 3.63 \text{ in.} - (1¼ \text{ in.} + ⅛ \text{ in.})$$

$$= 2.26 \text{ in.}$$

$$a_1 = \min(a_{calc}, p_{ext} - p_{fo})$$

$$= \min(1.77 \text{ in.}, 4¼ \text{ in.} - 2½ \text{ in.})$$

$$= 1.75 \text{ in.}$$

$$b_1 = p_{fo}$$

$$= 2½ \text{ in.}$$

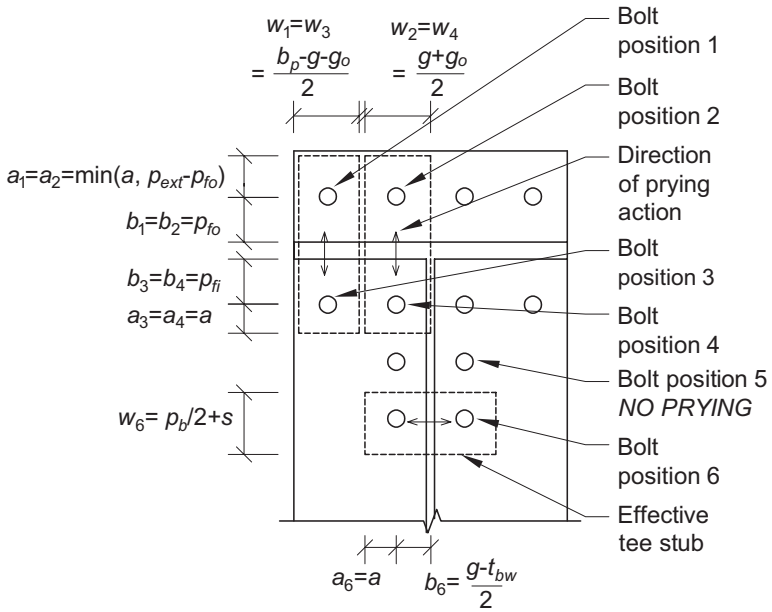

Fig. B-27. Effective tee-stub geometry for the 12-bolt MRE 1/3 unstiffened configuration.

Find forces related to prying, including the force, F_1', the prying force, $Q_{max,1}$, and the bolt tension contributing to flexural strength, P_{q1}.

$$F_1' = \frac{1}{b_1}\left[\frac{t_p^2 F_y}{4}(0.85w_1 + 0.8w_1') + \frac{\pi d_b^3 F_{nt}}{32}\right] \tag{3-26}$$

$$= \left(\frac{1}{2\text{½ in.}}\right)\left\{\left[\frac{(1\text{ in.})^2(50\text{ ksi})}{4}\right]\left[0.85(3.63\text{ in.}) + 0.8(2.26\text{ in.})\right] + \frac{\pi(1\text{¼ in.})^3(90\text{ ksi})}{32}\right\}$$

$$= 31.4 \text{ kips}$$

$$Q_{max,1} = \frac{w_1' t_p^2}{4a_1}\sqrt{F_y^2 - 3\left(\frac{F_1'}{w_1' t_p}\right)^2} \tag{3-23}$$

$$= \frac{(2.26\text{ in.})(1\text{ in.})^2}{4(1.75\text{ in.})}\sqrt{(50\text{ ksi})^2 - 3\left[\frac{31.4\text{ kips}}{(2.26\text{ in.})(1\text{ in.})}\right]^2}$$

$$= 14.2 \text{ kips}$$

$$P_{q1} = \max(P_t - Q_{max,1},\ T_b) \tag{3-27}$$

$$= \max(110\text{ kips} - 14.2\text{ kips},\ 81.0\text{ kips})$$

$$= 96.8 \text{ kips}$$

Prying forces for bolt positions 2 through 6 are calculated in a similar way using the effective tee-stub geometry shown in Figure B-27. Table B-13 gives the geometric parameters, related prying force, the usable strength for each bolt position, and reduction in bolt contribution factor, α_i. As described in Section 5.1.2, experiments have shown that bolts in the second interior row of configurations with three or more interior rows do not experience prying forces. However, they may not reach their full tensile strength. The bolt strength is taken equal to the bolt pretension for bolt position 5. The reduction factors for bolt locations that do not fully realize the bolt rupture strength before the first bolt fractures are $\alpha_1 = 0.50$, $\alpha_3 = 0.75$, $\alpha_5 = 0.75$, and $\alpha_6 = 0.50$.

Calculate the flexural strength for bolt rupture with prying action, M_q, using Equation 3-28. Then the design flexural strength is compared to the required flexural strength.

$$M_q = \sum_i \alpha_i P_{qi} n_i h_i \tag{3-28}$$

$$= 0.50(96.8\text{ kips})(2\text{ bolts})(38.1\text{ in.}) + 1.0(95.1\text{ kips})(2\text{ bolts})(38.1\text{ in.})$$

$$+ 0.75(97.0\text{ kips})(2\text{ bolts})(32.4\text{ in.}) + 1.0(95.3\text{ kips})(2\text{ bolts})(32.4\text{ in.})$$

$$+ 0.75(81.0\text{ kips})(2\text{ bolts})(28.6\text{ in.}) + 0.50(85.2\text{ kips})(2\text{ bolts})(24.9\text{ in.})$$

$$= 27{,}400 \text{ kip-in.}$$

LRFD	ASD
$\phi M_q = 0.75(27{,}400\text{ kip-in.})$ $= 20{,}600\text{ kip-in.} \geq M_u = 20{,}100\text{ kip-in.}$ **o.k.**	$\frac{M_q}{\Omega} = \frac{27{,}400\text{ kip-in.}}{2.00}$ $= 13{,}700\text{ kip-in.} \geq M_a = 13{,}400\text{ kip-in.}$ **o.k.**

Therefore, 1¼-in.-diameter Grade A325 bolts are sufficient.

Check Shear Yielding and Shear Rupture of the Extended Portion of the End Plate

For extended end-plate moment connections that are unstiffened, potential limit states that must be checked are shear yielding and shear rupture of the extended portion of the end plate. For the 12-bolt, multiple-row extended 1/3 four-wide/two-wide

Table B-13. Prying Action for the 12-Bolt MRE 1/3 Example						
Parameter	**Bolt Position 1**	**Bolt Position 2**	**Bolt Position 3**	**Bolt Position 4**	**Bolt Position 5**	**Bolt Position 6**
w_i (in.)	3.63	3.88	3.63	3.88		5.75
w_i' (in.)	2.26	2.51	2.26	2.51		4.38
a_i (in.)	1.75	1.75	1.77	1.77	*NO PRYING*	1.77
b_i (in.)	2.50	2.50	2.50	2.50		1.75
F_i' (kips)	31.4	33.4	31.4	33.4		69.8
$Q_{max,i}$ (kips)	14.2	15.9	14.0	15.7	0.0	25.8
P_{qi} (kips)	96.8	95.1	97.0	95.3	81.0	85.2
α_i	0.50	1.0	0.75	1.0	0.75	0.50

unstiffened end-plate moment connection, the shear demand is taken as one-third of the tension flange force because the exterior bolts represent one-third of the bolts. The shear strength is calculated in accordance with AISC *Specification* Section J4.2.

Calculate the shear demand on the extended portion of the end plate.

LRFD	ASD
$V_{up} = \frac{1}{3}\left(\frac{M_u}{d - t_{bf}}\right)$	$V_{ap} = \frac{1}{3}\left(\frac{M_a}{d - t_{bf}}\right)$
$= \frac{1}{3}\left(\frac{20{,}100 \text{ kip-in.}}{36 \text{ in.} - ¾ \text{ in.}}\right)$	$= \frac{1}{3}\left(\frac{13{,}400 \text{ kip-in.}}{36 \text{ in.} - ¾ \text{ in.}}\right)$
$= 190$ kips	$= 127$ kips

Calculate the nominal shear yielding strength.

$$R_n = 0.60F_yA_{gv} \qquad \text{(Spec. Eq. J4-3)}$$
$$= 0.60F_yb_pt_p$$
$$= 0.60(50 \text{ ksi})(15 \text{ in.})(1 \text{ in.})$$
$$= 450 \text{ kips}$$

Compare the design shear yielding strength to the shear demand. According to AISC *Specification* Section J4.2 for yielding of elements in shear, the resistance factor is $\phi = 1.00$, and the safety factor is $\Omega = 1.50$.

LRFD	ASD
$\phi R_n = 1.00(450 \text{ kips})$	$\frac{R_n}{\Omega} = \frac{450 \text{ kips}}{1.50}$
$= 450 \text{ kips} \quad \geq \quad V_{up} = 190 \text{ kips}$ **o.k.**	$= 300 \text{ kips} \quad \geq \quad V_{ap} = 127 \text{ kips}$ **o.k.**

Calculate the nominal shear rupture strength. The width of the extended portion of the end plate for use in the net section area is the width minus four effective hole diameters. The effective hole diameter is the hole diameter from AISC *Specification* Table J3.3 plus 1⁄16 in. The additional 1⁄16 in. accounts for damage around the hole caused by drilling, punching, or thermal cutting. For 1¼-in.-diameter bolts, the standard hole diameter, d_h, is 1⅜ in.

$$A_{nv} = \left[b_p - 4(d_h + 1/16) \right] t_p$$
$$= \left[15 \text{ in.} - 4(1\frac{3}{8} \text{ in.} + 1/16 \text{ in.}) \right] (1 \text{ in.})$$
$$= 9.25 \text{ in.}^2$$

$$R_n = 0.60 F_u A_{nv} \qquad \text{(Spec. Eq. J4-4)}$$
$$= 0.60(65 \text{ ksi})(9.25 \text{ in.}^2)$$
$$= 361 \text{ kips}$$

Compare the design shear rupture strength to the shear demand. Using AISC *Specification* Section J4.2 for rupture of elements in shear, the resistance factor is $\phi = 0.75$, and the safety factor is $\Omega = 2.00$.

LRFD	ASD
$\phi R_n = 0.75(361 \text{ kips})$ $= 271 \text{ kips} \geq V_{up} = 190 \text{ kips}$ **o.k.**	$\frac{R_n}{\Omega} = \frac{361 \text{ kips}}{2.00}$ $= 180 \text{ kips} \geq V_{ap} = 127 \text{ kips}$ **o.k.**

The extended portion of the 1-in.-thick end plate has sufficient resistance to shear yielding and shear rupture.

Check Shear Transfer at Bolt Holes

See Examples 5.3-1 or 5.3-2 for calculation procedures.

B. Check Beam to End-Plate Welds

The beam to end-plate welds shown in Figure B-26 are the same as shown in Figure 5-17. See Example 5.3-8 for weld strength checks.

The design shown in Figure B-26 is satisfactory for the required moment and shear force shown.

C. Column-Side Limit State Checks

See Example 5.3-1 or 5.3-2 for example column-side limit state check calculations.

Summary

The connection shown in Figure B-26 is adequate for the required moment and shear force.

EXAMPLE B.3-9—12-Bolt Extended Stiffened Thin End-Plate Example

Given:

The connection shown in Figure B-28 is a 12-bolt extended stiffened end-plate (12ES) connection for a built-up beam. The beam and plates are ASTM A572/A572M Grade 50 material. Bolts are Group 120 ASTM F3125/F3125M Grade A325, pretensioned. Weld electrodes are E70XX. The connection is to be evaluated as a thin end-plate design for the following required moments and forces:

	LRFD	ASD
Moment	$M_u = 20{,}100$ kip-in.	$M_a = 13{,}400$ kip-in.
Shear force	$V_u = 90.0$ kips	$V_a = 60.0$ kips

Solution:

From AISC *Manual* Table 2-4, the material properties are as follows:

ASTM A572/A572M Grade 50
F_y = 50 ksi
F_u = 65 ksi

From AISC *Specification* Table J3.2, the material properties of the bolts are as follows:

Group 120 ASTM F3125/F3125M 1⅛-in.-diameter Grade A325 pretensioned
F_{nt} = 90 ksi
F_{nv} = 54 ksi (Group 120 bolts with threads not excluded from the shear plane; thread condition N)

Beam
d = 36 in. t_{bw} = ⅜ in.
b_{bf} = 15 in. t_{bf} = ¾ in.

End-plate geometric properties:
b_p = 15 in.
t_p = ⅞ in.
g = 4 in.

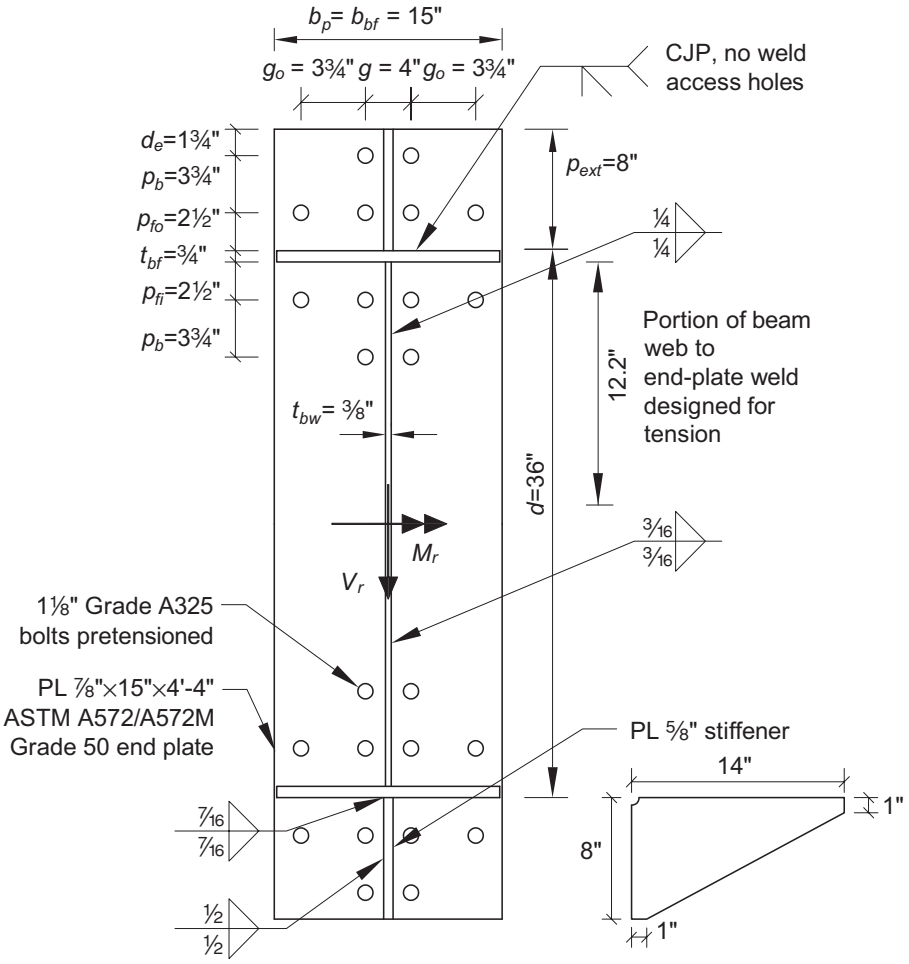

Fig. B-28. 12ES thin end-plate configuration for Example B.3-9.

g_o = 3¾ in.
p_{ext} = 8 in.
d_e = 1¾ in.
p_{fi} = 2½ in.
p_{fo} = 2½ in.
p_b = 3¾ in.
d_p = 52 in.

The distances from the centerline of the compression flange to the bolt lines, h_1, h_2, h_3, and h_4, are depicted in Table 5-18 and computed as:

$$h_1 = d - \frac{t_{bf}}{2} + p_{fo} + p_b$$
$$= 36 \text{ in.} - \frac{¾ \text{ in.}}{2} + 2½ \text{ in.} + 3¾ \text{ in.}$$
$$= 41.9 \text{ in.}$$

$$h_2 = d - \frac{t_{bf}}{2} + p_{fo}$$
$$= 36 \text{ in.} - \frac{¾ \text{ in.}}{2} + 2½ \text{ in.}$$
$$= 38.1 \text{ in.}$$

$$h_3 = d - \frac{3t_{bf}}{2} - p_{fi}$$
$$= 36 \text{ in.} - \frac{3(¾ \text{ in.})}{2} - 2½ \text{ in.}$$
$$= 32.4 \text{ in.}$$

$$h_4 = d - \frac{3t_{bf}}{2} - p_{fi} - p_b$$
$$= 36 \text{ in.} - \frac{3(¾ \text{ in.})}{2} - 2½ \text{ in.} - 3¾ \text{ in.}$$
$$= 28.6 \text{ in.}$$

$$b_{p,eff} \le b_{bf} + \max(t_p, 1 \text{ in.}) \quad (4\text{-}3)$$
$$\le 15 \text{ in.} + \max(⅞ \text{ in.}, 1 \text{ in.})$$
$$\le 16.0 \text{ in.}$$

$b_p = 15 \text{ in.} \le 16.0 \text{ in.}$ **o.k.**

$$b_{bf} \ge g + 2g_o \quad (4\text{-}2)$$
$$15 \text{ in.} \ge 4 \text{ in.} + 2(3¾ \text{ in.})$$
$15 \text{ in.} \ge 11.5 \text{ in.}$ **o.k.**

Beam flange to end-plate stiffener geometric properties:

$$h_{st} = p_{fo} + p_b + d_e$$
$$= 2½ \text{ in.} + 3¾ \text{ in.} + 1¾ \text{ in.}$$
$$= 8 \text{ in.}$$

$$L_{st} = \frac{h_{st}}{\tan 30^\circ} \tag{4-4}$$
$$= \frac{8 \text{ in.}}{\tan 30^\circ}$$
$$= 13.9 \text{ in.} \quad \leq \quad 14 \text{ in.} \quad \textbf{o.k.}$$

$$t_s \geq t_{bw}\left(\frac{F_{yb}}{F_{ys}}\right) \tag{3-36}$$
$$\geq (\tfrac{3}{8} \text{ in.})\left(\frac{50 \text{ ksi}}{50 \text{ ksi}}\right)$$
$$\geq \tfrac{3}{8} \text{ in.}$$
$$t_s = \tfrac{5}{8} \text{ in.} \quad \textbf{o.k.}$$

$$\frac{h_{st}}{t_s} = \frac{8 \text{ in.}}{\tfrac{5}{8} \text{ in.}}$$
$$= 12.8$$

$$\frac{h_{st}}{t_s} \leq 0.56\sqrt{\frac{E}{F_{ys}}} \tag{3-37}$$
$$\leq 0.56\sqrt{\frac{29{,}000 \text{ ksi}}{50 \text{ ksi}}}$$
$$\leq 13.5$$
$$\frac{h_{st}}{t_s} = 12.8 \quad \textbf{o.k.}$$

A. End-Plate and Bolt Design Verification

Determine if the specified end-plate thickness, ⅞ in., and 1⅛-in.-diameter Grade A325 bolts are sufficient using the thin end-plate/larger bolt diameter procedure.

Solve for the required end-plate thickness using Equations 5-5. First solve for the distance, s, and yield line parameter, Y_p, using Table 5-18.

$$s = \frac{\sqrt{b_p g}}{2}$$
$$= \frac{\sqrt{(15 \text{ in.})(4 \text{ in.})}}{2}$$
$$= 3.87 \text{ in.}$$

Because $s > d_e = 1\tfrac{3}{4}$, $s \geq p_{fo} = 2\tfrac{1}{2}$ in., and $p_{fi} = 2\tfrac{1}{2}$ in., the dimensions d_e, p_{fo}, and p_{fi} are used in the equation for the yield line parameter.

$$Y_p = \frac{b_p}{2}\left[h_2\left(\frac{1}{p_{fo}}\right)+h_3\left(\frac{1}{p_{fi}}\right)+h_4\left(\frac{1}{s}\right)-\frac{1}{2}\right]$$
$$+\frac{2}{g}\left[h_1(d_e+0.75p_b)+h_2(p_{fo}+0.25p_b)+h_3(p_{fi}+0.75p_b)+h_4(s+0.25p_b)\right]+\frac{5g}{4}$$
$$=\left(\frac{15\text{ in.}}{2}\right)\left[\frac{38.1\text{ in.}}{2\text{½ in.}}+\frac{32.4\text{ in.}}{2\text{½ in.}}+\frac{28.6\text{ in.}}{3.87\text{ in.}}-\frac{1}{2}\right]$$
$$+\left(\frac{2}{4\text{ in.}}\right)\left\{\begin{array}{l}(41.9\text{ in.})\left[1\text{¾ in.}+0.75(3\text{¾ in.})\right]\\+(38.1\text{ in.})\left[2\text{½ in.}+0.25(3\text{¾ in.})\right]\\+(32.4\text{ in.})\left[2\text{½ in.}+0.75(3\text{¾ in.})\right]\\+(28.6\text{ in.})\left[3.87\text{ in.}+0.25(3\text{¾ in.})\right]\end{array}\right\}+\frac{5(4\text{ in.})}{4}$$
$$=584\text{ in.}$$

Determine the required end-plate thickness using Equations 5-5. For extended end-plate configurations, $\gamma_r = 1.0$.

LRFD	ASD
$t_{p,reqd}=\sqrt{\dfrac{M_u}{\gamma_r\phi_b F_y Y}}$ $=\sqrt{\dfrac{20{,}100\text{ kip-in.}}{1.0(0.90)(50\text{ ksi})(584\text{ in.})}}$ $=0.875\text{ in.} \le \text{⅞ in.}$ **o.k.**	$t_{p,reqd}=\sqrt{\dfrac{\Omega_b M_a}{\gamma_r F_y Y}}$ $=\sqrt{\dfrac{1.67(13{,}400\text{ kip-in.})}{1.0(50\text{ ksi})(584\text{ in.})}}$ $=0.875\text{ in.} \le \text{⅞ in.}$ **o.k.**

Therefore, a ⅞-in.-thick end plate is sufficient.

Determine if the given bolt diameter of 1⅛ in. is sufficient. First calculate geometry of the effective tee stub; then calculate the related forces, F_i, Q_{max}, and P_{qi}; finally, calculate the required bolt diameter.

The bolts are specified as pretensioned. The minimum bolt pretension for a 1⅛-in.-diameter Grade A325 bolt is $T_b = 64$ kips. The nominal unthreaded body area of a 1⅛ in. bolt is $A_b = 0.994\text{ in.}^2$, and the nominal tensile stress for a Grade A325 bolt is $F_{nt} = 90$ ksi. The resulting nominal tensile strength of a 1⅛-in.-diameter Grade A325 bolt is:

$$P_t = F_{nt}A_b \qquad \text{(from } \textit{Spec.}\text{ Eq. J3-1)}$$
$$=(90\text{ ksi})(0.994\text{ in.}^2)$$
$$=89.5\text{ kips}$$

There are six unique bolt locations as labeled in Figure B-29. The orientation of the effective tee stubs is defined using the rules given in Section 5.1.2 and are shown in Figure B-29.

Calculate the bolt distance from bolt to edge of effective tee stub:

$$a = 3.62\left(\frac{t_p}{d_b}\right)^3 - 0.085\text{ in.} \qquad (3\text{-}24)$$
$$=3.62\left(\frac{\text{⅞ in.}}{1\text{⅛ in.}}\right)^3-0.085\text{ in.}$$
$$=1.62\text{ in.}$$

Bolt Position 1—Most Exterior Bolt

For bolt position 1 (see Figure B-29), calculate the geometry of the effective tee stub, including the width of the effective tee stub, w_1, the net effective width, w_1', and distance from effective tee stem to the bolt, b_1.

$$w_1 = d_e + \frac{p_b}{2}$$
$$= 1¾ \text{ in.} + \frac{3¾ \text{ in.}}{2}$$
$$= 3.63 \text{ in.}$$

$$w_1' = w_1 - (d_b + ⅛ \text{ in.}) \tag{5-7}$$
$$= 3.63 \text{ in.} - (1⅛ \text{ in.} + ⅛ \text{ in.})$$
$$= 2.38 \text{ in.}$$

$$a_1 = \min\left[a, (b_p - g)/2\right]$$
$$= \min\left[1.62 \text{ in.}, (15 \text{ in.} - 4 \text{ in.})/2\right]$$
$$= 1.62 \text{ in.}$$

$$b_1 = \frac{g - t_{bw}}{2}$$
$$= \frac{4 \text{ in.} - ⅜ \text{ in.}}{2}$$
$$= 1.81 \text{ in.}$$

Find forces related to prying, including the force, F_1', the prying force, $Q_{max,1}$, and the bolt tension contributing to flexural strength, P_{q1}.

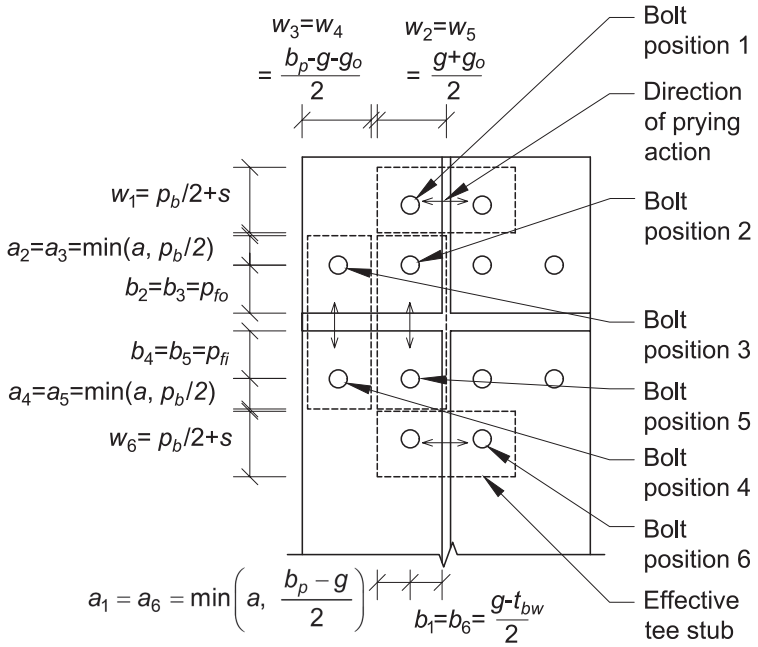

Fig. B-29. Effective tee-stub geometry for the 12ES configuration.

Table B-14. Prying Action for the 12-Bolt Extended Stiffened Example						
Parameter	**Bolt Position 1**	**Bolt Position 2**	**Bolt Position 3**	**Bolt Position 4**	**Bolt Position 5**	**Bolt Position 6**
w_i (in.)	3.63	3.88	3.63	3.63	3.88	5.75
w_i' (in.)	2.38	2.63	2.38	2.38	2.63	4.50
a_i (in.)	1.62	1.62	1.62	1.62	1.62	1.62
b_i (in.)	1.81	2.50	2.50	2.50	2.50	1.81
F_i' (kips)	33.3	25.7	24.1	24.1	25.7	51.8
$Q_{max,i}$ (kips)	11.7	14.3	12.9	12.9	14.3	23.7
P_{qi} (kips)	77.8	75.2	76.6	76.6	75.2	65.8
α_i	1.0	1.0	0.50	0.75	1.0	1.0

$$F_1' = \frac{1}{b_1}\left[\frac{t_p^2 F_y}{4}(0.85w_1 + 0.8w_1') + \frac{\pi d_b^3 F_{nt}}{32}\right] \quad (3\text{-}26)$$

$$= \left(\frac{1}{1.81 \text{ in.}}\right)\left\{\left[\frac{(⅞ \text{ in.})^2 (50 \text{ ksi})}{4}\right]\left[0.85(3.63 \text{ in.}) + 0.8(2.38 \text{ in.})\right] + \frac{\pi (1⅛ \text{ in.})^3 (90 \text{ ksi})}{32}\right\}$$

$$= 33.3 \text{ kips}$$

$$Q_{max,1} = \frac{w_1' t_p^2}{4a_1}\sqrt{F_y^2 - 3\left(\frac{F_1'}{w_1' t_p}\right)^2} \quad (3\text{-}23)$$

$$= \frac{(2.38 \text{ in.})(⅞ \text{ in.})^2}{4(1.62 \text{ in.})}\sqrt{(50 \text{ ksi})^2 - 3\left[\frac{33.3 \text{ kips}}{(2.38 \text{ in.})(⅞ \text{ in.})}\right]^2}$$

$$= 11.7 \text{ kips}$$

$$P_{q1} = \max(P_t - Q_{max,1}, T_b) \quad (3\text{-}27)$$

$$= \max(89.5 \text{ kips} - 11.7 \text{ kips},\ 64.0 \text{ kips})$$

$$= 77.8 \text{ kips}$$

Prying forces for bolt positions 2 through 6 are calculated in a similar way using the effective tee-stub geometry shown in Figure B-29. Table B-14 gives the geometric parameters, related prying force, the usable strength for each bolt position, and reduction in bolt contribution factor, α_i. The reduction factors for bolt locations that do not fully realize the bolt rupture strength before the first bolt fractures are $\alpha_3 = 0.50$ and $\alpha_4 = 0.75$.

Calculate the flexural strength for bolt rupture with prying action, M_q, using Equation 3-28. Then the design flexural strength is compared to the required flexural strength.

$$M_q = \sum_i \alpha_i P_{qi} n_i h_i \quad (3\text{-}28)$$

$$= 1.0(77.8 \text{ kips})(2 \text{ bolts})(41.9 \text{ in.}) + 1.0(75.2 \text{ kips})(2 \text{ bolts})(38.1 \text{ in.})$$

$$+ 0.5(76.6 \text{ kips})(2 \text{ bolts})(38.1 \text{ in.}) + 0.75(76.6 \text{ kips})(2 \text{ bolts})(32.4 \text{ in.})$$

$$+ 1.0(75.2 \text{ kips})(2 \text{ bolts})(32.4 \text{ in.}) + 1.0(65.8 \text{ kips})(2 \text{ bolts})(28.6 \text{ in.})$$

$$= 27{,}500 \text{ kip-in.}$$

LRFD	ASD
$\phi M_q = 0.75(27{,}500 \text{ kip-in.})$ $= 20{,}600 \text{ kip-in.} \quad \geq \quad M_u = 20{,}100 \text{ kip-in.} \quad$ **o.k.**	$\frac{M_q}{\Omega} = \frac{27{,}500 \text{ kip-in.}}{2.00}$ $= 13{,}800 \text{ kip-in.} \quad \geq \quad M_a = 13{,}400 \text{ kip-in.} \quad$ **o.k.**

Therefore, 1⅛-in.-diameter Grade A325 bolts are sufficient.

Check Shear Yielding and Shear Rupture of the Extended Portion of the End Plate

For extended end-plate moment connections that are stiffened, shear yielding and shear rupture of the extended portion of the end plate are not limit states.

Therefore, a ⅞-in.-thick end plate is sufficient.

Check Shear Transfer at Bolt Holes

See Example 5.3-1 or 5.3-2 for calculation procedures.

B. Check Beam to End-Plate Welds

The beam to end-plate welds shown in Figure B-28 are the same as shown in Figure 5-18. See Example 5.3-9 for weld strength checks.

The design shown in Figure B-28 is satisfactory for the required moment and shear force shown.

C. Column-Side Limit State Checks

See Example 5.3-1 or 5.3-2 for example column-side limit state check calculations.

Summary

The connection shown in Figure B-28 is adequate for the required moment and shear force.

Symbols

A_b	Nominal unthreaded body area of bolt, in.^{2}
A_b	Gross cross-sectional area of beam, in.^{2}
A_c	Gross cross-sectional area of column, in.^{2}
A_{fc}	Column compression flange area, in.^{2}
A_{ft}	Column tension flange area, in.^{2}
A_{gb}	Gross cross-sectional area of beam, in.^{2}
A_{gc}	Gross cross-sectional area of column, in.^{2}
A_{gcp}	Gross cross-sectional area of continuity plates, in.^{2}
A_n	Net area of end plate, in.^{2}
A_{net}	Net area of column web stiffener, in.^{2}
A_{nv}	Net area of extended unstiffened end plate subjected to shear, in.^{2}
A_w	Panel zone shear area, in.^{2}
A_{ws}	Area of end-plate stiffener for stiffened flush connections, in.^{2}
A_{wt}	Area of beam web and stiffeners in the vicinity of the tension bolts, in.^{2}
C_a	Ratio of required strength to available axial yield strength
$C_{a,stiff}$	Required strength for column web stiffeners using ASD load combinations, kips
C_{pr}	Factor to account for peak connection strength, including strain hardening
C_t	Factor to account for whether column is continuous past the connection
$C_{u,stiff}$	Required strength for column web stiffeners using LRFD load combinations, kips
C_v	Web shear buckling coefficient
D	Nominal dead load, kips
E	Young's modulus of elasticity of steel, ksi
F	Force, kips
F'	Bolt force associated with the plastic mechanism of effective tee stub, kips
F_{EXX}	Filler metal classification strength, ksi
F_{fsu}	Required axial strength for continuity plates, kips
F_{fu}	Factored beam flange force, kips
F_{nt}	Nominal bolt tensile strength, specified in *Specification* Table J3.2, ksi
F_{nv}	Nominal bolt shear strength, specified in *Specification* Table J3.2, ksi
F_u	Specified minimum tensile strength, ksi
F_{ub}	Specified minimum tensile strength of beam material, ksi
F_{up}	Specified minimum tensile strength of end-plate material, ksi
F_y	Specified minimum yield stress, ksi
F_{yb}	Specified minimum yield stress of beam material, ksi
F_{yc}	Specified minimum yield stress of column flange material, ksi
F_{ycp}	Specified minimum yield stress of continuity plate material, ksi
F_{yp}	Specified minimum yield stress of end-plate material, ksi
F_{ys}	Specified minimum yield stress of stiffener material, ksi
F_{yw}	Specified minimum yield stress of column web material, ksi
I	Moment of inertia in the plane of bending, in.^{4}
K_s	Initial rotational stiffness of the connection, kip-in./rad
L	Length of beam span, in.
L	Nominal live load, kips
L_c	Length of beam clear span, in.
L_h	Distance between beam plastic hinge locations, in.
L_n	Length of yield line, in.
L_{st}	Length of stiffener in stiffened extended end-plate connections, in.
L_{weld}	Length of weld, in.
$L_{weld,req}$	Required length of weld, in.

L_{ws} Length of end-plate stiffener in stiffened flush connections, in.

L_x Projection of the yield line length along the x-axis, in.

L_y Projection of the yield line length along the y-axis, in.

M Moment at beam end, kip-in.

M_a Required flexural strength using ASD load combinations, kip-in.

$M_{a,eq}$ Required flexural strength using ASD load combinations including $M_{r,axial}$, kip-in.

M_b Bolt moment, kip-in.

M_{cf} Nominal connection flexural strength for the limit state of column flange flexure, kip-in.

$M_{cf,s}$ Nominal connection flexural strength for the limit state of column flange flexure with column web stiffeners, kip-in.

$M_{cf,u}$ Nominal connection flexural strength for the limit state of column flange flexure without column web stiffeners, kip-in.

M_f Beam fixed end moment for service loads, kip-in.

M_f Moment at face of column associated with plastic hinging of beam, kip-in.

M_{fu} Beam fixed end moment for LRFD factored loads, kip-in.

M_{np} Nominal connection flexural strength for the limit state of bolt fracture with no prying action, kip-in.

M_p Plastic moment strength of the beam, kip-in.

M_{pl} Nominal connection flexural strength for the limit state of end-plate yielding, kip-in.

M_{pr} Probable maximum moment at plastic hinge, kip-in.

M_{p1} Plastic moment at face of tee stem, kip-in.

M_{p2} Plastic moment at bolt line, kip-in.

M_q Nominal connection flexural strength for the limit state of bolt fracture with prying action, kip-in.

M_r Required connection flexural strength, kip-in.

M_r^* Required flexural strength for sloped connections, kip-in.

$M_{r,axial}$ Connection equivalent required moment associated with beam axial force, kip-in.

M_s Beam end moment considering connection stiffness, kip-in.

M_u Required flexural strength using LRFD load combinations, kip-in.

$M_{u,eq}$ Required flexural strength using LRFD load combinations including $M_{r,axial}$, kip-in.

M_v Additional moment due to shear amplification from the location of the plastic hinge to the column centerline, kip-in.

P_a Concentrated force on the column from the beam bottom flange using ASD load combinations, kips

P_n Available compression yield strength of web stiffener plates/continuity plates, kips

$P_{n,stiff}$ Available yield strength of the stiffener plates, kips

P_q Bolt tensile strength adjusted for prying forces, kips

P_r Connection required axial strength, kips

P_r^* Required axial strength for sloped connections, kips

P_t Bolt ultimate tensile strength, kips

P_u Concentrated force on the column from the beam bottom flange using LRFD load combinations, kips

P_{ub} Beam axial tension/compression using LRFD load combinations, kips

P_{uc} Column axial tension/compression using LRFD load combinations, kips

$P_{uc,total}$ Total column axial tension/compression using LRFD load combinations, kips

$P_{u,max}$ Maximum compressive load which satisfies column web highly ductile criteria using LRFD load combinations, kips

P_y Axial yield strength of the column, kips

Q Bolt prying force, kips

Q_f Chord stress interaction parameter = 1.0 for wide flange shapes

Q_{max} Maximum possible bolt prying force, kips

R Seismic response modification coefficient from ASCE/SEI 7

R_a Required axial strength using ASD load combinations, kips

R_n Nominal strength, kips

$R_{n,brg}$ Nominal bolt bearing strength, kips

$R_{n,bt}$ Nominal bolt shear strength, kips

$R_{n,cs}$ Nominal strength of stiffened column flange to resist column flange flexure due to a concentrated load, kips

$R_{n,cu}$ Nominal strength of unstiffened column flange to resist column flange flexure due to a concentrated load, kips

$R_{n,lwc}$ Nominal column web local crippling strength, kips

$R_{n,lwy}$ Nominal column web local yielding strength, kips

R_u Required axial strength using LRFD load combinations, kips

R_{u1} Nominal tensile strength of continuity plates, kips

R_{u2} Nominal shear yield strength of continuity plates, kips

R_{u3} Panel zone available strength, kips

R_y Ratio of expected yield stress to specified minimum yield stress

S Nominal snow load, kips

S_h Distance from face of column to plastic hinge, in.

T_a Connection required axial tensile strength using ASD load combinations, kips

$T_{a,calc}$ Beam flange axial force calculated using ASD load combinations, kips

T_{af} Beam flange to end-plate weld required axial strength using ASD load combinations, kips

$T_{a,min}$ Minimum beam flange to end-plate weld required axial tensile strength using ASD load combinations, kips

$T_{a,stiff}$ Required tension strength for column web stiffeners using ASD load combinations, kips

$T_{a,ws}$ Required tension strength for web stiffener to end-plate connection using ASD load combinations, kips

T_{aw} Required axial strength for the beam web in the vicinity of the tension bolts using ASD load combinations, kips

T_{awd} Required axial strength for the beam web to end-plate weld in the vicinity of the tension bolts using ASD load combinations, kips

T_b Specified bolt pretension force equal to $T_{b,full}$ for fully pretensioned or value from Table 3-3 if snug tight, kips

$T_{b,full}$ Minimum bolt pretension for fully pretensioned bolts per *Specification* Table J3.1, kips

T_{nw} Required tensile strength for the stiffener to end-plate weld, kips

T_r Connection required axial tensile strength, kips

$T_{r,calc}$ Beam flange axial force, kips

T_{rw} Required strength for beam web tension yielding, kips

T_u Connection required axial tensile strength using LRFD load combinations, kips

$T_{u,calc}$ Beam flange axial force calculated using LRFD load combinations, kips

T_{uf} Beam flange to end-plate weld required axial strength using LRFD load combinations, kips

$T_{u,min}$ Minimum beam flange to end-plate weld required axial strength using LRFD load combinations, kips

$T_{u,stiff}$ Required tension strength for column web stiffeners using LRFD load combinations, kips

$T_{u,ws}$ Required tension strength for web stiffener to end-plate connection using LRFD load combinations, kips

T_{uw} Required axial strength for the beam web in the vicinity of the tension bolts using LRFD load combinations, kips

T_{uwd} Required axial strength for the beam web to end-plate weld in the vicinity of the tension bolts using LRFD load combinations, kips

T_{yf} Nominal axial yield strength of the beam flange, kips

T_{yw} Nominal axial yield strength of the beam web in the vicinity of the tension bolts, kips

V_a Connection required shear strength using ASD load combinations, kips

V_{ac} Column required shear strength using ASD load combinations, kips

V_{ap} Required shear strength on the extended portion of the end plate using ASD load combinations, kips

V_{aw} Required shear strength for the stiffener to beam flange weld using ASD load combinations, kips

$V_{gravity}$ Factored beam shear resulting from the load combination $1.2D + f_1L + 0.15S$, kips

V_n Nominal shear transfer strength, kips

V_{nw} Nominal shear strength for the stiffener to beam flange weld, kips

V_r Connection required shear strength, kips

V_r^* Required shear strength for sloped connections, kips

V_{rc} Column required shear strength, kips

V_u Connection required shear strength using LRFD load combinations, kips

V_{ub} Beam required shear strength using LRFD load combinations, kips

V_{uc} Column required shear strength using LRFD load combinations, kips

V_{up} Required shear strength on the extended portion of the end plate using LRFD load combinations, kips

V_{upz} Panel zone required shear strength, kips

V_{uw} Required shear strength for the stiffener to beam flange weld using LRFD load combinations, kips

W_E External work for yield line analysis, kip-in.

W_I Internal work for yield line analysis, kip-in.

Y_p End-plate yield line mechanism parameter, in.

Y_c Column flange yield line mechanism parameter, in.

Y_{cu} Yield line mechanism parameter for column flange with no column web stiffeners, in.

Y_{cs} Yield line mechanism parameter for column flange with column web stiffeners, in.

Z_b Nominal plastic section modulus of beam, in.^{3}

Z_c Nominal plastic section modulus of column, in.^{3}

Z_e Effective plastic section modulus of beam, in.^{3}

Z_p Plastic section modulus along the yield line, in.^{3}

$Z_{2effective}$ Effective plastic section modulus at the bolt line, in.^{3}

a Distance from bolt line to the prying force, in.

a Width of the panel zone, in.

a Calculated distance from bolt line to the prying force when not at an edge, in.

a_v Width of panel zone used to calculate panel zone shear area, in.

b Distance from bolt line to the stem of the effective tee stub, in.

b_{bf} Width of beam flange, in.

b_{cf} Width of column flange, in.

$b_{cf,eff}$ Effective width of column flange, in.

b_{cp} Width of cap plate, in.

b_f Width of beam flange, in.

b_p Width of end plate, in.

$b_{p,eff}$ Effective width of end plate, in.

b_s Width of stiffener plate, in.

c Distance between bolt lines on either side of tension flange for column yield line pattern, in.

$clip$ Length of column stiffener clip, in.

d Depth of beam, in.

d_b Nominal bolt diameter, in.

$d_{b,reqd}$ Required nominal bolt diameter, in.

d_c Depth of column, in.

d_e Extension of end plate beyond the outer bolt line, in.

d_h Effective bolt hole diameter, in.

d_p Height of end plate, in.

d_z Height of the panel zone, d-$2t_f$ of the deeper beam at the connection, in.

f_1 Load factor determined by the applicable building code for live loads but not less than 0.5

g Bolt gage, in.

g_o Gage between outer bolt lines in four-wide bolt patterns, in.

h Height of beam web; for webs of rolled sections, the clear distance between corner fillets; for welded built-up sections, the distance between flanges, in.

h Height of panel zone, in.

h_c Height of column web; for webs of rolled sections, the clear distance between corner fillets; for welded built-up sections, the distance between flanges, in.

h_{dp} Width of doubler plate, in.

h_{st} Height of stiffener above beam flange, in.

h_{ws} Width of end-plate stiffener in stiffened flush connections, in.

h_1 Distance from the center of the beam compression flange to the farthest load-carrying bolt line, in.

h_2 Distance from the center of the beam compression flange to the second-farthest load-carrying bolt line, in.

h_3 Distance from the center of the beam compression flange to the third-farthest load-carrying bolt line, in.

h_4 Distance from the center of the beam compression flange to the fourth-farthest load-carrying bolt line, in.

k_c Distance from outer face of column flange to web toe of fillet, equal to k_{des} for rolled shapes, in.

k_{des} Smallest value of k used in production, in.

k_{det} Value of k used in detailing, in.

k_v Panel zone shear buckling coefficient

k_1 Distance from web centerline to flange toe of fillet, in.

l_b Length of bearing, in.

l_c Clear distance, in the direction of the force, between the edge of hole and the edge of the adjacent hole or edge of material, in.

l_{ci} Clear distance, in the direction of the force, between the edge of hole and the edge of the adjacent hole or edge of material for interior bolt holes, in.

l_{cpf} Contact length between the continuity plates and column flange, in.

l_{cpw} Contact length between the continuity plates and column web, in.

l_{stiff} Length of column web stiffener, in.

l_t Height of beam web not included in the tension region, in.

l_w Length of the beam flange to end-plate weld, in.

l_w Length of the cap plate to panel zone weld, in.

l_{wt} Length of beam web to end-plate weld in the tension region, in.

l_{wv} Length of the beam web to end-plate fillet weld used to resist shear, in.

$l_{0.5w}$ Height of beam web for half of the beam depth, in.

m_p Plastic moment strength of a plate per unit length along a yield line, kip-in./in.

n Total number of tension bolts

n_b Number of bolts at the compression flange

n_{trib} Number of tension bolts adjacent to the web

p_b Center-to-center distance between bolt lines, in.

p_{cp} Distance from first inner bolt line to the inner face of column cap plate, in.

p_{ext} End-plate extension beyond the exterior face of beam tension flange, in.

p_f Distance from bolt line adjacent to the beam tension flange to the near face of beam tension flange, in.

p_{fi} Distance from first inner bolt line to inner face of beam tension flange, in.

p_{fo} Distance from first outer bolt line to outer face of beam tension flange, in.

p_s Distance from bolt line to face of end-plate stiffener, in.

p_{si} Distance from first inner bolt line to inner face of column stiffener, in.

p_{si} Distance from inner bolt line to face of end-plate stiffener, in.

p_{so} Distance from first outer bolt line to outer face of column stiffener, in.

p_{so} Distance from outer bolt line to face of end-plate stiffener, in.

q Uniform pressure applied to plate, ksi.

r_c Radius of stiffener clip, in.

r_n Bearing/tearout strength of an individual bolt, kips

r_{ni} Bearing/tearout strength of an individual interior bolt, kips

r_{no} Bearing/tearout strength of an individual outer bolt, kips

s Distance from the bolt line to an adjacent yield line where the plate extends beyond, in.

t End plate or column flange thickness, in.

t_{bf} Beam flange thickness, in.

t_{bw} Beam web thickness, in.

t_{cap} Thickness of cap plate, in.

t_{cf} Thickness of column flange, in.

$t_{cf,req}$ Required thickness of column flange, in.

t_{cp} Thickness of continuity plates, in.

$t_{cp,req}$ Required thickness of continuity plates, in.

t_{cw} Thickness of column web, in.

$t_{cw,req}$ Required thickness of column web, in.

t_{dp}	Thickness of doubler plates, in.
t_p	End-plate thickness, in.
$t_{p,req}$	Required end-plate thickness, in.
t_s	Stiffener thickness, in.
$t_{s,req}$	Required stiffener thickness, in.
t_{weld}	Leg dimension of fillet weld, in.
$t_{weld,req}$	Required leg dimension of fillet weld, in.
t_{ws}	Thickness of end-plate stiffener in stiffened flush connections, in.
w	Width of the effective tee stub, in.
w	Leg size of double fillet weld if used in the beam flange-to-end-plate weld, in.
w'	Width of effective tee stub minus the nominal bolt hole diameter, in.
w_{cp}	Width of continuity plate, in.
w_z	Width of the panel zone between column flanges, in.
Δ	Drift due to lateral forces, in.
Δ_{actual}	Peak drift due to unreduced lateral forces, in.
$\Delta_{elastic\ design}$	Elastic design drift due to lateral forces, in.
ΣM_{be}^*	Sum of the projections of the expected flexural strengths of the beams at the plastic hinge locations to the column centerline, kip-in.
ΣM_{pc}^*	Sum of the projections of the nominal flexural strengths of the columns (including haunches where used) above and below the joint to the beam centerline with a reduction for the axial force in the column, kip-in.
Ω	Safety factor
Ω	Safety factor for bolt rupture = 2.00
Ω	Safety factor for weld rupture = 2.00
Ω_b	Safety factor for flexure = 1.67
α	Reduction in bolt contribution for calculation of M_q connection flexural strength
α	1.0 (LRFD) or 1.6 (ASD)
α_s	1.0 (LRFD) or 1.5 (ASD)
δ	Virtual displacement used in yield line analysis, in.
δ_{max}	Average virtual displacement used in yield line analysis, in.
γ_r	Load factor to limit connection rotation at ultimate moment to 10% of simple span rotation; 0.80 for flush end-plate configurations and 1.0 for extended end-plate configurations
θ	Beam end rotation, rad
θ	Rotation at a yield line, rad
θ	Angle of loading measured from weld longitudinal axis, degrees
θ	Angle between the beam longitudinal axis and the end plate, degrees
θ_x	Rotation of facet n about the x-axis, rad
θ_y	Rotation of facet n about the y-axis, rad
θ_x	Component of yield line rotation about the x-axis, rad
θ_y	Component of yield line rotation about the y-axis, rad
λ	Width-to-thickness ratio for the element
λ_{hd}	Limiting width-to-thickness ratio for highly ductile compression elements
λ_r	Stiffener limiting width-to-thickness ratio for local buckling
$\sigma_{effective}$	Effective yield stress considering reduction for applied shear stress, ksi
ϕ	Resistance factor
ϕ	Resistance factor for weld rupture = 0.75
ϕ_b	Resistance factor for flexure = 0.90
ϕ_d	Resistance factor for ductile limit states = 1.00
ϕ_n	Resistance factor for nonductile limit states = 0.90
ϕ_r	Resistance factor for bolt rupture = 0.75
ϕ_v	Resistance factor for shear
4E	Four-bolt unstiffened extended end plate
4ES	Four-bolt extended stiffened end plate
8ES	Eight-bolt extended stiffened end plate
12ES	12-bolt extended stiffened end plate

References

Abar, B.M., Ghobadi, M.S., and Jazany, R.A. (2020), "Double Shear Bolted Bracket Moment Connections, Part 2: Four-Bolt Configuration Response Evaluation," *Journal of Constructional Steel Research*, Vol. 174.

Abel, M.S.M. and Murray, T.M. (1992), "Multiple Row, Extended Unstiffened End-Plate Connection Tests," Virginia Tech Structural Engineering Report No. CE/VPI-ST-02/04, Virginia Polytechnic Institute and State University, Blacksburg, Va.

Abel, M.S.M. and Murray, T.M. (1994), "Analytical and Experimental Investigation of the Extended Unstiffened Moment End-Plate Connection with Four Bolts at the Beam Tension Flange," Virginia Tech Structural Engineering Report No. CE/VPI-ST-93/08, Virginia Polytechnic Institute and State University, Blacksburg, Va.

Abidelah, A., Bouchair, A., and Kerdal, D.E. (2012), "Experimental and Analytical Behavior of Bolted End-Plate Connections without Stiffeners," *Journal of Constructional Steel Research*, Vol. 76, pp. 13–27.

Abolmaali, A., Kukreti, A., and Murray, T.M. (1984), "Finite Element Analysis of Two Tension Bolt Flush End-Plate Connections," FEARS Structural Engineering Laboratory Report No. FSEL/MBMA 84-01, University of Oklahoma, Norman, Okla.

Abolmaali, A., Matthys, J.H., Farooqi, M., and Choi, Y. (2005), "Development of Moment-Rotation Model Equations for Flush End-Plate Connections," *Journal of Constructional Steel Research*, Vol. 61, pp. 1,592–1,612.

Adey, B.T., Grondin, G.Y., and Cheng, J.J.R. (2000), "Cyclic Loading of End Plate Moment Connections," *Canadian Journal of Civil Engineering*, Vol. 27, pp. 683–701.

Agerskov, H. (1976), "High-Strength Bolted Connections Subject to Prying," *Journal of the Structural Division*, Vol. 102, No. 1, pp. 161–175.

Ahuja, V., Kukreti, A., and Murray, T.M. (1982), "Analysis of Stiffened End-Plate Connections Using the Finite Element Method," FEARS Structural Engineering Laboratory Report No. FSEL/AISC 82-01, University of Oklahoma, Norman, Okla.

AISC (1970), *Steel Construction Manual*, 7th Ed., American Institute of Steel Construction, New York, N.Y.

AISC (2017a), *Steel Construction Manual*, 15th Ed., American Institute of Steel Construction, Chicago, Ill.

AISC (2017b), *Design Examples*, Version 15.0, American Institute of Steel Construction, Chicago, Ill.

AISC (2018), *Seismic Design Manual,* 3rd Ed., American Institute of Steel Construction, Chicago, Ill.

AISC (2022a), *Code of Standard Practice for Steel Buildings and Bridges*, ANSI/AISC 303-22, American Institute of Steel Construction, Chicago, Ill.

AISC (2022b), *Prequalified Connections for Special and Intermediate Steel Moment Frames for Seismic Applications,* ANSI/AISC 358-22, American Institute of Steel Construction, Chicago, Ill.

AISC (2022c), *Seismic Provisions for Structural Steel Buildings*, ANSI/AISC 341-22, American Institute of Steel Construction, Chicago, Ill.

AISC (2022d), *Specification for Structural Steel Buildings*, ANSI/AISC 360-22, American Institute of Steel Construction, Chicago, Ill.

Alhendi, H. and Celikag, M. (2015a), "Behavior of Reverse-Channel and Double-Reverse-Channel Connections to Tubular Columns with HSS," *Journal of Constructional Steel Research*, Vol. 112, pp. 271–281.

Alhendi, H. and Celikag, M. (2015b), "Parametric Study on Moment-Rotation Characteristics of Reverse Channel Connections to Tubular Columns," *Journal of Constructional Steel Research*, Vol. 104, pp. 261–273.

Alhendi, H. and Celikag, M. (2015c), "Finite Element Prediction of Reverse Channel Connections to Tubular Columns Behavior," *Engineering Structures*, Vol. 100, pp. 599–609.

Al-Jabri, K.S., Lennon, T., Burgess, I.W., and Plank, R.J. (1998), "Behaviour of Steel and Composite Beam-Column Connections in Fire," *Journal of Constructional Steel Research*, Vol. 46, No. 1-3, pp. 308–309.

Al-Jabri, K.S., Seibi, A., and Karrech, A. (2006), "Modelling of Unstiffened Flush End-Plate Bolted Connections in Fire," *Journal of Constructional Steel Research*, Vol. 62, pp. 151–159.

Al-Rifaie, A., Guan, Z.W., Jones, S.W., and Wang, Q. (2017), "Lateral Impact Response of End-Plate Beam Column Connections," *Engineering Structures*, Vol. 151, pp. 221–234.

Al-Rifaie, A., Jones, S.W., Wang, Q.Y., and Guan, Z.W. (2018), "Experimental and Numerical Study on Lateral Impact Response of Concrete Filled Steel Tube Columns with End Plate Connections," *International Journal of Impact Engineering*, Vol. 121, pp. 20–34.

Anderson, D. and Najafi, A.A. (1994), "Performance of Composite Connections: Major Axis End Plate Joints," *Journal of Constructional Steel Research*, Vol. 31, pp. 31–57.

Anis, S., Tahir, M.M., Arizu, S., Shek, P.N., Tan, C.S., and Kueh, A.B.H. (2011), "Behaviour of Composite Beam with Trapezoid Web Profiled Steel Section in Sub-Assemblage Frame," *Advanced Materials Research*, Vol. 250–253, pp. 1,271–1,274.

Aribert, J.M. and Dinga, O.N. (2000), "Modeling and Experimental Investigation of Bolted Flush End-Plate Composite Beam-to-Column Joints," *Composite Construction in Steel and Concrete IV Conference*, Banf, Alberta.

ASCE (2022), *Minimum Design Loads and Associated Criteria for Buildings and Other Structures*, ASCE/SEI 7-22, American Society of Civil Engineers, Reston, Va.

ASTM (2015), *Standard Specification for "Twist Off" Type Tension Control Structural Bolt/Nut/Washer Assemblies, Alloy Steel, Heat Treated, 200 ksi Minimum Tensile Strength*, ASTM F3043-15, ASTM International, West Conshohocken, Pa.

ASTM (2016), *Standard Specification for Heavy Hex Structural Bolt/Nut/Washer Assemblies, Alloy Steel, Heat Treated, 200 ksi Minimum Tensile Strength*, ASTM F3111-16, ASTM International, West Conshohocken, Pa.

ASTM (2017), *Standard Specification for High Strength Structural Bolt Assemblies, Steel and Alloy Steel, Heat Treated, 144 ksi Minimum Tensile Strength, Inch Dimensions*, ASTM F3148-17a, ASTM International, West Conshohocken, Pa.

ASTM (2019a), *Standard Specification for Carbon Structural Steel*, ASTM A36/A36M-19, ASTM International, West Conshohocken, Pa.

ASTM (2019b), *Standard Specification for General Requirements for Rolled Structural Steel Bars, Plates, Shapes, and Sheet Piling*, ASTM A6/A6M-19, ASTM International, West Conshohocken, Pa.

ASTM (2019c), *Standard Specification for High-Strength Carbon-Manganese Steel of Structural Quality*, ASTM A529/A529M-19, ASTM International, West Conshohocken, Pa.

ASTM (2019d), *Standard Specification for High Strength Structural Bolts and Assemblies, Steel and Alloy Steel, Heat Treated, Inch Dimensions 120 ksi and 150 ksi Minimum Tensile Strength, and Metric Dimensions 830 MPa and 1040 MPa Minimum Tensile Strength*, ASTM F3125/F3125M-19e2, ASTM International, West Conshohocken, Pa.

ASTM (2020), *Standard Specification for Structural Steel Shapes*, ASTM A992/A992M-20, ASTM International, West Conshohocken, Pa.

ASTM (2021), *Standard Specification for High-Strength Low-Alloy Columbium-Vanadium Structural Steel*, ASTM A572/A572M-21e1, ASTM International, West Conshohocken, Pa.

Ataei, A. and Bradford, M.A. (2014), "Parametric Studies of Semi-Rigid Flush End Plate Joints with Concrete-Filled Steel Tubular Columns," *Applied Mechanics and Materials*, Vol. 553, pp. 588–593.

Ataei, A., Bradford, M.A., and Valipour, H.R. (2015a), "Moment-Rotation Model for Blind-Bolted Flush End-Plate Connections in Composite Frame Structures," *Journal of Structural Engineering*, Vol. 141, No. 9.

Ataei, A., Bradford, M.A., and Valipour, H.R. (2015b), "Experimental Study of Flush End Plate Beam-to-CFST Column Composite Joints with Deconstructable Bolted Shear Connectors," *Engineering Structures*, Vol. 99, pp. 616–630.

Ataei, A., Bradford, M.A., and Liu, X. (2016a), "Experimental Study of Flush End Plate Beam-to-Column Composite Joints with Precast Slabs and Deconstructable Bolted Shear Connectors," *Structures*, Vol. 7, pp. 43–58.

Ataei, A., Bradford, M.A., and Valipour, H.R. (2016b), "Finite Element Analysis of HSS Semi-Rigid Composite Joints with Precast Concrete Slabs and Demountable Bolted Shear Connectors," *Finite Elements in Analysis and Design*, Vol. 122, pp. 16–38.

Ataei, A., Bradford, M.A., and Liu, X. (2017), "Computational Modelling of the Moment-Rotation Relationship for Deconstructable Flush End Plate Beam-to-Column Composite Joints," *Journal of Constructional Steel Research*, Vol. 129, pp. 75–92.

Augusto, H., Castro, J.M., Rebelo, C., and Simoes da Silva, L. (2019), "Ductility-Equivalent Viscous Damping Relationships for Beam-to-Column Partial-Strength Steel Joints," *Journal of Earthquake Engineering*, Vol. 23, No. 5, pp. 810–836.

Augusto, H., Simoes da Silva, L., Rebelo, C., and Castro, J.M. (2017), "Cyclic Behaviour Characterization of Web Panel Components in Bolted End-Plate Steel Joints," *Journal of Constructional Steel Research*, Vol. 133, pp. 310–333.

AWS (2016), *Structural Welding Code—Seismic Supplement*, AWS D1.8/D1.8M:2016, American Welding Society, Miami, Fla.

AWS (2020), *Structural Welding Code—Steel*, AWS D1.1/D1.1M:2020, American Welding Society, Miami, Fla.

Aydin, A.C., Maali, M., Kilic, M., and Sagiroglu, M. (2015), "Experimental Investigation of Sinus Beams with End-Plate Connections," *Thin-Walled Structures*, Vol. 97, pp. 35–43.

Baei, M., Ghassemieh, M., and Goudarzi, A. (2012), "Numerical Modelling of End-Plate Moment Connection Subjected to Bending and Axial Forces," *Journal of Mathematics and Computer Science*, Vol. 4, No. 3, pp. 463–472.

Bahaari, M.R. and Sherbourne, A.N. (1994), "Computer Modelling of an Extended End-Plate Bolted Connection," *Computers & Structures*, Vol. 52, No. 5, pp. 879–893.

Bahaari, M.R. and Sherbourne, A.N. (1996), "Structural Behavior of End-Plate Bolted Connections to Stiffened Columns," *Journal of Structural Engineering*, Vol. 122, No. 8, pp. 926–935.

Bahaari, M.R. and Sherbourne, A.N. (1997), "Finite Element Prediction of End Plate Bolted Connection Behavior II: Analytic Formulation," *Journal of Structural Engineering*, Vol. 123, No. 2, pp. 165–175.

Bai, R., Chan, S.L., and Hao, J.P. (2015), "Improved Design of Extended End-Plate Connection Allowing for Prying Effects," *Journal of Constructional Steel Research*, Vol. 113, pp. 13–27.

Balc, R., Chira, A., and Chira, N. (2012), "Finite Element Analysis of Beam to Column End Plate Bolted Connection," *Acta Technica Napocensis: Civil Engineering & Architecture*, Vol. 55, No. 1, pp. 24–29.

Baumberger, A.M. (2005), "Finite Element Analysis of Shear in the Panel Zone of Steel Gable Frames," M.S. Thesis, Virginia Tech, Blacksburg, Va.

Beamish, M.J. and Butterworth, J.W. (1984), "Seismic Behaviour of Steel Portal Frame Knee Joints," University of Auckland, Department of Civil Engineering, Report No. 348, University of Auckland, Auckland, New Zealand.

Bjorhovde, R., Brozzetti, J., and Colson, A. (1987), "Classification of Connections," *Proceedings of Connections in Steel Structures—Behaviour, Strength and Design,* Cachan, France, pp. 388–391.

Bjorhovde, R., Colson, A., and Brozzeti, J. (1990), "Classification System for Beam-to-Column Connections," *Journal of Structural Engineering*, Vol. 116, No. 11, pp. 3,059–3,076.

Blumenbaum, S. and Murray, T.M. (2003), "Strength Evaluation of Four Extended Moment End-Plate Connections," Virginia Tech Structural Engineering and Materials Report No. CEE/VPI-ST-04/02, Virginia Polytechnic Institute and State University, Blacksburg, Va.

Blumenbaum, S. and Murray, T.M. (2004), "Response of Cyclically Loaded Extended End-Plate Moment Connections When Used with Welded Built-Up Sections," Virginia Tech Structural Engineering and Materials Report No. CEE/VPI-ST-04/02, Virginia Polytechnic Institute and State University, Blacksburg, Va.

Bond, D.E. and Murray, T.M. (1989), "Analytical and Experimental Investigation of a Flush Moment End-Plate Connection with Six Bolts at the Tension Flange," Virginia Tech Structural Engineering Report No. CE/VPI-ST-89/10, Virginia Polytechnic Institute and State University, Blacksburg, Va.

Boorse, M.R. and Murray, T.M. (1999), "Evaluation of the Inelastic Rotation Capability of Flush End-Plate Moment Connections," Virginia Tech Structural Engineering Report No. CE/VPI-ST 99/09, Virginia Polytechnic Institute and State University, Blacksburg, Va.

Borgsmiller, J.T. (1995), "Simplified Method for Design of Moment End-Plate Connections," M.S. Thesis, Virginia Tech, Blacksburg, Va.

Borgsmiller, J.T., Sumner, E.A., and Murray, T.M. (1995), "Extended Unstiffened Moment End-Plate Connection Tests," Virginia Tech Structural Engineering Report No. CE/VPI-95/13, Virginia Polytechnic Institute and State University, Blacksburg, Va.

Braconi, A., Bursi, O.S., Fabbrocino, G., Salvatore, W., Taucer, F., and Tremblay, R. (2008), "Seismic Performance of a 3D Full-Scale High-Ductile Steel-Concrete Composite Moment-Resisting Frame—Part II: Test Results and Analytical Validation," *Earthquake Engineering and Structural Dynamics*, Vol. 37, pp. 1,635–1,655.

Braconi, A., Elamary, A., and Salvatore, W. (2010), "Seismic Behaviour of Beam-to-Column Partial-Strength Joints for Steel-Concrete Composite Frames," *Journal of Constructional Steel Research*, Vol. 66, pp. 1,431–1,444.

Brown, N.D. and Anderson, D. (2001), "Structural Properties of Composite Major Axis End Plate Connections," *Journal of Constructional Steel Research*, Vol. 57, pp. 327–349.

Buzuleac, S.L. (2013), "Finite Element Analysis of Beam-Column Bolted End-Plate Connections in Steel Frames," *Buletinul Institutului Politehnic Din Iasi, Sectia Constructil Architectura*, Vol. 59, No. 4, pp. 117–129.

CEN (2005), *EN 1993-1-1—Eurocode 3: Design of Steel Structures*, European Committee for Standardization, Brussels, Belgium.

Cerfontaine, F. and Jaspart, J.P. (2002), "Analytical Study of the Interaction between Bending and Axial Force in Bolted Joints," *Eurosteel Conference*, Coimbra, Portugal, pp. 997–1,006.

Chasten, C.P., Lu, L.W., and Driscoll, G.C. (1992), "Prying and Shear in End-Plate Connection Design," *Journal of Structural Engineering*, Vol. 118, No. 5, pp. 1,295–1,311.

Chen, X. and Shi, G. (2016), "Finite Element Analysis and Moment Resistance of Ultra-Large Capacity End-Plate Joints," *Journal of Constructional Steel Research*, Vol. 126, pp. 153–162.

Chen, X. and Shi, G. (2018), "Experimental Study of End-Plate Joints with Box Columns," *Journal of Constructional Steel Research*, Vol. 143, pp. 307–319.

Chen, Y. and Wang, S. (2009), "Research on End-Plate Connection with Non-Completely Penetrated Welds," *Journal of Constructional Steel Research*, Vol. 65, pp. 228–236.

Choi, C.K. and Chung, G.T. (1996), "Refined Three Dimensional Finite Element Model for End-Plate Connections," *Journal of Structural Engineering*, Vol. 122, No. 11, pp. 1,307–1,316.

Coelho, A.M.G. and Bijlaard, F.S.K. (2007), "Experimental Behaviour of High Strength Steel End-Plate Connections," *Journal of Constructional Steel Research*, Vol. 63, pp. 1,228–1,240.

Coelho, A.M.G. and Bijlaard, F. (2010), "High Strength Steel in Buildings and Civil Engineering Structures: Design of Connections," *Advances in Structural Engineering*, Vol. 13, No. 3, pp. 413–429.

Coelho, A.M.G., Bijlaard, F.S.K., and Simoes da Silva, L. (2004), "Experimental Assessment of the Ductility of Extended End Plate Connections," *Engineering Structures*, Vol. 26, pp. 1,185–1,206.

Coelho, A.M.G., Simoes da Silva, L. and Bijlaard, F.S.K. (2006), "Ductility Analysis of Bolted Extended End Plate Beam-to-Column Connections in the Framework of the Component Method," *Steel and Composite Structures*, Vol. 6, No. 1, pp. 33–53.

Cristutiu, I.M. and Dubina, D. (2010), "Influence of Member Components on the Structural Performance of Beam-to-Column Joints of Pitched Roof Portal Frames with Class 3 and 4 Sections," *SDSS'Rio 2010 Stability and Ductility of Steel Structures*, Rio De Janeiro, Brazil, pp. 191–198.

Curtis, L.E. (1985), "Unstiffened and Washer Plate Stiffened Column Flanges at Moment End-Plate Connections," M.S. Thesis, University of Oklahoma, Norman, Okla.

Curtis, L.E. and Murray, T.M. (1989), "Column Flange Strength at Moment End-Plate Connections," *Engineering Journal*, Vol. 26, No. 2, pp. 41–50.

D'Aniello, M., Tartaglia, R., Costanzo, S., Campanella, G., Landolfo, R., and De Martino, A. (2018), "Experimental Tests on Extended Stiffened End-Plate Joints within Equal Joints Project," *Key Engineering Materials*, Vol. 763, pp. 406–413.

D'Aneillo, M., Tartaglia, R., Costanzo, S., and Landolfo, R. (2017), "Seismic Design of Extended Stiffened End-Plate Joints in the Framework of Eurocodes," *Journal of Constructional Steel Research*, Vol. 128, pp. 512–527.

Davis, D.B. (1996), "LRFD Evaluation of Full-Scale Metal Building Rigid Frame Tests," M.S. Thesis, Virginia Tech, Blacksburg, Va.

Davis, D.B., Simon, R., Shope, R., and Murray, T.M. (1995a), "Lateral Load Test of Kawada Industries Rigid Frames," Virginia Tech Structural Engineering and Materials Report No. CE/VPI-ST-95/15, Virginia Polytechnic Institute and State University, Blacksburg, Va.

Davis, D.B., Shope, R., Simon, R., and Murray, T.M. (1995b), "Gravity Loading Test of Kawada Industries Rigid Frame," Virginia Tech Structural Engineering and Materials Report No. CE/VPI-ST-95/14, Virginia Polytechnic Institute and State University, Blacksburg, Va.

De Lima, L.R.O., Simoes da Silva, L., da S. Vellasco, P.C.G., and de Andrade, S.A.L. (2004), "Experimental Evaluation of Extended Endplate Beam-to-Column Joints Subjected to Bending and Axial Force," *Engineering Structures*, Vol. 26, pp. 1,333–1,347.

Del Savio, A.A., Nethercot, D.A., Vellasco, P.C.G.S., de Lima, L.R.O., Andrade, S.A.L., and Martha, L.F. (2010), "An Assessment of Beam-to-Column Endplate and Baseplate Joints Including the Axial-Moment Interaction," *Advanced Steel Construction*, Vol. 6, No. 1, pp. 548–566.

Diaz, C., Victoria, M., Marti, P., and Querin, O.M. (2011), "FE Model of Beam-to-Column Extended End-Plate Joints," J*ournal of Constructional Steel Research*, Vol. 67, pp. 1,578–1,590.

Dinu, F., Marginean, I., and Dubina, D. (2017), "Experimental Testing and Numerical Modelling of Steel Moment-Frame Connections Under Column Loss," *Engineering Structures*, Vol. 151, pp. 861–878.

Dominisse, K. and Murray, T.M. (2004), "Strength Evaluation of Weak-Axis Extended Moment End-Plate Connection with Lightweight Concrete Slab," Virginia Tech Structural Engineering and Materials Report No. CEE/VPI-ST-04/03, Virginia Polytechnic Institute and State University, Blacksburg, Va.

Douty, R.T. and McGuire, W. (1965), "High Strength Bolted Moment Connections," *Journal of the Structural Division*, Vol. 91, No. 2, pp. 101–128.

Dunai, L., Fukumoto, Y., and Ohtani, Y. (1996), "Behaviour of Steel-to-Concrete Connections under Combined Axial Force and Cyclic Bending," *Journal of Constructional Steel Research*, Vol. 36, No. 2, pp. 121–147.

Eatherton, M.R., Chen, Y., Laknejadi, K., and Murray, T.M. (2017), "Using Longitudinal Stiffeners to Mitigate Buckling of Noncompact and Slender Beam Webs in Ductile Moment Frame Connections," *Annual Stability Conference Structural Stability Research Council*, San Antonio, Tex.

Eatherton, M.R., Nguyen, T.N., and Murray, T.M. (2021), "Yield Line Patterns for End-Plate Moment Connections," Virginia Tech Structural Engineering and Materials Report No. CE/VPI-ST-21/05, Virginia Polytechnic Institute and State University, Blacksburg, Va.

Eatherton, M.R., Toellner, B.W., Watkins, C.E., and Abbas, E. (2013), "The Effect of Powder Actuated Fasteners on the Seismic Performance of Protected Zones in Steel Moment Frames," Virginia Tech Structural Engineering and Materials Report No. CE/VPI-ST-13/05, Virginia Polytechnic Institute and State University, Blacksburg, Va.

El-Khoriby, S., Sakr, M.A., Khalifa, T.M., and Eladly, M.M. (2017), "Modelling and Behaviour of Beam-to-Column Connections under Axial Force and Cyclic Bending," *Journal of Constructional Steel Research*, Vol. 129, pp. 171–184.

El Sabbagh, A., Sharaf, T., Nagy, S., and El Ghandour, M. (2019), "Behavior of Extended End-Plate Bolted Connections Subjected to Monotonic and Cyclic Loads," *Engineering Structures*, Vol. 190, pp. 142–159.

Erfani, S., Asnafi, A.A., and Goudarzi, A. (2016), "Connection of I-Beam to Box-Column by a Short Stub Beam," *Journal of Constructional Steel Research*, Vol. 127, pp. 136–150.

Fanaie, N. and Monfared, M.N. (2016), "Cyclic Behavior of Extended End-Plate Connections with Shape Memory Alloy Bolts," *Structural Engineering and Mechanics*, Vol. 60, No. 3, pp. 507–527.

Fang, C., Yam, M.C.H., Lam, A.C.C., and Xie, L. (2014), "Cyclic Performance of Extended End-Plate Connections Equipped with Shape Memory Alloy Bolts," *Journal of Constructional Steel Research*, Vol. 94, pp. 122–136.

Farmani, M.A. and Ghassemieh, M. (2016), "Shape Memory Alloy-Based Moment Connections with Superior Self-Centering Properties," *Smart Materials and Structures*, Vol. 25, pp. 1–17.

FEMA (2000), *Recommended Seismic Design Criteria for New Steel Moment-Frame Buildings*, FEMA 350, Federal Emergency Management Agency, Washington D.C.

Fink, R.B., Sumner, E.A., and Murray, T.M. (2001), "Moment End-Plate to Column Flange Testing of Rack Components," Virginia Tech Structural Engineering and Materials Report No. CE/VPI-ST-01/07, Virginia Polytechnic Institute and State University, Blacksburg, Va.

Fisher, J.W., Lee, G.X., Yura, J.A., and Driscoll, G.C., Jr. (1963), *Plastic Analysis and Tests of Haunched Corner Connections*, Bulletin No. 91, Welding Research Council, Shaker Heights, Ohio.

Fleischman, R.B., Chasten, C.P., Lu, L.W., and Driscoll, G.C. (1989), "Top-and-Seat-Angle Connections and End-Plate Connections: Snug vs. Fully Pretensioned Bolts," ATLSS Report No. 89-06, Lehigh University, Bethlehem, Pa.

Fleischman, R.B., Chasten, C.P., Lu, L.W., and Driscoll, G.C. (1991), "Top-and-Seat-Angle Connections and End-Plate Connections: Snug vs. Fully Pretensioned Bolts," *Engineering Journal*, Vol. 28, No. 1, pp. 18–28.

Forest, R., and Murray, T.M. (1982), "Rigid Frame Studies Final Report Full Scale Frame Tests," FEARS Structural Engineering Laboratory Research Report No. FSEL/STAR 82-01, University of Oklahoma, Norman, Okla.

Francavilla, A.B., Latour, M., Piluso, V., and Rizzano, G. (2018), "Design of Full-Strength Full-Ductility Extended End-Plate Beam-to-Column Joints," *Journal of Constructional Steel Research*, Vol. 148, pp. 77–96.

Fu, F. and Lam, D. (2006), "Experimental Study on Semi-Rigid Composite Joints with Steel Beams and Precast Hollowcore Slabs," *Journal of Constructional Steel Research*, Vol. 62, pp. 771–782.

Fu, F., Lam, D., and Ye, J. (2008), "Modelling Semi-Rigid Composite Joints with Precast Hollowcore Slabs in Hogging Moment Region," *Journal of Constructional Steel Research*, Vol. 64, pp. 1,408–1,419.

Garoosi, A.M., Tahamouli Roudsari, M., and Hashemi, B.H. (2018), "Experimental Evaluation of Rigid Connection with Reduced Section and Replaceable Fuse," *Structures*, Vol. 16, pp. 390–404.

Ghaderi, M., Gerami, M., and Vahdani, R. (2020), "Performance Assessment of Bolted Extended End-Plate Moment Connections Constructed from Grade St-37 Steel Subjected to Fatigue," *Journal of Materials in Civil Engineering*, Vol. 32, No. 5.

Gerami, M., Saberi, H., Saberi, V., and Daryan, A.S. (2011), "Cyclic Behavior of Bolted Connections with Different Arrangements of Bolts," *Journal of Constructional Steel Research*, Vol. 67, pp. 690–705.

Ghassemieh, M., Baei, M., Kari, A., Goudarzi, A., and Laefer, D.F. (2015), "Adopting Flexibility of the End-Plate Connections in Steel Moment Frames," *Steel and Composite Structures*, Vol. 18, No. 5, pp. 1,215–1,237.

Ghassemieh, M., Jalalpour, M., and Gholampour, A.A. (2014b), "Numerical Evaluation of the Extended Endplate Moment Connection Subjected to Cyclic Loading," *Current Advances in Civil Engineering*, Vol. 2, No. 1, pp. 35–43.

Ghassemieh, M., Kukreti, A., and Murray, T.M. (1983), "Inelastic Finite Element Analysis of Stiffened End-Plate Moment Connections," FEARS Structural Engineering Laboratory Report No. FSEL/AISC 83-02, University of Oklahoma, Norman, Okla.

Ghassemieh, M., Shamim, I., and Gholampour, A.A. (2014a), "Influence of the Axial Force on the Behavior of Endplate Moment Connections," *Structural Engineering and Mechanics*, Vol. 49, No. 1, pp. 23–40.

Ghobarah, A., Korol, R.M., and Osman, A. (1992), "Cyclic Behavior of Extended End-Plate Joints," *Journal of Structural Engineering*, Vol. 118, No. 5, pp. 1,333–1,353.

Ghobarah, A., Osman, A., and Korol, R.M. (1990), "Behaviour of Extended End-Plate Connections under Cyclic Loading," *Engineering Structures*, Vol. 12, No. 1, pp. 15–27.

Ghobarah, A. and Ramadan, T. (1994), "Bolted Link-Column Joints in Eccentrically Braced Frames," *Engineering Structures*, Vol. 16, No. 1, pp. 33–41.

Gillman, C.L. (2004), "Finite Element Analysis of Shear in the Panel Zone of a Steel Gable Frame," M.S. Thesis, Virginia Tech, Blacksburg, Va.

Goudarzi, A., Ghassemieh, M., and Baei, M. (2012), "The Effect of Axial Force on the Behavior of Flush End-plate Moment Connections," *15th World Conference on Earthquake Engineering*, Lisbon, Portugal.

Gracia, J., Bayo, E., Ferrario, F., and Bursi, O. (2010a), "The Seismic Performance of a Semi-Rigid Composite Joints with a Double-Sided Extended End-Plate. Part II: Seismic Simulations," *Engineering Structures*, Vol. 32, pp. 397–408.

Gracia, J., Bayo, E., Ferrario, F., Bursi, O., Braconi, A., and Salvatore, W. (2010b), "The Seismic Performance of a Semi-Rigid Composite Joint with a Double-Sided Extended End-Plate. Part I: Experimental Research," *Engineering Structures*, Vol. 32, pp. 385–396.

Green, T. and Schlafly, T. (2011) "Design and Detailing Welded Skewed T-Joints," *Proceedings of the ASCE Structures Congress*, Las Vegas, Nev., April 14-16.

Griffiths, J.D. (1984), "End-Plate Moment Connections—Their Use and Misuse," With Errata, *Engineering Journal*, Vol. 21, No. 1, pp. 32–34.

Grogan, W. and Surtees, J.O. (1999), "Experimental Behaviour of End Plate Connections Reinforced with Bolted Backing Angles," *Journal of Constructional Steel Research*, Vol. 50, pp. 71–96.

Guo, B., Gu, Q., and Liu, F. (2006), "Experimental Behavior of Stiffened and Unstiffened End-Plate Connections under Cyclic Loading," *Journal of Structural Engineering*, Vol. 132, No. 9, pp. 1,352–1,357.

Guo, L., Wang, J., Wang, W., and Wang, C. (2020), "Cyclic Tests and Analyses of Extended Endplate Composite Connections to CFDST Columns," *Journal of Constructional Steel Research*, Vol. 167.

Hajjar, J.F., Leon, R.T., Gustafson, M.A., and Shield, C.K. (1988), "Seismic Response of Composite Moment-Resisting Connections. II: Behavior," *Journal of Structural Engineering*, Vol. 124, No. 8, pp. 877–885.

Hasan, R., Kishi, N., Chen, W.F., and Komuro, M. (1997), "Evaluation of Rigidity of Extended End-Plate Connections," *Journal of Structural Engineering*, Vol. 123, No. 12, pp. 1,595–1,602.

Hendrick, D., Kukreti, A.R., and Murray, T.M. (1984), "Analytical and Experimental Investigation of Stiffened Flush End-Plate Connections with Four Bolts at the Tension Flange," FEARS Structural Engineering Laboratory Report No. FSEL/MBMA 84-02, University of Oklahoma, Norman, Okla.

Hendrick, D., Kukreti, A., and Murray, T.M. (1985), "Unification of Flush End-Plate Design Procedures," FEARS Structural Engineering Laboratory Report No. FSEL/MBMA 85-01, University of Oklahoma, Norman, Okla.

Hendrick, R.A. (1983), "Column Strength at End-Plate Connections," M.S. Thesis, University of Oklahoma, Norman Okla.

Hong, J.K. and Uang, C.M. (2012), "Cyclic Testing of a Metal Building Moment Frame System with Web-Tapered Members," *Journal of Constructional Steel Research*, Vol. 70, pp. 248–255.

Hoseinzadeh, M., Saeidzadeh, M., and Momenzadeh, S. (2019), "Evaluation of Frication Strength Loss in Endplate Moment Connections with Skewed Beam," *International Journal of Steel Structures*, Vol. 19, No. 6, pp. 1,767–1,784.

Ioannides, S.A. and Tarpy, T.S. (1980), "Practical Application of Semi-Rigid Beam to Column End-Plate Connectors," *Applied Mathematical Modelling*, Vol. 4, No. 1, pp. 23–27.

Ismail, R.E.S., Fahmy, A.S., Khalifa, A.M., and Mohamed, Y.M. (2015), "Numerical Study on Ultimate Behaviour of Bolted End-Plate Steel Connections," *Latin American Journal of Solids and Structures*, Vol. 13, pp. 1–22.

Italiano, V.M. and Murray, T.M. (2001), "Behavior of Diagonal Knee Moment-End Plate Connections," Virginia Tech Structural Engineering Report No. CE/VPI-ST 01/01, Virginia Polytechnic Institute and State University, Blacksburg, Va.

Jain, N., Eatherton, M.R., and Murray, T.M. (2015), "Developing and Validating New Bolted End-Plate Moment Connection Configurations," Virginia Tech Structural Engineering and Materials Report No. CE/VPI-ST-15/08, Virginia Polytechnic Institute and State University, Blacksburg, Va.

Jaspart J.P., Braham, M., and Cerfontaine, F. (1999), "Strength of Joints Subjected to Combined Action of Bending Moment and Axial Force," *Eurosteel Conference*, CVUT Praha, Czech Republic, Paper No. A023.

Jenner, R., Densford, T., Astaneh-Asl, A., and Murray, T.M. (1985a), "Experimental Investigation of Rigid Frames Including Knee Connection Studies—Frame Assembly Tests," FEARS Structural Engineering Laboratory Report No. FSEL/MESCO 85-0l, University of Oklahoma, Norman, Okla.

Jenner, R., Densford, T., Astaneh-Asl, A., and Murray, T.M. (1985b), "Experimental Investigation of Rigid Frames Including Knee Connection Studies—Frame FR1 Tests," FEARS Structural Engineering Laboratory Report No. FSEL/MESCO 85-02, University of Oklahoma, Norman, Okla.

Jenner, R., Densford, T., Astaneh-Asl, A., and Murray, T.M. (1985c), "Experimental Investigation of Rigid Frames Including Knee Connection Studies—Frame FR2 Tests," FEARS Structural Engineering Laboratory Report No. FSEL/MESCO 85-03, University of Oklahoma, Norman, Okla.

Jerez, L. and Murray, T.M. (1980a), "Rigid Frame Studies Progress Report Full Scale Frame Tests SRL04 50 20/25 16/25," FEARS Structural Engineering Laboratory Report No. FSEL/MBMA 80-01, University of Oklahoma, Norman, Okla.

Jerez, L. and Murray, T.M. (1980b), "Rigid Frame Studies Progress Report Full Scale Frame Tests SRL0 60 40/25 20/20," FEARS Structural Engineering Laboratory Report No. FSEL/MBMA 80-02, University of Oklahoma, Norman, Okla.

Keikha, H. and Mofid, M. (2020), "Seismic Performance Evaluation of a Novel Bolted Flush End-Plate Beam Splice Connection," *Proceedings of the Institution of Civil Engineers—Structures and Buildings,* Vol. 173, No. 2, pp. 109–127.

Kennedy, N.A., Vinnakota, S., and Sherbourne, A.N. (1981), "The Split-Tee Analogy in Bolted Splices and Beam-Column Connections," *Proceedings of the International Conference: Joints in Structural Steelwork*, pp. 2.138–2.157.

Khonsari, S.V., Grayli, P.V., Ghorbani, A., and Moghaddam, A.R. (2018), "Behaviour of End-Plate Connections in 3D Frames under Fire Conditions: Experimental Study," *International Journal of Steel Structures*, Vol. 18, No. 3, pp. 734–749.

Kiamanesh, R. (2011), "On the Effects of Circular Bolt Patterns on the Behavior of the Extended End-Plate Connections," Ph.D. Dissertation, University of Texas at Arlington, Arlington, Tex.

Kiamanesh, R., Abolmaali, A., and Razavi, M. (2013), "Effect of Circular Bolt Pattern on Behavior of Extended End-Plate Connection," *Journal of Structural Engineering*, Vol. 139, No. 11, pp. 1,822–1,841.

Kline, D., Rojiani, K., and Murray, T.M. (1995), "Performance of Snug-Tight Bolts in Moment End-Plate Connections," Virginia Tech Structural Engineering Report No. CE/VPI-ST-89/04, Virginia Polytechnic Institute and State University, Blacksburg, Va.

Korol, R.M., Ghobarah, A., and Osman, A. (1990), "Extended End-Plate Connections under Cyclic Loading: Behaviour and Design," *Journal of Constructional Steel Research*, Vol. 16, No. 4, pp. 253–280.

Krawinkler, H. (1978), "Shear in Beam-Column Joints in Seismic Design of Steel Frames," *Engineering Journal*, Vol. 15, No. 3, pp. 82–91.

Krishnamurthy, N. (1978) "A Fresh Look at Bolted End-Plate Behavior and Design," *Engineering Journal*, Vol. 15, No. 2, pp. 39–49.

Krishnamurthy, N. and Graddy, D.E. (1976), "Correlation between 2- and 3-Dimensional Finite Element Analysis of Steel Bolted End-Plate Connections," *Computers and Structures*, Vol. 6, pp. 381–389.

Krolo, P., Grandic, D., and Bulic, M. (2016), "The Guidelines for Modelling the Preloading Bolts in the Structural Connection Using Finite Element Methods," *Journal of Computational Engineering*, Vol. 2016, pp. 1–8.

Kukreti, A.R. and Biswas, P. (1997), "Finite Element Analysis to Predict the Cyclic Hysteretic Behavior and Failure of End-Plate Connections," *Computers and Structures*, Vol. 65, No. 1, pp. 127–147.

Kukreti, A.R., Ghassemieh, M., and Murray, T.M. (1990), "Behavior and Design of Large-Capacity Moment End Plates," *Journal of Structural Engineering*, Vol. 116, No. 3, pp. 809–828.

Kukreti, A.R., Murray, T.M., and Abolmaali, A. (1987), "End-Plate Connection Moment-Rotation Relationship," *Journal of Constructional Steel Research*, Vol. 8, pp. 137–157.

Lachal, A., Aribert, J.M., and Ciutina, A. (2004), "Seismic Performance of End-Plate Moment Resisting Composite Joints," *Composite Construction in Steel and Concrete V Conference*, Mpumalanga, South Africa.

Leon, R.T., Hajjar, J.F., and Gustafson, M.A. (1988), "Seismic Response of Composite Moment-Resisting Connections. I: Performance," *Journal of Structural Engineering*, Vol. 124, No. 8, pp. 868–876.

Li, G.Q., Chen, L.Z., Li, J.T., and Lou, G.B. (2012a), "Modeling of End-Plate Bolted Composite Connection in Fire Considering Axial Force Effects," *Journal of Constructional Steel Research*, Vol. 76, pp. 133–143.

Li, J.T., Li, G.Q., Lou, G.B., and Chen, L.Z. (2012b), "Experimental Investigation on Flush End-Plate Bolted Composite Connection in Fire," *Journal of Constructional Steel Research*, Vol. 76, pp. 121–132.

Li, T.Q., Nethercot, D.A., and Choo, B.S. (1996a), "Behaviour of Flush End-Plate Composite Connections with Unbalanced Moment and Variable Shear/Moment Ratios—I. Experimental Behaviour," *Journal of Constructional Steel Research*, Vol. 38, No. 2, pp. 125–164.

Li, T.Q., Nethercot, D.A., and Choo, B.S. (1996b), "Behaviour of Flush End-Plate Composite Connections with Unbalanced Moment and Variable Shear/Moment Ratios—II. Prediction of Moment Capacity," *Journal of Constructional Steel Research*, Vol. 38, No. 2, pp. 165–198.

Liew, J.Y.R., Teo, T.H., and Shanmugam, N.E. (2004), "Composite Joints Subject to Reversal of Loading—Part 1: Experimental Study," *Journal of Constructional Steel Research*, Vol. 60, pp. 221–246.

Liew, J.Y.R., Teo, T.H., Shanmugam, N.E., and Yu, C.H. (2000), "Testing of Steel-Concrete Composite Connections and Appraisal of Results," *Journal of Constructional Steel Research*, Vol. 56, pp. 117–150.

Lim, C. (2009), "Low Cycle Fatigue Life Prediction of Four Bolt Extended Unstiffened End Plate Moment Connections," Ph.D. Dissertation, North Carolina State University, Raleigh, N.C.

Lim, C., Choi, W., and Sumner, E.A. (2012), "Low Cycle Fatigue Life Prediction Using a Four-Bolt Extended Unstiffened End Plate Connection," *Engineering Structures*, Vol. 41, pp. 373–384.

Liu, H., and Li, J. (2012), "Initial Stiffness Analysis of Steel Portal Frame End-Plate Connections Based on Finite Element Method," *Advanced Materials Research*, Vol. 446–449, pp. 867–870.

Loh, H.Y., Uy, B., and Bradford, M.A. (2004), "The Behaviour of Composite Joints Using Flush End Plate Connections—Part 1: Experimental Study," UNICIV Report No. R-424, University of New South Wales, Sydney, Australia.

Loh, H.Y., Uy, B., and Bradford, M.A. (2006), "The Effects of Partial Shear Connection in Composite Flush End Plate Joints Part 1—Experimental Study," *Journal of Constructional Steel Research*, Vol. 62, pp. 378–390.

Lopez, M., Loureiro, A., Gutierrez, R., and Reinosa, J.M. (2021), "A New Analytical Formulation for the Stiffness and Resistance of the Additional Plate in Bending in Beam-to-Beam Steel Joints," *Engineering Structures*, Vol. 228.

Loureiro, A., Moreno, A., Gutierrez, R., and Reinosa, J.M. (2012), "Experimental and Numerical Analysis of Three-Dimensional Semi-Rigid Steel Joints under Non-Proportional Loading," *Engineering Structures*, Vol. 38, pp. 68–77.

Luo, L., Du, M., Yuan, J., Shi, J., Yu, S., and Zhang, Y. (2020), "Parametric Analysis and Stiffness Investigation of Extended End-Plate Connection," *Materials*, Vol. 13, No. 5133.

Malakoutian, M., Berman, J.W., and Dusicka, P. (2013), "Seismic Response Evaluation of the Linked Column Frame System," *Earthquake Engineering and Structural Dynamics*, Vol. 42, pp. 795–814.

Mann, A.P. and Morris, L.J. (1979), "Limit Design of Extended End-Plate Connections," *Journal of the Structural Division*, Vol. 105, No. 3, pp. 511–526.

Mashaly, E., El-Heweity, M., Abou-Elfath, H., and Osman, M. (2011), "Behavior of Four-Bolt Extended End-Plate Connection Subjected to Lateral Loading," *Alexandria Engineering Journal*, Vol. 50, pp. 79–90.

Masika, R.J. and Dunai, L. (1995), "Behaviour of Bolted End-Plate Portal Frame Joints," *Journal of Constructional Steel Research*, Vol. 32, pp. 207–225.

Mays, T.W. and Murray, T.M. (1999), "Research on End-Plate Connections for Seismic Loading: An Update," *North American Steel Construction Conference*, Toronto, Canada, pp. 26-1–26-17.

Mays, T.W., Sumner, E.A., Plaut, R.H., and Murray, T.M. (2000), "Seismic Design of Sixteen-Bolt Extended Stiffened Moment End-Plate Connections," *Steel Structures in Seismic Areas (STESSA) Conference*, Montreal, Canada.

MBMA (2019), *Seismic Design Guide for Metal Building Systems: Based on the 2006 IBC*, 3rd Ed., Metal Building Manufactures Association, Cleveland, Ohio.

Meng, R.L. (1996), "Design of Moment End-Plate Connections for Seismic Loading," Ph.D. Dissertation, Virginia Tech, Blacksburg, Va.

Meng, R.L. and Murray, T.M. (1996), "Moment End-Plate Connections for Seismic Loading," Virginia Tech Structural Engineering Report No. CE/VPI-ST-96/04, Virginia Polytechnic Institute and State University, Blacksburg, Va.

Mohamadi-Shooreh, M.R. and Mofid, M. (2008), "Parametric Analyses on the Initial Stiffness of Flush End-Plate Splice Connections Using FEM," *Journal of Constructional Steel Research*, Vol. 64, pp. 1,129–1,141.

Mohamadi-Shooreh, M.R., Mofid, M., and McCabe, S.L. (2013), "Empirical Model of the Moment-Rotation Curve of Beam-to-Beam Bolted Flush Endplate Connections," *Journal of Structural Engineering*, Vol. 139, No. 1, pp. 66–72.

Moore, D.B. and Sims, P.A.C. (1986), "Preliminary Investigations into the Behaviour of Extended End-Plate Steel Connections with Backing Plates," *Journal of Constructional Steel Research*, Vol. 6, pp. 95–122.

Morrison, M., Quayyum, S., and Hassan, T. (2017), "Performance Enhancement of Eight Bolt Extended End-Plate Moment Connections under Simulation Seismic Loading," *Engineering Structures*, Vol. 151, pp. 444–458.

Morrison, M.L., Schweizer, D.Q., Quayyum, S., and Hassan, T. (2019), "An Unstiffened Eight-Bolt Extended End-Plate Moment Connection for Special and Intermediate Moment Frames," *Journal of Structural Engineering*, Vol. 145, No. 7.

Morrison, S.J., Astaneh-Asl, A., and Murray, T.M. (1985), "Analytical and Experimental Investigation of the Extended Stiffened Moment End-Plate Connection with Four Bolts at the Tension Flange," FEARS Structural Engineering Laboratory Report No. FSEL/MBMA 85-05, University of Oklahoma, Norman, Okla.

Morrison, S.J., Astaneh-Asl, A., and Murray, T.M. (1986), "Analytical and Experimental Investigation of the Multiple Row Extended Moment End-Plate Connection with Eight Bolts at the Beam Tension Flange," FEARS Structural Engineering Laboratory Report No. FSEL/MBMA 86-01, University of Oklahoma, Norman, Okla.

Mourad, S., Ghobarah, A., and Korol, R.M. (1994), "Dynamic Response of Hollow Section Frames with Bolted Moment Connections," *Engineering Structures*, Vol. 17, No. 19, pp. 737–748.

Mourad, S., Koral, R.M., and Ghobarah, A. (1996), "Design of Extended End-Plate Connections for Hollow Section Columns," *Canadian Journal of Civil Engineering*, Vol. 23, pp. 277–286.

Muresan, I.C. and Balc, R. (2015), "Finite Element Analysis of an Extended End-Plate Connection Using the T-Stub Approach," *International Conference on Numerical Analysis and Applied Mathematics*, Rhodes, Greece, pp. 850091-1–850091-4.

Murray, T.M. (1988), "Recent Developments for the Design of Moment End-Plate Connections," *Journal of Constructional Steel Research*, Vol. 10, pp. 133–162.

Murray, T.M. (1989), "Tests to Determine the Adequacy of A490 Bolts in Moment End-Plate Connections," Structural Engineers Inc. Report, Radford, Va.

Murray, T.M. and Borgsmiller, J.T. (1995), "Strength of Moment End-Plate Connections with Multiple Bolt Rows at the Beam Tension Flange," *Proceedings of the Connections in Steel Structures III Conference*, Trento, Italy.

Murray, T.M. and Kukreti, A.R. (1988), "Design of 8-Bolt Stiffened Moment End Plates," *Engineering Journal*, Vol. 25, No. 2, pp. 45–52.

Murray, T.M. and Shoemaker, W.L. (2002), *Flush and Extended Multiple-Row Moment End-Plate Connections*, Design Guide 16, AISC, Chicago, Ill.

Murray, T.M. and Sumner, E.A. (1999), "Brief Report of Steel Moment Connection Test—SAC Subtask 7.10, Testing and Analysis of Bolted End-Plate Connections," Virginia Tech Report, Virginia Polytechnic Institute and State University, Blacksburg, Va.

Murray, T.M. and Sumner, E.A. (2004), *Extended End-Plate Moment Connections—Seismic and Wind Applications*, Design Guide 4, AISC, Chicago, Ill.

Nemati, N., Le Houedec, D., and Zandonini, R. (2000), "Numerical Modelling of the Cyclic Behaviour of the Basic Components of Steel End Plate Connections," *Advances in Engineering Software*, Vol. 31, pp. 837–849.

Nia, M.M. and Moradi, S. (2020), "Limit State Behavior and Response Sensitivity Analysis of Endplate Steel Connections with Shape Memory Alloy Bolts," *Journal of Intelligent Material Systems and Structures*, Vol. 31, No. 18, pp. 2,071–2,087.

Nunes, P.C., de Lima, L.R.O., da Silva, J.G.S, da S. Vellasco, P.C.G., and de Andrade, S.A.L. (2007), "Parametrical Analysis of Extended Endplate Semi-Rigid Joints Subjected to Bending Moment and Axial Force," *Latin American Journal of Solids and Structures*, Vol. 4, No. 1, pp. 39–59.

Osman, A.M.G. (1991), "Extended End-Plate Beam-Column Joints in Seismic Moment Resisting Frames," Ph.D. Thesis, McMaster University, Hamilton, Ontario, Canada.

Packer, J.A. and Morris, L.J. (1977), "A Limit State Design Method for the Tension Region of Bolted Beam—Column Connections," *The Structural Engineer*, Vol. 55, No. 10, pp. 446–458.

Qian, Z.H., Tan, K.H., and Burgess, I.W. (2009), "Numerical and Analytical Investigations of Steel Beam-to-Column Joints at Elevated Temperatures," *Journal of Constructional Steel Research*, Vol. 65, pp. 1,043–1,054.

Qiang, X., Bijlaard, F.S.K., Kolstein, H., and Jiang, X. (2014a), "Behaviour of Beam-to-Column High Strength Endplate Connections under Fire Conditions—Part 1: Experimental Study," *Engineering Structures*, Vol. 64, pp. 23–38.

Qiang, X., Bijlaard, F.S.K., Kolstein, H., and Jiang, X. (2014b), "Behaviour of Beam-to-Column High Strength Steel Endplate Connections under Fire Conditions—Part 2: Numerical Study," *Engineering Structures*, Vol. 64, pp. 39–51.

Qiang, X., Jiang, X., Bijlaard, F., and Kolstein, H. (2016), "Performance Assessment on High Strength Steel Endplate Connections in Fire," *Journal of Structural Fire Engineering*, Vol. 7, No. 2, pp. 168–178.

Qiang, X., Jiang, X., Bijlaard, F.S.K., Kolstein, H., and Luo, Y. (2015), "Post-Fire Behaviour of High Strength Steel Endplate Connections—Part 2: Numerical Study," *Journal of Constructional Steel Research*, Vol. 108, pp. 94–102.

Radmehr, M. and Homami, P. (2020), "The Seismic Reliability Analysis of Moment Resisting Frames with Bolted End-Plate Connection," *Journal of Constructional Steel Research*, Vol. 171.

Ramadan, T. and Ghobarah, A. (1995), "Extended End-Plate Link-Column Joints in Eccentrically Braced Frames" *7th Canadian Conference on Earthquake Engineering*, Montreal, Canada, pp. 557–564.

Ramseyer, C. and Sherry, S.T. (2019), "Assessment of Partial Joint Penetration Welds on Bolted End-Plate Connections," *Engineering Structures*, Vol. 197.

RCSC (2020), *Specification for Structural Joints Using High-Strength Bolts*, Research Council on Structural Connections, Chicago, Ill.

Redmond, N.A. (2007), "Experimental and Analytical Investigation of the Shear Strength of Unstiffened Tapered Steel Members," M.S. Thesis, Virginia Tech, Blacksburg, Va.

Reza, M.A., Shanmugam, N.E., Badaruzzaman, W.H.W., and Dhakal, R.P. (2013), "Analysis of Connections in Composite Construction under Cyclic Loading," *Structures Congress*, Pittsburgh, Pa., pp. 1,975–1,986.

Ricles, J.M., Fisher, J.W., Lu, L.W., and Kaufmann, E.J. (2002), "Development of Improved Welded Moment Connections for Earthquake-Resistant Design," *Journal of Constructional Steel Research*, Vol. 58, 565–604.

Rodkey, R.W. and Murray, T.M. (1993a), "Twelve-Bolt Extended Unstiffened End-Plate Connection Test," Virginia Tech Structural Engineering Report No. CE/VPI-STG 93/09, Virginia Polytechnic Institute and State University, Blacksburg, Va.

Rodkey, R.W. and Murray, T.M. (1993b), "Eight-Bolt Extended Unstiffened End-Plate Connection Test," Virginia Tech Structural Engineering Report No. CE/VPI-STG 93/10, Virginia Polytechnic Institute and State University, Blacksburg, Va.

Ryan, J.C. (1999), "Evaluation of Extended End-Plate Moment Connections Under Seismic Loading," M.S. Thesis, Virginia Tech, Blacksburg, Va.

Ryan, J.C., Jr. and Murray, T.M. (1999), "Evaluation of the Inelastic Rotation Capability of Extended End-Plate Moment Connections," Virginia Tech Structural Engineering and Materials Report No. CE/VPI-ST 99/13, Virginia Polytechnic Institute and State University, Blacksburg, Va.

Saberi, H., Kheyroddin, A., and Gerami, M. (2014a), "Comparison of Bolted End Plate and T-Stub Connections Sensitivity to Bolt Diameter on Cyclic Behavior," *International Journal of Steel Structures*, Vol. 14, No. 3, pp. 633–647.

Saberi, V., Gerami, M., and Kheyroddin, A. (2014b), "Comparison of Bolted End Plate and T-Stub Connection Sensitivity to Component Thickness," *Journal of Constructional Steel Research*, Vol. 98, pp. 134–145.

Saberi, V., Gerami, M., and Kheyroddin, A. (2016), "Seismic Rehabilitation of Bolted End Plate Connections Using Post-Tensioned Tendons," *Engineering Structures*, Vol. 129, pp. 18–30.

Salmon, C.G., Johnson, J.E., and Malhas, F.A. (2009), *Steel Structures: Design and Behavior*, 5th Ed., Pearson, London, England.

Scheer, J., Pasternak, H., and Schween, T. (1991), "Structural Behavior of Stiffened Knee Joints with Thin Webs," *Journal of Structural Engineering*, Vol. 117, No. 9, pp. 2,600–2,619.

Schnupp, K.O. and Murray, T.M. (2003), "Seismic Evaluation of a 16-Bolt Flush Moment End-Plate Connection," Virginia Tech Structural Engineering and Materials Report No. CE/VPI-ST-03/02, Virginia Polytechnic Institute and State University, Blacksburg, Va.

Seek, M.W. and Murray T.M. (2008), "Seismic Strength of Moment End-Plate Connections with Attached Concrete Slab," *Connections VI Conference*, AISC, Chicago, Ill.

Shaker, F.M.F. and Elrahman, W.M.A. (2014a), "Analytical Behavior of Steel Pre-Tensioned Bolted Connections with Flushed and Extended End Plates under Bending," *World Applied Sciences Journal*, Vol. 30, No. 6, pp. 673–684.

Shaker, F.M.F. and Elrahman, W.M.A. (2014b), "Behavior of Flush and Extended End-Plate Beam-to-Column Joints under Bending and Axial Force," *World Applied Sciences Journal*, Vol. 30, No. 6, pp. 685–695.

Sheet, I.S. and Gunasekaran, U. (2013), "Seismic Performance of Moment End-Plate Connections to CFT Column under Cyclic Loading," *Advanced Materials Research*, Vol. 680, pp. 205–210.

Shek, P.N., Tahir, M.M., Sulaiman, A., and Tan, C.S. (2012), "Experimental Evaluation of Flush End-Plate Connection with Built-Up Hybrid Beam Section," *Advances in Structural Engineering*, Vol. 15, No. 2, pp. 331–341.

Shek, P.N., Tahir, M.M., Tan, C.S., and Kueh, A.B. (2011), "Experimental Investigation of End-Plate Connection with Cruciform Column Section," *Advanced Materials Research*, Vol. 250–253, pp. 3,730–3,733.

Shek, P.N., Tahir, M.M., Tan, C.S., and Sulaiman, A. (2013), "Experimental Investigation of Retrofitted Extended End-Plate Connections," *Applied Mechanics and Materials*, Vol. 284–287, pp. 1,330–1,333.

Sherbourne, A.N. and Bahaari, M.R. (1994), "3D Simulation of End-Plate Bolted Connections," *Journal of Structural Engineering*, Vol. 120, No. 11, pp. 3,122–3,136.

Sherbourne, A.N. and Bahaari, M.R. (1997), "Finite Element Prediction of End Plate Bolted Connection Behavior. I: Parametric Study," *Journal of Structural Engineering*, Vol. 123, No. 2, pp. 157–164.

Sherry, S. (2016), "Assessment of Partial Joint Penetration Welds on Bolted End-Plate Connections for Use in Intermediate Moment Frames," M.S. Thesis, University of Oklahoma, Norman, Okla.

Shi, G., Chen, X., and Wang, D. (2017), "Experimental Study of Ultra-Large Capacity End-Plate Joints," *Journal of Constructional Steel Research*, Vol. 128, pp. 354–361.

Shi, G., Shi, Y., and Wang, Y. (2007a), "Behaviour of End-Plate Moment Connections under Earthquake Loading," *Engineering Structures*, Vol. 29, pp. 703–716.

Shi, G., Shi, Y., and Wang, Y. (2007b), "Experimental and Theoretical Analysis of the Moment-Rotation Behavior of Stiffened End-Plate Connections," *Journal of Constructional Steel Research*, Vol. 63, pp. 1,279–1,293.

Shi, G., Shi, Y., Wang, Y., and Bijlaard, F.S.K. (2010), "Monotonic Loading Tests on Semi-Rigid End-Plate Connections with Welded I-Shaped Columns and Beams," *Advances in Structural Engineering*, Vol. 13, No. 2, pp. 215–229.

Shi, G., Shi, Y., Wang, Y., and Bradford, M.A. (2008), "Numerical Simulation of Steel Pretensioned Bolted End-Plate Connections of Different Types and Details," *Engineering Structures*, Vol. 30, pp. 2,677–2,686.

Shi, G., Shi, Y., Wang, Y., Li, S., and Chen, H. (2004), "Finite Element Analysis and Tests on Bolted End-Plate Connections in Steel Portal Frames," *Advances in Structural Engineering*, Vol. 7, No. 3, pp. 245–256.

Shi, Q., Yan, S., Kong, L., Bu, X., Wang, X., and Sun, H. (2019), "Seismic Behavior of Semi-Rigid Steel Joints—Major Axis T-Stub and Minor Axis End-Plate," *Journal of Constructional Steel Researc*h, Vol. 159, pp. 476–492.

Simoes da Silva, L.S. (2008), "Towards a Consistent Design Approach for Steel Joints under Generalized Loading," *Journal of Constructional Steel Research*, Vol. 64, pp. 1,059–1,075.

Simoes da Silva, L. and Coelho, A.M.G. (2001), "An Analytical Evaluation of the Response of Steel Joints under Bending and Axial Force," *Computers and Structures*, Vol. 79, pp. 873–881.

Simoes da Silva, L., Lima, L., Vellasco, P., and Andrade, S. (2001), "Experimental Behaviour of End-Plate Beam-to-Column Joints under Bending and Axial Force," *ECCS Technical Committee 10 Connections TWG 10.2*, UC/DEC/GCOM/2002-008/RR/JOINT and ECCS TC10-02-WG2/0xx.

Simoes da Silva, L., Lima, L.R.O., Vellasco, P.C.G., and Andrade, S.A.L. (2004), "Behaviour of Flush End-Plate Beam-to-Column Joints under Bending and Axial Force," *Steel and Composite Structures*, Vol. 4, No. 2, pp. 77–94.

Simoes da Silva, L., Simoes, R.D., and Cruz, P.J.S. (2001), "Experimental Behaviour of End-Plate Beam-to-Column Composite Joints under Monotonic Loading," *Engineering Structures*, Vol. 23, pp. 1,383–1,409.

Smith, M.D., Turner, K.A., and Uang, C.M. (2013), "Experimental Study of Cyclic Lateral-Torsional Buckling of Web-Tapered I-Beams," Final Report to the Metal Building Manufacturers Association, Structural Systems Research Report No. SSRP-12/06, University of California San Diego, San Diego, Calif.

Smith, M.D. and Uang, C.M. (2011), "Seismic Force Distribution for Metal Building Systems with Mezzanines," *Structures Congress*, Las Vegas, Nev., pp. 705–715.

Sokol, Z., Wald, F., Delabre, V., Muzeau, J.P., and Svarc, M. (2002), "Design of End Plate Joints Subject to Moment and Normal Force," *Third European Conference on Steel Structures-Eurosteel*, Coimbra, Portugal, pp. 1,219–1,228.

Spangler, D.D. and Murray, T.M. (1989a), "Experimental Investigation of Rigid Frame Knee Connections," Virginia Tech Structural Engineering Report No. CE/VPI-ST 89/01, Virginia Polytechnic Institute and State University, Blacksburg, Va.

Spangler, D.D. and Murray, T.M. (1989b), "P-Delta and Partial Knee Stiffness Effects of Rigid Primary Framing Systems," Virginia Tech Structural Engineering Report No. CE/VPI-ST 89/08, Virginia Polytechnic Institute and State University, Blacksburg, Va.

Srouji, R., Kukreti, A.R., and Murray, T. M. (1983), "Strength of Two Tension Bolt Flush End-Plate Connections," FEARS Structural Engineering Laboratory Report No. FSEL/MBMA 83-03, University of Oklahoma, Norman, Okla.

Srouji, R., Kukreti, A.R. and Murray, T. M. (1984), "Yield-Line Analysis of End-Plate Connections with Bolt Force Predictions," FEARS Structural Engineering Laboratory Report No. 83-05A, University of Oklahoma, Norman, Okla.

Steenhuis, M., Dol, C., and van Gorp, L. (1994), "Computerised Calculation of Force Distributions in Bolted End Plate Connections According to Eurocode 3," *Journal of Constructional Steel Research*, Vol. 31, pp. 135–144.

Stevens, R.T., Eatherton, M.R., amd Murray, T.M. (2020), "Effect of Stiffener Weld Detail on Cyclic Performance of End-Plate Moment Connections," Virginia Tech Structural Engineering and Materials, Report No. CE/VPI-ST-20/05 Virginia Polytechnic Institute and State University, Blacksburg, Va.

Straten, A., Maris, C., Vulcu, C., Dubina, D., and Neagu, C. (2016), "Prequalification Tests on Bolted Beam-to-Column Joints with Haunches," *Proceedings of the 8th International Workshop on Connections in Steel Structures (Connections VIII)*, Boston, Mass., May 24–26.

Strejcek, M., Reznicek, J., Tan, K.H., and Wald, F. (2011), "Behaviour of Column Web Component of Steel Beam-to-Column Joints and Elevated Temperatures," *Journal of Constructional Steel Research*, Vol. 67, pp. 1,890–1,899.

Structural Engineers Inc. (1984), "Multiple Row, Extended End Plate Connection Tests," Test Report, Norman, Okla.

Structural Engineers Inc. (1986), "Preliminary Experimental Investigation of Channel End-Plate Moment Connections," Test Report, Norman, Okla.

Sullivan, S.V., Charney, F.A., and Murray, T.M. (2006), "Performance of Diagonal Knee Connections with and without Stiffeners," Virginia Tech Structural Engineering Report No. CEE/VPI-ST06/02, Virginia Polytechnic Institute and State University, Blacksburg, Va.

Sumner, E.A. (2003), "Unified Design of Extended End-Plate Moment Connections Subject to Cyclic Loading," Ph.D. Dissertation, Virginia Tech, Blacksburg, Va.

Sumner, E.A., Borgsmiller, J.T., and Murray, T.M. (1995), "Experimental Investigation of Rigid Knee Joints," Virginia Tech Structural Engineering Research Report No. CE/VPI-95/12, Virginia Polytechnic Institute and State University, Blacksburg, Va.

Sumner, E.A., Mays, T.W., and Murray, T.M. (2000), "Cyclic Testing of Bolted Moment End-Plate Connections," SAC Report No. SAC/BD-00/21, Virginia Tech Structural Engineering Report No. CE/VPI-ST 00/03, Virginia Polytechnic Institute and State University, Blacksburg, Va.

Sumner, E.A. and Murray, T.M. (1995), "Experimental Investigation of Rigid Knee Joints—Addendum," Virginia Tech Structural Research Report No. CE/VPI-95/10, Virginia Polytechnic Institute and State University, Blacksburg, Va.

Sumner, E.A. and Murray, T.M. (2001a), "Experimental Investigation of the Multiple Row Extended 1/2 End-Plate Moment Connection," Virginia Tech Structural Engineering Report No. CE/VPI-ST-01/14, Virginia Polytechnic Institute and State University, Blacksburg, Va.

Sumner, E.A. and Murray, T.M. (2001b), "Experimental Investigation of Four Bolts Wide Extended End-Plate Moment Connections," Virginia Tech Structural Engineering and Materials Report No. CE/VPI-ST 01/15, Virginia Polytechnic Institute and State University, Blacksburg, Va.

Sumner, E.A. and Murray, T.M. (2002), "Behavior of Extended End-Plate Moment Connections Subjected to Cyclic Loading," *Journal of Structural Engineering*, Vol. 128, No. 4, pp. 501–508.

Sun, L., Liu, M., Liu, Y., Wang, P., Zhao, P., Zhao, H., Sun, J., and Shang, Y. (2020), "Studies on T-Shaped One-Side Bolted Connection to Hollow Section Column under Bending," *Journal of Constructional Steel Research*, Vol. 175.

Szabo, T., Eatherton, M.R., He, X., and Murray, T.M. (2017), "Study of a Twelve Bolt Extended Stiffened End-Plate Moment Connection," Virginia Tech Structural Engineering and Materials Report No. CE/VPI-ST-17/02, Virginia Polytechnic Institute and State University, Blacksburg, Va.

Tahir, M.M., Juki, I., Yong, L.H., Mohammad, S., and Ngian, S.P. (2011), "Finite Element Analysis of Flush End-Plate Connections Connected to Column Web," *International Journal of Steel Structures*, Vol. 11, No. 3, pp. 247–258.

Tahir, M.M., Mohammadhosseini, H., Ngian, S.P., and Effendi, M.K. (2018), "I-Beam to Square Hollow Column Blind Bolted Moment Connection: Experimental and Numerical Study," *Journal of Constructional Steel Research*, Vol. 148, pp. 383–398.

Tao, Z., Li, W., Shi, B.L., and Han, L.H. (2017), "Behaviour of Bolted End-Plate Connections to Concrete-Filled Steel Columns," *Journal of Constructional Steel Research*, Vol. 134, pp. 194–208.

Tartaglia, R., D'Aniello, M., Rassati, G.A., Swanson, J.A., and Landolfo, R. (2018a), "Full Strength Extended Stiffened End-Plate Joints: AISC vs Recent European Design Criteria," *Engineering Structures*, Vol. 159, pp. 155–171.

Tartaglia, R., D'Aniello, M., Rassati, G.A., Swanson, J., and Landolfo, R. (2018b), "Influence of Composite Slab on the Nonlinear Response of Extended End-Plate Beam-to-Column Joints," *Key Engineering Materials*, Vol. 762, pp. 818–825.

Tartaglia, R., D'Aniello, M., Zimbru, M., De Martino, A., and Landolfo, R. (2019), "Robustness of Seismically Pre-Qualified Extended Stiffened Beam-to-Column Joints," *Proceedings of the 7th ECCOMAS Thematic Conference on Computational Methods in Structural Dynamics and Earthquake Engineering (COMPDYN)*, Crete, Greece, June 24–26.

Thai, H.T., Vo, T.P., Nguyen, T.K., and Pham, C.H. (2017), "Explicit Simulation of Bolted Endplate Composite Beam-to-CFST Column Connections," *Thin-Walled Structures*, Vol. 119, pp. 749–759.

Thompson, B.G. and Murray, T.M. (1975), "End-Plate Connection Tests and Analysis," School of Civil Engineering and Environmental Science Report, University of Oklahoma, Norman, Okla.

Tsai, K.C. and Popov, E.P. (1990), "Cyclic Behavior of End-Plate Moment Connections," *Journal of Structural Engineering*, Vol. 116, No. 11, pp. 2,917–2,930.

Uang, C.M., Smith, M.D., and Shoemaker, W.L. (2011), "Earthquake Simulator Testing of Metal Building Systems," *Structures Congress*, Las Vegas, Nev., pp. 693–704.

Urbonas, K. and Daniunas, A. (2005), "Component Method Extension to Steel Beam-to-Beam and Beam-to-Column Knee Joints under Bending and Axial Forces," *Journal of Civil Engineering and Management*, Vol. XI, No. 3, pp. 217–224.

Urbonas, K. and Daniunas, A. (2006), "Behaviour of Semi-Rigid Steel Beam-to-Beam Joints under Bending and Axial Forces," *Journal of Constructional Steel Research*, Vol. 62, pp. 1,244–1,249.

Van-Long, H., Jean-Pierre, J., and Jean-Fracois, D. (2015), "Extended End-Plate to Concrete-Filled Rectangular Column Joint Using Long Bolts," *Journal of Constructional Steel Research*, Vol. 113, pp. 156–168.

Vega, G. and Xiao, R. (2014), "Advanced Study of Non-Linear Semi-Continuous Beam-Column Endplate Connection and Metal-Decking Floor Modelling," *Journal of Constructional Steel Research*, Vol. 95, pp. 191–197.

Vulcu, C., Don, R., Ciutina, A., and Dubina, D. (2017), "Numerical Investigation of Moment-Resisting Slim-Floor Beam-to-Column Connections," *Proceedings of the Eight International Conference on Composite Construction in Steel and Concrete*, Jackson Hole, Wyo., July 29–Aug 2.

Wald, F. and Švarc, M. (2001), "Experiments with End Plate Joints Subject to Moment and Normal Force," *Contributions to Experimental Investigation of Engineering Materials and Structures*, CTU reports No. 2–3, Prague, Czech Republic, pp. 1–13.

Wang, A.J. (2010), "A Study on Composite End-Plate Connections with Flexible Tensile Reinforcements and Shear Connectors," *Canadian Journal of Civil Engineering*, Vol. 37, pp. 1,437–1,450.

Wang, A.J. (2012), "A Study on Semi-Continuous Composite Beams with Realistic Modelling of End-Plate Connections," *Australian Journal of Structural Engineering*, Vol. 13, No. 3, pp. 259–277.

Wang, H., Huo, J., Liu, Y., Elchalakani, M., and Zhu, Z. (2021), "Dynamic Performance of Composite Beam-Column Connections Subjected to Impact Loadings," *Journal of Constructional Steel Research*, Vol. 178.

Wang, J. and Chen, L. (2012), "Experimental Investigation of Extended End Plate Joints to Concrete-Filled Steel Tubular Columns," *Journal of Constructional Steel Research*, Vol. 79, pp. 56–70.

Wang, J., Chen, X., and Han, L.H. (2011), "Structural Behaviour of Blind Bolted Connection to Concrete-Filled Steel Tubular Columns," *Advanced Materials Research*, Vol. 163-167, pp. 591–595.

Wang, J., Chen, X., and Hou, H. (2012a), "Experimental Study of Blind Bolted Joints to Concrete-Filled Thin-Walled Steel Tubular Columns under Cyclic Loading," *Applied Mechanics and Materials*, Vol. 166–169, pp. 78–82.

Wang, J., Chen, X., and Shen, J. (2012b), "Performance of CFTST Column to Steel Beam Joints with Blind Bolts under Cyclic Loading," *Thin-Walled Structures*, Vol. 60, pp. 69–84.

Wang, J. and Guo, S. (2012), "Structural Performance of Blind Bolted End Plate Joints to Concrete-Filled Thin-Walled Steel Tubular Columns," *Thin-Walled Structures,* Vol. 60, pp. 54–58.

Wang, J., Pan, X., and Peng, X. (2017), "Pseudo-Dynamic Tests of Assembly Blind Bolted Composite Frames to CFST Columns," *Journal of Constructional Steel Research*, Vol. 139, pp. 83–100.

Wang, J. and Pang, Y. (2017), "Experimental and Numerical Analyses of Blind Bolted Moment-Resisting Composite Joints to CFST Columns with RC Slab," *International Journal of Steel Structures*, Vol. 17, No. 3, pp. 909–938.

Wang, J. and Spencer, B.F. (2013), "Experimental and Analytical Behavior of Blind Bolted Moment Connections," *Journal of Constructional Steel Research*, Vol. 82, pp. 33–47.

Wang, J., Uy, B., Li, D., and Sopng, Y. (2020), "Progressive Collapse Analysis of Stainless Steel Composite Frames with Beam-to-Column Endplate Connections," *Steel and Composite Structures*, Vol. 36, No. 4, pp. 427–446.

Wang, J. and Zhang, N. (2017), "Performance of Circular CFST Column to Steel Beam Joints with Blind Bolts," *Journal of Constructional Steel Research*, Vol. 130, pp. 36–52.

Wang, J., Zhang, N., and Guo, S. (2016a), "Experimental and Numerical Analysis of Blind Bolted Moment Joints to CFTST Columns," *Thin-Walled Structures*, Vol. 109, pp. 185–201.

Wang, J., Zhu, H., Uy, B., Ptel, V., Aslani, F., and Li, D. (2018), "Moment-Rotation Relationship of Hollow-Section Beam-to-Column Steel Joints with Extended End-Plates," *Steel and Composite Structures*, Vol. 29, No. 6, pp. 717–734.

Wang, J.F., Han, L.H., and Uy, B. (2009a), "Hysteretic Behaviour of Flush End Plate Joints to Concrete-Filled Steel Tubular Columns," *Journal of Constructional Steel Research*, Vol. 65, pp. 1,644–1,663.

Wang, J.F., Han, L.H., and Uy, B. (2009b), "Behaviour of Flush End Plate Joints to Concrete-Filled Steel Tubular Columns," *Journal of Constructional Steel Research*, Vol. 65, pp. 925–939.

Wang, S. and Chen, Y. (2009), "Initial Stiffness and Moment Resistance of Reinforced Joint with End-Plate Connection," *Frontiers of Architecture and Civil Engineering in China*, Vol. 3, No. 4, pp. 345–351.

Wang, Y.C. and Davies, J.M. (2003), "An Experimental Study of the Fire Performance of Non-Sway Loaded Concrete-Filled Steel Tubular Column Assemblies with Extended End Plate Connections," *Journal of Constructional Steel Research*, Vol. 59, pp. 819–838.

Wang, Z.B., Tao, Z., Li, D.S., and Han, L.H. (2016b), "Cyclic Behaviour of Novel Blind Bolted Joints with Different Stiffening Elements," *Thin-Walled Structures*, Vol. 101, pp. 157–168.

Wei, G., Koutromanos, I., Murray, T.M., and Eatherton, M.R. (2019), "Investigation of Partial Tension Field Action in Gable Frame Panel Zones," *Journal of Constructional Steel Research*, Vol. 162, pp. 1–11.

Wei, Z. and Qian, L. (2011), "Design Approach of Stiffeners and Model of the Initial Stiffness in Extended End-Plate Connection," *Advanced Materials Research*, Vol. 243–249, pp. 942–947.

Wheeler, A.T., Clarke, M.J., and Hancock, G.J. (2000), "FE Modeling of Four-Bolt, Tubular End-Plate Connections," *Journal of Structural Engineering*, Vol. 126, No. 7, pp. 816–822.

Wheeler, A.T., Clarke, M.J., and Hancock, G.J., (2003), "Design Model for Bolted Moment End Plate Connections Joining Rectangular Hollow Sections Using Eight Bolts," Department of Civil Engineering Research Report No. R827, University of Sydney, Sydney, Australia.

Wheeler, A.T., Clarke, M.J., Hancock, G.J., and Murray, T.M. (1997), "Design Model for Bolted Moment End Plate Connections Using Rectangular Hollow Sections," Department of Civil Engineering Research Report No. R745, University of Sydney, Sydney, Australia.

Wheeler, A.T., Clarke, M.J., Hancock, G.J., and Murray, T.M. (1998), "Design Model for Bolted Moment End Plate Connections Joining Rectangular Hollow Sections," *Journal of Structural Engineering*, Vol. 124, No. 2, pp. 164–173.

Xiao, Y., Choo, B.S., and Nethercot, D.A. (1996), "Composite Connections in Steel and Concrete. Part 2—Moment Capacity of End Plate Beam to Column Connections," *Journal of Constructional Steel Research*, Vol. 37, No. 1, pp. 63–90.

Xu, L. (2001), "Second-Order Analysis for Semirigid Steel Frame Design," *Canadian Journal of Civil Engineering*, Vol. 28, pp. 59–76.

Xu, L., Pan, J., Cai, J., Wu, D., and Li, Y. (2019), "Mechanical Behavior of Flat CFST Column to Steel Beam Joints under Reversed Cyclic Loading," *Engineering Structures*, Vol. 198.

Xu, M., Gao, S., Zhang, S., and Li, H. (2018), "Experimental Study on Bolted CFST-Column Joints with Different Configurations in Accommodating Column-Loss," *Journal of Constructional Steel Research*, Vol. 151, pp. 122–131.

Yam, M.C.H., Fang, C., Lam, A.C.C., and Zhang, Y. (2015), "Numerical Study and Practical Design of Beam-to-Column Connections with Shape Memory Alloys," *Journal of Constructional Steel Research*, Vol. 104, pp. 177–192.

Yang, B. and Tan, K.H. (2014), "Behavior of Composite Beam-Column Joints in a Middle-Column-Removal Scenario: Experimental Tests," *Journal of Structural Engineering*, Vol. 140, No. 2.

Yang, B., Tan, K.H., and Xiong, G. (2015), "Behaviour of Composite Beam-Column Joints under a Middle-Column-Removal Scenario: Component-Based Modelling," *Journal of Constructional Steel Research*, Vol. 104, pp. 137–154.

Yang, B., Tan, K.H., Xiong, G., and Nie, S.D. (2016), "Experimental Study about Composite Frames under an Internal Column-Removal Scenario," *Journal of Constructional Steel Research*, Vol. 121, pp. 341–351.

Yang, P. and Eatherton, M.R. (2014), "A Phenomenological Component-Based Model to Simulate Seismic Behavior of Bolted Extended End-Plate Connections," *Engineering Structures*, Vol. 75, pp. 11–26.

Yee, Y.L. and Melchers, R.E. (1986), "Moment-Rotation Curves for Bolted Connections," *Journal of Structural Engineering*, Vol. 112, No. 3, pp. 615–635.

Young, J. and Murray, T.M. (1997), "Experimental Investigation of Positive Bending Moment Strength of Rigid Knee Connections," Virginia Tech Structural Engineering Research Report No. CE/VPI-ST 97/08, Virginia Polytechnic Institute and State University, Blacksburg, Va.

Zahmatkesh, F. and Talebi, E. (2010), "The Performance of Bolted Slant Endplate Connections Subjected to Temperature Increase," *ASME 2010 10th Biennial Conference on Engineering Systems Design and Analysis*, Istanbul, Turkey.

Zarat-Basir, M., Eatherton, M.R., and Murray, T.M. (2020), "Testing of Stiffened and Unstiffened Twelve-Bolt Extended End-Plate Moment Connections," Virginia Tech Structural Engineering and Materials, Report No. CE/VPI-ST-20/01, Virginia Polytechnic Institute and State University, Blacksburg, Va.

Zeinoddini-Meimand, V., Ghassemieh, M., and Kiani, J. (2014), "Finite Element Analysis of Flush End Plate Moment Connections under Cyclic Loading," *International Journal of Civil, Environmental, Structural, Construction and Architectural Engineering*, Vol. 8, No. 1, pp. 96–104.

Zhang, H., Su, M., Lian, M., Cheng, Q., Guan, B., and Gong, H. (2020), "Experimental and Numerical Study on the Seismic Behavior of High-Strength Steel Framed-Tube Structures with End-Plate Connected Replaceable Shear Links," *Engineering Structures*, Vol. 223.

Zhao, J. (2013), "Model of the Initial Stiffness in Extended End-Plate Connection," *Applied Mechanics and Materials*, Vol. 321–324, pp. 1,766–1,769.

Zhuling, Y., Baolong, C., and Ke, Z. (2012), "Analysis on the Seismic Behavior of Extended End-Plate Connections of Steel Frame Structure," *Applied Mechanics and Materials*, Vol. 193–194, pp. 1,405–1,413.

Smarter. Stronger. Steel.

American Institute of Steel Construction
312.670.2400 | www.aisc.org

D839-23